# PRINCIPLES AND CASE STUDIES OF SIMULTANEOUS DESIGN

# PRINCIPLES AND CASE STUDIES OF SIMULTANEOUS DESIGN

**WILLIAM L. LUYBEN**

AIChE®

WILEY

A JOHN WILEY & SONS, INC., PUBLICATION

Published by John Wiley & Sons, Inc., Hoboken, New Jersey
Published simultaneously in Canada



***Library of Congress Cataloging-in-Publication Data:***

Luyben, William L.
Principles and case studies of simultaneous design / William L. Luyben.
p. cm.
Includes bibliographical references and index.
ISBN 978-0-470-92708-3 (cloth)
1. Chemical engineering. 2. Engineering design. I. Title.
TP155.L884 2010
660′.2812–dc22

2010036834

Printed in the United States of America

eBook ISBN: 978-1-118-00163-9
oBook ISBN 978-1-118-00165-3
ePub ISBN: 978-1-118-00164-6

10 9 8 7 6 5 4 3 2 1

The book is dedicated to all the past, present and future
Lehigh “kick-ass” engineers.

# CONTENTS

# PREFACE

Process design involves the development of an effective flowsheet to transform reactants into products in a profitable, safe, environmentally friendly, and controllable plant. Coming up with the best topology of process units is a synthesis problem. It involves science, art, innovation, intuition, inspiration, experience, and common sense. Success also requires a lot of hard work and, at times, a little luck. The designer usually has many criteria to satisfy, many of which are conflicting.

Despite the predictions of many skeptics, chemical process design remains a vital area in chemical engineering. The recognition of the importance of energy and environmental problems, and the interaction between the two, has renewed interest in the design of energy-efficient process plants.

The goal of this book is to present some general design principles in a concise form that should aid the engineer in completing the daunting task of developing an effective flowsheet and control structure. A rich variety of case studies are presented that illustrate in an in-depth and quantitative way the application of these general principles.

Effective development of a chemical process requires the simultaneous consideration of both steady-state economic and dynamic controllability aspects of the process. We call this "simultaneous design." It is one of the main features of this book.

Detailed case studies are presented of ten complex processes that contain a variety of features commonly occurring in many important industrial plants. In-depth, economic steady-state designs are developed that satisfy an economic objective function such as minimizing total annual cost of both capital and energy. Complete, detailed flowsheets and Aspen Plus files are provided. Conventional proportional-integral (PI) plantwide control structures are developed and tested for their ability to maintain product quality during typically large disturbances. Complete Aspen Dynamics files of the dynamic simulations are provided.

There are many comprehensive design books, but none of them provides a significant number of examples of detailed economic design and accompanying dynamic plantwide control of typically complex industrial processes. Most of the current design books are

"encyclopedic" in nature, in that they cover a very wide spectrum of topics associated with process design. In addition to discussing flowsheet development and equipment design, these textbooks go into a lot of detail in areas that are certainly important but not as technically essential to process design as those presented in this book. The coverage of economics in many of these books includes elegant methods of economic analysis, most of which can hardly be justified by the uncertainties in market predictions. Many chapters in these books are devoted to a host of other somewhat peripheral subjects, such as written and oral skills, ethics, "green" engineering, and product design. The engineer is easily overwhelmed by the sheer size of such a book, and it is difficult to sort out the essentials.

In this book, I intended to cut through this maze of information and present the essential principles of design and control in a brief, readable form that can be easily comprehended by students and engineers in the chemical, petroleum, and biochemical industries. The detailed case studies should provide concrete examples of the application of these design and control principles.

I hope you find this book useful for practical engineering applications and that the subject matter is interesting, important, challenging, and presented in a readable manner. Good luck in your engineering careers. Keep the faith!

WILLIAM L. LUYBEN

# NOMENCLATURE

| | |
|---|---|
| $\Re$ | reaction rate |
| $\tau_F$ and $\tau_R$ | time constants |
| $\tau_{\mathrm{I}}$ | controller integral time (min) |
| $A$ | area |
| A, B, C, D | for generic chemical reactants |
| $A_{\mathrm{C}}$ | condenser area ($m^2$) |
| $A_{\mathrm{R}}$ | reboiler area ($m^2$) |
| BB | butane–butylene |
| B1 | bottoms (B2, etc.) |
| $B_{\mathrm{tot}}$ | total butanol stream |
| $C$ | concentration |
| C1 | column 1 (C2, etc.) |
| $C_4$ | $iC_4$, $nC_4$ |
| CSTR | continuous stirred-tank reactor |
| $D$ | distillate flowrate (kmol/h) |
| $D$ | diameter |
| D1 | distillate (D2, etc.) |
| $D_2/R_2$ | ratio |
| DEB | diethyl benzene |
| DIB | deisobutanizer |
| DIPA | di-isopropyl amine |
| DME | dimethyl ether |
| DP | depropanizer |
| EB | ethyl benzene |
| $F$ | feed flowrate (kmol/h) |

*Principles and Case Studies of Simultaneous Design*, First Edition. William L. Luyben

| | |
|---|---|
| FC | flow controller |
| FEHE | feed-effluent heat exchanger |
| FFE | flowrate of fresh ethylene feed |
| HDA | hydrodealkylation process |
| HP | high-pressure steam |
| HX | heat exchanger |
| ID | column diameter (m) |
| IPA | isopropanol |
| $k_1$ and $k_2$ | specific reaction rates |
| K1 | compressor 1 (K2, etc.) |
| $K_C$ | controller gain (dimensionless) |
| $k_F k_R$ | loop gain |
| $L$ | length |
| LP | low-pressure steam |
| MH | 2-methyl-1-heptene |
| MHOH | 2-methyl-2-heptanol |
| MIPA | mono-isopropyl amine |
| MMH | 2-methoxy-2-methylheptane |
| MP | medium-pressure steam |
| MTBE | methyl tert-butyl ether |
| $M_{tot}$ | methyl acetate/methanol stream |
| NF | feed stage |
| NT | total number of stages |
| OP | controller output signal |
| $P$ | pressure |
| PDIB | *p*-diisopropyl benzene |
| PI | proportional-integral controller |
| $Q$ | heat input |
| $Q_C$ | condenser duty (MW) |
| $Q_R$ | reboiler duty (MW) |
| $R$ | reflux flowrate (kmol/h) |
| R/F | reflux-to-feed ratio |
| R1 | reactor 1 (R2, etc.) |
| ROI | return on investment |
| RR | reflux ratio ($R/D$) |
| RVP | Reid vapor pressure |
| SP | setpoint signal |
| SVD | singular value decomposition |
| TAC | total annual cost ($10^6$ \$/y) |
| $T_B$ | base temperature (K) |
| TC | temperature controller |
| $T_D$ | reflux-drum temperature (K) |
| THF | tetrahydrofuran |
| $T_R$ | reactor temperature (K) |
| $U$ | overall heat-transfer coefficient |
| VLE | vapor–liquid equilibrium |
| VPC | valve position controller |
| $V_R$ | reactor size ($m^3$) |
| $Y$ | output |
| $zn(j)$ | column $n$ feed composition (mole fraction $j$) |

# CHAPTER 1

# INTRODUCTION

In this first chapter we discuss what process design is all about, some of its history and technical triumphs, and what the future may hold. The essential features of design are summarized, and its vital role in the development of our modern society is discussed.

## 1.1 OVERVIEW

The function of chemical process design is to take the chemistry that has been discovered by a chemist in small-scale laboratory experiments and end up with a large plant-scale process that efficiently and safely produces large quantities of a useful product. The chemist works with grams of material in test tubes and Parr bombs. The final plant produces millions of kilograms per year of products and requires large equipment (reactors sometimes as large as 100 $m^3$ and distillation columns 50 m in height and 5 m in diameter). The scale-up factor is often many orders of magnitude.

How the chemist handles the small quantities of chemicals in the laboratory equipment is usually much different from how the engineer deals with the enormous amounts of chemicals in an industrial plant. Basic geometry tells us that the surface-to-volume ratio of a cylinder decreases as the total volume increases. So, as larger and larger reactor vessels are used, the jacket heat-transfer area gets smaller relative to the reaction heat that must be transferred between the jacket and the material in the reactor. Smaller areas require larger differential temperature driving forces for heat transfer, which makes dynamic control more difficult, as we will demonstrate in subsequent chapters. So scale-up is one of the important aspects of process design.

The chemist often conducts batch experiments. Reactants are placed in a test tube and heated to reaction temperature. The changes in composition with time are obtained. The

*Principles and Case Studies of Simultaneous Design*, First Edition. William L. Luyben

effects of the important reaction parameters on these time trajectories are determined: temperature, pressure, initial reactant concentrations, and quantity of catalyst. Kinetic mechanisms are deduced from this batch data, and kinetic relationships and parameters are obtained that fit the experimental data. However, many industrial processes operate continuously, not in batch mode. So the engineer has to use the batch chemical data from the chemist and apply it to continuously operating reactors.

The chemist usually starts with essentially pure reactants and does not worry about separating the mixture of products and reactants that result from the laboratory experiments. These separations are critical to the technical success and economic viability of a large-scale plant. High-purity products must be produced with little variability in product quality. Reactants must be recovered and recycled. By-products must be recovered and disposed of in an economic and pollution-free way.

The separation aspects of a chemical plant often dominate the economics. As many of the case studies presented in subsequent chapters demonstrate, there are important trade-offs between the costs and performance in the reaction section of the process and the costs and performance in the separation section of the process.

The most fundamental process design trade-off is between reactor size and recycle flowrate. The larger the reactor, the smaller the required recycle flowrate. Large reactors increase capital investment in reactor vessels and catalyst. But small recycle flowrates reduce capital investment in separation equipment (distillation columns and heat exchangers) and reduce energy costs in the separation units. So there is a "sweet spot" at which this trade-off gives the "best" flowsheet in terms of economic objectives.

Chemists use nice, pure chemical reactants. The feed streams in many industrial plants frequently are not pure. They can contain chemically inert components that will build up in the unit if not purged out. Undesirable by-products may also be generated that must be removed.

These issues are only a small fraction of the challenges faced by the engineer in developing a process design. The final flowsheet is inevitably a compromise among many competing factors. The process that is built must be economically attractive, it must be safe, and it must be dynamically operable.

This book emphasizes the need to consider both steady-state economics and dynamic controllability through all stages of process development. We call this theology *simultaneous design*. The desirability of combining steady-state and dynamic design has been discussed in process design circles since the pioneering work of Page Buckley at DuPont in the 1950s. Papers and books have been written. Talks have been presented. Symposia have been run. The advantages of coupling design and control have been clearly identified. The simulation tools (software and hardware) are available. Design and control methodology has been developed and documented.

However, it appears that little of this "theology" has been implemented in senior design courses. In almost all chemical engineering departments, process designs are developed with little or no consideration of whether or not the process is controllable. In my opinion, this represents a major flaw in the education of chemical engineers. Old war stories abound of multimillion-dollar plants that have been built but could never be economically and safely operated because of dynamic instabilities.

All the case studies presented in this book combine detailed economics investigations and quantitative dynamic simulation studies. Effective plant-wide control structures are developed that can handle the large disturbances often experienced in industrial processes.

## 1.2 HISTORY

Chemical process design probably goes back to prehistoric times, when ancient man developed methods for providing food, clothing, and shelter from the raw materials available. The methods and tools were crude by present-day standards, but they were probably considered cutting-edge, high-tech in those days. Making beer and baking bread were (and still are) important chemical processes. Producing soap, tanning leather, and making tools involved crude forms of process design. The Egyptians invented papyrus, the forerunner of paper, way back in 4000 BC.

Chemistry developments built slowly in early civilizations. Copper, bronze, and iron tools and weapons were developed, which facilitated providing food by hunting and tilling the soil. Progress became more rapid through biblical times and the Middle Ages as more and more chemicals were discovered that were useful to mankind. Gunpowder was produced in China around 800 AD. The primary energy source during all these many years was renewable, sustainable, and carbon-neutral wood.

But advances in chemistry accelerated rapidly starting in the eighteenth and nineteenth centuries. Industrial and university chemical research centers were discovering a vast variety of chemicals that had potential value to improve the quality of human life. The production of ammonia for use in agricultural fertilizer produced substantial increases in food production. The Bessemer process for converting iron into steel was developed. Nitroglycerin and TNT were invented. Nobel invented dynamite in 1866. Coal was the primary energy source during this period, and it also was the source of many chemical raw materials. This period was when much coal chemistry was developed.

At the beginning of the twentieth century there was an explosion of activity in chemical process design. Petroleum and natural gas became the principle energy sources as well as the sources of raw materials. The vast variety of hydrocarbons that occur in crude oil or that are produced in refineries in the cracking and reforming processes provided both inexpensive raw materials and energy for the chemical industry.

The intense demands made by two world wars also spurred chemical process design. The development of the atomic bomb in the Manhattan Project relied heavily on a number of complex chemical reaction and separation steps invented by chemical process engineers. The post-World War II expansion of the chemical industry around the world presented enormous challenges and opportunities to process design and control engineers. A drive along the Houston Ship Channel gives some indication of the size of the petroleum and chemical industry. This “mecca” of process design owes it location to cheap gas and oil.

The energy situation has changed drastically in the last several decades. Supply and demand as well as political issues have created rapid increases in gas and oil prices. Most of the new chemical plants are being built in locations that have large gas and oil resources (mostly in the Middle East) or locations with rapidly developing economies (Asia). The need for energy-efficient process design is now more important than ever.

Environmental concerns have also become major drivers in process design. The concern about carbon dioxide emissions has spurred activity in the design of chemical recovery processes for possible sequestration. Reducing the formation of polluting by-products has required significant modifications in many process designs. The new flowsheets feature more extensive recycling to suppress undesirable products or the use of new solvents.

“Times are a-changing” has been an appropriate characterization of process design for many years, and there is no indication that the situation will change. The need for innovative,

efficient, economical process design is as strong now as it ever was. So be assured, you are not wasting your time studying and working on process design.

A good process design engineer must have a solid grasp of technical fundamentals, a healthy portion of common sense, a familiarity with practical fluid mechanics (plumbing), the ability to think "out of the box," a strong element of tenacity, and the willingness to work hard.

## 1.3 BOOKS

The first textbooks dealing with process design began appearing shortly after the formal birth of chemical engineering as a distinct discipline. The 1934 book by Vilbrandt, *Chemical Engineering Plant Design*,[1] appears to be the first textbook dealing with the subject. Topics discussed include mechanical details of equipment and buildings, plant geographic location, and accounting. The 1974 book by Guthrie, *Process Plant Estimating Evaluation and Control*,[2] presented a wealth of material on estimating capital and operating costs in chemical plants. The 1985 book by Peters and Timmerhaus, *Plant Design and Economics for Chemical Engineers*,[3] was the pioneering design text that covered a wide variety of important topics in process design. In 1968, the insightful *Strategy of Process Engineering* by Rudd and Watson[4] developed some of the fundamentals of process flowsheet development. The idea of "conceptual process design" as opposed to "detailed process design" was the result of the pioneering work of Jim Douglas.[5]

A host of textbooks have appeared in recent years that are widely used in senior design courses and represent good reference sources. A partial list is provided at the end of this chapter.[6–13]

However, these books are almost encyclopedic in nature. They attempt to cover all facets of process design, sometimes in excruciating detail. The student finds it difficult to filter out the important "water droplets" from the "ocean" of information and words in these voluminous textbooks. I hope this book is successful in presenting only the essential technical principles that underlie chemical process design.

## 1.4 TOOLS

There has been tremendous progress in the computational, writing, and graphical tools available for the process design engineer. In the early days of my career (1955), there were only mechanical calculators, slide rules, Leroy lettering sets, and manual typewriters. Computers were not in use by practicing engineers. Engineering calculations were done by hand. Graphical methods were employed where possible. No process simulation software was available.

About this time, analog and digital computers began to appear in industry and in universities. Each company began to develop its own process simulation software. Many large chemical companies (Monsanto, DuPont, Exxon) had proprietary simulators, which could only handle steady-state design.

The Monsanto Company developed FLOWTRAN in the late 1960s. It was made available to universities and other companies in 1973. Over the next several decades a number of process simulators appeared, each with increased capability and improved user-friendliness. Simulators that could handle dynamics and the computers having the required computational speed and memory finally appeared on the scene in the late 1990s.

The current state of process simulation is greatly advanced from where it was fifty years ago. Almost all companies make extensive use of process simulators in both the design and the operation of chemical plants. Steady-state simulation studies are routinely used. A growing number of companies also incorporate dynamic simulations in their design development.

Almost all chemical engineering departments in universities include steady-state process simulation in their design courses. However, it appears that only a tiny handful of departments even mention dynamic plantwide control studies in their design courses. In my opinion, this is a major technical flaw in a design course. To find the "best" design, the dynamic controllability must be investigated.

The advances in other tools have also been enormous. Generating figures in PowerPoint or Visio sure beats struggling with the old Leroy lettering set. Word processing greatly facilitates technical writing. Mathematical tools like MATLAB, MathCad, and Mathematica make technical calculations simple and powerful. Spreadsheets are also widely used.

## REFERENCES


1. Vilbrandt, F. C. *Chemical Engineering Plant Design*, McGraw-Hill, New York, 1934.
2. Guthrie, K. M. *Process Plant Estimating Evaluation and Control*, Craftsman Book, Carlsbad, CA, 1974.
3. Peters, M. S., Timmerhaus, K. D. *Plant Design and Economics for Chemical Engineers*, McGraw-Hill, New York, 1958.
4. Rudd, D. F., Watson, C. C. *Strategy of Process Engineering*, John Wiley & Sons, New York, 1968.
5. Douglas, J. M. *Conceptual Design of Chemical Processes*, McGraw-Hill, New York, 1988.
6. Ulrich, G. D. *A Guide to Chemical Engineering Process Design and Economics*, John Wiley & Sons, New York, 1984.
7. Biegler, L. T., Grossmann, I. E., Westerberg, A. W. *Systematic Methods of Chemical Process Design*, Prentice-Hall, Englewood Cliffs, NJ, 1997.
8. Turton, R., Bailie, R. C., Whiting, W. B., Shaelwitz, J. A. *Analysis, Synthesis and Design of Chemical Processes*, 2nd Edition, Prentice Hall, Englewood Cliffs, NJ, 2003.
9. Dimian, A. C. *Integrated Design and Simulation of Chemical Processes*, Elsevier, New York, 2003.
10. Duncan, T. M., Reimer, J. A. *Chemical Engineering Design and Analysis: An Introduction*, Cambridge University Press, New York, 1998.
11. Seider, W. D., Seader, J. D., Lewin, D. R. *Product & Process Design Principles*, John Wiley & Sons, Hoboken, NJ, 2004.
12. Towler, G., Sinnott, R. *Chemical Engineering Design: Principles, Practice and Economics of Plant and Process Design*, Elsevier, New York, 2008.
13. Dimian, A. C., Bildea, C. S. *Chemical Process Design: Computer-Aided Case Studies*, Wiley-VCH, New York, 2008.

# CHAPTER 2

# PRINCIPLES OF REACTOR DESIGN AND CONTROL

The reaction section of a chemical plant is typically the heart of the process. Here is where the basic chemical transformations of raw materials into products are conducted. The reaction section must be well designed so that the conversion of reactants and the yield of desired products is high, and the dynamic stability of the reactor is guaranteed. Reactors can present major safety and dynamic controllability problems if the reactions are exothermic and irreversible. Many industrial accidents have resulted from poor design and operation of chemical reactors.

In this chapter we discuss basic principles of reactor design and control since the two features are intimately connected. Failure to explore reactor dynamics can lead to catastrophic results.

## 2.1 BACKGROUND

Reactors occur in many flavors, but we limit our discussion to continuous systems. *Continuous stirred-tank reactors* (CSTR) and tubular reactors are the most common types. The reactors may or may not contain catalysts. The phases in the reactors can be liquid or vapor. The reactors can be adiabatic or involve heat transfer (cooling or heating). Multiple reactors of the same or different types can be operated in series or parallel. The fresh feed streams of reactants can enter the process as gases or liquids.

There are also many types of reactions: endothermic, exothermic, irreversible, reversible, consecutive, simultaneous, homogeneous, heterogeneous, and so on. The type of reaction and the type of reactor exercises a very strong impact on the design of both the reaction section and the separation section of the process.

*Principles and Case Studies of Simultaneous Design*, First Edition. William L. Luyben

## 2.2 PRINCIPLES DERIVED FROM CHEMISTRY

A look at the stoichiometry and the kinetic parameters of the reactions can immediately yield a lot of information about what conditions should be favorable to facilitate the production of desired products. Stoichiometry and the kinetic parameters also determine the general topology of the process in terms of the need for recycles.

### 2.2.1 Heat of Reaction

Basic kinetics tells us that all specific reaction rates increase with temperature, but chemical equilibrium constants for reversible reactions can either increase or decrease with temperature depending on the heat of reaction.

***Endothermic Reactions.*** Endothermic reactions have positive heats of reaction, so they soak up heat. If the reactor is adiabatic, temperatures will *decrease* from the inlet to the outlet in a tubular reactor. If heat transfer is used in the reactor, heat must be transferred *into* the reactor from a higher-temperature heat source to maintain temperatures.

The chemical equilibrium constant of an endothermic reaction increases as temperature increases. High reactor temperatures increase both specific reaction rates and chemical equilibrium constants. Therefore, conversion is enhanced by running at the highest possible temperature. This means that a small reactor can be used.

So the optimum design of endothermic reactors is relatively easy. You simply operate at the highest possible temperature. Maximum temperature may be limited by a variety of constraints: catalyst degradation, materials of construction, undesirable side reactions that occur at high temperatures, thermal degradation, pressure limitations, and so on.

Many processes with endothermic reaction that operate at high temperatures use multiple adiabatic reactors in series with intermediate furnaces to heat up the process stream to some optimum maximum inlet reactor temperature. The number of reactors and their sizes are important design optimization variables.

Endothermic reactions rarely present control problems. Temperature runaways seldom occur because a temperature increase raises reaction rates, which in turn tend to soak up heat and reduce temperatures. Thus endothermic reactions are self-regulatory.

***Exothermic Reactions.*** Exothermic reactions have negative heats of reaction, so they generate heat. If the reactor is adiabatic, temperatures will *increase* from the inlet to the outlet in a tubular reactor. If heat transfer is used in the reactor, heat must be transferred *out of* the reactor into a lower-temperature heat sink to maintain temperatures.

The chemical equilibrium constant of an exothermic reaction *decreases* as temperature increases. This presents a problem. High reactor temperatures are needed to achieve reasonably large specific reaction rates so that fairly high conversions can be attained. On the other hand, if the temperature is too high, we run into a chemical equilibrium constraint, which means the reaction stops and conversion is limited.

The optimum design of exothermic reversible reactions involves a trade-off between reactor temperature and reactor size. Low temperature can permit high conversion, but a large reactor has to be used. Many processes with this type of reaction are designed with multiple reactors in a series. The first reactors operate at high temperature to get the reactions going. The later reactors operate at lower temperatures so as to avoid the chemical equilibrium constraint.

Reactors with exothermic reactions can present major dynamic control problems. If the exothermic reactions are *reversible*, temperature runaways are usually not an issue because of the self-regulation wrapped up in the chemical equilibrium constraint. If a temperature increase occurs, heat will be generated, which will increase temperature further. However, at some point the forward and the reverse reaction rates will approach each other. The net reaction rate will go to zero, and the temperature will stop climbing.

However, if the exothermic reactions are *irreversible*, there is the potential for temperature runaways. So the system that can present difficult dynamic control problems is one in which the reactions are *irreversible* and *exothermic*. If a temperature increase occurs, heat will be generated, which will increase temperature further and result in a further increase in reaction rate and heat generation. Open-loop unstable reactors can occur and can run away to dangerously high temperature levels. Pressure will build up, safety valves or rupture disks will open, and serious safety and pollution problems may result.

The other necessary ingredient for this instability scenario is a reactor that is operating at low to modest levels of conversion. If the conversion is very high, the concentration of reactant in the reactor will be low. There is very little "fuel" around to cause the reactions to run away. The small amount of reactant will be consumed before dangerous temperatures are reached. This limiting reactant condition is frequently used to provide concentration self-regulation in reaction systems with two reactants and very large activation energies. The high temperature sensitivity can be mitigated by running with only a small concentration of one of the two reactants.

### 2.2.2 Reversible and Irreversible Reactions

Some aspects of reversible and irreversible reactions have been discussed in the previous section. The impact on reactor design and control was examined. However, the distinction between the two types of reactions also has a strong effect on the topology of the process flowsheet.

***Reversible.*** If the reactions are reversible, it almost always necessary to design a plant with recycles. The reactor effluent will always contain reactants, which must be recovered and recycled because of the strong economic impact of reactant cost. Therefore the flowsheet with a reversible reaction has one or several recycle streams. The number of recycle streams depends on the number of reactants and the methods used for separating them from the products.

For example, suppose the chemistry is the reversible reaction $A + B \Leftrightarrow C$ and suppose distillation is used to separate the reactor effluent containing all three components. If the volatilities of A and B are larger than C, a single distillation column can be used with a single recycle stream (the distillate) containing A and B. On the other hand, if the volatilities are such that A is the lightest, C is the intermediate, and B is the heaviest, two distillation columns and two recycle streams will be required. Using the direct separation sequence, a recycle stream of A would be taken overhead in the first column and a recycle stream of B would come from the bottom of the second column.

***Irreversible.*** If the reactions are irreversible, high conversions can be attained if reactor temperature and/or reactor size can be made large enough. Reactor temperatures have constraints, as mentioned in the previous section. If the specific reaction rate is still small at this maximum temperature, a very large single reactor would be required to achieve

high conversion. Using multiple reactors in series with decreasing reactant concentrations in successive stages would reduce total volume requirements.

In some cases, the achievable conversions can be high enough to not require any recycle streams. Essentially all of the reactants are consumed. However, in many situations, it turns out to be more economical to use a flowsheet topology with smaller reactors and a separation section with recycle even when the reactions are irreversible.

### 2.2.3 Multiple Reactions

In most processes, more than just a single reaction occurs. Some reactions are good, making the desired product. Some reactions are bad, making undesired by-products that reduce the yield of the desired product and thereby waste reactant and present expensive waste-disposal problems.

In this section we consider a number of common situations. The desirable and undesirable reactions can be simultaneous or consecutive.

***Simultaneous Reactions.*** Consider the hypothetical reaction system with two simultaneous reactions:

$$\begin{aligned} A + B &\longrightarrow C \\ 2A &\longrightarrow D \end{aligned} \tag{2.1}$$

Component C is the desired product. Component D is the bad guy. Looking at this stoichiometry, it is immediately obvious that we need to keep the concentration of A in the reactor low so as to suppress the production of D. The implication of this observation is that we need a large excess of component B to keep the concentration of A small. Therefore the flowsheet topology must include a recycle stream of component B.

For a given reactor temperature, there is a trade-off between the yield of C and the amount of B recycle. If the undesired product D is difficult to get rid of or presents a safety or environmental hazard, we want to make a very small amount of it. Therefore a large B recycle must be used. The capital and energy cost of the separation section and the cost of the reactant raw materials have to be balanced by the costs and risks of handling and disposing of component D.

Of course reactor temperature can also affect conversions and yields. The optimum reactor temperature depends on the activation energies of the two reactions. If the activation energy of the desirable reaction is larger than the activation energy of the undesirable reaction, high reactor temperatures improve yield. If the situation is reversed, low reactor temperatures improve selectivity (more C is made compared to D). However, if reactor temperatures are too low, the specific reaction rate is so small that reactant conversion is low unless very large reactors are used.

The latter situation is very common: low temperatures favor the desired product. So many process designs require trade-offs among the design optimization variables of temperature, reactor size, and recycle. This is a common theme in many of the process case-studies presented in later chapters of this book.

***Consecutive Reactions.*** Consider the hypothetical reaction system with two consecutive reactions:

$$\begin{aligned} A + B &\longrightarrow C \\ A + C &\longrightarrow D \end{aligned} \tag{2.2}$$

Component C is the desired product, and component D is the undesired product. It is again obvious that the concentration of component A must be kept small. So all the ideas presented in the previous section also apply in these types of reactions.

Reactor temperature selection depends on the relative values of the two activation energies. The same trade-offs among temperature, size, and recycle apply.

## 2.3 PRINCIPLES DERIVED FROM PHASE OF REACTION

Reactions occur in either the liquid phase or the gas phase. Liquid-phase reactions are carried out in either CSTRs or tubular reactors. Typical residence times vary from a few minutes to tens of minutes because reactor mass hold-up can be fairly large due to the high liquid density. Most gas-phase reactions are carried out in tubular reactors, since you cannot stir gas. Typical residence times are seconds because of the small vapor density.

Having liquid-phase reactions implies liquid feed streams into the reactor and liquid recycle streams. Having vapor-phase reactions implies gas streams entering and leaving the reactor. The original fresh feeds and the recycle streams to a gas-phase reactor can be either liquid or vapor. If they are liquid, they must be vaporized and preheated to the required reactor inlet temperature in heat exchangers. Attempting to both vaporize and superheat a liquid stream can lead to severe hydraulic problems due to slug flow during the transition from liquid to vapor. These problems can be avoided by using a separate heat exchanger (kettle reboiler) as a vaporizer, which generates saturated vapor, and then a downstream heat exchanger to superheat the gas to the desired reactor inlet temperature.

Fluid mechanics tells us that orders of magnitude less energy is required to pump a liquid than to compress a vapor. So, if a reactor feed stream needs to be a high-pressure gas and if it is originally a liquid, the liquid stream should be pumped up to the required pressure and then vaporized. If the recycle stream is a gas and must be compressed, the pressure drops through the reactor and other units in the gas recycle loop should be kept as small as possible. There is an engineering trade-off between compression costs needed to provide enough pressure drop (velocity) in heat-transfer units for reasonable heat-transfer coefficients and the capital cost of heat exchanger area. Since heat-transfer film coefficients are small in gas systems, heat exchangers tend to be quite large compared to liquid systems in which higher heat-transfer coefficients can be attained by providing more pressure drop, which is inexpensively provided by pumping.

Another aspect of gas-phase reactions is the selection of which reactant to design for high per-pass conversion. Consider the reversible gas-phase reaction $A + B \Leftrightarrow C$, where B is a high-boiling component that is supplied in the liquid phase, while A is a low-boiling gas. There must always be some reactant in the reactor effluent, since the reaction is reversible and complete conversion of both reactants in not possible.

We could design the process for a high conversion of A or a high conversion of B. Which is better? If we feed an excess of A, there will be lots of A coming out of the reactor. This component is a low-boiling component and cannot be condensed inexpensively using cooling water, so a gas recycle stream of A will have to be compressed, which is expensive. Alternatively we could feed an excess of B. This is a high-boiling component that can be condensed and pumped up to the required pressure before vaporizing. Pumping is inexpensive. Vaporization requires significant energy but it may be at a low enough temperature to require relatively inexpensive low-pressure steam. Compression requires high-level energy (electric power or high-pressure steam) that is expensive. So the question of which

is better depends on the relative costs and amounts of energy and capital required in the two alternatives.

Gas-phase systems that require compression are unavoidable in many processes. The work required to compress a gas from a suction pressure $P_1$ to a discharge pressure $P_2$ is a minimum if the compression is isothermal. But compressors operate adiabatically. So the design of a gas compressor configuration usually involves a series of compressors and intercoolers. After the first stage of compression, the gas is cooled to as low a temperature as attainable with cooling water in a heat exchanger. Remember that the adiabatic compression of an ideal gas is given by the following equation.

$$W = \frac{\gamma R T_1}{\gamma - 1}\left[\left(\frac{P_2}{P_1}\right)^{\gamma - 1/\gamma} - 1\right] \tag{2.3}$$

The suction temperature $T_1$ directly affects the work, so the compressor system should be designed for low inlet temperatures. The number of compression stages used is a balance between energy costs and capital investment in compressors and heat exchangers. A useful heuristic in a system with $N$ stages of compression, with an initial feed pressure of $P_0$ and a final pressure of $P_N$, is to make the compression ratio in each stage $(P_N/P_0)^{1/N}$.

## 2.4 DETERMINING KINETIC PARAMETERS

The most difficult part of any process design and the essential simulation is getting reliable reaction kinetic parameters. The commercial simulators provide almost none of this type of data in their libraries, so the designer must go to the laboratory or the literature or the pilot plant or the operating plant to find information.

Using reliable laboratory data in which you have confidence is clearly the most desirable approach. But in many situations, particularly at the conceptual design stage, the process designer must rely on literature data. This can be a real pain, since authors report their results using a variety of units, and the process simulators often require very specific units. The Aspen Plus simulator used in this book requires that overall reaction rates must be given in either "kmoles per second per cubic meters of reactor volume" or "kmoles per second per kilogram of catalyst" in the reactor. Also, if concentrations are given in partial pressures, they must be in terms of Pascals. Translating literature data into these units is not a trivial job but can be speeded by using MathCad or other equation-manipulating software.

### 2.4.1 Thermodynamic Constraints

The first thing to investigate for any reaction system is the chemical thermodynamic constraints. Using AspenTech software, this is easy to achieve by using the RGIBBS reactor model, which minimizes the free energy of the system to solve for the concentration of reactants and products at chemical equilibrium. Clearly no kinetic reactions can give conversions greater than this.

Place the RGIBBS reactor on the Aspen Plus flowsheet and connect a feed stream of reactants. Specify temperature and pressure, and the model will predict the compositions leaving the reactor. These results are independent of reactor size and would be obtained if

the reactor were infinitely large for any kinetic expression. They provide an upper limit to what can be achieved.

This procedure is very useful in exploring the effects of changing temperature and pressure on conversion, yield, and selectivity. The designer can quickly get a feel for how temperature and pressure affect reactor performance in the chemical system under study. The results from an RGIBBS reactor are essentially the same as those of any kinetic reactor in which the kinetics are fast.

Another useful application of the RGIBBS reactor is to calculate the temperature dependence of the chemical equilibrium constant $K_{EQ}$. You simply make a series of runs over a range of temperatures and calculate $K_{EQ}$ from the concentrations (activities) at each temperature. For example, if the vapor-phase reaction is $A + B \Leftrightarrow C + D$, and the forward and reverse reactions are first-order in the partial pressures of the components, at each temperature the chemical equilibrium constant is

$$K_{EQ} = \frac{P_C P_D}{P_A P_B} \tag{2.4}$$

Then a plot of the logarithm of $K_{EQ}$ versus the reciprocal of the absolute temperature should give a straight line from which an equation for $K_{EQ}$ can be obtained.

$$\ln(K_{EQ}) = A + \frac{B}{T} \tag{2.5}$$

Sometimes literature data only give information on the forward reaction rate. The reverse reaction rate can be calculated from the $K_{EQ}$ equation developed from the RGIBBS runs.

### 2.4.2 Kinetic Parameters from Plant Data

Operating data from a pilot plant or a commercial plant, which is preferable to laboratory data, is sometimes available. In this situation, it is possible to calculate kinetic parameters that fit this data if it includes essential information like temperature, pressure, reactor size, throughput, conversion, and yield. There are elegant data regression methods available that can be applied for this job. Aspen Plus has this capability. However, it is often sufficient to assume some quite simple kinetic model with parameters that can be easily calculated from plant data. In many cases, these simple models capture the macroscopic effect of reaction parameters with sufficient fidelity to permit their use in process design calculations.

## 2.5 PRINCIPLES OF REACTOR HEAT EXCHANGE

Continuous stirred-tank reactors and tubular reactors have different heat-transfer configurations, display different dynamic characteristics, and present different dynamic control problems and design issues.

### 2.5.1 Continuous Stirred-Tank Reactors

A CSTR is usually a cylindrical agitated vessel containing reacting liquids. The most simple way to transfer heat is through the wall of the vessel into a surrounding jacket. The rate of

heat transfer depends on the circumferential area of the vertical wall, the overall heat-transfer coefficient and the differential temperature driving force between the temperature of the liquid in the vessel and the temperature of the cooling or heating medium in the jacket. Note that the aspect ratio (length-to-diameter ratio) of the vessel is an important parameter. For a given volume, the heat-transfer area increases as we increase the aspect ratio, which is good from a dynamic control standpoint. However, a long skinny tank is difficult keep well mixed, which is a requirement in a CSTR. So a typical aspect ratio for reactors is two.

There are several alternative heat-transfer arrangements in CSTRs. A coil can be installed inside the vessel. The diameter of this internal coil cannot be small because of mechanical strength issues, and the coil cannot interfere with mixing. An increase in heat-transfer area of about 30% can be achieved. Large increases in area can be obtained by pumping the liquid in the reactor vessel through an external heat exchanger. The flowrate of this circulating stream is set at a high value to keep the whole system well mixed. Another alternative arrangement for exothermic reaction systems is to use evaporative cooling. The pressure in the reactor is set so that the liquid will boil at reaction temperatures. The latent heat of vaporization is supplied by the exothermic heat of reaction. Vapor from the reactor flows to a condenser, and the liquid is returned to the reactor.

The key process design parameter in reactors is *heat-transfer area*. Reactor dynamic stability depends on having plenty of area so that rapid and large changes in heat-transfer rates can be achieved, which permit disturbances to be handled. As previously discussed, reactors with exothermic irreversible reactions are the major troublemakers. Large area means a small temperature difference between the reactor temperature and cooling medium temperature in the jacket, coil, or external heat exchanger. When a disturbance occurs, the flowrate of the cooling medium is changed, which can produce a big change in the differential temperature driving force and thus make a big change in the heat-transfer rate. Reactor stability is directly related to heat-transfer area. A quantitative study of this issue is given in Luyben.[1]

In CSTR systems the feed temperature has a minor effect on reactor performance, both steady-state and dynamic. The liquid is perfectly mixed, so there is a single temperature to control. As discussed below, feed temperature is much more important in tubular reactors.

### 2.5.2 Tubular Reactors

Tubular reactors are distributed systems with temperatures and compositions changing down the length of the reactor. If they are designed for adiabatic operation, the reactor is a vessel with or without beds of solid catalyst. They also can be designed as multitube heat exchangers so that cooling or heating occurs between the reacting process phase and the heating or cooling medium. Reactants typically flow inside the small-diameter tubes (filled with catalyst if the reactions are heterogeneous), and the cooling or heating medium is on the shell side.

***Adiabatic Tubular Reactors.*** Since no heat is removed or added in an adiabatic reactor, temperatures will increase down the length of the reactor if the reactions are exothermic, or temperatures will decrease if the reactions are endothermic. The inlet temperature is a critical design parameter in both cases.

Let us consider first the endothermic case. We want the highest inlet temperature attainable because both specific reaction rates and chemical equilibrium constants increase with temperature. So the process is designed to come into the reactor at the highest possible

temperature. If the temperature decrease is large, reaction rates will decrease toward the end of the reactor and chemical equilibrium constraints may be encountered. In this case, a number of adiabatic tubular reactors with intermediate heating may be required to achieve the desired conversion.

If the reactions are exothermic, we have similar problems but in the opposite direction. Temperature increases down the length of the reactor. In most systems there are constraints on the maximum temperature that can be tolerated anywhere in the reactor. For a given inlet temperature and a given desired per-pass conversion and given inlet compositions, the adiabatic temperature rise is fixed. So the inlet conditions must be adjusted to not exceed the maximum temperature limitation.

Suppose the conversion and the inlet compositions are fixed. The obvious thing to do is to adjust in the inlet temperature so that the exit temperature does not exceed the maximum temperature. However, if the inlet temperature is low, the specific reaction rate near the inlet end of the reactor will be small. Temperature will increase only very slowly as the process fluid moves down through the reactor. It will take a large reactor to attain the desired conversion. So there is an important trade-off between tubular reactor inlet temperature and reactor size.

In many applications, the most economically attractive design flowsheet uses multiple adiabatic tubular reactors in series with intermediate cooling so that reasonable reactor sizes can be used. There is an optimum inlet reactor temperature for each reactor. The exit temperatures of all reactors are set at the maximum. The number of reactors and the sizes of reactors needed to achieve an overall desired conversion can be determined to minimize capital investment in reactor vessels and heat exchangers.

An alternative to intermediate cooling is to use *cold shot* cooling. In this arrangement, a fraction of the cold feed stream entering the first reactor is bypassed around the reactor and mixed with the hot stream leaving the reactor to bring the inlet temperature of the second reactor down to the required level. If three reactors are used, the same method is used at the outlet of the second stage.

There is another design parameter than can be used to avoid high temperatures in a tubular reactor. The feed composition can be adjusted so that the adiabatic temperature rise is small enough to avoid exceeding the temperature limitation. If the concentration of one or more of the reactants is kept small, the adiabatic temperature rise will be small. The low reactant concentration can be achieved by having an excess of other components in the inlet feed gas to act as thermal sinks that soak up the heat of reaction. Of course this method requires that these other components be recovered and recycled, which translates into a more expensive separation section in terms of capital investment and energy costs. So adiabatic tubular reactors have a large number of design optimization variables that must be considered.

***Tubular Reactors with Heat Transfer.*** Tubular reactors are often designed as tube-in-shell heat exchangers so that heat can be transferred into or out of the process stream as it flows through the reactor. The diameter of the multiple tubes used in these reactors should be as small as possible so that the heat-transfer area is maximized per unit of volume. Mechanical strength limitations usually set this minimum diameter at about 1 inch.

The number of tubes used and their length depend on the required reactor volume (or amount of catalyst) to achieve the desired conversion and pressure drop considerations. Of course pressure drop is very important in gas systems because of the high cost of compression.

The inlet temperature in a tubular reactor with heat transfer is much less critical because the heat transfer will bring the process stream to a temperature at which reaction rates are adequate.

If heating is required, a high-temperature heat source is used on the shell side of the reactor: steam, DOWTHERM, molten salt, or a hot process stream, depending on the required temperature level. If cooling is required, a low-temperature heat sink is used: cooling water, steam, or a cool process stream, depending on the required temperature level. If the cooling/heating medium is cooled/heated by sensible heat (change in temperature), the temperature of the medium varies with length in the reactor. Countercurrent or cocurrent flow can be used. If the cooling/heating medium undergoes a phase change (e.g., condensing steam or vaporizing boiler-feed water), the temperature on the medium side is essentially constant at the boiling-point temperature of the medium at the shell-side pressure.

### 2.5.3 Feed-Effluent Heat Exchangers

An important aspect of heat transfer in reactor systems is managing the energy requirements for getting the reactor up to its optimum temperature and cooling the reactor effluent before feeding it into the separation section. The simple arrangement of using independent heat exchangers to heat the reactor feed and to cool the reactor effluent can consume a lot of energy.

A common design is to use the hot reactor effluent to supply some or all of the heat needed to preheat the cold feed. Figure 2.1 shows a typical set-up. A bypass of cold feed around

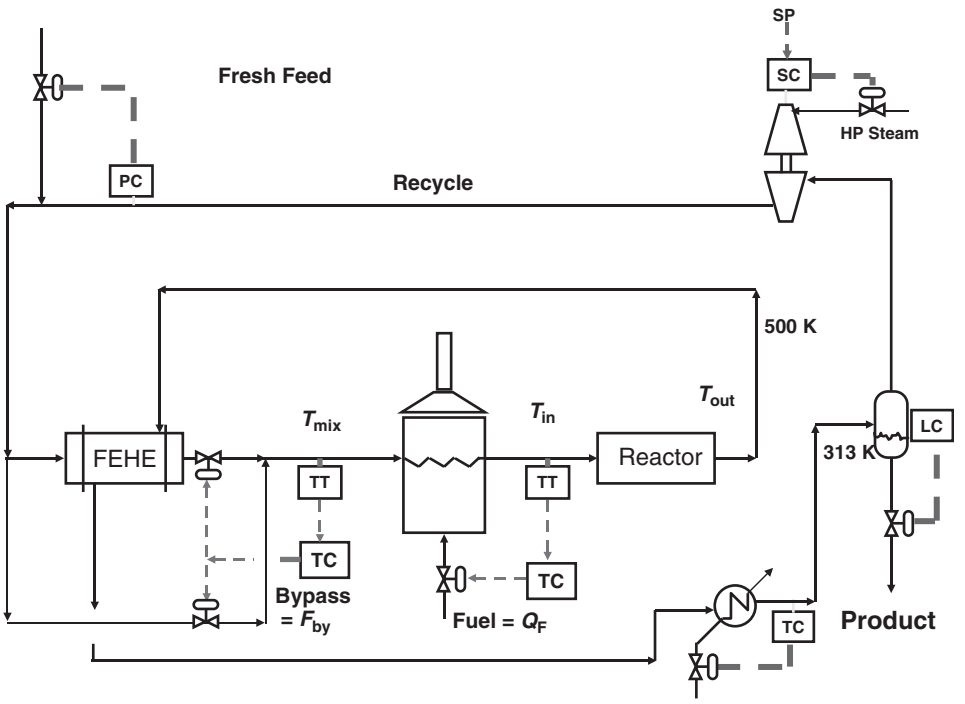


**Figure 2.1.** Inlet temperature control with furnace.

the heat exchanger is manipulated to control the temperature of blended stream entering the furnace. The reactor inlet temperature is controlled by manipulating the firing rate in the furnace. This process configuration and control structure can handle very large disturbances because the bypass will prevent a reactor runaway (too high temperature) and the furnace will prevent a reactor quench (too low temperature).

## 2.6 HEURISTIC DESIGN OF REACTOR/SEPARATION PROCESSES

The dominant trade-off in chemical process design is between reactor size and recycle flowrate. Big reactors require larger capital investments in vessels and catalyst, but they result in smaller recycle flowrates for a given yield, which means lower capital investments and energy costs in the separation section of the process. Small reactors have reverse effects. Therefore, an economic optimum exists that balances the costs of the reaction section and the separation section of the process.

In this section we present a heuristic approach to quickly determine this optimum trade-off during preliminary conceptual design. The basic idea is to start with a very large reactor and find the recycle flowrate required to meet some specified conversion/yield/selectivity criterion. This is the minimum recycle flowrate. Then a heuristic similar to that used in distillation column design is employed. The actual recycle flowrate is set equal to 1.2 times the minimum, and the reactor and separation sections are designed with this recycle. The heuristic recycle ratio has some dependence on the phase equilibrium (decreases as relative volatility decreases) and catalyst cost (increases as catalyst cost increases).

The process studied has a CSTR, two distillation columns, and one recycle stream. Two consecutive reactions ($A + B \rightarrow C$ and $A + C \rightarrow D$) produce a desired product C and an undesired product D. Achieving high selectivity requires low concentrations of A and C, so there is a large recycle of mostly B. Relative volatilities are assumed to be $\alpha_A > \alpha_B > \alpha_C > \alpha_D$, so there is one recycle from the overhead of the first distillation column containing unreacted A and B. The second column separates C and D.

### 2.6.1 Introduction

As we will discus in Chapter 3, in the design of distillation columns there is a classical trade-off between the number of trays and the reflux ratio required to achieve a specified separation. Simple heuristic optimization rules are widely and effectively used to quickly find an approximate economic design at the conceptual design stage of the project. The two most often applied alternative heuristics are

1. Set the actual number of trays equal to twice the minimum number.
2. Set the actual reflux ratio equal to 1.2 times the minimum reflux ratio.

In many processes, either of these two alternative rules produces a design that is reasonably close to the real economic optimum, which can be found by rigorously evaluating designs with varying numbers of trays and finding the design that minimizes total annual costs (capital plus energy). Using more trays increases column height and capital investment in the vessel, but more trays reduce energy cost and capital investment in heat exchangers.

Many chemical processes feature a reaction section coupled with a separation section through recycle streams. In the design of these multiunit processes, the dominant design

issue is the classical trade-off between the size of the reactor and amount of recycle required to achieve a specified conversion, yield, or selectivity in the overall process.

It would be useful to have a simple heuristic approach to this trade-off that could provide some guidance for initial flowsheet development at the conceptual process design stage. The purpose of this section is to propose such a simple heuristic method.

### 2.6.2 Process Studied

Figure 2.2 shows the flowsheet of the process. The equipment sizes and conditions shown are the economic optimum developed later in this chapter for the base-case conditions: a selectivity specification of 100 (kmoles C produced divided by kmoles D produced), kinetic parameters of $k_1 = 25$ and $k_2 = 1$, relative volatilities between adjacent components of 2 and catalyst price of \$10/kg.

***Reactor.*** The molar holdup of the CSTR reactor is a 35 kmol. Two irreversible reactions occur with specific reaction rates $k_1$ and $k_2$.

$$\begin{aligned} &\mathrm{A} + \mathrm{B} \longrightarrow \mathrm{C} \\ &\Re 1 = V_\mathrm{R} * k_1 * z_\mathrm{A} * z_\mathrm{B} \end{aligned} \tag{2.6}$$

$$\begin{aligned} &\mathrm{A} + \mathrm{C} \longrightarrow \mathrm{D} \\ &\Re 2 = V_\mathrm{R} * k_2 * z_\mathrm{A} * z_\mathrm{C} \end{aligned} \tag{2.7}$$

where $z_j$ = mole fraction component $j$ in the reactor
$V_\mathrm{R}$ = reactor molar holdup

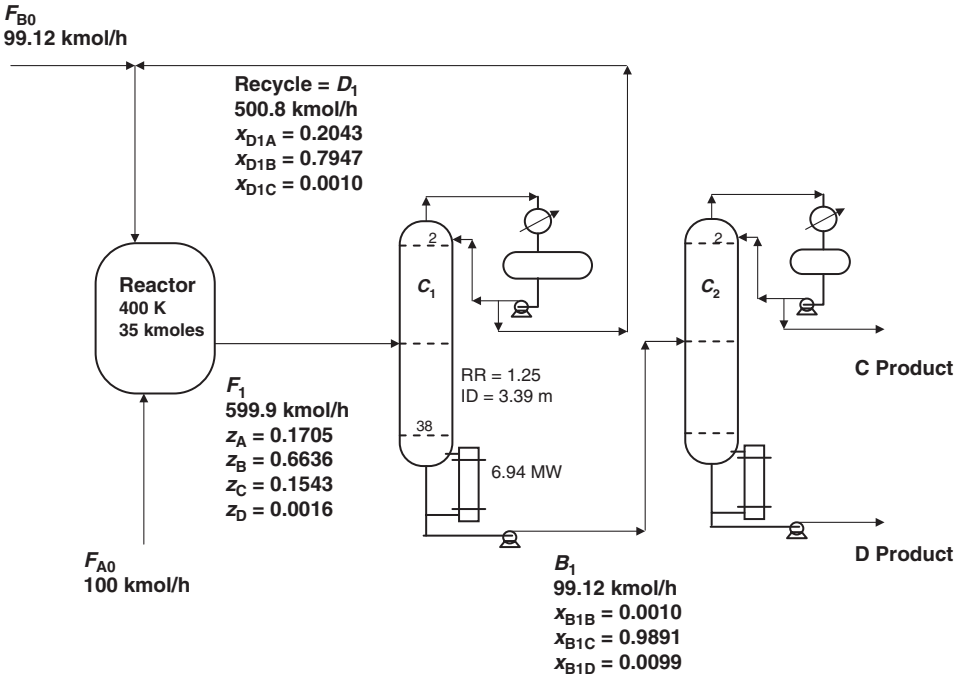


**Figure 2.2.** Flowsheet ($k_1 = 15$, selectivity = 100; \$10/kg; $\alpha = 2$).

This type of basic kinetic system is very commonly encountered in many real industrial processes. The desired product C is formed by the first reaction, but it can react further to produce an undesired product D. Therefore, the concentrations of A and C must be kept small to achieve the desired selectivity by running with an excess of B, thus requiring a large recycle. Two fresh feed streams of pure A and pure B are fed to the reactor ($F_{A0}$ and $F_{B0}$) in addition to the recycle stream from the top of the first column (D1).

Selectivity is defined as the moles of the desired component C produced, divided by the moles of the undesired component D produced.

$$\text{Selectivity} = \frac{\text{moles C}}{\text{moles D}} = \frac{x_{B1C}}{x_{B1D}} \tag{2.8}$$

where $x_{B1j}$ = mole fraction of component $j$ in the bottoms stream of the first distillation column C1.

The fresh feed of reactant A is fixed at $F_{A0} = 100$ kmol/h in all cases. The fresh feed of B is calculated for each case by solving the nine nonlinear simultaneous algebraic equations describing the reactor and column for the specified conditions (reactor size, desired selectivity, and kinetic parameters).

The equations describing the reactor are:

$$F_{A0} + D_1 * x_{D1A} = F_1 * z_A + \Re 1 + \Re 2 \tag{2.9}$$

$$F_{B0} + D_1 * x_{D1B} = F_1 * z_B + \Re 1 \tag{2.10}$$

$$D_1 * x_{D1C} = F_1 * z_C - \Re 1 + \Re 2 \tag{2.11}$$

$$0 = F_1 * (1 - z_A - z_B - z_C) - \Re 2 \tag{2.12}$$

The composition of C in the $D_1$ recycle is assumed to be $x_{D1C} = 0.001$. The five specified variables are $F_{A0}$, $V_R$, $x_{D1C}$, $k_1$, and $k_2$. The eight unknown variables in these four equations are $F_{B0}$, $z_A$, $z_B$, $z_C$, $D_1$, $x_{D1A}$, $x_{D1B}$, and $F_1$. Note that the reactions are nonequimolar, so there is a reduction in the molar flows into and out of the reactor. Each reaction consumes 2 mol of reactants while making 1 mol of product.

***Column C1.*** The reactor effluent is fed to a distillation column whose job is to recycle unreacted A and B back to the reactor and send a mixture of products C and D downstream to the second distillation column. Constant relative volatilities are assumed with reactant A and B lighter than products C and D.

$$\alpha_A > \alpha_B > \alpha_C > \alpha_D \tag{2.13}$$

With these phase equilibria relationships, the separation section has one recycle from the top of column C1.

The sizing and cost analysis for the column use the Fenske equation to find the minimum number of trays and the Underwood equations to find the minimum reflux ratio. The separation is between components B and C. All A is assumed to go overhead ($x_{B1A} = 0$). The impurity of B in the bottoms is set at $x_{B1B} = 0.001$.

Then the number of trays is set at twice the minimum, and the required reflux ratio is set at 1.2 times the minimum for estimating the capital costs (column shell, condenser, and

reboiler) and the energy cost (reboiler heat input at \$7.78/GJ). Standard column sizing and cost relationships are used.[2,3]

The equations describing the column are given below. They are solved simultaneously with those of the reactor to find the unknowns.

$$F_1 = D_1 + B_1 \tag{2.14}$$

$$F_1 * z_A = D_1 * x_{D1A} \tag{2.15}$$

$$F_1 * z_B = D_1 * x_{D1B} + B_1 * x_{B1B} \tag{2.16}$$

$$F_1 * z_C = D_1 * x_{D1C} + B_1 * x_{B1C} \tag{2.17}$$

The additional unknown variable not in the previous list of eight is $x_{B1B}$. Therefore, we have a system of nine unknowns. But Eqs. (2.9) through (2.12) and Eqs. (2.14) through (2.17) give us only eight equations.

***Solution Method.*** The method for solving these equations for the reactor and column linked together with the recycle stream is to fix the total flowrate of the fresh feed of B plus the recycle $D_1$.

$$\text{Total} = F_{B0} + D_1 \tag{2.18}$$

With the variable Total fixed, Eq. (2.18) provides an additional equation. The MATLAB function *fsolve* was used to solve these nine nonlinear simultaneous algebraic equations for a given case.

Then an iterative procedure (interval halving) was used to change Total until a desired specification (Selectivity) was achieved for the case (fixed $V_R$, $k_1$, and $k_2$). Figure 2.3a shows results from these calculations for the case when a selectivity of 100 is specified with three different kinetic parameters $k_1 = 15$, 25, and 50. The $k_2$ is 1 in all cases. The ordinate is the recycle flowrate $D_1$ (Total $- F_{B0}$). The abscissa is reactor molar holdup. Figure 2.3b gives other important variables.

More recycle is needed to achieve a specified selectivity for a fixed reactor size as the specific reaction rate $k_1$ is reduced. Small values of $k_1$ lead to larger concentrations of A in the reactor ($z_A$) but smaller concentrations of C ($z_C$) and D ($z_D$).

The *key feature* of these plots (and the basis for the heuristic proposed) is that the required recycle flowrate levels out at some minimum value as reactor size is made very large. We define the asymptotic recycle flowrate as the minimum recycle. It can be expressed as a ratio to the fresh feed of A to put it in dimensionless form. For example, for the $k_1 = 25$ case, the minimum recycle is 425 kmol/h for a fresh feed of $F_{A0} = 100$ kmol/h. So the minimum recycle ratio $R_{min}$ is 4.25.

The curves shown in Figure 2.3a are similar to those seen in the classical plots of reflux ratio versus trays in distillation design. At any point on the curve, the products from the process are exactly the same, but equipment (reactor and column) and energy (reboiler heat input) are different. So where is the optimum point on the curve? We address this question next for a number of different cases to see if there is some simple relationship between the economic optimum recycle flowrate and the minimum. The minimum recycle flowrate can be easily determined by running a case with a very large reactor.

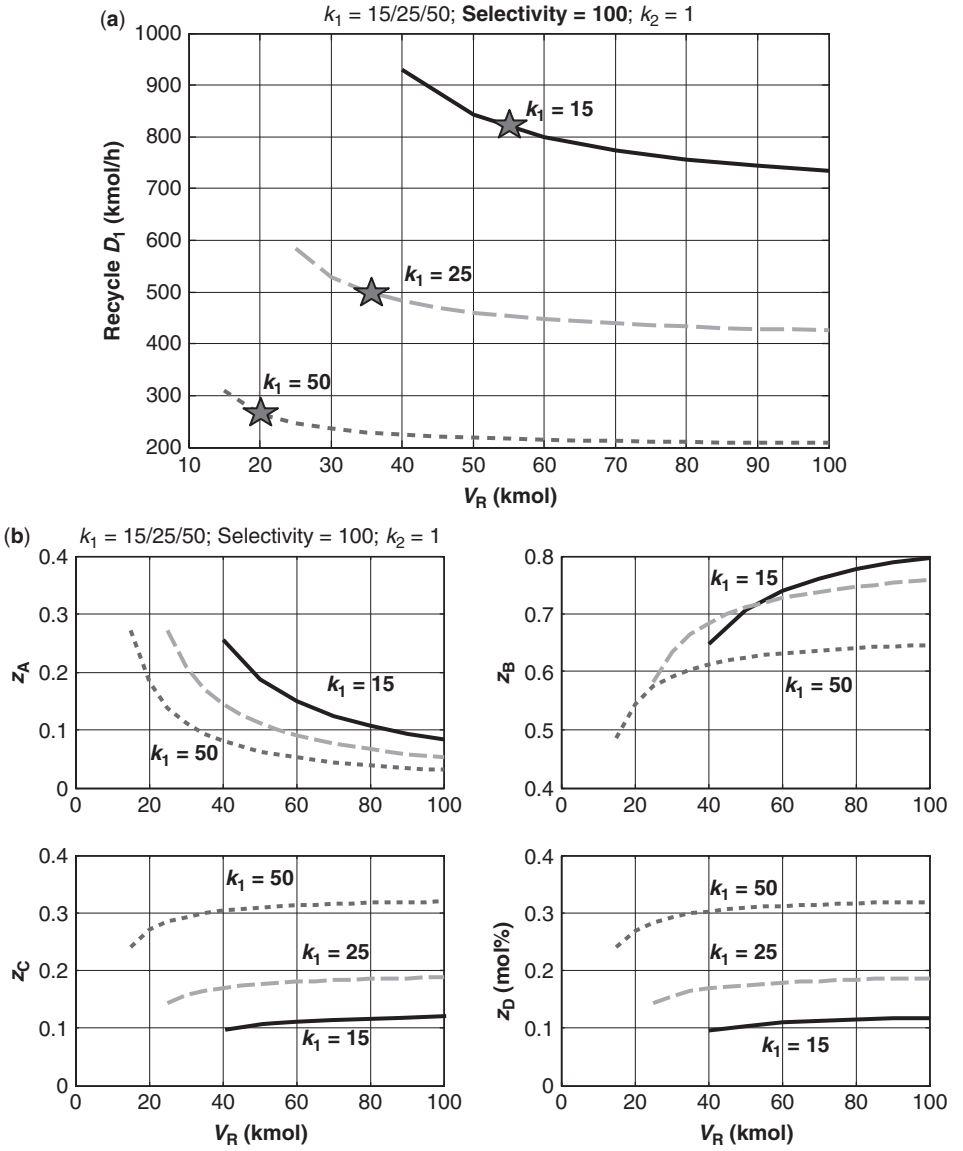


**Figure 2.3.** (a) Required recycle for 100 selectivity. (b) Other variables for 100 selectivity.

### 2.6.3 Economic Optimization

One of the famous "Douglas Doctrines" is that energy and capital can usually be spent to improve yield and selectivity.[2] This result is easily demonstrated by comparing the annual cost of raw materials and the annual value of products with annual capital and energy costs. The former are typically orders-of-magnitude larger than the latter. This translates into designs for most processes that feature very high conversion, yield, and selectivity. We cannot afford to waste raw materials, so conversions in the range of 99% are typical. We cannot afford to incur expensive waste disposal problems by producing undesired products, so selectivities of 100 are typical.

The precise best values for these criteria are strongly dependent on market prices for raw materials and finished products. Estimates of market prices are often far from reliable. The predictive success of marketing analysts is usually lower than that of the meteorologist's success at forecasting tomorrow weather or the stock market analyst's success at predicting what the stock market will do in the next year.

In order to avoid these uncertainties, we take the approach that the designer will specify a reasonable criterion, such as a selectivity of 100. Then a plant can be designed that meets this criterion with the minimum total annual cost (TAC). Pricing of feed streams and products is avoided.

Total annual cost is the sum of the energy cost plus the annual cost of the capital investment using a payback period. In this work, a payback period of 3 years and the installed cost of equipment are used.

$$\text{TAC} = \text{Energy cost} + \frac{\text{Capital installed investment}}{\text{Payback period}} \tag{2.19}$$

For the flowsheet considered in Figure 2.2, we are concerned with the reactor and the first column. The second column does not change from case to case for a specified selectivity. Capital investment is required for the reactor vessel, catalyst, column vessel, reboiler, and condenser. Energy cost depends on reboiler duty.

Table 2.1 gives sizing and costing results for several cases with selectivity fixed at 100, which corresponds to a yield of 98%. The cost of catalyst is \$10/kg, and the relative volatility between all adjacent components is 2. Three values of $k_1$ (15, 25, and 50 $h^{-1}$) are explored. In all cases, the required recycle decreases as reactor size increases. This reduces energy cost but the larger reactor increases total capital cost.

The optimum reactor size and the optimum recycle flowrate decrease as $k_1$ increases. The optimum designs are indicated in Figure 2.3a by the stars. Notice that the minimum recycle flowrates for the three values of $k_1$ are 720 kmol/h for $k_1 = 15\ h^{-1}$, 425 kmol/h for $k_1 = 25\ h^{-1}$ and 210 kmol/h for $k_1 = 50\ h^{-1}$. The economic optimum recycle flowrates are 818 kmol/h for $k_1 = 15\ h^{-1}$, 500.8 kmol/h for $k_1 = 25\ h^{-1}$, and 264.6 kmol/h for $k_1 = 50\ h^{-1}$. The three ratios of optimum-to-minimum are 1.14, 1.18, and 1.26, respectively.

These results suggest that the proposed heuristic of 1.2 may be valid for preliminary conceptual design.

### 2.6.4 Other Cases

A number of other cases were explored to see the impact of other design parameters on the heuristic ratio. We would expect that a more expensive catalyst would shift the optimum to smaller reactors and larger recycle flowrates. We would expect that more difficult separations (smaller relative volatilities) would shift the optimum to large reactors and smaller flowrates. These are studied below. First, we see if the specified selectivity has any effect on the optimum-to-minimum recycle ratio.

***Selectivity.*** Figure 2.4 shows what happens when the selectivity is reduced from 100 to 50 with the other parameters fixed. The yield is reduced from 98 to 96%. Optimum reactor sizes do not change much, but recycle flowrates are much lower. However, minimum recycle flowrates are also smaller, so how is the ratio of optimum to minimum affected?

With the selectivity set at 50, the minimum recycle flowrates for the three values of $k_1$ (as shown in Figure 2.4a) are 360 kmol/h for $k_1 = 15\ h^{-1}$, 220 kmol/h for $k_1 = 25\ h^{-1}$ and 110

**TABLE 2.1 Sizing and Economics for Selectivity = 100**

| | $k_1 = 15\ h^{-1}$ | | |
|---|---|---|---|
| $V_R$ | 50 kmol | 55 kmol | 60 kmol |
| Recycle $D_1$ (kmol/h) | 842.3 | 818.0 | 799.8 |
| Reactor ($10^6$ \$) | 0.2652 | 0.2814 | 0.2971 |
| Catalyst ($10^6$ \$) | 1.250 | 1.375 | 1.500 |
| Column diameter (m) | 4.315 | 4.275 | 4.245 |
| Column ($10^6$ \$) | 1.185 | 1.175 | 1.168 |
| Heat exchangers ($10^6$ \$) | 1.078 | 1.065 | 1.055 |
| Total capital ($10^6$ \$) | 3.777 | 3.896 | 4.020 |
| Total energy ($10^6$ \$/yr) | 2.752 | 2.701 | 2.663 |
| TAC ($10^6$ \$/yr) | 4.011 | **4.000** | 4.003 |
| | $k_1 = 25\ h^{-1}$ | | |
| $V_R$ | 30 kmol | 35 kmol | 40 kmol |
| Recycle $D_1$ (kmol/h) | 529.8 | 500.8 | 482.6 |
| Reactor ($10^6$ \$) | 0.1930 | 0.2124 | 0.2308 |
| Catalyst ($10^6$ \$) | 0.7498 | 0.8747 | 1.000 |
| Column diameter (m) | 3.452 | 3.394 | 3.356 |
| Column ($10^6$ \$) | 0.9312 | 0.9176 | 0.9090 |
| Heat exchangers ($10^6$ \$) | 0.8063 | 0.7886 | 0.7774 |
| Total capital ($10^6$ \$) | 2.680 | 2.793 | 2.917 |
| Total energy ($10^6$ \$/yr) | 1.761 | 1.702 | 1.665 |
| TAC ($10^6$ \$/yr) | 2.655 | **2.633** | 2.637 |
| | $k_1 = 50\ h^{-1}$ | | |
| $V_R$ | 15 kmol | 20 kmol | 25 kmol |
| Recycle $D_1$ (kmol/h) | 310.3 | 264.8 | 246.3 |
| Reactor ($10^6$ \$) | 0.1253 | 0.1499 | 0.1723 |
| Catalyst ($10^6$ \$) | 0.3749 | 0.5000 | 0.6248 |
| Column diameter (m) | 2.659 | 2.544 | 2.496 |
| Column ($10^6$ \$) | 0.6980 | 0.6724 | 0.6620 |
| Heat exchangers ($10^6$ \$) | 0.5743 | 0.5421 | 0.5290 |
| Total capital ($10^6$ \$) | 1.772 | 1.864 | 1.988 |
| Total energy ($10^6$ \$/yr) | 1.045 | 0.9564 | 0.9209 |
| TAC ($10^6$ \$/yr) | 1.636 | **1.578** | 1.584 |

kmol/h for $k_1 = 50\ h^{-1}$. The economic optimum recycle flowrates are 447.2 kmol/h for $k_1 = 15\ h^{-1}$, 277.0 kmol/h for $k_1 = 25\ h^{-1}$ and 145.8 kmol/h for $k_1 = 50\ h^{-1}$. The three ratios of optimum-to-minimum are 1.24, 1.26, and 1.33, respectively. The ratio increases slightly as selectivity is lowered.

Figure 2.5 shows what happens when the selectivity is increased from 100 to 150 with the other parameters fixed. The yield is increased from 98 to 99%. Optimum reactor size doesn't change much, but recycle flowrates are much higher. However, minimum recycle flowrates are also larger, so how is the ratio of optimum to minimum affected?

With the selectivity set at 150, the minimum recycle flowrates for the three values of $k_1$ (as shown in Figure 2.5a) are 1100 kmol/h for $k_1 = 15\ h^{-1}$, 640 kmol/h for $k_1 = 25\ h^{-1}$ and 320 kmol/h for $k_1 = 50\ h^{-1}$. The economic optimum recycle flowrates are 1189 kmol/h for

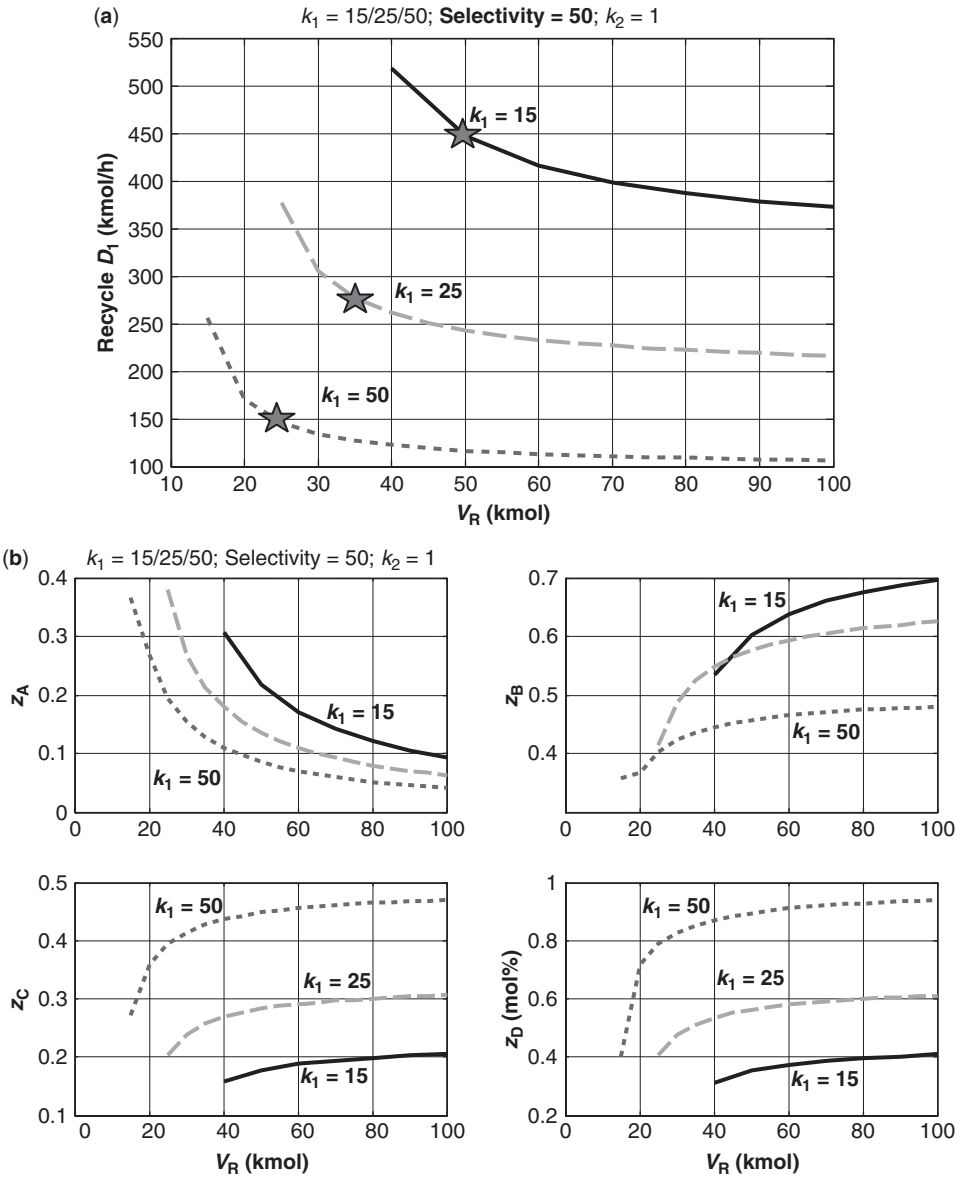


**Figure 2.4.** (a) Required recycle for 50 selectivity. (b) Other variables for 50 selectivity.

$k_1 = 15\ \text{h}^{-1}$, 709.1 kmol/h for $k_1 = 25\ \text{h}^{-1}$ and 364.3 kmol/h for $k_1 = 50\ \text{h}^{-1}$. The three ratios of optimum-to-minimum are 1.11, 1.08, and 1.14, respectively. The ratio decreases slightly as selectivity is raised.

These results indicate that a heuristic of 1.2 should be fairly adequate for initial estimates in conceptual design over a wide range of selectivities.

In the next section we explore the effect of other design parameters that are expected to cause some shift in the heuristic ratio. Note that the minimum recycle flowrate depends on the values of $k_1$ and selectivity specified and not on catalyst price or relative volatility.

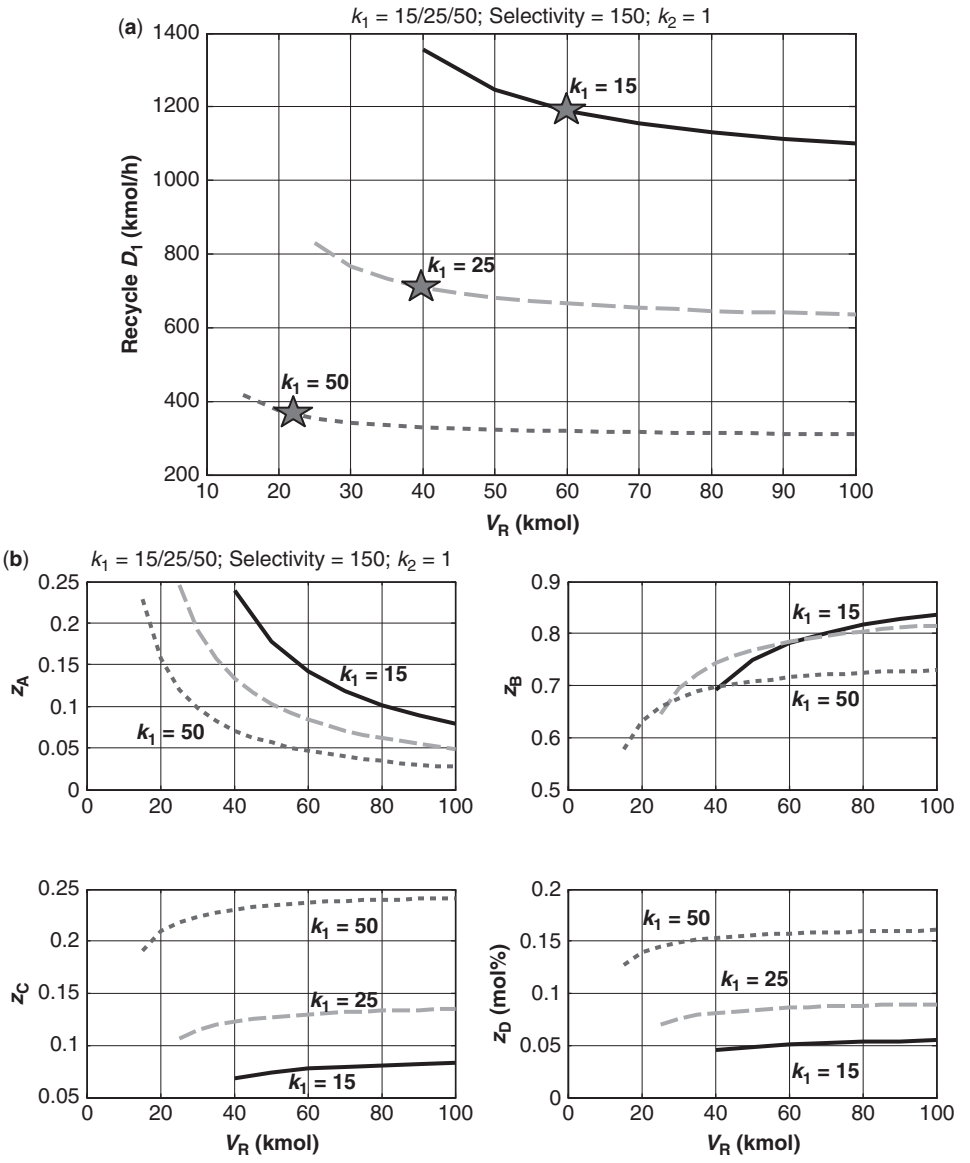


**Figure 2.5.** (a) Required recycle for 150 selectivity. (b) Other variables for 150 selectivity.

***Catalyst Cost.*** A catalyst cost of \$10/kg has been used in the all the previous cases. Increasing the price of the catalyst should make the reaction section more expensive, so the economic optimum would be expected to shift to somewhat higher recycle flowrates. Figure 2.6 shows that this is what occurs. These results use the base-case values of selectivity = 100, $k_1 = 25$, and relative volatility = 2.

The optimum reactor size decreases and the recycle flowrate increases as the catalyst becomes more expensive. Naturally TAC also increases. The lower right graph in Figure 2.6 shows that the optimum-to-minimum recycle ratio increases from 1.2 up to 1.4

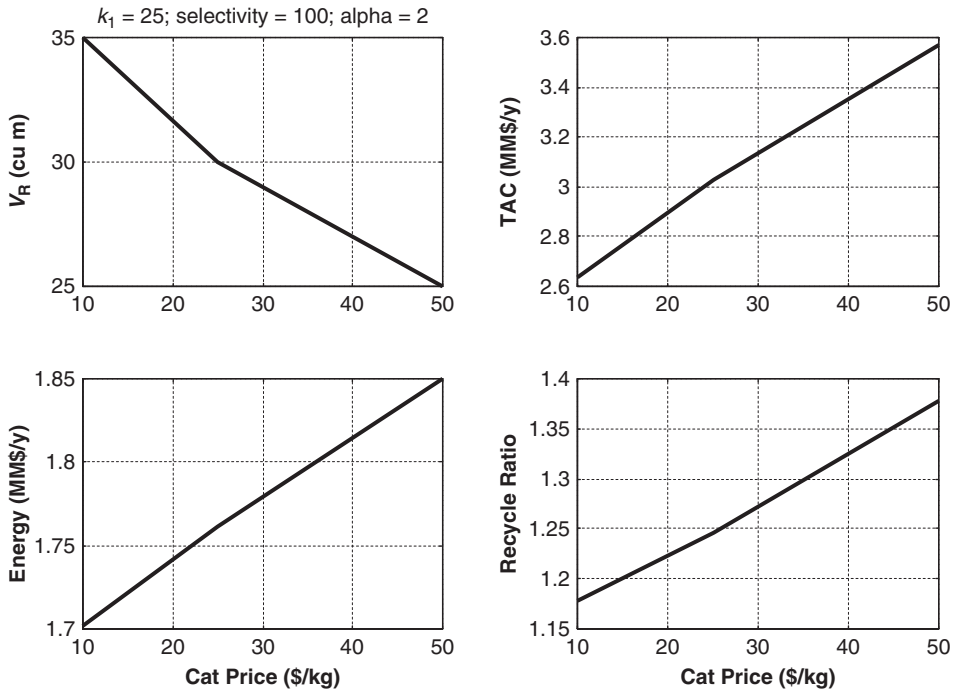


**Figure 2.6.** Effect of catalyst price.

as the catalyst increases in cost by a factor of five. So the heuristic value will depend on the cost of the catalyst.

***Relative Volatility.*** A relative volatility of 2 between adjacent components has been used in all the previous cases ($\alpha_A = 8$; $\alpha_B = 4$; $\alpha_C = 2$; $\alpha_D = 1$). Decreasing relative volatilities will make separations more difficult and the separation section more expensive, so the economic optimum would be expected to shift to somewhat smaller recycle flowrates.

Figure 2.7 gives results for a number of cases in which the relative volatilities are modified. The abscissa is relative volatility between adjacent components. For example, a relative volatility of 1.2 means that $\alpha_A = 1.728$, $\alpha_B = 1.44$, $\alpha_C = 1.2$, $\alpha_D = 1$.

Optimum reactor sizes, energy consumption (a direct indication of recycle flowrate), and TAC all increase as relative volatilities are made smaller. The lower right graph in Figure 2.7 shows that the optimum-to-minimum recycle ratio decreases from 1.2 down to less than 1.1 as relative volatility decreases from 2 to 1.2. Therefore a lower value for the heuristic should be used when separations are more difficult.

***Separation Sequence.*** The flowsheet shown in Figure 2.2 features a single recycle stream coming from the first column because the volatilities of the reactants A and B are bigger than the volatilities of the products C and D. In some systems, the phase equilibria are such that one of the products has a volatility that is larger than or intermediate between the volatilities of the two reactants. In that situation, two recycle streams would be required and more distillation columns would be needed. The separation costs would therefore be

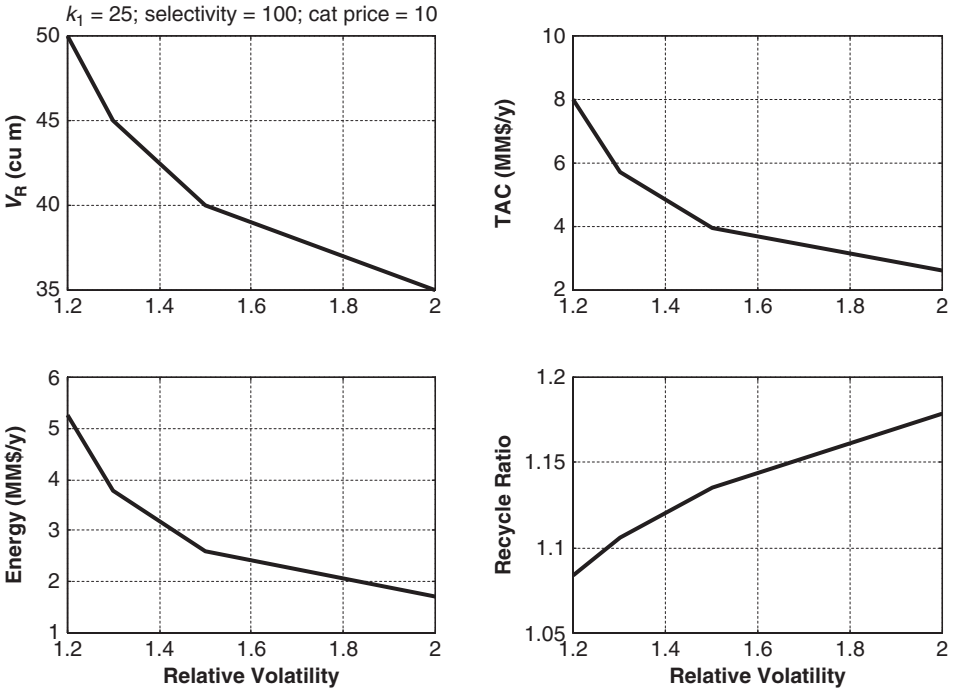


**Figure 2.7.** Effect of relative volatility.

larger and a lower heuristic ratio should be used (1.1 instead of 1.2). The next section considers such a case.

### 2.6.5 Real Example

Hypothetical chemical examples have been considered in previous sections. To see if the proposed heuristic method works on a real chemical example, the process to make the gasoline additive 2-methoxy-2-methylheptane (MMH) is studied. Chapter 12 studies this process in detail and the optimum design of this process is presented there and in a paper by the author.[4] The chemistry involves the liquid-phase reversible reaction of methanol with 2-methyl-1-heptene (MH) to form MMH. However, methanol and MH also undergo an undesirable reaction to form dimethyl ether (DME) and 2-methyl-2-heptanol (MHOH). Thus the system has two undesirable products.

Figure 2.8 shows the flowsheet with the economic optimum design conditions and equipment sizes. The first undesirable byproduct (DME) is very volatile, so it is removed in the first column. Then the excess reactants are removed out the top of the second column for recycle back to the reactor. The desired product MMH is separated from the second undesired byproduct (MHOH) in a third column. So the separation section is more complex and inherently more expensive than the simple system shown in Figure 2.2. Therefore, a somewhat small heuristic optimum-to-minimum recycle ratio is expected.

The economic optimum design has 50 kmol/h of fresh methanol and a recycle flowrate of 79.99 kmol/h with a 12 $m^3$ reactor. The specifications for the various streams are described in detail in a paper by the author.[4]

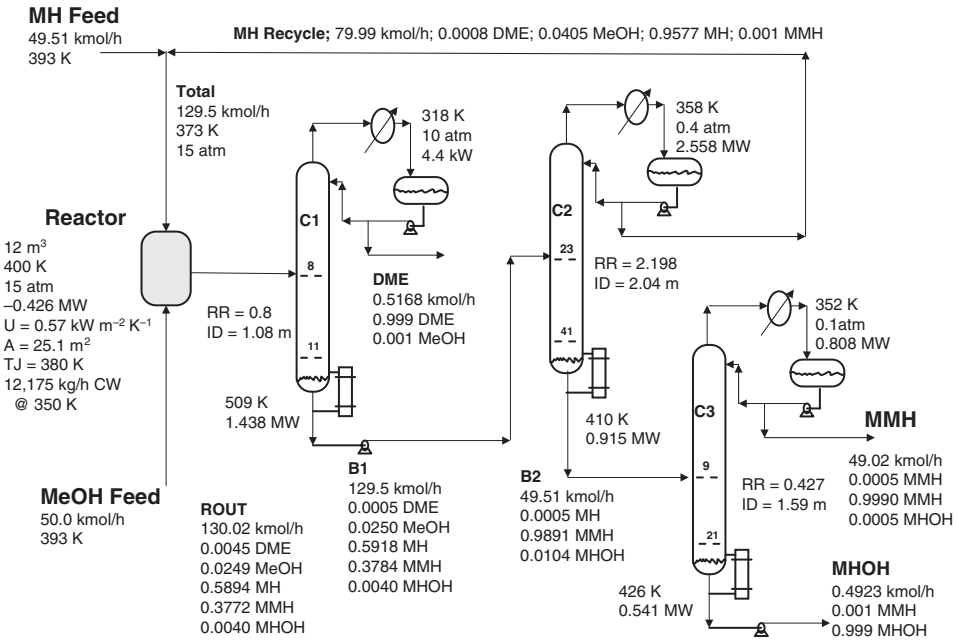


**Figure 2.8.** MMH flowsheet.

The yield of the process is defined as the flowrate of the MMH product stream from the second column (D2) divided by the fresh methanol feed. In the optimum design $D_2$ is 49.02 kmol/h, giving a selectivity of 0.9803 when the reactor is 12 $m^3$.

Simulation runs were made with increasingly larger reactors while holding the yield of MMH at 0.9803 by varying the recycle flowrate. A reactor size of 15 $m^3$ resulted in a lower recycle flowrate ($D_2 = 75.99$ kmol/h). A reactor size of 20 $m^3$ resulted in an even lower recycle flowrate ($D_2 = 73.69$ kmol/h). Increasing reactor size still further made no change in the required recycle flowrate. Therefore, the minimum recycle flowrate is about 74 kmol/h while the economic optimum recycle flowrate is about 80 kmol/h.

The correct optimum-to-minimum recycle ratio in the MMH process is 1.08, which is very close to the 1.1 that the proposed heuristic method would have used in light of the more complex separation section.

## 2.7 CONCLUSION

Some important design and control principles have been discussed in this chapter. The nature of the chemistry tells us a lot about what kind of process flowsheet will be needed to efficiently produce products. The type of equipment and the operating conditions in both the reaction section and the separation section of the process depend on the chemistry: stoichiometry, heat of reaction, reaction phase, and reaction type.

Reactor control can be challenging when exothermic irreversible reactions occur in reactors operating with low conversions. The availability of "fuel" with lots of reactants in the reactor can lead to temperature runaways (instability) unless the reactor is carefully designed with adequate heat-removal area.

A simple heuristic approach to determine economic optimum designs of chemical process with reaction and separation sections has been proposed and tested. The chemistry assumes completing reactions with desired and undesired products being formed that force a design with recycle to attain specified yield or selectivity. The minimum recycle flowrate is determined by using very large reactors. Then the actual recycle flowrate is set at 1.1 to 1.2 times the minimum, depending on the cost of the catalyst, the relative volatilities, and the complexity of the separation section.

## REFERENCES

1. Luyben, W. L. *Chemical Reactor Design and Control*, John Wiley & Sons, Hoboken, NJ, 2007.
2. Douglas, J. M. *Conceptual Design of Chemical Processes*, McGraw-Hill, New York, 1988.
3. Turton, R., Bailie, R. C., Whiting, W. B., Shaelwitz, J. A. *Analysis, Synthesis and Design of Chemical Processes*, 2nd Edition, Prentice Hall, Englewood Cliffs, NJ, 2003.
4. Luyben, W. L. "Design and control of the methoxy-methyl-heptane process," *Ind. Eng. Chem. Res.* 2010, **49**, 6164–6175.

# CHAPTER 3

# PRINCIPLES OF DISTILLATION DESIGN AND CONTROL

The separation section of the process has the job of taking the reactor effluent and producing reactant, recycle and product streams at their required purities. There are many separation techniques: distillation, extraction, absorption, adsorption, gas diffusion through membranes, pervaporation, crystallization. The most widely applied and dominant separation technique is distillation, so we will discuss this very important separation technology in this chapter. The design and control of the separation section of a process depends heavily on the design and control of the reaction section. And vice versa.

In this chapter we discuss basic principles of distillation design and control. Distillation columns are somewhat more complex to design because there are more design optimization variables: pressure, total number of trays, feed-tray location, reflux ratio (RR), and product composition specifications. But there are a number of heuristics that have been developed over the years that are quite effective and simplify the design optimization problems.

On the other hand, the control of distillation columns is somewhat easier and in a sense less critical because distillation columns display well-behaved, stable, dynamic responses. Temperature runaways do not occur. However, tight control of the product streams leaving the columns is important to product-quality issues. Their multivariable nature introduces a measure of complexity compared to simple control of a single temperature in a reactor.

There are a wide variety of distillation columns because chemical components have a wide range of boiling points. Columns operate from vacuum conditions (10 mm Hg) to high pressure (20 atm). Temperature levels vary from cryogenic conditions to 600 K.

There are a number of optimization variables in distillation design that must be determined. In the following section, several approaches to finding the "best" column design are presented.

*Principles and Case Studies of Simultaneous Design*, First Edition. William L. Luyben

## 3.1 PRINCIPLES OF ECONOMIC DISTILLATION DESIGN

The optimum economic design of a distillation column involves the classical trade-off between trays and energy. As the number of trays is increased, the capital investment in the column vessel increases because of the increasing height. On the other hand, the energy consumption in the reboiler decreases, which decreases energy costs and capital investment in the heat exchangers (reboiler and condenser). In addition, it reduces the required diameter of the column since vapor rates are lower.

Before this trade-off can be quantitatively explored, the pressure of the column must be specified. The standard distillation design problem is to find the "best" column given the following specified variables:

1. Feed flowrate, composition, and thermal conditions (temperature and pressure)
2. Distillate composition in terms of heavy-key impurity
3. Bottoms composition in terms of light-key impurity

The variables that must be determined so as to satisfy some economic objective functions are:

1. Operating pressure
2. Total trays
3. Feed-tray location

Once the "best" values of these three design optimization variables have been found, all the other dependent variables of the column are fixed. The temperatures, compositions, and flowrates on all trays are now known, as well as the heat duties in the reboiler and condenser.

### 3.1.1 Operating Pressure

Pressure selection is usually pretty straightforward. Most, but not all, chemical vapor-liquid separations get easier (have higher relative volatilities) as temperature decreases. So we want a low pressure that gives low temperatures. However, lower column pressures also give lower reflux-drum and condenser temperatures. Temperatures down to about 120 °F can be achieved by using inexpensive cooling water. Operating at lower temperatures lower than this would require the use of expensive refrigerant in the condenser for heat removal. So there is a lower limit to the economic pressure.

There are chemical systems that display the opposite volatility dependence on temperature (pressure). The water/acetic acid system is an important example. The selection of pressure in these systems is a balance between the amount of energy used and its cost. The temperature in the base of the column increases as pressure increases, requiring a higher-temperature, more-expensive heat source.

A different constraint occurs in some chemical separations. There may be a maximum temperature limitation above which bad things can happen: thermal decomposition, coke formation, polymerization. The ethyl benzene/styrene separation is an important example. Styrene polymerization limits temperatures in the column.

The base temperature is the highest in the column, so the pressure must be set such that the temperature in the base, as determined by the bottoms composition, does not exceed the

temperature limit. The pressure drop through the trays sets the reflux-drum pressure, which is lower than the base pressure. The reflux-drum temperature is then determined by the distillate composition at this pressure. If this temperature is below that attainable by the use of cooling water, expensive refrigeration must used. These conditions mean that the separation is doubly expensive in terms of energy. We have to provide expensive heat in the reboiler and remove expensive heat in the refrigerated condenser.

Vacuum operation is often required in these maximum-temperature separations. Vacuum pressures give very small vapor densities, which translate into large-diameter columns. Vacuum pumps or steam-jet ejectors are needed to remove inert components from the condenser.

### 3.1.2 Heuristic Optimization

Once the pressure is fixed, the number of stages must be determined. Heuristic rules can be easily applied to get ballpark estimates of the optimum economic design. The two alternatives are:

1. Use twice the minimum number of trays, or
2. Use 1.2 times the minimum reflux ratio (RR)

These limiting conditions can be found analytically in systems with constant relative volatilities by use of the classical Fenske and Underwood equations. However, they can also be easily found in any real system using a simulator. The feed conditions are specified, and the compositions of the distillate and bottoms products are held at their specified values. In Aspen Plus this is achieved by using *Design Spec/Vary* functions.

The number of trays is specified at a large number, giving a required RR. The number of trays is increased until the RR stops decreasing. This is the minimum RR.

Then the number of trays is reduced until the required RR starts to drastically increase. This is the minimum number of trays.

### 3.1.3 Rigorous Optimization

A rigorous optimum design is determined by changing the total number of stages over a range of values. With the distillate and bottoms composition held at their specified values, the required reboiler heat input, the condenser duty, height of the column, and the diameter of the column are calculated for each case. The feed-tray location is varied for each choice of total stages until the location that minimizes reboiler energy is found.

The heat exchanger heat-transfer rates are then used to calculate heat-transfer areas using reasonable overall heat-transfer coefficients and differential temperature driving forces.

The information is then used to calculate the capital cost of the column vessel and the heat exchangers (reboiler and condenser). Energy cost is dominated by reboiler heat input as long as refrigeration is not used in the condenser.

*Total annual cost* (TAC) is a simple and effective economic objective function that can be applied to each individual column. Total annual cost is the sum of the annual cost of energy plus the annual cost of capital. The latter term is the capital investment divided by a payback period. Numerical examples of these calculations are given in many of the case studies discussed in subsequent chapters.

### 3.1.4 Feed Preheating and Intermediate Reboilers and Condensers

In addition to heat transfer in the reboiler and condenser, other heat exchangers are frequently used to reduce energy costs.

***Feed Preheating.*** If a hot process stream is available with a temperature higher than that of the feed temperature, it may be desirable to install a heat exchanger to preheat the feed using this hot stream. A hotter feed results in lower reboiler heat input and higher condenser heat removal. Since the latter is usually cheap, the capital investment in an addition heat exchanger may be justified.

Since the bottoms stream from the column is usually hotter than the feed, the bottoms is frequently used for this purpose. However, if the bottoms is feeding a downstream column, we would not want to "rob Peter to pay Paul."

We also might consider preheating the feed using steam. If steam at lower pressure than that used in the reboiler can be used in the preheater, the economics may be favorable because the lower-pressure steam is less expensive. Do not make the mistake of designing a system with a feed preheater that uses the same pressure steam as that used in the reboiler. The total energy cost will be higher in this situation because heat added in the reboiler has more effect on separation than heat added in the preheater.

***Intermediate Reboilers and Condensers.*** Instead of adding all the heat at the very base of the column, where the temperature is the highest and the most expensive heat source is required, it sometimes pays to use an intermediate reboiler located farther up the column, where the temperatures are lower. At this higher location, a lower-temperature, less expensive heat source can be used.

Conversely, instead of removing all the heat at the top of the column where the temperature is the lowest and the heat is thrown away into cooling water, it sometimes pays to use an intermediate condenser (pumparound) locate farther down in the column where the temperatures are higher. At this location and higher temperature, the heat can be transferred into a process stream that needs to be heated.

The use of intermediate condensers and reboilers is frequently seen in columns with large temperature differences from top to bottom. Petroleum fractionators are good examples of this configuration.

### 3.1.5 Heat Integration

The thermodynamic efficiencies of distillation columns are low. Almost all the energy added in the reboiler is removed in the condenser. The efficiency can be greatly improved by using "multiple-effect" distillation columns.

Multiple-effect evaporators are widely used to remove water from salt/water mixtures. A series of evaporators are designed with the process stream flowing from stage to stage. Water is boiled off in each stage by operating successive stages at lower and lower pressures. In the lowest pressure stage, the water vapor is condensed using cooling water in a heat exchanger. The heat supplied to this stage is the water vapor boiled off in the upstream stage, which is at a higher temperature so that it can be condensed in the jacket of the final stage evaporator. This cascading of stages, using the vapor from an upstream stage as the heat input to the next stage, is continued with progressively higher temperatures in each stage. The final stage gets its heat from high-pressure steam. In theory, if the steam required to remove a given amount

of water is $F_S$, the steam required to remove the same amount of water in an N-stage evaporator configuration is $F_S/N$.

The same idea can be applied to distillation columns, if it is possible to operate one column at high temperatures (high pressure) and another column at lower temperatures (low pressure). The overhead vapor from the high-temperature column is condensed in a condenser/reboiler heat exchanger that generates vapor in a low-temperature column. Significant reductions in energy consumption can be achieved in many separations by the use of heat integration.

Heat-integrated systems come in many flavors. The most common situation is when there are two columns making different separations in which the reflux-drum temperature of one column is sufficiently higher than the base temperature of the second column so as to provide reasonable differential temperature driving force for heat transfer without requiring an excessively large heat-transfer area. The condenser heat duty in the high-temperature column and the reboiler duty in the low-temperature column should be similar in magnitude. Any difference in the duties can be easily handled by using either an auxiliary reboiler in the low-temperature column or an auxiliary condenser in the high-temperature column.

In many applications, a two-column heat-integrated system is used instead of a single column for the same separation job. There are several configurations of this type. The feed can be split and fed into the two columns, one operating at high pressure and the other operating at low pressure. The low-pressure column has a water-cooled condenser. The high-pressure column has a steam-heated reboiler. The pressures are adjusted so a 20 to 30 K temperature difference is achieved between the reflux-drum temperature in the high-pressure column and the base temperature in the low-pressure column. The feed split can be adjusted so that the condenser duty in the high-pressure column is exactly equal to the reboiler duty in the low-pressure column. Specification distillate and bottoms products are removed from both columns.

Another common configuration sends the entire feed stream to one of the columns. The distillate from this column is about half of the lighter component. The bottoms stream is fed to the second column, which takes the rest of the lighter component out the top and all the heavier component out the bottom. Either the first or the second column can be the high-pressure column with the other column the low-pressure column. Heat integration can be in direction of flow (first column at high pressure) or in the reverse direction to the process flow (second column at high pressure).

For this type of heat-integrated system to be economical, the difference in the boiling point between the light and heavy components cannot be large. Otherwise the pressure difference necessary to achieve the condenser and reboiler temperatures would be large, which would result in a high temperature in the base of the high-pressure column and require an expensive heat source. The high pressure would also reduce relative volatilities in most systems, which would increase energy consumption.

## 3.2 PRINCIPLES OF DISTILLATION CONTROL

In this section we discuss the development of effective distillation control structures. A simple two-product distillation column is studied. Once the column is built, the number of trays and the feed-tray location are fixed. We assume the feed flowrate is set by an upstream unit.

There are three *inventory* variables that must be controlled: pressure, liquid level in the reflux drum, and liquid level in the base. There are five control valves available: condenser cooling water, reboiler steam, reflux, distillate, and bottoms. Three of these must be used to control the three inventory variables. That leaves two control valves available to control two variables.

Ideally, the two variables to control would be the compositions of the distillate (heavy-key impurity) and the bottoms (light-key impurity). These are the variables that were used to design the column in the first place. A "dual-composition" control structure is the ideal scheme but is seldom implemented in industry because online composition measurements are usually expensive, require high maintenance, and can introduce significant delays in the control loop, particularly if gas chromatographs are used.

Therefore many distillation columns are controlled using temperature measurements, which are inexpensive, reliable, and relatively fast. Do we need to control two temperatures or will one be sufficient? And if we use temperatures, where is the best location for their measurement?

### 3.2.1 Single-End Control

Many industrial distillation columns use some type of single-end temperature control because of its simplicity and low maintenance cost. However, this simple structure may not provide effective control for some columns. Even if a single-end control structure is possible, we have to decide how to select the other control degree of freedom. The most common choices are holding a constant *reflux-to-feed ratio* (R/F) or holding a constant *reflux ratio* (RR).

It is important to note that either of these ratio-control structures should be effective, from a steady-state standpoint, for feed flowrate disturbances. As feed flowrate changes, all flows ratio directly and composition and temperatures throughout the column end up at the same values (neglecting any changes in pressure and tray efficiencies). However, for feed composition changes, the compositions and temperatures in the column change at the new steady state with both product purities held constant. So the choice between the RR and R/F structure must be based on feed composition disturbances.

***Selecting Reflux Ratio or Reflux-to-Feed Ratio.*** To aid in making this choice, a series of steady-state simulation runs can be made in which the effects of changes in feed composition on the required changes in R/F ratio and RR are determined while holding both products at their specified compositions.

If the required changes in the R/F are very small, a single-end control structure with R/F held constant may be effective. If the required changes in the RR are very small, a single-end control structure with RR held constant may be effective. If there are significant changes in both, we may have to use a dual-end control structure.

***Selecting Temperature/Composition Control Tray Location.*** Another important issue in distillation control is the location of the tray on which temperature is to be controlled in a single-end structure. There are many methods for making this selection, but a simple and effective approach is to select a tray at a point where there are significant changes in temperature from tray to tray.

Another useful method is to find the sensitivity of tray temperatures to changes in a manipulated variable. For example, suppose we are exploring a control structure in which

reflux-drum level is controlled by manipulating distillate flowrate, base level is controlled by manipulating bottoms flowrate, and pressure is controlled by manipulating condenser heat removal (cooling water flowrate). The two remaining control variables are reflux and reboiler heat input. We fix the reflux flowrate and make a small (0.1%) change in the reboiler heat input. The resulting changes in the tray temperatures from the original steady state are calculated. The tray with the largest changes in temperature may be a good spot to use for temperature control.

A third useful method is called the *invariant temperature* approach. Feed composition is varied over the expected range of values with both the distillate and bottoms held at their specified compositions. Temperature profiles are plotted for each feed composition. If there are trays with temperatures that do not change for different feed compositions, these trays may be good locations to control.

The most elegant method for control-tray location is *singular value decomposition* (SVD). The steady-state gains between all the tray temperatures and the two manipulated variables ($\Delta T_n/\Delta R$ and $(\Delta T_n/\Delta Q_R)$ are calculated, and the $N \times 2$ matrix is decomposed using software such as MATLAB into three matrices $\mathbf{u}\sigma\mathbf{V}^T$. The two $\mathbf{u}$ vectors are plotted against tray numbers. The trays with the largest magnitudes of $\mathbf{u}$ indicate locations in the column that can provide effective control. More details can be found in Luyben.[1]

In columns separating components with low relative volatilities, it is often not possible to use temperatures because there is very little change from tray to tray. Pressure changes from tray to tray may have more effect than composition. In these cases, direct composition control is often required.

Distillation wisdom suggests that it is more effective to control the *impurity* of a stream than the purity because there is more change in the composition of the impure component for a change in the manipulated variable. The steady-state gain is higher, which offers the potential for tighter control.

A comment on what composition to control may be useful. Intuitively we would select the composition of the product stream. But if the product purity is high (the impurity level is very small), it may be difficult to get an accurate online measurement. The high purity also may result in very nonlinear dynamic responses. An effective and practical method for dealing with this problem is to move away from the end of the column and control the composition on an intermediate tray where the impurity is larger and can be more accurately measured. Nonlinearity problems are also reduced.

***Controller Tuning.*** Once the structure has been established, the single-end temperature or composition controller must be tuned in a consistent and repeatable way. First, make sure that realistic lags or deadtimes are inserted in the dynamic simulation loop. Temperature controllers should use 1-min deadtimes. Composition controllers should use 3- to 5-min deadtimes. Failure to insert these dynamic lags or deadtimes will result in a prediction of controller performance that is unrealistically better than what is attainable in the real plant in which these dynamic elements are always present due to measurement and valve dynamics.

The relay-feedback test is an effective way to determine the ultimate gain and period of a loop. This test can be easily conducted in Aspen Dynamics software. Controller tuning parameters are then easily calculated from the ultimate properties using whatever tuning rules you prefer. The conservative Tyreus–Luyben tuning is quite appropriate for distillation columns, where rapid and oscillatory swings in the manipulated variables can cause major hydraulic problems (flooding or weeping).

### 3.2.2 Dual-End Control

If the analysis discussed in the previous section indicates that single-end control is inadequate, two temperature controllers or two composition controllers or one temperature controller and one composition controller may be required. In this situation the engineer must be a little more cautious about controller tuning. The two loops are inherently interacting. Tuning one loop with the other on manual and then doing the same with the other loop may lead to an unstable system when both loops are put on automatic.

An effective and practical way to handle this problem is to use *sequential* tuning. The fastest loop is tuned first with the other controller(s) on manual. This is usually the loop with reboiler heat input as the manipulated variable. Changes in vapor rates travel up through the column rapidly, so changing reboiler heat input quickly affects the temperature and compositions on all trays. Changes in reflux, on the other hand, affect conditions in the column slowly because of the liquid hydraulic lags. It takes 3 to 6 s per tray to have a change in liquid *inflow* change the liquid *outflow* on a tray. So a change in reflux flowrate at the top of a 40-tray column may take 2 to 4 min to show up on the bottom trays.

Once the fast loop is tuned, keep it on automatic and tune the next fastest loop. This procedure is applied in many of the case studies presented in subsequent chapters.

### 3.2.3 Alternative Control Structures

The discussions in the previous sections have assumed that the reflux-drum level is controlled by distillate flowrate and base level is controlled by bottoms flowrate. This structure is the most widely used for a number of reasons. The major reason is that it provides attenuation of flow disturbance down through a series of process units because proportional-only level control provides gradual, nonoscillatory variations in the product streams feeding downstream units. In a multiunit process this can help to provide stable operation with reduced variability in product quality.

However, there are situations where other structures should be used. The most frequently occurring case is when the RR is high. If the RR is greater than about 3, the reflux-drum level should be controlled by reflux flowrate, not distillate flowrate. This switch is needed because any small change in the vapor coming overhead in the column will require a large change in the distillate flowrate since it is a factor of 4 times smaller than the vapor.

With reflux holding reflux-drum level, the distillate flowrate can be set in different ways. If it is used to control a temperature or composition, the tuning of the reflux-drum level controller should be proportional only with a gain of 5 instead of the normal value of 2. We want the reflux to change fairly quickly when the distillate is changed because reflux is really what is affecting temperature or composition.

If the distillate is manipulated to hold a constant RR, the flowrate of the reflux is measured and sent to a multiplier with a constant that is the reciprocal of the desired RR. The output signal from the multiplier is the setpoint signal of the distillate flow controller.

An interesting dilemma crops up in a high RR column when the single-end analysis indicates that a R/F control structure is better than a RR control structure. How do we resolve the conflicting objectives of wanting an R/F structure (which fixes the reflux for a fixed-feed flowrate) but not wanting to control reflux-drum level with the small distillate stream?

An effective solution is to control reflux-drum level with reboiler heat input and control a tray temperature (or composition) near the top of the column with the distillate flowrate. Reboiler heat input affects the pressure in the condenser. If the pressure controller is on

automatic, the increase in reboiler heat input will increase pressure, and the pressure controller will increase condenser heat removal (increase cooling water), which condenses more vapor and increases the liquid level in the reflux drum. The type and tuning of the reflux-drum level controller are different than the normal proportional-only controller with a gain of 2. A *proportional-integral* (PI) controller should be used, and a relay-feedback test must be run to tune this level loop because the dynamics of the column and the condenser pressure controller are nested inside the level loop. Fortunately, these high RR columns usually occur when the amount of the light component in the feed is small. The resulting temperature profile shows a break near the top of the column that can be effectively controlled by manipulating distillate flowrate. Note that the reflux-drum level loop is nested inside the temperature loop. The variable that is really affecting temperature is vapor boilup, which is changed by the level controller as the level is affected by changes in distillate flowrate.

## 3.3 CONCLUSION

Some of the important principles of distillation design and control have been summarized in this chapter. Quantitative examples of the application of these principles are given in the case studies presented in subsequent chapters.

Efficient design and effective control of the separation section of a chemical process are vital to its profitable and safe operation. Distillation is the dominant separation method used in the chemical-processing industries. The concepts presented in this chapter and in the previous chapter, which covered reactors, should be integrated into a complete design of the entire process.

## REFERENCE

1. Luyben, W. L. *Distillation Design and Control Using Aspen Simulation*, John Wiley & Sons, Hoboken, NJ, 2006.

# CHAPTER 4

# PRINCIPLES OF PLANTWIDE CONTROL

One of the biggest challenges to the successful development of a chemical process is finding an effective plantwide control structure. All of the units in a process must "dance together" in a stable harmonious manner. Small ripples in the reaction section should not be transmitted into the separation section, and vice versa.

Some practical methods to achieve stable regulatory-level control of complex multiunit processes are discussed in this chapter. They have been effectively applied over many years in a large number of processes. The presence of recycle streams needs special attention. Recycle streams can be gas or liquid. Gas recycle usually requires compression, which is expensive in terms of both energy and capital investment. But these increases in cost may be justified if improvements in yield can be realized, and by-product safety and environmental problems can be avoided.

The development of a plantwide control structure is not a trivial task. Typical processes can have many variables that must be controlled and many valves that must be driven by some control signal. Single-input–single-output proportional-integral controllers are widely used in industry. A process may have 30 to 50 loops to configure (select controlled/manipulated variable pairings and controller tuning constants). With 30 loops there are 30-factorial possible combinations of the variables. So an exhaustive enumeration of all possible pairings is untenable. Common sense, experience, and process control wisdom can reduce the possible pairings to a manageable number with dynamic performance that can be evaluated using dynamic simulation.

The first law of plantwide control is that it is easy to find a control structure that will **not** work! There are several alternative plantwide control structures that do work. The best structure depends on the control objectives of the plant, which in turn depend on the business objectives of the company. For example, if the product from the plant is to be provided to a downstream customer at whatever flowrate the customer desires at any point in time, an

*Principles and Case Studies of Simultaneous Design*, First Edition. William L. Luyben

"on-demand" plantwide control structure must be developed. The inventory loops (liquid levels and pressures) would be set up to work their way backwards from the product leaving the process to the fresh feed streams coming into the process.

In this chapter we summarize some basic concepts and features of the plantwide control problem. Then, we give a few simple examples of plantwide control structures that work, and some that do not work. More extensive quantitative examples are provided in the case-study processes given in subsequent chapters.

## 4.1 HISTORY

In the middle of the twentieth century, after World War II, there was a tremendous worldwide demand for chemicals for reconstruction in war-torn countries around the world and for improvement in the standard of living. A surge in the development and construction of chemical plants occurred. Driven by cheap oil and gas, these designs emphasized production using minimum capital. Energy conservation was a secondary concern.

With little experience in handling the complex multiunit processes that were developed, designers often resorted to the conservative approach of placing intermediate surge tanks between adjacent units so that disturbances and shutdowns in one unit did not immediately affect other units.

An abrupt change occurred in the 1970s with the oil embargo and the resulting order-of-magnitude increase in energy prices. Now process designs had to be optimized with consideration given to expensive energy. In addition, the international demand for capital investment made the luxury of installing intermediate surge tanks uneconomical. The control structure had to provide stable regulatory control with all the units tightly coupled together. Another reason for reducing inventories was that this reduces the potential for safety and environmental hazard. Process "intensification" has become an important consideration in plant design.

Since recycle streams are major sources of potential dynamic control problems, we discuss some of the effects of recycle.

## 4.2 EFFECTS OF RECYCLE

One of the important uses of recycle streams is to suppress the production of undesirable by-products. Minimizing the amounts of toxic or dangerous undesirable components has become increasingly important with tighter pollution and safety standards.

### 4.2.1 Time Constants of Integrated Plant with Recycle

One of the basic issues with recycle stream is that they can produce a drastic slowdown in the dynamic response of the entire integrated plant. Distillation columns and reactors normally have transient responses that last for tens of minutes to several hours. Inserting a recycle stream can lengthen the transient response of the coupled process to days.

To quantify this effect, consider the idealized process shown in Figure 4.1. We assume that the input $U$ affects the output $Y$ through a simple first-order lag transfer function. There is also a recycle that moves from the output of the process back into the inlet of the

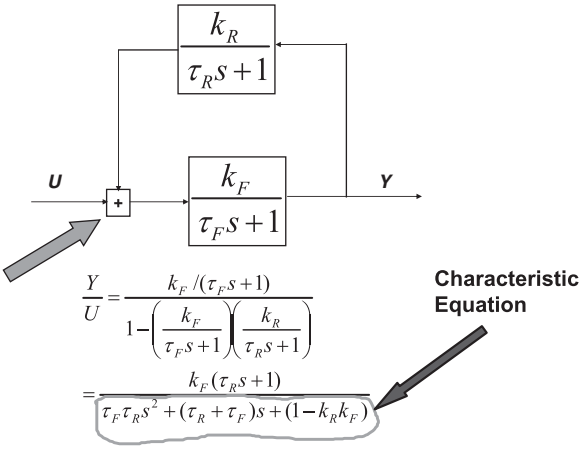


**Figure 4.1.** Process with recycle.

process. So the total input to the forward transfer function block is the sum of the original input and the recycle signal.

A little algebra leads to the transfer function describing the entire system. The characteristic equation is the denominator of the transfer function. Figure 4.2 shows that the second-order system has a time constant that depends on the time constants of the individual components ($\tau_F$ and $\tau_R$) and on the product of the two gains $k_F k_R$ (the loop gain). It is clear that the overall time constant of the process gets larger and larger as the value of the loop gain approaches unity.

Figure 4.3 shows results of a simulation of this simple system for a step change in input. The individual time constants of each lag have values of 1 unit of time. The time constant of a first-order system is the time it takes the output to get to 62.3% of the final steady-state value. The strong influence of the loop gain on the system time constant is clearly shown. When the loop gain is 0.9, the process time constant is over 20 units of time, which is a factor of 20 times the time constant of the individual units.

### 4.2.2 Recycle Snowball Effect

The flowrates of recycle streams are often very sensitive to small disturbances. This is called the "snowball" effect. A small change in some variable, for example fresh feed flowrate, can

$$\left(\frac{\tau_F\tau_R}{1-k_F k_R}\right)s^2+\left(\frac{\tau_F+\tau_R}{1-k_F k_R}\right)s+1=0$$

$$\tau^2 s^2+2\tau\varsigma s+1=0$$

**As "$k_F k_R$" approaches "1", time constant increases!**

**Figure 4.2.** Characteristic equation.

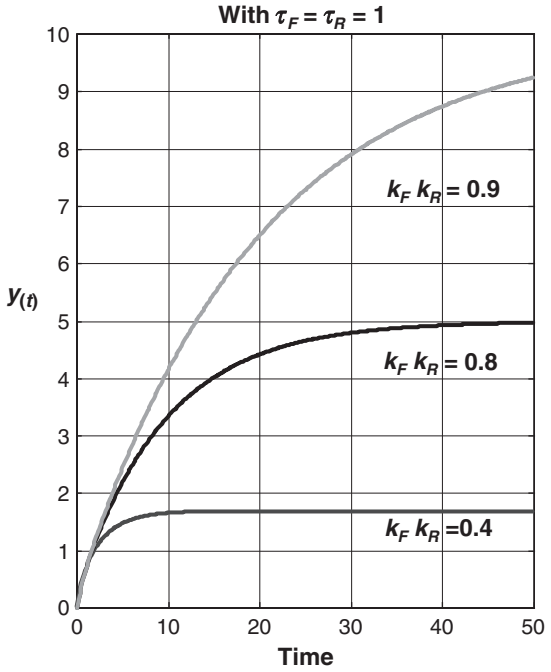


**Figure 4.3.** Effect of recycle loop gain.

produce a very large change in the resulting flowrate of the recycle stream. Amplification factors of 3 are quite common, that is, a 10% change in feed flowrates results in a 30% change in recycle flowrate.

Since the recycle stream is coming from a distillation column, the loading in this column must change drastically. Vapor rates may get so high that the column floods or we run out of reboiler or condenser capacity.

Snowballing occurs because the conditions in the reactor have to change to accommodate the disturbance. Increasing fresh feed 10% requires that reaction rates in the reactor must increase by 10%. If the volume and the temperature in the reactor are fixed, the only way a 10% increase in reaction rate can be attained is by significant changes in the compositions of reactants in the reactor. Higher reactant concentrations are needed, which means that the recycle of reactant must increase.

A simple example clearly illustrates the problem. Figure 4.4a shows a flowsheet with a reactor and a distillation column. The chemistry is A + B → C. The fresh feed is initially 50 mol/min of A and 50 mol/min of B. The product stream from the column must be 50 mol/min of C. Suppose the recycle of A and B from the column back to the reactor consists of 50 mol/min of A and 50 mol/min of B. The total feed to the reactor is 100 mol/min of A and 100 mol/min of B. Therefore the reactor effluent is 50 mol/min of A, 50 mol/min of B, and 50 mol/min of C. The concentrations of reactants in the reactor are $z_A = z_B = 50/150 = 0.3333$. The recycle flowrate is 100 mol/min (the sum of A and B).

We assume that the reaction rate is first order in the two reactant mole fractions ($\Re_C = kV_R z_A z_B$). The temperature and holdup in the reactor are fixed. These parameters are such that 50 mol/min of C are produced with a $z_A z_B$ product of compositions of (0.3333) (0.3333) = 0.1111.

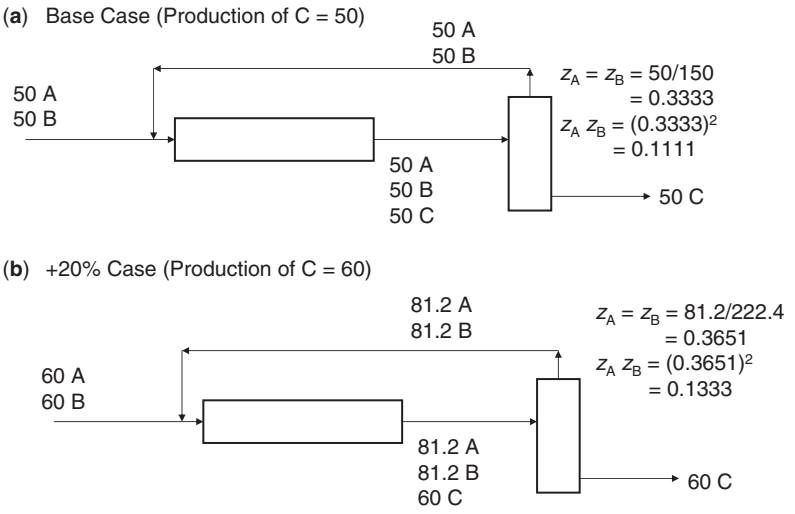


**Figure 4.4.** "Snowball" effect.

Now suppose we want to produce 20% more C. This means we must feed in 60 mol/min of A and 60 mol/min of B to make 60 mol/min of C. It also means that the $z_A z_B$ product of compositions must increase by 20% from 0.1111 up to 0.1333 if reactor temperature and holdup are unchanged. What is the new recycle flowrate?

The new values of $z_A$ and $z_B$ must be $\sqrt{0.1333} = 0.3651$. A little algebra shows that the amount of A in the reactor effluent with an equal amount of B and with a C of 60 mol/min of must be 81.2 mol/min of A. Therefore the recycle flowrate must increase from the initial 100 mol/min of the mixture of A and B to a 162.4 mol/min of mixture of A and B. A 20% increase in throughput requires a 62% increase in recycle!

Now that we understand the potential problem, how do we prevent it? A simple practical way to prevent drastic changes in the loading of the separation section is to use a plantwide control structure that places a *flow controller* somewhere in a liquid recycle loop. Simple examples are given later in this chapter, and more complex examples are presented in the case studies covered in subsequent chapters.

## 4.3 MANAGEMENT OF FRESH FEED STREAMS

A key feature of plantwide control structures is where and how the fresh feed streams are introduced into the process. Assuming that the separation section is doing its job of keeping the losses of reactants to negligible amounts, the reactant components that are fed into the process in the fresh feed streams must be completely consumed by the reactions occurring in the reaction section. We cannot feed more reactants than the reactor can convert to products.

### 4.3.1 Fundamentals

The conversion of reactant depends on conditions in the reactor and its size. If we attempt to feed into the process more than can be reacted, the system will fill up with excess reactant and

shut down. So managing the fresh feeds is a critical issue that the control structure must effectively handle.

If the fresh feed is a gas, it may be fed into a circulating gas loop, perhaps on pressure control. The system pressure gives a good indication of whether or not the gaseous reactant is being consumed at the rate we are feeding it. Rising pressure says too much is being fed. Dropping pressure say too little is being fed. So the pressure controller will effectively handle the issue of feeding exactly enough gaseous reactant.

If the fresh feed is a liquid, it may be fed directly into the reaction section or it may be fed into the separation section at a location where the component tends to accumulate. Distillation column bases or reflux drums are common locations. The liquid level gives an indication of whether or not the liquid reactant is being consumed at the rate we are feeding it. Increasing liquid level says too much is being fed. Dropping liquid level says we need to feed in more.

The fresh feed management problem becomes more complex when there are several reactant components involved in the chemistry. Then an almost perfect stoichiometric balance among the reactants must be maintained.

### 4.3.2 Process with Two Recycles and Two Fresh Feeds

To illustrate these issues, let us consider a process that is fairly simple but is representative of many industrial processes. The chemistry involves two reactants (A and B) producing product C. Figure 4.5 gives the flowsheet. The two reactants are fed into the process in two fresh feed streams $F_{A0}$ and $F_{B0}$. The irreversible reaction occurs in the liquid phase

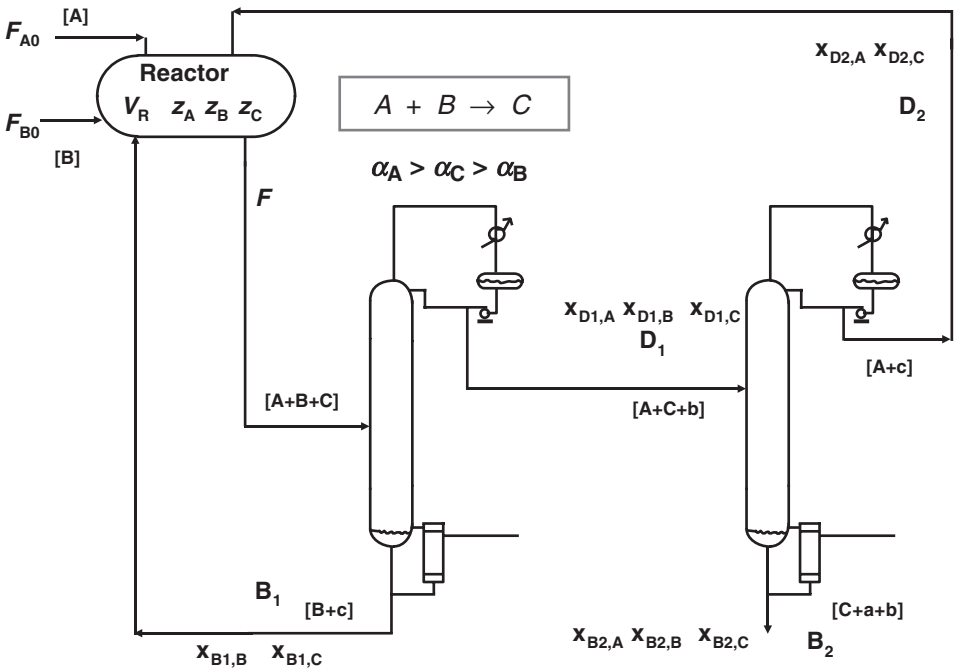


**Figure 4.5.** Process with two recycles and two fresh feeds.

in an isothermal, constant-holdup CSTR. The per-pass conversion is modest, so the reactor effluent $F$ contains significant concentrations of both reactants ($z_A = 0.13$ and $z_B = 0.25$). These reactant must be separated from the product and recycled.

The relative volatilities are assumed to be $\alpha_A > \alpha_C > \alpha_B$. Because product C is the intermediate-boiling component, two recycle streams must be produced in two distillation columns. The "indirect" separation scheme is selected, in which a recycle stream of B comes out the bottom of the first distillation column and a recycle stream of A comes out the top of the second distillation column. The product C is removed out the bottom of the second column.

The reaction is first order in each of the reactant concentrations: $z_A$ mole fraction A and $z_B$ mole fraction B). As discussed in the previous section, the second-order reaction rate $\Re$ depends on the product of the two concentrations.

$$\Re = V_R k z_A z_B$$

where $V_R$ is the molar reactor holdup and $k$ is the temperature-dependent specific reaction rate. We assume that reactor temperature is fixed, which fixes $k$. For a desired rate of production, the size of the reactor is minimized when the product $z_A z_B$ is maximized. The maximum product of these terms would occur when the two mole fractions are both 0.5. Of course there is some product in the reactor effluent with mole fraction $z_C$. Adjusting the $z_A$ and $z_B$ to be equal would minimize the required reactor volume.

However, we need to also consider the economics of the separation section. Recycling component A requires that all of it in the reactor effluent must be vaporized twice (once in each column). Recycling component B involves no vaporization since it goes out the bottom of the first column. So the energy costs in the separation section are lower if the system is designed with $z_B$ larger than $z_A$. Figure 4.6 shows how several design parameters vary with the design value of $z_B$. At the economic optimum, the B recycle from the bottom of the first column (B1) is larger than the A recycle from the top of the second column (D2).

There are several plantwide control structures that work in this process (and many that do *not* work). Several alternatives are presented to illustrate alternative fresh feed management techniques. You will observe that all of the workable control schemes use information from inside the process to detect any imbalance in the stoichiometry and to use feedback control to correct any problem.

***CS1.*** Figure 4.7 shows an effective plantwide control structure CS1. Both recycles are flow controlled, so snowballing is prevented. The liquid level in the base of the first column is controlled by manipulating the fresh feed of B ($F_{B0}$). The liquid level in the reflux drum of the second column is controlled by manipulating the fresh feed of A ($F_{A0}$). These levels tell us if we are feeding too little or too much of each reactant. Production rate is adjusted by simultaneously changing the setpoint signals to both of the recycle flow controllers.

***CS2.*** Figure 4.8 shows an alternative plantwide control structure CS2 that also works in this process. The key feature is a composition measurement in the reactor to detect changes in the inventory of one of the reactant ($z_B$). A composition controller manipulates the fresh feed of reactant B. The reactor level controller manipulates the fresh feed of reactant A. Snowballing is prevented by flow controlling the reactor effluent that is feeding the distillation column.

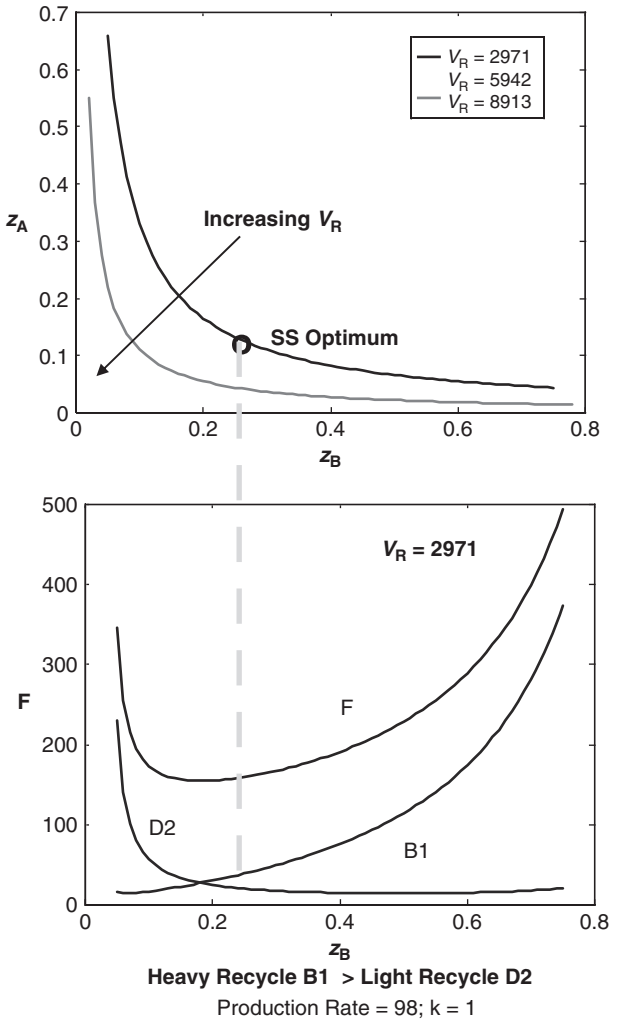


**Figure 4.6.** Optimum economic steady-state design.

Both control structures CS1 and CS2 are effective because they use measured information inside the process to keep track of a least one reactant composition so that precisely the correct amount of reactant is fed to balance the stoichiometry *down to the last molecule.* Even a tiny imbalance in the amounts of the two reactants fed into the system will result in a slow but steady buildup of the component in excess, which will eventually lead to a plant shutdown as recycle flowrates hit constraints.

In both of these control structures there is no direct setting of the throughput, which may strike some as a disadvantage. Let us look at another alternative control structure in which throughput can be directly set.

***CS3.*** Figure 4.9 shows a structure in which the flowrate of fresh A is fixed. If we want to change production rate, we simply change the setpoint of the flow controller. Snowballing is prevented by flow controlling the reactor effluent.

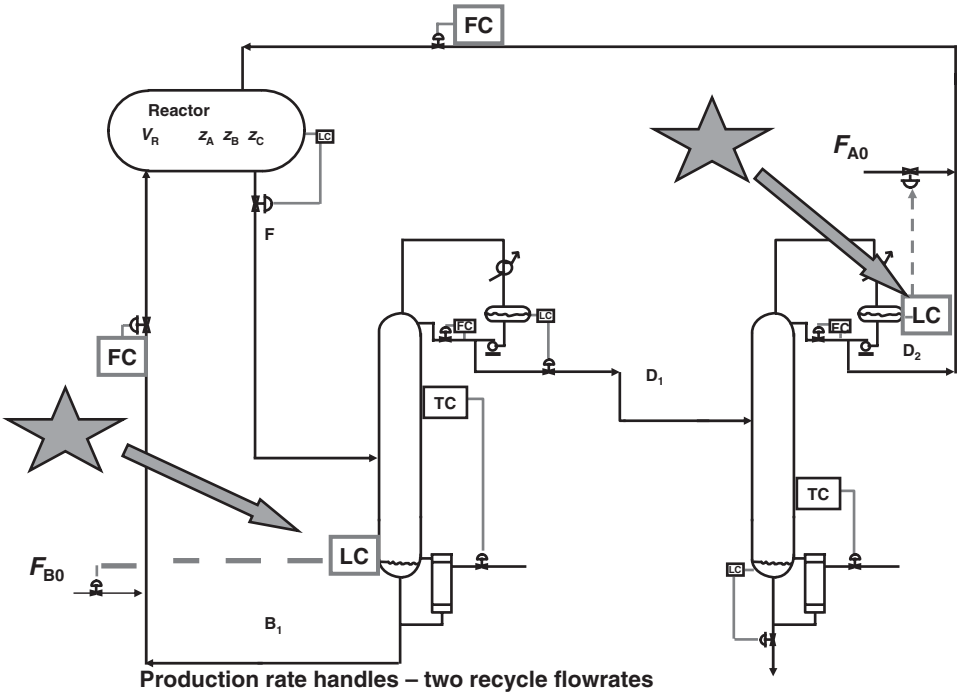


**Figure 4.7.** CS1: Both recycles flow-controlled.

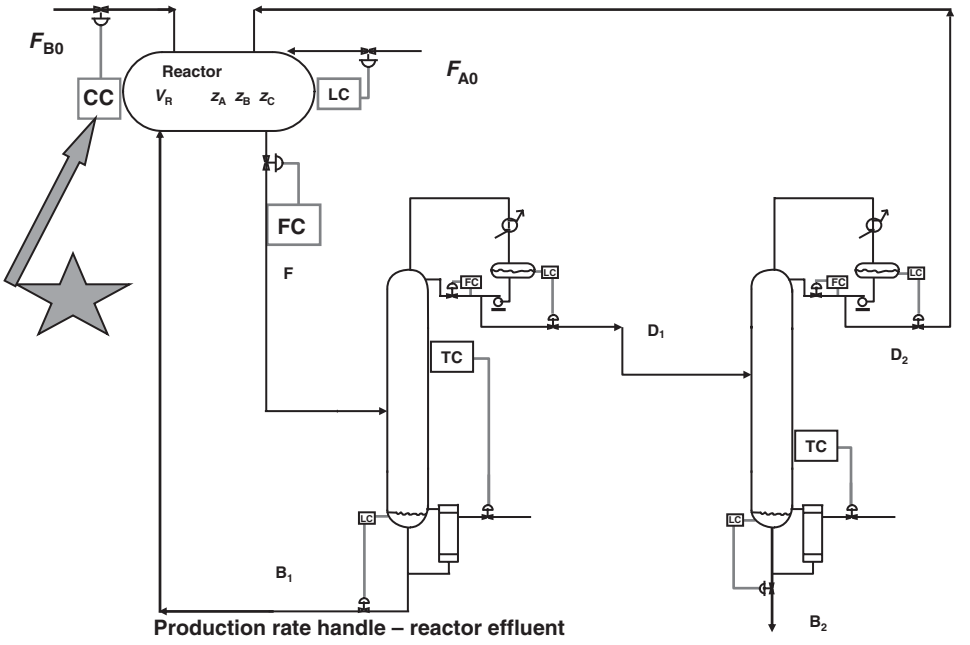


**Figure 4.8.** CS2: Reactor composition controlled.

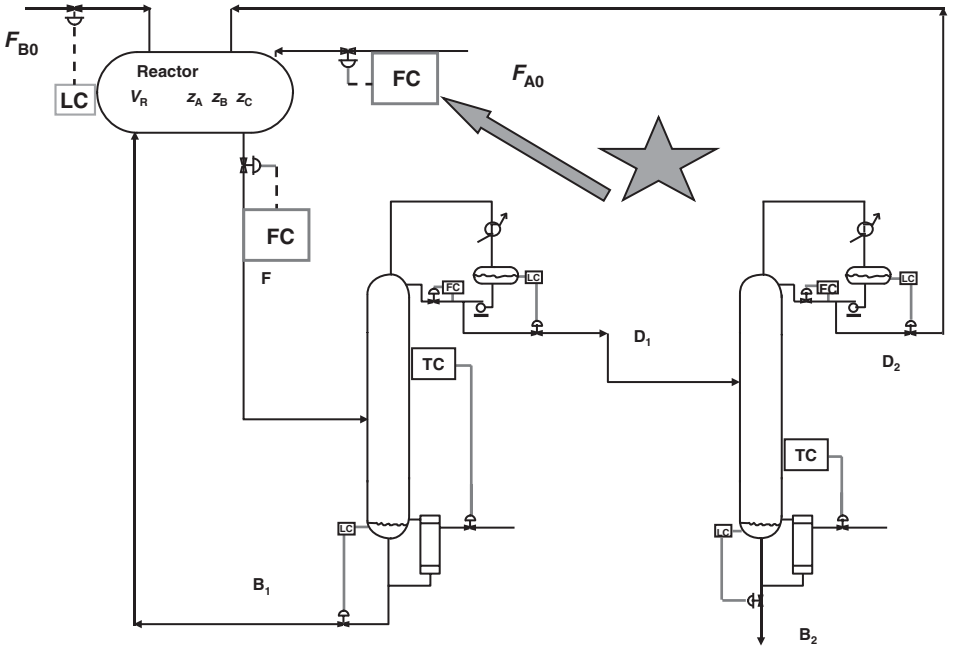


**Figure 4.9.** CS3: Fresh feed flow-controlled.

Does this structure work? Figure 4.10 shows what happens when a very small 2% increase in $F_{A0}$ is made. Reaction rate in the reactor must increase by 2%. This is achieved by the increase in $z_A$ from 0.13 to 0.155. Notice, however, that there is a decrease in $z_B$, which is a forewarning of potential trouble.

Now let's impose a more realistically large disturbance. Figure 4.11 gives results for a relatively small 5% increase in the $F_{A0}$ flow. The reaction rate in the reactor must increase by 5%. The composition of A increases, but the composition of B decreases. The increase in $F_{A0}$ has increased the level in the reactor, so the level controller has decreased the flow of B into the reactor. There is no combination of reactor compositions that makes the $z_A z_B$ product high enough. The system fills up with A as the recycle of A ($D_2$) gets larger and larger. The fresh feed of B eventually falls to zero.

Notice that it takes 6 days for the imbalance in reactants to finally produce a process shutdown. If a 10% disturbance is made, the time to shutdown is reduced to 3 days.

This simple example demonstrates that the plantwide control structure must be able to detect any imbalance in the stoichiometry and have a mechanism for correcting the problem.

***CS4.*** The final control structure to be considered is one that has appeared in several published papers. Figure 4.12 shows a structure in which the fresh feed flowrate of A is fixed and the fresh feed flowrate of B is ratioed to it. This may seem like a simple way to handle the stoichiometry problem. It may even seem to work in computer simulations.

In the real world, however, this scheme will not work. The accuracy with which flowrates can be measured in an industrial plant is 10% (if we are lucky). Remember that the stoichiometry *must be balanced down to the last molecule*.

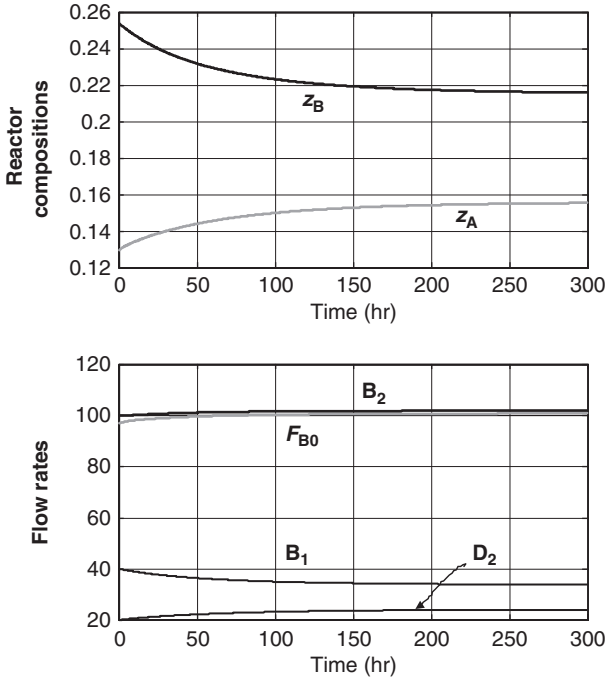


**Figure 4.10.** CS3 for 2% increase in $F_{A0}$.

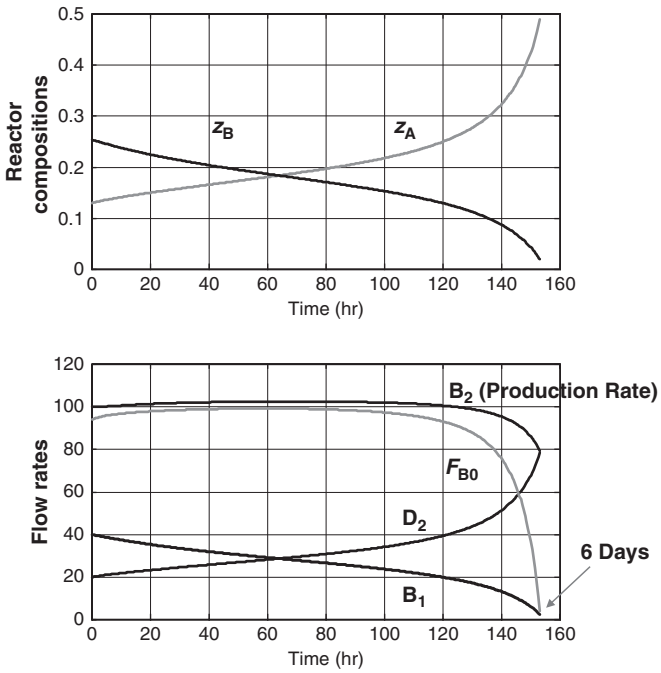


**Figure 4.11.** CS3 for 5% increase in $F_{A0}$.

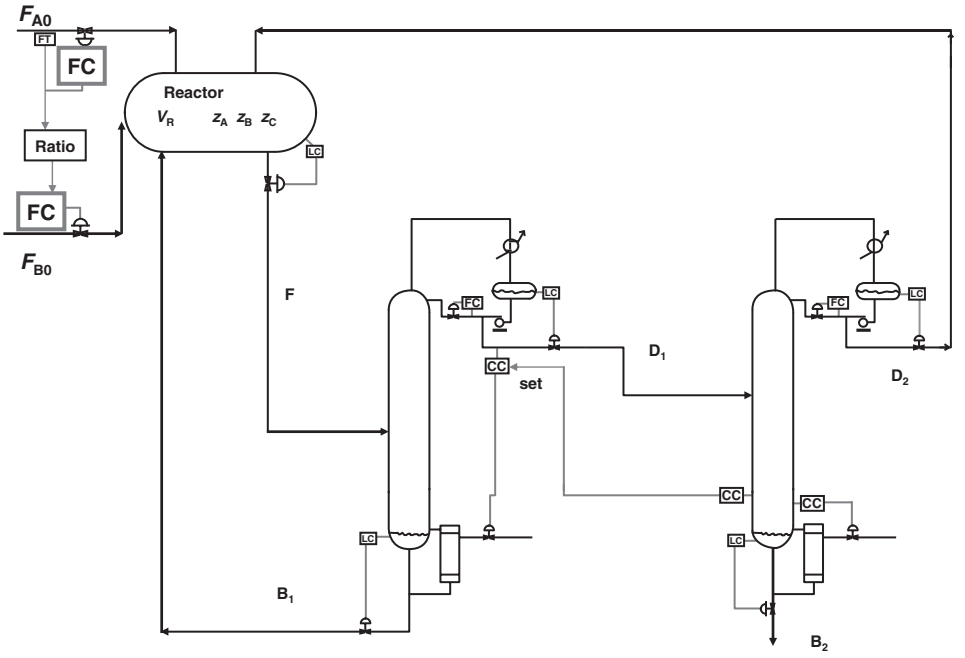


**Figure 4.12.** CS4 ratio structure.

This structure will not work even in simulations if there are changes in the compositions of the fresh feeds, which is almost always the case in operating plants.

## 4.4 CONCLUSION

We have laid the framework and enumerated the basic concepts for being able to develop effective, stable plantwide control structures in complex processes with multiple units and recycle streams. These ideas are applied in the case studies presented in subsequent chapters.

# CHAPTER 5

# ECONOMIC BASIS

The case studies presented in the rest of the chapters in this book use a consistent set of methods and relationships for sizing equipment, estimating equipment capital investment, and specifying energy costs at different temperature levels. The equations, correlations, and parameter values are taken from the useful books by Douglas[1] and Turton et al.[2]

## 5.1 LEVEL OF ACCURACY

Engineering economics are applied at many levels ranging from very crude "back-of-the-envelope" order-of-magnitude estimates to the reasonably precise estimates needed to get the money to proceed with buying equipment and constructing the plant. The most precise estimates strive to have an accuracy of $\pm 10\%$.

However, long before the project reaches the stage of actually committing to the expenditure of hundreds of millions of dollars, a long series of preliminary scouting studies must be made to see if there is any possibility of making money.

This book is aimed at the conceptual design stage where the main purpose is to compare alternative flowsheet designs and operating parameters. So precise economic estimates of capital and energy costs are not required. Ballpark numbers are good enough to decide which of the many alternative flowsheet arrangements looks the best.

At later stages in the project, more precision is required. But we should remember that even though fairly accurate estimates of equipment and energy costs can be generated, the profitability of the process depends very heavily on the ability of the marketing department to provide estimates of the cost of raw materials and the potential selling price of the products. Marketing estimates usually are worse than even the shaky weather forecasts made by a battery of meteorologists.

*Principles and Case Studies of Simultaneous Design*, First Edition. William L. Luyben

So very simple economic analysis approaches are taken in this book. There are dozens of books that concentrate on cost estimation. There are quite rigorous computer software packages available for cost estimation. AspenTechn provides the ICARUS Process Estimation software, which can be used when precision is required. The CAPCOST program given in Turton et al.[2] can also be used.

## 5.2 SIZING EQUIPMENT

Each major piece of equipment in the process must be designed, which means we need to know how big it is. The diameters and lengths of vessels used as reactors, columns, and tanks must be determined. These dimensions depend on the flowrates in the equipment. The heat-transfer area required in heat exchangers must be determined based on realistic estimates of overall heat-transfer coefficients, heat-transfer rates, and differential temperature driving forces. Compressor capital cost depends directly on the work required to achieve the compression ratio and throughput specified.

### 5.2.1 Vessels

***Columns.*** Vertical cylindrical vessels are used for distillation, absorption, and liquid–liquid extraction. Columns can have trays or packing. When trays are used, the tray spacing must be specified. To provide enough room for someone to crawl inside the column for repairs and maintenance, a typical value of tray spacing is 2 ft.

Packed columns are separated into several sections of packing with liquid redistribution every 20 ft or so. The height of a theoretical tray must be estimated to determine the total length of the vessel.

Aspen Plus calculates the diameter of the vessel. Knowing the diameter and the height, the capital cost can be found using the equations given in Section 5.3.

***CSTRs.*** The total volume is optimized during steady-state design. The aspect ratio (length-to-diameter) is usually about two. The larger the aspect ratio, the larger the jacket heat-transfer area, which helps dynamic control. But the reactor mixing can be adversely affected if the aspect ratio is too large.

***Adiabatic Tubular Reactors.*** These units are vessels that are either empty (if the reactions are homogeneous) or packed with solid catalyst (if the reactions are heterogeneous). The aspect ratio of the vessel is set at about 10 so that the flow patterns through the vessel are approximately plug flow (no axial or radial gradients in compositions or temperature).

***Cooled Tubular Reactors.*** A tubular reactor with heat transfer is essentially a tube-in-shell heat exchanger. The process fluid is inside the tubes with the catalyst, and the cooling or heating medium is on the shell side. The total tube volume is set by the required reactor volume (or amount of catalyst). The smaller the diameter of the tubes, the larger the heat-transfer area per total volume. Mechanical strength issues usually limit the minimum tube diameter to about 1 inch. The length of the tubes and the number of tubes is selected so that the pressure drop through the reactor is not too large. This is particularly important in gas systems because compression cost varies directly with pressure drop.

***Liquid Surge Tanks.*** Reflux drums and column bases in distillation columns and absorbers are sized to provide 5 min of liquid holdup when the vessel is half full, based on the total liquid stream entering the tank.

***Flash Tanks.*** There are two criteria that must be evaluated when sizing a flash tank. The diameter may be set by the requirement of 5 min of liquid holdup. Or it may be set by a maximum superficial vapor velocity up through the vessel to minimize liquid entrainment. An F factor of 0.5 (in engineering units) is used. An aspect ratio of 2 is commonly used.

$$\text{F factor} = V_{\max}(\text{ft/sec})\sqrt{\rho_V(\text{lb/ft}^3)} = 0.5$$

***Decanters.*** More holdup time is required in decanters to give the two liquid phases plenty of time to settle into light and heavy phases. Holdup times of 20 to 30 min are often used.

### 5.2.2 Heat Exchangers

Heat exchangers of many types are used in chemical processes. Tube-in-shell heat exchangers are the most common, but plate heat exchangers are sometimes used when fouling is not a problem because they provide more heat-transfer area and lower pressure drop per volume of vessel. Fired furnaces are used when high temperatures are required. Many heat exchangers heat or cool process material using utilities (steam or cooling water). Other heat exchangers transfer heat between process streams.

To find the capital cost of a heat exchanger, we only need the heat-transfer area. But to get the area we need the heat duty, the overall heat-transfer coefficient, and the differential temperature driving force. The heat duty is obtained directly from the simulation. The overall heat-transfer coefficient depends on the phases on the two sides of the heat exchanger. Table 5.1 gives typical values.

The differential temperature driving force varies with the temperature level. The higher the temperature, the larger the economic optimum differential temperature. A useful heuristic is to use a $\Delta T$ that is about 5% of the absolute temperature. This provides a reasonable compromise between investment in heat exchanger area and energy costs of high-temperature or low-temperature heat sources or sinks. For example, if a heat exchanger operates around 200 °C (473 K), the minimum approach temperature at the limiting end of the heat exchanger should be about 24 K. In cryogenic service, a small $\Delta T$ is used because the low temperature is attained by expensive compression.

**TABLE 5.1 Overall Heat-Transfer Coefficients**

| | Btu $hr^{-1}$ $ft^{-2}$ $F^{-1}$ | kW $m^{-2}$ $K^{-1}$ | kcal $hr^{-1}$ $m^{-2}$ $K^{-1}$ |
|---|---|---|---|
| Gas–gas | 30 | 0.17 | 150 |
| Gas–condensing vapor | 50 | 0.28 | 240 |
| Gas–vaporizing liquid | 50 | 0.28 | 240 |
| Liquid–liquid | 100 | 0.57 | 490 |
| Liquid–condensing vapor | 150 | 0.85 | 730 |
| Liquid–vaporizing liquid | 150 | 0.85 | 730 |

The condenser of a distillation column using cooling water has a heat sink that comes in at 90 °F and leaves at 110 °F. A log-mean $\Delta T$ is used with the two differences between the reflux-drum temperature and these two cooling-water temperatures.

### 5.2.3 Compressors

The power requirements of a compression system depend on the compression ratio and the suction temperature. Compressors are driven by steam turbines (using high-pressure steam) or electric motors. In either case the energy is high level and expensive. As discussed in Chapter 2, compressor suction temperatures should be kept low. Multistage compression systems use intercooling to more closely approach isothermal compression. Equal compression ratios are used in each stage. Compressor power requirements are obtained from the simulation.

### 5.2.4 Pumps, Valves, and Piping

Since the work of pumping liquids is usually small and the cost of a pump is usually much smaller than that the major vessels, pumping cost can usually be neglected in the conceptual design stage. The same is true for valves and piping.

## 5.3 EQUIPMENT CAPITAL COST

Two types of capital equipment costs are presented in cost estimation references. Bare-module cost is the cost of the equipment itself. Installed cost is the cost of the equipment plus all the costs of installing it in the process. The equations given below are for installed costs.

Of course, the total capital cost of a plant includes many expenditures beyond the investment in the major pieces of equipment. These include site preparation, off-site units (boiler house, raw material and product tankage, piping, buildings for staff, maintenance shops). The total investment in a typical plant is about 3 to 4 times the cost of the major equipment. In this book, a small 3-year payback period is used to account for this factor. An alternative approach would be to increase the capital cost of the equipment by 3 and use a 9-year payback period.

The equations given below are taken from Douglas[1] and Turton et al.[2] All costs are in US dollars. Conventional carbon steel materials of construction and modest pressure levels are assumed. If these assumptions are not valid for your process, the appropriate correction factors can be found in Douglas.[1] Correction factors during periods of rapid inflation should also be applied.

### 5.3.1 **Vessels** (diameter and length in meters)

$$\text{Capital cost} = 17{,}640(D)^{1.066}(L)^{0.802}$$

### 5.3.2 **Heat Exchangers** (area in square meters)

$$\text{Capital cost} = 7296(A)^{0.65}$$

### 5.3.3 **Compressors** (work in horsepower)

$$\text{Capital cost} = (1293)(517.3)(3.11)(\text{hp})^{0.82}/280$$

## 5.4 ENERGY COSTS

The cost of energy depends on the temperature level of the heat source or sink. Electrical energy is the most expensive. Low-pressure steam is the least expensive.

Low-pressure steam (6 bar, 87 psia, 160 °C/433 K/320 °F) = \$7.78/GJ
Medium-pressure steam (11 bar, 160 psia, 184 °C/457 K/363 °F) = \$8.22/GJ
High-pressure steam (42 bar, 611 psia, 254 °C/527 K/490 °F) = \$9.88/GJ
Electricity = \$16.8/GJ
Refrigeration:
Chilled water at 5 °C, returned at 15 °C = 4.43/GJ
Refrigerant at −20 °C = 7.89/GJ
Refrigerant at −50 °C = 13.11/GJ

## 5.5 CHEMICAL COSTS

Estimation of capital and energy costs can usually be made with reasonable accuracy (±20%). Estimation of the costs of raw materials and the selling price of products is usually subject to much more uncertainty.

A useful source of chemical prices is: http://www.icis.com/StaticPages/Students.htm.

## REFERENCES

1. Douglas, J. M. *Conceptual Design of Chemical Processes*, McGraw-Hill, New York, 1988.
2. Turton, R., Bailie, R. C., Whiting, W. B., Shaelwitz, J. A. *Analysis, Synthesis and Design of Chemical Processes*, 2nd Edition, Prentice Hall, Englewood Cliffs, NJ, 2003.

# CHAPTER 6

# DESIGN AND CONTROL OF THE ACETONE PROCESS VIA DEHYDROGENATION OF ISOPROPANOL

Now that the fundamental principles of plantwide simultaneous design and control have been discussed, we are ready to illustrate their application to a number of typically complex industrial processes. We begin with the acetone process.

Acetone is produced via several alternative processes, one of which is the dehydrogenation of isopropanol. The endothermic gas-phase reaction converts isopropanol to acetone and hydrogen. The process consists of a vaporizer, heated tubular reactor, flash tank, absorber, and two distillation columns. The liquid fresh feed is a mixture of isopropanol (IPA) and water. It is combined with a small IPA/water recycle stream, vaporized, and fed into the vapor-phase reactor, which is heated by high-temperature molten salt. Reactor effluent is cooled and fed to a flash tank. The gas from the tank contains most of the hydrogen but also some acetone. This gas is fed to an absorber in which a water stream is used to recover acetone. The liquid streams from the base of the absorber and the flash tank are fed to the first distillation column, which produces high-purity acetone out the top. There is also a vapor vent stream leaving the reflux drum of this column to remove the small amount of hydrogen dissolved in the feed. The second distillation column produces a high-purity water bottoms and a distillate with a composition near the isopropanol/water azeotrope, which is recycled back to the vaporizer.

In this process there are a number of interacting design optimization variables that illustrate some interesting design trade-offs. Removing the hydrogen without losing too much product acetone is the main challenge. Losses can occur in both the absorber off-gas and the column vent. Raising absorber pressure decreases off-gas losses but increases vent losses. Raising absorber pressure has several other effects. It raises the vaporizer pressure, which raises the required temperature and cost of the vaporizer heat source. It adversely affects kinetics because the reaction is nonequimolar and conversion decreases

*Principles and Case Studies of Simultaneous Design*, First Edition. William L. Luyben

with increasing pressure. A higher reactor temperature is required to achieve the desired conversion.

In this chapter, we develop the economically optimum design considering capital costs, energy costs, and raw material costs, and then develop a plantwide control structure capable of effectively handling large disturbances in production rate.

## 6.1 PROCESS DESCRIPTION

Figure 6.1 shows the acetone process described in Turton et al.[1] The authors provide a good description of the basic units in the process with equipment sizes and operating conditions. Their intent is not to determine the optimum design but to illustrate a typical multiunit chemical process that features a reaction section coupled with a separation section and connected by a recycle stream.

The fresh feed contains 34.81 kmol/h of IPA. Notice that the absorber is operated at low pressure (1.5 atm), which results in a loss of acetone in the off-gas of 2.52 kmol/h (7.2% loss). The acetone lost in the vent stream from the first distillation column reflux drum is small (0.0335 kmol/h) because there is very little hydrogen in the column feed at the low operating pressure in the flash drum and absorber.

We will consider in Section 6.3 a revised flowsheet in which the absorber pressure is raised to reduce off-gas acetone losses. However, higher pressure increases dissolved hydrogen in the column feed and results in larger losses of acetone in the vent stream.

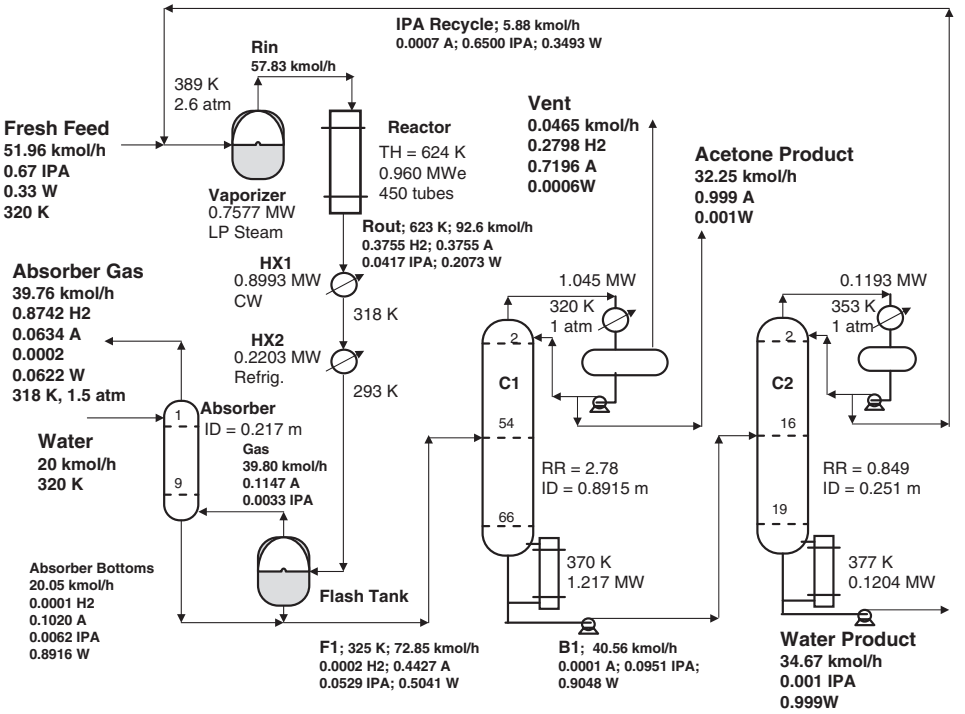


**Figure 6.1.** Turton et al. design.

### 6.1.1 Reaction Kinetics

The production of acetone involves the dehydrogenation of IPA in a high-temperature gas-phase reactor.

$$(CH_3)_2CHOH \rightarrow (CH_3)_2CO + H_2 \tag{6.1}$$

Turton et al.[1] assumed the reaction to be irreversible and specified that the per-pass conversion of IPA is 90% to prevent side reactions. The reaction occurs in the vapor phase in the presence of a solid catalyst (assumed to have 0.5 void fraction and a 2000 $kg/m^3$ solid density).

Using the reactor size and kinetics given in Turton et al. gives the 90% conversion specified by the authors if the presence of the solid catalyst is neglected. Of course, the catalyst is present, so a bigger reactor would have to be used to give the same conversion.

The kinetics used by Turton et al. are also unrealistic in that the reaction cannot be irreversible. If it were irreversible, we could operate at high pressure, which would raise the concentration of IPA and drive the reaction toward the products. But Le Châtelier's principle tells us that raising pressure should drive the reaction toward the reactant since there are two moles of product generated from one mole of reactant.

In an attempt to modify the kinetics so as to capture these realistic effects, an RGIBBS reactor was run in Aspen Plus to find the effect of pressure on conversion. At 623 K (the temperature in the Turton flowsheet), the RGIBBS equilibrium conversion is 97.1% at 2 atm. This should be compared with the 90% conversion in the Turton design. As pressures are raised to 5, 10, and 15 atm, the equilibrium conversions decrease to 93.3%, 87.8%, and 83.2%, respectively. Clearly, the effect of pressure must be considered.

The kinetics were modified to assume a reversible reaction, as shown in Eq. (6.2).

$$(CH_3)_2CHOH \Leftrightarrow (CH_3)_2CO + H_2 \tag{6.2}$$

The forward and reverse overall reaction rates are given in Eq. (6.3), with units of kmol $s^{-1}$ $m^{-3}$.

$$\begin{aligned} \Re_F &= C_{IPA} k_F e^{-72{,}380/RT} \\ \Re_R &= C_{acetone} C_{H2} k_R e^{-9480/RT} \end{aligned} \tag{6.3}$$

The activation energy of the forward reaction used is the value given in Turton et al. (72,380 kJ/kmol). The activation energy of the reverse reaction was calculated using the heat of reaction (+62,900 kJ/kmol).

$$\lambda = E_F - E_R \tag{6.4}$$

An empirical trial-and-error procedure was employed to find the unknown values of the preexponential factors $k_F$ and $k_R$ that satisfied two conditions. First, they should give approximately the same pressure dependence of conversion in a large tubular reactor as predicted by RGIBBS. Second, they should give a 90% conversion when used in the Turton tubular reactor (including the presence of catalyst). Table 6.1 shows the parameters used in the rest of this study. To be consistent with the assumption made by Turton, the conversion in the reactor is held at 90% as other design parameters are changed.

**TABLE 6.1 Reaction Kinetics**

| | Turton | Modified Reversible | |
|---|---|---|---|
| | Irreversible | Forward | Reverse |
| $k$ | $3.51 \times 10^5$ | $22 \times 10^6$ | 1,000 |
| $E$ (kJ/kmol) | 72,380 | 72,380 | 9,480 |
| Concentration terms (kmol/m$^3$) | $C_{IPA}$ | $C_{IPA}$ | $C_{acetone}C_{H2}$ |

### 6.1.2 Phase Equilibrium

Two phase equilibrium features dominate the separations required in this process. The first is the high volatility of hydrogen compared to the other components. After the mixture leaving the reactor is cooled, it is flashed in the separator. Most of the hydrogen goes into the gas stream, but a small amount is dissolved in the liquid. This hydrogen ends up in the condenser of the first distillation column and would require a very low temperature to condense. Therefore a small vent stream is removed from the top of the reflux drum. Any acetone in this vent stream is lost and only has fuel value.

The second important phase equilibrium feature is the existence of an azeotrope in the IPA/water system. The normal boiling points of IPA and water are 355.4 and 373 K, respectively. The azeotrope contains 67.32 mol% IPA at 1 atm and 353.4 K. Figure 6.2 gives the *Txy* and *xy* diagrams for IPA/water at atmospheric pressure. UNIQUAC physical properties are used in the Aspen simulations. The existence of the azeotrope means that the IPA that is unconverted in the reactor and recycled from the top of the second distillation column will have a composition close to the azeotropic composition. The separation is fairly easy, so the column will not require many trays and can run with a low reflux ratio (RR).

The normal boiling point of acetone is 329.4 K, so it is the low boiler in the system, if hydrogen is disregarded. Figure 6.3 gives the *Txy* and *xy* diagrams for acetone and water at atmospheric pressure. There is no azeotrope, but there is a pinch at the high acetone end of the diagrams. This means that producing high-purity acetone will require a column with many trays and a fairly high RR.

Figure 6.4 shows the ternary diagram for the acetone/IPA/water system at 1 atm. There are two distillation regions. The feed to the first distillation column lies in the lower region. The residue curves indicate that a high-purity acetone can be produced in the distillate, and the bottoms will be a mixture of mostly IPA and water. The location of the feed, distillate, and bottoms stream compositions for the first distillation are shown and lie on a straight line.

Figure 6.4 also gives results from the Aspen Conceptual Design program. The feed composition is specified at 44.3 mol% acetone, 5.3 mol% IPA, and 50.4 mol% water. The three compositions specified are $x_{D(W)} = 0.001$, $x_{D(IPA)} = 0.000001$ and $x_{B(A)} = 0.0001$. Setting the RR at 3.9 produces a column with 50 stages feeding on stage 45. These results are similar to those of the Turton design.

## 6.2 TURTON FLOWSHEET

Figure 6.1 shows the flowsheet of the process with the equipment sizes and conditions presented by Turton et al.[1] The fresh liquid feed is 51.96 kmol/h of a mixture that is 67 mol% IPA and 33 mol% water.

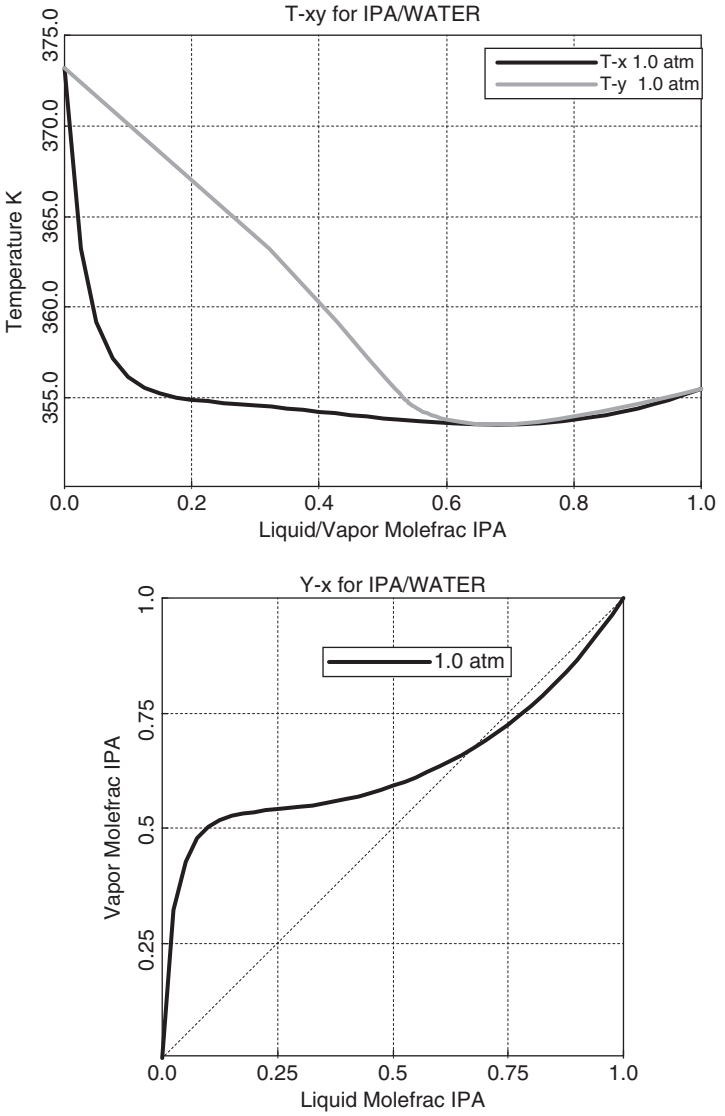


**Figure 6.2.** VLE for IPA/Water at 1 atm.

### 6.2.1 Vaporizer

The fresh feed is fed into a vaporizer along with 5.88 kmol/h of a recycle stream that is 65 mol% IPA and 35 mol% water. The vaporizer operates at 2.6 atm and 389 K in this design because the absorber downstream is operated at low pressure (1.5 atm). Low-pressure steam at 433 K can be used as the heat source in the vaporizer with a cost of \$7.78/GJ.

If the pressure in the absorber is raised to improve acetone recovery, the pressure and temperature in the vaporizer will increase. At higher pressures, the vaporizer will have to use more expensive medium-pressure steam (457 K at \$8.22/GJ) or high-pressure steam (527 K at \$9.83/GJ). These alternate operating conditions are considered in the next section.

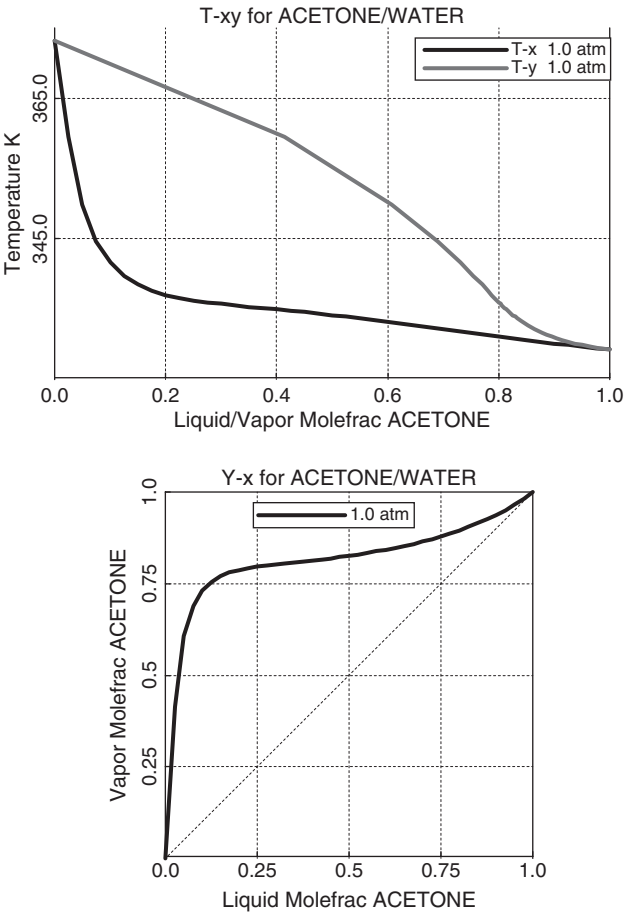


**Figure 6.3.** VLE for Acetone/Water at 1 atm.

### 6.2.2 Reactor

The vapor stream is fed into a tubular reactor containing 450 tubes, 0.0504 m in diameter and 6.096 m in length. The endothermic heat of reaction is provided by a hot molten salt heating medium at 624 K. The heat duty is 0.960 MW, which is assumed to be provided by a fired furnace at a price of \$9.83/GJ. The catalyst in the reactor tube has a void fraction of 0.5 and a solid density of 2000 $kg/m^3$.

The heat-transfer coefficient in the reactor is 60 $W\ m^{-2}\ K^{-1}$. Temperatures in the reactor vary with length. Figure 6.5 shows the reactor temperature profile. Reactor exit temperature is 623 K. Since the reaction is endothermic, the higher the temperature, the larger the chemical equilibrium constant. As we will see in the next section, if reactor pressure is increased, which drives the reaction toward the reactant, the reactor temperature must be increased to maintain the same conversion.

### 6.2.3 Heat Exchangers, Flash Tank, and Absorber

The hot reactor effluent is cooled with cooling water to 318 K and then cooled to 293 K using refrigeration. A low temperature helps to reduce the loss of acetone in the gas stream leaving

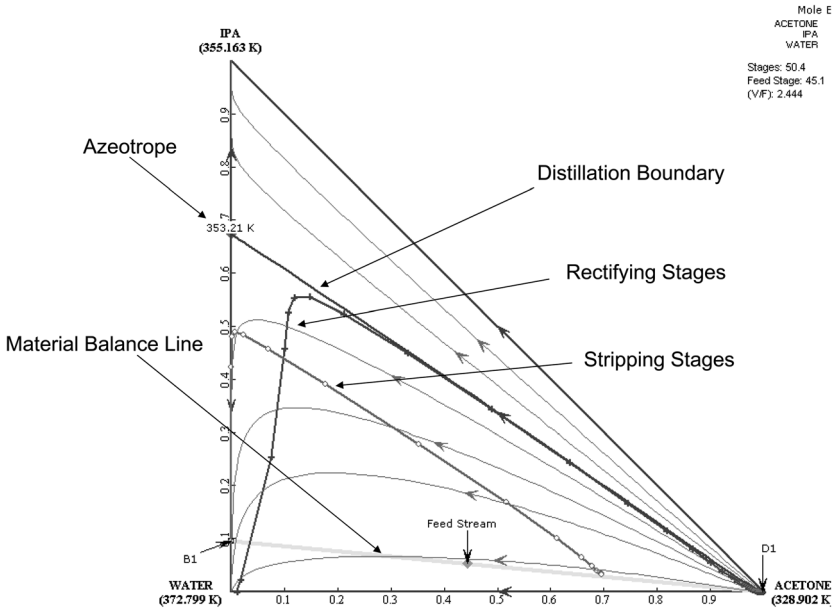


**Figure 6.4.** Ternary diagram for acetone/IPA/water.

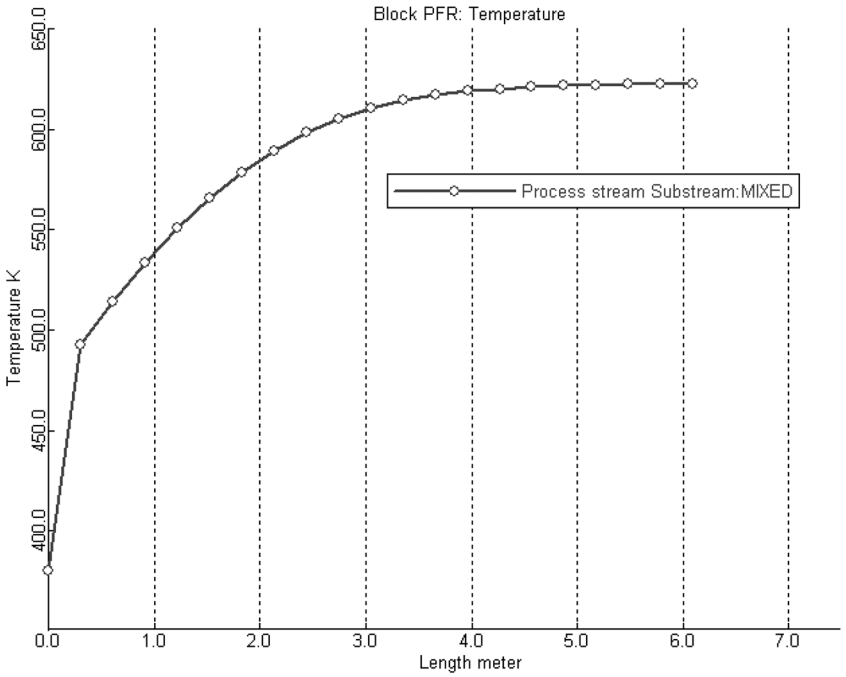


**Figure 6.5.** Turton et al. reactor temperature profile.

the flash tank and, subsequently, in the absorber off-gas. But refrigeration is much more expensive than cooling water. If the absorber and flash tank were run at higher pressure, refrigeration would not be required. The refrigeration load is 0.22 MW at a cost of \$4.43/GJ at this temperature level.

The two-phase mixture from the partial condenser is sent to a flash drum. The vapor stream is fed into the bottom of a 10-stage absorber. Water is fed on the top tray at 20 kmol/h and 320 K. The off-gas from the absorber is mostly hydrogen, but 2.52 kmol/h of acetone are lost in this stream (39.76 kmol/h with 6.34 mol% acetone). The diameter of the absorber is 0.217 m.

The liquid from the flash tank and the liquid from the base of the absorber are fed to the first distillation column. They both are mixtures of acetone, IPA, and water with a small amount of dissolved hydrogen (0.02 mol% $H_2$ in the flash-tank liquid and 0.01 mol% $H_2$ in the absorber bottoms). This hydrogen goes overhead in the first distillation column and will blanket the condenser unless vented off. With the low-pressure operation of the flash tank and absorber, the acetone lost in the vent stream is quite low (0.0335 kmol/h of acetone). Raising the pressure in the flash tank and absorber will decrease the acetone losses in the absorber off-gas but increase the acetone losses in the column vent.

### 6.2.4 Acetone Column C1

The column in the Turton design has 67 stages and is fed on stage 54, which is the optimum feed stage to minimize reboiler heat input. The operating pressure is 1 atm, which gives a reflux-drum temperature of 320 K so cooling water can be used in the condenser. The RR required to achieve the design specification of 99.9 mol% acetone is 2.78. The specification for the bottoms is 0.01 mol% acetone impurity. The column diameter is 0.8915 m and the reboiler heat input is 1.217 MW.

### 6.2.5 Water Column C2

The column has 20 stages and is fed on stage 16. The operating pressure is 1 atm, which gives a reflux-drum temperature of 353 K. The RR is low (RR = 0.849). Energy consumption 0.120 MW, and the column diameter is 0.251 m. The design specifications are 0.1 mol% IPA in the bottoms (the water product) and 65 mol% IPA in the distillate (reasonably close to the azeotropic composition).

## 6.3 REVISED FLOWSHEET

The design discussed in the previous section has not been optimized from the standpoint of economics. The loss of acetone is quite high. Refrigeration is required in one heat exchanger. An obvious parameter to vary is the absorber pressure. Figure 6.6 gives the revised flowsheet for a design in which the absorber pressure is raised to 17 atm.

### 6.3.1 Effect of Absorber Pressure

As previously mentioned, raising absorber pressure should reduce acetone losses in the absorber off-gas. But it will raise the pressure in the reactor, which adversely affects conversion. In order to keep conversion at 90%, reactor temperatures will have to be increased. There may be a maximum temperature limitation due to loss of catalyst activity. Howard[2]

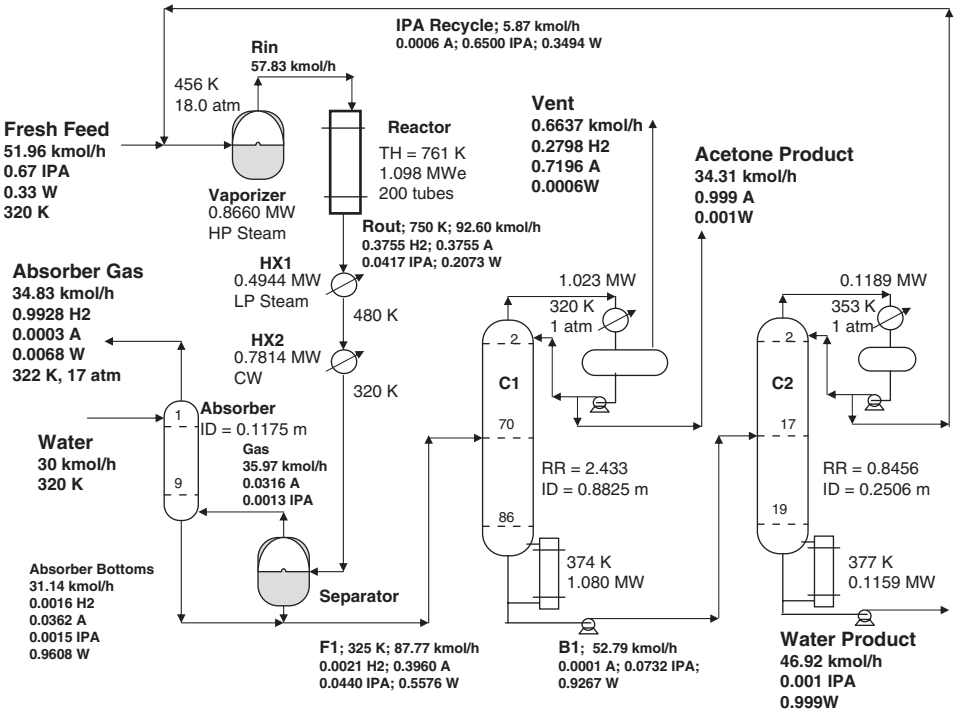


**Figure 6.6.** 17-atm design.

gives a typical reactor operating temperature of 673 to 773 K, so we will assume that the temperature of the hot medium heating the reactor cannot be higher than 760 K. Notice that the temperature of the heating medium in the Turton design is 624 K, which is far below this limitation.

Raising absorber pressure will also raise the pressure and temperature in the vaporizer, which means a higher-temperature, more expensive energy source must be used. On the other hand, a higher pressure in the absorber should mean some steam can be generated from the hot reactor effluent. In addition, cooling water instead of refrigeration can be used in the condenser because a low temperature is not required at the higher pressure.

Table 6.2 shows the effects of absorber pressure on a number of parameters. As absorber pressure increases, the acetone losses in the absorber off-gas decrease, but the acetone losses in the distillation column reflux-drum vent increase. The minimum total loss occurs at an absorber pressure of 17 atm.

At this pressure, the vaporizer temperature has increased to 456 K from the Turton design of 389 K. Low-pressure steam at 433 K can be used in the Turton design, in which the heat duty in the vaporizer is 0.7577 MW. High-pressure steam at 527 K must be used in the 17-atm design, in which the heat duty is 0.866 MW. Low-pressure steam costs \$7.78/GJ. High-pressure steam costs \$9.83/GJ. Therefore, vaporizer energy cost is higher in the 17-atm design.

However, low-pressure steam can be generated in the first heat exchanger by the hot gases leaving the reactor instead of wasting the heat by using cooling water. The heat duty in this steam generator is 0.4944 MW, which constitutes an energy credit. In addition, refrigeration

**TABLE 6.2 Effect of Absorber Pressure[a]**

| Absorber Pressure (atm) | Off-Gas Acetone Loss (kmol/h) | Vent Acetone Loss (kmol/h) | Total Acetone Loss (kmol/h) | Vaporizer Temperature (K) | Reactor Heating Medium Temperature (K) |
|---|---|---|---|---|---|
| 5 | 2.336 | 0.1033 | 2.469 | 409 | 676 |
| 7 | 1.270 | 0.1953 | 1.465 | 420 | 695 |
| 9 | 0.7679 | 0.2152 | 0.9831 | 429 | 710 |
| 11 | 0.4858 | 0.2711 | 0.7569 | 437 | 723 |
| 13 | 0.3110 | 0.3269 | 0.6487 | 444 | 734 |
| 15 | 0.1990 | 0.3826 | 0.5816 | 450 | 743 |
| 17 | 0.1241 | 0.4383 | **0.5624** | 456 | 752 |
| 19 | 0.0745 | 0.4938 | 0.5683 | 461 | 760 |
| 21 | 0.0422 | 0.5493 | 0.5915 | 466 | 767 |

[a]Water flowrate = 20 kmol/h; 300 reactor tubes.

is not needed in the second heat exchanger. The Turton design requires 0.2203 MW of refrigeration at a cost of \$4.2/GJ.

Increasing absorber pressure also requires an increase in reactor temperature to maintain the desired 90% per-pass conversion of IPA. Reactor energy consumption increases from 0.960 MW in the Turton design to 1.098 MW in the 17-atm design. An energy cost of \$9.83/GJ is assumed in all designs.

The higher reactor temperatures require an increase in the temperature of the heating medium in the reactor. If there is a maximum catalyst temperature constraint, this may impose a constraint on the maximum absorber pressure. In the Turton design, the temperature of the heating medium is 624 K. In the 17-atm design, the temperature of the heating medium is 761 K. Literature values of operating temperature indicate a range from 673 to 773 K, so the 17-atm design falls under this limit (see Howard[2]).

### 6.3.2 Effect of Water Solvent and Absorber Stages

The two design optimization parameters in the absorber are the flowrate of the water and the number of stages. Very little improvement in acetone recovery was observed by increasing the number of stages above 10.

Increasing the water flowrate should recover more acetone, but it may increase vent losses and increase heat duties in the distillation column. More water consumption will increase water procurement costs, but process water is very inexpensive (\$0.067/1000 kg). A flowrate of 30 kmol/h corresponds to a water bill of only \$317/yr.

Table 6.3 shows the effect of water flowrate on acetone losses and reboiler heat duties. Acetone loss is minimized using 30 kmol/h of water in the absorber. There is a very small 2% increase in reboiler duty in the first distillation column in going from 20 to 30 kmol/h. Reboiler duty in the second column is essentially constant.

### 6.3.3 Effect of Reactor Size

The final design optimization variable in the reaction section of the process is reactor size. Since conversion in the reactor is fixed at 90% and reactor pressure is fixed at 17.5 atm by the absorber pressure of 17 atm, the required reactor temperature does not change as the

**TABLE 6.3 Effect of Absorber Water**[a]

| Absorber Water (kmol/h) | Off-Gas Acetone Loss (kmol/h) | Vent Acetone Loss (kmol/h) | Total Acetone Loss (kmol/h) | Reboiler Duty C1 (MW) | Reboiler Duty C2 (MW) |
|---|---|---|---|---|---|
| 20 | 0.1241 | 0.4383 | 0.5624 | 1.066 | 0.1158 |
| 25 | 0.0522 | 0.4581 | 0.5103 | 1.073 | 0.1158 |
| 28 | 0.0225 | 0.4698 | 0.4923 | 1.078 | 0.1158 |
| 30 | 0.0103 | 0.4776 | **0.4879**[b] | 1.080 | 0.1159 |
| 32 | 0.0040 | 0.4854 | 0.4894 | 1.083 | 0.1159 |
| 35 | 0.0008 | 0.4970 | 0.4978 | 1.088 | 0.1160 |

[a]Absorber pressure = 17 atm; 300 reactor tubes.
[b]Minimum acetone losses.

number of tubes is changed. The required heat duty also does not change. So the only thing that increases as the number of tubes is decreased is the temperature of the heating medium. Since high-temperature energy is assumed to be used in providing this heat (fired furnace), the temperature level does not affect energy cost.

However, it does affect the wall temperatures in the reactor, which could affect catalyst activity if a high temperature limitation exists. The literature suggests a limit of 773 K (see Howard[2]).

Using 300, 250, 200, 150, and 100 tubes in the reactor gives heating medium temperatures of 752, 754, 761, 778, and 826 K, respectively. Therefore, a reactor with 200 tubes is selected to be well under the maximum catalyst temperature limitation. The capital cost of the reactor in the Turton design with 450 tubes is $378,000. The capital cost of the 200-tube reactor is $223,000.

Reactor temperature and composition profiles are given in Figure 6.7.

### 6.3.4 Optimum Distillation Design

The number of trays in the distillation columns in the 17-atm design were determined to produce the minimum total annual cost (TAC). Capital and energy costs were calculated for a range of number of stages. Table 6.4 presents these results.

The optimum number of stages in the first column (C1) was found to be 87, which is 20 more than in the Turton design. The optimum number of stages in the second column (C2) was found to be 20, which is the same as in the Turton design.

Temperature profiles for both columns are given in Figure 6.8.

## 6.4 ECONOMIC COMPARISON

The basis for the economic and sizing calculations have been discussed in Chapter 5 and are taken from Turton et al.[1] and Douglas[3]. Table 6.5 summarizes this information.

Table 6.6 gives detailed information on equipment size, energy consumption, and capital investment for the Turton and 17-atm designs. Figure 6.1 gives the Turton flowsheet. Figure 6.6 gives the 17-atm flowsheet.

The first column in Table 6.6 gives economic results for the original Turton design. Total capital investment is $1,764,000. The total energy cost is $842,000/yr (energy consumption in columns, reactor, refrigerated condenser, and vaporizer).

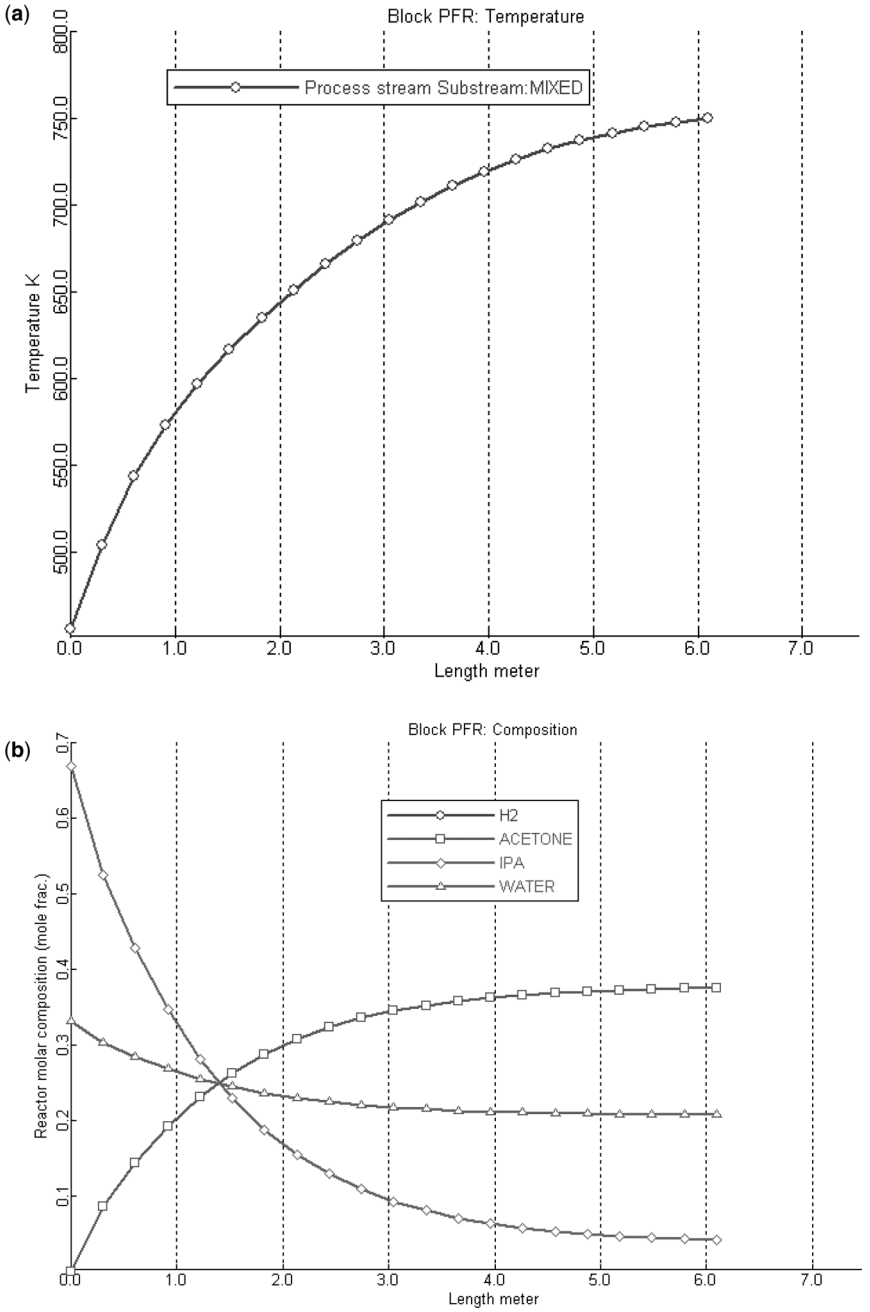


**Figure 6.7.** (a) Reactor temperature profile for 17-atm design. (b) Reactor composition profiles for 17-atm design.

The second column in Table 6.6 gives economic results for the case where the pressure in the absorber is raised to 17 atm. Total capital investment is $1,415,000. The total energy cost is $780,000/yr (energy consumption in columns, reactor, and vaporizer with an energy credit for low-pressure steam generated).

**TABLE 6.4 Optimum Distillation Column Design**

| | | | | |
|---|---|---|---|---|
| Column C1 | | | | |
| NT | 67 | 77 | 87 | 97 |
| ID ($m^2$) | 0.932 | 0.905 | 0.8847 | 0.868 |
| $Q_{R1}$ (MW) | 1.188 | 1.128 | 1.085 | 1.050 |
| $Q_{C1}$ (MW) | 1.135 | 1.072 | 1.027 | 0.9893 |
| TAC ($10^6$ \$/yr) | 0.5075 | 0.5014 | **0.4996**[a] | 0.5001 |
| Column C2 | | | | |
| NT | 15 | 20 | 25 | |
| ID ($m^2$) | 0.262 | 0.2505 | 0.2465 | |
| $Q_{R1}$ (MW) | 0.1255 | 0.1159 | 0.1133 | |
| $Q_{C1}$ (MW) | 0.1298 | 0.1189 | 0.1150 | |
| TAC ($10^6$ \$/yr) | 0.05546 | **0.05461**[a] | 0.05606 | |

[a]Minimum TAC.

In addition to these favorable energy and capital investment numbers, the 17-atm design produces 34.31 kmol/h of acetone product, compared to the 32.25 kmol/h produced in the Turton flowsheet. Using an acetone price of \$0.50/lb, the increase in annual product sales is \$1,150,000.

Raising the absorber pressure provides a much more economically attractive design. Capital investment and energy consumption are lower, and product yield is increased.

## 6.5 PLANTWIDE CONTROL

The steady-state Aspen Plus model shown in Figure 6.6 does not include pumps and control valves. The first step in studying dynamics using a pressure-driven dynamic simulation is to add these items and to determine the volumes of all vessels. The units with dynamics include the vaporizer, the reactor, the flash drum, the absorber, and the two distillation columns. Of course, the size of the reactor is known from the steady-state design. The other units are sized to provide 5 min of liquid holdup at the 50% level. The units with liquid surge capacity are the reflux drums and column bases in the distillation columns, the vaporizer, the absorber base, and the flash tank. The reactor is simulated as a tubular reactor with a constant-temperature heating medium. The distillation columns and the absorber are simulated using the Aspen *Radfrac* model. Heat exchangers are simulated using the Aspen *Heater* model. The vaporizer and flash tank are simulated using the Aspen *Flash2* model.

### 6.5.1 Control Structure

Figure 6.9 shows the plantwide control structure developed for this process using plantwide process control methodology (see Luyben et al.[4]). Conventional PI controllers are used in all loops. The various loops are listed below with their controlled and manipulated variables.

1. Fresh feed of the mixture of IPA and water is flow controlled. This is the throughput handle.
2. Vaporizer level is controlled by vaporizer heat input. There is no liquid outlet stream.
3. Reactor outlet temperature is controlled by the temperature of the molten salt.
4. The temperature of the stream leaving the steam generator is controlled by manipulating the generation rate of low-pressure steam.

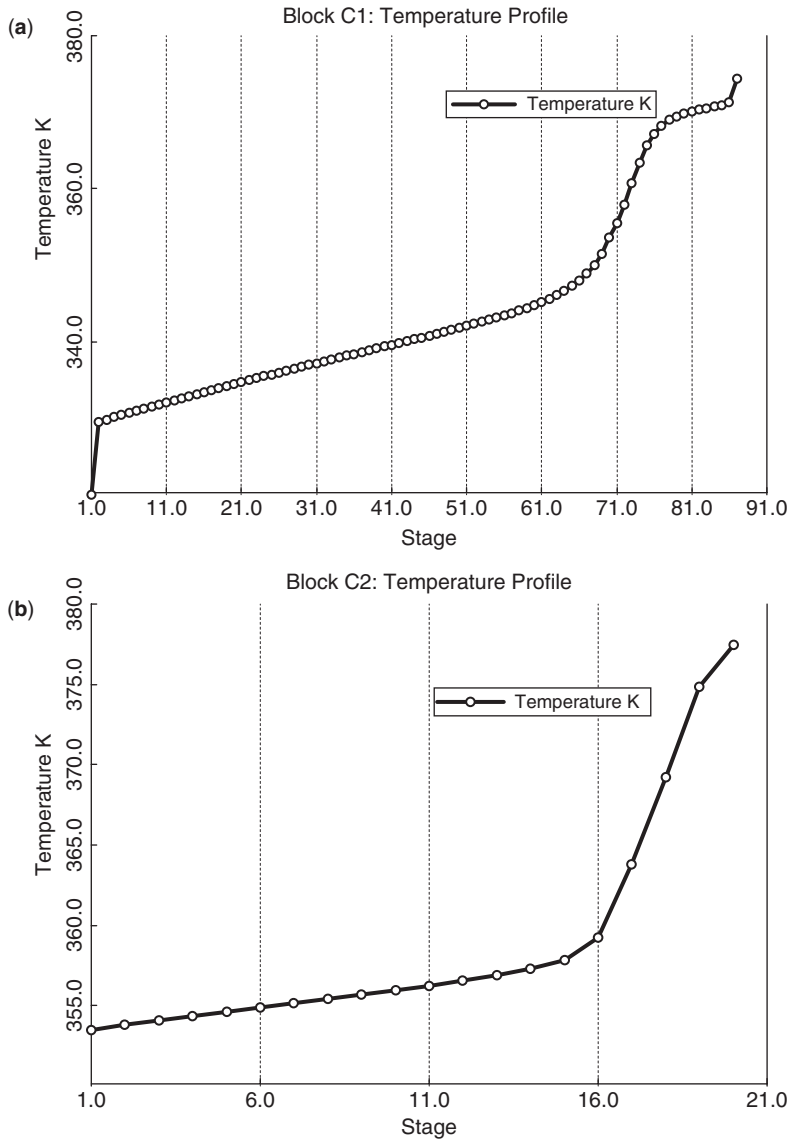


**Figure 6.8.** (a) Column C1 temperature profile. (b) Column C2 temperature profile.

5. The temperature of the stream leaving the condenser is controlled by manipulating the flowrate of cooling water.
6. The liquid level in the flash tank is controlled by manipulating the liquid leaving the bottom of the vessel.
7. The pressure in the absorber is controlled by manipulating the flowrate of the off-gas. This holds the pressure in the system all the way back to the vaporizer.
8. The liquid level in the base of the absorber is controlled by manipulating the liquid leaving the bottom of the absorber.

**TABLE 6.5 Basis of Economics and Equipment Sizing**

Column diameter: Aspen tray sizing
Column length: NT trays with 2-ft spacing plus 20% extra length
Column vessel (diameter and length in meters)
Capital cost = 17,640 $(D)^{1.066}$ $(L)^{0.802}$

*Condensers (area in $m^2$)*
Heat-transfer coefficient = 0.852 kW/K-$m^2$
Differential temperature = reflux-drum temperature − 310 K
Capital cost = 7296 $(A)^{0.65}$

*Reboilers (area in $m^2$)*
Heat-transfer coefficient = 0.568 kW/K − $m^2$
Differential temperature = 403 K − base temperature
Capital cost = 7296 $(A)^{0.65}$

*Reactor (heated)*
Heat-transfer coefficient = 60 W K-$m^2$
Differential temperature = $T_H - T_R(z)$
Capital cost = 7296 $(A)^{0.65}$

*Vaporizer (area in $m^2$):*
Heat-transfer coefficient = 0.568 kW/K-$m^2$
Differential temperature = $T_S - T_{vaporizer}$
Capital cost = 7296 $(A)^{0.65}$

*Flash tank (diameter and length in meters)*
Capital cost = 17,640 $(D)^{1.066}$ $(L)^{0.802}$

*Absorber (diameter and length in meters)*
Diameter: Aspen tray sizing
Length: NT trays with 2 ft spacing plus 20% extra length
Vessel (diameter and length in meters)
Capital cost = 17,640 $(D)^{1.066}$ $(L)^{0.802}$

*Energy costs*
Fired furnace = \$9.83/GJ
HP steam = \$9.83/GJ
MP steam = \$8.22/GJ
LP steam = \$7.78/GJ
Refrigeration = \$4.42/GJ

$$\text{TAC} = \frac{\text{Capital cost}}{\text{Payback period}} + \text{Energy cost}$$

Payback period = 3 yr

9. The flowrate of water to the top of the absorber is ratioed to the gas feed coming into the absorber from the flash tank.
10. Pressures in the two distillation columns are controlled by condenser heat removals.
11. Base levels in the distillation columns are controlled by bottoms flowrates.
12. Reflux drum level in the first column is controlled by manipulating reflux flowrate because of the fairly high RR.

**TABLE 6.6 Economic Comparison**

| | | Turton Design | 17-atm Design |
|---|---|---|---|
| Absorber pressure | atm | 1.5 | 17.0 |
| Reactor tubes | — | 450 | 200 |
| Reactor area | $m^2$ | 434 | 193 |
| Reactor capital investment | $10^6$ $ | 0.3782 | 0.2232 |
| Reactor energy (fired furnace) | MW | 0.960 | 1.098 |
| Reactor energy cost | $10^6$ $/yr | 0.2976 | 0.3398 |
| HX1 energy | MW | 0.8993 | 0.4944 |
| HX1 area | $m^2$ | 11.3 | 20.6 |
| HX1 capital investment | $10^6$ $ | 0.0353 | 0.0521 |
| HX1 energy credit (LP steam) | $10^6$ $/yr | — | 0.1213 |
| Vaporizer energy | MW | 0.7577 | 0.866 |
| Vaporizer area | $m^2$ | 73.0 | 34.8 |
| Vaporizer capital investment | $10^6$ $ | 0.1185 (LP steam) | 0.07335 (HP steam) |
| Vaporizer energy cost | $10^6$ $/yr | 0.1859 | 0.2685 |
| Condenser energy | MW | 0.2203 | 0.7814 |
| Condenser area | $m^2$ | 12.66 | 14.72 |
| Condenser capital investment | $10^6$ $ | 0.0380 | 0.0419 |
| Condenser energy cost | $10^6$ $/yr | 0.0307 (refrigeration) | — |
| Separator capital investment | $10^6$ $ | 0.0146 | 0.0158 |
| Absorber capital investment | $10^6$ $ | 0.0171 | 0.00888 |
| C1 area reboiler | $m^2$ | 64.9 | 65.6 |
| C1 area condenser | $m^2$ | 123 | 120 |
| C1 HX capital investment | $10^6$ $ | 0.276 | 0.274 |
| C1 shell capital investment | $10^6$ $ | 0.428 | 0.424 |
| C1 energy cost | $10^6$ $/yr | 0.2086 | 0.2650 |
| C2 area reboiler | $m^2$ | 8.31 | 8.00 |
| C2 area condenser | $m^2$ | 4.18 | 4.17 |
| C2 HX capital investment | $10^6$ $ | 0.0474 | 0.0466 |
| C2 shell capital investment | $10^6$ $ | 0.0319 | 0.0319 |
| C2 energy cost | $10^6$ $/yr | 0.0205 | 0.0284 |
| Total capital | $10^6$ $ | 1.764 | 1.415 |
| Total energy | $10^6$ $/yr | 0.8420 | 0.7801 |
| TAC | $10^6$ $/yr | 1.430 | 1.252 |

13. Distillate flowrate in the first column is ratioed to reflux flowrate with the ratio being adjusted by a distillate composition controller.
14. The temperature on stage 75 in the first column is controlled by manipulating reboiler heat input.
15. The reflux drum level in the second column is controlled by manipulating the distillate flowrate.
16. The reflux flowrate in the second column is ratioed to the column feed.
17. The temperature on stage 17 in the second column is controlled by manipulating reboiler heat input.

Items 12, 13, and 16 require some discussion.

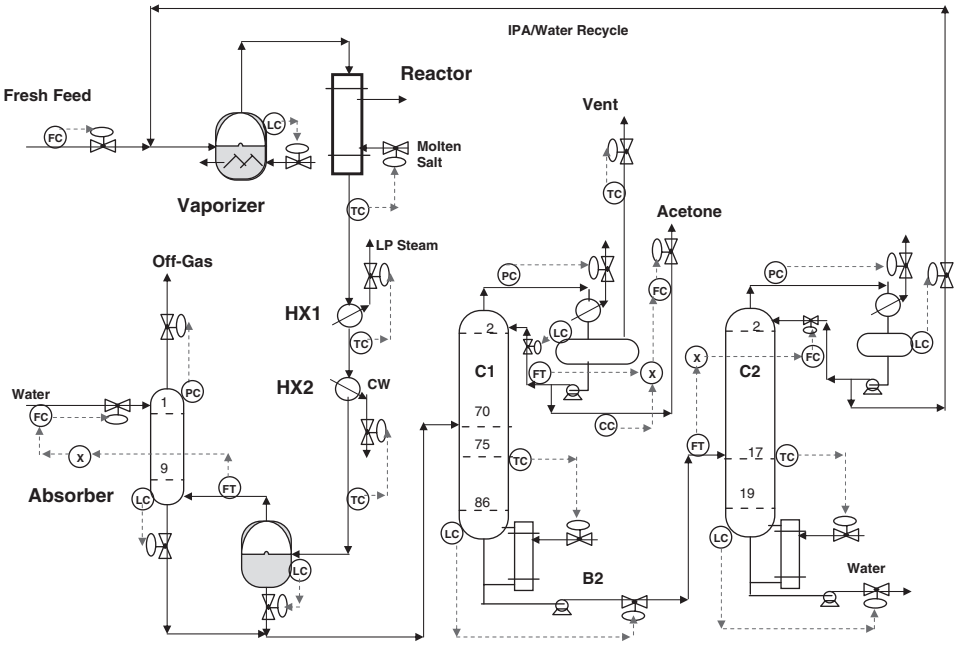


**Figure 6.9.** Plantwide control structure.

### 6.5.2 Column Control Structure Selection

Most distillation columns use some type of single-end temperature control for reasons of simplicity and low maintenance cost. However, this simple structure may not provide effective control for some columns. Even if a single-end control structure is possible, we have to decide how to select the other control degree of freedom. Normally there is a choice between holding a constant RR or holding a constant reflux-to-feed (R/F) ratio.

***Selecting Reflux Ratio or Reflux-to-Feed Ratio.*** To explore this question, a series of steady-state runs were made in which the effects of changes in feed composition on the required changes in R/F ratio and RR were determined while holding both products at their specified composition.

Table 6.7 gives results of these calculations for the two distillation columns. In the first distillation column (C1), the feed compositions of the light-key component acetone and the heavy-key component IPA are varied around the design point (39.6 mol% acetone and 4.40 mol% IPA). As more acetone and less IPA are fed to the column, the R/F ratio increases about 5%. On the other hand, the RR hardly changes at all. This indicates that a single-end control structure with a fixed RR may provide effective control.

In the second distillation column (C2), the feed compositions of the light-key component IPA and the heavy-key component water are varied around the design point (7.32 mol% IPA and 92.68 mol% water). The required changes in both the R/F ratio and the RR in this column are fairly large. Therefore a single-end structure may not be effective. However, the performance of this column is not as critical as that of the first column since the distillate is recycled and the loss of IPA in the bottoms is quite small. A R/F structure is used in

**TABLE 6.7 Column Control Structure Selection**

| | Feed Composition | Reflux-to-Feed Ratio | Reflux Ratio |
|---|---|---|---|
| C1 | 0.37602 Acetone<br>0.06401 IPA | 0.9222 | 2.436 |
| Design | 0.39602 Acetone<br>0.04401 IPA | 0.9696 | 2.433 |
| | 0.41602 Acetone<br>0.02401 IPA | 1.018 | 2.432 |
| C2 | 0.05317 IPA<br>0.94675 Water | 0.07986 | 0.9935 |
| | 0.06317 IPA<br>0.93675 Water | 0.08293 | 0.8658 |
| Design | 0.07317 IPA<br>0.92675 Water | 0.09407 | 0.8459 |
| | 0.08317 IPA<br>0.91675 Water | 0.1061 | 0.8383 |
| | 0.09317 IPA<br>0.90675 Water | 0.1185 | 0.8345 |

this column, and the results given in the next section indicate that this structure provides adequate control.

***Selecting Temperature Control Tray Location.*** Another important issue in control structure selection is the location of the tray used for temperature control. A simple approach that usually works quite well is to select a location where the temperatures are changing significantly from tray to tray. Looking at the temperature profile for the first column (C1) given in Figure 6.8a, we can see that there is a significant slope in the temperature profile near the base of the column. Stage 75 is selected for single-end temperature control with a fixed RR. Reboiler heat input is manipulated to control this tray temperature.

It is important to note that a high-purity acetone distillate product is required from this column. The purity of the bottoms is less important because any acetone that drops out the bottom will be go overhead in the next column and be recycled back to the reactor in the recycle stream. Conventional distillation control wisdom suggests that to achieve effective inferential composition control of the distillate by using a tray temperature, a tray near the top of the column should be controlled. However, the break in the temperature in this column is near the bottom. For this reason, single-end temperature control may not be effective in this application. We will demonstrate this problem in the next section and show that a composition controller is required to maintain high-purity acetone.

Looking at the temperature profile for the second column (C2) given in Figure 6.8b, we can see that there is a significant slope in the temperature profile near the base of the column. Stage 17 is selected for single-end temperature control with a fixed RR. Reboiler heat input is manipulated to control this tray temperature. Since the important objective in this column is to prevent loss of IPA out the bottoms low, a tray location near the bottom should be effective.

### 6.5.3 Dynamic Performance Results

All liquid level controllers are proportional only using $K_C = 2$. There is one exception to this level control tuning. A gain of 4 is used in the reflux-drum level controller in the second

column. The level sets the distillate, which is a recycle stream. Using a higher gain helps to speed up the overall dynamics of the recycle system. The required changes in the flowrate of the recycle stream occur more quickly with the higher gain, which helps to drive the overall process to its new steady state in less time.

Deadtimes of 3 min are used in the reactor exit temperature loop and in the composition loop. Deadtimes of 1 min are used in the column temperature loops. Temperature and composition loops are tuned using relay-feedback tests (as comprehensively described by Yu[5]) and Tyreus-Luyben tuning rules. Table 6.8 gives controller tuning parameters for the three major temperature loops and for the composition loop.

The initial control structure tested did not use the composition controller. The first column had a single temperature controller and a fixed RR. Figure 6.10 gives results for 20% increases (solid lines) and 20% decreases (dashed lines) in the fresh feed flowrate. Stable regulator control is achieved for these large disturbances.

However, as the third graph on the left shows, the impurity of water in the acetone distillate product from the first column ($x_{D1(w)}$) deviates significantly from the specified 0.1 mol% (on a relative basis).

Figure 6.11 gives results for the same disturbances with the composition controller in service. The composition controller adjusts the RR to drive distillate impurity to the specified value. Notice that the distillate-to-reflux ratio is increased as feed flowrate increases. This corresponds to a lower RR. Keep in mind that the stage 75 temperature controller is maintaining temperature, so this column has dual-end control.

The compositions of the bottoms and distillate products in the second column depart somewhat from their specifications, but as previously discussed, tight control of these streams is not vital.

An alternative to using dual-end control with a composition analyzer is to overpurify the acetone product so that it remains above the purity specifications despite disturbances. This would increase energy consumption in the first distillation column. For example, changing the water impurity level to 0.05 mol% would require an increase in the reboiler duty in the first column of 5.7%.

Figure 6.12 gives results for other disturbances using the dual-end structure. The solid lines are for a change in reactor exit temperature from 750 to 740 K. Reactor conversion is lower, so there is an increase in the recycle stream ($D_2$). More energy is required in the reboiler of the second column.

The dashed lines in Figure 6.12 are for a change in the absorber pressure from 17 to 15 atm. The second graph on the right shows that the composition of acetone in the absorber

**TABLE 6.8 Controller Parameters**

| | TCR | TC1 | TC2 | CC |
|---|---|---|---|---|
| SP | 750 K | 365.6 K | 363.8 K | 0.001 mole fraction water |
| Transmitter range | 700–800 K | 300–400 K | 300–400 K | 0–0.001858 mole fraction water |
| OP | 764.6 K | 258.2 kcal/s | 28.23 kcal/s | 0.40375 $D_2/R_2$ ratio |
| OP range | 700–800 K | 0–516 kcal/s | 0–55 kcal/s | 0–1 $D_2/R_2$ ratio |
| Deadtime | 3 min | 1 min | 1 min | 3 min |
| $K_C$ | 0.359 | 2.63 | 2.41 | 1.51 |
| $\tau_I$ | 14.6 min | 14.5 min | 10.6 min | 76.6 min |

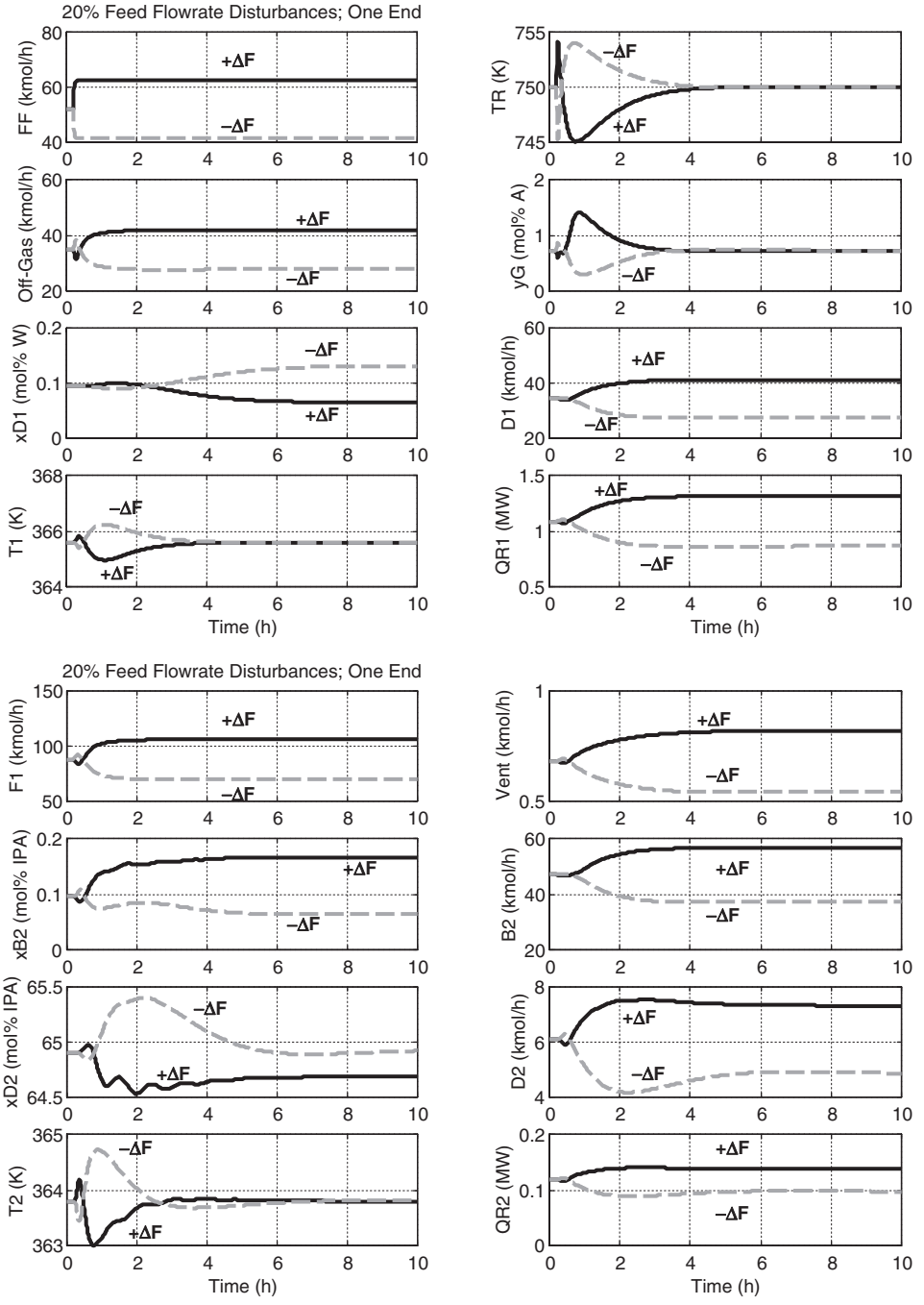


**Figure 6.10.** Feed flowrate disturbances with single-end temperature control.

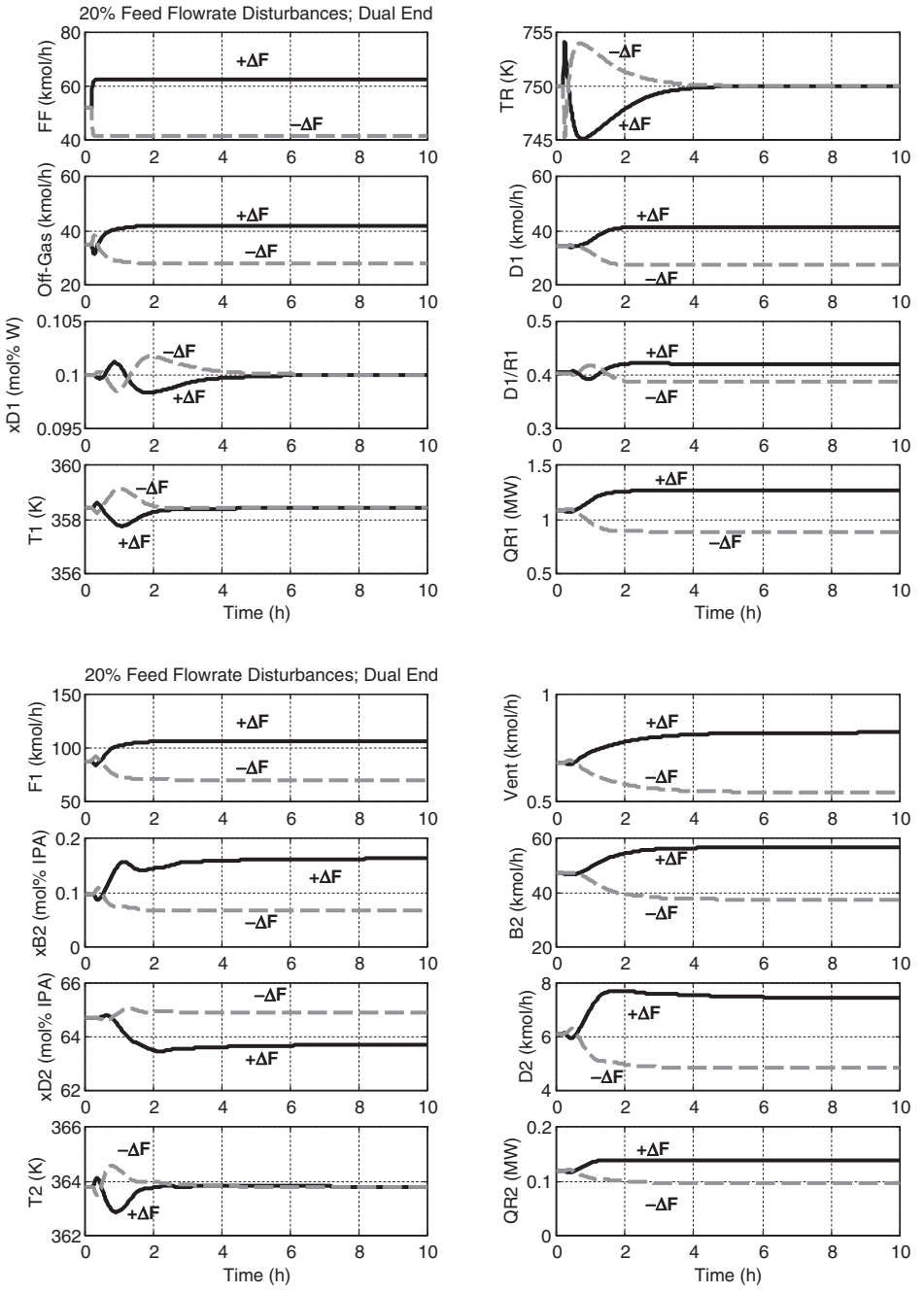


**Figure 6.11.** Feed flowrate disturbances with dual-end control.

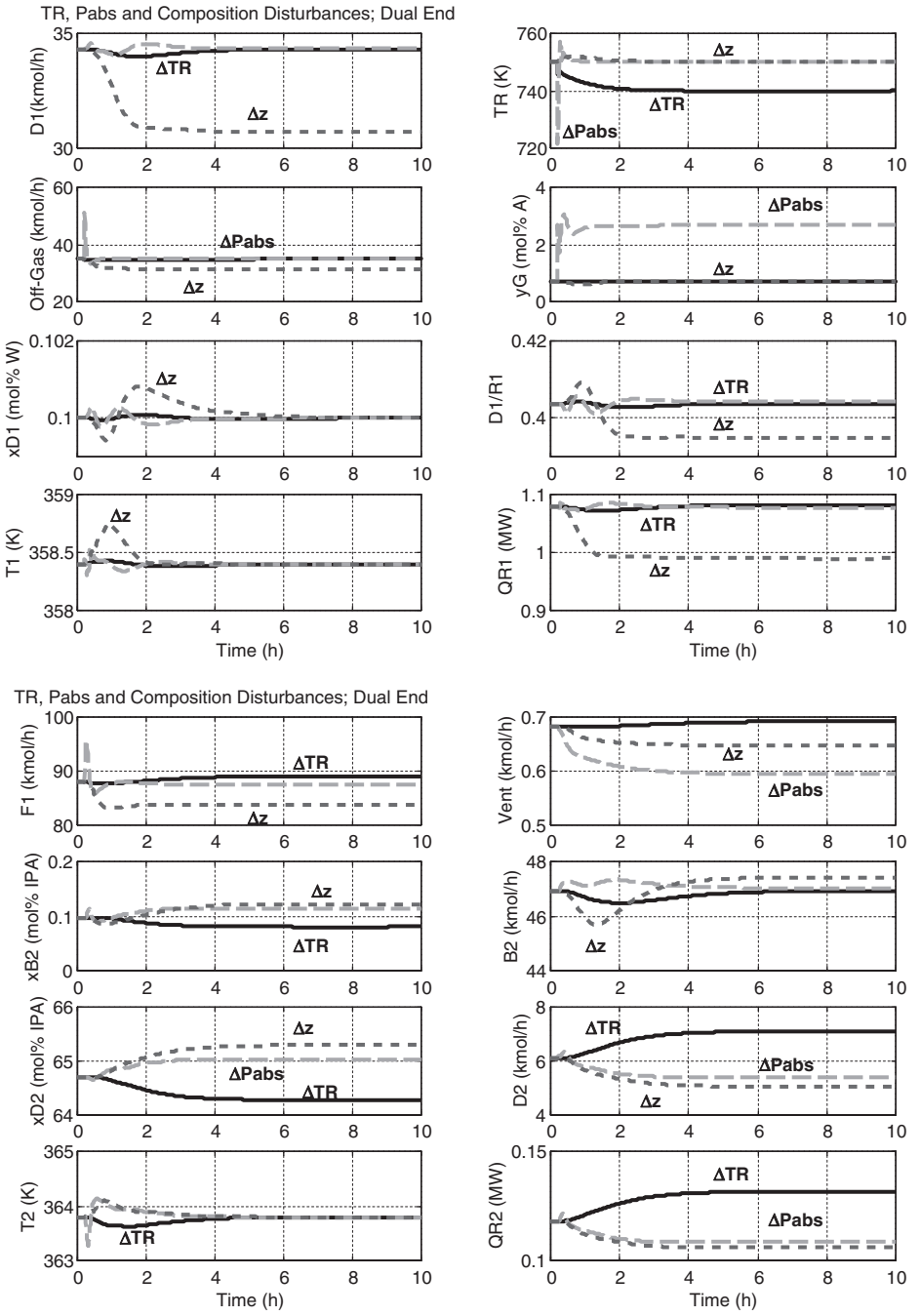


**Figure 6.12.** Disturbances in reactor temperature, absorber pressure, or feed composition.

off-gas yG increases from 0.66 mol% up to almost 3 mol%. The vent stream decreases from 0.66 kmol/h to about 0.60 kmol/h.

The dotted lines in Figure 6.12 are for a change in the fresh feed composition from 67 to 60 mol% IPA with a corresponding increase in water concentration. With less IPA fed, the production rate of acetone decreases ($D_1$), less energy is needed in the reboiler of the first column ($Q_{R1}$), and a higher RR is required in the first column (lower $D_1/R_1$ ratio).

The proposed dual-end control structure handles all these large disturbances quite well with the acetone product held close to its specified purity.

## 6.6 CONCLUSION

The acetone process illustrates a number of interesting design trade-offs. Effective removal of the very light hydrogen product, while minimizing loss of the acetone product, is the main feature of this process. There is an optimum absorber pressure that balances the opposing effects of pressure on losses in the absorber off-gas stream and losses in the distillation column vent stream. High pressure also adversely affects reaction kinetics, so reactor temperature must be increased as pressure is increased.

Effective dynamic control of the multiunit process is achieved by the use of conventional controllers. To insure close control of the high-purity acetone product, a dual-end control structure must be used. Large disturbances in throughput, feed composition, reactor temperature, and absorber pressure are well handled.

## REFERENCES

1. Turton, R., Bailie, R. C., Whiting, W. B., Shaelwitz, J. A. *Analysis, Synthesis and Design of Chemical Processes*, 2nd Edition, Prentice Hall, Englewood Cliffs, NJ, 2003.
2. Howard, W. L. Acetone, in *Kirk-Othmer Encyclopedia of Chemical Technology*, Vol. 1, John Wiley & Sons, 2001, p. 160.
3. Douglas, J. M. *Conceptual Design of Chemical Processes*, McGraw-Hill, New York, 1988.
4. Luyben, W. L., Tyreus, B. D., Luyben, M. L. *Plantwide Process Control*, McGraw-Hill, New York, 1999.
5. Yu, C. C. *Autotuning of PID Controllers*, 2nd Edition, Springer, London, 2006.

# CHAPTER 7

# DESIGN AND CONTROL OF AN AUTO-REFRIGERATED ALKYLATION PROCESS

The alkylation of $C_4$ olefins with isobutane to produce high octane $C_8$ components ("alkylate") is a very important process in many oil refineries. The Kellogg process uses a sulfuric acid catalyst in a series of agitated reactors that must operate at temperatures requiring refrigeration because high temperatures favor undesirable side reactions. The reactors are cooled by boiling the liquid in the reactor, compressing the vapor and condensing it, and returning the liquid back to the reactor. A large excess of isobutane, which requires a large recycle stream, is used to suppress undesirable reactions. Inert components (propane and *n*-butane) that enter in the fresh feed streams must be purged from the system. Two distillation columns are used, one of which has a vapor sidestream in addition to distillate and bottoms streams.

This chapter studies a simplified version of the auto-refrigerated alkylation process and demonstrates the design trade-offs and interactions among design optimization variables such as reactor size, reactor temperature, compressor work, and isobutane recycle. Large reactors permit lower temperatures for a given olefin conversion, which improves selectivity. However, low reactor temperatures produce a low reactor pressure, which increases compressor work. Higher isobutane recycle improves selectivity but increases energy consumption and equipment sizes in the separation section. So the optimum economic design must balance the capital costs of reactors and distillation columns with the energy costs of compression and reboiler heat inputs. The locations where the fresh feed streams enter the process also affect the design.

An effective plantwide control structure is also developed that handles large disturbances in throughput and feed compositions. The structure has several uncommon control features: control of two compositions and one temperature in the sidestream column and a proportional-only temperature control in the other column.

*Principles and Case Studies of Simultaneous Design*, First Edition. William L. Luyben

## 7.1 INTRODUCTION

The alkylation of $C_3$ and $C_4$ olefins with isobutane to produce an alkylate product of high value is widely used in oil refineries around the world. The alkylation process was developed in 1930s and provided high-octane aviation fuel during World War II. Today these units produce an "alkylate" product that is a valuable gasoline blending component.

There are two alkylation processes using different catalysts: tetrahydrofuran (THF) and sulfuric acid. They have different advantages and disadvantages. The sulfuric acid process is more environmentally friendly but must operate at low reactor temperatures that require expensive refrigeration. The THF process does not require refrigeration but poses more of a pollution risk.

In this chapter, the sulfuric acid process is studied. There are a number of design optimization variables, which interact in terms of their effects on conversion, selectivity, capital investment, and operating costs. The operating cost is primarily energy consumption in distillation column reboilers, but the refrigeration compressor is another significant energy consumer.

If a bigger reactor is used, reactor temperatures can be lower, which improves selectivity while achieving the same olefin conversion. However, lower reactor temperatures mean lower reactor pressures because the reactors operate at their bubble-point pressure. Since the compressor discharge pressure is set by the temperature (120 °F) that can be achieved in a water-cooled condenser, lower reactor pressure requires more compressor work. So both reactor and compressor capital investment increase and compressor energy consumption increases as reactor size is increased. On the other hand, selectivity can also be increased by using more isobutane recycle, but this increases capital investment and energy costs in the separation section. Therefore the design must find an economic balance among reactor size, reactor temperature, and isobutane recycle.

Another interesting feature of the alkylation process is the need to purge from the process two inert components that enter with the fresh feed streams. Significant amounts of both propane and normal butane are contained in the multicomponent olefin feed stream (typically coming from a catalytic cracking unit) and the makeup butane feed that is needed to provide the stoichiometric amount of isobutane to react with the olefin. These inert components must have a way to exit the process, or they will build up and shut down the unit.

## 7.2 PROCESS DESCRIPTION

The alkylation process studied in this paper is a simplified version of the actual industrial process. The olefin is assumed to be 1-butene, which enters in a butane–butylene (BB) fresh feed stream that also contains propane, isobutane, and *n*-butane. There is more 1-butene in this feed than there is isobutane, so the reaction stoichiometry requires another source of additional isobutane to provide the necessary amount. This fresh $C_4$ stream typically comes from a saturated light-ends unit, and it also contains some propane and *n*-butane. The desired product is assumed to be *iso*-octane. An undesirable product is assumed to be dodecane.

The liquid phase sulfuric acid is neglected in this study. In the real plant, a large stream of acid is circulated in the system. A small spent acid stream is continuously withdrawn, and fresh sulfuric acid makeup is continuously added, since there are undesirable reactions that contaminate the acid.

### 7.2.1 Reaction Kinetics

The production of *iso*-octane ($iC_8$) involves the liquid-phase reaction of 1-butene with isobutane in a series of low-temperature agitated reactors in the presence of a second liquid phase of sulfuric acid.

$$C_4H_8 + C_4H_{10} \longrightarrow C_8H_{18} \tag{7.1}$$

We assume that there is also a sequential reaction of *iso*-octane and 1-butene to form an undesirable high-molecular weight component (dodecane, $C_{12}H_{26}$).

$$C_8H_{18} + C_4H_8 \longrightarrow C_{12}H_{26} \tag{7.2}$$

In reality, there are many complex reactions forming several chemical components. The simplified kinetics used in this chapter are those suggested by Mahajanam et al.[1] We believe they capture the important features of the chemical system and their effects on process design and control.

Table 7.1 gives the reaction kinetics assumed in this chapter. All reaction rates have units of kmol $sec^{-1}$ $m^{-3}$ (consistent with Aspen simulation requirements). Concentration units are molarity. Notice that the activation energy of the undesirable reaction is larger than that of the desirable reaction. Therefore, low reactor temperatures improve selectivity. In addition, selectivity is improved by keeping the concentration of 1-butene and *iso*-octane low in the reactor. This can be achieved by using a large excess of isobutane, but the excess must be recovered and recycled. The 1-butene concentration can also be kept low by distributing the BB feed among the several reactors that operate in series. So all of the recycle isobutane is fed to the first reactor, and the BB fresh feed is split equally among the three reactors used in the flowsheet discussed later.

These reactions are exothermic, so the heat of reaction must be taken into account. The reactors are auto-refrigerated, removing heat by boiling the organic liquid phase in the reactor. The inlet streams entering the reactors are warmer than the reactors, so the sensible heat must also be removed by vaporization.

### 7.2.2 Phase Equilibrium

There are two basic separations required: propane/isobutane and isobutane/*n*-butane. The Choa-Seader physical property package is used in the Aspen simulations. Figure 7.1a gives the *Txy* diagram for the propane/isobutane system at 220 psia, the pressure required if cooling water is used in the condenser. This separation is fairly easy, so the resulting distillation column does not require a large number of trays. Figure 7.1b gives the *Txy* diagram for the isobutane/*n*-butane system at 95 psia, the pressure required if cooling water is used in the condenser. This separation is quite difficult, so a column with a significant number of

**TABLE 7.1 Alkylation Reaction Kinetics**

| | $\Re 1$ | $\Re 2$ |
|---|---|---|
| $k$ | $1.663 \times 10^6$ | $4.158 \times 10^{12}$ |
| $E$ (kcal/kmol) | 15,356 | 19,444 |
| Concentration terms (kmol/$m^3$) | $iC_4/C_4^=$ | $iC_8/C_4^=$ |

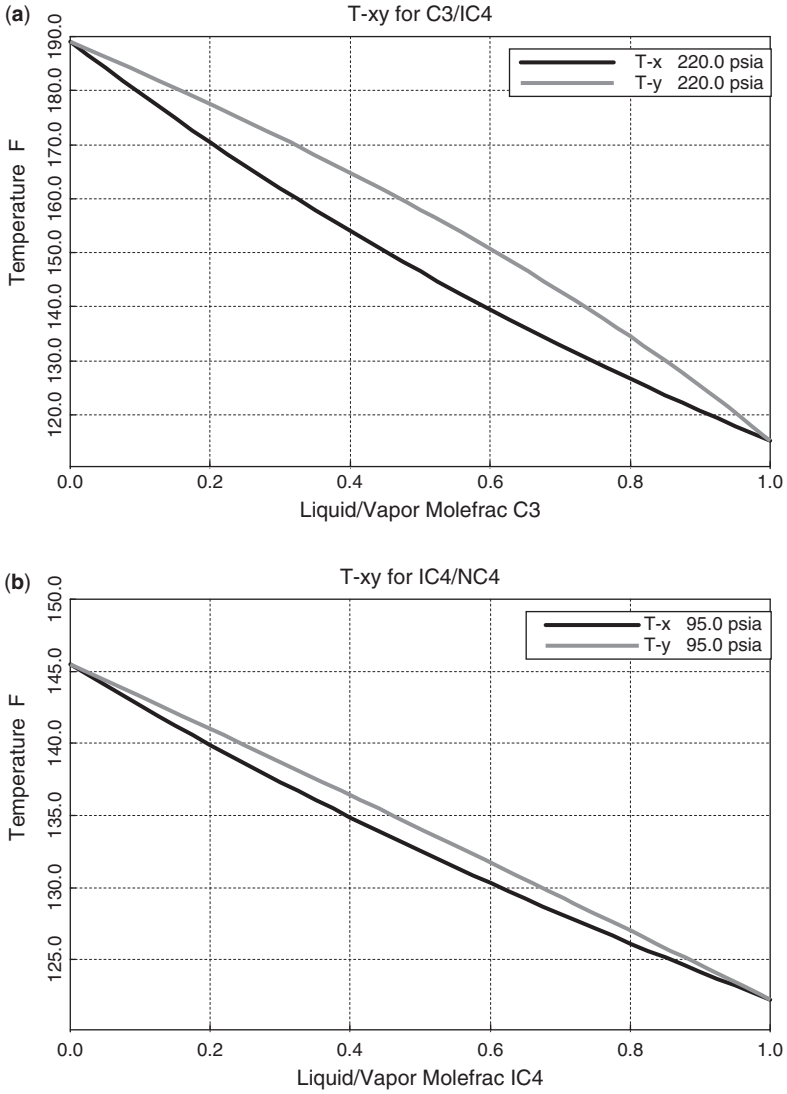


**Figure 7.1.** *Txy* diagrams for (a) propane/isobutane at 220 psia, and (b) isobutane/*n*-butane at 95 psia.

trays is required. In a later section, the optimum designs of these two columns are developed based on minimizing total annual cost (capital and energy).

### 7.2.3 Flowsheet

Figure 7.2 shows the flowsheet of the alkylation process with the equipment sizes and conditions that is the economic optimum, as discussed in Section 7.4. In the simulation, we use three adiabatic continuous stirred-tank reactors (CSTR) reactors in series. In the real process, there is one large vessel with multiple compartments in which the liquid

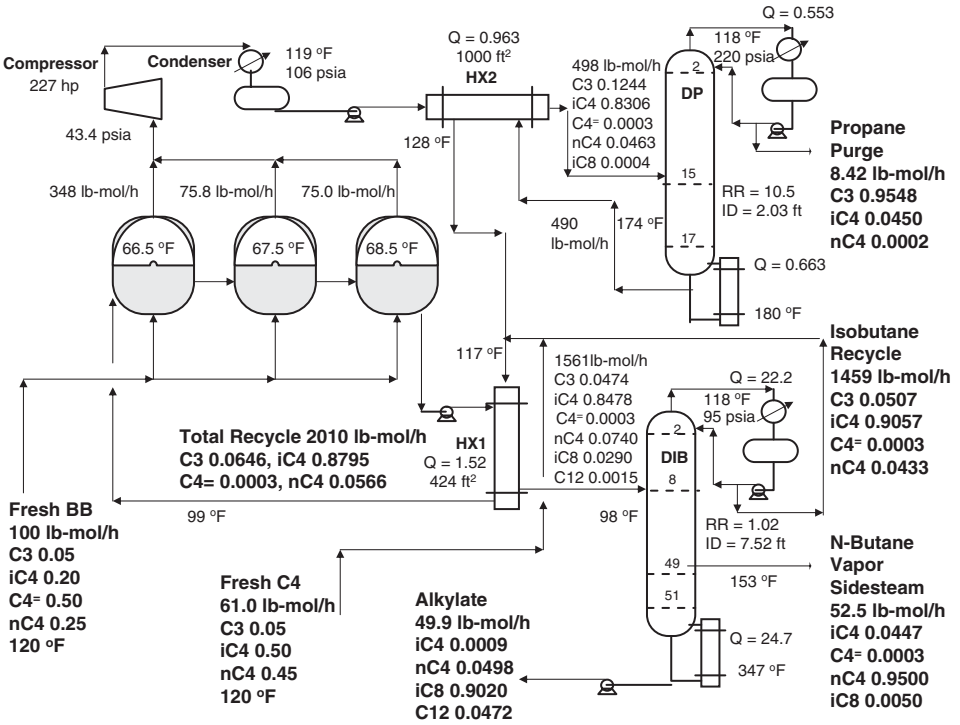


**Figure 7.2.** Alkylation flowsheet.

flows from one compartment to the next. Each compartment is vigorously agitated to contact the liquid acid phase with the organic liquid phase. There is no heat removal from the reactors. The exothermic heat of reaction and the sensible heat of cooling the inlet streams are removed by the latent heat of vaporization involved in boiling the liquid and generating vapor.

The volume of liquid in each of the simulated reactors is specified (to be optimized). The reactor is assumed to be half full of liquid, and reaction occurs only in the liquid phase. The total volume of the reactor vessel used for calculating the vessel cost is therefore six times the volume of liquid in each of the three reactors. An aspect ratio of $L_R/D_R = 10$ is assumed for determining the dimensions of the reactor vessel.

The fresh BB feed is split into three equal parts, and these are fed into each of the three simulated reactors. The total isobutane recycle stream is cooled in a heat exchanger HX1, using the cool reactor effluent, and fed into the first reactor.

The vapor streams from each reactor are combined and compressed. The compressor raises the pressure of the gas stream to a high enough value (106 psia) so that the bubble-point temperature of the mixture of organic components is about 120 °F, which permits the use of cooling water in the condenser.

The total reactor vapor has a composition of about 12 mol% propane, so this stream is fed to a depropanizer (DP) distillation column to purge out the propane that enters in the two fresh feed streams. The DP produces a distillate with a composition of 95 mol% propane. The column operates at 220 psia so that cooling water can be used in the condenser. The feed is preheated in a heat exchanger (HX2) with the hotter bottoms

stream. This heat exchanger is designed by specifying that the hot exit stream is 130 °F. The bottoms composition is about 10 mol% propane. It is then combined with the distillate from the next column and the fresh $C_4$ feed. This combined stream is fed back to the first reactor, first passing through a heat exchanger (HX1) to cool it. An alternative flowsheet is considered later in this paper in which the fresh $C_4$ feed is introduced at a different location.

The liquid stream from the last reactor is heated in the HX1 heat exchanger and fed into a large deisobutanizer (DIB) distillation column. This heat exchanger is designed by specifying a cold exit temperature of 100 °F. The distillate from the DIB is recycled back to the reactors with an impurity specification of 4.3 mol% *n*-butane. A vapor sidestream is removed near the bottom of the column to purge *n*-butane from the process. The purity of this sidestream is set at 95 mol% *n*-butane. Alkylate ($iC_8$) is removed in the bottoms stream along with the undesired component ($C_{12}$). A small amount of *n*-butane is also included in the bottoms alkylate stream since some butane can be blended into gasoline to meet the Reid vapor pressure (RVP) specification. The composition of *n*-butane in the bottoms is 5 mol%.

The selectivity of the process is measured by the amounts of $iC_8$ and $C_{12}$ in the alkylate stream. Selectivity can be adjusted by changing reactor temperatures or by changing isobutane recycle. This issue is discussed in the following section.

A high conversion of 1-butene is desired since it means low concentrations of 1-butene in the reactors, which suppress the undesirable side reaction. A specification of 0.5 lb-mol/h of 1-butene in the liquid effluent from the last reactor is used to keep conversion high.

### 7.2.4 Design Optimization Variables

This process has a very large number of design optimization variables. The most important are reactor size, reactor temperature, isobutane recycle, and the number of trays in the two columns. The purity specifications for the product and recycle streams are also potential design optimization variables.

A heuristic approach is taken to reduce the number of variables so that only the most significant can be quantitatively assessed. Most of the heuristics apply to the distillation columns, where long experience with column design permits the selection of reasonable product specifications that trade off impurity levels with energy costs. The compositions of the alkylate product, the butane product, and the propane product are set at those found in a typical alkylation plant.

Some *n*-butane can be dropped down into the alkylate as limited by RVP specifications. The amount of isobutane lost in the *n*-butane product cannot be too large because isobutane is worth more than *n*-butane, but achieving higher *n*-butane purity increases energy consumption in the DIB since the $iC_4/nC_4$ separation is difficult. Similar logic suggests that a reasonable specification for the $nC_4$ impurity in the $iC_4$ recycle from the top of the DIB is about 4.3 mol%.

In the DP, the distillate is LPG sold for domestic and industrial heating. A typical specification of 4.3 mol% isobutane impurity is selected. There is no hard specification for the DP bottoms since it is recycled back to the reactors. Achieving higher $iC_4$ concentrations requires more stages and more energy. A reasonable value of 8.8 mol% propane impurity in the bottoms is selected as a typical value.

The remaining design optimization variables are the most important ones: reactor size, reactor temperature, and $iC_4$ recycle. These are quantitatively evaluated in the next section.

## 7.3 DESIGN OF DISTILLATION COLUMNS

A common procedure for optimizing a distillation column is to determine the values of the design optimization variables that minimize total annual cost. The parameters that must be given are the feed conditions and the desired product specifications. The design optimization variables include pressure, total number of trays, feed tray location, and sidestream tray location.

In this hydrocarbon system, decreasing pressure increases relative volatilities, so the selection of pressure is straightforward. We minimize it subject to the use of cooling water.

To use the common design procedure we must know the feed conditions. These are unknown at the beginning of the design. The parameter that has the greatest effect on the column feeds is the isobutane recycle. So some initial studies are conducted with some arbitrary recycle flowrates for different size reactors, optimizing each column under these changing conditions. The final optimum design is shown in Figure 7.2. The optimization procedure is discussed below for each column using the feed conditions that are quite similar to those found in the final design.

The sizing relationships and cost estimations for the equipment are discussed in Chapter 5 and are summarized in Table 7.2.

### 7.3.1 Depropanizer

The pressure is set at 220 psia. The feed conditions used in the optimization are 481 lb-mol/h at 171 °F and 239 psia with a composition of 10.32 mol% propane, 84.48 mol% isobutane, 0.02 mol% butene, 5.14 mol% *n*-butane, and 0.04 mol% *iso*-octane.

The product specifications are 4.33 mol% isobutane in the distillate and 8.81 mol% propane in the bottoms. Distillate flowrate and reflux ratio (RR) are varied to achieve these specifications as the total number of trays and the feed tray are varied.

The separation is fairly easy, so a fairly small column is required. However, note that the distillate flowrate is quite small compared to the feed flowrate. The resulting RR is high.

Table 7.3 gives results for three DP columns with a total number of stages of 12, 17, and 22, respectively. The feed tray location is optimized for each of these columns by finding the location that minimizes reboiler heat input. As more trays are used, energy cost decreases monotonically. However, as more trays are used, capital cost initially decreases and then begins to increase. This is caused by the relative costs of decreasing column diameter and heat exchanger area as more trays are added versus the cost of building a taller column. Eventually the increase in the height of the vessel becomes more important, and capital costs increase.

A 17-stage DP fed on Stage 15 shows the minimum total annual cost.

### 7.3.2 Deisobutanizer

The pressure is set at 95 psia. The feed conditions used in the optimization are 1579 lb-mol/h at 98 °F and 145 psia with a composition of 4.01 mol% propane, 84.99 mol% isobutane, 0.02 mol% butene, 7.97 mol% *n*-butane, 2.86 mol% *iso*-octane, and 0.15 mol% dodecane.

The separation between isobutane and *n*-butane is difficult, so a fairly large column is required. However, note that the distillate flowrate is large compared to the feed flowrate. The resulting RR is low even for this difficult separation.

**TABLE 7.2 Basis of Economics and Equipment Sizing**

Column diameter: Aspen tray sizing
Column length: NT trays with 2-ft spacing plus 20% extra length
Column vessel (diameter and length in meters)
Capital cost = 17,640 $(D)^{1.066}$ $(L)^{0.802}$

*Condensers (area in $m^2$)*
Heat-transfer coefficient = 0.852 kW/K-$m^2$
Differential temperature = 13.9 K
Capital cost = 7296 $(A)^{0.65}$

*Reboilers (area in $m^2$)*
Heat-transfer coefficient = 0.568 kW/K-$m^2$
Differential temperature = 34.8 K
Capital cost = 7296 $(A)^{0.65}$

*Reactor (diameter and length in meters)*
Half full of liquid, three compartments
Aspect ratio = 10
Capital cost = 17,640 $(D)^{1.066}$ $(L)^{0.802}$

Compressor capital cost = $(1293)(517.3)(3.11)(\text{hp})^{0.82}/280$

*Energy cost*
LP steam = \$6.08/GJ

$$\text{TAC} = \frac{\text{Capital cost}}{\text{Payback period}} + \text{Energy cost}$$

Payback period = 3 yr

The separation between *n*-butane and *iso*-octane is easy, so the sidestream is withdrawn close to the bottom of the column. Note that the sidestream is a vapor to take advantage of the lower concentrations of the heavier components ($iC_8$ and $C_{12}$) in the vapor phase compared to their concentrations in the liquid phase.

The product specifications are 4.33 mol% *n*-butane in the distillate, 95 mol% *n*-butane in the vapor sidestream, and 4.98 mol% *n*-butane in the bottoms. Distillate flowrate, sidestream flowrate, and RR are varied to achieve these three specifications as the total number of trays and the sidestream withdrawal stage and the feed tray are varied.

**TABLE 7.3 Column Optimization**

| | DP | | | DIB | | |
|---|---|---|---|---|---|---|
| NT | 12 | 17 | 22 | 42 | 52 | 62 |
| NF | 11 | 15 | 19 | 6 | 8 | 9 |
| NS | — | — | — | 39 | 49 | 69 |
| ID (ft) | 2.67 | 2.16 | 2.14 | 7.72 | 7.46 | 7.42 |
| $Q_R$ ($10^6$ Btu/h) | 1.84 | 0.840 | 0.809 | 24.0 | 22.7 | 22.5 |
| $Q_C$ ($10^6$ Btu/h) | 1.64 | 0.641 | 0.606 | 21.7 | 20.4 | 20.2 |
| Capital ($10^6$ \$) | 0.231 | 0.168 | 0.185 | 1.52 | 1.59 | 1.70 |
| Energy ($10^6$ \$/yr) | 0.103 | 0.0472 | 0.0455 | 1.35 | 1.28 | 1.26 |
| TAC ($10^6$ \$/yr) | 0.1804 | **0.1033** | 0.1069 | 1.855 | **1.804** | 1.830 |

Table 7.3 gives results for three DIB columns with a total number of stages of 42, 52, and 62, respectively. The feed tray location and the sidestream withdrawal stage are optimized for each of these columns by finding the locations that minimize reboiler heat input. Notice that energy cost decreases monotonically as more trays are added. Capital cost increases monotonically as more trays are added in this tall column.

A 52-stage DIB fed on Stage 6 with sidestream withdrawn from Stage 49 shows the minimum total annual cost.

## 7.4 ECONOMIC OPTIMIZATION OF ENTIRE PROCESS

There are several aspects associated with optimizing a complex process with many design optimization variables.

### 7.4.1 Flowsheet Convergence

The alkylation process is typical of many chemical processes that feature multiple units connected by recycle streams. The convergence of these flowsheets using any commercial simulation software can be quite difficult. Such was the case in this system. We were unable to get the Aspen Plus simulation to converge with the isobutane recycle stream connected.

However, we were successful in using the technique of exporting the file from steady-state Aspen Plus into Aspen Dynamics and making the desired connections in the dynamic simulation (see Luyben[2]). With a plantwide control structure in place, the dynamic simulation was run out until all variables stopped changing with time. The process is quite slow due to the recycle stream. It took over 48 h of process time to come to a steady state. The results shown in Figure 7.2 are from the converged dynamic simulation.

### 7.4.2 Yield

The yield of the process is defined as the production rate of the desired product $iC_8$ divided by the total of the $iC_8$ and $C_{12}$ produced. A value of 95% is used as the desired yield.

Yield is affected by reactor size, reactor temperature, and isobutane recycle. The effects of reactor size and isobutane recycle on yield are shown in Figure 7.3. These results are from cases in which the olefin conversion has been held constant (0.5 lb-mol/h of butene in the liquid stream from the last reactor) by adjusting reactor temperature.

As the reactor size is increased (increasing reactor capital cost), less recycle is required (reducing capital and energy costs in the DIB distillation column). However, increasing the size of the reactor produces a lower reactor temperature for the fixed conversion. The lower temperature means a lower compressor suction pressure, so compression costs increase (both capital and energy).

### 7.4.3 Effect of Reactor Size

Figure 7.4 gives results for different reactor sizes with both yield and conversion fixed. Conversion is fixed by adjusting reactor temperature. Yield is fixed by adjusting isobutane recycle.

An increase in reactor size produces decreases in isobutane recycle, reactor temperature, reactor pressure, and energy consumption in the DIB reboiler. However, compressor power

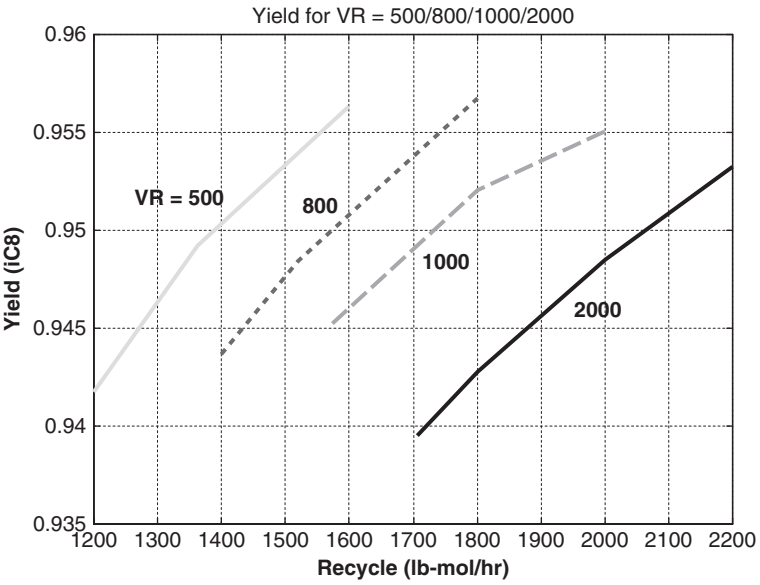


**Figure 7.3.** Effects of recycle and reactor size on yield.

increases. The net effect of all the variables on TAC is shown in the bottom right graph in Figure 7.4. Total annual cost decreases for reactor sizes all the way down to 300 $ft^3$. Note that capital investment increases as reactor size increases, and energy costs decrease as reactor size increases.

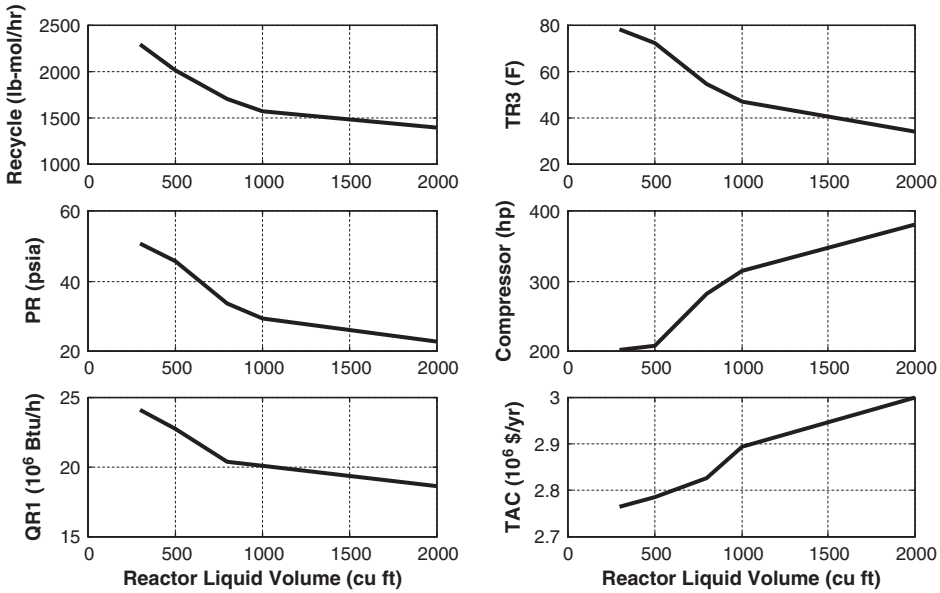


**Figure 7.4.** Effect of reactor size with fixed yield and conversion.

**TABLE 7.4 Economic Effects of Reactor Size[a]**

| Individual Reactor Liquid Volume | $ft^3$ | 300 | 500 | 800 | 1000 | 2000 |
|---|---|---|---|---|---|---|
| Recycle | lb-mol/h | 2300 | 2010 | 1700 | 1570 | 1390 |
| Reactor temperature ($T_{R3}$) | °F | 78.5 | 72.3 | 54.8 | 47 | 34 |
| Reactor pressure | psia | 50.6 | 45.7 | 33.5 | 29.2 | 22.6 |
| Reboiler heat input ($Q_{R1}$) | $10^6$ Btu/h | 24.1 | 22.7 | 20.4 | 20.1 | 18.6 |
| Compressor power | hp | 202 | 207 | 281 | 314 | 380 |
| Total capital | $10^6$ $ | 3.7859 | 4.0898 | 4.4186 | 4.7081 | 5.1800 |
| Total energy | $10^6$ $/yr | 1.5035 | 1.4205 | 1.3536 | 1.3240 | 1.2700 |
| TAC | $10^6$ $/yr | 2.766 | 2.784 | 2.826 | 2.893 | 3.000 |

[a]Selectivity = 95%.

Reactor size is denoted as the liquid volume in one of the three reactors. Each reactor is half full of liquid. So for a case labeled as $V_R = 300\ ft^3$, the total volume of the single large reactor with three compartments is 1800 $ft^3$ (6.12 ft in diameter and 61.2 feet in length).

### 7.4.4 Optimum Economic Design

Do the results shown in Figure 7.4 mean that the 300 $ft^3$ liquid holdup per reactor is the best of these designs? To answer this question, we look at the incremental capital investment required to go from a small reactor system up to the next size reactor and the corresponding savings in energy cost.

Table 7.4 gives more details of the breakdown between capital costs and energy costs for various reactor sizes. Note that it takes additional capital investment to build a plant with a larger reactor, but the larger reactor plant has lower energy cost.

For example, the 300 $ft^3$ design requires a total capital investment of $3,785,900 while the 500 $ft^3$ design capital is $4,089,800. The difference is $303,900 in incremental investment. The annual energy costs of the 300 and 500 $ft^3$ designs are $1,503,500 per year and $1,420,500 per year, respectively. This gives a savings of $83,000 per year.

The incremental return on investment is $83,000/$303,900 = 0.27, which is a reasonable return on investment in most companies. Therefore, it pays to build the more expensive 500 $ft^3$ process.

Performing the same calculation to see if it pays to build the 800 $ft^3$ plant instead of the 500 $ft^3$ plant shows a difference in capital investment of $4,418,600 − $4,089,800 = $328,800 and a difference in energy cost of $1,420,500/year − $1,353,600/year = $66,900/year. The incremental investment is larger and the incremental savings are smaller in this case than in the previous. The incremental return on investment is $66,900/$328,800 = 0.20, which is approaching the minimum return on investment required in some companies. Repeating these calculations for moving up to the 1000 $ft^3$ process yields an incremental return on investment of only 10%.

## 7.5 ALTERNATIVE FLOWSHEET

The flowsheets considered up to this point combined the small fresh $C_4$ stream with the very large recycle isobutane recycle stream and fed the total back into the first reactor. This is the typical arrangement in many chemical plants for the introduction of fresh feed. The fresh $C_4$ stream is only 61.0 lb-mol/h, while the recycle stream is 1459 lb-mol/h. One would think that little would be gained by introducing this small stream at any other location.

However, the isobutane purity of the fresh $C_4$ stream is only 50 mol%, while the purity of the recycle is 90.6 mol% isobutane. Therefore, we are mixing an impure stream with a purer stream. The relative flowrates are so different that one would expect this to have little effect.

This turns out not to be the case. The energy consumption in the DIB can be significantly reduced (from $24.7 \times 10^6$ Btu/h to $16.7 \times 10^6$ Btu/h) by feeding the fresh $C_4$ stream into the DIB column. It is fed at a location (Stage 36) where the tray composition is about 50 mol% isobutane, which matches the composition of the fresh $C_4$ feed.

The reason for this unexpected effect is the extreme sensitivity of the energy requirement in the DIB on its feed composition. Table 7.5 shows how reflux and RR must change as the composition of the feed to the DIB changes. The three product streams are held at their specified values: $x_{D1}(nC_4) = 0.05$, $y_S(nC_4) = 0.95$ and $x_{B1}(nC_4) = 0.0493$. Very small changes in the light- and heavy-key components ($iC_4$ and $nC_4$) require very large changes in the RR and reflux-to-feed (R/F) ratio. As the *n*-butane composition changes from 6.81 mol% to 5.51 mol%, the RR and R/F ratio both decrease by a factor of ten. This extreme sensitivity to feed composition is a unique feature of this DIB.

The revised flowsheet is shown in Figure 7.5. A comparison with the original flowsheet (Figure 7.2) shows that the DIB feed composition has changed from 7.40 to 5.81 mol% $nC_4$ and 84.78 to 86.21 mol% $iC_4$. The result is a decrease in the RR from 1.02 to 0.246, which drops the reboiler heat input from $24.7 \times 10^6$ Btu/h to $16.7 \times 10^6$ Btu/h.

The modified flowsheet was converged for other cases with different reactor volumes, and Table 7.6 compares results for the two flowsheets. In all cases, significant reductions in DIB reboiler heat input are observed. Note that the isobutane composition of the feed to the DIB increases in all cases when the fresh $C_4$ stream is fed to the column and not directly into the reactor. These small feed composition changes result in large changes reboiler duty.

**TABLE 7.5 Effect of DIB Column Feed Composition**[a]

| | | | Base | | |
|---|---|---|---|---|---|
| $z_1(C_3)$ | 0.0479 | 0.0479 | 0.0479 | 0.0479 | 0.0479 |
| $z_1(iC_4)$ | 0.8531 | 0.8581 | 0.8631 | 0.8651 | 0.8661 |
| $z_1(nC_4)$ | **0.0681** | 0.0631 | 0.0581 | 0.0561 | **0.0551** |
| $z_1(C_4^=)$ | 0.0003 | 0.0003 | 0.0003 | 0.0003 | 0.0003 |
| $z_1(iC_8)$ | 0.0291 | 0.0291 | 0.0291 | 0.0291 | 0.0291 |
| $z_1(C_{12})$ | 0.0015 | 0.0015 | 0.0015 | 0.0015 | 0.0015 |
| R/F | 0.7481 | 0.5168 | 0.2497 | 0.1296 | 0.0651 |
| RR | 0.7776 | 0.534 | 0.2565 | 0.1328 | 0.0666 |
| $Q_{R1}(10^6$ Btu/h) | 22.47 | 19.74 | 16.58 | 20.76 | 19.80 |

[a]Feed = 1560 lb-mol/h. $x_B(nC_4) = 0.05$, $y_S(nC_4) = 0.95$, $x_D(nC_4) = 0.0433$.

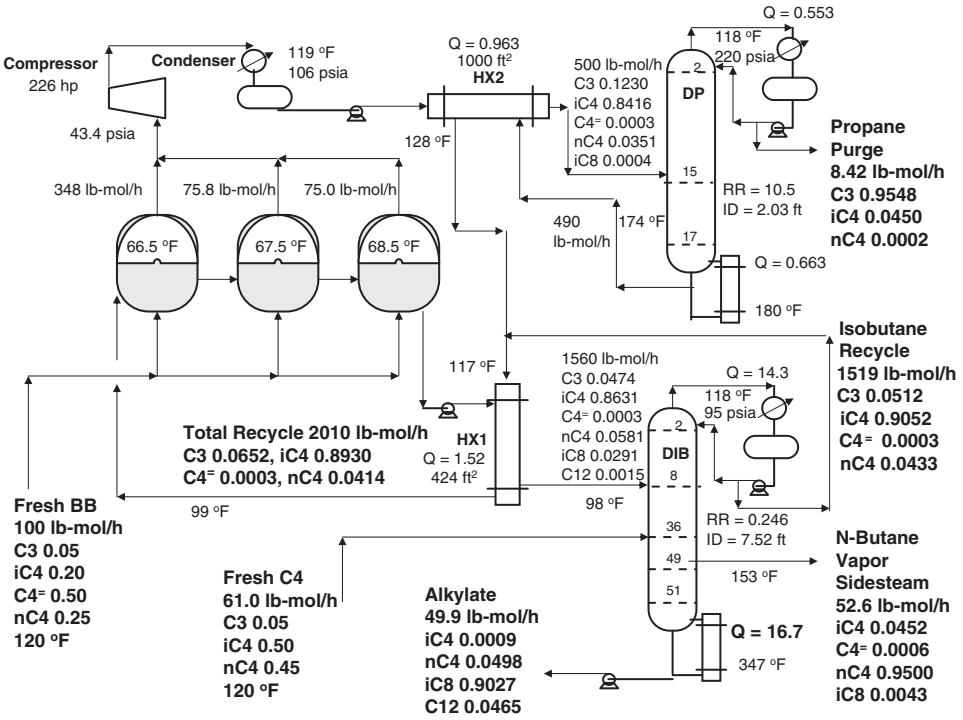


**Figure 7.5.** Alkylation flowsheet for fresh $C_4$ fed to DIB.

The new flowsheet will have somewhat different economics, so the selection of the optimum reactor size may be slightly altered. The energy and capital costs of the DIB will be lower for all cases. The DP is essentially unaffected by the change. Note in Table 7.6 that the difference in reboiler duty $Q_{R1}$ between the original and modified flowsheets is about $8 \times 10^6$ Btu/h for the small reactors ($V_R = 300$ and 500 ft$^3$), but this difference is smaller for the larger reactor cases ($6 \times 10^6$ Btu/h for the $V_R = 800$ ft$^3$ case and $5.7 \times 10^6$ Btu/h for the $V_R = 1000$ ft$^3$ case). This indicates that there is less to be saved in energy by going to larger reactors.

Reworking the economics with the smaller DIB results in a smaller incremental savings in energy between the 300 and 500 ft$^3$ cases ($1,065,200 − $1,008,700 = $56,500 per year). The incremental increase in total capital is $3,700,100 − $3,452,000 = $248,100, which

**TABLE 7.6 Comparison of Original and Modified Flowsheets**

| Individual Reactor Liquid Volume | ft$^3$ | | 300 | 500 | 800 | 1000 |
|---|---|---|---|---|---|---|
| $Q_{R1}$ | $10^6$ Btu/h | Original | 24.1 | 24.7 | 20.8 | 20.1 |
| | | Modified | 16.3 | 16.7 | 14.8 | 14.4 |
| $z_{1(iC_4)}$ | mol% | Original | 85.66 | 84.78 | 83.99 | 83.24 |
| | | Modified | 87.09 | 86.31 | 85.79 | 85.32 |
| $z_{1(nC_4)}$ | mol% | Original | 7.59 | 7.40 | 8.68 | 9.17 |
| | | Modified | 6.12 | 5.81 | 6.62 | 7.00 |

gives a return on investment of 18%. Therefore the 500 $ft^3$ design may not be the economic optimum.

The flowsheet used to study dynamics and control is the 500 $ft^3$ reactor case with the fresh $C_4$ fed to the DIB.

## 7.6 PLANTWIDE CONTROL

The flowsheet shown in Figure 7.5 does not include all the pumps and control valves needed in the process. The first step in studying dynamics using a pressure-driven dynamic simulation is to add these items and to determine the volumes of all vessels. The reactor sizes and column diameters are known, but the liquid surge capacities of the column reflux drums, column bases, and refrigerant drum must be specified. These are all sized to provide 5 min of holdup when at 50% level. The tube-side and shell-side volumes of the heat exchangers HX1 and HX2 are calculated from the known heat-transfer areas and assuming 2-inch diameter tubes, 20 ft in length. Shell volume is assumed to be equal to tube volume. Figures 7.6 and 7.7 give temperature and composition profiles in the two distillation columns.

### 7.6.1 Control Structure

Figure 7.8 shows the plantwide control structure developed for this process using plantwide process control methodology (see Luyben[3]). Conventional PI controllers are used in all loops. The various loops are listed below with their controlled and manipulated variables.

1. Fresh BB feed is flow controlled and split equally among the three reactors. This is the throughput handle. The flowrate of the total BB is measured and fed into a flow controller that manipulates the valve in the line to the first reactor. The total BB flow signal is also sent into a multiplier with a constant set at 0.3333. The output signal of the multiplier is the setpoint signal to two flow controllers that manipulate the appropriate valves in the BB feed lines to the other two reactors.
2. Total isobutane recycle (distillate from the DIB plus bottoms from the DP) is flow control with the setpoint of the flow controller coming from a multiplier. The input signal to the multiplier is the total BB flowrate. The constant in the multiplier is the desired recycle-to-BB ratio.
3. The liquid levels in each reactor are controlled by manipulating the liquid stream leaving the reactor.
4. The temperature in the third reactor ($T_{R3}$) is controlled by manipulating compressor work.
5. The pressure in the refrigerant drum is controlled by manipulating heat removal in the refrigerant condenser.
6. The level in the refrigerant drum is controlled by manipulating the feed to the DP.
7. The pressures in both columns are controlled by condenser heat removal.
8. Base levels in both columns are controlled by manipulating the bottoms flowrates.
9. Reflux-drum level in the DP is controlled by manipulating the reflux flowrate since this column has a large RR because of the small distillate stream that is purging out the propane from the system.

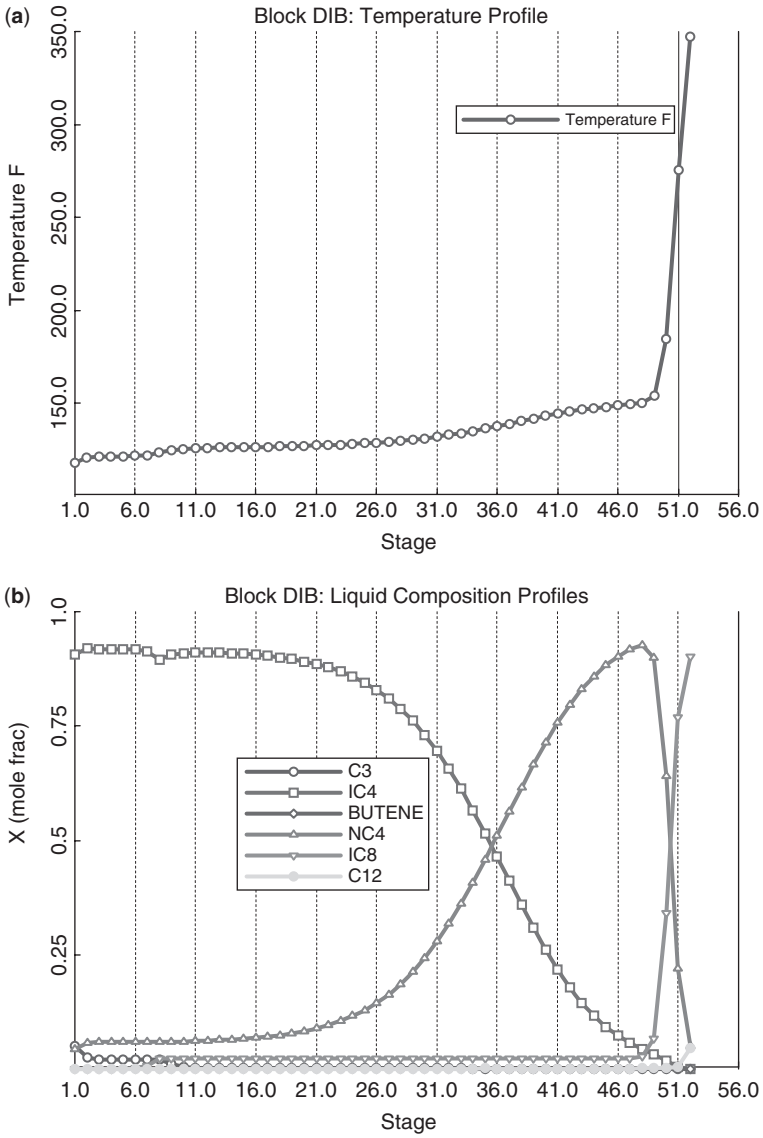


**Figure 7.6.** (a) DIB temperature profile. (b) DIB composition profiles.

10. The distillate flowrate in the DP is adjusted to maintain a constant RR. This is achieved by measuring the reflux flowrate, sending this flow signal into a multiplier that is set at the reciprocal of the RR and sending the output signal of the multiplier to a distillate flow controller as its setpoint signal.
11. The temperature on Stage 5 in the DP is controlled by manipulating the reboiler heat input. Stage 5 is selected because this is where the slope of the temperature profile is large (see Figure 7.7a).
12. Reflux-drum level in the DIB is controlled by manipulating the fresh $C_4$ feed stream.

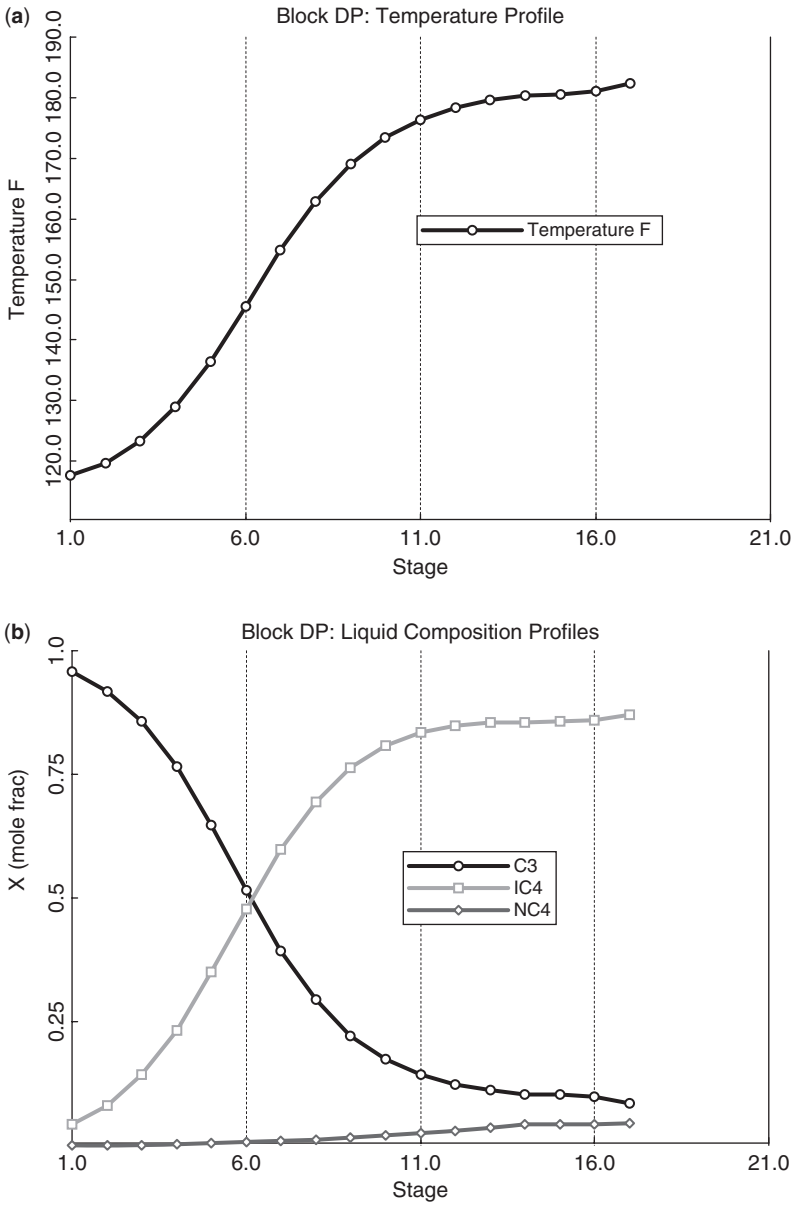


**Figure 7.7.** (a) DP temperature profile. (b) DP liquid composition profile.

13. The composition of the *n*-butane impurity in the DIB distillate is controlled by manipulating the DIB reflux flowrate.
14. The composition of the *n*-butane purity in the DIB vapor sidestream is controlled by manipulating the sidestream flowrate.
15. The temperature on Stage 50 in the DIB is controlled by manipulating reboiler heat input. This location is selected by looking at the temperature profile shown in Figure 7.6a.

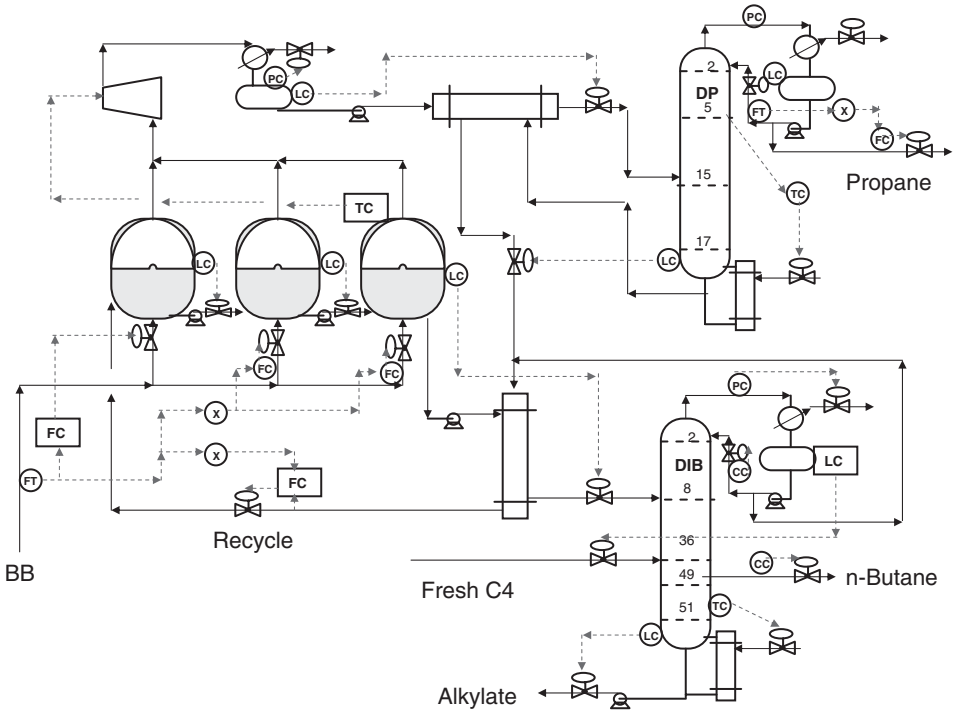


**Figure 7.8.** Plantwide control structure.

Item 12 above is one of the key plantwide control features of this structure. The fresh $C_4$ feed required to balance the reaction stoichiometry is fed into the system by looking at the inventory of isobutane in the reflux drum of the DIB. If more 1-butene is coming into the process in the BB fresh feed than the isobutane that is coming into the process in the BB fresh feed and the fresh $C_4$ feed, the level in the DIB will decrease. So this signal provides a good indication of isobutane inventory in the system and can be used to make a feedback control adjustment.

Note that there is no direct effect of fresh $C_4$ feed flowrate on the reflux-drum liquid level in the DIB since the feed is a liquid. Changing the feed affects the temperature on Stage 50, and the temperature controller then adjusts reboiler heat input, which then affects reflux-drum level. So the temperature loop is "nested" inside the level loop. The temperature loop must be on automatic for the level loop to work.

The other unusual features of this control structure are Items 13 and 14 above. Two composition controllers are used in the DIB. The composition controller on the distillate is needed because of the extreme sensitivity of the DIB to changes in feed composition, as discussed earlier. Very large changes in reflux flow are required to handle disturbances. In fact, in some situations, the reflux flowrate goes to zero, and the column becomes a simple stripping column.

The composition controller on the sidestream is needed because the temperature profile in the column between the top and the sidestream drawoff location is very flat due to the small relative volatility between isobutane and *n*-butane.

### 7.6.2 Controller Tuning

Deadtimes of 1 min are inserted in temperature loops. Deadtimes of 3 min are inserted in composition loops. The very convenient relay-feedback feature in Aspen Dynamics is used to find ultimate gains and periods. The Tyreus-Luyben tuning rules are used.

The tuning of the three interacting controllers in the DIB is performed sequentially. First the distillate and sidestream composition controllers are put on manual, and the Stage 50 temperature controller is tuned. Then, with the temperature controller on automatic and the distillate composition controller still on manual, the sidestream composition controller is tuned. Finally, with the other two controllers on automatic, the distillate composition controller is tuned. Table 7.7 gives controller parameters for the important loops.

The tuning of the temperature loop in the DP is quite unusual. The response of the column was found to be a long-period oscillation if any integral action was used in the temperature controller. Figure 7.9 illustrates this effect. The disturbance is a 10% increase in BB fresh feed. Three different tuning constants are used in the DP temperature controller TC2, which manipulates reboiler heat input. The relay-feedback tests gave constants for a PI controller of $K_C = 2.5$ and $\tau_I = 2.5$ min. Results using these settings are shown as the dashed lines. The DP response is a long-period (4 h) oscillation with increasing amplitude, indicating instability.

Increasing the integral time to 30 min (shown in the dotted lines) increases the period of oscillation to 7 h, but the magnitude of the oscillation is slowly decaying. The solid lines give the response when a proportional-only temperature controller is used with $K_C = 5$ (about half the ultimate gain).

These results are due to the system acting as a pure integrator with respect to propane. A very small amount comes in with the fresh feeds, and it all must leave from the DP. If a PI controller is used, the process is an integrator and the controller has another integrator. Two integrators in series make the feedback control problem difficult. A simple solution to this problem is to use a proportional-only temperature controller. The inherent offset of a proportional-only controller did not adversely affect the performance of the column. Propane purity was held quite close to its specification despite the offset in the temperature controller.

All liquid level loops are proportional with $K_C = 2$, except the DP reflux-drum level control that used a $K_C = 5$ due to the use of reflux to control level. Higher gains could have been used in the level controllers in the reactors to keep a more constant volume for reactions.

**TABLE 7.7 Controller Parameters**

| | Reactor | Deisobutanizer Stage 50 | Deisobutanizer Sidestream | Deisobutanizer Distillate | Depropanizer Stage 5 |
|---|---|---|---|---|---|
| | TCR | TC1 | CC$y_S$ | CC$x_D$ | TC2 |
| SP | 68.5 °F | 162.2 °C | 0.95 $nC_4$ | 0.0433 $nC_4$ | 136.4 °F |
| Transmitter range | 0–100 °F | 100–200 °C | 0.9–1 | 0–0.1 | 100–200 °F |
| OP | 227 hp | 3.37 Gcal/h | 61 lb-mol/h | 85 Klb/h[a] | $0.66 \times 10^6$ Btu/h |
| OP range | 0–826 hp | 0–1.68 Gcal/h | 0–150 lb-mol/h | 0–171 Klb/h | 0–$1.76 \times 10^6$ Btu/h |
| Deadtime | 1 min | 1 min | 3 min | 3 min | 1 min |
| $K_C$ | 6.8 | 0.20 | 2.8 | 4.9 | 5 |
| $\tau_I$ (min) | 9.2 | 6.6 | 46 | 28 | 9999 |

[a]Mass flowrate of reflux.

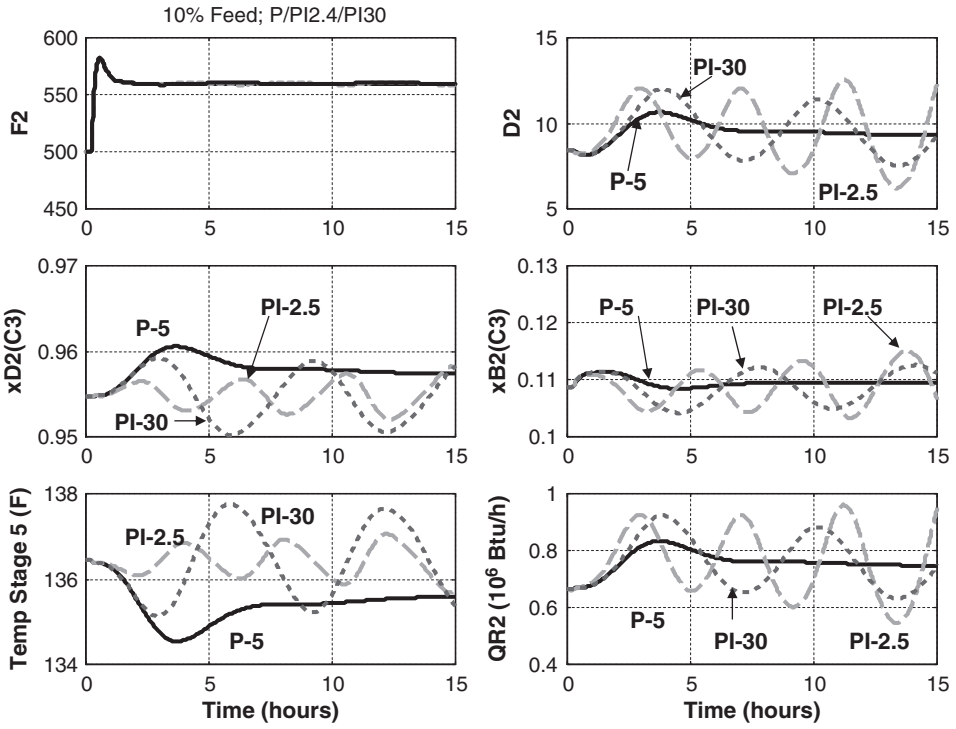


**Figure 7.9.** Depropanizer temperature control (P and PI).

However, using gains of two results in more constant residence times and also helps to smooth out flow disturbances.

### 7.6.3 Dynamic Performance

Figure 7.10 shows the responses of the entire process for 20% disturbances in the setpoint of the total BB feed flow controller. The solid lines are for a 20% increase. The dashed lines are for a 20% decrease. Stable regulator control is achieved by the control structure with the three product streams held close to their desired specifications.

Notice the large changes in the fresh $C_4$ flowrate. This variable controls the liquid level in the DIB reflux drum. The change in BB feed immediately changes the recycle flowrate due to the ratio. This affects the level in the reflux drum. For the 20% *increase* in throughput, the fresh $C_4$ feed goes through a dynamic transient where the flowrate increases by a factor of three.

For the 20% *decrease* in throughput, the fresh $C_4$ feed shuts off completely for almost 5 h. The output signal from the proportional level controller ($K_C = 2$) goes to zero when the level reaches 25% of scale. The design value of 5 min of holdup is sufficiently large to let the system ride through this disturbance without losing liquid level in the reflux drum. Remember the reflux-drum level loop has the Stage 50 temperature loop nested inside it, so the dynamics are not fast. A larger reflux drum may be necessary for larger disturbances.

The proportional temperature controller in the DP is able to hold the composition of the distillate product quite close to desired purity. Notice that there are large changes in the

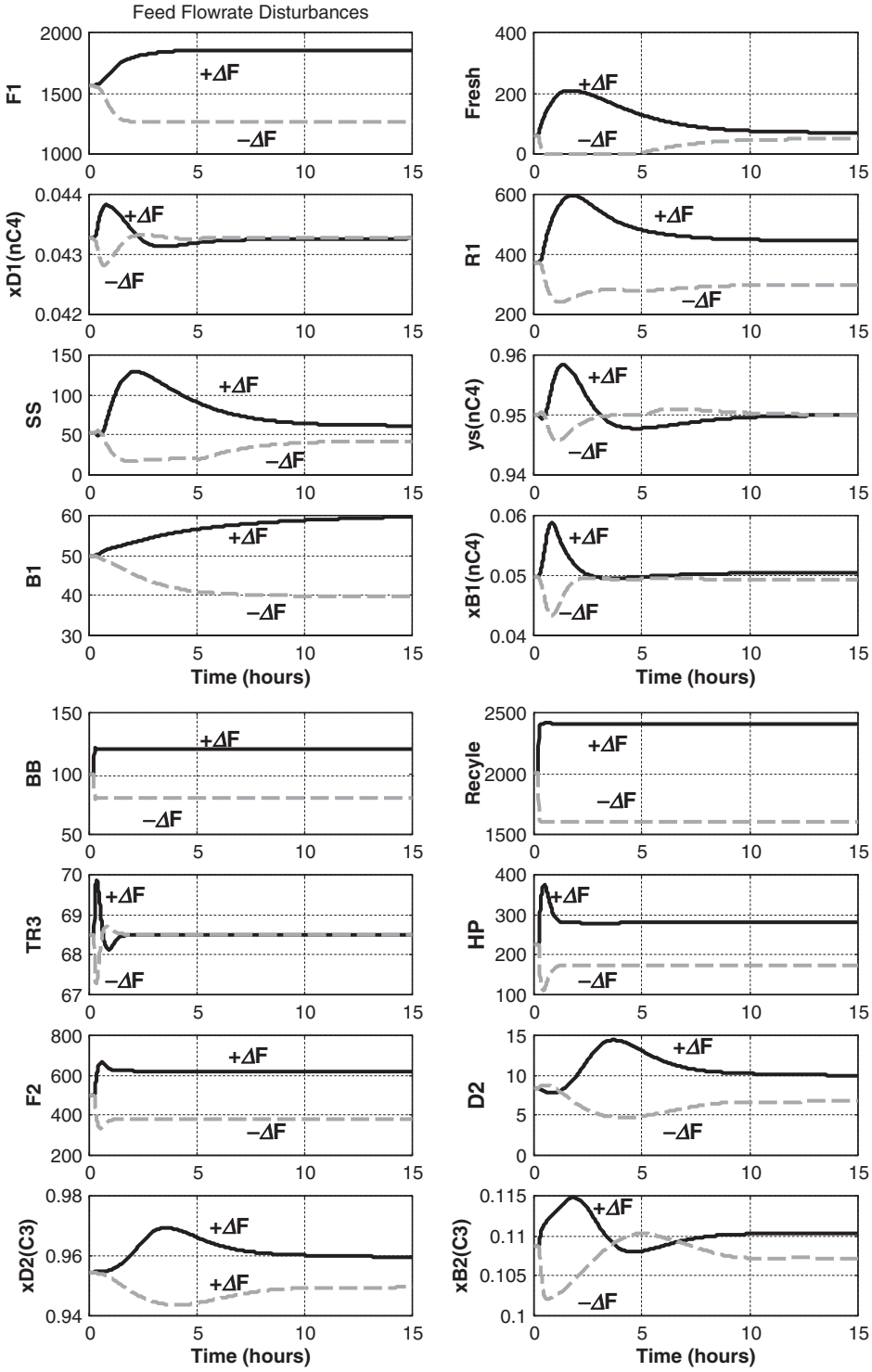


**Figure 7.10.** 20% disturbances in BB fresh feed.

flowrate of the vapor sidestream from the DIB. The control valve in this line must be sized for this rangeability.

Figure 7.11 gives results for two composition disturbances. The solid lines are for a change in the fresh BB feed composition. The 1-butene composition is increased from 50 to 55 mol%, while the isobutane composition is reduced from 20 to 15 mol%. Thus more olefin is fed, which should produce more alkylate and require more isobutane. But less isobutane comes in with this stream, so an increase in the fresh $C_4$ stream must occur to satisfy the reaction stoichiometry. The top right graph in Figure 7.11 shows that the fresh $C_4$ feed increases. More alkylate ($B_1$) is produced. Since there is more reaction occurring, compressor horsepower increases to maintain reactor temperature.

The dashed lines in Figure 7.11 are for a disturbance in the composition of the fresh $C_4$ feed. The isobutane composition is reduced from 50 to 45 mol%, while the propane composition is increased from 5 to 10 mol%. Since the same amount of 1-butene is coming into the process, the same amount of isobutane is needed for reaction. This means that the fresh $C_4$ stream, with its lower isobutane concentration, must increase to provide the same amount of isobutane. It also means that much more propane and *n*-butane will enter the system and need to be purged. These effects are clearly seen in Figure 7.11. Recycle and BB flowrates and compressor power are unchanged. Fresh $C_4$ increases, alkylate production (B1) stays the same, propane purge (D2) increases, and sidestream (SS) increases.

Figure 7.12 shows the controller faceplates from the Aspen Dynamics simulation. Notice that there are three flow controllers on cascade: the total isobutane recycle flow controller ($FC_{tot}$), the sidestream flow controller (FCS), and the DP distillate flow controller (FCD2). These controllers receive their setpoint signals from multipliers or other controllers.

These results demonstrate that the proposed plantwide control structure provides effective dynamic control of the alkylation process in the face of quite large disturbances.

## 7.7 CONCLUSION

The alkylation process exhibits some interesting design and control features. It provides a classical example of the engineering trade-off between reactor size and recycle flowrate. Achieving high olefin conversion requires large reactors or high temperatures. Achieving high selectivity for the alkylate product requires low temperatures or high recycle flowrates.

Auto-refrigerated cooling using a compressor adds an additional feature to the analysis. Since low reactor temperature reduces reactor pressure, compressor work increases as reactor temperature is lowered when using larger reactors.

An apparently minor change in the flowsheet has a big effect on the energy requirements. Feeding the fresh $C_4$ feed into the DIB instead of directly into the reactor causes a significant reduction in reboiler heat input to this column. The energy consumption in the DIB is very sensitive to its feed composition, and mixing the fresh $C_4$ stream (50 mol% isobutane concentration) with the recycle stream (90 mol% isobutane) affects concentrations in the reactor and DIB feed.

Effective dynamic control of the multiunit process is achieved by the use of conventional controllers. The total isobutane recycle flowrate is ratioed to the olefin feed stream. Deisobutanizer reflux-drum level is controlled by the flowrate of fresh $C_4$ fed into the column. This loop depends on the temperature loop, so its action is fairly slow. A proportional-only temperature controller is used in the DP to prevent cycling due to having two integrators in the loop since the process acts as a pure integrator in terms of propane

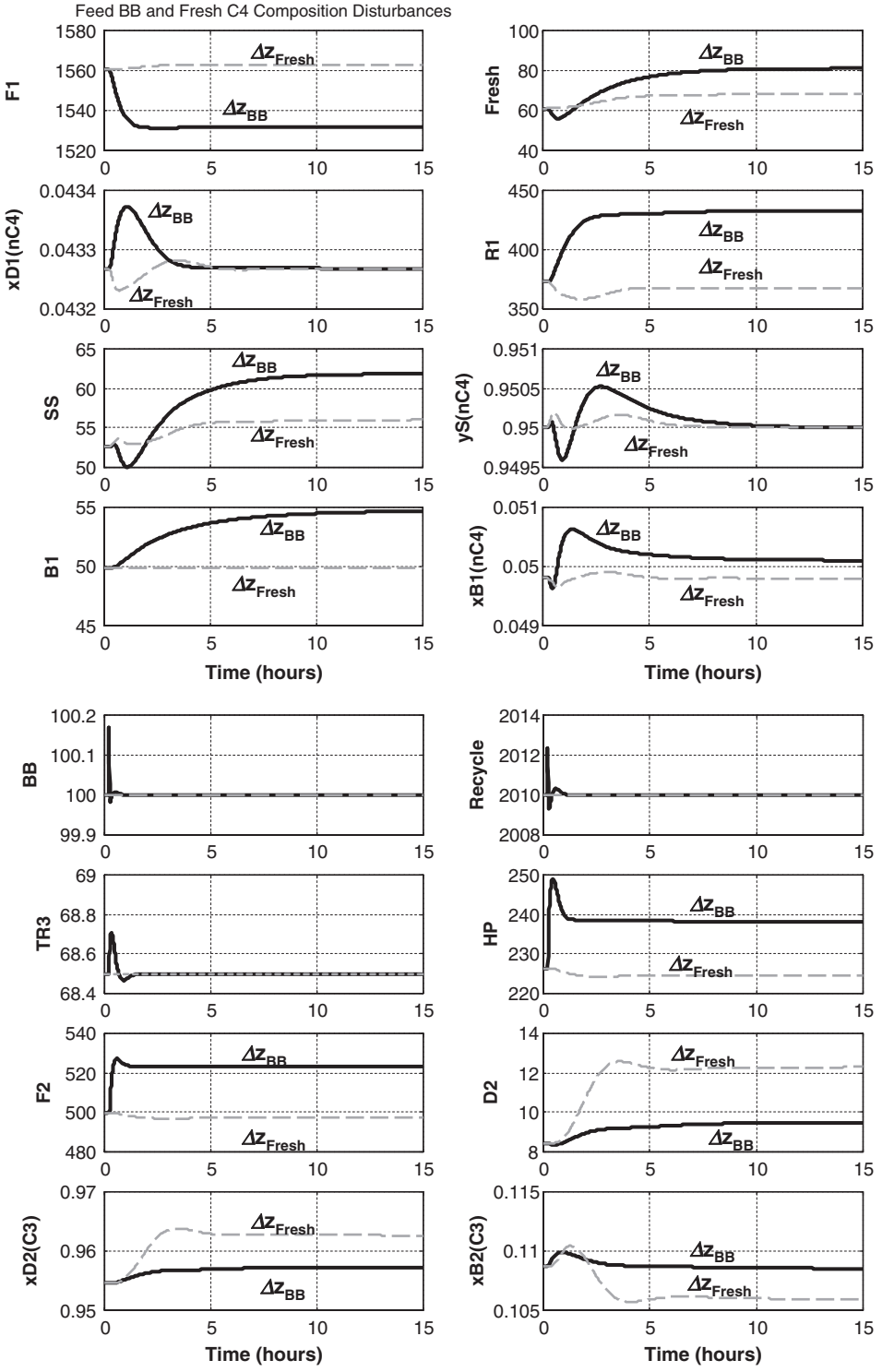


**Figure 7.11.** Disturbances in BB composition or fresh $C_4$ composition.

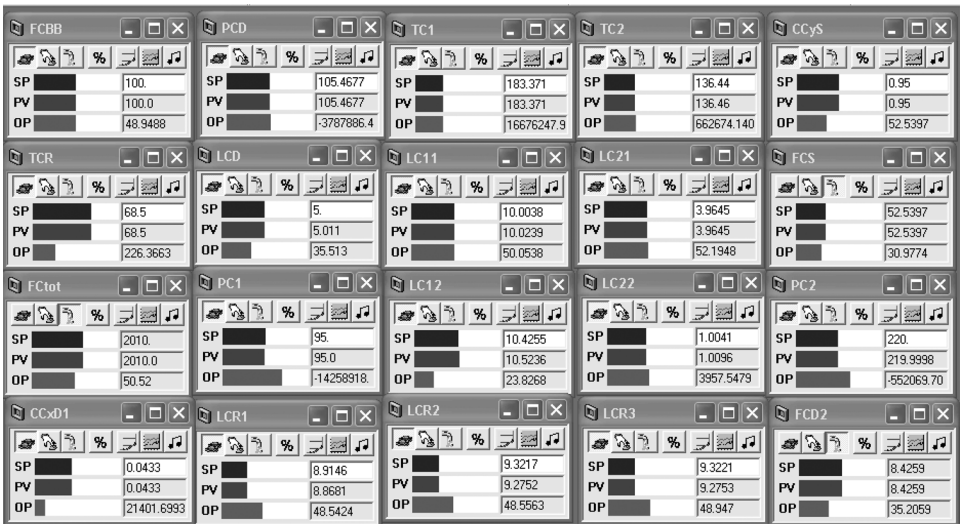


**Figure 7.12.** Controller faceplates.

accumulation. Large disturbances in throughput and feed compositions are handled with products held close to their specified values.

## REFERENCES

1. Mahajanam, R. V., Zheng, A., Douglas, J. M. A shortcut method for control variable section and its application to the butane alkylation process, *Ind. Eng. Chem. Res.* 2001, **40**, 3208.
2. Luyben, W. L. Use of dynamic simulation to converge complex process flowsheets, *Chem. Eng. Ed.* 2004, **38**, 2.
3. Luyben, W. L., Tyreus, B. D., Luyben, M. L. *Plantwide Process Control*, McGraw-Hill, New York, 1999.

# CHAPTER 8

# DESIGN AND CONTROL OF THE BUTYL ACETATE PROCESS

Butyl acetate can be produced by the reaction of methyl acetate with butanol in a reversible, liquid-phase, mildly exothermic reaction. Methanol is the second product. The chemical equilibrium constant is less than unity, so the reactor effluent contains significant amounts of the reactants, which must be recovered for recycle back to the reactor. The volatilities are such that there are three distillation columns and two recycle streams. The nonideal vapor–liquid equilibrium (VLE) results in two azeotropes that must be considered. The first column (C1) takes the two light components overhead (methyl acetate and methanol) and the two heavy components out the bottom (butanol and butyl acetate). The C1 distillate is fed to a second column that produces product methanol out the bottom and a recycle stream of the methyl acetate/methanol azeotrope in the distillate. The C1 bottoms is fed to a third column that produces product butyl acetate out the bottom and a recycle stream of butanol in the distillate.

Since the butanol recycle is vaporized only once and the methyl acetate recycle is vaporized twice, we would intuitively expect the economically optimum design of this process to feature larger butanol recycle flowrates than methyl acetate recycle flowrates.

This chapter demonstrates that this expectation is not fulfilled. The butanol recycle column must be operated at high pressure to avoid the butanol/butyl acetate azeotrope, so a higher-temperature, more costly heat source is needed to recycle butanol. Other design optimization variables include reactor temperature, reactor size, and butanol recycle composition. A plantwide control structure is also developed, and its effectiveness in the face of very large disturbances is demonstrated by dynamic simulation.

*Principles and Case Studies of Simultaneous Design*, First Edition. William L. Luyben

## 8.1 INTRODUCTION

Jimenez and Costa-Lopez[1] reported work on the production of butyl acetate and methanol by reacting methyl acetate and butanol in a reactive distillation column. The feed stream was a mixture of methyl acetate and methanol, which came from an upstream poly vinyl alcohol process. They proposed reacting the methyl acetate with butanol to form butyl acetate and methanol. This liquid-phase reaction is reversible with an equilibrium constant of about unity. Kinetics are quite fast, and heat effects are small.

In their first paper, Jimenez and Costa-Lopez[2] gave useful information dealing with reaction equilibrium and kinetics, which are used in this chapter. In their second paper, they studied a four-column process in which the key unit was a reactive distillation column (Jimenez and Costa-Lopez[1]). The presence of a minimum boiling azeotrope between methyl acetate and methanol prevents the use of just a single reactive column because any unreacted methyl acetate that leaves the reaction zone will go out the top of the column with the methanol.

Jimenez and Costa-Lopez[1] claimed that an extractive agent (*o*-xylene) must be added to the reactive distillation column. Of course this means the entrainer must be recovered in a subsequent column. In addition, there is the inevitable contamination of products with small amounts of the entrainer. Gangadwala et al.[3] studied a reactive distillation process for the production of butyl acetate from the reaction of butanol with acetic acid.

Luyben et al.[4] studied both a conventional multiunit flowsheet and a reactive distillation flowsheet for butyl acetate production. They used simplified and heuristic economic optimization to develop the two flowsheets.

In this chapter, we extend previous work by examining in more detail the conventional process with a reactor and three distillation columns. Rigorous economic analysis is used to determine the optimum flowrates of the two recycle streams. The conclusion is counterintuitive: the optimum methyl acetate recycle is larger than the butanol recycle.

A plantwide dynamic control structure is developed and tested. The commercial simulation products AspenPlus and AspenDynamics are used in this study.

## 8.2 CHEMICAL KINETICS AND PHASE EQUILIBRIUM

### 8.2.1 Chemical Kinetics and Chemical Equilibrium

The liquid-phase reversible reaction considered is

$$\mathrm{MeAc} + \mathrm{BuOH} \iff \mathrm{MeOH} + \mathrm{BuAc}$$

The kinetics for the forward and reverse reactions are based on those given by Jimenez and Costa-Lopez.[1] Their reaction rates are given in units of $\mathrm{mol/min/g_{cat}}$ and must be converted to units acceptable to Aspen Plus, which are $\mathrm{kmol/s/m^3}$ of reactor volume. Assuming a catalyst bulk density of $2000\ \mathrm{kg/m^3}$, the kinetic expressions used are given below with the overall reaction rate $\Re$ having first-order dependence on the two reactants and products. Concentrations are in molality ($\mathrm{kmol/m^3}$). Activation energies are in kJ/kmol and temperature is in K.

$$\begin{aligned} \Re &= k_F C_{\mathrm{MeAC}} C_{\mathrm{BuOH}} - k_R C_{\mathrm{MeOH}} C_{\mathrm{BuAc}} \\ k_F &= 7 \times 10^6 e^{-71{,}960/RT} \\ k_R &= 9.467 \times 10^6 e^{-72{,}670/RT} \end{aligned} \tag{8.1}$$

Notice that the activation energies are essentially the same, which means that the heat of reaction is small and also that the equilibrium constant decreases only slightly with increasing temperature.

Figure 8.1 shows the temperature dependence of the forward and reverse specific reaction rates ($k_F$ and $k_R$) and the chemical equilibrium constant ($K_{EQ}$). Later in the chapter we will justify the selection of a reactor temperature of 350 K so that specific reaction rates are high enough to drive the reaction essentially to equilibrium in a small 4 $m^3$ continuous stirred-tank reactor (CSTR).

Notice that the forward reaction rate depends on the product of the two reactant concentrations $C_{MeAc}C_{BuOH}$. The same production rate can be achieved by having any number of reactant concentrations, just so the product of the concentrations is the same. Methanol concentration could be large and butanol concentration could be small. Or the reverse could be true. These concentrations depend on the relative flowrates of the two recycles.

The second-order reaction and system are similar to that studied almost two decades ago using ideal vapor liquid equilibrium (Tyreus and Luyben[5]). In this previous work, there were two recycle streams, one heavy recycle stream from the bottom of the first distillation column and a second light recycle stream from the top of another distillation column. The economics favored using a larger amount of heavy recycle than light recycle because the heavy recycle did not have to be vaporized. This result is intuitive, and we would expect it to be generally true in many processes with similar chemistry, phase equilibrium, and flowsheet topology.

The process considered in the present work uses real chemicals that exhibit nonideal VLE behavior and require energy inputs with different costs, depending on the temperature level in the base of the column. The result of these differences between ideal and nonideal systems is the counterintuitive result that there should be more light recycle than heavy recycle.

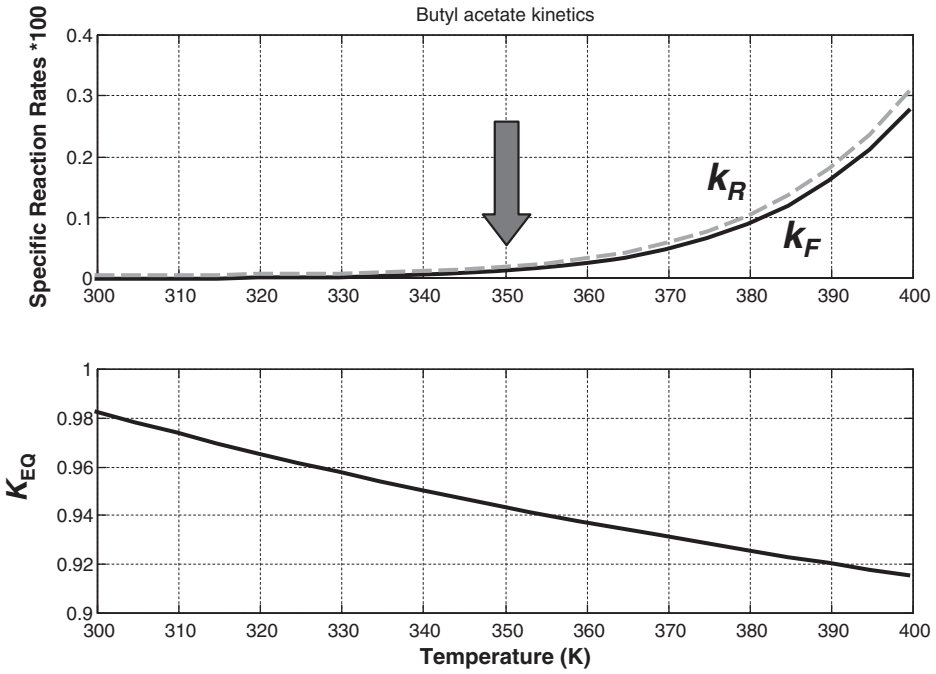


**Figure 8.1.** BuAc kinetics.

### 8.2.2 Vapor–Liquid Equilibrium

The phase equilibrium of this four-component system is complex because of the existence of two binary azeotropes. Using NRTL physical properties (as recommended by Jimenez and Costa-Lopez[1]), Aspen Plus predicts two binary azeotropes:

1. Methyl acetate and methanol form a homogeneous minimum-boiling azeotrope with composition of 66.13 mol% methyl acetate at 1.1 atm and 329.2 K. See Figure 8.2.
2. Butanol and butyl acetate form a homogeneous minimum-boiling azeotrope with composition of 78.06 mol% butanol at 1 atm and 389.9 K. See Figure 8.3a. At 2 atm, the azeotropic composition is 95.72 mol% butanol. The azeotrope disappears when the pressure is *raised* to about 3 atm. However, a severe pinch in the high butanol end of the *xy* curve still exists. An operating pressure of 4 atm is used in this study to lessen the pinch (see Figure 8.3b), but a distillate purity of only 90 mol% butanol is found to be the economic optimum for the butanol recycle stream. At 4 atm pressure, the base temperature in the distillation column of 459 K requires the use of high-pressure steam (42 atm).

The first azeotrope means that any columns that are separating methyl acetate from methanol can produce high-purity methanol in the bottoms but can only produce a distillate that has a composition near the azeotropic composition. In this work, the methyl acetate recycle column is specified to produce a distillate with a composition of 64 mol% methyl acetate. A column pressure of 1.1 atm gives a reflux-drum temperature of 329 K, which permits the use of cooling water in the condenser.

The second azeotrope has an unusual pressure dependence. In most chemical systems, increasing pressure moves the composition of the azeotrope to the left (it becomes less rich in the lighter component). But the opposite effect is displayed in the butanol/butyl acetate system, as shown in Figure 8.3. In this study, the butanol column separating butanol and butyl acetate operates at 4 atm. If this separation were conducted at lower pressure, the

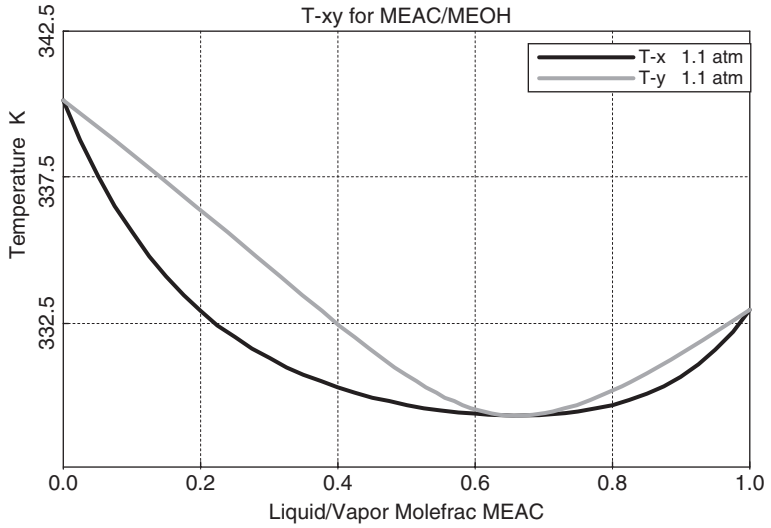


**Figure 8.2.** Methyl acetate/methanol VLE at 1.1 atm.

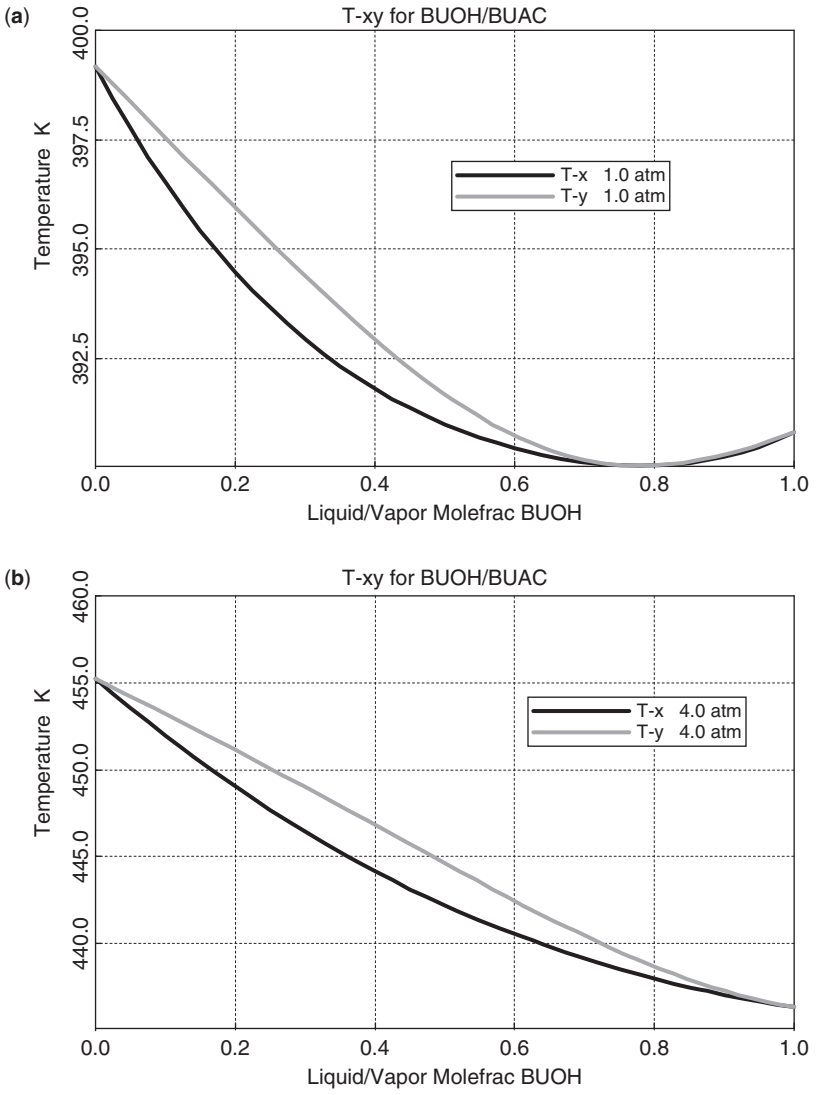


**Figure 8.3.** Butanol/butyl acetate VLE (a) at 1 atm, and (b) 4 atm.

butanol recycled back to the reactor would have a higher concentration of the impurity butyl acetate. This would reduce the per-pass conversion and require larger recycle flows.

However, the disadvantage of operating at high pressure is a high base temperature in the distillation column. It would be 399 K if the column were operated at 1 atm, but base temperature increases to 459 K when operating at 4 atm. This means that high-pressure steam at about 527 K must be used in the reboiler (42 atm steam), which is more expensive than the 433 K (6 atm) steam that could be used with a low-pressure column.

However, there is an advantage in operating a high-pressure butanol/butyl acetate column. The reflux-drum temperature at 4 atm is 437 K, which is high enough to permit heat integration with one of the other columns in the process (the methanol column C2,

which has a reboiler temperature of about 344 K). The use of heat integration is not included in this study but would obviously reduce energy consumption.

The butanol/butyl acetate separation is somewhat difficult and therefore requires a distillation column with a modest reflux ratio (RR = 1.92) and a modest number of stages (47).

## 8.3 PROCESS FLOWSHEET

Figure 8.4 gives the flowsheet of the process after economic optimization, to be discussed in Section 8.4. Flowsheet stream conditions, equipment sizes, and heat exchanger heat duties are provided.

### 8.3.1 Reactor

Fresh feed with composition 60 mol% methyl acetate and 40 mol% methanol and flowrate 100 kmol/h is fed into a 4 $m^3$ reactor, which operates at 350 K and 5 atm. The residence time in the reactor is about 6 min since the kinetics are fast and chemical equilibrium is quickly attained. Fresh butanol (59.4 kmol/h) is added to a butanol recycle stream (120.6 kmol/h, 90 mol% butanol, 10 mol% butyl acetate) to give a total butanol stream ($B_{tot}$) of 180 kmol/h, which is fed into the reactor. A methyl acetate/methanol recycle (171.2 kmol/h, 64 mol% methyl acetate, 36 mol% methanol) is combined with the feed stream (100 kmol/h), giving a total methyl acetate/methanol stream ($M_{tot}$) of 271.2 kmol/h, which is fed to the reactor. These two total streams ($B_{tot}$ and $M_{tot}$) will be the major design optimization variables. The

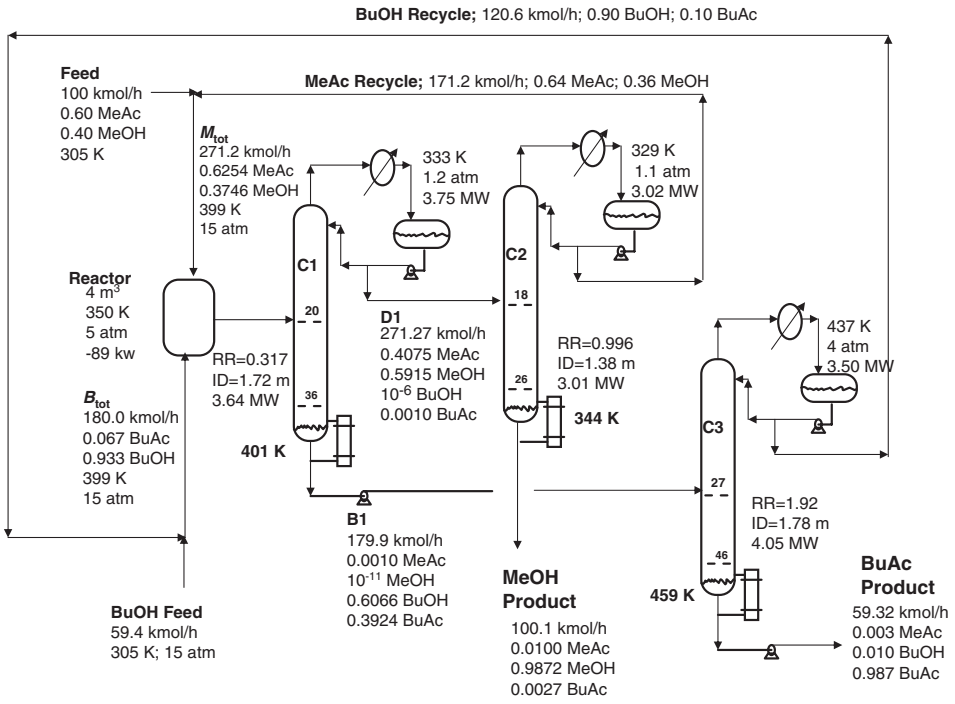


**Figure 8.4.** Proposed flowsheet.

per-pass conversion of methyl acetate is about 34%. A small amount of heat (89 kW) must be removed from the reactor.

### 8.3.2 Column C1

Reactor effluent is fed to column C1, which splits the two light components from the two heavy components. Methyl acetate and methanol are taken overhead while butanol and butyl acetate leave in the bottoms. The column has 37 stages and is fed on Stage 20. We use the Aspen tray-numbering convention of counting trays from the top with the condenser as Stage 1.

The specifications for this column are somewhat unusual. The key components are not adjacent in terms of boiling points. The normal boiling points of methyl acetate, methanol, butanol, and butyl acetate are 330.1, 337.8, 390.8, and 399.3 K, respectively. So the separation in this column should be to keep butanol from going overhead and methanol from going out the bottom. But as the stream data given in Figure 8.4 show, the concentration of butanol in the distillate is much lower than the concentration of butyl acetate. In the bottoms, the concentration of methanol is much lower than the concentration of methyl acetate. This odd behavior may be the result of the azeotropes. The specification for the distillate is 0.1 mol% butyl acetate.

The specification for the bottoms is that the sum of the methanol and the methyl acetate is 0.1 mol%. For some values of parameters, the dominant impurity in the bottoms is methanol, but for other values of parameters, the dominant impurity in the bottoms is methyl acetate. The sum of the compositions is obtained in the *Radfrac* model in Aspen Plus by selecting both components as the *Selected component* in the *Design spec* feature.

The required RR in column C1 is 0.317 and reboiler heat duty is 3.64 MW. Low-pressure steam is used in the reboiler (433 K at 6 atm) since the base temperature is 401 K. The column operates with a condenser pressure of 1.2 atm, which gives a reflux-drum temperature of 333 K and permits the use of cooling water in the condenser.

### 8.3.3 Column C2

The distillate stream from column C1 is fed to column C2, which produces high-purity (98.72 mol%) methanol out the bottom and a distillate stream with a composition (64 mol% methyl acetate) near the azeotrope. The distillate is recycled back to the reactor at a rate of 171.2 kmol/h. The column has 27 stages and is fed on Stage 18.

The specifications are 64 mol% methyl acetate in the distillate and 0.1 mol% methyl acetate in the bottoms. To achieve these specifications, the RR is 0.996 and reboiler heat duty is 3.01 MW. Low-pressure steam is used in the reboiler since the base temperature is 344 K. The column operates with a condenser pressure of 1.1 atm, which gives a reflux-drum temperature of 329 K and permits the use of cooling water in the condenser.

### 8.3.4 Column C3

The bottoms from C1 is fed to column C3, which produces high-purity (98.7 mol%) butyl acetate out the bottom and a butanol-rich distillate (90 mol%) that is recycled back to the reactor at a rate of 120.6 kmol/h. The column has 47 stages and is fed on Stage 27.

The specifications are 0.1 mol% butanol in the bottoms and 10 mol% butyl acetate in the distillate. To achieve the specifications, the RR is 1.92 and reboiler heat duty is 4.05 MW.

Since the base temperature is 459 K, high-pressure steam (527 K at 42 atm) must be used in the reboiler.

The column operates with a condenser pressure of 4 atm, which gives a reflux-drum temperature of 437 K. As noted earlier, this temperature is high enough to permit heat integration with the low-temperature reboiler (344 K) in column C2.

The total energy consumption of the three columns in this flowsheet is 10.7 MW, not considering any heat integration. Using a price of \$7.78/GJ for low-pressure steam (columns C1 and C2) and \$9.83/GJ for high-pressure steam (column C3), the total energy cost of the process is \$2,888,000/yr.

Figures 8.5 through 8.7 give temperature and composition profiles for the three distillation columns. The control system developed later in Section 8.5 will use these temperature profiles to select appropriate trays for temperature control.

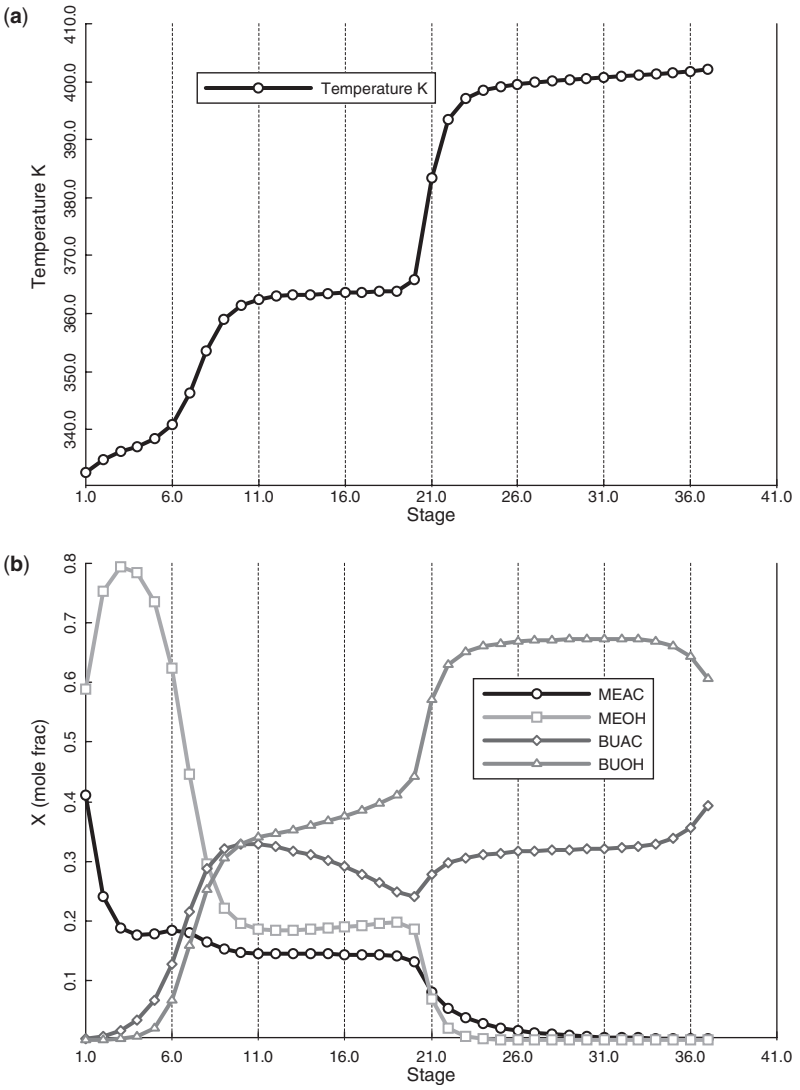


**Figure 8.5.** Column C1 (a) temperature profile, and (b) composition profiles.

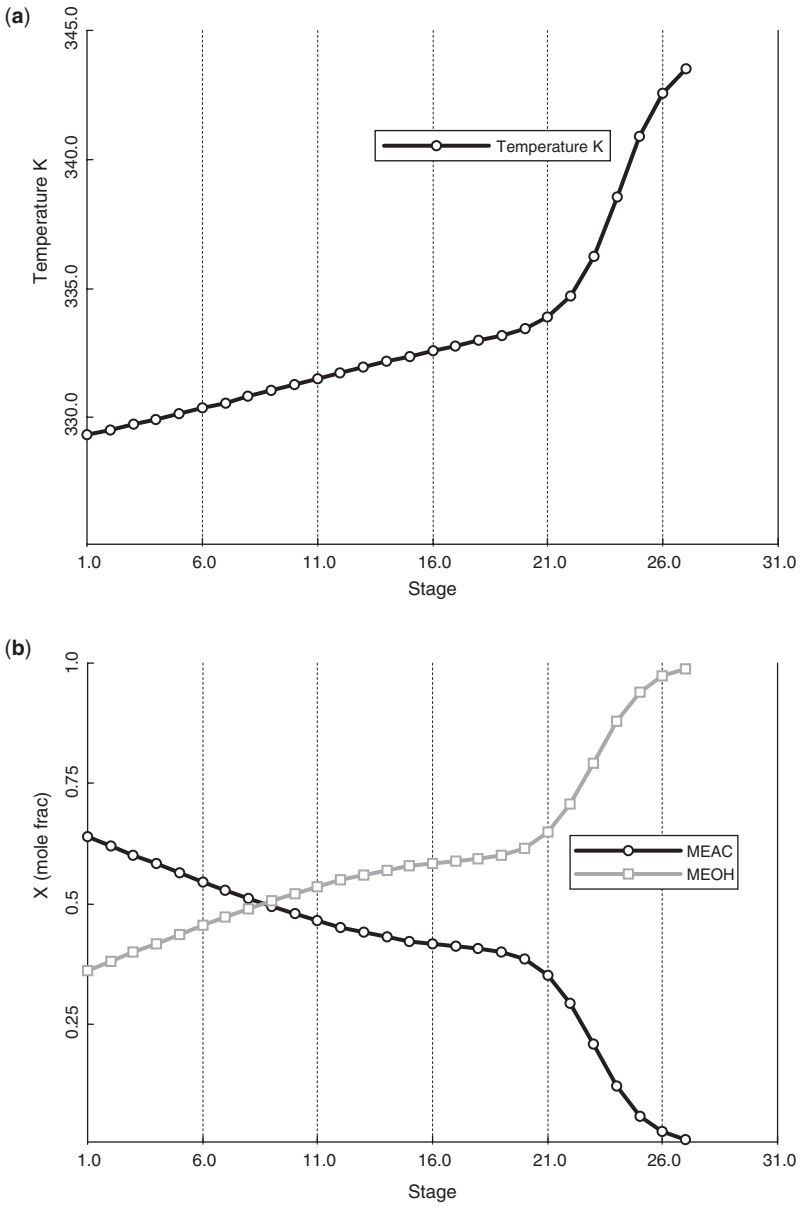


**Figure 8.6.** Column C2 (a) temperature profile, and (b) composition profiles.

### 8.3.5 Flowsheet Convergence

Convergence of steady-state simulators when recycle streams are present can be very difficult. The butyl acetate process has two recycle streams, which can present problems. However, successful and robust convergence was achieved by using the strategy of fixing the total butanol flowrate $B_{\text{tot}}$ entering the reactor (see Figure 8.4) by varying the fresh feed of butanol. A *Flowsheet design spec* in Aspen Plus is used for this objective.

The fresh feed stream, which is a mixture of methyl acetate and methanol, is fixed at 100 kmol/h. A value of $B_{\text{tot}}$ is specified, and the flowsheet is converged. There is a

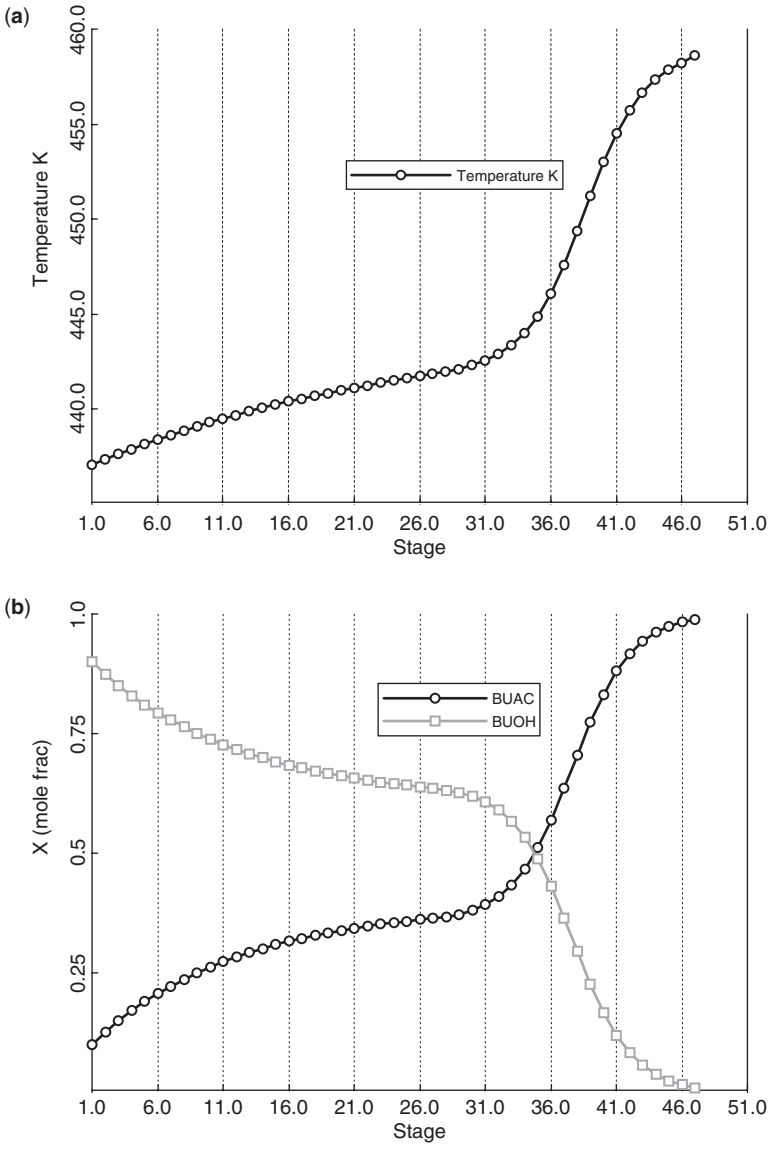


**Figure 8.7.** Column C3 (a) temperature profile, and (b) composition profiles.

unique value of the methyl acetate/methanol azeotrope recycle that is required to convert essentially all the methyl acetate in the feed stream into butyl acetate. The recycle is the distillate D2 from column C2. The sum of the fresh feed and the recycle is labeled $M_{\text{tot}}$.

In the next section we will see the effects of selecting various values of $B_{\text{tot}}$ on the required $M_{\text{tot}}$ and the resulting economics of the process. As $B_{\text{tot}}$ is increased, $M_{\text{tot}}$ decreases. Increasing $B_{\text{tot}}$ increases separation costs in column C3, but the corresponding decreases in $M_{\text{tot}}$ reduce the separation costs in column C2. So there is a trade-off between these two variables.

## 8.4 ECONOMIC OPTIMUM DESIGN

The butyl acetate process has a large number of design optimization variables: two recycle flowrates, reactor size and temperature, number of trays in each column, feed-tray locations, and two recycle compositions. The major trade-off is between heavy recycle (distillate D3, the butanol recycle from column C3) and light recycle (distillate D2, the methyl acetate/methanol azeotrope recycle from column C2). In the following sections, we consider all of these variables and their effects on the economics of the process.

Total annual cost (TAC) is used as the economic parameter to be minimized since it takes into account both capital and energy costs. Table 8.1 gives the relationships used for sizing equipment and for determining capital and energy costs as given in Chapter 5.

The fresh feed flowrate of the methyl acetate/methanol mixture is fixed in all cases at 100 kmol/h. This feed stream contains 60 kmol/h of methyl acetate, so the amount of butyl acetate leaving the process is essentially 60 kmol/h in all cases since the losses of methyl acetate are kept very small by the separations specified in the distillation columns. There are 40 kmol/h of methanol entering in the fresh feed stream. The reaction generates 60 kmol/h of methanol. So the methanol leaving from the bottom of column C2 is essentially 100 kmol/h.

### 8.4.1 Reactor Size and Temperature

As shown in Figure 8.1, the chemical equilibrium constant decreases slightly with increasing reactor temperature, so low reactor temperature increases conversion. However, specific reaction rates at low temperatures are small, so reaction kinetics limit conversion.

**TABLE 8.1 Basis of Economics and Equipment Sizing**

Column diameter: Aspen tray sizing
Column length: NT trays with 2-ft spacing plus 20% extra length
Column and reactor vessel (diameter and length in meters)
Capital cost $= 17{,}640(D)^{1.066}(L)^{0.802}$

*Condensers (area in $m^2$)*
Heat-transfer coefficient $= 0.852\ \text{kW/K-m}^2$
Differential temperature = Reflux-drum temperature − 310 K
Capital cost $= 7296\ (A)^{0.65}$

*Reboilers (area in $m^2$)*
Heat-transfer coefficient $= 0.568\ \text{kW/K-m}^2$
Differential temperature = 34.8 K
Capital cost $= 7296\ (A)^{0.65}$

*Energy cost*
LP steam $= \$7.78/10^6$ GJ
HP steam $= \$9.83/10^6$ GJ

$$\text{TAC} = \frac{\text{Capital cost}}{\text{Payback period}} + \text{Energy cost}$$

Payback period = 3 yr

Table 8.2 shows the effects of changing reactor temperature or reactor size. Total butanol ($B_{tot}$) is fixed at 180 kmol/h. In the upper table, reactor volume is set at 2 $m^3$ and reactor temperature is varied. The methyl acetate plus fresh feed flowrate ($M_{tot}$) is used as a simple measure of separation costs. $M_{tot}$ reaches a minimum at about 350 K, so this reactor temperature is selected.

In the lower table, reactor temperature is fixed at 350 K and reactor volume is varied. $M_{tot}$ decreases as reactor size is increased, but there is little change when reactor volume exceeds about 4 $m^3$, so this volume is selected.

### 8.4.2 Butanol Recycle and Composition

With reactor temperature set at 350 K and reactor volume fixed at 4 $m^3$, the design optimization variable $B_{tot}$ was changed over a range of values, and the economics of the process were evaluated. These calculations were repeated for several values of the butyl acetate impurity in the butanol recycle from column C3. Capital costs include the reactor, three distillation columns, three condensers, and three reboilers. Energy costs are the reboiler heat inputs of the three columns. The cost of the low-pressure steam used in the reboilers of columns C1 and C2 is \$7.78/GJ. The cost of the high-pressure steam used in the reboiler of column C3 is \$9.83/GJ.

Figure 8.8 give results over a broad range of butanol recycle flowrates and for three values of butanol recycle composition. The butanol recycle is expressed in terms of $B_{tot}$, which is the total butanol fed to the reactor (sum of distillate D3 from column C3 and fresh feed of butanol).

The upper left graph shows that $M_{tot}$ decreases as $B_{tot}$ increases. The separation load is shifting from column C2 (the origin of the methyl acetate recycle) to column C3 (the origin of the butanol recycle). Remember that the composition of the D2 distillate stream is close to the azeotrope. Increasing the butyl acetate impurity $x_{D3(BuAc)}$ in the butanol

**TABLE 8.2 Effect of Reactor Temperature and Size**

| VR = 2 $m^3$ | |
|---|---|
| TR (K) | $M_{tot}$ (kmol/h)[a] |
| 330 | 277.03 |
| 340 | 272.17 |
| **350** | **272.17** |
| 360 | 273.11 |
| 370 | 274.56 |
| 380 | 276.03 |
| 390 | 277.58 |
| 400 | 279.14 |
| TR = 350 K | |
| VR ($m^3$) | $M_{tot}$ (kmol/h)[a] |
| 0.5 | 278.27 |
| 1 | 274.22 |
| 2 | 272.17 |
| 3 | 271.48 |
| **4** | **271.16** |
| 5 | 270.98 |
| 6 | 270.84 |

[a] $B_{tot}$ = 180 kmol/h.

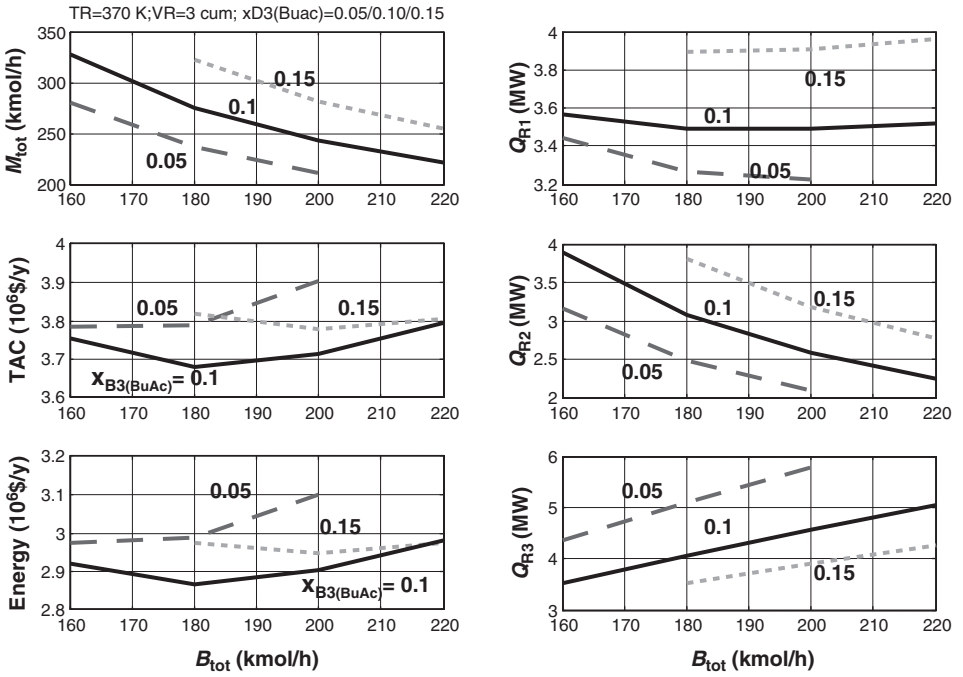


**Figure 8.8.** Effect of BuOH recycle flowrate and composition.

recycle increases the amount of methyl acetate that must be recycled back to the reactor to maintain the specified production rate of products.

The three graphs on the right show how the reboiler heat inputs are affected. The energy required in column C1 ($Q_{R1}$) doesn't change much as $B_{tot}$ changes but does increase slightly as butyl acetate impurity increases. As $B_{tot}$ increases, the energy required in column C2 ($Q_{R2}$) to produce the $M_{tot}$ decreases since $M_{tot}$ decreases, but the energy required in column C3 ($Q_{R3}$) increases.

The butyl acetate impurity has opposite effects on $Q_{R2}$ and $Q_{R3}$. Increasing impurity requires more $M_{tot}$, so $Q_{R2}$ *increases*. Increasing impurity makes the separation in column C3 easier, so $Q_{R3}$ *decreases*.

The middle and bottom graphs on the left side of Figure 8.8 show the net effects of these variables on TAC and total energy cost. Both of these variables go through a minimum at about 180 kmol/h of $B_{tot}$, so this flowrate is selected for the final design. Butyl acetate impurities in the butanol recycle of less than or greater than 10% lead to increases in TAC and energy costs.

The flowsheet shown in Figure 8.4 is the proposed design. The flowrate of $B_{tot}$ is 180 kmol/h, and the impurity in the butanol recycle is 10 mol% butyl acetate. Note that the recycle of the heavy component butanol is *smaller* (120.6 kmol/h) than the recycle of the light component methyl acetate (171.2 kmol/h).

### 8.4.3 Distillation Column Design

In the heuristic discussed in Luyben et al.,[4] approximate methods were used to pick the number of trays in the three columns and feed-tray locations. A more rigorous approach

will be presented in this chapter. The total number of trays is varied in each column to find the minimum TAC. The feed-tray location that minimizes reboiler heat input is found for each value of total stages.

The results show only slight changes from those used in the original work. Column C1 stages are increased from 32 to 37. Column C2 stages are reduced from 32 to 27. Column C3 stages are reduced from 52 to 47.

### 8.4.4 System Economics

The total capital investment in the revised plant is \$2,425,000. The total energy cost is \$2,888,000/yr. Table 8.3 compares the original process with the revised process.

The feed flowrate used in the original paper was 58.1 kmol/h, while the feed flowrate used in this work is 100 kmol/h. Therefore, all flowrates and energy consumptions reported in the original paper were scaled up by a factor of 100/58.1. All capital costs were scaled up using the 0.6 power of this ratio. Column diameters were scaled up using the 0.5 power of this ratio.

**TABLE 8.3 Economic Comparison**

| | | Original | Revised |
|---|---|---|---|
| Flows | BuOH recycle (kmol/h) | 162.5 | 120.6 |
| | MeAc recycle (kmol/h) | 122.7 | 171.2 |
| | $B_{tot}$ (kmol/h) | 222.7 | 180 |
| | $M_{tot}$ (kmol/h) | 222.5 | 271.2 |
| C1 | ID (m) | 1.68[c] | 1.716 |
| | NT | 32 | 37 |
| | NF | 16 | 20 |
| | $Q_C$ (MW) | 3.53[a] | 3.75 |
| | $Q_R$ (MW) | 3.49[a] | 3.64 |
| C2 | ID (m) | 1.20[c] | 1.384 |
| | NT | 32 | 27 |
| | NF | 16 | 18 |
| | $Q_C$ (MW) | 2.19[a] | 3.019 |
| | $Q_R$ (MW) | 2.22[a] | 3.014 |
| C3 | ID (ft) | 2.13[c] | 1.785 |
| | NT | 52 | 47 |
| | NF | 26 | 27 |
| | $Q_C$ (MW) | 4.97[a] | 3.50 |
| | $Q_R$ (MW) | 5.59[a] | 4.05 |
| Reactor | Size ($m^3$) | 9.77[a] | 4.0 |
| Capital | ($10^6$ \$) | 3.38[b] | 2.425 |
| Energy | (MW) | 11.30[a] | 10.70 |
| Energy cost[d] | ($10^6$ \$/yr) | 3.135 | 2.888 |

[a]Flowrates, reactor size, and energy scaled by ratio of feed flowrates (100/58.1).
[b]Capital scaled by ratio of feed flowrates to 0.6 power.
[c]Column diameters scaled by ratio of feed flowrates to 0.5 power.
[d]Energy cost using LP steam for $Q_{R1}$ and $Q_{R2}$; HP steam for $Q_{R3}$.

Table 8.3 shows the revised flowsheet has smaller butanol recycle (162.5 to 120.6 kmol/h) but larger methyl acetate recycle (122.7 compared to 171.2 kmol/h). More material goes overhead in columns C1 and C2, so the heat inputs in these columns are larger in the revised flowsheet ($Q_{R1}$ increases from 3.49 to 3.64 MW and $Q_{R2}$ increases from 2.22 to 3.01 MW). Both of these reboilers use low-pressure steam.

The smaller butanol recycle in the revised flowsheet reduces heat input in column C3. Table 8.3 shows that reboiler heat input $Q_{R3}$ deceases from 5.59 MW in the original flowsheet to 4.05 MW in the revised design. This reboiler uses high-pressure, expensive steam.

The total energy consumption in the revised flowsheet is only slightly lower (11.30 MW compared to 10.70 MW), but the total cost of energy is significantly smaller: \$2,888,000/yr in the revised flowsheet versus \$3,135,000/yr in the original.

The capital cost of the vessels and heat exchangers in columns C1 and C2 are larger in the revised flowsheet because diameters are larger and heat-transfer rates are larger. However, these costs in column C3 are lower because the diameter and heat-transfer rates of C3 are smaller. Since column C3 has more stages than the other columns, its capital cost is larger. The net effect is a smaller total capital in the revised design (\$2,425,000 vs. \$3,380,000).

In the Section 8.5, a plantwide control system is developed and tested for the revised flowsheet.

## 8.5 PLANTWIDE CONTROL

A plantwide control scheme was developed and tested for large disturbances in throughput and feed composition. Proportional integral controllers are used for flows, pressures, and temperatures. Proportional controllers are used for all liquid levels. Deadtimes of 1 min are inserted in the column temperature controllers. Relay-feedback tests are run to determine ultimate gains and periods of the column temperature controllers, and the Tyreus–Luyben controller tuning settings are used.

In all three columns, the effectiveness of using single-end temperature control was explored by using a steady-state "feed-sensitivity analysis." Changes in light- and heavy-key component feed compositions to the column were made, with the distillate and bottoms compositions held at their specified values. The required changes in RR and reflux-to-feed (R/F) ratio were examined. If either of these showed little change with variations in feed composition, a single-end structure might be considered effective.

The location of the tray that will have its temperature controlled was selected by finding the location in the temperature profile in each column where there was a large change in temperature from tray to tray.

### 8.5.1 Column C1

Table 8.4 gives results of the feed-sensitivity analysis. The light-key component is methanol, and the heavy-key component is butanol. The specifications are 0.1 mol% butyl acetate in the bottoms and 0.1 mol% of total methanol and methyl acetate in the distillate. The top part of Table 8.4 shows that there are significant changes in both RR and R/F. So, single-end control may not be effective. This is verified by the dynamic simulation given in Section 8.5.5. Initially, a RR structure will be used.

**TABLE 8.4 Feed Composition Sensitivity Analysis**

| | Feed Composition (Mole Fraction) | Reflux Ratio | Reflux-to-Feed Ratio |
|---|---|---|---|
| C1 | MeOH = 0.3356<br>BuOH = 0.2818 | 0.2434 | 0.1414 |
| Design | MeOH = 0.3556<br>BuOH = 0.2618 | 0.3173 | 0.1908 |
| | MeOH = 0.3756<br>BuOH = 0.2418 | 0.2381 | 0.1480 |
| C2 | MeAc = 0.3875<br>MeOH = 0.6114 | 1.030 | 0.6170 |
| Design | MeAc = 0.4075<br>MeOH = 0.5914 | 0.9960 | 0.6298 |
| | MeAc = 0.4275<br>MeOH = 0.5714 | 0.9649 | 0.6407 |
| C3 | BuOH = 0.5865<br>BuAc = 0.4125 | 1.979 | 1.282 |
| Design | BuOH = 0.6065<br>BuAc = 0.3925 | 1.919 | 1.286 |
| | BuOH = 0.6265<br>BuAc = 0.37925 | 1.857 | 1.286 |

Figure 8.5a shows that there is a significant change in the temperature profile near Stage 22, so this stage is selected for temperature control.

### 8.5.2 Column C2

The middle section of Table 8.4 gives results of the feed-sensitivity analysis. The light-key component is methyl acetate, and the heavy-key component is methanol. The specifications are 0.1 mol% methyl acetate in the bottoms and 64 mol% methyl acetate in the distillate. The changes in both RR and R/F are fairly small. So, single-end control should be effective. The R/F ratio structure is used.

Figure 8.6a shows that there is a significant change in the temperature profile near Stage 25, so this stage is selected for temperature control. This stage is near the bottom of the column, and the methanol product is withdrawn from bottom of the column. So, inferential composition control using temperature should be effective as long as the amount of butyl acetate (or butanol) leaving the top of C1 does not increase. This issue will be considered in Section 8.5.5.

### 8.5.3 Column C3

The bottom section of Table 8.4 gives results of the feed-sensitivity analysis. The light-key component is butanol, and the heavy-key component is butyl acetate. The specifications are 0.1 mol% butanol in the bottoms and 10 mol% butyl acetate in the distillate. The R/F is almost constant, so a single-end control structure should be effective with R/F held constant.

Figure 8.7a shows that there is a significant change in the temperature profile near Stage 41, so this stage is selected for temperature control. This stage is fairly close to the

bottom of the column, and the butyl acetate product is withdrawn from bottom of the column. So, inferential composition control using temperature should be effective. Even if some methyl acetate or methanol should drop out the bottom of C1, these light components will go overhead in C3 and get recycled. They should not affect butyl acetate product purity.

### 8.5.4 Plantwide Control Structure

The control scheme developed for the process is shown in Figure 8.9. The important loops from a plantwide control perspective are the two flow controllers FCM and FCB that control the flowrates of the total methyl acetate and total butanol streams fed to the reactor. The various loops are outlined below:

1. The flowrate of the stream $M_{tot}$ is measured and the flowrate of the fresh methyl acetate/methanol feed is manipulated to keep the total flow at its desired setpoint (271.2 kmol/h at base-case conditions). This total flow is the sum of the fresh feed plus the distillate D2 from column C2. This distillate flow is manipulated to control the level in the C2 reflux drum. If this level increases, the distillate flowrate will increase. But since the total flowrate is fixed, the flowrate of the fresh feed will be reduced by the FCM flow controller.

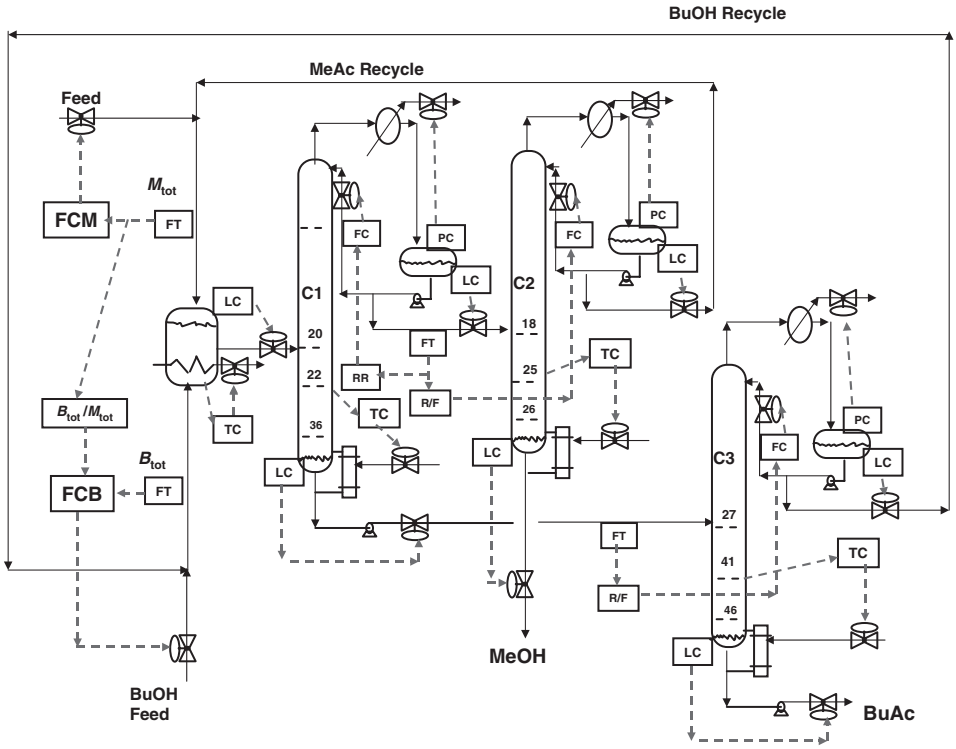


**Figure 8.9.** Initial plantwide control structure.

2. The flowrate of the stream $B_{tot}$ is measured and the flowrate of the fresh butanol feed *BUOH Feed* is manipulated to keep the total flow at its desired setpoint (180 kmol/h at base-case conditions). This total flow is the sum of the fresh butanol feed plus the distillate D3 from column C3. This distillate flow is manipulated to control the level in the C3 reflux drum. If this level increases, the distillate flowrate will increase. But since the total flowrate is fixed, the flowrate of the fresh butanol feed will be reduced by the FCB flow controller. The setpoint of the FCB controller comes from a multiplier. Thus, the total butanol flowrate is ratioed to the total methyl acetate flowrate.
3. Reactor temperature is controlled by manipulating cooling water to the jacket.
4. Reactor liquid level is controlled by manipulating liquid from the reactor.
5. Pressures in all three columns are controlled by manipulating condenser heat removals.
6. Base liquid levels in all three columns are controlled by manipulating bottoms flowrates.
7. Reflux-drum level in column C1 is controlled by manipulating distillate flowrate, which is fed to column C2.
8. The RR in column C1 is controlled by measuring distillate flowrate and sending this signal to a multiplier whose other input is the desired RR (0.317). The output signal from the multiplier is the setpoint of a flow controller on the reflux.
9. The temperature on Stage 22 in column C1 is controlled at 387.2 K by manipulating reboiler heat input.
10. The temperature on Stage 25 in column C2 is controlled at 340.9 K by manipulating reboiler heat input.
11. The reflux in column C2 is ratioed to the feed.
12. The temperature on Stage 41 in column C3 is controlled at 454.5 K by manipulating reboiler heat input.
13. The reflux in column C3 is ratioed to the feed.

The production rate handle in this process is the setpoint of the FCM controller. Table 8.5 gives controller parameters for the column temperature loops.

### 8.5.5 Dynamic Performance

The effectiveness of this plantwide control structure is demonstrated by subjecting the process to feed flowrate and feed composition disturbances. Figure 8.10 gives results for a 20% step decrease in the setpoint of flow controller FCM. At time equal 0.2 h, the setpoint is decreased from 271.2 to 216.9 lb-mol/h (a 20% decrease). The dashed lines are when the control structure outlined above is used.

The top left graph shows that a large transient increase in the butyl acetate impurity going overhead in column C1 occurs. The C1 distillate composition $x_{D1(BuAc)}$ peaks at about 1.7 mol% butyl acetate, which is far from its normal 0.1 mol%. The butyl acetate goes into the downstream column and produces a large transient drop in the purity of the methanol product $x_{B2(MeOH)}$ leaving in the bottoms (top right graph). The reason for this poor performance is the effect of the large step decrease in feed to column C1. The middle left graph in Figure 8.10 shows that the temperature (T1) on Stage 22 rises, which drives butyl acetate overhead.

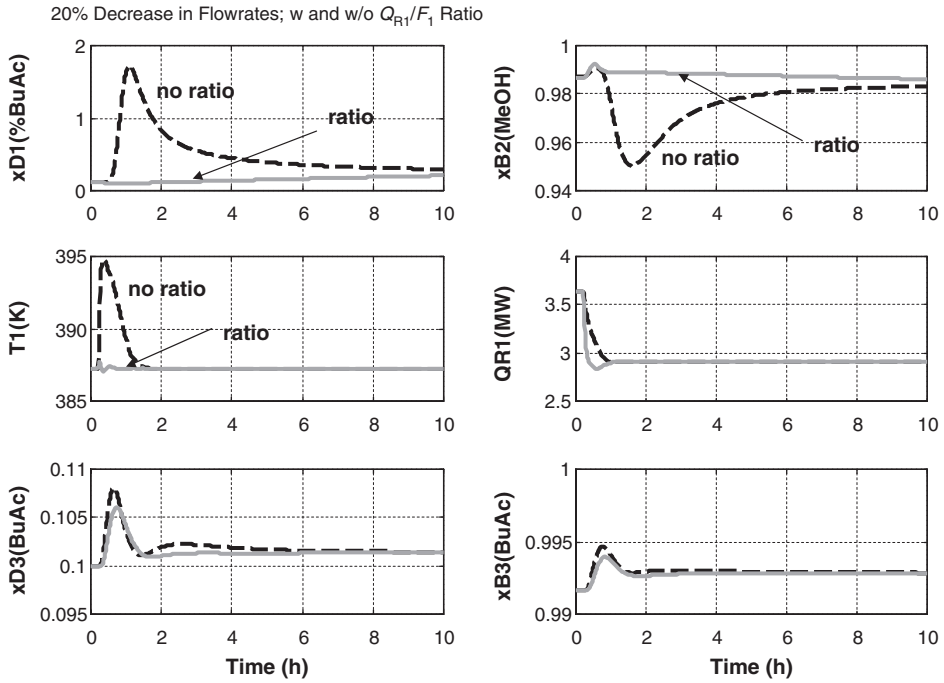


**Figure 8.10.** Effect of $Q_{R1}/F_1$ ratio; 20% decrease in flowrate.

***$Q_{R1}/F_1$ Ratio Control.*** The obvious solution to this problem is to use a steam-to-feed feedforward ratio so that the change in feed flowrate will immediately cause an appropriate change in reboiler heat input. The solid lines in Figure 8.10 demonstrate the improvement realized by using this revised control structure. The rise in Stage 22 temperature is greatly reduced for the 20% drop in throughput, and little butyl acetate is driven overhead. So the use of the $Q_{R1}/F_1$ ratio is included in the plantwide control structure. The temperature controller must be retuned for this modified control structure in which the temperature controller output signal is one of the inputs to the multiplier $Q_{R1}/F_1$. The other input is the feed to column C1.

The dynamic response of the process was found to be quite good for changes in throughput. Both product streams ($B_2$ and $B_3$) were held close to their specifications. Figure 8.11 gives a number of important variables throughout the system. The solid lines are for a 20% increase in throughput. The dashed lines are for a 20% decreases. Stable regulatory control is achieved. The purity of methanol product $B_2$ is held quite close to 98.7 mol% methanol specification, despite some changes in the butyl acetate going overhead in column C1. The purity of the butyl acetate product $B_3$ is maintained close to its specification.

However, when feed composition disturbances were introduced, the methanol product purity was not held constant. Figure 8.12 gives results when the feed composition is changed at time equal 0.2 hours. The solid lines are when the feed is changed from 60 mol% methyl acetate and 40 mol% methanol to 70 mol% methyl acetate and 30 mol% methanol. The dashed lines are when the feed is changed from 60 mol% methyl acetate and 40 mol% methanol to 50 mol% methyl acetate and 50 mol% methanol.

When methyl acetate feed concentration increases, more butyl acetate goes overhead in column C1 (upper left graph in Figure 8.12, $x_{D1(BuAc)}$). This appears as a heavy impurity

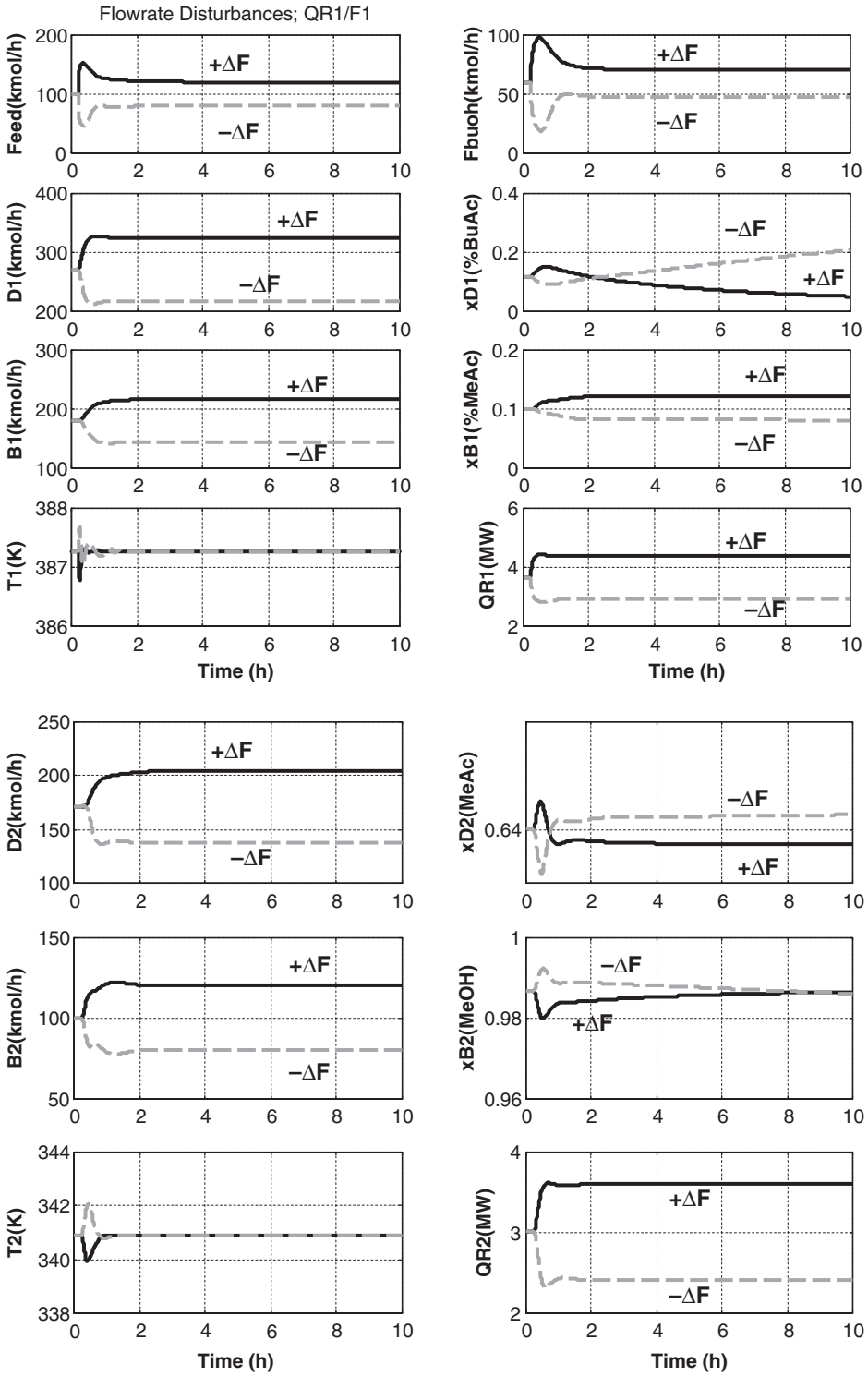


**Figure 8.11.** 20% flowrate disturbances.

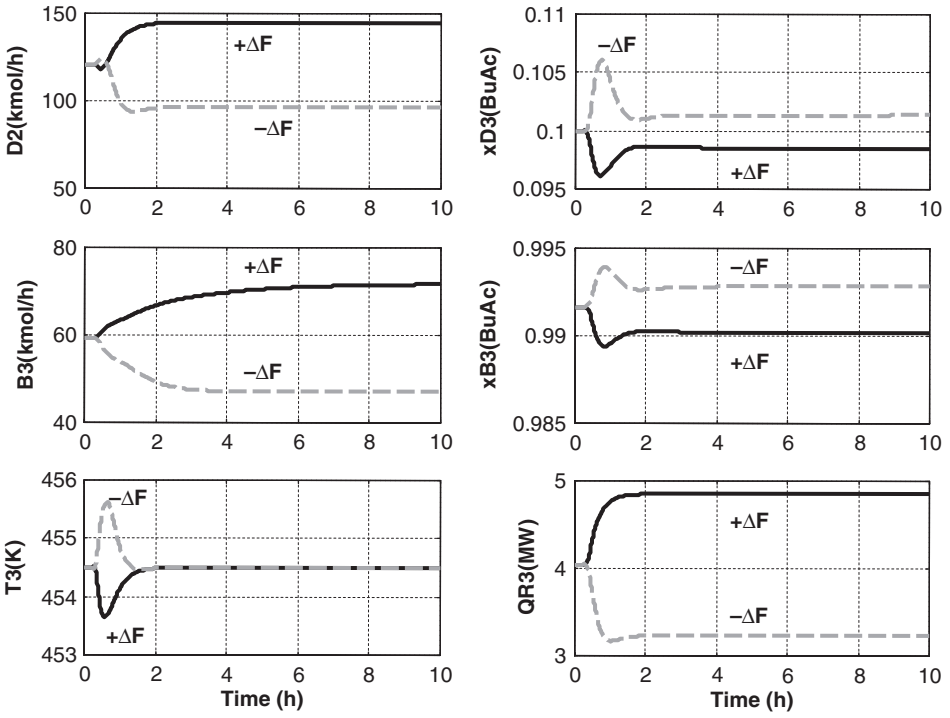


**Figure 8.11.** *Continued.*

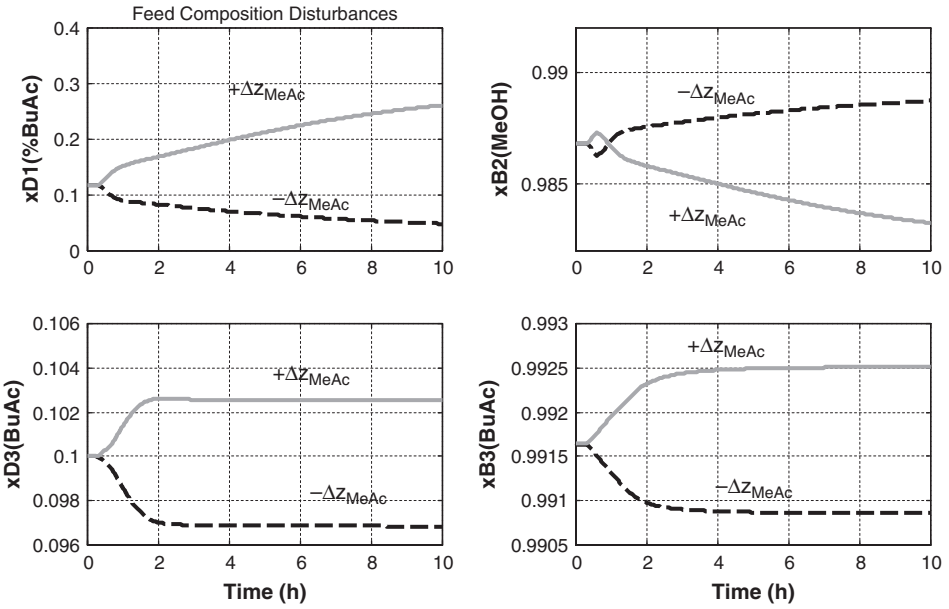


**Figure 8.12.** Feed composition disturbances.

**TABLE 8.5 Controller Parameters**

| | TC1 | TC2 | TC3 | TC11(Dual) | TC12(Dual) |
|---|---|---|---|---|---|
| Controlled variable | Stage 22 temperature in C1 | Stage 25 temperature in C2 | Stage 41 temperature in C3 | Stage 22 temperature | Stage 7 temperature |
| Manipulated variable | Reboiler heat input $Q_{R1}$ | Reboiler heat input $Q_{R2}$ | Reboiler Heat input $Q_{R3}$ | $Q_{R1}/F_1$ | Reflux ratio |
| SP | 387.2 K | 340.9 K | 454.5 K | 387.2 K | 338.8 K |
| Transmitter range | 350–450 K | 300–400 K | 350–450 K | 350–450 K | 300–400 K |
| OP | 869.5 kcal/s | 719.8 kcal/s | 968.0 kcal/s | 0.02905 GJ/kmol | 0.317 GJ/kmol |
| OP range | 0–1500 kcal/s | 0–1439 kcal/s | 0–2000 kcal/s | 0–0.1 GJ/kmol | 0–1 GJ/kmol |
| Deadtime | 1 min | 1 min | 1 min | 1 min | 1 min |
| $K_C$ | 0.46 | 3.71 | 2.9 | 0.236 | 16.0 |
| $\tau_I$ | 10.6 min | 6.6 min | 9.2 min | 10.6 min | 13.2 min |

in the methanol product leaving the bottom of column C3, and reduces methanol purity (upper right graph, $x_{B2(\mathrm{MeOH})}$).

These results are not unexpected, as previously discussed. The feed sensitivity analysis predicted that a single-end control structure may not work well because both RR and R/F ratio must change in the face of feed composition disturbances to maintain product compositions. A two-end control structure is required in column C1. The new tuning parameters are included in Table 8.5.

***Dual Temperature Control.*** Fortunately, the temperature profile in column C1 shown in Figure 8.5a has two breaks, one near the bottom (Stage 22) and one near the top (Stage 7).

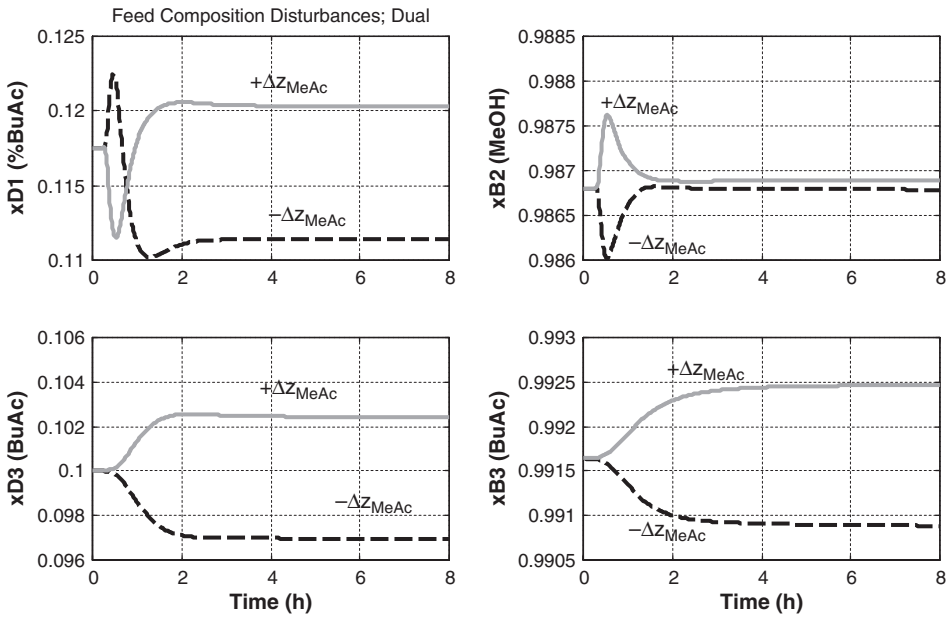


**Figure 8.13.** Feed composition disturbances with C1 dual-temperature control.

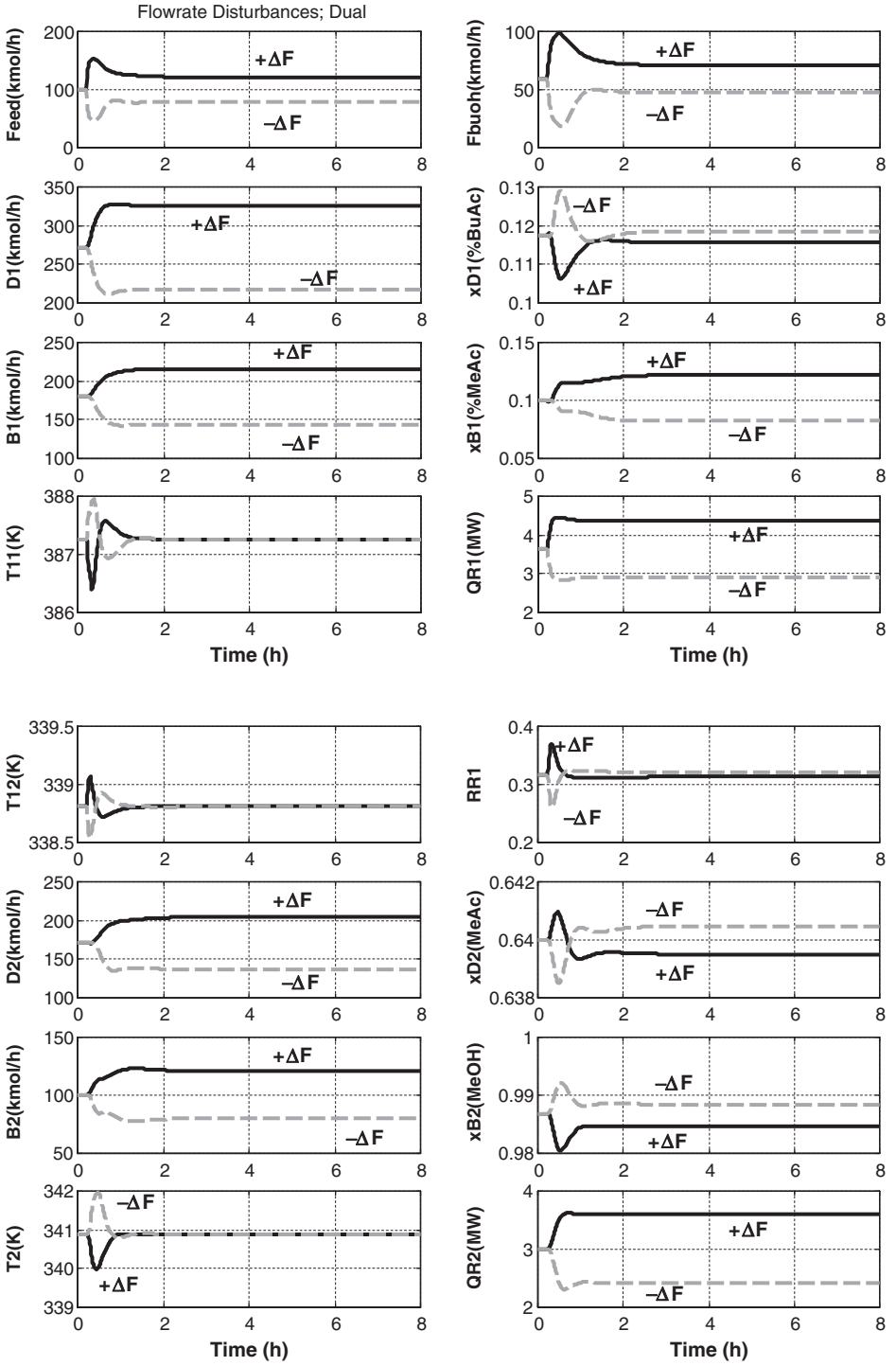


**Figure 8.14.** 20% feed flowrate disturbances; dual temperature control.

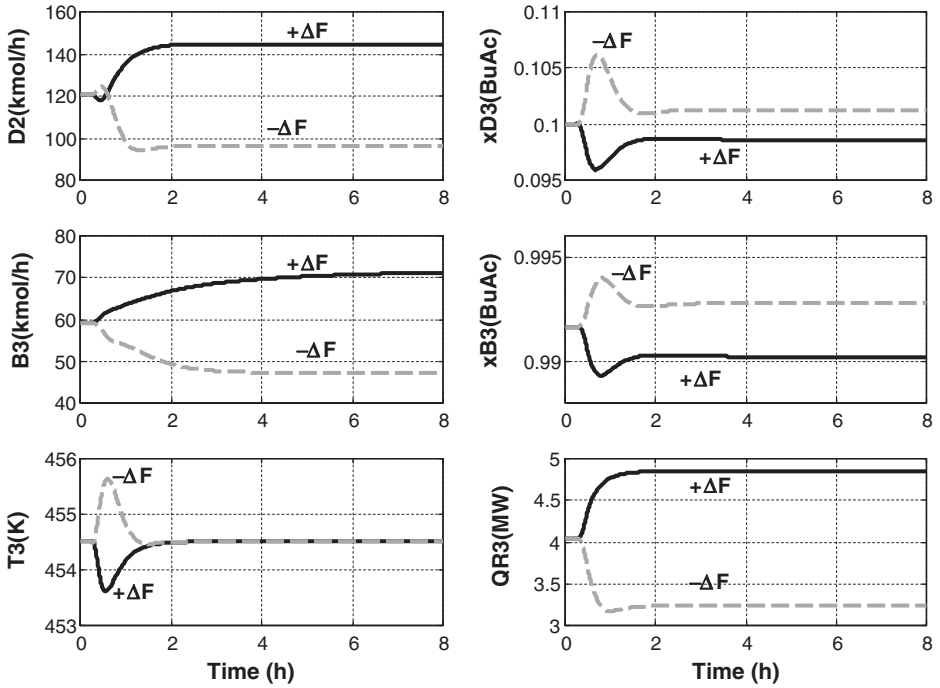


**Figure 8.14.** *Continued.*

So two temperature controllers can be used in column C1. The TC11 controller manipulates reboiler heat input to control Stage 22 temperature. The TC12 controller manipulates RR to control Stage 7 temperature.

These two loops interact, so a sequential tuning procedure is used. The T22-$Q_{R1}/F_1$ loop is tuned first, with the other loop on manual. Then the T7-RR1 loop is tuned with the other loop on automatic. Table 8.5 gives controller parameters for this dual-temperature control structure.

Figure 8.13 shows the improvement in handling feed composition disturbances achieved by the use of the dual-temperature control structure in column C1. The disturbances are the same as those used in Figure 8.12. The purity of the methanol product is held very close to its specification because butyl acetate impurity does not go overhead in column C1. The Stage 7 temperature controller adjusts the RR to achieve this objective. Notice that the time scales in Figures 8.12 and 8.13 are different. The dual-temperature control structure speeds up the dynamics of the process because it prevents butyl acetate impurity from going overhead in column C1 and affecting the downstream column C2.

Figures 8.14 and 8.15 show how important variables throughout the process change dynamically in the face of large disturbances in feed flowrate and feed composition when the dual-temperature control structure is used in column C1. Notice that the second temperature controller in column C1 is changing the RR1.

The final plantwide control structure is given in Figure 8.16. The dynamic simulation results demonstrate the effectiveness of this control structure to handle large disturbance and maintain both products very close to their specifications.

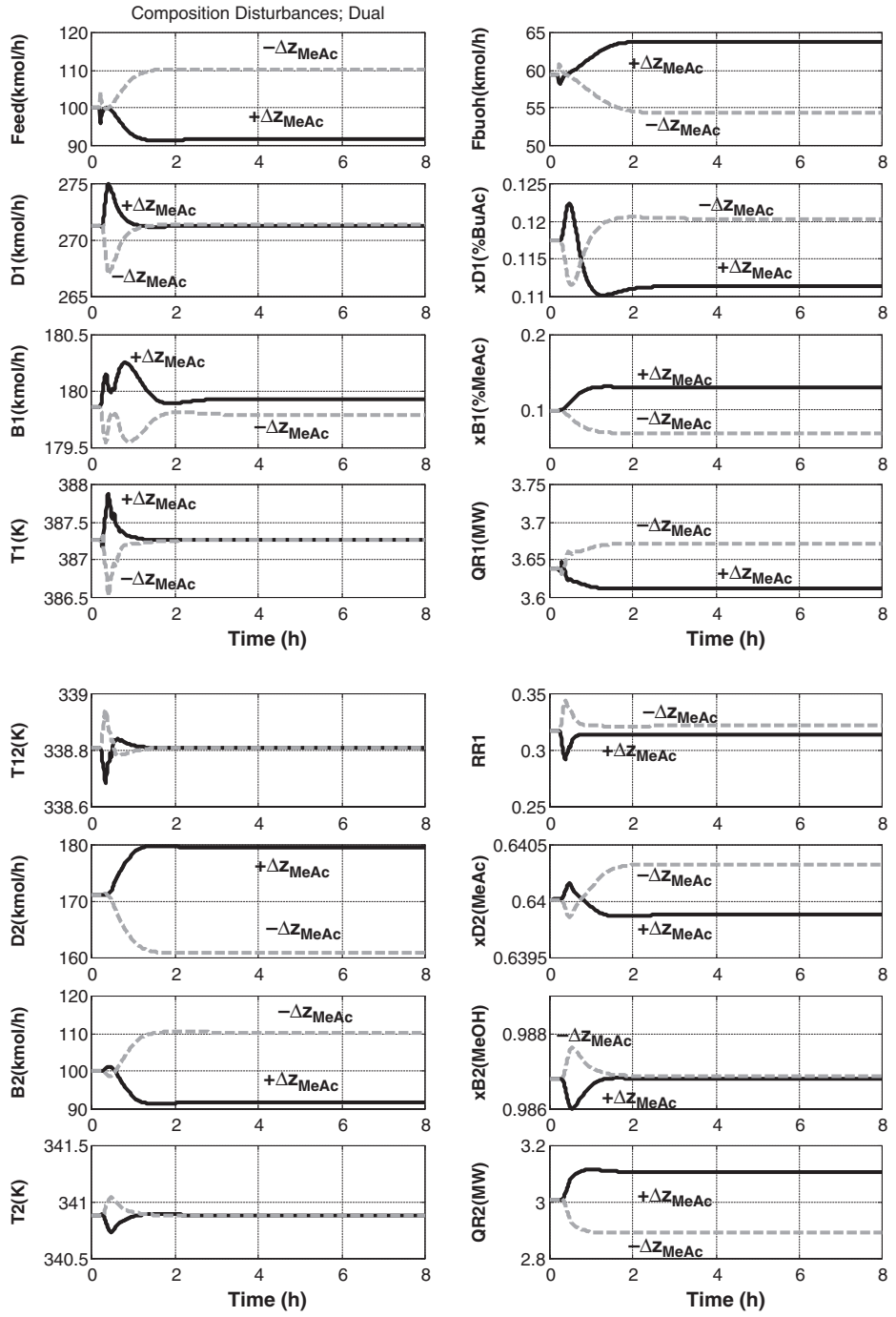


**Figure 8.15.** Feed composition disturbances; dual temperature control.

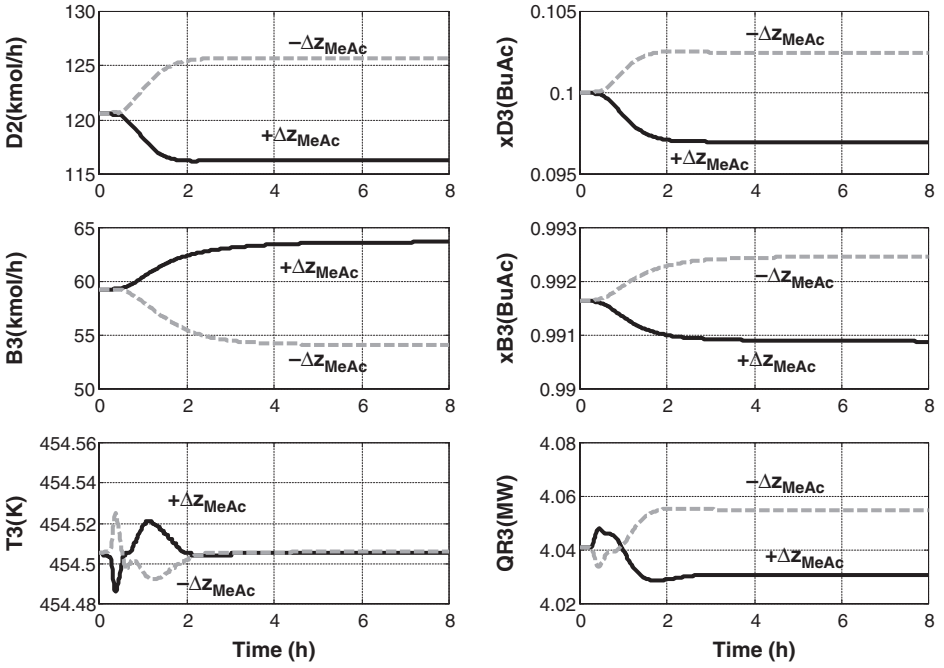


**Figure 8.15.** *Continued.*

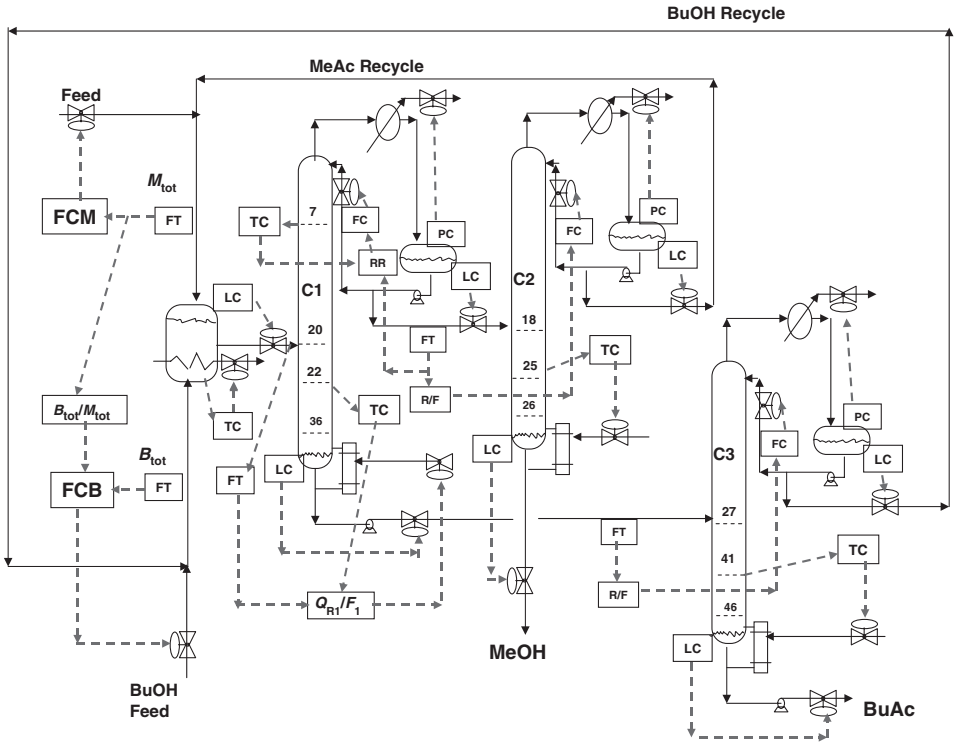


**Figure 8.16.** Final plantwide control structure.

## 8.6 CONCLUSION

The design and control of a butyl acetate process have been studied. There is a trade-off between the two recycle streams. Rigorous economic optimization indicates that, contrary to expectations, the flowrate of the light recycle should be larger than the flowrate of the heavy recycle. This result is due to two factors. First, the separation in the heavy recycle column is more difficult. Second, a higher-temperature energy source is needed in the heavy recycle column.

The plantwide control structure fixes the total flowrates of the two reactants fed to the reactor. The fresh feed streams are manipulated to satisfy the reaction stoichiometry and the reaction capability of the system. Two of the distillation columns can use single-end control. The third column requires dual-temperature control to maintain product purities in the face of feed composition disturbances.

## REFERENCES

1. Jimenez, L., Costa-Lopez, J. The production of butyl acetate and methanol via reactive and extractive distillation. II. Process modeling, dynamic simulation and control strategy, *Ind. Eng. Chem. Res.* 2002, **41**, 6735.
2. Jimenez, L., Costa-Lopez, J. The production of butyl acetate and methanol via reactive and extractive distillation. I. Chemical equilibrium, kinetics and mass-transfer issues, *Ind. Eng. Chem. Res.* 2002, **41**, 6663.
3. Gangadwala, J., Kienle, A., Stein, E., Mahajani, S. Production of butyl acetate by catalytic distillation: Process design studies, *Ind. Eng. Chem. Res.* 2004, **43**, 136.
4. Luyben, W. L., Pszalgowski, K. M., Schaefer, M. R., Siddons, C. Design and control of conventional and reactive distillation processes for the production of butyl acetate, *Ind. Eng. Chem. Res.* 2004, **43**, 8014–8025.
5. Tyreus, T. D., Luyben, W. L. Dynamics and control of recycle systems: 4. Ternary systems with one or two recycle streams, *Ind. Eng. Chem. Res.* 1993, **32**, 1154–1162.

# CHAPTER 9

# DESIGN AND CONTROL OF THE CUMENE PROCESS

The chemistry of the cumene process features the desired reaction of benzene with propylene to form cumene and the undesirable reaction of cumene with propylene to form *p*-diisopropyl benzene (PDIB). Both reactions are irreversible. Since the second has a higher activation energy than the first, low reactor temperatures improve selectivity of cumene. However, low reactor temperatures result in low conversion of propylene for a given reactor size or require a large reactor for a given conversion. In addition, selectivity can be improved by using an excess of benzene to keep cumene and propylene concentrations low, but this increases separation costs. Therefore, the process provides an interesting example of plantwide economic design optimization in which there are many classical engineering trade-offs: reactor size versus temperature, selectivity versus recycle flowrate, and reactor size versus recycle flowrate. Design optimization variables affect both energy costs and capital investment. They also affect the amount of reactants required to produce a specified amount of cumene product. The economic effect of reactant consumption is very large, an order of magnitude greater than the impact of energy or capital.

The process is presented in the design book by Turton et al.[1] and consists of a cooled tubular reactor and two distillation columns. The liquid fresh feeds and the benzene recycle stream are vaporized, preheated, and fed into the vapor-phase reactor, which is cooled by generating steam. Reactor effluent is cooled and fed to the first column, which produces a distillate stream of benzene that is recycled back to the reactor. The second column separates the desired cumene product from the undesired *p*-diisopropyl benzene.

In this chapter, we develop the economically optimum design considering capital costs, energy costs, and raw material costs and develop a plantwide control structure capable of effectively handling large disturbances in production rate.

*Principles and Case Studies of Simultaneous Design*, First Edition. William L. Luyben

## 9.1 INTRODUCTION

The cumene process illustrates some interesting design optimization features and principles. The two dominant design optimization variables are reactor size and benzene recycle. Increasing either one reduces the amount of undesirable by-product that is produced, but increasing either of these variables raises capital and/or energy costs.

Of more importance is the effect of these design optimization variables on conversion and selectivity, which translates into changes in the amounts of the reactants required to produce a fixed amount of cumene. For example, if a bigger reactor is used, reactor temperature can be lower, which improves selectivity while achieving the same conversion and also reduces the amount of raw materials. If the reactor is inexpensive (cheap catalyst), the optimum design is a large reactor. However, if the reactor is expensive, the optimum design is a small reactor.

As Douglas[2] pointed out (Douglas Doctrine) two decades ago, the costs of raw materials and products are usually much larger than the costs of energy or capital in a typical chemical process. Therefore, the process must be designed (investing capital and paying for energy) so as to not waste feedstocks or lose products (particularly in the form of undesirable products). Process economics dictate that the conversion of reactant must be quite high. These principles are clearly illustrated in the cumene process in several ways.

1. The fresh propylene feed stream contains some propane impurity, which is inert in the reactor and must have a place to get out of the process. Since the separation of propylene and propane is difficult, the economics strongly favor designing the reactor for a very high conversion of propylene. The propane and any unreacted propylene are flashed off and burned, so they only have fuel value. High propylene conversion can be achieved by either running at high temperatures or increasing the size of the reactor. The former increases the production of undesirable by-product. The latter increases capital cost.
2. The undesirable by-product is also burned, so it only has value as fuel. Since it takes reactants to produce this product instead of producing cumene, there is a strong incentive to keep its production rate small.

The economic analysis presented in the chapter will show that raw material fresh feed costs are an order of magnitude larger than energy or annual capital costs.

## 9.2 PROCESS STUDIED

The cumene process is described in Turton et al.[1] in a fair amount of detail. The basic flowsheet is presented, and the kinetics of the reactions are given. This latter information is quite useful since it is often difficult to find kinetic information in the literature. The authors provide a good description of the basic units in the process with equipment sizes and operating conditions. Their intent is not to determine the optimum design but to illustrate a typical multiunit chemical process that features a reaction section coupled with a separation section and connected by a recycle stream.

### 9.2.1 Reaction Kinetics

The production of cumene (isopropyl benzene) involves the reaction of benzene with propylene in a high-temperature, high-pressure, gas-phase reactor.

$$C_6H_6 + C_3H_6 \longrightarrow C_9H_{12} \tag{9.1}$$

**TABLE 9.1 Reaction Kinetics**

| | $\Re 1$ | $\Re 2$ |
|---|---|---|
| $k$ | $2.8 \times 10^7$ | $2.32 \times 10^9$ |
| $E$ (kJ/kmol) | 104,174 | 146,742 |
| Concentration terms (kmol/m$^3$) | $C_P C_B$ | $C_C C_P$ |

There is also a sequential reaction of cumene and propylene to form PDIB.

$$C_9H_{12} + C_3H_6 \longrightarrow C_{12}H_{18} \tag{9.2}$$

Table 9.1 gives the reaction kinetics provided by Turton et al.[1] All reaction rates have units of kmol s$^{-1}$ m$^{-3}$. Concentration units are molarity. The reactions occur in the vapor phase in the presence of a solid catalyst (assumed to have 0.5 void fraction and a 2000 kg/m$^3$ solid density). The reactor is run at high pressure (25 bar) since the moles of reactants are more than the moles of product (Le Châtelier's principle).

Notice that the activation energy of the undesirable reaction is larger than that of the desirable reaction. Therefore low reactor temperatures improve selectivity. In addition, selectivity is improved by keeping the concentration of cumene and propylene low in the reactor. This can be achieved by using a large excess of benzene, but the excess must be recovered and recycled.

### 9.2.2 Phase Equilibrium

Assuming that a separation between propylene and propane is uneconomical, the only separations required are achieved fairly easily by distillation. The normal boiling points of benzene, cumene, and PDIB are 80.1, 152.4, and 209.8 °C, respectively. The NRTL physical property package is used in the Aspen simulations used in this chapter. Figure 9.1 gives the *Txy* diagrams for the benzene/cumene system and for the cumene/PDIB system at atmospheric pressure. The curves are fairly fat, so the required number of trays and the reflux ratios (RR) in the distillation columns are fairly low.

### 9.2.3 Flowsheet

Figure 9.2 shows the flowsheet of the process with the equipment sizes and conditions used by Turton et al.[1] The fresh feed streams of benzene and mixed $C_3$ (propylene and propane) enter the process as liquids. The fresh feed flowrate of the $C_3$ feed is set at 110 kmol/h. The composition of this feed is 95 mol% propylene and 5 mol% propane. Since propane does not react, the (110)(0.05) = 5.5 kmol/h of propane must leave the process somewhere. It is vented in a gas stream from the flash drum.

The fresh feed of benzene is 104.2 kmol/h. Note that if there were only the cumene reaction [Eq. (9.1)] and if all the propylene were converted and none were lost, the fresh feed flowrate of the pure benzene would have to satisfy the stoichiometry of the reaction: (110)(0.95) = 94.5 kmol/h. But some of the propylene is consumed in the second reaction and some is lost. The result is a benzene fresh feed flowrate of 104.2 kmol/h, which shows that over 10 kmol/h of benzene is being undesirably consumed or lost. The production rate of cumene is 92.86 kmol/h in the Turton et al. design.

The liquid fresh feeds are combined with a liquid recycle stream (benzene recycle D1, the distillate from the first column C1) and fed into a vaporizer. The total benzene fed to the

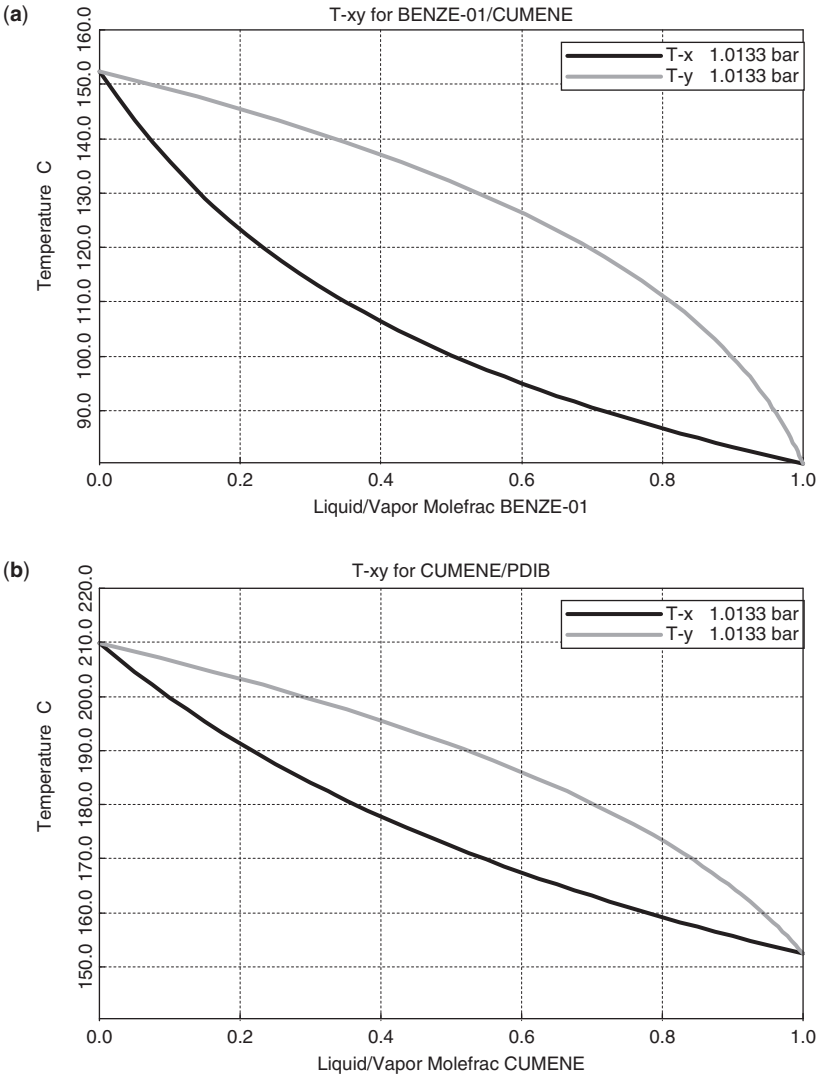


**Figure 9.1.** *Txy* diagrams for (a) benzene/cumene, and (b) cumene/PDIB.

reactor (sum of fresh plus recycle) is 207 kmol/h. The saturated gas leaves the vaporizer at 209 °C and 25 bar. It is preheated in two heat exchangers. The first recovers heat from the hot reactor effluent at 427 °C. The second adds additional heat to bring the reactor inlet temperature up to 360 °C.

***Reaction Section.*** The reactor is a cooled tubular reactor that generates high-pressure steam from the exothermic reactions. There are 342 tubes, 0.0763 m in diameter and 6 m in length. They are filled with a solid catalyst with a void fraction of 0.5 and a solid density of 2000 kg/m$^3$. The temperature on the steam side of the reactor is 360 °C. An overall heat transfer coefficient of 0.065 kW m$^{-2}$ K$^{-1}$ is used. We assume that the reactor inlet temperature is set to the same value as the coolant (steam) temperature in the reactor.

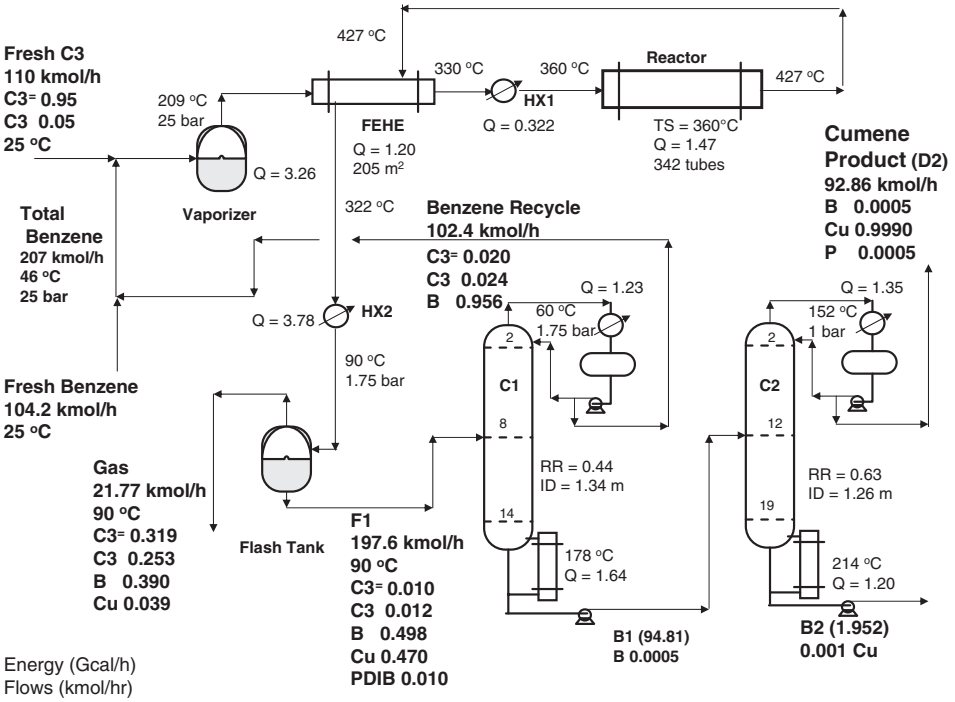


**Figure 9.2.** Turton et al. design.

Reactor effluent leaves at 427 °C, is cooled to 322 °C in the feed-effluent heat exchanger (FEHE) and sent to a condenser in which it is cooled to 90 °C using cooling water. The two-phase stream from the heat exchanger is fed to a flash tank. The gas from the tank is used as fuel. The liquid is fed into the first distillation column C1.

It is important to note that this gas stream in the Turton et al. design is very large (21.77 kmol/h), and it contains a large concentration of unreacted propylene (31.9 mol% propylene). Clearly this operation would be quite uneconomical because of the excessively large losses of the raw material propylene.

As we will show in the optimization studies in Section 9.3, the propylene conversion must be drastically increased. There are 8.9 kmol/h of propylene in the reactor effluent in the Turton et al. design, which has a reactor inlet temperature and a steam temperature of 360 °C. It is a simple matter to increase the propylene conversion by increasing these two temperatures. However, the higher temperature will increase the production of the undesirable product. So it may be more economical to increase the size of the reactor (use more tubes), which would give a higher propylene conversion but at a lower temperature. This is one of the important design trade-offs in the cumene process.

***Benzene Recycle Column C1.*** This column has 15 stages and is fed on stage 6, which is the optimum feed stage to minimize reboiler heat input. The operating pressure is 1.75 bar, which gives a reflux-drum temperature of 60 °C, so cooling water can be used in the condenser. The RR is small (0.44). The distillate is mostly benzene and is recycled back to the reactor. Its composition is 95.6 mol% benzene with small amounts of propylene and propane that are in the liquid from the flash drum.

The design specification is to keep benzene from dropping out the bottom and affecting the purity of the cumene product leaving in the distillate of the downstream column. Since the specified cumene purity is 99.9 mol%, a very small benzene composition in the bottoms (0.05 mol%) is required. The column diameter is 1.36 m, and the reboiler heat input is 1.64 Gcal/h. Both of these increase if more benzene recycle is used.

***Cumene Product Column C2.*** This column has 20 stages and is fed on stage 12. The operating pressure is 1 bar, which gives a reflux-drum temperature of 152 °C. The RR is low (0.63). Energy consumption 1.2 Gcal/h, and the column diameter is 1.26 m.

The design specification is to attain high-purity cumene in the distillate and minimize the loss of cumene in the bottoms. The bottoms composition is set at 0.1 mol% cumene. The distillate composition is 99.9 mol% cumene using the 0.63 RR.

Notice that the bottoms B2 flowrate is 1.952 kmol/h in this flowsheet. This represents a loss of reactants, and the stream only has fuel value. The production of the undesired product can be reduced by lowering reactor temperatures (which would require a larger reactor) or increasing benzene recycle (which would require a larger distillation column C1 and would increase energy consumption in the vaporizer and in the C1 reboiler).

## 9.3 ECONOMIC OPTIMIZATION

The design discussed in Section 9.2 has not been optimized from the standpoint of economics. The low conversion of propylene in the reactor and the subsequent loss of propylene in the gas stream is an obvious issue that must be considered.

Of the 104.5 kmol/h of propylene in the fresh feed, the amount lost in the gas stream is 6.94 kmol/h. So reactor propylene conversion is only 93%. In addition, the production of 1.952 kmol/h of the undesirable product consumes 3.904 kmol/h of propylene. So the conversion of propylene to the desired product cumene is only 90%.

### 9.3.1 Increasing Propylene Conversion

As previously mentioned, propylene conversion in the reactor can be easily increased by increasing reactor inlet temperature $T_{in}$ and steam temperature $T_S$. However, selectivity will be adversely affected.

Figure 9.3 gives a flowsheet in which the reactor inlet temperature and coolant temperature have been increased from 360 °C to 374 °C. Notice that the production rate of cumene is kept the same as the original case ($D_2 = 92.86$ kmol/h). The gas stream is greatly reduced from 21.77 to 10.10 kmol/h. The concentration of propylene in the gas stream drops from 31.9 to 5.4 mol%. Therefore, much less fresh propylene is fed into the system; fresh benzene feed drops from 104.2 to 99.81 kmol/h. This represents a very large savings in raw material costs, as we will quantify in Section 9.3.4.

Notice, however, that the higher reactor temperatures also result in a higher production of the undesirable product. The flowrate of the bottoms B2 from column C2 increases from 1.952 to 2.588 kmol/h, so the loss of both propylene and benzene that this stream represents increases.

How can we keep propylene conversion high but reduce the production of the undesired product? There are two ways to achieve these objectives. The temperatures in the reactor could be lowered if a bigger reactor were used. Or the recycle of benzene could be increased.

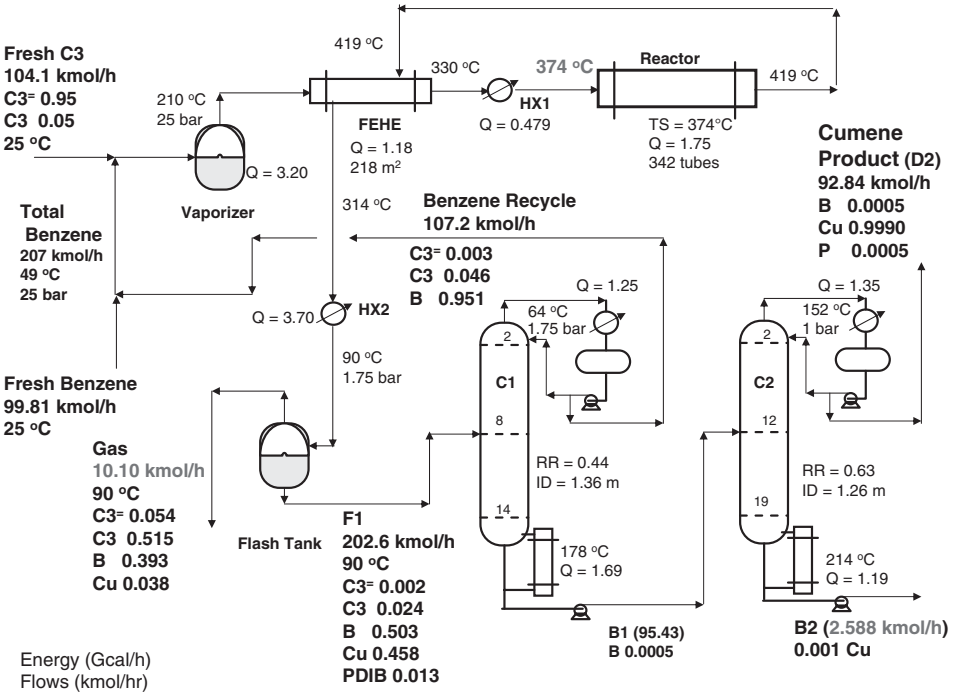


**Figure 9.3.** Conversion 99%.

Both of these involve higher capital and/or energy costs. In Section 9.3.4, we quantify the economic effects of these two design optimization variables while maintaining a high propylene conversion.

### 9.3.2 Effects of Design Optimization Variables

To get some feel for the effects of reactor size and benzene recycle, a series of runs were made in which one of the two design optimization variables was changed over a range of values while holding the other variable constant. In these runs, the fresh feed of the propylene/propane stream was held constant at the original value of 110 kmol/h (Turton et al. 2003). Note that the production rate of cumene D2 is not held constant in this series of runs.

Figure 9.4 shows how changes in the benzene recycle affect a number of important variables. The total benzene feed to the reactor is the sum of the fresh benzene feed and the recycle benzene, which is the distillate D1 of the first distillation column. The top left graph shows that the production of the undesirable product (PDIB in B2) decreases as more benzene is recycled. The middle left graph shows that the production of the desired product (cumene in D2) also increases. These very beneficial effects are offset by the required increase in the energy consumption in the column C1 reboiler ($Q_{R1}$) and in the vaporizer ($Q_{vaporizer}$), as shown in the bottom two graphs. In addition, the production of gas increases. Notice that the reactor temperatures must be increased as more material flows through the reactor to maintain the 99% propylene conversion because of the smaller residence time. Despite the higher temperatures, selectivity improves because of the higher benzene concentrations in the reactor.

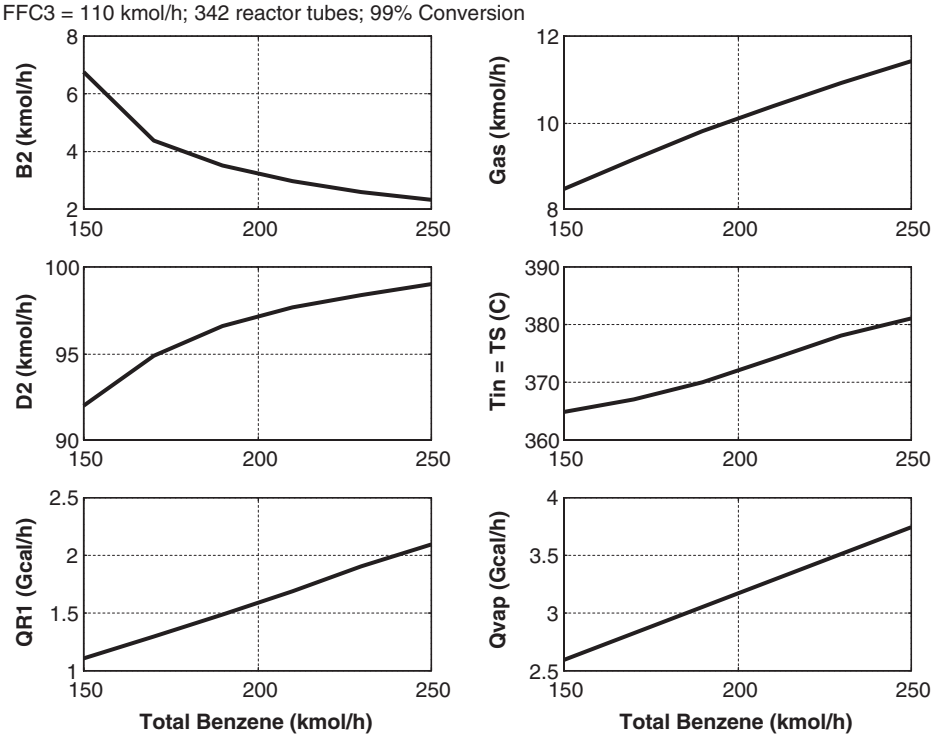


**Figure 9.4.** Effect of benzene recycle.

Figure 9.5 shows how changes in reactor size impact the performance of the system. As the number of reactor tubes is increased, more cumene is produced and less undesirable product must be burned. There is also a small decrease in gas flowrate. The important effect of making the reactor larger is that lower reactor temperatures can be used to achieve the same 99% propylene conversion, as shown in bottom right graph of Figure 9.5. Comparing the results in Figure 9.4 with those in Figure 9.5 shows that the lower reactor temperatures have the beneficial effects of making more cumene, less undesirable product, and less gas.

These preliminary scoping studies indicate that reactor size has a stronger impact on performance than benzene recycle. Of course, increasing either of these variables means an increase in capital and/or energy costs. In order to quantify the economics of these design optimization variables, we must quantitatively estimate the capital cost of equipment (heat exchangers, reactor vessel, catalyst, and distillation columns), the operating cost of energy (vaporizer, preheater, and reboilers), and the cost of purchasing the two raw materials (propylene and benzene).

### 9.3.3 Economic Basis

The sizing and cost estimation for the equipment is given in Chapter 5 and summarized in Table 9.2. The reactor capital cost is based on its heat exchange area and the amount of catalyst it contains. The very important effect of the price of catalyst is explored later in this chapter. As we would expect, expensive catalyst favors a small reactor design while inexpensive catalyst leads to a large reactor with many tubes.

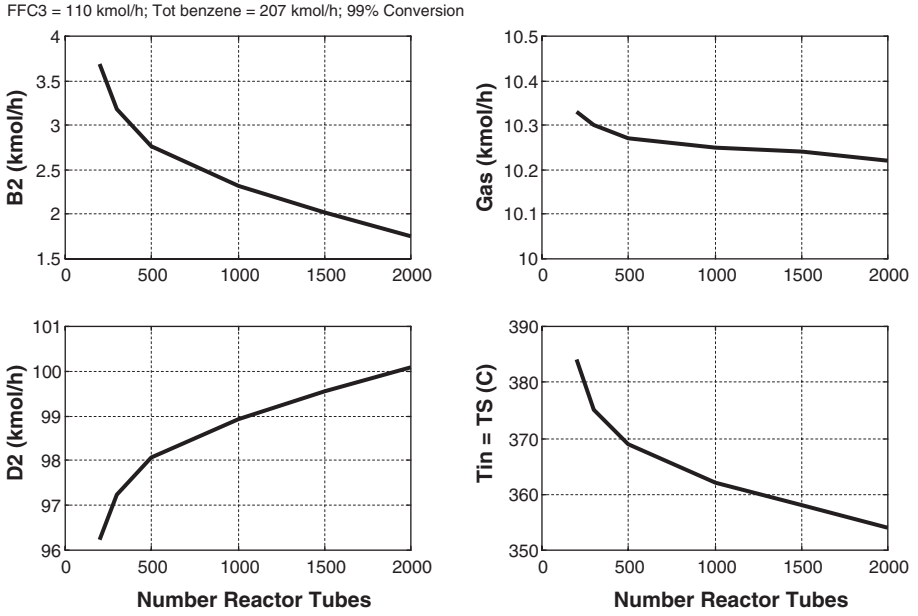


**Figure 9.5.** Effect of reactor size.

High-pressure steam (254 °C with a cost of \$9.83/GJ) is used in the vaporizer and in both reboilers because of their high temperatures. The very high reactor inlet temperatures (360 °C) require a high-temperature heating medium or electricity, so a cost of \$16.8/GJ is used. Steam generated in the reactor is assumed to be worth \$6.67/GJ.

The cost of raw materials is based on data from the Internet Web site www.icis.com (provided by Miles Julian, DuPont Engineering Department, retired). Propylene is priced at \$0.37/lb (34.3 \$/kmol), and benzene is priced at \$2.90/gal (68.6 \$/kmol).

There are two waste streams that are burned and carry a fuel credit in the economic analysis. The bottoms stream from column C2 is essentially pure PDIB. Its heat of combustion is estimated to be 1624 kcal/mol. The gas stream contains propylene, propane, benzene, and cumene. The heats of combustion of these components are 460, 485, 747, and 1183 kcal/mol, respectively.

The values of these streams were estimated by calculating the amount of air needed to completely combust each component to water and carbon dioxide, with 5% excess oxygen. The molar flowrates and heat capacities of each component were used to find the sensible heat needed to increase the combustion gas temperature from 25 to 285 °C (the assumed stack gas temperature). This sensible heat was subtracted from the heat of combustion to find the net heating value of each component. Using \$6/GJ value of energy, the calculated heating values of propylene, propane, benzene, cumene, and PDIB used in the economic analysis are \$10.4, \$10.9, \$27.9, \$26.6, \$36.5/kmol, respectively.

### 9.3.4 Economic Optimization Results

Table 9.3 gives detailed information for a number of alternative designs. All of these cases produce the same amount of cumene ($D_2 = 92.86$ kmol/h). But the equipment sizes and fresh feed flowrates are different in each case.

**TABLE 9.2 Basis of Economics and Equipment Sizing**

Column diameter: Aspen tray sizing
Column length: NT trays with 2 ft spacing plus 20% extra length
Column vessel (diameter and length in meters)

$$\text{Capital cost} = 17{,}640(D)^{1.066}(L)^{0.802}$$

*Condensers (area in $m^2$)*

Heat-transfer coefficient $= 0.852\ \text{kW/K-m}^2$
Differential temperature $= 13.9\ \text{K}$
Capital cost $= 7296(A)^{0.65}$

*Reboilers, FEHE, and preheater (area in $m^2$)*

Heat-transfer coefficient $= 0.568\ \text{kW/K-m}^2$
Differential temperature $= 34.8\ \text{K}$
Capital cost $= 7296(A)^{0.65}$

*Reactor (cooled)*

Heat-transfer coefficient $= 0.065\ \text{kW/K-m}^2$
Differential temperature $= T_R(z) - T_S$
Capital cost $= 7296(A)^{0.65}$

*Energy cost*

HP steam $= \$9.83/10^6\ \text{GJ}$

$$\text{TAC} = \frac{\text{Capital cost}}{\text{Payback period}} + \text{Energy cost}$$

Payback period $= 3\ \text{yr}$

Capital costs of equipment, energy costs, fuel credits and raw material costs are provided. The results in this table use a catalyst price of \$10/kg. The effect of catalyst price is explored later in this section.

***Turton Design.*** The first column in Table 9.3 gives economic results for the original Turton et al. design. Total capital investment is \$2,070,000. The net total energy cost is \$2,240,000/yr (energy consumption in columns, heat exchangers, and vaporizer reduced by the steam generated in the reactor and reduced by the fuel credits from burning B2 and gas).

The dominating factor is the cost of raw materials. The fresh C3 feed at 110 kmol/h and fresh benzene feed at 104.2 kmol/h cost a total of \$95,660,000/yr! There are fairly large fuel credits from burning gas and B2, but these are swamped by the cost of the purchased reactants. The low propylene conversion gives a molar flowrate of 9 kmol/h of propylene in the reactor effluent, and this is lost in the gas stream.

***High Conversion Design.*** The second column in Table 9.3 gives economic results for the case where propylene conversion has been increased by raising reactor temperatures. Propylene conversion in the reactor is raised by specifying a much smaller molar flowrate

**TABLE 9.3 Economic Effects of Design Optimization Variables**[a]

| | | Turton et al.[1] Design | Conversion 99% | Increase Benzene Recycle | Increase Reactor Size | Economic Optimum |
|---|---|---|---|---|---|---|
| Reactor tubes | | 342 | 342 | 342 | 1000 | 1500 |
| Total benzene recycle | kmol/h | 207 | 207 | 250 | 207 | 207 |
| $T_{in} = T_S$ | °C | 360 | 374 | 382 | 363 | 358 |
| $T_{out}$ | °C | 427 | 419 | 428 | 364 | 358.5 |
| Gas | kmol/h | 21.77 | 10.10 | 11.12 | 10.01 | 9.979 |
| B2 | kmol/h | 1.952 | 2.588 | 1.898 | 1.85 | 1.550 |
| FFC3 | kmol/h | 110.0 | 104.1 | 102.6 | 102.55 | 101.93 |
| FFB | kmol/h | 104.2 | 99.81 | 100.24 | 99.07 | 98.78 |
| C1 capital | $10^6$ $ | 0.407 | 0.414 | 0.455 | 0.389 | 0.407 |
| C1 energy | $10^6$ $/yr | 0.591 | 0.609 | 0.767 | 0.609 | 0.607 |
| C2 capital | $10^6$ $ | 0.338 | 0.338 | 0.339 | 0.338 | 0.338 |
| C2 energy | $10^6$ $/yr | 0.429 | 0.429 | 0.429 | 0.429 | 0.429 |
| HX1 capital | $10^6$ $ | 0.0201 | 0.0261 | 0.0322 | 0.0212 | 0.0192 |
| HX1 energy | $10^6$ $/yr | 0.0500 | 0.0744 | 0.103 | 0.0542 | 0.0464 |
| HX2 capital | $10^6$ $ | 0.0700 | 0.0690 | 0.0691 | 0.0609 | 0.0601 |
| Vaporizer capital | $10^6$ $ | 0.222 | 0.219 | 0.241 | 0.219 | 0.219 |
| Vaporizer energy | $10^6$ $/yr | 1.18 | 1.15 | 1.33 | 1.16 | 1.15 |
| FEHE capital | $10^6$ $ | 0.232 | 0.242 | 0.245 | 0.369 | 0.354 |
| Reactor vessel capital | $10^6$ $ | 0.410 | 0.410 | 0.410 | 0.823 | 1.07 |
| Catalyst @ $10/kg | $10^6$ $ | 0.374 | 0.374 | 0.374 | 1.09 | 1.64 |
| Reactor steam credit | $10^6$ $/yr | 0.359 | 0.350 | 0.401 | 0.545 | 0.401 |
| Fuel credit B2 | $10^6$ $/yr | 0.624 | 0.828 | 0.607 | 0.592 | 0.713 |
| Fuel credit gas | $10^6$ $/yr | 3.41 | 1.61 | 1.87 | 1.60 | 1.59 |
| Feed C3 cost | $10^6$ $/yr | 33.051 | 31.274 | 30.828 | 30.813 | 30.627 |
| Feed benzene cost | $10^6$ $/yr | 62.612 | 59.979 | 60.230 | 59.535 | 59.36 |
| Total capital | $10^6$ $ | 2.07 | 2.09 | 2.16 | 3.31 | 4.11 |
| Total energy | $10^6$ $/yr | 2.24 | 2.26 | 2.63 | 2.24 | 2.23 |
| TAC | $10^6$ $/yr | 94.204 | 91.427 | 91.539 | 90.961 | 90.883 |

[a]Cumene production $D_2 = 92.85$ kmol/h.

of 0.9 kmol/h in the reactor effluent, which is achieved by adjusting the reactor inlet and steam temperature (raised from 360 to 374 °C).

There is little change in total capital investment or energy, and fuel credits are reduced. Gas flowrate is cut in half, but the production of the undesirable product increases somewhat (B2 changes from 1.952 to 2.588 kmol/h because of the higher reactor temperatures).

However, the flowrates of the raw materials are both reduced, which produces a very large reduction in the cost of raw materials. The fresh $C_3$ feed is reduced from 110 to 104.1 kmol/h

and fresh benzene feed drops from 104.2 to only 99.81 kmol/h (see also Figure 9.3). The raw material cost is cut from \$95,660,000/yr to \$91,250,000/yr! Remember that the production rate of cumene is the same in both of these flowsheets.

These results illustrate very dramatically the Douglas Doctrine that process designs must minimize the losses of raw material and products.

***Higher Benzene Recycle.*** The third column in Table 9.3 gives economic results for the case where benzene recycle is increased from 207 to 250 kmol/h of total benzene fed to the reactor. High propylene conversion is maintained by raising reactor temperatures to 382 °C. Higher temperatures are required because of the smaller residence time in the reactor.

Total capital and energy costs both increase due to a larger vaporizer and a larger recycle column (C1). Production of the undesirable product is reduced, despite the higher reactor temperatures because of the higher benzene concentrations in the reactor. Gas flowrate is slightly higher.

The fresh feed flowrates change in different directions. Less propylene fresh feed is required, but more benzene fresh feed is needed. The net result is a slight reduction in the raw material costs of about \$200,000/yr. The total annual cost (TAC) that combines all these factors increases from \$91,427,000/yr in the previous case to \$91,539,000 in this higher benzene recycle case.

So, increasing benzene recycle does not improve the economics of the process because more capital and more energy are required.

***Larger Reactor.*** The fourth column in Table 9.3 gives economic results for the case in which reactor size is increased. The number of reactor tubes is increased from 342 to 1000. Total benzene recycle is set at the base-case 207 kmol/h. This larger reactor will be more expensive in terms of vessel cost (more heat-transfer area) and catalyst cost. However, a larger reactor should permit lower reactor temperatures, which should improve selectivity. Propylene conversion is kept at 99%.

Table 9.3 shows that reactor temperatures can be reduced to 363 °C with this larger reactor, compared to the second column, where 374 °C is required with the base-case number of tubes. Gas production is about the same, but the production of undesirable product is reduced to 1.85 kmol/h. Energy cost is about the same, but capital cost increases due to the larger reactor.

However, both fresh feed flowrates are reduced, which cuts raw material costs to \$90,348,000/yr. The economic results show a TAC of \$90,961,000/yr, which is better than the smaller reactor case.

So, increasing the number of tubes from 342 to 1000 improves the economics. What happens for larger reactors? Figure 9.6 gives results for a range of number of reactor tubes for a constant production rate of cumene. These results are different than those shown in Figure 9.5, in which the production rate of cumene is not fixed, but the flowrate of fresh propylene is fixed. Propylene conversion is 99%, total benzene recycle is 207 kmol/h, and catalyst price is \$10/kg in this figure.

There is a minimum in the TAC curve at 1500 reactor tubes, where the increasing cost of capital is balanced by the reduction in raw material cost. Energy cost changes very little with reactor size. Energy consumption depends primarily on benzene recycle.

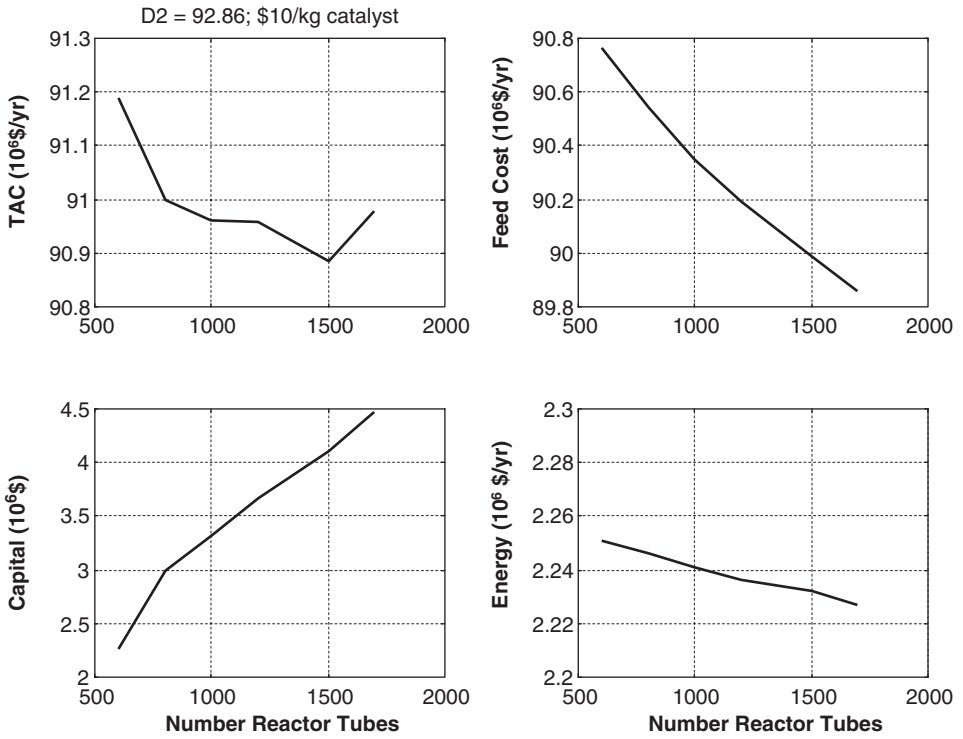


**Figure 9.6.** Effect of reactor size for fixed production rate.

***Effect of Catalyst Price.*** All of the results given in Table 9.3 and Figure 9.6 are based on a catalyst price of \$10/kg. Since catalyst price has a major impact on capital cost, it will affect the optimum economic design.

Figure 9.7 shows the effect of catalyst price on TAC over a range of reactor sizes. As catalyst price increases, the optimum number of reactor tubes decreases. But even with a very expensive catalyst, the optimum number of reactor tubes is substantially larger than the original Turton et al. design.

Figure 9.8 gives flowsheet conditions for the optimum 1500-tube reactor case assuming \$10/kg catalyst cost. The last column in Table 9.3 gives details of the economics and conditions for this case.

Figure 9.9 gives the temperature and composition profiles in the reactor for the optimum case. Figures 9.10 and 9.11 give temperature and composition profiles for columns C1 and C2.

## 9.4 PLANTWIDE CONTROL

The units with dynamics include the vaporizer, heat exchangers, reactor, flash drum, and distillation columns. Reflux drums, column bases, the vaporizer, and the flash drum are sized to provide 5 min of holdup when at 50% level. The tube-side and shell-side volumes of the FEHE are calculated using the heat-transfer area of 460 $m^2$ and assuming 0.0762 m

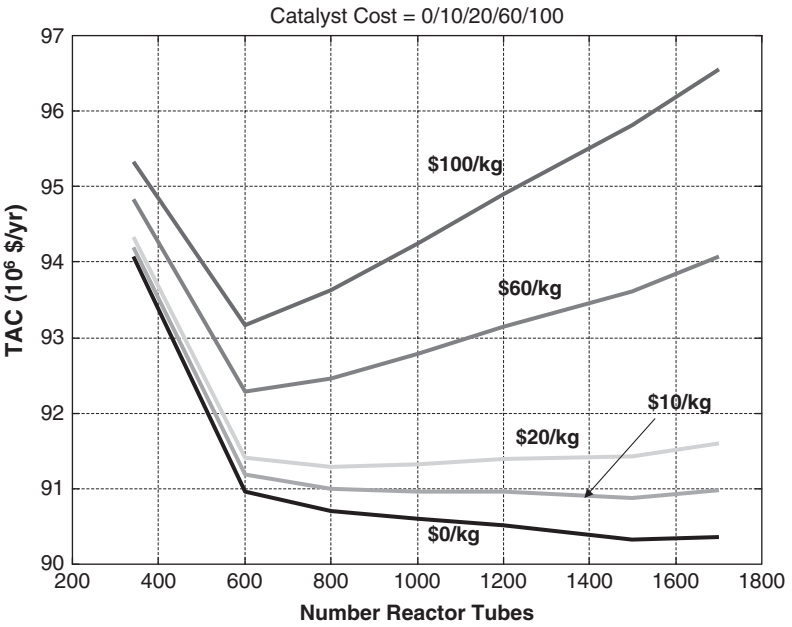


**Figure 9.7.** Effect of reactor size and catalyst cost on TAC for fixed production rate.

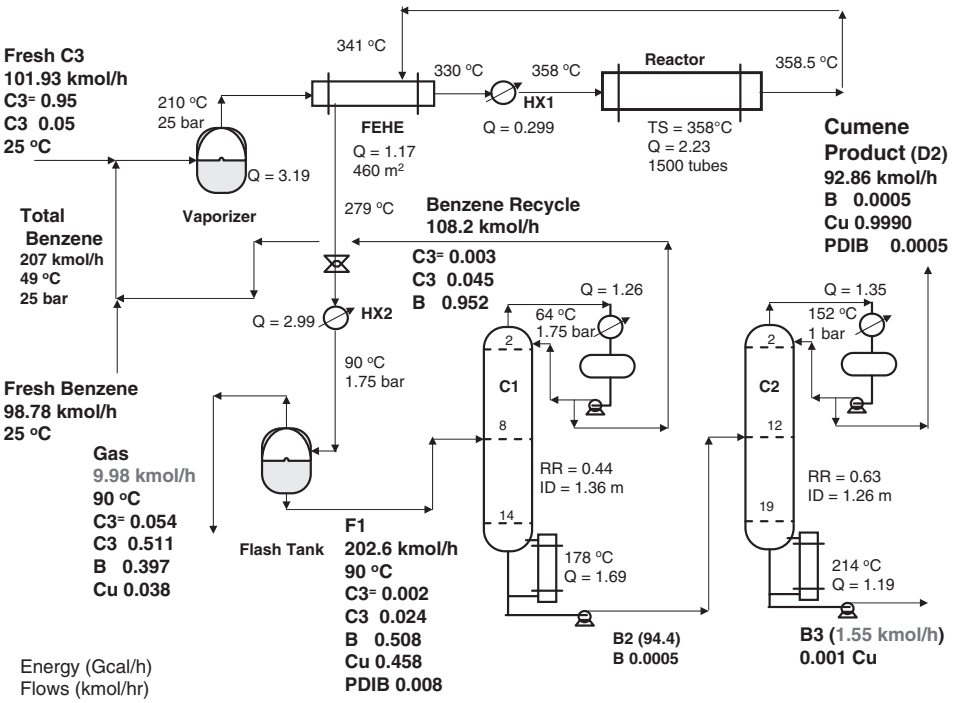


**Figure 9.8.** Optimum design for \$10/kg catalyst (1500 tubes, 207 total benzene).

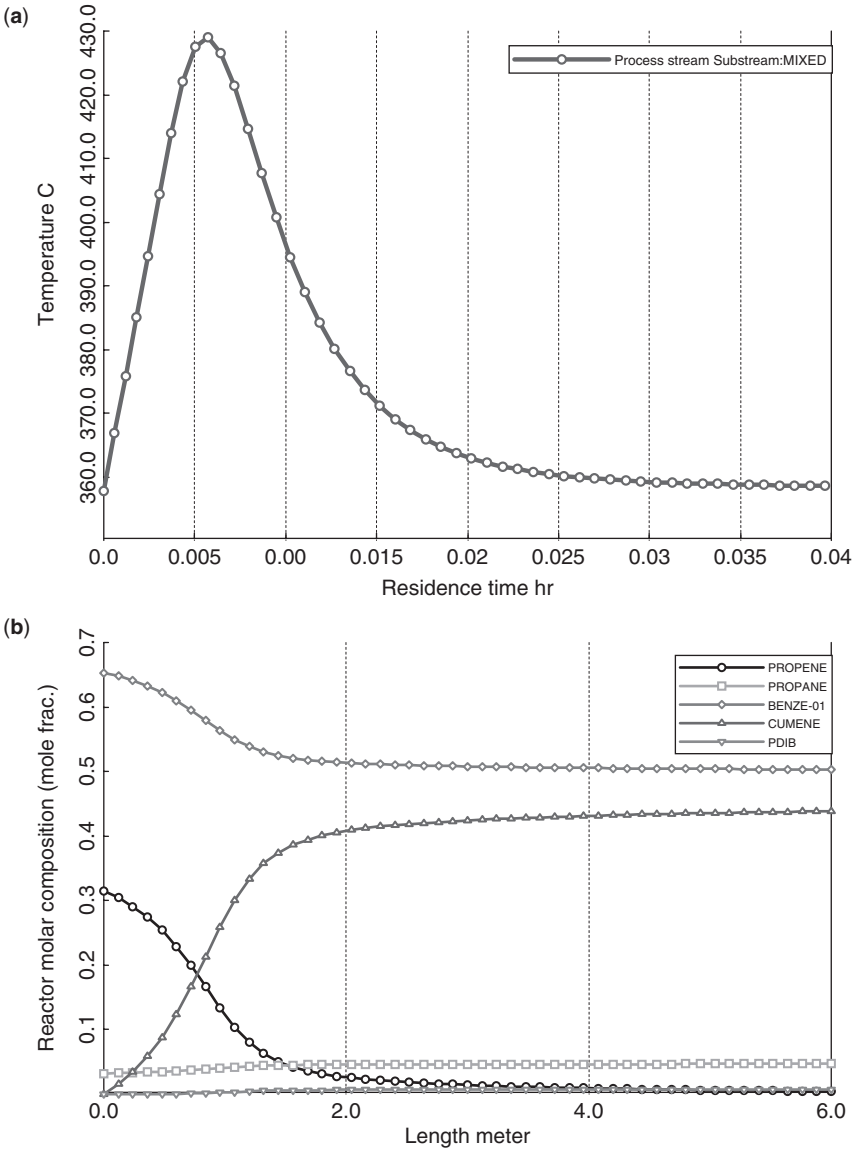


**Figure 9.9.** (a) Reactor temperature profile. (b) Reactor composition profiles.

in diameter tubes, 6 m in length. The tube volume is 8.76 $m^3$ in 320 tubes. Shell volume is assumed equal to tube volume. The volume of HX2 is 0.5 $m^3$, based on its heat-transfer area of 25.6 $m^3$. The volume of the vaporizer is 4.59 $m^3$, and the volume of the flash drum is 4.15 $m^3$.

Figure 9.12 shows the plantwide control structure developed for this process using process control methodology.[3,4] Conventional PI controllers are used in all loops. The various loops are listed below with their controlled and manipulated variables.

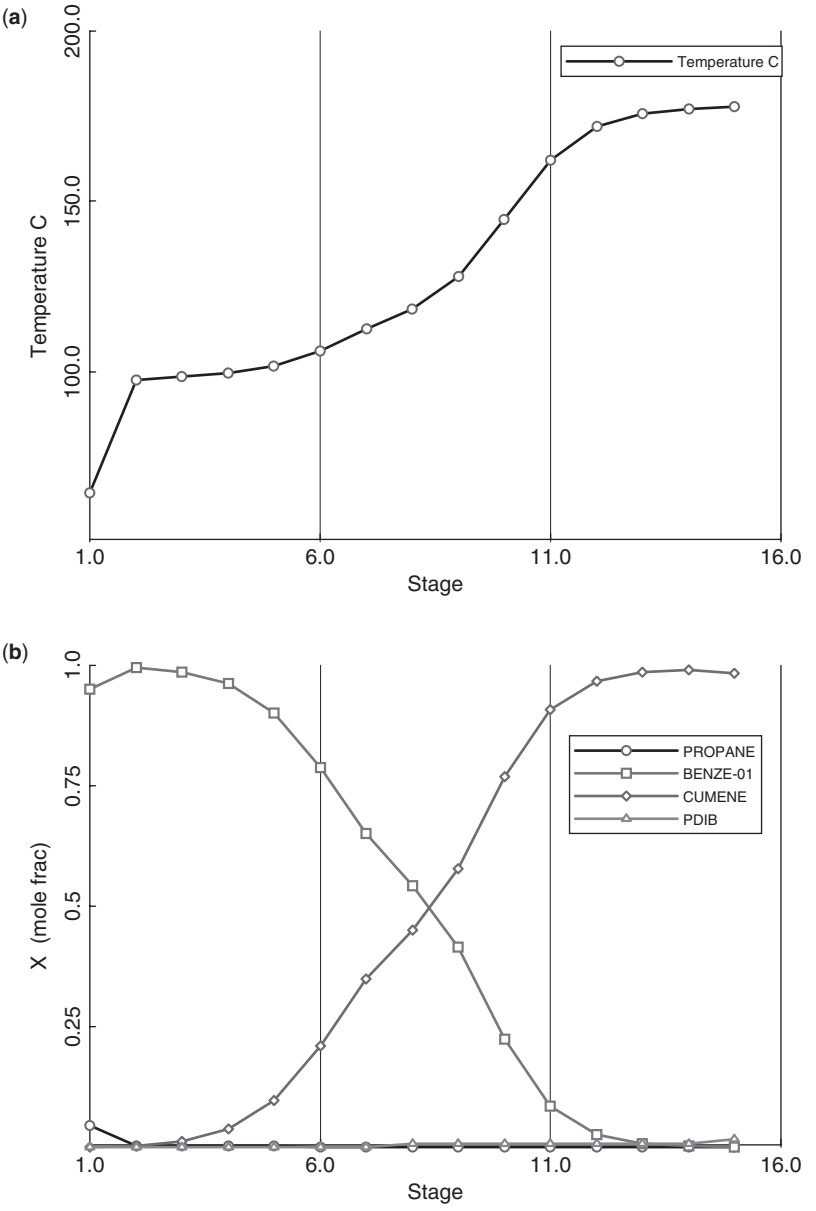


**Figure 9.10.** (a) Column C1 temperature profile. (b) Column C1 composition profiles.

1. Fresh C3 feed is flow-controlled. This is the throughput handle.
2. Total benzene (fresh feed plus benzene recycle D1 from column C1) is ratioed to the C3 flowrate. The fresh feed of benzene is manipulated to achieve the desired total flowrate of total benzene.
3. Vaporizer level is controlled by vaporizer heat input. There is no liquid outlet stream.
4. Reactor inlet temperature is controlled by heat input to HX1.

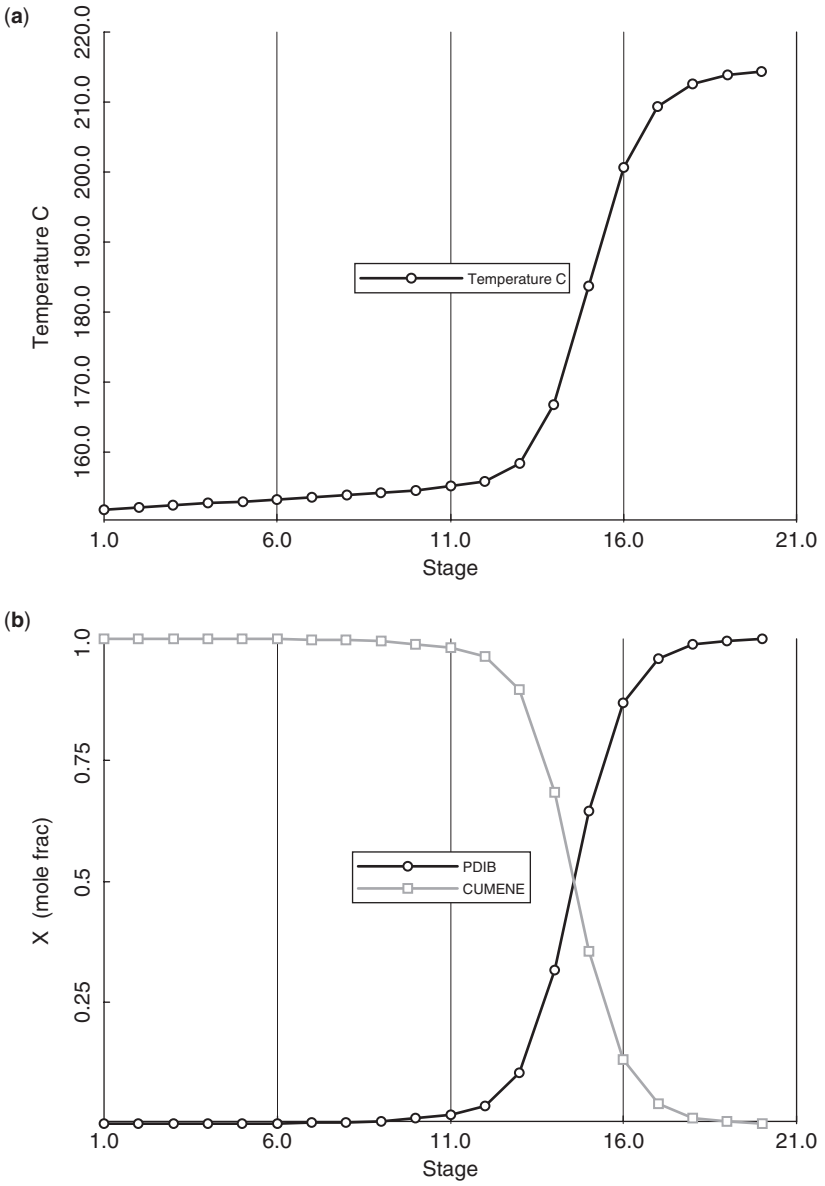


**Figure 9.11.** (a) Column C2 temperature profile. (b) Column C2 composition profiles.

5. Reactor exit temperature is controlled by manipulating the pressure (temperature) of the steam being generated on the shell side of the tubular reactor.
6. The back pressure on the reactor system is controlled by manipulating the control valve located after the FEHE. This valve drops the pressure from 23 bar in the reactor to 2 bar in the flash tank.
7. Temperature leaving the condenser HX2 is controlled by heat removal.
8. The level in the flash tank is controlled by manipulating the flowrate of liquid leaving the tank and going to column C1.

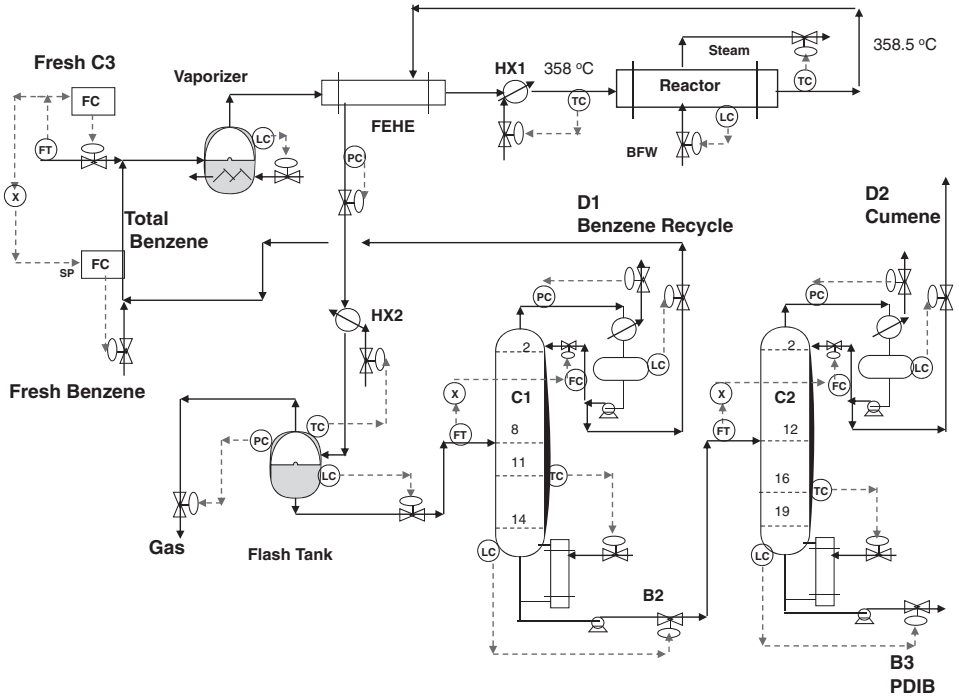


**Figure 9.12.** Plantwide control structure.

9. The pressure in the flash tank is controlled by manipulating the gas stream.
10. Pressures in all columns are controlled by condenser heat removal.
11. Base levels in all columns are controlled by bottoms flowrates.
12. Reflux-drum levels in all columns are controlled by distillate flowrates.
13. Reflux flowrates are ratioed to column feed.
14. The temperature on stage 11 in column C1 is controlled by manipulating reboiler heat input. This location is selected by looking at the temperature profile shown in Figure 9.10a.
15. The temperature on stage 16 in column C1 is controlled by manipulating reboiler heat input. This location is selected by looking at the temperature profile shown in Figure 9.11a.

Item 2 is one of the key plantwide control features of this structure. The total flowrate of benzene is controlled. Note that the flowrates of the fresh benzene and the recycle benzene are about the same in magnitude (98.78 and 108.2 kmol/h) in this flowsheet. The flowrate of the fresh feed is used to control the total with the distillate from column C1 being used to control the reflux-drum level in this column. In another process in which the flowrate of the fresh feed is much smaller than the recycle, this structure would not be effective. In that situation, the total should be controlled by manipulating the flowrate of the recycle, and the liquid level in the reflux drum should be controlled by manipulating the fresh feed stream. It is important to realize that changing the fresh feed flowrate has an immediate effect on the reflux-drum level, even though it is not introduced into the drum. Changing

**TABLE 9.4 Temperature Controller Parameters**

| | Reactor Exit | Recycle Column C1 Stage 11 | Product Column C2 Stage 16 |
|---|---|---|---|
| | TCR | TC1 | TC2 |
| SP | 358.5 °C | 162.2 °C | 200.6 °C |
| Transmitter range | 300–400 °C | 100–200 °C | 150–250 °C |
| OP | 358 °C | 3.37 Gcal/h | 3.37 Gcal/h |
| OP range | 300–400 °C | 0–1.68 Gcal/h | 0–1.18 Gcal/h |
| Deadtime | 1 min | 1 min | 1 min |
| $K_C$ | 2.4 | 0.66 | 0.51 |
| $\tau_I$ (min) | 11 | 11 | 23 |

fresh feed affects total flow, so the total flow controller adjust the distillate flow to hold the total flow constant. Therefore the reflux-drum level is immediately affected.

All liquid level controllers are proportional only using $K_c = 2$. The reactor exit temperature loop and column temperature loops contain 1-min deadtimes and are tuned using relay-feedback tests and Tyreus–Luyben tuning rules. Table 9.4 gives controller tuning parameters for various cases. Figure 9.13 shows the controller faceplates from the Aspen Dynamics simulation. Note that the flow controller on the total benzene is on cascade, receiving its setpoint from the multiplier that gets it input from the flow transmitter on the fresh C3 feed.

The effectiveness of this structure is demonstrated in Figures 9.14, 9.15, and 9.16 for several large disturbances. In Figure 9.14, the setpoint of the C3 fresh feed flow controller is changed at time equal 0.2 h. The solid lines are responses for a 20% increase, and the dashed lines are for a 20% decrease. Stable regulatory control is achieved with the product quality of the cumene product $x_{D2(cumene)}$ being maintained above the desired 99.9 mol% specification [$x$D2(C)]. An increase in fresh feed results in the production of more gas and more undesirable product B2. The temperature of the steam $T_S$ in the reactor must be reduced to hold the same exit temperature. Column temperatures are well controlled. There is a fairly large dynamic transient in the composition of the undesirable product $x_{B2(PDIB)}$. This could be greatly reduced by using a steam-to-feed ratio in column C2 with the ratio reset by the column temperature controller.

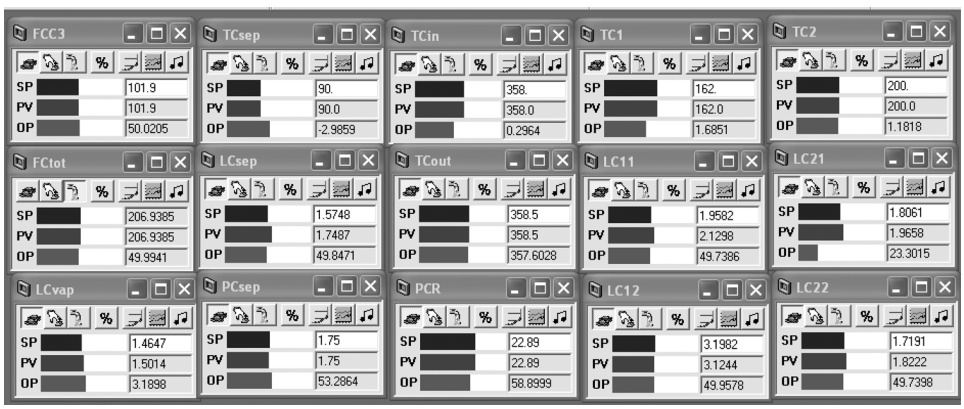


**Figure 9.13.** Controller faceplates.

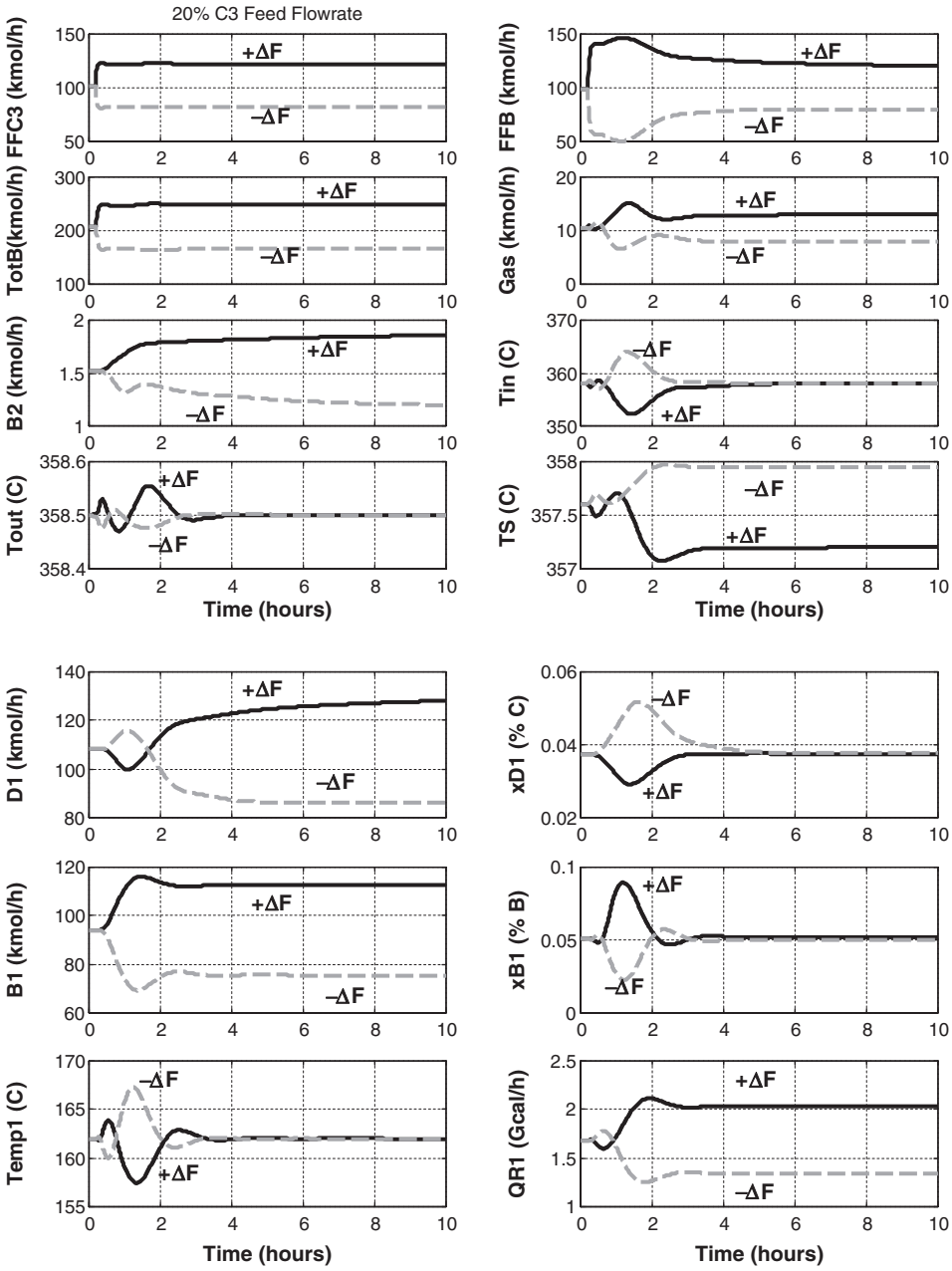


**Figure 9.14.** Twenty percent C3 fresh feed flowrate disturbances.

Figure 9.15 gives responses for disturbances in the composition of the fresh C3 feed. The solid lines indicate when more propane is fed. The feed composition is changed from 95 to 93 mol% propylene with a corresponding increase in propane from 5 to 7 mol% propane. The dashed lines indicate when less propane is fed (5 mol% changed to 3 mol% propane).

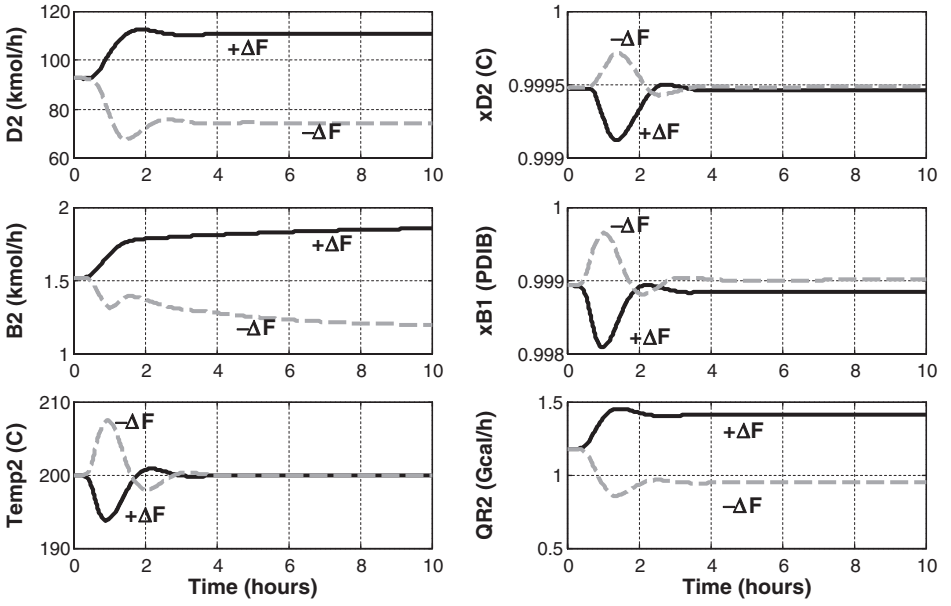


**Figure 9.14.** *Continued.*

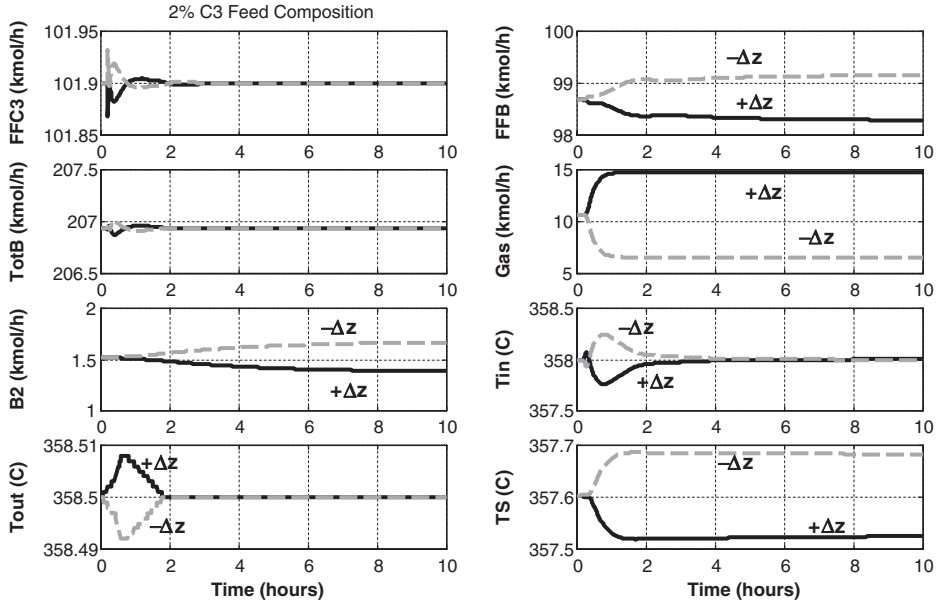


**Figure 9.15.** Propylene fresh feed composition disturbances.

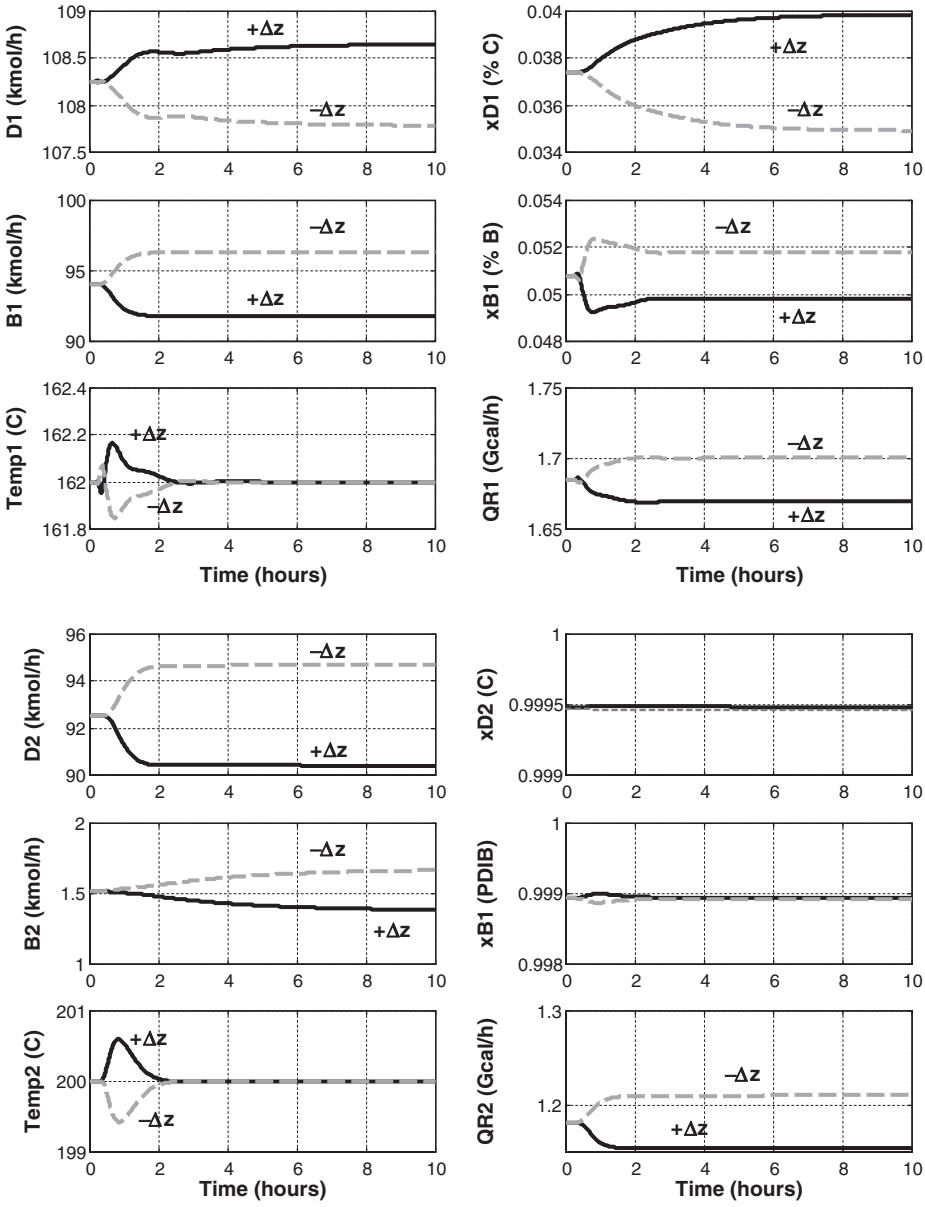


**Figure 9.15.** *Continued.*

The control structure handles this disturbance well. When more propane enters the system, the flowrate of fresh benzene is gradually reduced. More gas is removed and less cumene is produced. Benzene recycle increases, which results in a small decrease in the production of the undesirable product.

The final disturbance is a change in the setpoint of the reactor exit temperature controller. Figure 9.16 gives responses for a change from 358 to 365 °C (solid lines) and for a change

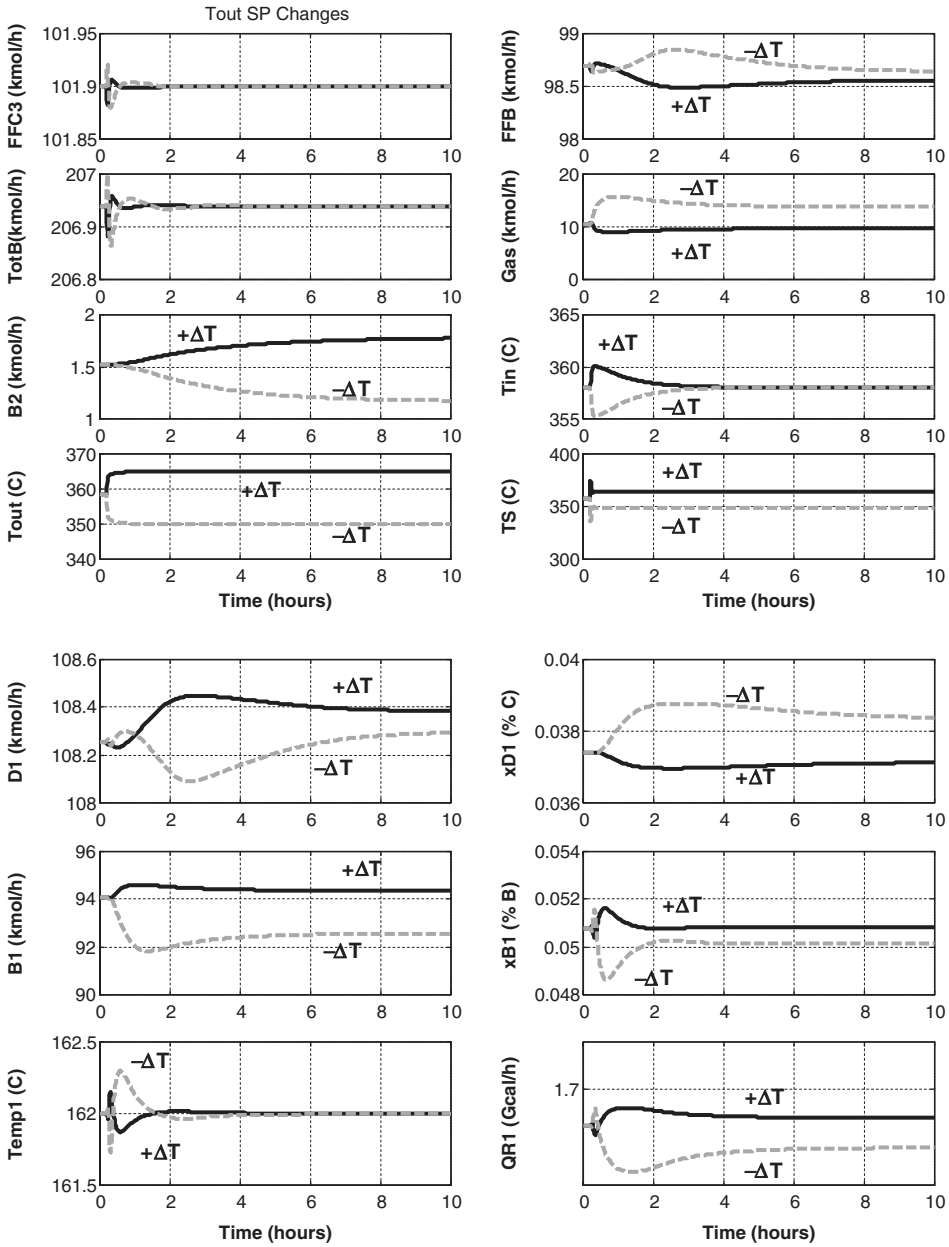


**Figure 9.16.** Disturbances in reactor exit temperature setpoint.

from 358 to 350 °C (dashed lines). As expected, increasing reactor temperature produces more undesirable product B2. There is little change in the cumene production (D2) for an increase in reactor temperature, but there is a significant decrease for a decrease in reactor temperature. This occurs because the lower conversion of propylene in the reactor produces a large increase in the gas.

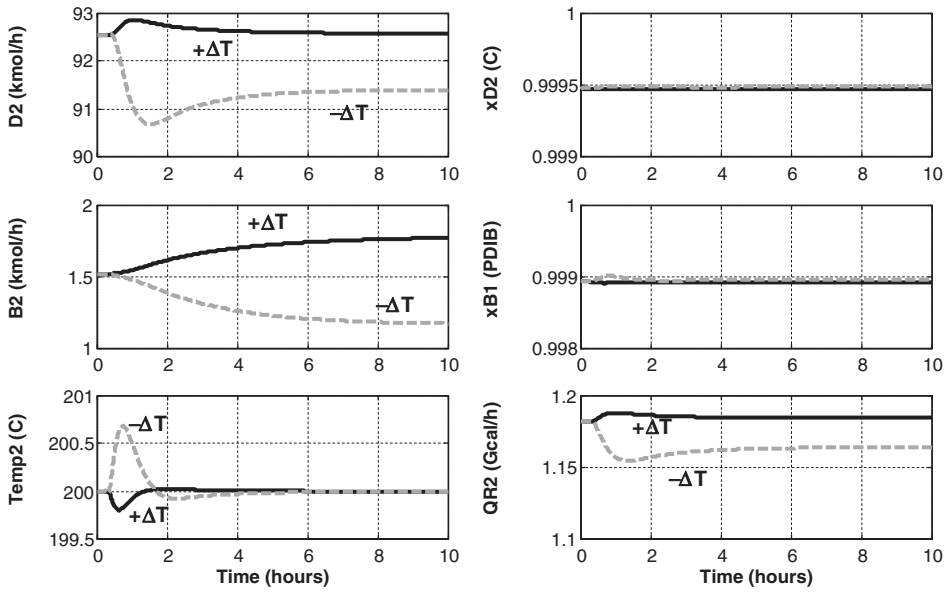


**Figure 9.16.** *Continued.*

## 9.5 CONCLUSION

The cumene process exhibits some interesting design and control features. It provides a classical example of the engineering trade-off between reactor size and recycle flowrate. Design optimization variables affect capital and energy costs. But they also affect conversion and selectivity, which have a very large impact on raw material costs. The economics of the cumene process illustrate that reducing reactant losses and the production of undesirable products can produce savings that are much larger than capital or energy costs.

Effective dynamic control of the multiunit process is achieved by the use of conventional controllers and a control structure that fixes the total benzene feed to the reactor (fresh feed plus recycle). Large disturbances in throughput and feed compositions are handled with products held close to their specified values.

## REFERENCES

1. Turton, R., Bailie, R. C., Whiting, W. B., Shaelwitz, J. A. *Analysis, Synthesis and Design of Chemical Processes*, 2nd Edition, Prentice Hall, Englewood Cliffs, NJ, 2003.
2. Douglas, J. M. *Conceptual Design of Chemical Processes*, McGraw-Hill, New York, 1988.
3. Luyben, W. L. *Distillation Design and Control Using Aspen Simulation*, John Wiley & Sons, Hoboken, NJ, 2006.
4. Luyben, W. L., Tyreus, B. D., Luyben, M. L. *Plantwide Process Control*, McGraw-Hill, New York, 1999.

# INDEX




*Principles and Case Studies of Simultaneous Design*, First Edition. William L. Luyben

# CHAPTER 10

# DESIGN AND CONTROL OF THE ETHYL BENZENE PROCESS

The ethyl benzene process involves the reaction of benzene with ethylene to form the desired ethyl benzene (EB) product. However, ethylene can also react with EB to form an undesired product of diethyl benzene (DEB) if reactor temperatures or ethylene concentrations are high.

An unusual feature of the EB process is the ability to recycle "to extinction" all the DEB formed in the reactor (no net DEB product produced) since DEB reacts with benzene to form EB. Since DEB is the highest boiling component in the system, it comes out the bottom of the two distillation columns, so there is little energy penalty in having a large DEB recycle. Recycling benzene is more expensive because it goes overhead in the first distillation column.

In this chapter, the economic optimum steady-state design, which minimizes total annual cost (TAC: capital and energy), and an effective plantwide control structure are developed.

## 10.1 INTRODUCTION

Ethyl benzene is an important commodity chemical. Much of its production is used to make styrene. The process considered in this chapter has two reactors in series, two distillation columns, and two liquid recycle streams. Thus, it provides a nice example of a multiunit complex process that is typical of many chemical plants found in industry.

An interesting and unusual feature of the EB process is the recycle to extinction of the DEB by-product. A significant amount of DEB circulates through the system, and the per-pass EB selectivity is quite low. But the overall selectivity is essentially 100% since all of the fresh reactant feeds (ethylene and benzene) end up leaving in the single product stream as EB.

*Principles and Case Studies of Simultaneous Design*, First Edition. William L. Luyben

In this chapter, we present the details of the process, discuss the important economic trade-offs in its steady-state design, and demonstrate the effectiveness of a plantwide control structure. It is hoped that other workers will find the EB process useful in their research for testing other design and control methodologies.

The EB process provides a good example of the application of several fundamental principles of design. We can look at the chemistry and immediately know that there will be a trade-off between reactor size and selectivity because the activation energy of the undesirable reaction is larger than that of the desirable reaction. So, low reactor temperatures will be favored, but this requires larger reactors for a given conversion. The chemistry also tells right up front that there will be a trade-off between recycle costs and selectivity because the concentrations of the components that react in the undesirable reaction must be kept small. These design trade-offs are discussed in detail in this chapter.

## 10.2 PROCESS STUDIED

Figure 10.1 shows the flowsheet studied in this chapter. The process is a modified version of a process that was explored earlier (see Luyben[1]), when it was used to illustrate dynamic plantwide simulation methods. The economics of the design were not considered in this previous work. Kinetic parameters have been adjusted to give reasonable rates of generation of the two components of interest (EB and DEB) in the reactors.

The EB process involves sparging gaseous ethylene into the liquid phase of the first of two continuous stirred-tank reactors (CSTR) in series. Both reactors operate at high pressure (20 atm) to maintain liquid in the reactor at the high temperatures required for reasonable

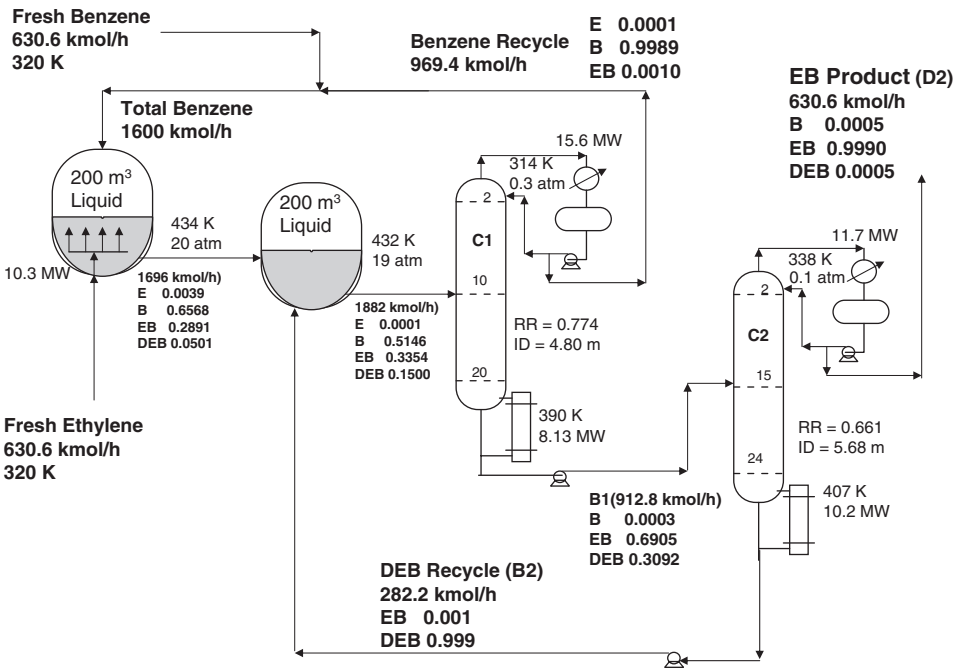


**Figure 10.1.** Ethyl benzene flowsheet.

reaction rates (433 K). A large liquid benzene stream is also fed to the first reactor. The heat of the exothermic reaction is removed by generating 2.5 atm steam in this reactor.

The effluent from the first reactor is fed into the second reactor along with a recycle stream of DEB. This reactor is adiabatic. The effluent from the second reactor is fed to a distillation column that produces a distillate that is mostly benzene, which is recycled to the first reactor along with the fresh feed of makeup benzene. The bottoms stream is a mixture of EB and DEB. It is fed to a second distillation column, which produces an EB distillate and a DEB bottoms that is recycled back to the second reactor.

Note that a two-reactor flowsheet is used so that high conversion of the ethylene can be achieved in the first reactor and conditions are favorable in the second reactor for the reaction of DEB back to EB (higher concentration of DEB).

### 10.2.1 Reaction Kinetics

The production of EB involves the liquid-phase reaction of ethylene with benzene

$$C_2H_4 + C_6H_6 \longrightarrow C_8H_{10} \tag{10.1}$$

There are other undesirable reactions that we assume can be represented by the formation of DEB from the reaction of EB with ethylene.

$$C_8H_{10} + C_2H_4 \longrightarrow C_{10}H_{14} \tag{10.2}$$

A third reaction also occurs, in which DEB reacts with benzene to form EB.

$$C_{10}H_{14} + C_6H_6 \longrightarrow 2C_8H_{10} \tag{10.3}$$

This reaction makes it possible to recycle the DEB back to the second reactor where an excess of benzene exists and drives the reaction to the right to produce EB. Thus, there is essentially no DEB leaving the system despite the fact that a large amount is produced in the first reactor and passes through the two distillation columns.

Table 10.1 gives the reaction kinetics assumed in this study. All reaction rates have units of kmol $s^{-1}$ $m^{-3}$ (consistent with Aspen simulation requirements). Concentration units are molarity (kmol/$m^3$).

Notice that the activation energy of the undesirable reaction (reaction 2) is larger than that of the desirable reaction. Therefore, low reactor temperatures improve selectivity. In addition, selectivity is improved by keeping low concentrations of ethylene and EB in the reactor. This can be achieved by using a large excess of benzene, but the excess must be recovered and recycled.

A high conversion of ethylene in the first reactor is desired so that the ethylene concentration is low. This reduces the production of DEB and results in only a small amount of

**TABLE 10.1 Ethyl Benzene Reaction Kinetics**

| | $\Re 1$ | $\Re 2$ | $\Re 3$ |
|---|---|---|---|
| $k$ | $1.528 \times 10^6$ | $2.778 \times 10^7$ | 1000 |
| $E$ (cal/mol) | 17,000 | 20,000 | 15,000 |
| Concentration terms (kmol/$m^3$) | $C_E C_B$ | $C_E C_{EB}$ | $C_B C_{DEB}$ |

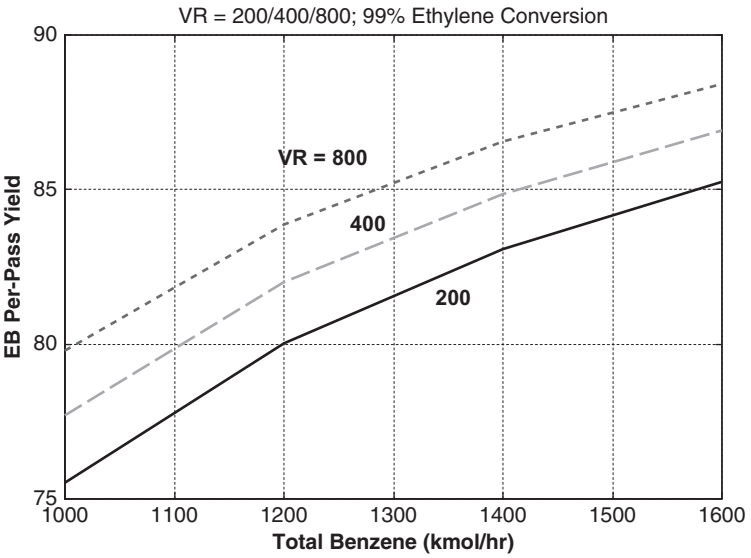


**Figure 10.2.** Per-pass yield.

ethylene that is recycled in the benzene recycle stream. Ethylene conversion is set at 99% for all the cases considered by adjusting the temperature of the first reactor.

Figure 10.2 illustrates how the important design optimization variables affect EB yield, which is defined as the molar flowrate of EB leaving the reactor divided by the sum of the molar flowrates of EB and DEB. This is *per-pass* yield, not the overall yield of the entire process. Yield is increased by increasing the recycle flowrate of benzene or by increasing reactor size. The larger the reactor, the lower the temperature required for the fixed ethylene conversion of 99%. The 200 $m^3$ reactor requires temperatures around 430 K. The 400 $m^3$ reactor requires temperatures around 416 K. The 800 $m^3$ reactor requires temperatures around 403 K. Lower temperature favors EB production because of the higher activation energy of the DEB reaction.

### 10.2.2 Phase Equilibrium

The two separations required are the removal of benzene from EB and the removal of EB from DEB. The Choa–Seader physical property package is used in the Aspen simulations. The normal boiling points of these components are 353 K for benzene, 409 K for EB, and 457 K for DEB. The significant differences mean that the two distillation columns have a fairly small number of trays and required a low reflux ratio (RR). In Section 10.3 of this chapter, the optimum designs of these two columns are developed based on minimizing TAC. The design optimization variables are pressure, number of trays, and feed locations.

Notice that the normal boiling points are considerably higher than the temperatures that can be achieved in a water-cooled condenser (314 K). This means that the columns could be operated under vacuum conditions, if this is economically attractive. This question is quantitatively addressed in Section 10.3.1.

### 10.2.3 Flowsheet

Figure 10.1 shows the flowsheet of the EB process with the equipment sizes and conditions that are the economic optimum, as discussed in the next section. Reactors of equal size are assumed. The economic optimum combination of reactor size and benzene recycle flowrate is reactors containing 200 $m^3$ of liquid (half full) and a total benzene stream of 1600 kmol/h. The total benzene stream is the distillate from the first column (969.4 kmol/h) and the fresh benzene feed.

The two fresh feeds (ethylene and benzene) are each 630.6 kmol/h, as is the production rate of EB since only a negligible amount of DEB leaves the system. Essentially all of the ethylene and benzene reactants leave as EB product in the distillate D2 from the second column.

The first reactor operates at 434 K and 20 atm. It is cooled by generating steam. About 80.5 kmol/h of DEB are generated in the first reactor along with 464.4 kmol/h of EB, leaving 6.3 kmol/h of unreacted ethylene. So the per-pass EB yield is only 85% in the first reactor.

$$\text{EB yield} = \frac{464.4}{464.4 + 80.5} = 0.852$$

The first reactor is cooled by generating steam in internal cooling coils. The temperature of the saturated steam is 414 K, with a reactor temperature of 434 K. In the Aspen Dynamics simulation, the heat removal option is *constant medium temperature.* A heat-transfer coefficient of 203 cal $s^{-1}$ $m^{-2}$ $K^{-1}$ is assumed, which requires 602 $m^2$ of heat-transfer area to remove the $2.46 \times 106$ cal/s of heat. Jacket heat-transfer area in the reactor (diameter = 7.53 m and length = 6.34 m) is only 151 $m^2$, so internal coils or an external heat exchanger are required.

The effluent from the first reactor is fed into the second reactor, in which essentially all the DEB generated in the first reactor is converted to EB by reaction with benzene. The recycle DEB from the bottom of the second column is also fed into the second reactor at a molar flowrate of 282.2 kmol/h. The DEB leaving in the effluent of the second reactor is this same 282.2 kmol/h. So, the second reactor is able to convert essentially all the DEB formed in the first reactor back to EB. Thus, the DEB is recycled to extinction.

The effluent from the second reactor is at high pressure and high temperature. It is fed into the first distillation column C1. The high feed temperature results in the vapor load in the rectifying section being higher than that in the stripping section. Notice that the condenser heat duty (15.6 MW) is much higher than the reboiler duty (8.13 MW) because of the high temperature of the feed stream. The first column has 21 stages and a reflux ratio of 0.774. It operates under moderate vacuum at 0.3 atm, which gives a reflux-drum temperature of 314 K and permits the use of cooling water in the condenser. The base temperature is 390 K, which permits the use of low-pressure steam (433 K, 4 atm) in the reboiler. The distillate is mostly benzene, which is mixed with the fresh benzene makeup feed and recycled to the first reactor. Figure 10.3 gives temperature and composition profiles in column C1.

The second column C2 has 25 stages and a RR of 0.661. It operates under low vacuum at 0.1 atm, which gives a reflux-drum temperature of 338 K and permits the use of cooling water in the condenser. The base temperature is 407 K, which permits the use of low-pressure steam in the reboiler. The distillate is high-purity EB (99.9 mol%). The bottoms B2 is recycled to the second reactor. Figure 10.4 gives temperature and composition profiles in column C2.

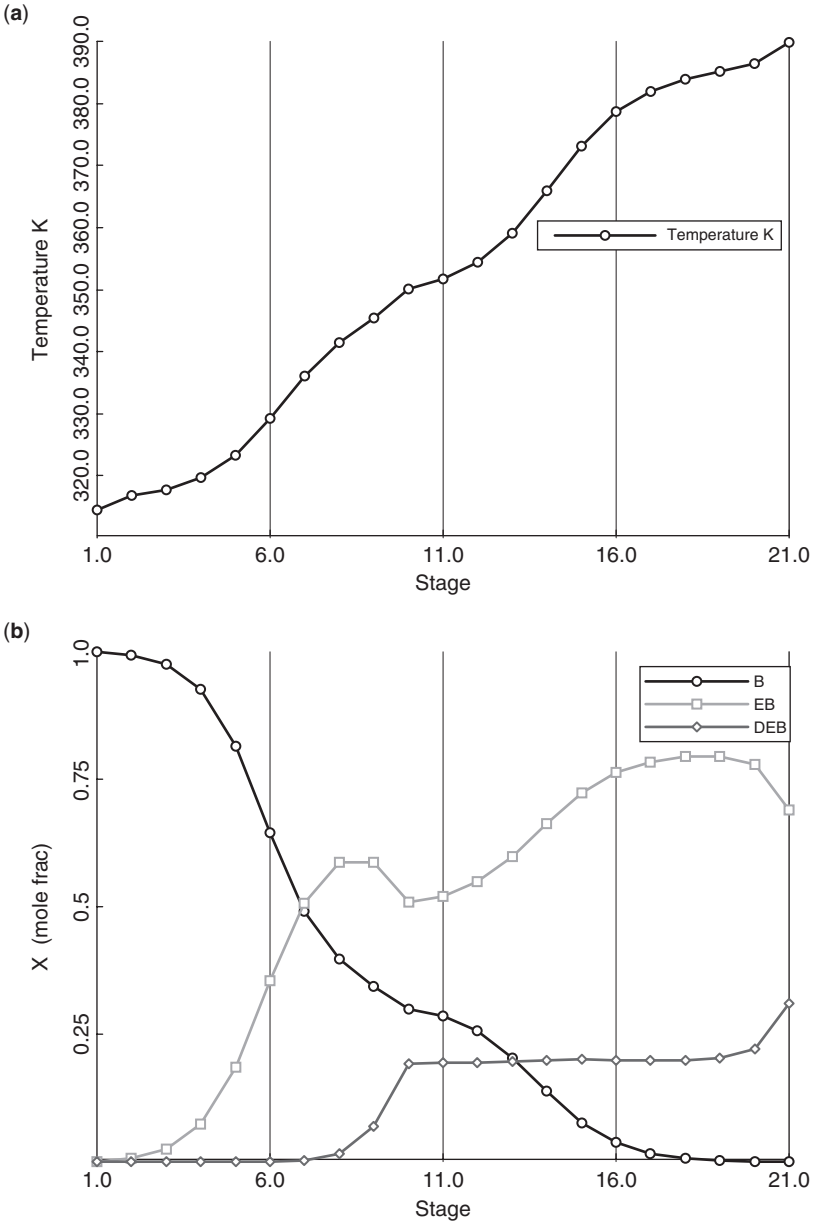


**Figure 10.3.** C1 (a) temperature profile, and (b) composition profiles.

## 10.3 DESIGN OF DISTILLATION COLUMNS

A common procedure for optimizing the design of a distillation column is to determine the values of the design optimization variables that minimize TAC (see Table 10.2). The parameters that must be given are the feed conditions and the desired product specifications.

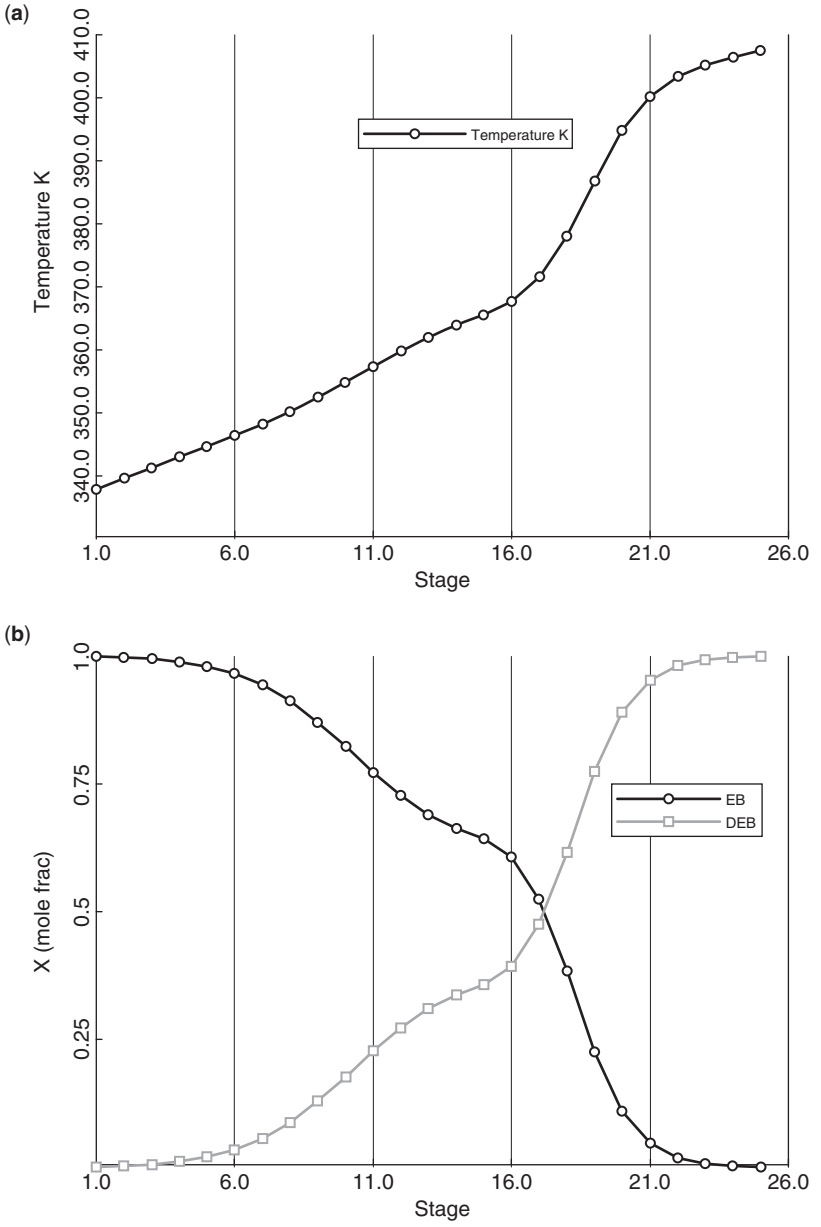


**Figure 10.4.** C2 (a) temperature profile, and (b) composition profiles.

The design optimization variables include pressure, total number of trays, and feed-tray location.

An iterative sequential optimization procedure was used to optimize the entire process. First, preliminary estimates of reactor conditions were used to determine distillation column feed compositions and flowrates. The columns were then optimized for these

**TABLE 10.2 Basis of Economics and Equipment Sizing**

Column diameter: Aspen tray sizing using double-pass trays
Column length: NT trays with 2 ft spacing plus 20% extra length
Column vessel (diameter and length in meters)
Capital cost $= 17{,}640(D)^{1.066}(L)^{0.802}$

*Condensers (area in $m^2$)*
Heat-transfer coefficient $= 0.852\ \text{kW/K-m}^2$
Differential temperature = Reflux-drm Temperature − 310 K
Capital cost $= 7296(A)^{0.65}$

*Reboilers (area in $m^2$)*
Heat-transfer coefficient $= 0.568\ \text{kW/K-m}^2$
Differential temperature = Steam temperature − Base temperaute
Capital cost $= 7296(A)^{0.65}$

*Reactor (diameter and length in meters)*
Half full of liquid
Aspect ratio = 1
Capital cost $= 17{,}640(D)^{1.066}\ (L)^{0.803}$

*Energy cost*
LP steam (433 K) = \$7.78/GJ
MP steam (457 K) = \$8.22/GJ
HP steam (537 K) = \$9.83/GJ
Value of steam generated in reactor:
LP steam (410 K) = \$6.00/GJ

$$\text{TAC} = \frac{\text{Capital cost}}{\text{Payback period}} + \text{Energy cost}$$

Payback period = 3 yr

values. Next, the overall process was optimized in terms of reactor size and recycle flowrates using the preliminary column designs. Once new column feed conditions were determined, the columns were reoptimized and the procedure repeated until design optimization variables stopped changing.

In many systems, decreasing pressure increases relative volatilities, which decrease energy requirements. This can reduce steam consumption and capital investment in column shell and in heat exchanger area (condenser and reboiler). Since the components to be separated in this system have fairly high normal boiling points, pressure can be reduced to vacuum conditions.

Lower pressure also gives a lower base temperature, which means a lower-temperature, less expensive energy source can be used in the reboiler or the area of the reboiler can be smaller. However, lower column pressure gives a lower condenser temperature, which increases the required area in the condenser. All of these interacting effects must be quantitatively evaluated.

### 10.3.1 Column Pressure Selection

A number of cases are run with different operating pressures to assess the economic impact of pressure. The sizing relationships and cost estimations for the equipment are based on

information from Douglas[2] and Turton et al.[3] and are summarized in Table 10.2. Note that the cost of steam at different pressures is given.

The feed flowrates and compositions used in these cases are those found in the final optimum design. The number of trays and the feed-tray locations are also those found in the final optimum design (see Figure 10.1). The determination of the optimum number of trays is discussed in Section 10.3.2.

The specifications for the design of column C1 are 0.1 mol% EB in the distillate and a ratio of benzene to EB in the bottoms of 0.0005. This latter specification is needed to make sure the purity of the final EB product leaving the second column can be achieved. Distillate flowrate and RR are varied to achieve these specifications for each case. The specifications for the design of column C2 are 0.1 mol% EB in the bottoms and 0.05 mol% DEB in the distillate.

Table 10.3 gives detailed results for both columns over a range of pressures. Note that the pressure of the steam used in the reboiler changes from case to case. In both columns, energy costs decrease as pressure is decreased because reboiler heat inputs decrease. In addition, lower-pressure, less expensive steam can be used as base temperatures ($T_B$) decrease. As shown in Figure 10.5, column C1 diameters increase monotonically as pressure decreases. However, in column C2, there is an initial decrease in diameter before it begins to increase as

**TABLE 10.3 Column Pressure Selection**

| | C1 21/11 | | | | | |
|---|---|---|---|---|---|---|
| Pressure (atm) | 0.1 | 0.3 | 0.4 | 0.5 | 0.7 | 1.0 |
| $T_D$ (K) | 289 | 316 | 324 | 331 | 341 | 353 |
| $T_R$(K) | 373 | 392 | 398 | 405 | 415 | 426 |
| Steam | LP | LP | LP | LP | MP | HP |
| ID (m) | 6.5 | 4.80 | 4.44 | 4.17 | 3.85 | 3.62 |
| $Q_R$ (Mcal/s) | 1.57 | 1.91 | 2.11 | 2.17 | 2.40 | 2.69 |
| $Q_C$ (Mcal/s) | 3.89 | 3.72 | 3.69 | 3.66 | 3.63 | 3.63 |
| AR ($m^2$) | – | 343 | 443 | 570 | 420 | 638 |
| AC ($m^2$) | – | 3040 | 1292 | 854 | 574 | 414 |
| Capital ($10^6$ \$) | – | 2.44 | 1.86 | 1.76 | 1.44 | 1.36 |
| Energy ($10^6$ \$/yr) | – | 1.97 | 2.17 | 2.23 | 2.60 | 2.92 |
| TAC ($10^6$ \$/yr) | – | 2.77 | 2.788 | 2.80 | 3.08 | 3.37 |

| | C2 22/13 | | | | |
|---|---|---|---|---|---|
| Pressure (atm) | 0.1 | 0.3 | 0.5 | 0.7 | 1.0 |
| $T_D$ (K) | 338 | 369 | 386 | 397 | 411 |
| $T_R$ (K) | 405 | 426 | 440 | 451 | 464 |
| Steam | MP | MP | MP | MP | HP |
| ID (m) | 5.78 | 4.44 | 4.17 | 4.17 | 4.20 |
| $Q_R$ (Mcal/s) | 2.30 | 2.74 | 3.05 | 3.31 | 3.65 |
| $Q_C$ (Mcal/s) | 2.90 | 2.95 | 3.04 | 3.13 | 3.27 |
| AR ($m^2$) | 325 | 648 | 258 | 328 | 426 |
| AC ($m^2$) | 508 | 245 | 196 | 176 | 159 |
| Capital ($10^6$ \$) | 1.72 | 1.49 | 1.20 | 1.22 | 1.27 |
| Energy ($10^6$ \$/yr) | 2.49 | 2.97 | 3.96 | 4.29 | 4.73 |
| TAC ($10^6$ \$/yr) | 3.07 | 3.46 | 4.35 | 4.70 | 5.16 |

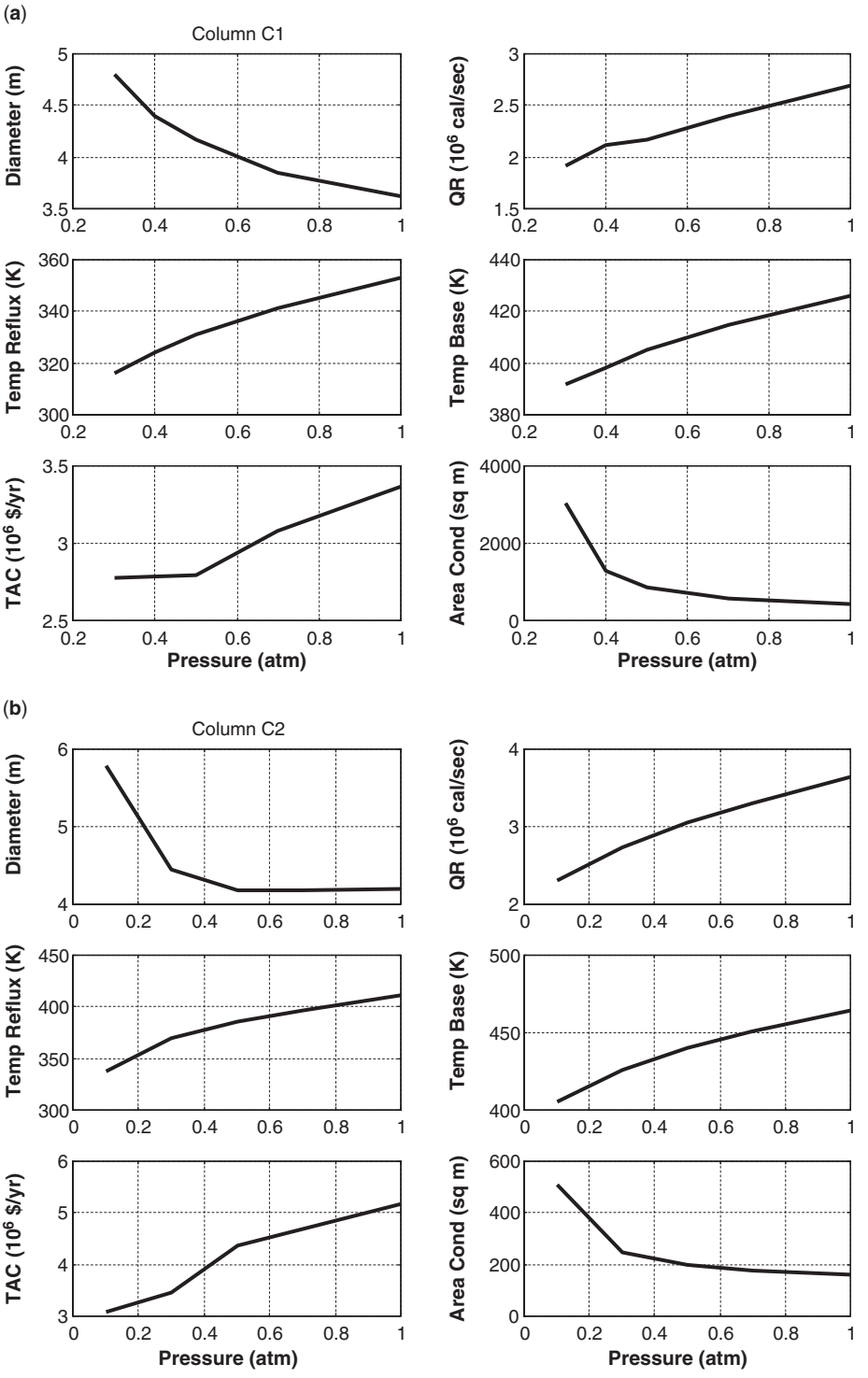


**Figure 10.5.** Effect of pressure for (a) C1, and (b) C2.

**TABLE 10.4 Column Tray Number Optimization**

| | C1 (0.3 atm) | | | C2 (0.1 atm) | | |
|---|---|---|---|---|---|---|
| NT | 16 | **21** | 26 | 22 | **25** | 32 |
| NF | 8 | 10 | 13 | 13 | 15 | 18 |
| ID (m) | 5.14 | 4.81 | 4.77 | 5.82 | 5.78 | 5.64 |
| $Q_R$ ($10^6$ cal/s) | 2.26 | 1.96 | 1.95 | 2.55 | 2.46 | 2.44 |
| $Q_C$ ($10^6$ cal/s) | 4.07 | 3.73 | 3.68 | 2.93 | 2.83 | 2.77 |
| Shell ($10^6$ \$) | 0.653 | 0.776 | 0.929 | 0.992 | 1.10 | 1.33 |
| Heat exchangers ($10^6$ \$) | 1.78 | 1.67 | 1.66 | 0.756 | 0.739 | 0.732 |
| Total capital ($10^6$ \$) | 2.43 | 2.45 | 2.58 | 1.75 | 1.84 | 2.06 |
| Energy ($10^6$ \$/yr) | 2.32 | 2.01 | 2.00 | 2.77 | 2.67 | 2.65 |
| TAC ($10^6$ \$/yr) | 3.131 | **2.828** | 2.864 | 3.348 | **3.282** | 3.333 |

pressure is reduced. This is due to the interaction between vapor flowrates, which decrease as pressure decreases, and vapor velocities, which increase as vapor density decreases. Notice the rapid increase in the required condenser area as pressures are reduced; this is due to the smaller temperature difference between cooling water (310 K) and the reflux-drum temperature. Pressures lower than 0.3 atm cannot be used in column C1 if cooling water is to be the heat-removal medium.

It is assumed that the minimum practical pressure is 0.1 atm (76 mm Hg) in the condenser. Therefore, the pressure selected for column C2 is 0.1 atm, and for column C1 it is 0.3 atm.

Only steady-state issues have been considered in this analysis. However, running distillation columns under vacuum can significantly impact dynamic control strategies. In a vacuum column, the pressure changes from tray to tray are a significant portion of the total pressure. Tray pressure drop changes with vapor rates, so pressures on the column trays can vary, which affects tray temperatures. Therefore, it is sometimes necessary to use direct composition control instead of temperature control. A practical alternative in some systems is to use "pressure-compensated" temperature control.

### 10.3.2 Number of Column Trays

Having established the operating pressures in the columns, we must find the economic optimum number of trays. Using more trays reduces reboiler heat input, which reduces column diameter and heat exchanger area (reboiler and condenser). But using more trays increases the height of the column, which increases capital cost.

Table 10.4 gives results for both columns over a range of tray numbers. The pressure in C1 is 0.3 atm. The pressure in C2 is 0.1 atm. The feed-tray location is optimized for each case by minimizing reboiler heat input. Increasing the number of trays reduces energy cost and the capital cost of the heat exchangers. However, the capital cost of the vessel shell increases as more trays are used.

Total annual cost is minimized by using a 21-stage C1 column and a 25-stage C2 column.

## 10.4 ECONOMIC OPTIMIZATION OF ENTIRE PROCESS

The design optimization variables in the EB process are reactor size and benzene recycle flowrate. Ethylene conversion in the first reactor is fixed at 99%. Increasing reactor size means lower reactor temperatures, better EB yield, and lower DEB recycle flowrates. The

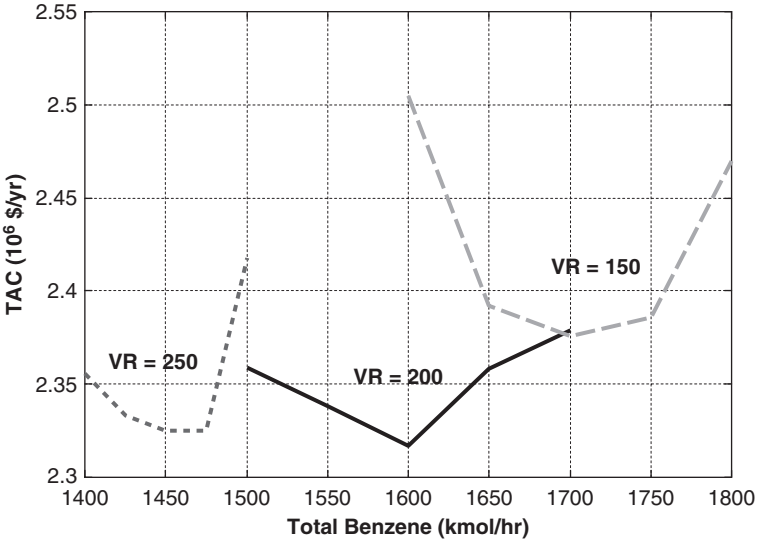


**Figure 10.6.** Effect of benzene recycle and reactor size on TAC.

result is higher reactor capital cost but lower separation costs. Increasing benzene recycle also gives better EB yield and lower DEB recycle, but separation costs increase because recycling benzene is more expensive than recycling DEB since benzene must be vaporized and taken overhead in the first distillation column. The DEB recycle, on the other hand, comes out the bottom of both distillation columns and does not have to be vaporized.

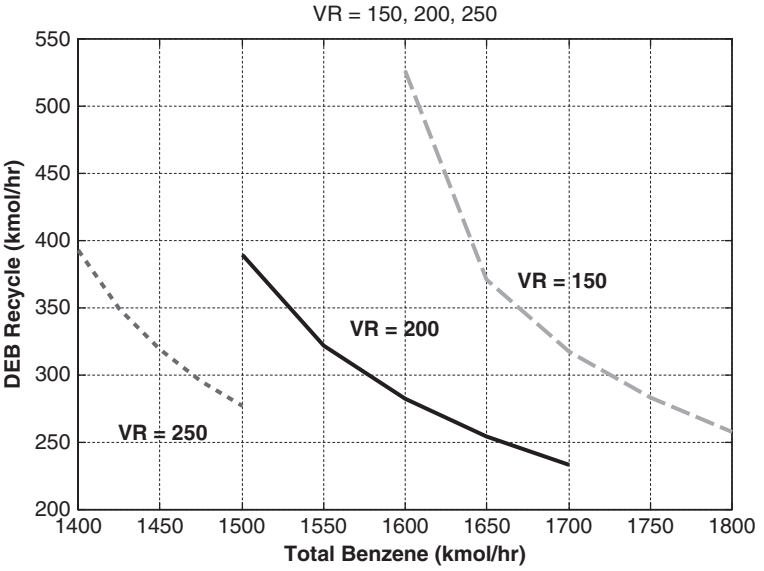


**Figure 10.7.** Effect of benzene recycle and reactor size on DEB recycle.

Figure 10.6 shows the economic impact of these two variables. The minimum TAC is achieved using 200 $m^3$ reactors and a total benzene flowrate of 1600 kmol/h. Figure 10.7 shows the effect of the two design optimization variables on the recycle flowrate of DEB from the bottom of column C2. Bigger reactors and higher benzene recycle flowrates produce less DEB in the reactor and result in smaller DEB recycle. Table 10.5 provides more detailed information about the alternative designs.

**TABLE 10.5 Effects of Reactor Size and Recycle**

| | | | |
|---|---|---|---|
| $V_R = 150$ ($m^3$) | | | |
| Total benzene (kmol/h) | **1600** | **1700** | **1800** |
| DEB recycle (kmol/h) | 525.9 | 317.3 | 258.0 |
| $T_{R1}$ (K) | 440 | 442 | 442 |
| ID1 (m) | 4.99 | 5.03 | 5.15 |
| $Q_{R1}$ ($10^6$ cal/s) | 2.09 | 2.01 | 2.07 |
| $Q_{C1}$ ($10^6$ cal/s) | 4.02 | 4.09 | 4.29 |
| ID2 (m) | 6.10 | 5.74 | 5.64 |
| $Q_{R2}$ ($10^6$ cal/s) | 2.83 | 2.49 | 2.40 |
| $Q_{C2}$ ($10^6$ cal/s) | 3.21 | 2.86 | 2.77 |
| Total energy cost ($10^6$ \$/yr) | 0.941 | 0.846 | 0.867 |
| Total capital ($10^6$ \$) | 4.69 | 4.59 | 4.88 |
| TAC ($10^6$ \$/yr) | **2.505** | **2.376** | **2.470** |
| $V_R = 200$ ($m^3$) | | | |
| Total benzene (kmol/h) | **1500** | **1600** | **1700** |
| DEB recycle (kmol/h) | 389.6 | 282.2 | 233.3 |
| $T_{R1}$ (K) | 433 | 434 | 434 |
| ID1 (m) | 4.70 | 4.80 | 4.93 |
| $Q_{R1}$ ($10^6$ cal/s) | 1.92 | 1.94 | 2.02 |
| $Q_{C1}$ ($10^6$ cal/s) | 3.58 | 3.74 | 3.94 |
| ID2 (m) | 5.86 | 5.68 | 5.61 |
| $Q_{R2}$ ($10^6$ cal/s) | 2.60 | 2.44 | 2.37 |
| $Q_{C2}$ ($10^6$ cal/s) | 2.97 | 2.80 | 2.73 |
| Total energy cost ($10^6$ \$/yr) | 0.761 | 0.725 | 0.778 |
| Total capital ($10^6$ \$) | 4.79 | 4.77 | 4.80 |
| TAC ($10^6$ \$/yr) | **2.359** | **2.317** | **2.379** |
| $V_R = 250$ ($m^3$) | | | |
| Total benzene (kmol/h) | **1400** | **1450** | **1500** |
| DEB recycle (kmol/h) | 393.1 | 319.0 | 276.9 |
| $T_{R1}$ (K) | 427 | 427 | 428 |
| ID1 (m) | 4.50 | 4.54 | 4.60 |
| $Q_{R1}$ ($10^6$ cal/s) | 1.85 | 1.84 | 1.87 |
| $Q_{C1}$ ($10^6$ cal/s) | 3.28 | 3.34 | 3.43 |
| ID2 (m) | 5.87 | 5.74 | 5.67 |
| $Q_{R2}$ ($10^6$ cal/s) | 2.61 | 2.50 | 2.43 |
| $Q_{C2}$ ($10^6$ cal/s) | 2.98 | 2.86 | 2.79 |
| Total energy cost ($10^6$ \$/yr) | 0.696 | 0.673 | 0.766 |
| Total capital ($10^6$ \$) | 4.98 | 4.96 | 4.96 |
| TAC ($10^6$ \$/yr) | **2.356** | **2.325** | **2.418** |

## 10.5 PLANTWIDE CONTROL

The flowsheet shown in Figure 10.1 does not include all the pumps and control valves needed in the process. The first step in studying dynamics using a pressure-driven dynamic simulation is to add these items and to determine the volumes of all vessels. The reactor sizes and column diameters are known, but the liquid surge capacities of the column reflux drums and column bases must be specified. These are all sized to provide 5 min of holdup when at 50% level. The steady-state conditions found in the dynamic simulation using Aspen Dynamics have only minor differences from those found in the steady-state simulation using Aspen Plus. The most significant difference is the DEB recycle B2, which is 282.2 kmol/h in Aspen Plus and 251.2 kmol/h in Aspen Dynamics.

Figure 10.8 shows the plantwide control structure developed. Conventional PI controllers are used in all loops. The recycles and the EB product are streams from the two distillation columns, so we first discuss the control schemes used for these units.

### 10.5.1 Distillation Column Control Structure

Most industrial distillation columns use inferential temperature control instead of the ideal direct composition control because of practical issues of reliability, expense and high maintenance when dealing with online analyzers. In many columns, a single temperature controller is used to maintain a temperature on an appropriate tray by manipulating reboiler heat input. Several methods for selecting the best tray have been proposed, but the simplest is to use the location where the temperature profile is steep. Then a reflux-to-feed (R/F) ratio

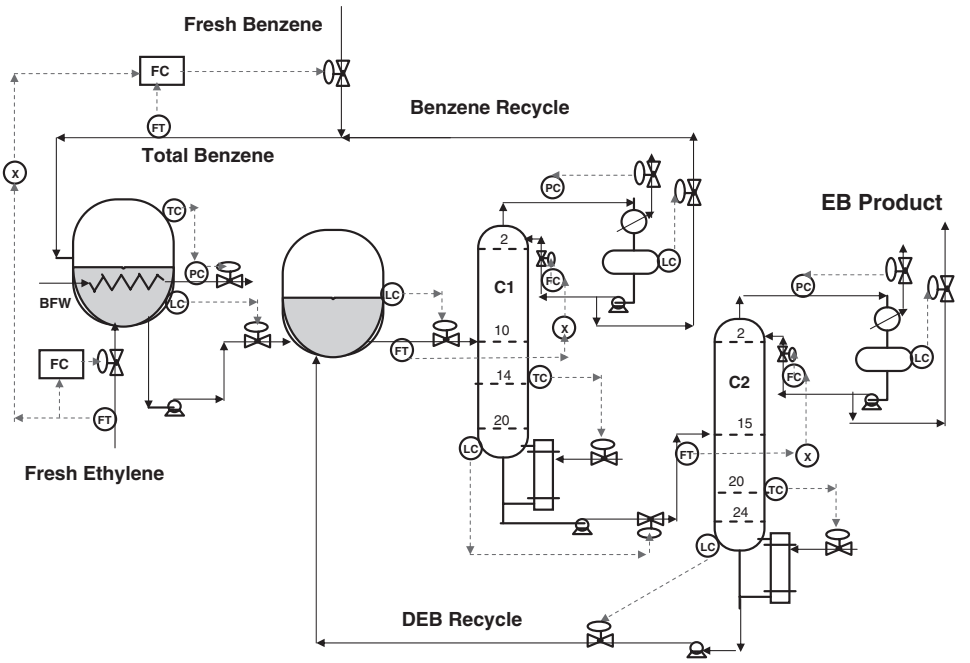


**Figure 10.8.** Ethyl benzene plantwide control structure.

or a reflux ratio structure is selected based on which can better handle feed composition disturbances. This approach is employed for the two columns in this study.

Figure 10.3a gives the temperature profile in column C1. The primary control objective in this column is to keep the benzene from dropping out the bottoms, so temperature in the lower part of the column should be used. The location where temperatures are changing rapidly from tray to tray is around stage 14, so the temperature on this stage is controlled by reboiler heat input. Figure 10.4a gives the temperature profile in column C2. The location where temperatures are changing rapidly from tray to tray is around stage 20, so the temperature on this stage is controlled by reboiler heat input.

Now we must decide whether to use the R/F ratio structure or the RR structure. From a steady-state perspective, either scheme can handle feed flowrate disturbances since all flowrates just ratio up or down with feed flowrate (if changes in pressure and tray efficiencies are neglected). However, their performances with feed composition changes are quite different.

To see which is better, feed compositions are changed around their design conditions in a steady-state simulation in which the two product streams are held at their specified values. In Aspen Plus, this is achieved by using the *Design Spec/Vary* feature. Table 10.6 gives the required changes in R/F and RR as feed compositions are changed in terms of the light- and heavy-key components in the two columns. In column C1 the key components are benzene and EB. In column 2 the key components are EB and DEB.

The results given in Table 10.6 indicate that R/F structures are better than RR structures in both columns. They are more effective in column C2 than in column C1 since the RR changes are only 3% in the former but 15% in the latter. The performances of the R/F structures are evaluated in Section 10.5.4.

### 10.5.2 Plantwide Control Structure

The various loops shown in Figure 10.8 are listed below with their controlled and manipulated variables.

1. Fresh ethylene feed is flow-controlled
2. The total benzene (distillate from column C1 plus fresh benzene) is flow-controlled by manipulating the fresh benzene feed. The setpoint of the flow controller comes from a

**TABLE 10.6 Effect of Column Feed Compositions**

| C1 | | Base | | Percentage Change Over Range |
|---|---|---|---|---|
| $z_{1(B)}$ | 0.4601 | 0.5102 | 0.5601 | – |
| $z_{1(EB)}$ | 0.3825 | 0.3325 | 0.2825 | – |
| R/F | 0.4332 | 0.4018 | 0.3725 | 15% |
| RR | 0.9407 | 0.7870 | 0.6644 | 35% |
| **C2** | | **Base** | | **Percentage Change Over Range** |
| $z_{2(EB)}$ | 0.6283 | 0.6783 | 0.7283 | – |
| $z_{2(DEB)}$ | 0.3714 | 0.3214 | 0.2714 | – |
| R/F | 0.4655 | 0.4582 | 0.4530 | 3% |
| RR | 0.6753 | 0.6216 | 0.7406 | 18% |

multiplier. The input signal to the multiplier is the fresh ethylene flowrate. The constant in the multiplier is the desired total benzene-to-ethylene ratio.

3. The liquid levels in each reactor are controlled by manipulating the liquid streams leaving the reactor.
4. The temperature in the first reactor ($T_{R1}$) is controlled by changing the setpoint of a steam pressure controller. Not shown in Figure 10.8 are the details of adding boiler feed water to maintain a liquid level in the steam drum and reactor coils.
5. The pressures in both columns are controlled by condenser heat removal.
6. Base levels in both columns are controlled by manipulating bottoms flowrates.
7. Reflux-drum levels in both columns are controlled by manipulating flowrates of the distillate stream. Reflux ratios are small in both columns, so using distillate instead of reflux is an acceptable choice (see Luyben[4]).
8. The temperature on stage 14 in column C1 is controlled by manipulating reboiler heat input.
9. The temperature on stage 20 in column C2 is controlled by manipulating reboiler heat input.

### 10.5.3 Controller Tuning

Deadtimes of 1 min are inserted in column temperature loops. A deadtime of 3 min is used in the reactor temperature loop because of the dynamics of the steam coils and steam drum with the steam pressure controller. The very convenient relay-feedback feature in Aspen Dynamics is used to find ultimate gains and periods. The Tyreus–Luyben tuning rules are used. Table 10.7 gives controller tuning parameters.

Reactor level controllers are proportional with $K_c = 5$. Column base and reflux-drum level loops are proportional with $K_c = 2$.

### 10.5.4 Dynamic Performance

Figure 10.9 shows the responses of the entire process for 20% disturbances in the setpoint of the ethylene feed flow controller. The solid lines are for a 20% increase. The dashed lines are for a 20% decrease. An increase in fresh ethyl feed produces increases in benzene fresh feed (FFB) and the EB product (D2), while flowrates increase throughout the plant. The purity of

**TABLE 10.7 Controller Parameters**

| | Reactor | C1 Stage 14 | C2 Stage 20 | VPC |
|---|---|---|---|---|
| | TCR1 | TC1 | TC2 | FCB2 |
| SP | 433.7 K | 365.8 K | 394.5 K | 251.2 kmol/h |
| Transmitter range | 400–500 K | 300–400 K | 350–450 K | 0–500 kmol/h |
| OP | 414.9 K | 1.99 $10^6$ cal/s | 2.42 $10^6$ cal/s | 2.537 kmol/kmol |
| OP range | 350–450 K | 0–6.6 $10^6$ cal/s | 0–6.6 $10^6$ cal/s | 0–5 kmol/kmol |
| Deadtime | 3 min | 1 min | 1 min | 0 min |
| $K_C$ | 1.5 | 0.54 | 1.5 | 0.6 |
| $\tau_I$ (min) | 26 | 13 | 9.2 | 9999 |

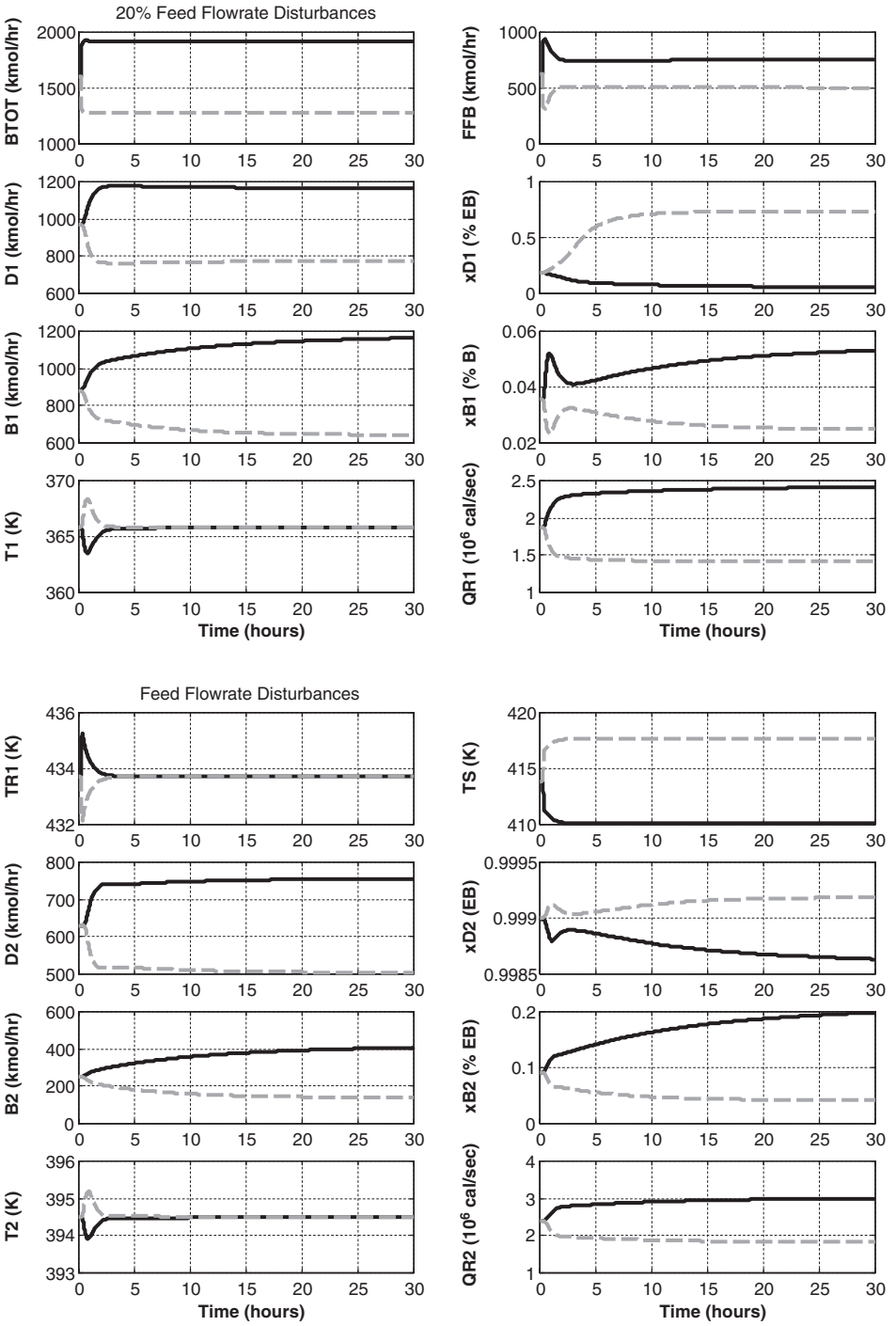


**Figure 10.9.** Ethylene feed flowrate disturbances.

the EB product $x_{D2(EB)}$ is maintained quite close to its specified value of 99.9 mol% for these large disturbances.

Notice the large change in the DEB recycle flow (B2) from the second column. It increases from 251 up to 415 kmol/h, a 65% increase for the 20% increase in ethylene fresh feed. This is a classical example of the "snowball effect" (a small change in throughput results in a large change in recycle flowrate. We return to this issue in the next section.

Figure 10.10 shows responses for two different feed composition disturbances. The solid lines indicate when the fresh benzene composition is changed from pure benzene to 95 mol% benzene and 5 mol% EB. For this disturbance, since the ethylene fresh feed is constant, the fresh feed of benzene must be increased to provide the benzene reactant required by the reaction stoichiometry. The same amount of EB is produced in the reactors, but there is some EB in the benzene fresh feed. So the distillate D2 from the second column increases. There is a fairly small change in the DEB recycle (B2), increasing from 251 to 319 kmol/h.

The other more significant disturbance (shown as dashed lines in Figure 10.10) is when the fresh benzene composition is changed from pure benzene to 95 mol% benzene and 5 mol% DEB. We are putting into the system more DEB that must be converted into EB in the second reactor since DEB is recycled to extinction. There is a very large increase in B2 that climbs from 251 to almost 600 kmol/h after 30 h. The purity of the EB product in D1 drops well below its specification because there is more benzene dropping out the bottom of the first column [see $x_{B1(B)}$]. In addition, the temperature controllers in both columns are unable to maintain their setpoints because of the gradual ramp disturbances that these columns see. Reboiler heat inputs are increasing, but temperatures hang below their setpoints.

The control structure shown in Figure 10.8 cannot handle this severe and difficult disturbance. Are there better control structures?

### 10.5.5 Modified Control Structure

The control structure shown in Figure 10.8 handles most disturbances fairly well but results in large changes in the DEB recycle flowrate. The disturbance in which DEB impurity is added into the fresh benzene feed cannot be handled because of extremely large changes in DEB recycle needed to recycle this component to extinction.

Several modified control structures were tested to overcome these problems. The generation of DEB depends on both reactor temperature and DEB concentrations in the reactors. Since reactor volumes are fixed by the steady-state design, reactor temperature cannot be reduced without adversely affecting ethylene conversion. However, DEB concentrations can be affected by changing benzene recycle. Figure 10.7 illustrates the strong dependence of DEB recycle flowrate on total benzene flowrate. This suggests that using benzene recycle to lessen the impact of large DEB recycle flowrates may be possible.

In the original control structure, the total benzene flowrate is ratioed to the fresh ethylene flowrate using a fixed ratio. Therefore total benzene recycle is only changed if there is a change in the ethylene fresh feed flowrate. A modified control structure was developed that adjusts this ratio on the basis of changes in the DEB recycle flowrate (B2). This structure is a type of *valve position controller* (VPC). The B2 flowrate signal is the process variable signal to a proportional-only controller with a setpoint signal that is the steady-state value of the B2 flowrate (251.2 kmol/h). The controller output signal of this controller is the total benzene to fresh ethylene feed ratio (2.537 at design conditions) and is fed into the multiplier. The other input to the multiplier is the flowrate of the ethylene fresh feed.

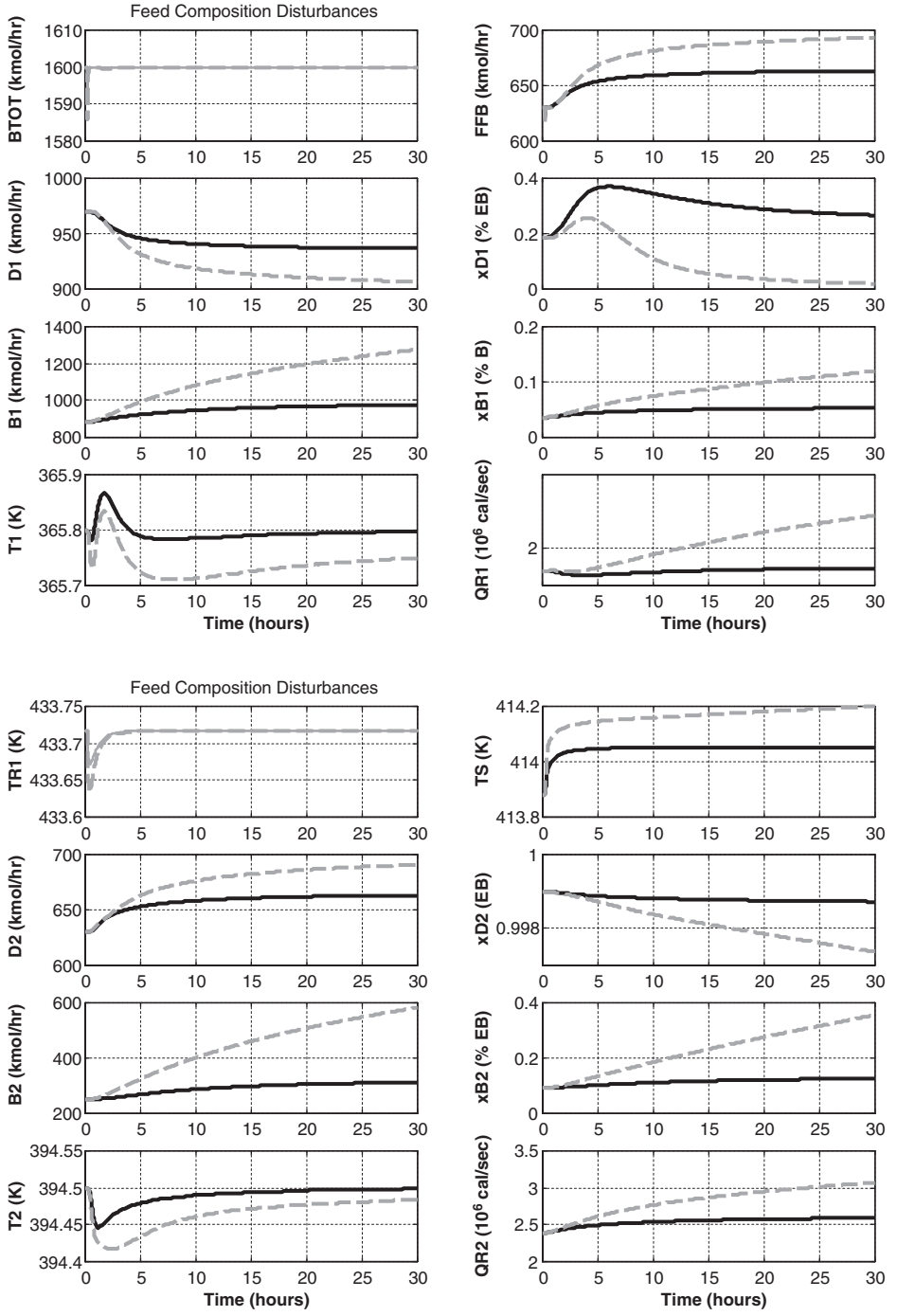


**Figure 10.10.** Feed composition disturbances.

A proportional-only VPC controller is used because we do not want to maintain a constant B2 flowrate. We merely want to change benzene recycle somewhat to reduce the magnitude of the changes in DEB recycle. Several values of controller gain were evaluated using gains from 0.1 to 1. A controller gain of $K_c = 0.6$ was found to give good dynamic responses with very little oscillation. (See Table 10.7.)

Figure 10.11 shows the modified control structure with the VPC controller adjusting the $B_{tot}$/FFE ratio. All other loops are unchanged. No retuning of temperature loops is required.

Figure 10.12 compares the responses of the system using the original structure (dashed lines) and the VPC structure (solid lines). The disturbance is the severe addition of DEB impurity into the fresh benzene feed. The original structure cannot handle this disturbance. The VPC structure handles it very well. Instead of a large buildup of DEB recycle, there is only a modest increase (from 251 to 337 kmol/h) because the benzene recycle has been increased from 1600 to 1978 kmol/h instead of remaining constant at 1600 kmol/h in the original control structure. Ethyl benzene product purity ($x_{D2}$) is held very close to its specification. The composition of benzene in the bottoms of C1 is kept small with the VPC control structure instead of increasing significantly as it did in the original structure. The EB impurity in the recycled DEB stream is also kept small in the VPC control structure instead of increasing significantly as it did in the original structure.

The effect of the control structure change on reactor temperature control is interesting. Since benzene recycle is increased in the VPC control structure, and this stream is colder than the temperature of the first reactor, less heat has to be removed. The result is an increase in the required steam temperature $T_S$.

Figures 10.13 to 10.15 give direct comparisons of the responses of the original control structure and the VPC control structure for the same feed flowrate and feed composition

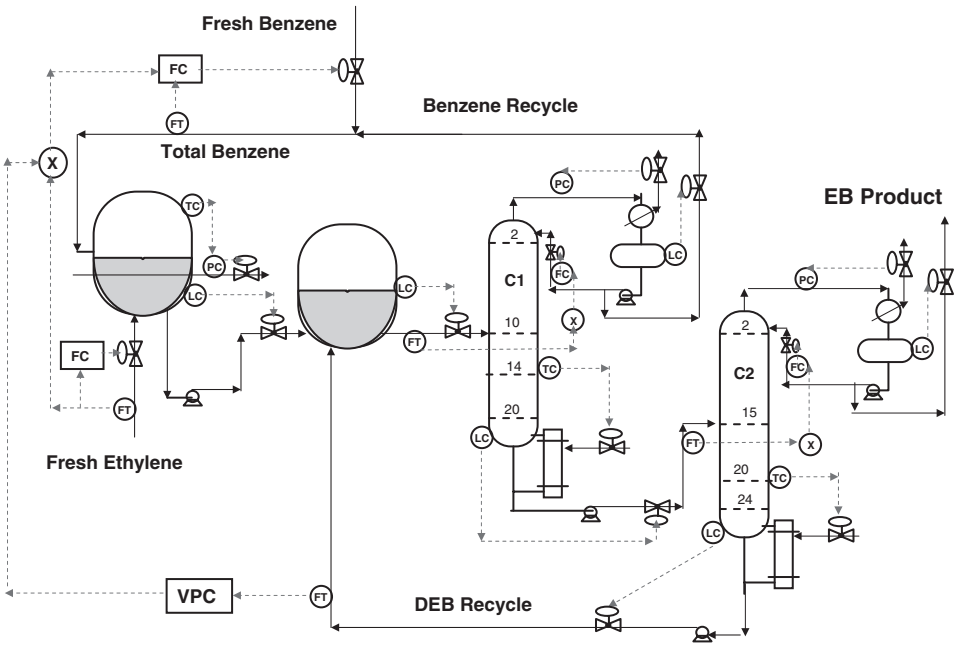


**Figure 10.11.** Modified plantwide control structure using VPC.

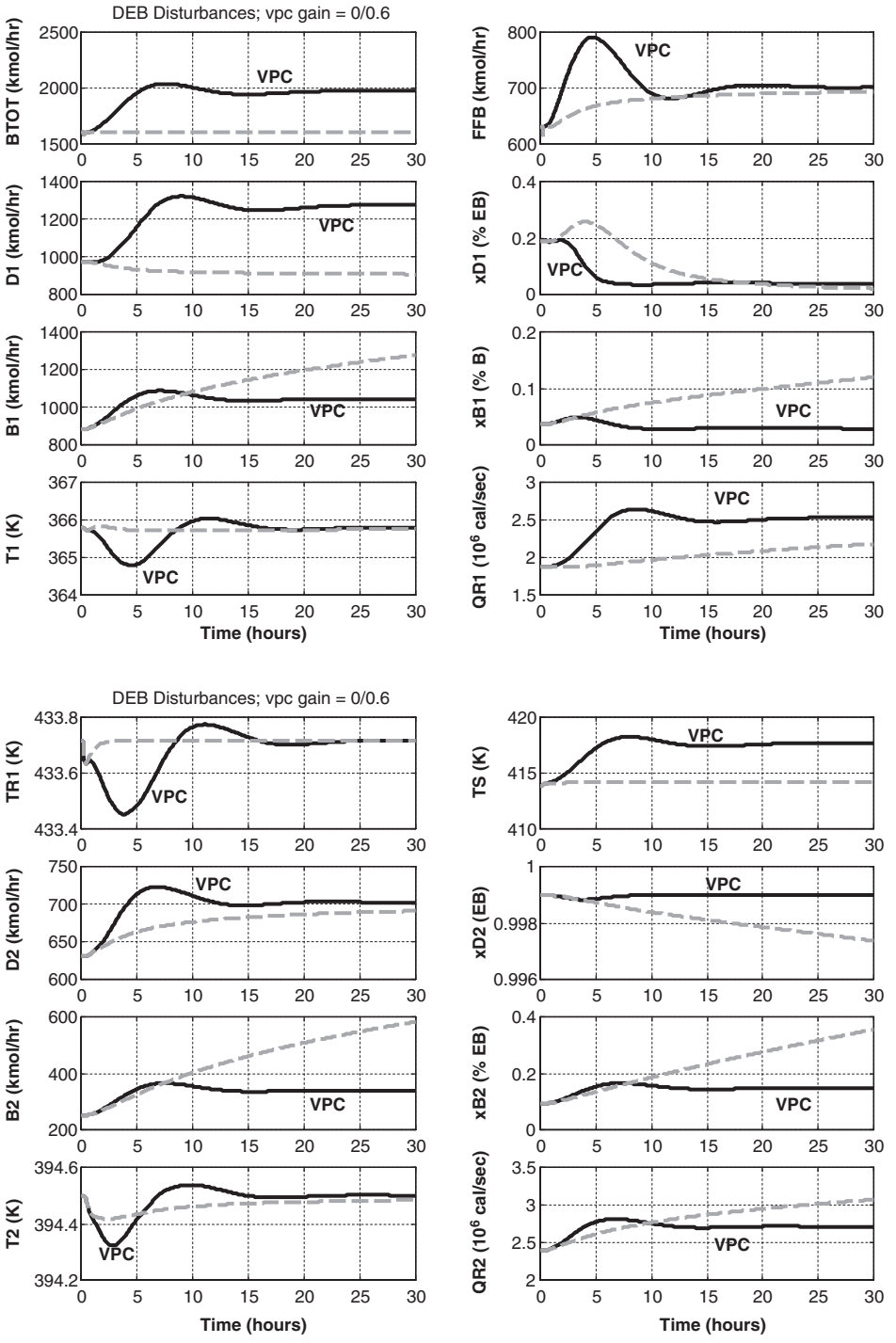


**Figure 10.12.** DEB feed composition disturbance with and without VPC.

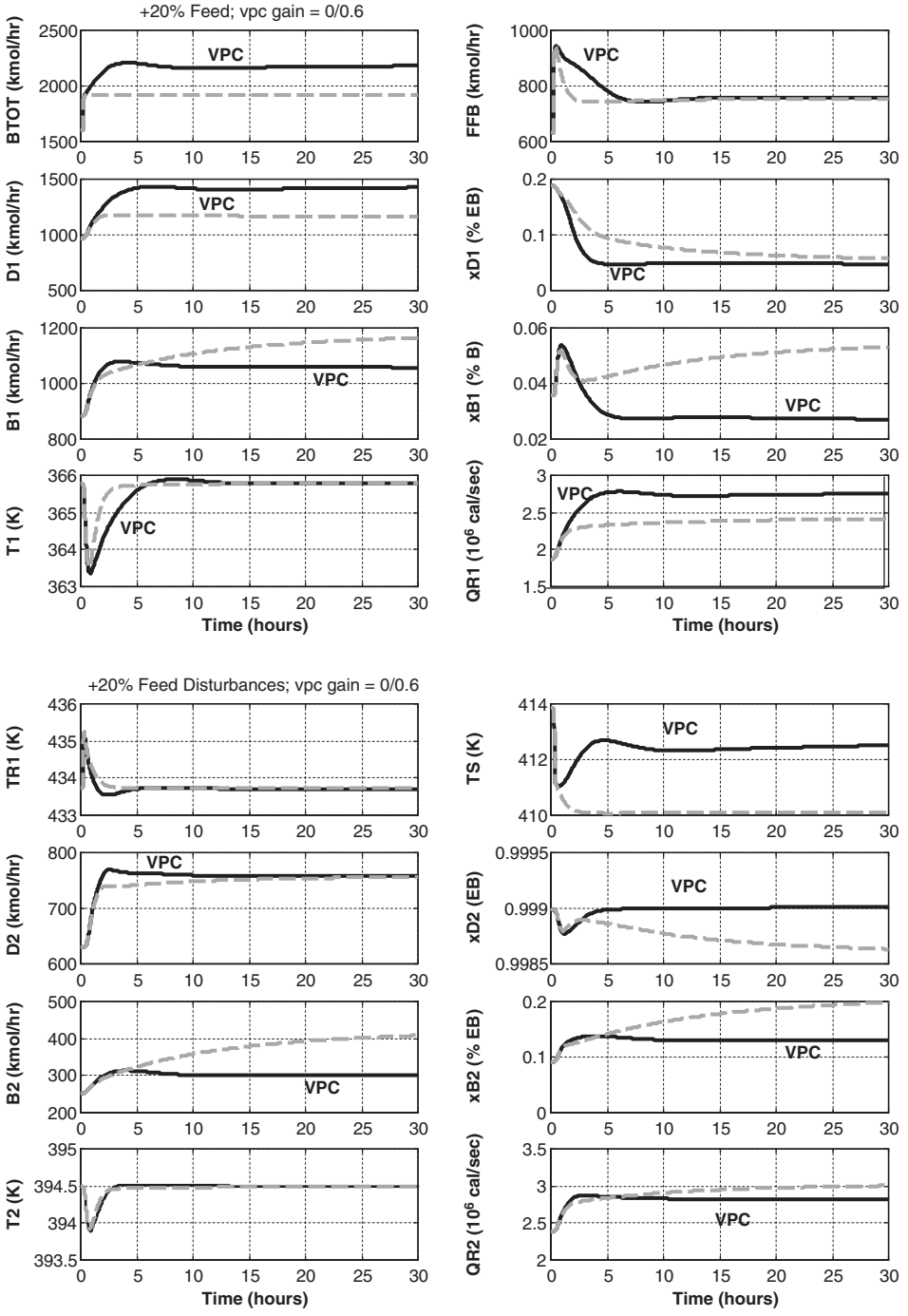


**Figure 10.13.** +20% feed flowrate disturbance with and without VPC.

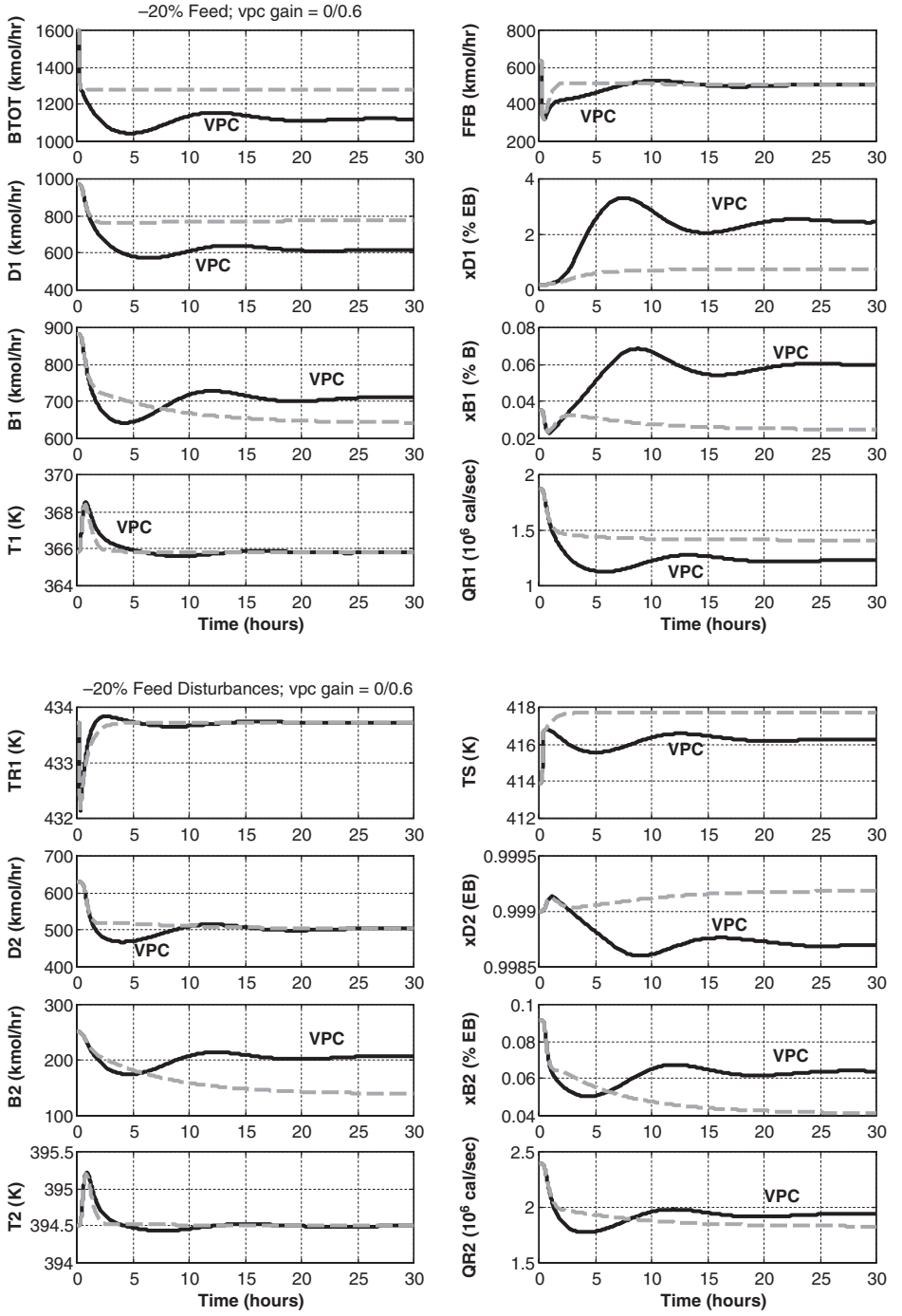


**Figure 10.14.** −20% feed flowrate disturbance with and without VPC.

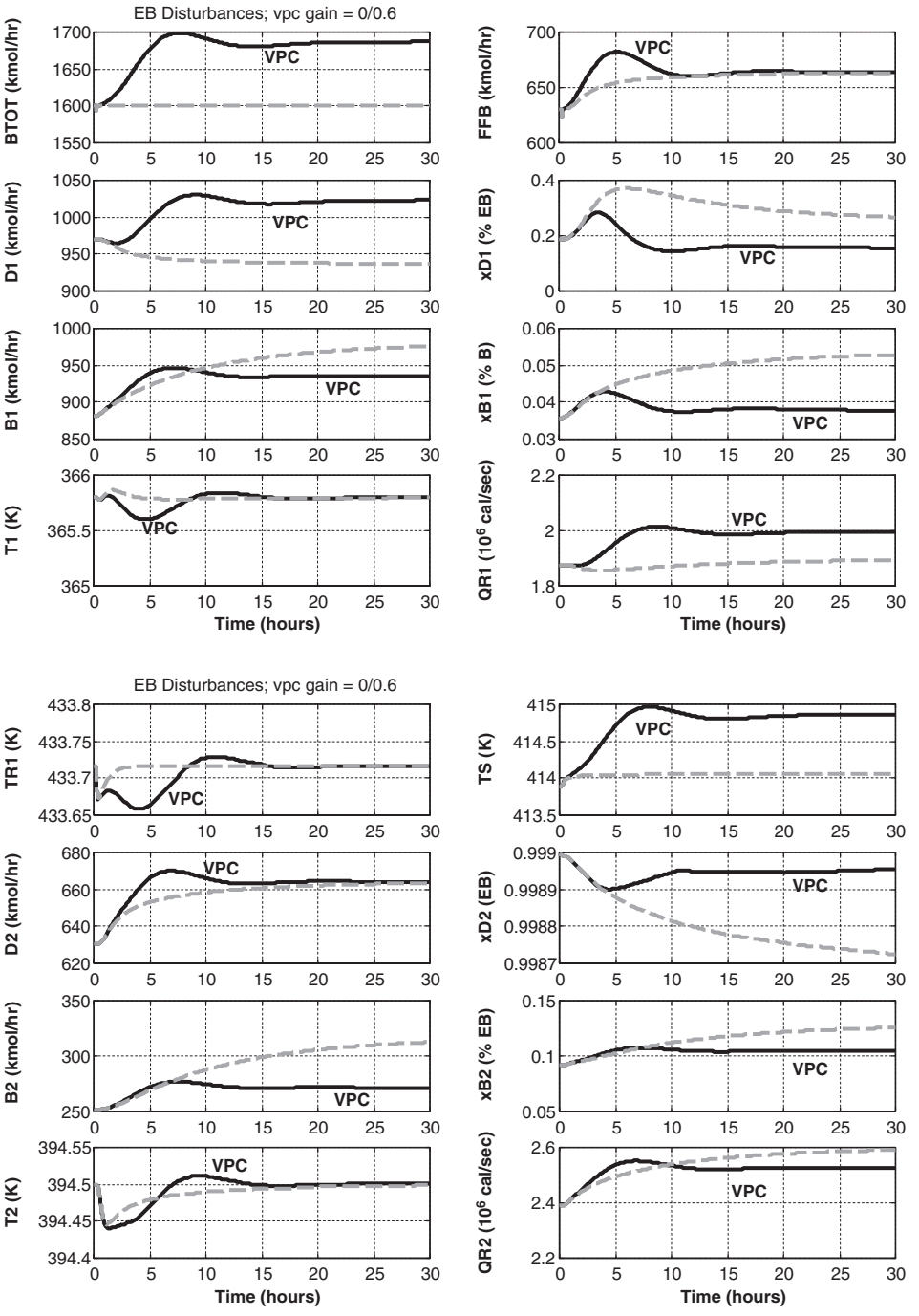


**Figure 10.15.** EB feed composition disturbance with and without VPC.

disturbances. The VPC control structure provides improved dynamic control in terms of tighter product quality control and smaller changes in the DEB recycle flowrate.

These results demonstrate that the proposed plantwide control structure provides effective dynamic control of the EB process in the face of quite large disturbances.

## 10.6 CONCLUSION

The design and control of an interesting multiunit process have been explored. The two-reactor, two-column, two-recycle process presents challenging problems. The EB process displays several unusual features. The most unusual is the recycling to extinction of an undesirable by-product (DEB). Significant design trade-offs between reactor size and recycle flowrates exist that require detailed economic analysis to find the optimum design that balances the competing effects of the design optimization variables.

Effective dynamic control of the multiunit process is achieved by the use of conventional controllers but configured in an unusual control structure. The straight-forward structure that simply ratios the total benzene recycle to the ethylene feed stream leads to very large changes in the recycle of the DEB and fails for some disturbances. A modified valve-position-control structure solves these problems by changing the benzene-to-ethylene ratio in response to changes in the DEB recycle flowrate. Very large disturbances can be effectively handled with the EB purity being maintained very close to its specification.

## REFERENCES

1. Luyben, W. L. *Plantwide Dynamic Simulators in Chemical Processing and Control*, Marcel Dekker, New York, 2002.
2. Douglas, J. M. *Conceptual Design of Chemical Processes*, McGraw-Hill, New York, 1988.
3. Turton, R., Bailie, R. C., Whiting, W. B., Shaeiwitz, J. A. *Analysis, Synthesis and Design of Chemical Processes*, 2nd Edition, Prentice Hall, Englewood Cliffs, NJ, 2003.
4. Luyben, W. L. *Distillation Design and Control Using Aspen Simulation*, John Wiley & Sons, Hoboken, NJ, 2006.

# CHAPTER 11

# DESIGN AND CONTROL OF A METHANOL REACTOR/COLUMN PROCESS

Methanol is one of the prime candidates for providing an alternative to petroleum-based liquid transportation fuels. It can be made from any renewable biomass hydrocarbon source by partial oxidation in an oxygen-blown gasifier to produce synthesis gas, which is then converted into methanol.

The purpose of this chapter is to develop the economically optimal design of a methanol reactor/distillation column system with three gas recycle streams to produce high-purity methanol from synthesis gas. The economics consider capital costs, energy costs, the value of the methanol product, and the heating value of a vent stream that is necessary for purging off inert components entering in the feed. A plantwide control structure is developed that is capable of effectively handling large disturbances in production rate and synthesis gas composition. The unique features of this control scheme are no control of pressure in the reactor/recycle gas loop and a high-pressure override controller to handle stoichiometric imbalances in the composition of the synthesis gas feed.

## 11.1 INTRODUCTION

Global economic, environmental, and political forces have increased interest in developing sources of liquid transportation fuels that are not petroleum based. Renewable biomass has the potential to provide an alternative energy source that offers many long-term advantages over petroleum. Biomass can be converted into synthesis gas by gasification, and the synthesis gas can be efficiently converted into methanol using existing technology. It is possible that, in the not too distant future, most liquid-consuming transportation vehicles (cars, trucks, trains, and airplanes) may use methanol as their energy source. Olah et al.[1] propose

*Principles and Case Studies of Simultaneous Design*, First Edition. William L. Luyben

a "methanol economy" as a more practical approach compared to the widely discussed "hydrogen economy" because existing liquid fuel infrastructure (pipelines and tanks) could be used with little modification and the safety concerns associated with hydrogen could be avoided.

This chapter studies the process used to convert synthesis gas into methanol. A cooled tubular reactor is used to react hydrogen with the carbon monoxide and carbon dioxide in the synthesis gas to produce methanol. Water is a by-product. The gas-phase exothermic reactions are conducted in a packed tubular reactor, which is cooled by generating steam. A large gas recycle stream is required to obtain high overall conversion. A distillation column separates methanol from water.

A fixed amount of synthesis gas is fed into the system, and the effects of the many design optimization variables on the yield of methanol, the energy costs, and the capital costs are evaluated. These variables include reactor pressure, reactor size, concentration of inert components in the recycle gas, and pressure in a flash tank upstream of the column. The purpose of the flash tank is to keep light components that would blanket the condenser from entering the column.

The investigation reveals that the economics are dominated by methanol yield. Energy costs and capital costs are an order of magnitude smaller than the value of the product. The major energy cost is compression of the synthesis gas, so the optimum reactor operating pressure is a trade-off between compression costs and methanol yield. Reactor temperature is set so that high-pressure steam can be produced in the reactor. Reactor size is a trade-off between reactor and catalyst capital investment and recycle compression costs (energy and capital). Inert component concentration in the recycle gas is a trade-off between methanol yield (reactant losses in the vent) and compression costs. Selection of pressure in the flash tank is a trade-off between compressor costs in two compressors that are affected in opposite directions by varying flash tank pressure.

## 11.2 PROCESS STUDIED

Figure 11.1 shows the flowsheet of the process. The equipment sizes and conditions shown are the economic optimum developed in Section 11.6. The Aspen RK-Aspen physical properties model is used in all units of the process, except in the distillation column in which the van Laar equations are used to calculate liquid activity coefficients.

### 11.2.1 Compression and Reactor Preheating

Synthesis gas at 51.2 bar is compressed in a two-stage compression system to 110 bar. The fresh feed is mostly hydrogen, carbon dioxide, and carbon monoxide, but it also contains small amounts of methane and nitrogen. The inert components must be purged out of the system. The two feed compressors consume a total of 8.98 MW of electric energy.

Three recycle gas streams are added and the total gas stream enters a feed-effluent heat exchanger (FEHE) at 53 °C. The hot reactor effluent at 266 °C transfers 43.9 MW of heat into the cold stream, which heats it to 144 °C. The required area is 2157 $m^2$ using an overall heat-transfer coefficient of 144 $kcal\,h^{-1}\,m^{-2}\,K^{-1}$. The gas is then heated to 150 °C in a reactor preheater (HX3), which has a duty of 2.99 MW and uses medium-pressure steam (184 °C and 11 bar).

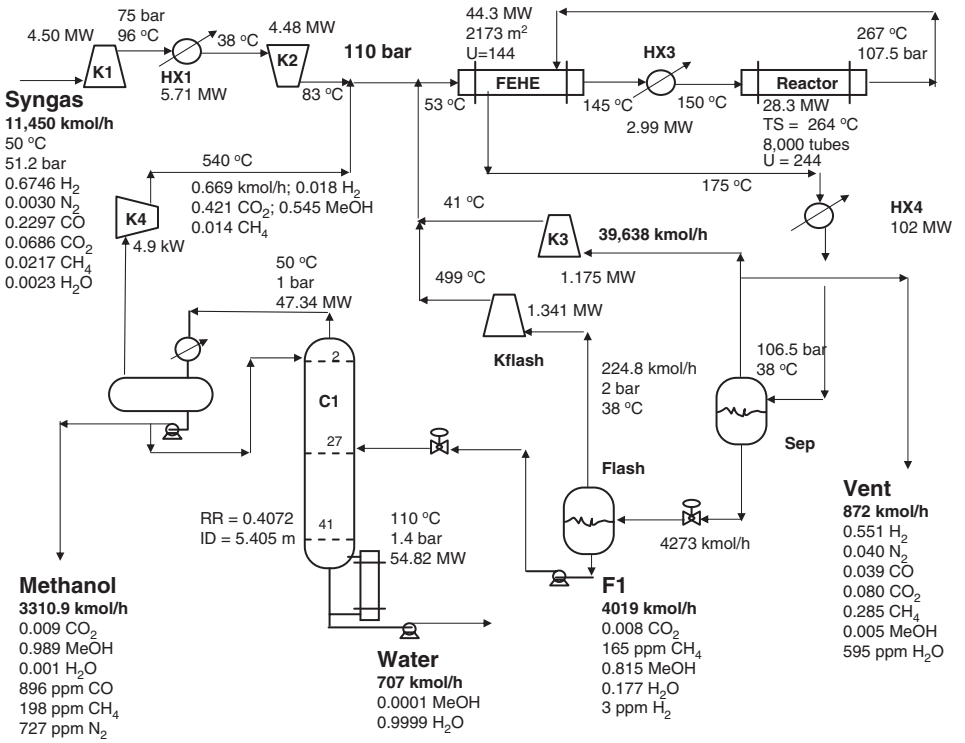


**Figure 11.1.** Methanol flowsheet.

### 11.2.2 Reactor

The packed tubular reactor has 8000 tubes with length 12.2 m and diameter 0.03675 m. The reactor is cooled by generating high-pressure steam (254 °C and 42 bar), so the reactor temperatures through the tubes climb to a peak of about 280 °C. The reactor effluent is at 266 °C. The heat transfer rate is 28.3 MW, using an overall heat-transfer coefficient of 244 kcal $h^{-1}$ $m^{-2}$ $K^{-1}$. The catalyst has a density of 2000 kg/$m^3$ and the reactor void volume is 0.5. The reaction kinetics are discussed in Section 11.3. The reasons for the selections of temperature, pressure, and reactor size are discussed in Section 11.6.

### 11.2.3 Separator, Recycle, and Vent

After the reactor effluent is cooled to 174 °C in the FEHE, it is further cooled to 38 °C and partially condensed in a water-cooled heat exchanger with a heat duty of 102 MW. The stream is separated in a tank operating at 106.6 bar and 38 °C. The total pressure drop around the gas loop (heat exchangers and reactor) is 3.4 bar.

Most of the vapor stream is compressed back up to 110 bar and recycled. The recycle compressor work is 1.10 MW. The gas recycle flowrate is 38,465 kmol/h for the 11,450 kmol/h of synthesis gas feed (recycle-to-feed ratio = 3.36). A small fraction (0.022) is vented off at a flowrate of 865 kmol/h. This is where the inert methane and nitrogen in the synthesis gas fresh feed are removed from the system. The concentration of methane and nitrogen in the vent and recycle streams are 28.5 and 4 mol%, respectively. These compositions should be compared with the 2.17 mol% methane and 0.3 mol%

nitrogen in the fresh synthesis gas feed. The inerts are allowed to build up so that the losses of the reactants (hydrogen, carbon monoxide, and carbon dioxide) are kept small.

The hydrogen that is lost in the vent stream is 6.17% of the hydrogen in the synthesis gas feed. The carbon monoxide lost is 1.23% of the carbon dioxide in the synthesis gas feed. The carbon dioxide lost is 8.75%. The yield of methanol from the carbon monoxide and carbon dioxide in the synthesis gas feed is 96%.

### 11.2.4 Flash and Distillation

The liquid from the separator contains significant amounts of light components because of the high pressure in the separator. The concentration of hydrogen is 0.2 mol%, the concentration of methane is 1.2 mol%, and the concentration of carbon dioxide is 3.9 mol%. If this stream were fed directly into the distillation column, these inert components would build up in the condenser and blanket the condenser. Either a high pressure or a low temperature would be needed in the condenser, which may require the use of expensive refrigeration.

Therefore, a flash tank is used to remove most of the light components before the stream is fed into the column. The flash tank is operated at 2 bar. The gas (224.8 kmol/h) is compressed to 110 bar and recycled to the reactor. The compressor power is 1.341 MW.

The liquid from the flash tank is pumped into a 42-stage distillation column on stage 27. The column operates at 1 bar, and a reflux-drum temperature of 50 °C is used so that cooling water can be used in the condenser. A small vapor stream from the top of the reflux drum recycles the small amount of inert components entering the column. This small vapor stream (0.0669 kmol/h) is compressed back up to 110 bar (work is 4.9 kW).

There are three specifications in this column. Two specifications set the compositions of the bottoms (0.01 mol% methanol) and the distillate (0.1 mol% water). The third specification sets the reflux-drum temperature at 50 °C, which establishes the amount of vapor that must be removed from the top of the reflux drum for compression and recycle.

The methanol/water separation is reasonably easy, so the required reflux ratio (RR) is only 0.407. Reboiler energy is 54.8 MW. Low-pressure steam (160 °C and 6 bar) can be used in the reboiler since the base temperature is 110 °C.

## 11.3 REACTION KINETICS

The chemistry of the methanol process involves the reaction of both carbon dioxide and carbon monoxide with hydrogen.

$$\begin{aligned} CO + 2H_2 &\iff CH_3OH \\ CO_2 + 3H_2 &\iff CH_3OH + H_2O \end{aligned} \tag{11.1}$$

The kinetics are given by vanden Bussche and Froment[2] in the following form by using the water-shift reaction.

$$\begin{aligned} CO_2 + 3H_2 &\iff CH_3OH + H_2O \\ CO_2 + H_2 &\iff CO + H_2O \end{aligned} \tag{11.2}$$

The reactions are exothermic and use a solid catalyst. The kinetics are described by LHHW-type equations (Langmuir–Hinshelwood–Hougen–Watson). Conversion of the

reaction rate equations and their units given in the original paper into the form required by Aspen Plus is a daunting task. The original data use pressures in bar and reaction rates in kmol $min^{-1}$ $kg^{-1}$ catalyst. These must be transformed to Pascals. This transformation was provided by Emmanuel Lejeune (AspenTech), and his invaluable assistance is gratefully acknowledged.

The LHHW kinetic structure has the form

$$\Re = (\text{Kinetic term})\frac{(\text{Driving-force term})}{(\text{Adsorption term})} \tag{11.3}$$

The reaction rate for the first reaction for the production of methanol from carbon dioxide is given in Eq. (11.4).

$$\Re_1 = (k_4 p_{CO_2} p_{H_2})\frac{\left[1 - \frac{1}{K_{E1}}\left(\frac{p_{CH_3OH} p_{H_2O}}{p_{CO_2} p_{H_2}}\right)\right]}{\left[1 + k_3\left(\frac{p_{H_2O}}{p_{H_2}}\right) + k_1\sqrt{p_{H_2}} + k_2 p_{H_2O}\right]^3} \tag{11.4}$$

The reaction rate for the water-shift reaction is given in Eq. (11.5).

$$\Re_2 = (k_5 p_{CO_2})\frac{\left[1 - \frac{1}{K_{E2}}\left(\frac{p_{CO} p_{H_2O}}{p_{CO_2} p_{H_2}}\right)\right]}{\left[1 + k_3\left(\frac{p_{H_2O}}{p_{H_2}}\right) + k_1\sqrt{p_{H_2}} + k_2 p_{H_2O}\right]} \tag{11.5}$$

Table 11.1 gives the kinetic and adsorption parameters entered into the Aspen LHHW reaction model to implement these kinetics. Note that the activation energy of the first reaction when put in LHHW form turns out to be negative, which makes no physical sense.

Since the reactions are exothermic, the chemical equilibrium constants decrease with increasing temperature. Therefore, low reactor temperatures should improve conversion, provided they are not so low that the specific reaction rates are too small. For a given reactor size and a desired conversion, recycle flowrate increases as reactor temperatures are lowered, which mean higher compressor work.

The reactor is simulated in Aspen using the RPLUG model with a *constant medium temperature* as the dynamic heat-transfer selection. The reactor is cooled by generating saturated steam, and the temperature of the boiling water on the shell side of the reactor tubes is the same at all axial positions. The selection of the medium temperature inferentially sets the reactor temperature profile.

The medium temperature is set at 264 °C so that high-pressure steam (254 °C and 42 bar) can be generated. Thus, one of the important design optimization variables (reactor temperature) is established a priori so that valuable high-pressure steam can be generated, which can be used to drive compressors.

## 11.4 OVERALL AND PER-PASS CONVERSION

With the design conditions and equipment sizes shown in Figure 11.1, there are 28,920 kmol/h of hydrogen entering the reactor, 4066 kmol/h of carbon monoxide and 3976 kmol/h of carbon dioxide. The corresponding component flowrates leaving the reactor

**TABLE 11.1 Kinetic LHHW Parameters**

$\Re 1$ ($CO_2 + 3H_2 \rightarrow CH_3OH + H_2O$)
- Kinetic factor $k = 1.07 \times 10^{-3}$
  $E = -36{,}696$ kJ/kmol
- *Driving-force expressions*
  - Term 1
    - Concentration exponents for reactants: $CO_2 = 1$; $H_2 = 1$
    - Concentration exponents for products: $CH_3OH = 0$; $H_2O = 0$
    - Coefficients: A = −23.02581; B = C = D = 0
  - Term 2
    - Concentration exponents for reactants: $CO_2 = 0$; $H_2 = -2$
    - Concentration exponents for products: $CH_3OH = 1$; $H_2O = 1$
    - Coefficients: A = 24.388981; B = −7059.7258; C = D = 0
- *Adsorption expression*
  - Adsorption term exponent = 3
  - Concentration exponents
    - Term 1: $H_2 = 0$; $H_2O = 0$
    - Term 2: $H_2 = -1$; $H_2O = 1$
  - Adsorption constants
    - Term 1: A = 0, B = 0, C = 0, D = 0
    - Term 2: A = 8.1471087, B = 0, C = 0, D = 0

$\Re 2$ ($CO_2 + H_2 \rightarrow CO + H_2O$)
- Kinetic factor $k = 1.22 \times 10^{9}$
  $E = 94765$ kJ/kmol
- *Driving-force expressions*
  - Term 1
    - Concentration exponents for reactants: $CO_2 = 1$; $H_2 = 0$
    - Concentration exponents for products: $CO = 0$; $H_2O = 0$
    - Coefficients: A = −11.512952; B = C = D = 0
  - Term 2
    - Concentration exponents for reactants: $CO_2 = 0$; $H_2 = -1$
    - Concentration exponents for products: $CO = 1$; $H_2O = 1$
    - Coefficients: A = −16.184871; B = 4773.2589; C = D = 0
- *Adsorption expression*
  - Adsorption term exponent = 1
  - Concentration exponents
    - Term 1: $H_2 = 0$; $H_2O = 0$
    - Term 2: $H_2 = -1$; $H_2O = 1$
  - Adsorption constants
    - Term 1: A = 0, B = 0, C = 0, D = 0
    - Term 2: A = 8.1471087, B = 0, C = 0, D = 0

are 21,673, 1468, and 3292 kmol/h, which means that the per-pass conversion of hydrogen is 25%, the per-pass conversion of carbon monoxide is 64%, and the per-pass conversion of carbon dioxide is 17%.

The overall conversion of the carbon monoxide and carbon dioxide in the fresh synthesis gas feed to methanol is 96%. There are 2630 kmol/h of carbon dioxide and 785 kmol/h of carbon monoxide in the synthesis gas, totaling 3415 kmol/h. The methanol in the distillate product is 3278 kmol/h.

There are 2 mol of hydrogen needed to react with the carbon monoxide, and 3 mol of hydrogen needed to react with the carbon dioxide. If there were complete conversion of all the carbon dioxide and carbon monoxide in the synthesis gas feed, the hydrogen consumed in the reactions would be $2630 \times 2 + 786 \times 3 = 7616$ kmol/h of hydrogen. The hydrogen supplied in the fresh synthesis gas feed is 7724 kmol/h. So there is a small excess. The overall conversion of hydrogen to produce methanol is quite high (98.6%).

These high conversions of reactants indicate that the design has achieved only small losses of the valuable reactants, despite the need to purge out the inert components in the fresh feed (methane and nitrogen). The economics discussed in Section 11.6 demonstrate that energy and capital can be expended to improve yield so that losses of reactants and products are very small. Douglas[3] established this principle in his pioneering work on conceptual process design over two decades ago.

It should be noted that an alternative design could be developed if medium or low-pressure steam were generated in the reactor. Low-pressure steam (160 °C and 6 bar) could be generated if the medium temperature were set at 170–180 °C, and this steam could be used in the reboiler of the distillation column. The resulting lower reactor temperatures would result in a smaller reactor and less recycle. This alternative design is not considered in this chapter.

## 11.5 PHASE EQUILIBRIUM

There are two vapor-liquid flash separations in the process. The Aspen Flash2 model is used in the separator block and the flash block. Most of the light components are removed in the vapor streams leaving these vessels, but small amounts of light components are dissolved in the liquid streams. This is what necessitates the need for the flash tank and the vapor stream from the reflux drum.

The methanol/water separation is nonideal but fairly easy. The van Laar equations are used in the distillation column. Figure 11.2 gives a *Txy* diagram at 1 bar pressure.

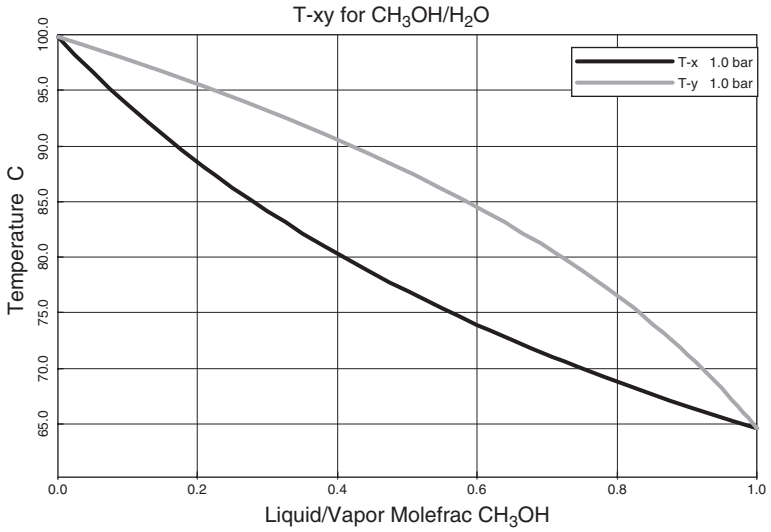


**Figure 11.2.** *Txy* diagram for methanol/water at 1 bar.

## 11.6 EFFECTS OF DESIGN OPTIMIZATION VARIABLES

The methanol process has a number of design optimization variables that impact energy and capital economics in conflicting ways. We explore these effects quantitatively in this section.

### 11.6.1 Economic Basis

The economics consider both capital investment (compressors, heat exchangers, reactor, catalyst, separator tank, flash tank, and column) and energy costs (compressor work, steam used in the reactor preheater, and reboiler duty in the column). Table 11.2 summarizes the sizing and cost basis used in this analysis. These parameters are taken from Douglas[3] and Turton et al.[4]

The compressors use electricity at \$16.8/GJ. The reactor preheater uses medium-pressure steam at \$8.22/GJ. The column reboiler uses low-pressure steam at \$7.78/GJ.

There are two credits in the economics. One is for the steam generated in the reactor. It is at high-pressure but is saturated, not superheated, so \$6/GJ is assumed for its value. The second is the heating value of the vent stream, which contains mostly hydrogen and methane with some carbon monoxide. These components can be burned to recover heat. The amount of air to completely combust each component, the component heats of

**TABLE 11.2 Basis of Economics and Equipment Sizing**

Column diameter: Aspen tray sizing
Column length: NT trays with 2-ft spacing plus 20% extra length
Column vessel (diameter and length in meters)
  Capital cost $= 17{,}640(D)^{1.066}(L)^{0.802}$
*Condensers (area in $m^2$)*
  Heat-transfer coefficient $= 0.852$ kW/K-$m^2$
  Differential temperature = Reflux-drum temperature − 303 K
  Capital cost $= 7296(A)^{0.65}$
*Reboiler (area in $m^2$)*
  Heat-transfer coefficient $= 0.568$ kW/K-$m^2$
  Differential temperature = 34.8 K
  Capital cost $= 7296(A)^{0.65}$
*Reactor and FEHE (area in $m^2$)*
  Capital cost $= 7296(A)^{0.65}$
  Heat-transfer coefficient FEHE $= 144$ kcal $h^{-1}$ $K^{-1}$ $m^{-2}$
  Heat-transfer coefficient reactor $= 244$ kcal $h^{-1}$ $K^{-1}$ $m^{-2}$
Catalyst cost = \$10/kg
Compressor capital cost $= (1293)(517.3)(3.11)(\text{hp})^{0.82}/280$
*Energy cost*
  LP steam = \$7.78/GJ
  MP steam = \$8.22/GJ
  HP saturated steam from reactor = \$6.00/GJ
  Electricity = \$16.8/GJ

$$\text{TAC} = \frac{\text{Capital cost}}{\text{Payback period}} + \text{Energy cost}$$

Payback period = 3 yr

combustion, and the mean heat capacities of the resulting nitrogen, carbon dioxide, and water gas stream are used to find the heating value of the vent stream (0.331 kJ/kmol). The sensible heat of changing the combustion products from ambient up to a 260 °C stack gas temperature is subtracted from the heat of combustion. A value of \$6/GJ is used for this fuel.

The assessment of economics uses the income derived from the process for a fixed amount of synthesis gas fed. The value of methanol is assumed to be \$2/gallon (\$21/kmol). In all cases the fresh feed of synthesis gas is fixed at 11,450 kmol/h. As design parameters change, the amount of product methanol changes, the amount of venting changes, the amount of reactor steam changes, and the energy consumption changes (compressors, reactor preheater, and column reboiler).

We define income as the sum of the value of the methanol produced plus the value of the vent and reactor steam credits minus the energy costs minus the annual capital cost.

$$\begin{aligned}\text{Income} = {} & (\text{Flowrate methanol})(\$\ \text{Value}) + (\text{Flowrate vent})(\$\ \text{Value}) \\ & + (\text{Reactor steam})(\$\ \text{Value}) - (\text{Work of 5 compressors})(\$/\text{MW}) \\ & - (\text{Reboiler energy})(\$/\text{MW}) - \left(\frac{\text{Total capital}}{3}\right)\end{aligned} \tag{11.6}$$

Total capital investment includes the cost of the five compressors, the intercooler between the feed compressors, the FEHE, the reactor preheater, the reactor with catalyst, the cooler/condenser, the separator vessel, the flash drum, the distillation column vessel, the condenser, and the reboiler.

We choose to look at income instead of profit because this avoids having to assign a value for the synthesis gas feed. The incremental increase in income when changing a design parameter and the incremental increase in the required capital investment are evaluated to see if the incremental return on investment is sufficient to justify the investment.

As the numbers given in the following sections will reveal, the value of the product is an order of magnitude larger that the cost of energy and capital. Douglas[3] pointed out this basic design principle many years ago. Small increases in product yield are worth more than the corresponding required increases in capital and energy to achieve them. This is true up to a point.

In the following sections, the effects of variables on the economics of the process are studied one at a time to present a clear picture of the trends. After each variable is explored, the dominant variables are varied in an iterative procedure to arrive at the optimum values of the design variables.

### 11.6.2 Effect of Pressure

High pressure in the reactor favors the production of methanol because of the increase in reactant partial pressures. Both reactions are nonequimolar with fewer molecules of products than reactants. So Le Châtelier's principle would indicate that high pressure drives the reactions to the right. At a given recycle flowrate, the higher the pressure, the smaller the reactor can be, which reduces reactor vessel and catalyst capital investment. With a given reactor size, the higher the pressure, the smaller the recycle flowrate can be, which reduces recycle compression energy and recycle compressor capital investment.

However, the higher the pressure, the more compression of the feed synthesis gas is required. The synthesis gas is assumed to be supplied at 51.2 bar from an upstream unit. A two-stage compressor system is used with intermediate cooling. Following the common design heuristic, the compression ratio is specified to be the same in both stages. For a given synthesis gas pressure $P_1$ and a system pressure $P_2$, the compression ratio in each stage of a two-stage compression system is $\sqrt{P_2/P_1}$.

Figure 11.3 and Table 11.3 show the effects of changing pressure on a number of important variables. These results are generated with the other design optimization variables set at reasonable initially guessed values. The number of reactor tubes is 5000, the flash tank pressure is 10 bar, and the vent/recycle split fraction is 0.025. This split affects the composition of the inert components in the recycle gas. The number of stages in the distillation column is set at 42 with feed on stage 20. All of these variables will be optimized later.

The top left graph in Figure 11.3 shows that compressor work in the feed compressors increases as system pressure is increased. The work in the first compressor (K1) is shown, and the work in the second compressor (K2) is essentially the same as K1. The changes in compressor work are quite significant and impact both energy cost (expensive electrical energy at \$16.8/GJ) and compressor capital investment (see Table 11.2).

On the other hand, the top right graph in Figure 11.3 shows that required recycle flowrate decreases as pressure increases. This reduces the cost of compression of the gas recycle in compressor K3 (second graph from the top on the left in Figure 11.3). The net effect is an increase in total capital cost and total energy cost (third graphs from the top in Figure 11.3).

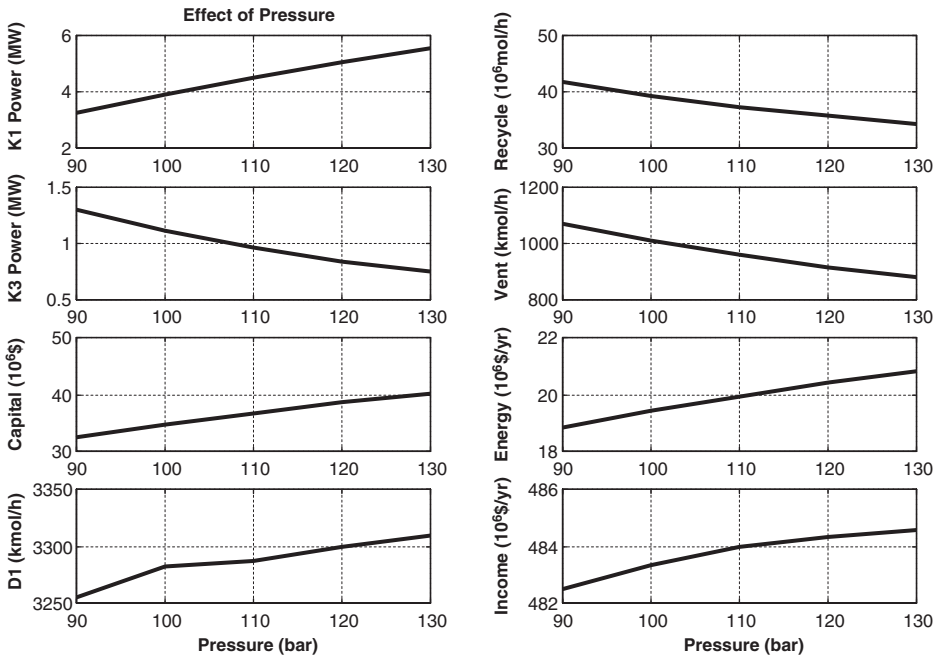


**Figure 11.3.** Effect of reactor pressure.

**TABLE 11.3 Effect of Pressure**[a]

| System Pressure (bar) | 90 | 100 | 110 | 120 | 130 |
|---|---|---|---|---|---|
| Compressor K1 (MW) | 3.254 | 3.901 | 4.499 | 5.053 | 5.571 |
| Compressor K2 (MW) | 3.254 | 3.899 | 4.483 | 5.037 | 5.559 |
| Compressor K3 (MW) | 1.303 | 1.109 | 0.958 | 0.841 | 0.747 |
| $D_1$ (kmol/h) | 3254.7 | 3272.7 | 3287.3 | 3299.5 | 3309.7 |
| Vent (kmol/h) | 1069.0 | 1008.8 | 957.9 | 915.9 | 879.0 |
| Recycle (kmol/h) | 41,690 | 39,343 | 37,358 | 35,720 | 34,281 |
| $Q_{HX1}$ (MW) | 4.444 | 5.101 | 5.709 | 6.272 | 6.798 |
| Total capital ($\$10^6$) | 32.55 | 34.74 | 36.70 | 38.53 | 40.21 |
| Total energy ($\$10^6$/yr) | 18.83 | 19.41 | 19.92 | 20.42 | 20.86 |
| Income ($\$10^6$/yr) | 482.48 | 483.34 | 483.96 | 484.33 | 484.57 |
| Incremental capital ($) | – | 2,192,000 | 1,961,100 | 1,830,000 | 1,679,000 |
| Incremental income ($/yr) | – | 860,000 | 618,000 | 373,000 | 239,000 |
| Incremental ROI (%) | – | 39.2 | 31.5 | 20.4 | 14.2 |

[a]5000 tubes, 10 bar flash, 0.025 split.

The bottom two graphs of Figure 11.3 show that the production rate (D1) of the methanol product gradually increases as pressure is increased, which produces a gradual rise in income despite the increases in both energy cost and capital cost. Remember that the feed of synthesis gas is fixed. The increase in product is accompanied by a corresponding decrease in the vent rate (second graph on the right in Figure 11.3). Due to the improvement in kinetics, there are smaller losses of reactants in the vent stream as pressure increases.

However, capital investment increases as pressure rises, so we need to see if the incremental investment is justified by the incremental increase in income. The detailed numbers are presented in Table 11.3. Moving from 90 to 100 bar provides a $860,000 per year increase in income and requires a $2,192,200 increase in capital investment. The incremental return on investment is a healthy 39%.

Evaluating the move from 100 to 110 bar shows a 31% incremental return on incremental investment. Going from 110 to 120 bar yields a 20% return, and going from 120 to 130 bar yields a 14% return. These results clearly demonstrate that there is a point of diminishing returns for investing capital. A system pressure of 110 bar is selected as the design value.

### 11.6.3 Effect of Reactor Size

Using a pressure of 110 bar and holding the other design optimization variables constant, the effect of changing the number of tubes in the reactor is explored. Tube diameter is kept constant at the smallest practical value (0.03675 m) to provide the maximum heat-transfer area per unit volume. Tube length is kept constant to provide a reasonable pressure drop through the reactor (1.5 bar).

Increasing reactor size will increase capital investment in both the multi-tube vessel and the catalyst inside the tubes. However, the per-pass conversion should increase, so the required recycle flowrate would decrease. This will decrease compressor work in the recycle compressor K3 and also decrease its capital cost.

Figure 11.4 shows the effect on several important variables of changing the number of reactor tubes. The upper left graph shows that capital investment in the reactor vessel, catalyst, and K3 compressor increases as more tubes are used. All the other units are essentially

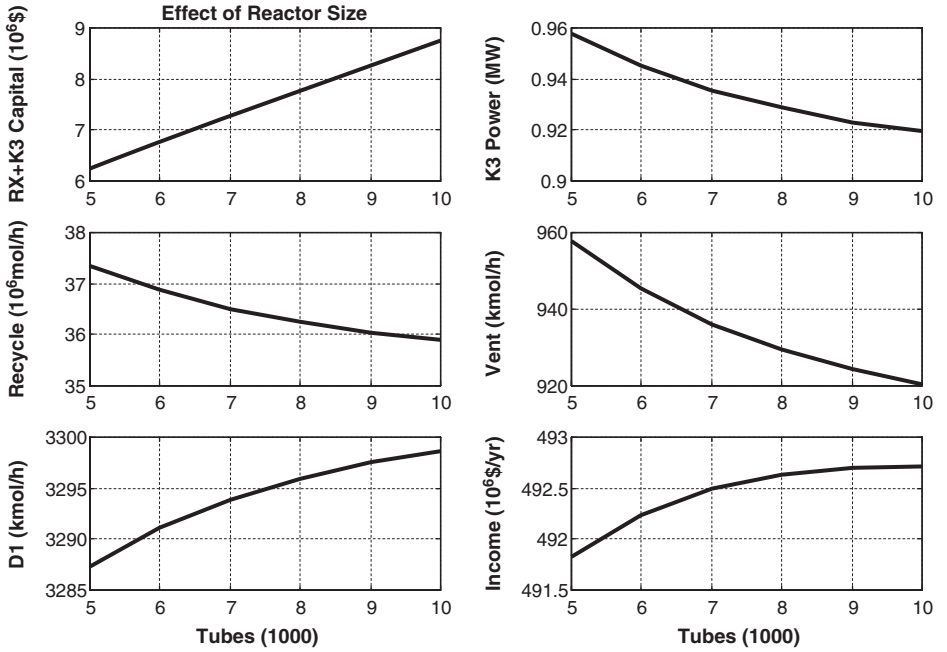


**Figure 11.4.** Effect of reactor size.

unaffected by changes in reactor size. The middle left graph shows that there is a decrease in recycle, which results in a decrease in work in the recycle compressor K3 (top right graph) and its capital cost. The effect of increases in reactor vessel and catalyst capital is larger than the effect of decreases in compressor capital, so the total capital investment in these two units increases.

The larger reactor improves the yield of methanol, as reflected in the gradual increase in the distillate (D1), which is the methanol product stream (bottom left graph in Figure 11.4). The vent flowrate decreases as the product flowrate increases (middle right graph in Figure 11.4) because the flowrate of synthesis gas is fixed.

Income increases gradually, but the rate of increase slows down as more tubes are added. Table 11.4 gives details of the economics. Return on investment calculations show a gradual decrease in the incremental return on incremental investment. Going from 7000 to 8000 tubes gives a 28% return. Going from 8000 to 9000 gives a small 14% return on investment.

A reactor with 8000 tubes is selected.

### 11.6.4 Effect of Vent/Recycle Split

All previous designs have used a vent-to-recycle split of 0.025. The resulting inert component compositions in the vent stream are about 26 mol% methane and 3 mol% nitrogen. The remaining components represent losses of the reactants hydrogen, carbon monoxide, and carbon dioxide. Lowering the split ratio (less venting) will increase the composition of the inert components in the vent and reduce reactant losses in the vent, which only has fuel value.

**TABLE 11.4 Effect of Reactor Size**[a]

| Tube Number | 5000 | 6000 | 7000 | 8000 | 9000 | 10,000 |
|---|---|---|---|---|---|---|
| Recycle (kmol/h) | 37,351 | 36,869 | 36,507 | 36,247 | 36,044 | 35,897 |
| $D_1$ (kmol/h) | 3287.34 | 3291.09 | 3293.93 | 3295.96 | 3297.52 | 3298.66 |
| Compressor K3 (MW) | 0.9580 | 0.9453 | 0.9356 | 0.9289 | 0.9231 | 0.9197 |
| Vent (kmol/h) | 957.7 | 945.4 | 936.1 | 929.4 | 924.2 | 920.4 |
| Reactor + K3 capital ($\$10^6$) | 6.238 | 6.7592 | 7.2705 | 7.7751 | 8.2705 | 8.7618 |
| Income ($\$10^6$/yr) | 491.83 | 492.23 | 493.49 | 492.63 | 492.70 | 492.71 |
| Incremental capital ($) | – | 521,200 | 511,300 | 504,600 | 495,400 | 491,300 |
| Incremental income ($/yr) | – | 400,000 | 260,000 | 140,000 | 70,000 | 10,000 |
| Incremental ROI (%) | – | 77 | 51 | 28 | 14 | 2 |

[a]110 bar, 10 bar flash, 0.025 split.

On the other hand, having higher inert concentrations in the recycle gas going to the reactor will adversely affect kinetics and require higher recycle flowrates, which will increase recycle compressor costs. So there is a trade-off between vent losses and recycle compressor energy and capital costs.

In order to accurately show the effects of higher recycle gas flowrates around the gas loop, pressure drops through the various units in the loop are varied with recycle flowrate. The base-case pressure drop around the loop is 3 bar: 0.5 bar through both sides of the FEHE, 1.5 bar through the reactor, 0.1 bar through the reactor preheater, and 0.4 bar through the condenser. The base-case recycle flowrate is 36,200 kmol/h. Pressure drops change with the square of the flowrate changes. The discharge pressure of the feed compressors is kept at 110 bar.

Figure 11.5 shows that recycle flowrates increase as the split ratio is *decreased* (second graph from the top on the left), as does the work of the recycle compressor K3 (top right graph). Vent rates decrease, and methanol product rates increase as the split ratio is decreased. But both capital investment and energy costs increase when the split ratio is decreased. A split ratio of 0.022 gives the maximum income.

Moving from a split ratio of 0.023 down to 0.022 gives an incremental increase in income of $620,000/yr and requires only a $25,000 increase in capital investment. Moving from 0.022 down to 0.021 produces a *decrease* in income, while at the same time increasing capital investment. Therefore, a split ratio of 0.022 is selected.

### 11.6.5 Effect of Flash-Tank Pressure

A flash-tank pressure of 10 bar has been used in all the previous designs. This design optimization variable is now explored with all the other variables fixed: 110 bar pressure, 8000 tubes, and a split ratio of 0.022.

The flash tank's job is to keep inert components out of the distillation column. The lower the flash pressure, the fewer inert components entering the column, which reduces the vapor coming off the top of the reflux drum, thus reducing costs of the compressor K4 on this stream. On the other hand, lowering flash pressure results in more vapor leaving the flash tank, which increases energy and capital cost of the compressor (Kflash) that is recycling this stream back to the 110-bar reactor pressure. So there is a trade-off between the cost of the two compressors, which are affected in opposite ways by flash pressure.

Figure 11.6 illustrates all these trends. The top left graph shows that the vapor V1 from the reflux drum of the distillation column decreases as flash pressure is decreased. This

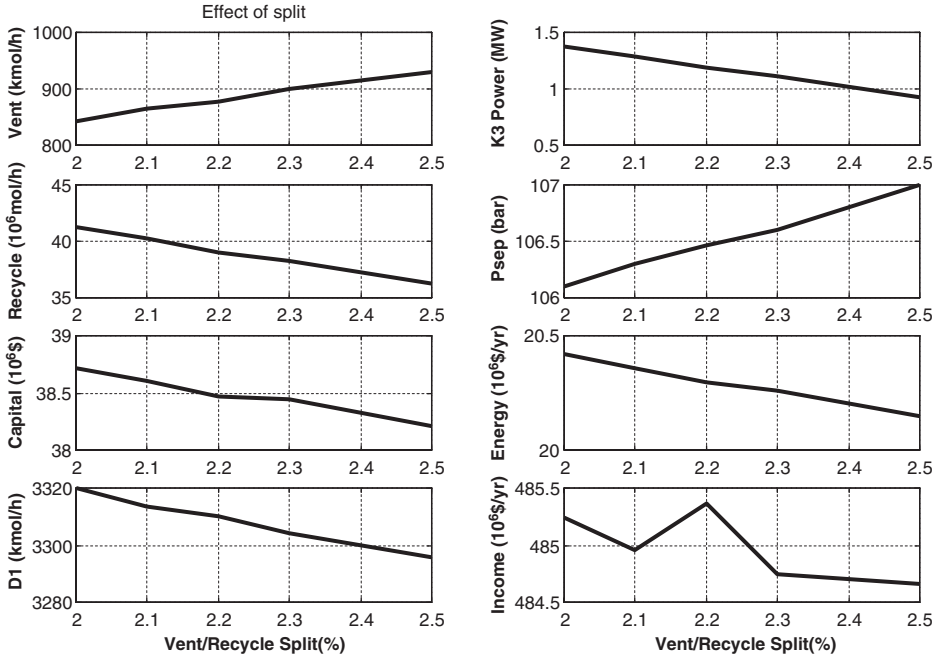


**Figure 11.5.** Effect of vent/recycle split.

reduces the work in compressor K4. Once flash pressure gets down to 2 bar, there are only very small amounts of inert components entering the column.

However, the flowrate of vapor leaving the flash tank increases as flash pressure is decreased, as shown by the increase in compressor work (middle left graph in Figure 11.6). Going from 2 bar to 1 bar results in a rapid change in Kflash compressor work. A pressure of 2 bar gives the maximum income and at the same time gives the minimum capital investment. So the flash drum pressure is set at 2 bar.

It is interesting to note that there is additional advantage of running a low flash-drum pressure. The reduction in the amount of inert components coming into the reflux drum of the column improves the purity of the methanol product. The specification used is 0.1 mol% water in the distillate, but there is some carbon dioxide present in the liquid product. With a flash-drum pressure of 2 bar, the carbon dioxide composition is 0.9 mol% in the distillate, which gives a methanol purity of 98.9 mol%. With a flash-drum pressure of 1.5 bar, the carbon dioxide composition is 0.7 mol% in the distillate, which gives a methanol purity of 99.2 mol%. With a flash-drum pressure of 1 bar, the carbon dioxide composition is 0.5 mol% in the distillate, which gives a methanol purity of 99.4 mol%. So, if very high purity methanol is desired, a low flash-drum pressure would be required.

### 11.6.6 Optimum Distillation Column Design

The last design optimization variable explored is the number of stages and the feed-stage location in the distillation column. The values that minimize TAC were determined. The results are shown in Table 11.5. The optimum feed stage is found for each case by determining the feed stage that minimizes reboiler heat input.

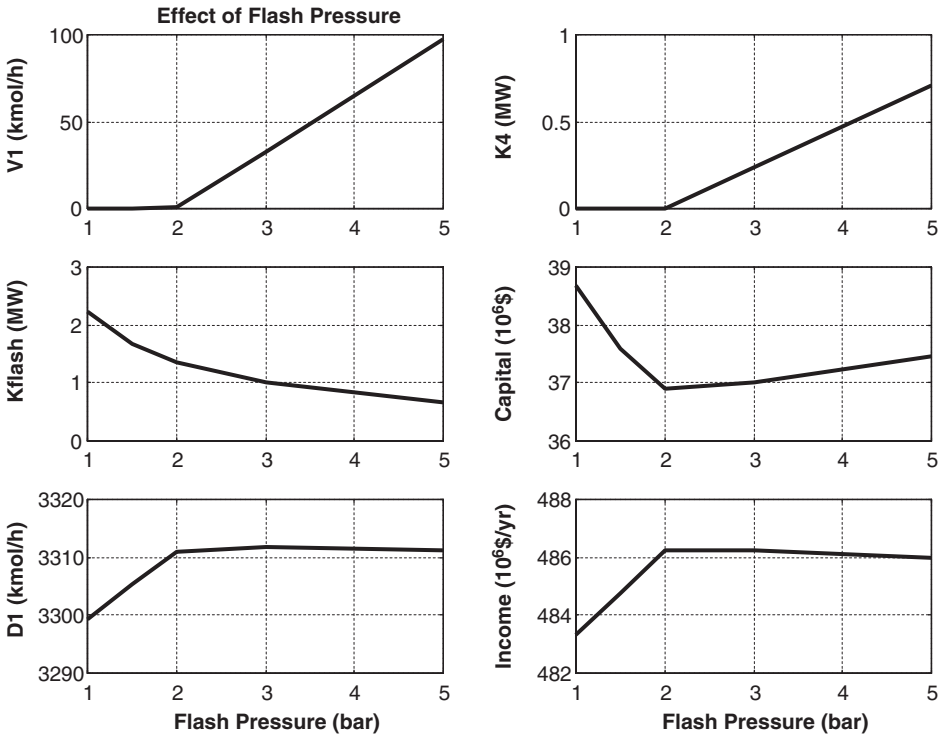


**Figure 11.6.** Effect of flash tank pressure.

As the number of total stages is increased, energy costs and heat exchanger capital costs decrease, but the capital cost of the shell increases. Total capital increases with increasing stages. The 42-stage column has the lowest TAC.

Note that the variation of the economic objective function (TAC) with total stages is quite modest, with less than 1% change over the entire range from 32 to 52 stages. Thus, a rigorous determination of precisely the optimum number of stages, narrowing it down to a precision of a single stage, is unnecessary.

**TABLE 11.5 Optimum Distillation Column Design**

| | | | |
|---|---|---|---|
| NT | 32 | 42 | 52 |
| $NF_{opt}$ | 19 | 27 | 30 |
| ID (m) | 5.979 | 5.806 | 5.674 |
| $Q_R$ (MW) | 59.85 | 54.27 | 54.26 |
| $Q_C$ (MW) | 48.45 | 47.83 | 47.79 |
| Area reboiler ($m^2$) | 2770 | 2741 | 2740 |
| Area condenser ($m^2$) | 2838 | 2802 | 2800 |
| Capital costs ($10^6$ \$) | | | |
| Shell | 1.318 | 1.623 | 1.928 |
| Reboiler and condenser | 2.542 | 2.523 | 2.522 |
| Energy cost ($10^6$ \$/yr) | 13.46 | 13.32 | 13.31 |
| TAC ($10^6$ \$/yr) | 14.75 | **14.70** | 14.80 |

Figure 11.7 gives the temperature and composition profiles in the distillation column. These will be used in developing a control structure in the next section.

The flowsheet shown in Figure 11.1 shows the final design. The system pressure is 110 bar, the reactor has 8000 tubes, the vent/recycle split is 0.022, the flash-drum pressure is 2 bar, and the column has 42 stages. An effective plantwide control scheme for the process is developed and tested in the next section.

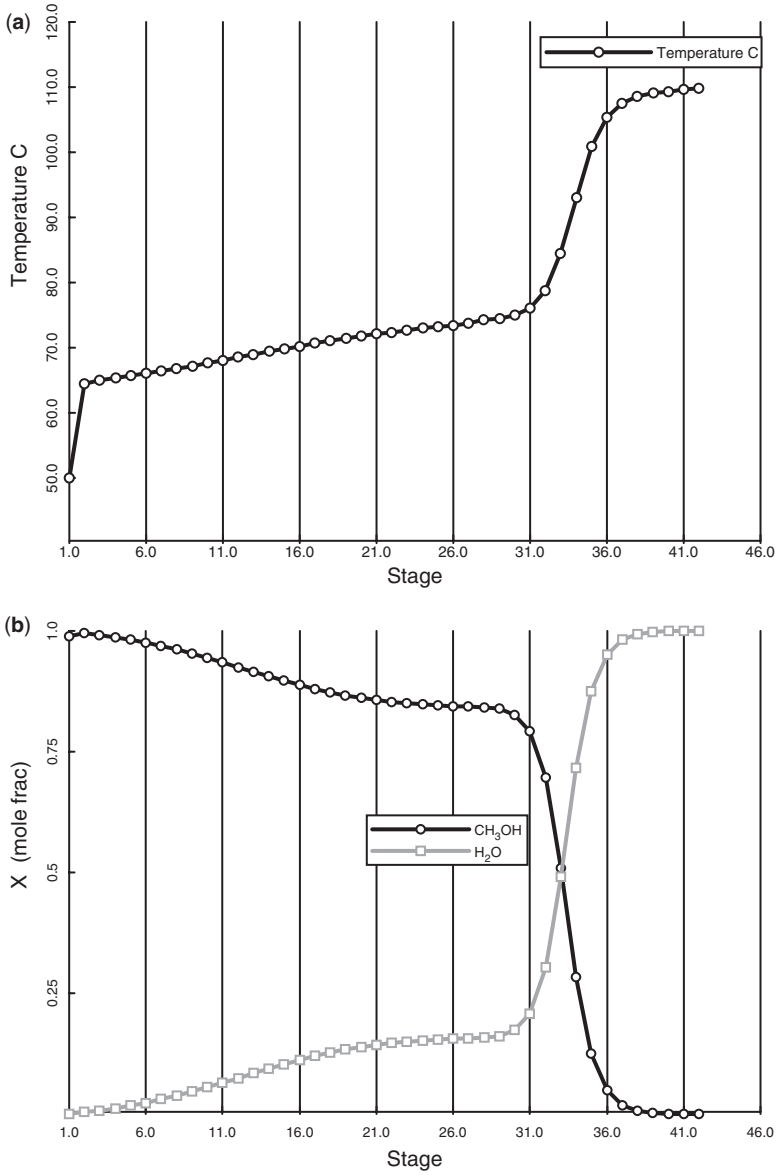


**Figure 11.7.** (a) Column temperature profile. (b) Column composition profiles.

## 11.7 PLANTWIDE CONTROL

Before exporting the steady-state Aspen Plus simulation into Aspen Dynamics, the size of the reflux drum and column base in the distillation column are determined to provide 5 min of liquid holdup at 50% level. The size of the reactor and column vessel are known from the steady-state design. The sizes of the separator and flash drum were also determined during steady-state design so that their capital investment costs could be calculated. The size of the separator is set by the maximum superficial vapor velocity, using the gas flowrate and its density. An $F$ factor of 0.5 is used (in English engineering units). The diameter is 6.5 m, since there is a very large gas recycle stream. The size of the flash tank is set by 5 min of liquid holdup (2.8 m in diameter, 5.6 m in length). The compressors and heat exchangers are assumed have negligible dynamic lags.

The development of the plantwide control structure presented below is based on the heuristic procedure proposed a decade ago (see Luyben et al.[5]), which has been successfully applied to many industrial processes.

### 11.7.1 Control Structure

Figure 11.8 shows the plantwide control structure developed for this process. Conventional PI controllers are used in all loops. All level loops are proportional with $K_C = 2$. Flow controllers that manipulate compressors use a gain of 0.5 and an integral time of 0.5 min. The column tray temperature controller has a 1-min deadtime. The reactor temperature loop has a 2-min deadtime to account for the steam generation dynamics. The composition controller has a 3-min deadtime. These temperature and composition controllers are tuned by using

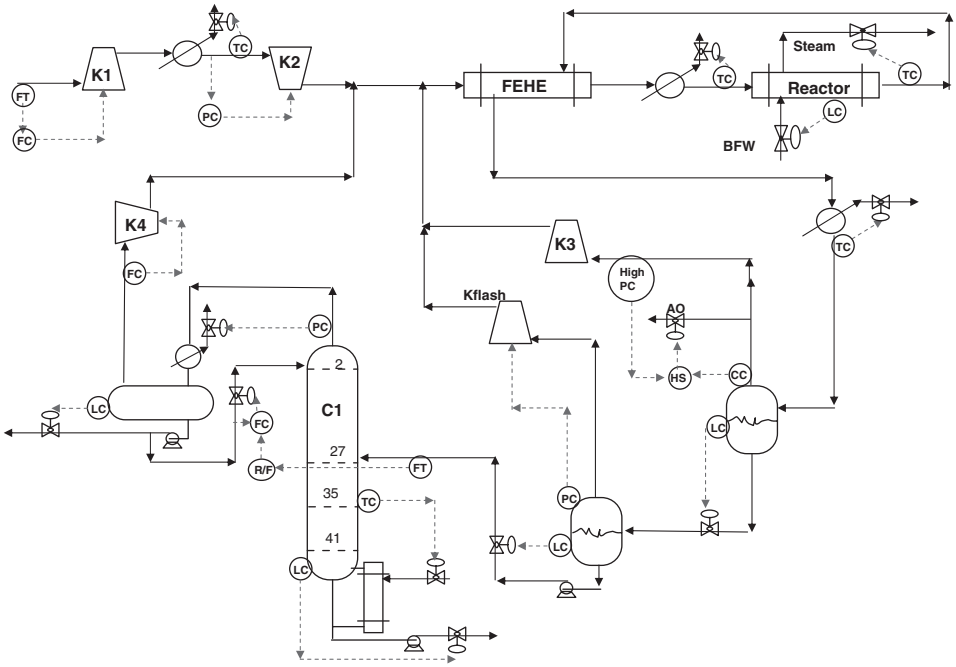


**Figure 11.8.** Plantwide control structure.

relay-feedback tests to obtain ultimate gains and periods, and then applying Tyreus-Luyben tuning rules.

All of the loops are listed below with their controlled and manipulated variables.

1. The synthesis gas is flow-controlled by manipulating work to compressor K1. If the synthesis gas is being generated in an upstream gasification unit, a pressure controller in that unit typically would change the setpoint of the flow controller.
2. The temperature of the compressed gas leaving the interstage cooler is controlled by manipulating heat removal in the heat exchanger (cooling water).
3. The suction pressure of the second compressor K2 is controlled by manipulating its compressor work.
4. The reactor inlet temperature is controlled by manipulating the heat input to the reactor preheater (medium-pressure steam).
5. Reactor exit temperature is controlled by manipulating the temperature of the cooling medium on the shell side of the reactor in the Aspen plug-flow reactor model. Physically this corresponds to adjusting the setpoint of a steam back-pressure controller and bringing in BFW to hold the liquid level on the shell of the reactor vessel.
6. The temperature of the gas leaving the condenser and going into the separator is controlled by manipulating the heat removal (cooling water) in the condenser.
7. A composition controller manipulates the control valve in the vent stream to maintain the composition of methane in the gas recycle.
8. A high-pressure override controller can also change the position of the control valve in the vent line if the separator pressure exceeds some specified value. A high selector determines which signal will position the vent valve. The setup and the need for this controller are discussed in Section 11.7.3.
9. The liquid level in the separator is controlled by manipulating the liquid flowrate from the separator into the flash tank.
10. The pressure in the flash tank is controlled by manipulating work in the Kflash compressor, which recycles the gas back to the reactor.
11. The liquid level in the flash tank is controlled by manipulating the liquid flowrate from the flash tank into the distillation column.
12. Base liquid level in the column is controlled by manipulating bottoms flowrate. This is the water product stream leaving the process.
13. Reflux-drum level is controlled by manipulating distillate flowrate. This is the methanol product stream leaving the process.
14. The reflux is ratioed to the feed to the column using a multiplier that adjusts the setpoint of a flow controller on the reflux. The feed flowrate is the other input to the multiplier.
15. Column pressure is controlled by manipulating condenser heat removal (cooling water).
16. The temperature on stage 35 is controlled by manipulating reboiler heat input (low-pressure steam).
17. The small vapor stream from the top of the reflux drum is flow-controlled by manipulating work in compressor K4.

Note that the throughput is set by the synthesis gas flowrate into the process, and inventory loops are in the direction of flow. Note also that the pressure in the system is *not*

controlled but floats up and down as throughput and synthesis gas composition change. Further discussions and the rationale for the important loops are given in Section 11.7.3.

### 11.7.2 Column Control Structure Selection

For reasons of simplicity and low maintenance cost, many industrial distillation columns use some type of single-end temperature control. However, this simple structure may not provide effective control for some columns. Even if a single-end control structure is possible, we have to decide how to select the other control degree of freedom. The most common choices are holding a constant reflux-to-feed (R/F) ratio or holding a constant reflux ratio (RR).

***Selecting Reflux Ratio or Reflux-to-Feed Ratio.*** To explore this question, a series of steady-state runs are made in which the effects of changes in feed composition on the required changes in R/F ratio and RR are determined while holding both products at their specified compositions. Table 11.6 gives results of these calculations.

The required changes in the R/F ratio are only about 3% over the entire range of feed compositions from 86.5 to 76.5 mol% methanol. An appropriate change in the water feed composition is made as the methanol composition is varied. The required changes in the RR are much larger (about 16%). Therefore, from a steady-state standpoint, the R/F control structure should handle feed composition disturbances better than the RR control structure.

***Selecting Temperature/Composition Control Tray Location.*** Another important issue in distillation control is the location of the tray with the temperature that is to be controlled in a single-end structure. There are many methods for making this selection, but a simple and effective approach is to select a tray where there are significant changes in temperature from tray to tray.

Figure11.7a shows a large change in the temperature profile in the lower part of the column. Stage 35 is selected, which has a temperature of 101 °C. The controller parameters that result from relay-feedback testing are given in Table 11.7.

### 11.7.3 High-Pressure Override Controller

As the dynamic simulation results presented in the next section will demonstrate, there is no need for an override controller when disturbances in throughput occur. The design values of the composition of the synthesis gas provide the necessary balance between the carbon monoxide and carbon dioxide fed and the hydrogen fed so as to satisfy the stoichiometry of the two reactions. For 1 mol of carbon monoxide, 2 mol of hydrogen are required. For 1 mol of carbon dioxide, 3 mol of hydrogen are required.

**TABLE 11.6 Column Control Structure Selection**

| | Feed Composition | Reflux-to-Feed Ratio | Reflux Ratio |
|---|---|---|---|
| | 0.86517 MeOH<br>0.12674 $H_2O$ | 0.3355 | 0.3771 |
| Design | 0.81517 MeOH<br>0.17674 $H_2O$ | 0.3297 | 0.4071 |
| | 0.76517 MeOH<br>0.22674 $H_2O$ | 0.3394 | 0.385 |

**TABLE 11.7 Controller Parameters**

| | TCRX | TC1 | CC Vent | High PC |
|---|---|---|---|---|
| Controlled variable | Reactor exit temperature | Stage 35 temperature | Recycle gas composition | Separator pressure |
| Manipulated variable | Steam temperature | Reboiler heat input | Signal to high selector on vent valve position | Signal to high selector on vent valve position |
| SP | 267 °C | 101 °C | 0.258 mole fraction $CH_4$ | 130 bar |
| Transmitter range | 200–300 °C | 50–150 °C | 0–0.5 mole fraction $CH_4$ | 120 – 140 bar |
| OP | 264 °C | 45.38 Gcal/h | 14.77% | 0% |
| OP range | 200–300 °C | 0–90.77 Gcal/h | 0–100% | 0–100% |
| Deadtime | 2 min | 1 min | 3 min | – |
| $K_C$ | 0.456 | 1.37 | 5.0 | 5 |
| $\tau_I$ | 9.2 min | 9.2 min | 56 min | – |

There are 2630 kmol/h of carbon monoxide in the synthesis gas that require 5260 kmol/h of hydrogen. There are 785.3 kmol/h of carbon dioxide in the synthesis gas that require 2356 kmol/h of hydrogen. Thus, the total hydrogen required to completely react all the carbon monoxide and carbon dioxide is 7616 kmol/h. The hydrogen in the synthesis gas feed is 7839 kmol/h, so there is a slight excess, which leaves the system in the vent stream along with the unreacted carbon monoxide and carbon dioxide.

If the synthesis gas composition changes such that this delicate stoichiometric balance no longer holds, the component(s) in excess will build up and pressure will increase in the system. Remember that the feed into the system is flow-controlled. Therefore, a strategy to handle this problem is required.

An override controller is a simple way to achieve this objective. The vent valve is air-to-open (fails shut). A high selector chooses between the higher of two signals. The first signal comes from the composition controller. This signal normally sets the vent valve position. The second signal comes from the high-pressure override controller, which has an output signal that only increases and takes over the vent valve when the separator pressure get above 120 bar. The override controller is proportional-only, with a gain of 5 and a normal output signal of 0%. As pressure changes from 120 to 140 bar, its output signal changes from 0 to 100%. At some pressure, this output will exceed the signal coming from the composition controller and begin opening the vent valve.

The synthesis gas composition disturbances discussed below demonstrate the effectiveness of the proposed control structure.

### 11.7.4 Dynamic Performance Results

Several large disturbances are made to test the ability of the proposed plantwide control structure. These disturbances include synthesis gas feed flowrate and synthesis gas composition (adding more inert methane or changing the relative amounts of the reactants).

***Throughput Disturbances.*** Figure 11.9 gives results for 20% changes in the setpoint of the synthesis gas flow controller. The solid lines are 20% increases; the dashed lines are 20% decreases. The disturbances are made at 0.2 h.

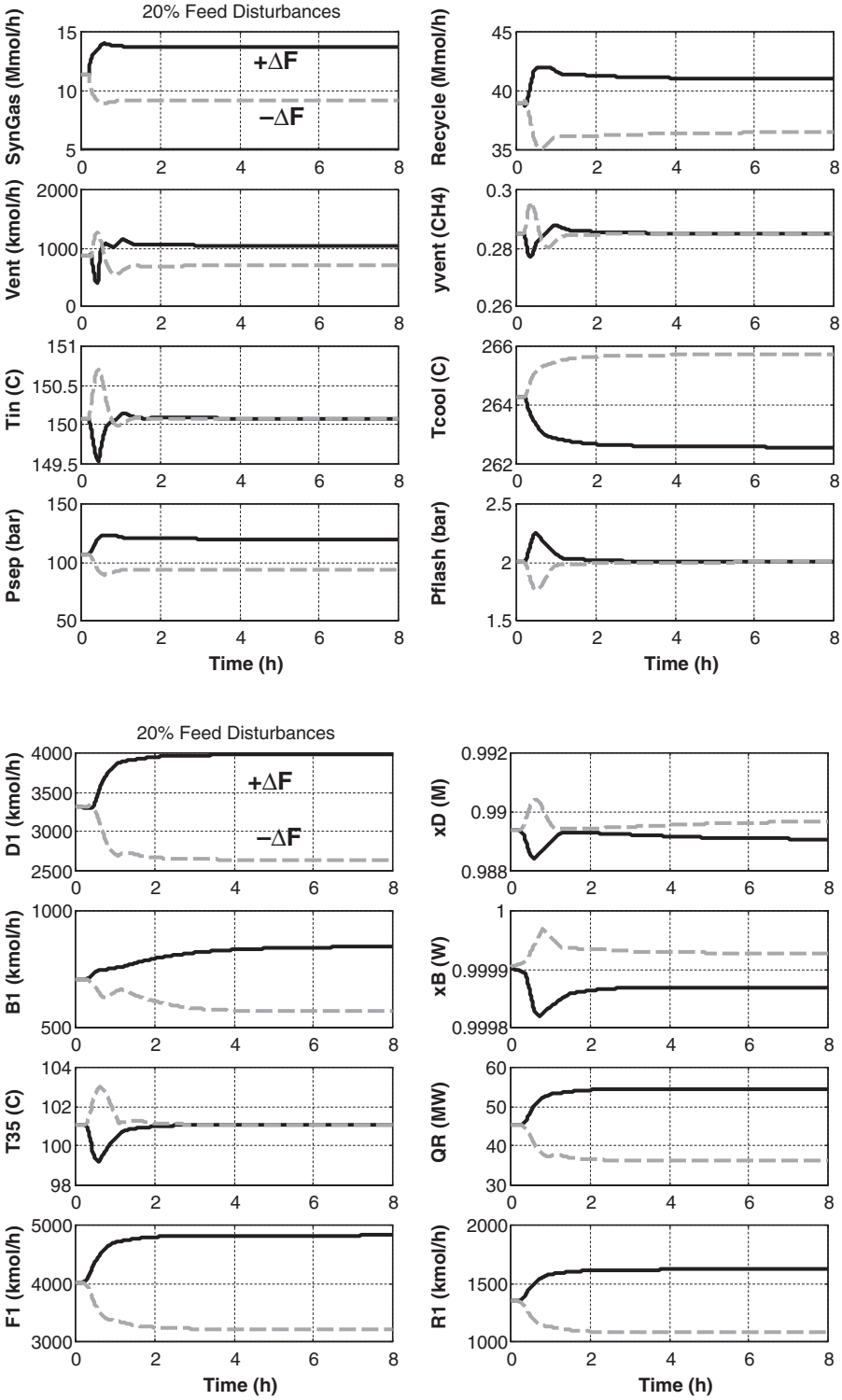


**Figure 11.9.** 20% feed flowrate disturbances.

Stable regulatory control is achieved. Notice that the pressure in the separator ($P_{sep}$) rises up to a new steady-state level for increases in throughput and drops to a lower level for decreases in throughput. The pressure in the gas loop (FEHE, preheater, reactor, and separator) is *not* controlled in this plantwide control structure, but varies with conditions in the reactor that affect reaction rates.

Recycle, distillate, and bottoms flowrates increase as throughput increases. The coolant temperature ($T_{cool}$) in the reactor decreases as throughput increases, so that the increased heat removal can be achieved by providing a larger differential temperature driving force.

Stage 35 temperature is well controlled by manipulating reboiler heat input (T35). The R/F ratio system changes the column reflux R1 as the feed to the column F1 changes.

Of primary importance, the compositions of the two products leaving the process are held quite close to their specified values. The distillate composition $x_{D(M)}$ and the bottoms water composition $x_{B(W)}$ remain near their specifications.

***Methane Impurity in Synthesis Gas Feed.*** Figure 11.10 gives results for changes in the methane impurity in the synthesis gas. The design value of this inert impurity is 2.17 mol% methane. The design hydrogen feed composition is 67.46 mol% hydrogen. The solid lines show results for an increase in methane impurity to 3.17 mol% and an appropriate decrease in hydrogen composition to 66.46 mol%. The dashed lines show results for a decrease in methane impurity to 1.17 mol% and an appropriate increase in hydrogen composition to 68.46 mol%.

First, let us consider the effects of increasing the methane impurity in the synthesis gas. There is a substantial increase in the vent flowrate (Vent), which results in higher losses of the reactants. Consequently, less methanol D1 and water B1 are produced. The pressure in the system goes down ($P_{sep}$). Product purities are held close to their specifications.

Now consider the effects of decreasing the methane impurity in the synthesis gas. More products are made because the vent flowrate decreases, meaning smaller losses of reactants. Product purities are again held close to their specifications.

However, this disturbance shows the need for the high-pressure override controller. Notice that the recycle gas methane composition is *not* held at its setpoint (yvent) but drifts downward. This occurs because the pressure in the gas loop $P_{sep}$ starts to increase. When the pressure gets up to 120 bar, the override controller takes over and opens the vent valve to maintain system pressure.

***Reactant Concentrations in Synthesis Gas Feed.*** Figure 11.11 also demonstrates the need for the override controller. The disturbances are changes in the carbon monoxide, carbon dioxide, and hydrogen compositions in the feed.

*Carbon Monoxide to Carbon Dioxide Ratio.* The solid line gives results for the case in which the feed contains more carbon dioxide and less carbon monoxide. Carbon dioxide is changed from 6.858 to 8.858 mol%. Carbon monoxide is changed from 22.97 to 20.97 mol%.

As expected, more water is produced (B1 increases), since there is more carbon dioxide. The amount of methanol produced (D1) decreases slightly because the vent rate increases from 872 to 939 kmol/h, so reactant losses increase. There is a slight drop in methanol purity.

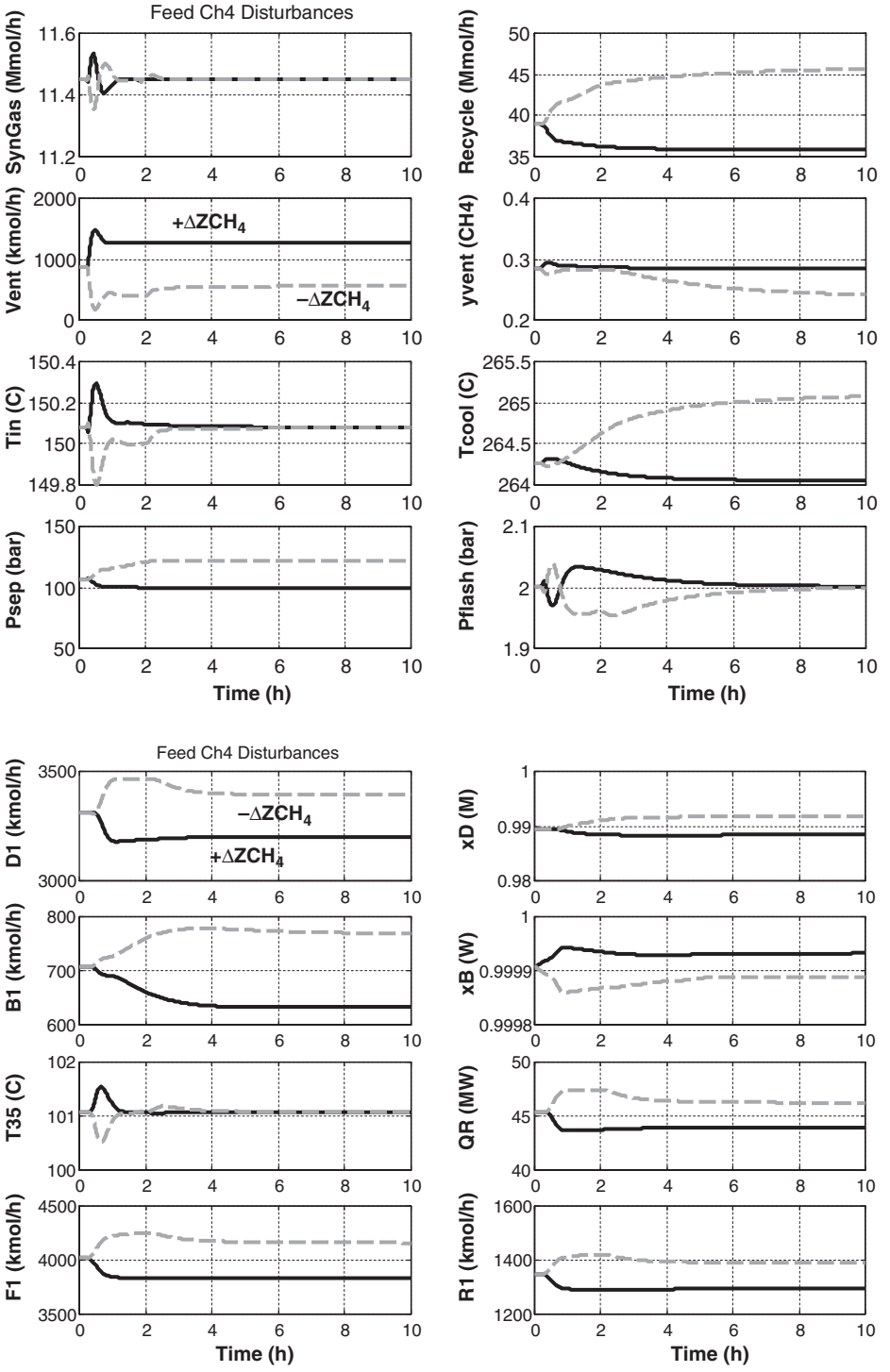


**Figure 11.10.** Feed methane composition disturbances.

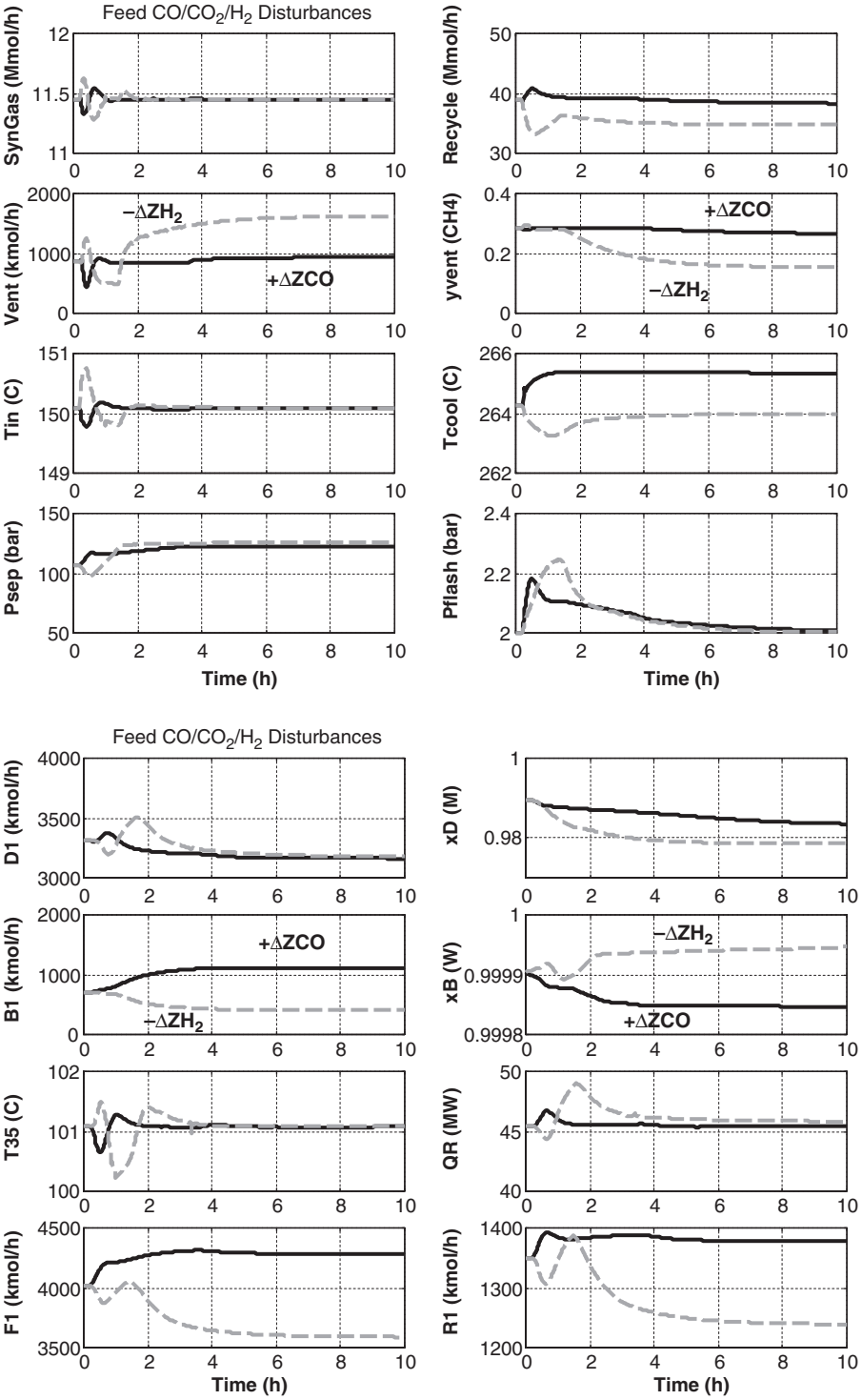


**Figure 11.11.** Feed hydrogen composition disturbances.

Pressure increases from 110 to 115.9 bar, so the override controller does not come into play for this disturbance. The vent methane composition controller is able to maintain the desired 28.5 mol% methane.

Since carbon dioxide consumes more hydrogen than carbon monoxide, the amount of hydrogen lost in the vent drops from 479 to 207 kmol/h for this disturbance. On the other hand, the amount of carbon dioxide lost increases from 69.8 to 206.9 kmol/h.

*Hydrogen to Carbon Ratio.* The dashed lines in Figure 11.11 give results when the synthesis gas composition is changed from 67.46 to 61.46 mol% hydrogen, 22.97 to 25.97 mol% carbon monoxide, and 6.86 to 9.86 mol% carbon dioxide. This disturbance increases the demand for hydrogen by feeding in more carbon monoxide and carbon dioxide, but provides less hydrogen.

The result is an initial drop in pressure ($P_{sep}$), as the hydrogen is consumed at a higher rate. However, it does not take long for the pressure to start increasing because the carbon monoxide and carbon dioxide are not being consumed due to the shortage of hydrogen. When the pressure builds up to 120 bar, the override controller take over the vent valve and removes gas from the system. The vent methane composition is not controlled and drops from 28.5 to 15.4 mol% methane.

The reactor pressure eventually levels out at 131 bar with a very large vent rate (1623 kmol/h). Large losses of reactants in the vent stream occur, so the production of methanol drops from 3311 to 3178 kmol/h. The water produced drops from 707 to 411 kmol/h. The loss of carbon dioxide in the vent climbs from 69.8 kmol/h to a whopping 673 kmol/h. The high reactor pressure requires a huge increase in the work of the Kflash compressor from 1.015 to 8.77 MW.

These results demonstrate the need to provide precise control of the synthesis gas feed by varying conditions in upstream units. For example, if the synthesis gas is being generated from coal in a gasifier, there will be a shortage of hydrogen since coal has a hydrogen-to-carbon ratio of about one. The synthesis gas is typically split into two streams. One is sent directly to the methanol plant. The other stream is sent to a water–gas shift reactor unit to produce more hydrogen and carbon dioxide from water and carbon monoxide. Then the carbon dioxide is removed from the gas, typically using amine scrubbing. The resulting hydrogen-rich stream is combined with the other synthesis gas stream, and the total is fed to the methanol process. The fraction of the synthesis gas fed to the water–gas shift unit must be precisely set, so that the methanol plant feed has the correct amount of hydrogen for reaction with the carbon dioxide and carbon monoxide it contains.

## 11.8 CONCLUSION

The methanol process presents some interesting design and control features. Design trade-offs exist between reactor pressure and feed compressor energy, between reactor size and recycle flowrate, between venting rate and reactant losses, and between flash pressure and flash compression energy.

The plantwide control structure has the unusual feature of permitting the pressure in the reactor to vary as conditions change. A high-pressure override controller is needed to handle imbalances in the stoichiometry of the reactants in the synthesis gas feed.

## REFERENCES

1. Olah, G. A., Goeppert, A., Suryn Prakash, G. K. *Beyond Oil and Gas: The Methanol Economy*, Wiley-VCH, Chichester, UK, 2006.
2. vanden Bussche, K. M., Froment, G. F. A steady-state kinetic model for methanol synthesis and the water gas shift reaction on a commercial $Cu/ZnO/Al_2O_3$ catalyst, *J. Catalysis* 1996, **161**, 1–10.
3. Douglas, J. M. *Conceptual Design of Chemical Processes*, McGraw-Hill, New York, 1988.
4. Turton, R., Bailie, R. C., Whiting, W. B., Shaelwitz, J. A. *Analysis, Synthesis and Design of Chemical Processes*, 2nd Edition, Prentice Hall, Englewood Cliffs, NJ, 2003.
5. Luyben, W. L., Tyreus, B. D., Luyben, M. L. *Plantwide Process Control*, McGraw-Hill, New York, 1999.

# CHAPTER 12

# DESIGN AND CONTROL OF THE METHOXY-METHYL-HEPTANE PROCESS

The chemical 2-methoxy-2-methylheptane (MMH) has been proposed as a gasoline additive to replace methyl tert-butyl ether (MTBE) in order to avoid groundwater contamination. The chemistry involves the liquid-phase reversible reaction of methanol with 2-methyl-1-heptene (MH) to form MMH. However, methanol and MH also undergo an undesirable reaction to form dimethyl ether (DME) and 2-methyl-2-heptanol (MHOH).

The activation energies of the two competing reactions favor high reactor temperature, which is limited by catalyst activity to 400 K. Yield of the desired product is increased by either increasing reactor size or keeping the concentration of methanol in the reactor low by using a large excess of MH in the reactor. The latter strategy results in a large recycle flowrate of MH, which increases separation costs. Thus, this process demonstrates the classic design trade-off between reactor costs and separation costs.

The purpose of this chapter is to explore the economics and the dynamics of this process. The cost of the MH raw material and the values of the products are somewhat uncertain. Therefore, the approach adopted in this chapter is to design the process for a specified yield of MMH. For a given yield, there are optimum values of reactor size and recycle flowrate that minimize total annual cost (TAC). The flowsheet features a continuous stirred-tank reactor (CSTR), three distillation columns, and one recycle stream.

A plantwide control structure is also developed that is capable of effectively handling large disturbances in production rate and operating parameters. The limiting reactant (methanol) is flow-controlled to set the production rate. The fresh feed of the other reactant (MH) is fed to maintain a fixed total flowrate of MH (fresh feed plus recycle).

## 12.1 INTRODUCTION

Griffin et al.[1] studied the effect of competing reversible reactions on the optimum operating policies for plants with recycle. Economically optimal designs were developed for a given

*Principles and Case Studies of Simultaneous Design*, First Edition. William L. Luyben

kinetic system with the reactor designed to be liquid-full. Then, the optimum reactor volume when operating at production rates other than the design value was determined. Some systems always operate with full reactors. With other chemistry, operating with the reactor only partially full is the economic optimum. No control issues were explored by these authors.

The case study presented by Griffin et al.[1] has two competing reactions, one producing the desired product and the second producing undesired products. Their paper provided only sketchy information about the flowsheet and the economics, but it does provide the reaction kinetics and the desired production rate. We use this information as the basis for our study in this chapter.

## 12.2 PROCESS STUDIED

Figure 12.1 shows the flowsheet of the process. The equipment sizes and conditions shown are the economic optimum developed later in this chapter for a 99% yield of MMH. The Aspen UNIQUAC physical properties model is used in all units of the process. Since MMH and MHOH are not in the Aspen data bank, pseudo components were generated from the molecular structures of these two molecules.

### 12.2.1 Reactor

The reactor is a 12 $m^3$ CSTR operating at 400 K and 12 atm. A fresh methanol stream (MeOH) is fed at 50 kmol/h. Fresh MH is fed to the reactor at 49.51 kmol/h and combined with a recycle stream from a downstream distillation column to give a total of 129.5 kmol/h

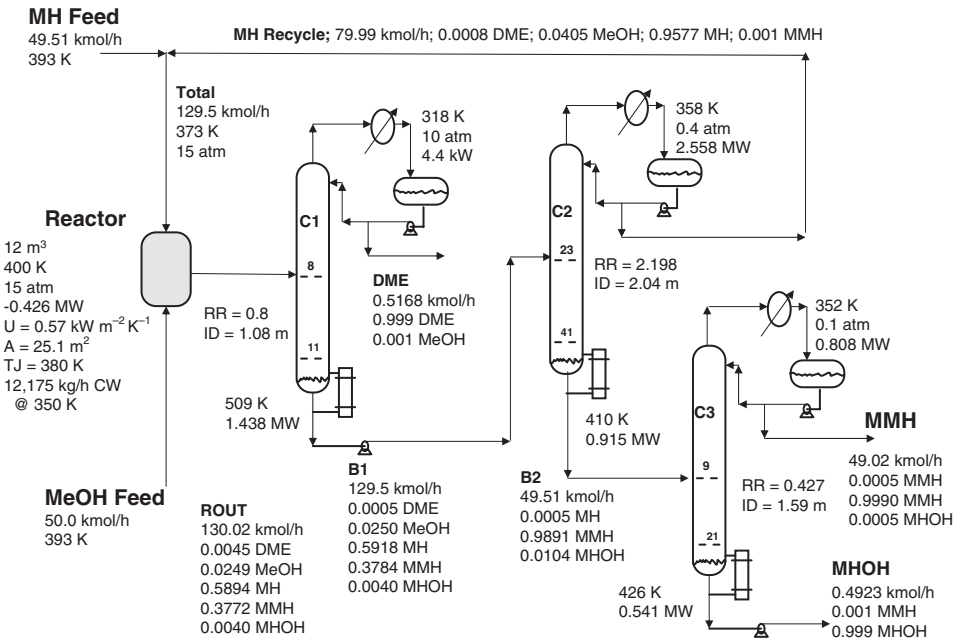


**Figure 12.1.** Flowsheet.

of MH fed to the reactor. Concentrations in the reactor are 0.45 mol% DME, 2.49 mol% MeOH, 58.94 mol% MH, 37.72 mol% MMH, and 0.40 mol% MHOH. The low methanol concentration is needed to achieve the desired 99% yield of MMH. The reactor effluent is 130.02 kmol/h. Thus, the per-pass conversion of methanol is 93.9% and the per-pass conversion of MH is 39.2%.

### 12.2.2 Column C1

The reactor effluent is fed on stage 8 of a 12-stage distillation column. Aspen notation is used with the reflux drum being stage 1. The column operates at 10 atm, which gives a reflux-drum temperature of 318 K and permits the use of cooling water in the condenser. The distillate product is a small stream of 0.5168 kmol/h of 99.9 mol% DME. The separation between DME and methanol is easy, so the reflux ratio is small (RR = 0.8) and few stages are required.

The base temperature is 509 K, so high-pressure steam is required in the reboiler (42 bar, 527 K). The reboiler duty is 1.438 MW, but the condenser duty is only 0.0044 MW because of the very small distillate flowrate and low RR. Most of the reboiler heat goes to increase the sensible heat of the feed from 400 K up to the base temperature of 509 K. Column diameter is 1.08 m.

### 12.2.3 Column C2

The bottoms from the first column is fed to column C2, which separates the product MMH from the recycle MH. The distillate is 79.94 kmol/h, with a composition of 0.1 mol% MMH, 1.35 mol% MeOH, and 98.55 mol% MH. The bottoms is a mixture of the product MMH and the impurity MHOH. The bottoms specification is 0.05 mol% MH.

The column has 42 stages and is fed on stage 23. It operates under vacuum conditions (0.4 atm) with a reflux-drum temperature of 358 K. The required RR to achieve the specified separation is 2.198. Base temperature is 410 K, so medium-pressure steam can be used in the reboiler (11 bar, 457 K). Column diameter is 2.04 m.

### 12.2.4 Column C3

The third column has 22 stages and is fed on stage 14. The distillate is the MMH product (49.02 kmol/h) with a purity of 99.9 mol% MMH. The bottoms is 0.4923 kmol/h of by-product MHOH with an purity of 99.9 mol%.

The column operates under vacuum (0.1 atm). The reflux-drum temperature is 352 K, and the base temperature is 426 K using medium-pressure steam. The RR is 1.59, and the reboiler duty is 0.541 MW. Column diameter is 1.59 m.

## 12.3 REACTION KINETICS

The chemistry involves the reversible reaction of methanol with the unsaturated compound MH to form MMH. The molecular structures of these components are shown in Figure 12.2.

$$CH_3OH + C_8H_{16} \Longleftrightarrow C_9H_{20}O \tag{12.1}$$

**MH**: 2-methyl-1-heptene ($C_8H_{16}$)

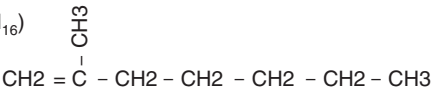

**MMH**: 2-methoxy-2-methylheptane ($C_9H_{20}O$)

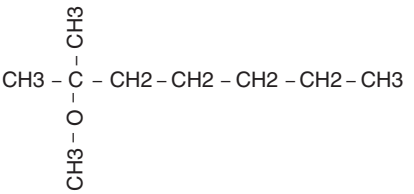

**MHOH**: 2-methyl-2-heptanol ($C_8H_{18}O$)

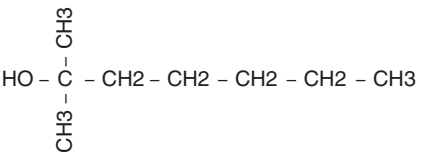

**Figure 12.2.** Molecular structures.

There is also an undesirable irreversible reaction of methanol and MH to form DME and MHOH.

$$2CH_3OH + C_8H_{16} \longrightarrow C_2H_6O + C_8H_{18}O \tag{12.2}$$

The overall reaction rates have units of kmol $s^{-1}$ $kg^{-1}$. Concentrations are in terms of mole fractions.

$$\Re_1 = k_{1F} x_{MeOH} x_{MH} - k_{1R} x_{MMH} \tag{12.3}$$

$$\Re_2 = k_2 (x_{MeOH})^2 \tag{12.4}$$

Table 12.1 gives the kinetic parameters for these reactions based on the information given in Griffin et al.[1]

Notice that the activation energy of the forward MMH reaction is larger than that of the reverse reaction, which means that high reactor temperatures should favor conversion. Griffin et al. state that the upper temperature limit of the resin catalyst is about 400 K.

To achieve a high yield of MMH, the methanol concentration must be kept low in the reactor, which implies a large recycle of MH from the separation section. In the optimized flowsheet for a 99% yield (see Figure 12.1), the methanol concentration in the reactor is only 2.49 mol% while the MH concentration is 58.94 mol%.

**TABLE 12.1 Kinetic Parameters**

| Overall Reaction Rates | kmol $s^{-1}$ $kg_{cat}^{-1}$ | $\Re 1$ Forward | $\Re 1$ Reverse | $\Re 2$ |
|---|---|---|---|---|
| $k$ | kmol $s^{-1}$ $kg_{cat}^{-1}$ | $6.7 \times 10^7$ | $2.1 \times 10^{-6}$ | $1.3 \times 10^9$ |
| $E$ | kJ/kmol | 90,000 | 900 | 105,900 |
| Concentrations | mole fraction | $x_{MH} x_{MEOH}$ | $x_{MMH}$ | $(x_{MeOH})^2$ |

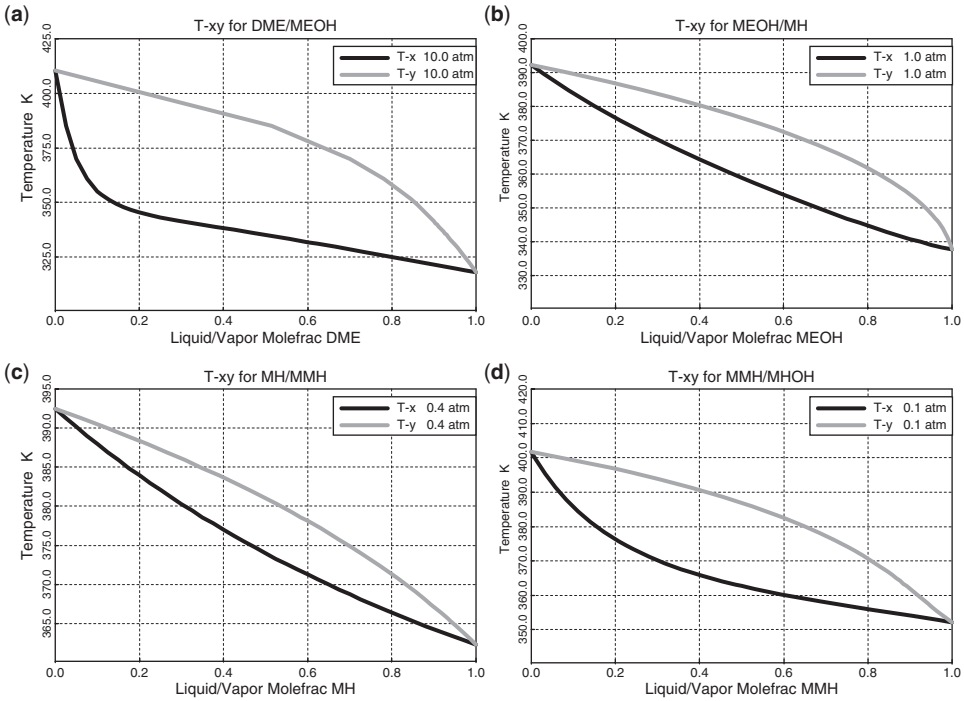


**Figure 12.3.** *Txy* diagrams for (a) DME/MeOH at 10 atm, (b) MeOH/MH at 1 atm, (c) MH/MMH at 0.4 atm, and (d) MMH/MHOH at 0.1 atm.

## 12.4 PHASE EQUILIBRIUM

The boiling points of the five components involved in the MMH process are quite different, so the separations are fairly easy: DME = 248.2 K, MeOH = 337.5 K, MH = 392.2 K, MMH = 424.4 K, and MHOH = 471.4 K.

Figure 12.3 gives *Txy* diagrams for several binary pairs. Figure 12.3a is for DME/MeOH at 10 atm, the operating pressure in the first column. Figure 12.3b is for MeOH/MH at 1 atm, and shows that no azeotrope is predicted. These components are not separated since they are both recycled back to the reactor in a single stream (the distillate from the second column). Figure 12.3c is for MH/MMH at 0.4 atm, the operating pressure in the second column. Figure 12.3d is for MMH/MHOH at 0.1 atm, the operating pressure in the third column.

## 12.5 DESIGN OPTIMIZATION

In order to do a rigorous economic analysis, the cost of the raw materials and the value of the products must be known or estimated. In this system, these values are quite uncertain. In the paper by Griffin et al.,[1] the fresh feed stream of MH is assumed to be pure. In reality, this unsaturated compound would probably be produced in a refinery by catalytic cracking in which a number of other similar components would be simultaneously generated. Separating out pure MH would probably be quite difficult and expensive. Therefore, the

cost of the MH raw material is somewhat uncertain. Likewise, the values of the MMH, DME, and MHOH produced have a fair amount of uncertainty associated with them.

Therefore, the approach adopted in this chapter is to design the process for a specified *yield* of MMH. For a given yield, there are optimum values of reactor size and recycle flowrate that minimize TAC.

### 12.5.1 Economic Basis

The economic analysis considers both capital investment (heat exchangers, reactor, catalyst, and columns) and energy costs (steam used in the reboilers). Table 12.2 summarizes the sizing and cost basis used in this analysis. These parameters are taken from Douglas[2] and Turton et al.[3]

### 12.5.2 Reactor Size versus Recycle Trade-Off

The dominant design optimization variables in the MMH process are reactor size and recycle flowrate. Figure 12.4 illustrates the effects of these two variables on the yield of MMH. For all these cases, the fresh feed of methanol is fixed at 50 kmol/h. The total MH fed to the reactor (fresh feed plus recycle, which is the distillate from column C2) is fixed by using the *Flowsheet design specification* feature in Aspen Plus. The desired flowrate of the total

**TABLE 12.2 Basis of Economics and Equipment Sizing**

Column diameter: Aspen tray sizing
Column length: NT trays with 2-ft spacing plus 20% extra length
Column vessels (diameter and length in meters)
$\text{Capital cost} = 17{,}640(D)^{1.066}(L)^{0.802}$

*Condensers (area in $m^2$)*
$\text{Heat-transfer coefficient} = 0.852\ \text{kW m}^{-2}\ \text{K}^{-1}$
Differential temperature = Reflux-drum temperature − 310 K
$\text{Capital cost} = 7296(A)^{0.65}$

*Reboilers (area in $m^2$)*
$\text{Heat-transfer coefficient} = 0.568\ \text{kW m}^{-2}\ \text{K}^{-1}$
Differential temperature = 34.8 K
$\text{Capital cost} = 7296(A)^{0.65}$

*Reactor vessel (diameter and length in meters)*
Aspect ratio = 2
$\text{Capital cost} = 17{,}640(D)^{1.066}(L)^{0.802}$
Catalyst cost = \$10/kg

*Energy costs*
LP steam = \$7.78/GJ
MP steam = \$8.22/GJ
HP steam = \$9.88/GJ

$$\text{TAC} = \frac{\text{Capital cost}}{\text{Payback period}} + \text{Energy cost}$$

Payback period = 3 yr

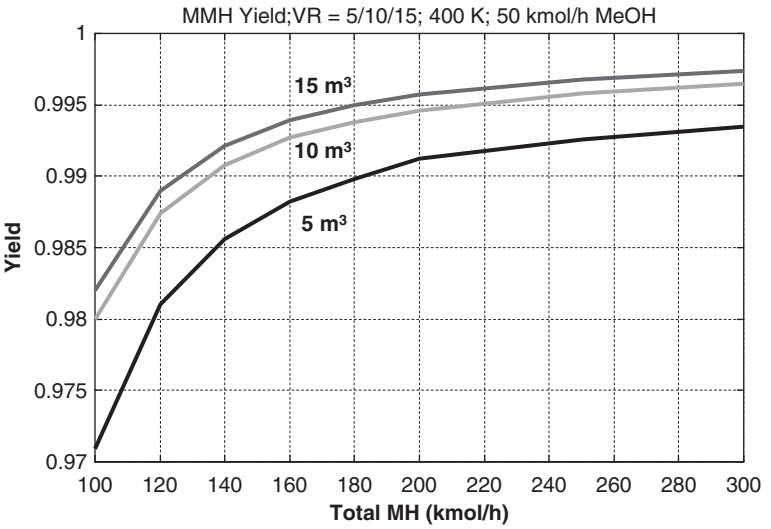


**Figure 12.4.** Effect of recycle and reactor size on MMH yield.

stream is specified and the flowrate of the fresh MH is varied to achieve this design specification.

There are also design specifications on each of the three columns. These specifications are:

Column C1: 0.1 mol% MeOH in distillate and RR = 0.8

Column C2: 0.1 mol% MMH in distillate and 0.05 mol% MH in bottoms

Column C3: 0.05 mol% MHOH in distillate and 0.1 mol% MMH in bottoms

The flowsheet is converged for these conditions, giving the resulting flowrates of the fresh MH and the MMH product (distillate D3 from column C3). The MMH yield is then calculated.

$$\text{Yield} = \frac{\text{Flowrate of MMH product}}{\text{Flowrate of MH fresh feed}} = \frac{\text{D3}}{\text{FFMH}} \tag{12.5}$$

Note that the fresh feed of methanol is fixed at 50 kmol/h, but the fresh feed of MH varies with the total MH recycle selected and other conditions in the process.

The results shown in Figure 12.4 are generated with the three distillation columns optimized in terms of operating pressure, total number of stages, and feed-stage location. The design of the columns is discussed in Section 12.6.

For a given reactor size, the yield of MMH increases as the flowrate of recycle MH increases. For a given flowrate of MH recycle, yield increases as reactor size increases. If a desired yield is selected, which will depend strongly on the cost of raw materials and the values of the products, there are many combinations of reactor size and recycle that can achieve the same yield.

For example, suppose a yield of 99% is desired. Figure 12.5 shows that there are many possible alternative designs. Using a small 5 $m^3$ reactor requires a total MH flowrate of

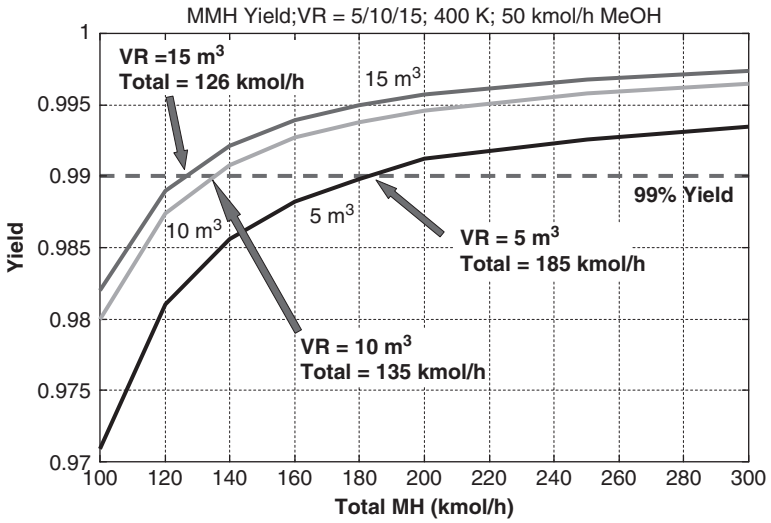


**Figure 12.5.** Alternative values of recycle and reactor size for 99% MMH yield.

185 kmol/h. Using a larger 15 $m^3$ reactor requires a total MH flowrate of only 126 kmol/h. A small reactor keeps the capital cost of the reactor vessel and catalyst small, but the large recycle results in high capital and energy costs of the separation section. Therefore an economic trade-off exists between reactor size and recycle flowrate.

To select the economic "best" design requires sizing all the equipment and evaluating capital and energy costs. The economic optimization function selected is TAC, which considers both capital and energy cost.

$$\text{TAC(\$/yr)} = \text{Annual energy cost} + \frac{\text{Capital investment}}{\text{Payback period}} \tag{12.6}$$

Results for reactors of various sizes are shown in Figure 12.6. In all these cases, the yield of MMH is 99%. The required total MH flowrate (recycle plus D2) is shown in the bottom right graph. The design that gives the minimum TAC has a 12-$m^3$ reactor with a total MH flowrate to the reactor of 129.5 kmol/h. The TAC of this optimum flowsheet is \$1,351,000/yr. Note that selecting a different desired yield will lead to a different optimum design. For example, a yield of 98% leads to an optimum flowsheet with a smaller reactor (10 $m^3$) and a smaller total MH flowrate (100 kmol/h). As we would expect, the TAC of the 98% yield process is lower (\$1,190,000/yr) than the 99% yield process.

Energy costs decrease as reactor size increases. Capital initially decreases as reactor size increases because of reductions in the capital cost of the distillation columns (vessel plus heat exchangers). However, the increasing cost of the reactor vessel and catalyst eventually begin to increase capital cost. The flowsheet for this design is shown in Figure 12.1. Table 12.3 gives details of equipment sizes, parameter values and costs for three alternative designs with reactor sizes of 10, 12, and 15 $m^3$. The second distillation column is the largest in terms of vessel height and diameter, so it has the highest capital investment. However, the first distillation column has the largest energy cost because the heat duty is the largest and expensive high-pressure steam is required.

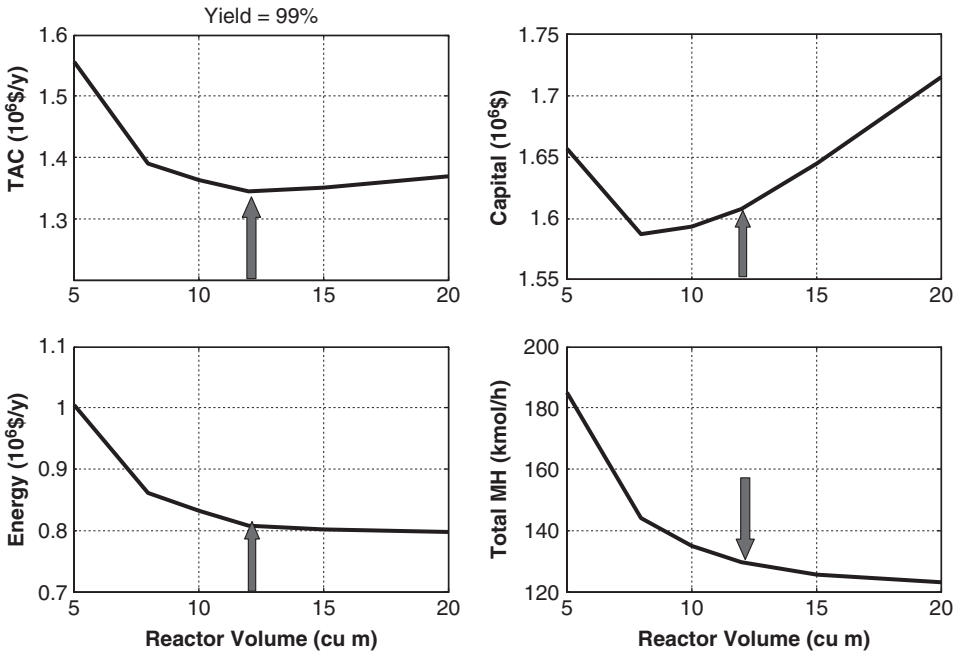


**Figure 12.6.** Optimum reactor size and recycle for 99% MMH yield.

**TABLE 12.3 Comparison of Alternative Designs for 99% Yield**

| Reactor Size ($m^3$) | 10 | 12 | 15 |
|---|---|---|---|
| Total MH recycle (kmol/h) | 135.0 | 129.5 | 125.5 |
| Reactor ($10^6$ \$) | 0.09737 | 0.1091 | 0.1253 |
| Catalyst ($10^6$ \$) | 0.1000 | 0.1200 | 0.1500 |
| Column C1 ID (m) | 1.093 | 1.084 | 1.084 |
| $Q_R$ (MW) | 1.481 | 1.442 | 1.417 |
| $Q_C$ (MW) | 0.0044 | 0.0044 | 0.0044 |
| Vessel capital cost ($10^6$ \$) | 0.09567 | 0.09483 | 0.09483 |
| HX capital cost ($10^6$ \$) | 0.1309 | 0.1276 | 0.1275 |
| Energy cost ($10^6$ \$/yr) | 0.4614 | 0.4424 | 0.4415 |
| Column C2 ID (m) | 2.075 | 2.044 | 2.024 |
| $Q_R$ (MW) | 0.9375 | 0.9147 | 0.898 |
| $Q_C$ (MW) | 2.639 | 2.558 | 2.502 |
| Vessel capital cost ($10^6$ \$) | 0.5760 | 0.5668 | 0.5609 |
| HX capital cost ($10^6$ \$) | 0.2168 | 0.2129 | 0.2100 |
| Energy cost ($10^6$ \$/yr) | 0.2300 | 0.2244 | 0.2203 |
| Column C3 ID (m) | 1.590 | 1.589 | 1.589 |
| $Q_R$ (MW) | 0.5422 | 0.5426 | 0.5427 |
| $Q_C$ (MW) | 0.8075 | 0.8079 | 0.8079 |
| Vessel capital cost ($10^6$ \$) | 0.2487 | 0.2486 | 0.2486 |
| HX capital cost ($10^6$ \$) | 0.1284 | 0.1284 | 0.1285 |
| Energy cost ($10^6$ \$/yr) | 0.1486 | 0.1407 | 0.1407 |
| Total capital ($10^6$ \$) | 1.5938 | 1.6082 | 1.6455 |
| Total energy cost ($10^6$ \$/yr) | 0.8320 | 0.80752 | 0.8025 |
| TAC ($10^6$ \$/yr) | 1.3633 | **1.3436** | 1.3510 |

## 12.6 OPTIMUM DISTILLATION COLUMN DESIGN

There are two aspects to finding the optimum design of a distillation column. The first is the optimum operating pressure. The second is the optimum number of stages and feed-stage location.

### 12.6.1 Column Pressures

***Column C1.*** The distillate is high-purity, low-boiling DME with a normal boiling point of 248.2 K. Operating at atmospheric pressure would require expensive refrigeration in the condenser. So, the operating pressure is set at 10 atm, which gives a reflux-drum temperature of 318 K and permits the use of cooling water. The resulting reboiler temperature is high (509 K), which requires the use of high-pressure steam.

Since the condenser duty is very small (only 4.4 kW) compared to the reboiler duty, there is the possibility that running the column at a lower pressure might be economical. This would require expensive refrigeration in the condenser, but reboiler duty would be reduced because of the lower sensible heat required due to the smaller difference between the feed temperature and the base temperature. This alternative was briefly explored assuming operation at 4 atm. The resulting reflux-drum temperature of 285 K would require 253 K refrigerant at \$7.89/GJ. The base temperature drops from 509 to 457 K, which still requires high-pressure steam. But the reboiler duty decreases from 1.438 to 1.315 MW. The cost of 4.4 kW of refrigeration is only \$1100/yr. The savings in reboiler cost is about \$38,000/yr. This alternative design was not considered in the economic analysis, since this chapter is a comparative study in which this option would have essentially the same effect on all designs.

***Column C2.*** The distillate is mostly MH, with a small amount of methanol. The normal boiling point of MH is 392.2 K, so operation at vacuum conditions is possible, if it is advantageous. Operating at 0.6 atm gives a base temperature of 420 K, which requires *medium-pressure* steam (457 K at \$8.22/GJ). The reboiler energy at 0.6 atm is 0.9793 MW. The diameter of the column is 1.929 m.

Running at 0.4 atm reduces the base temperature to 410 K, which permits the use of *low-pressure* steam (433 K at \$7.78/GJ). In addition, the reboiler energy requirement drops to 0.9147 MW. However, the diameter of the column increases to 2.044 m because of the lower vapor density at the lower pressure. The upper part of Table 12.4 gives results over a range of pressures for column C2. Operation at 0.4 atm gives the smallest TAC.

***Column C3 Pressure.*** The distillate is mostly MMH, which has a normal boiling point of 424.4 K. The lower part of Table 12.4 gives results over a range of pressures for column C3. As pressure is lowered, reboiler energy decreases but column diameter and capital increase. Medium-pressure steam can be used when operating at the lower pressures.

A minimum practical operating pressure is assumed to be 0.1 atm in the reflux drum. Operation at this pressure gives the smallest TAC.

### 12.6.2 Number of Stages

The number of stages sets the column height and directly impacts the capital cost of the vessel. The typical effect of adding more trays is to reduce energy costs and capital investment in heat exchangers. Each of the columns is examined below. It should be noted that the

**TABLE 12.4 Effect of Operating Pressure**

| Column C2 Pressure | 0.2 | 0.3 | 0.4 | 0.5 | 0.6 |
|---|---|---|---|---|---|
| $Q_R$ (MW) | 0.8432 | 0.8799 | 0.9147 | 0.9475 | 0.9793 |
| $T_R$ (K) | 399 | 405 | 410 | 416 | 420 |
| $Q_C$ (MW) | 2.655 | 2.599 | 2.558 | 2.527 | 2.527 |
| $T_C$ (K) | 339 | 350 | 358 | 365 | 365 |
| Diameter (m) | 2.484 | 2.217 | 2.044 | 1.929 | 1.929 |
| Capital ($10^6$ \$) | 0.9818 | 0.851 | 0.7792 | 0.7336 | 0.7066 |
| Energy ($10^6$ \$/yr) | 0.2069 | 0.2159 | 0.2244 | 0.2456 | 0.2539 |
| | (LP) | (LP) | (LP) | (MP) | (MP) |
| TAC ($10^6$ \$/yr) | 0.5342 | 0.4995 | **0.4842** | 0.4982 | 0.4894 |
| Column C3 Pressure | 0.1 | 0.2 | 0.5 | | |
| $Q_R$ (MW) | 0.5195 | 0.6281 | 0.8421 | | |
| $T_R$ (K) | 426 | 436 | 456 | | |
| $Q_C$ (MW) | 0.8113 | 0.8378 | 0.9193 | | |
| $T_C$ (K) | 352 | 371 | 400 | | |
| Diameter (m) | 1.593 | 1.361 | 1.152 | | |
| Capital ($10^6$ \$) | 0.3764 | 0.3296 | 0.2995 | | |
| Energy ($10^6$ \$/yr) | 0.1347 | 0.1628 | 0.2624 | | |
| | (MP) | (MP) | (HP) | | |
| TAC ($10^6$ \$/yr) | **0.2601** | 0.2727 | 0.3622 | | |

variation of the economic objective function (TAC) with total stages is usually quite modest. Therefore, a rigorous determination of precisely the optimum number of stages, narrowing it down to a precision of a single stage, is unnecessary.

***Column C1.*** This column is quite unusual in many respects. The distillate is a very small stream of the DME impurity that is generated in the reactor. With a 99% yield of MMH, the distillate is only 0.5168 kmol/h out of a feed to the column of 130.0 kmol/h. Despite this small distillate flowrate, only a very low RR (0.8) is required to achieve the 0.1 mol% methanol impurity in the distillate because of the large difference in boiling points. This results in a very small condenser duty (0.004 MW). However, the reboiler duty is not negligible (1.438 MW) because the feed is at 400 K while the bottoms stream leaves at 507 K.

Easy separation also means few trays are required. The fewer the trays, the lower the base pressure and, consequently, the lower the base temperature. So, in this atypical column, fewer trays actually reduces reboiler duty and column diameter. Table 12.5 gives results for several total number of stages. A practical limit of at least 10 trays is assumed.

**TABLE 12.5 Distillation Column C1 Design**

| $N_T$ | 12 | 17 | 22 |
|---|---|---|---|
| $N_{Fopt}$ | 9 | 14 | 19 |
| ID (m) | 0.9651 | 0.9684 | 0.9699 |
| $Q_R$ (MW) | 1.411 | 1.415 | 1.418 |
| $Q_C$ (MW) | 0.004 | 0.004 | 0.004 |

$P = 10$ atm.

**TABLE 12.6 Distillation Column C2 Design**

| | | | |
|---|---|---|---|
| $N_T$ | 32 | 42 | 52 |
| $N_{Fopt}$ | 17 | 23 | 25 |
| ID (m) | 2.105 | 2.044 | 2.015 |
| $Q_R$ (MW) | 1.039 | 0.9147 | 0.8645 |
| $Q_C$ (MW) | 2.701 | 2.558 | 2.491 |
| Capital costs ($10^6$ \$) | 0.6759 | 0.7667 | 0.8695 |
| Energy cost ($10^6$ \$/yr) | 0.2549 | 0.2244 | 0.2121 |
| TAC ($10^6$ \$/yr) | 0.4802 | **0.4800** | 0.5019 |

$P = 0.4$ atm.

Therefore, a 12-stage column is selected, since it gives the smallest reboiler duty and the smallest capital investment (smallest diameter and smallest height).

***Column C2.*** This column gives typical results. The more trays used, the lower the energy consumption, but the higher the capital cost. Table 12.6 gives results that indicate a 42-stage column is the economic optimum in terms of TAC. The operating pressure is 0.4 atm.

***Column C3.*** Table 12.7 gives results for column C3 operating at 0.1 atm. Energy decreases as more trays are added, but capital investment increases. The 22-stage column is the economic optimum in terms of TAC.

### 12.6.3 Column Profiles

The temperature and composition profiles for all three columns are given in Figures 12.7 through 12.9. Notice that Figure 12.7a shows a very large temperature change in column C1 (318 to 509 K) because of the large difference in boiling points. This implies that "average temperature" control may be required to reduce the process gain and avoid saturation of the temperature signal.

Figure 12.8a shows that there are two breaks in the temperature profile, so it may be possible to use dual-temperature control if this structure is required. Figure 12.9a shows that there is only one break in the temperature profile in column C3, so only single-end temperature control is possible in this column, which provides the final separation between the product (MMH) and one of the by-products (MHOH).

**TABLE 12.7 Distillation Column C3 Design**

| | | | |
|---|---|---|---|
| $N_T$ | 17 | 22 | 27 |
| $N_{Fopt}$ | 6 | 9 | 12 |
| ID (m) | 1.647 | 1.593 | 1.580 |
| $Q_R$ (MW) | 0.5751 | 0.5195 | 0.5138 |
| $Q_C$ (MW) | 0.8672 | 0.8113 | 0.8056 |
| Capital costs ($10^6$ \$) | 0.3393 | 0.3764 | 0.4219 |
| Energy cost ($10^6$ \$/yr) | 0.1491 | 0.1347 | 0.1332 |
| TAC ($10^6$ \$/yr) | 0.2622 | **0.2601** | 0.2738 |

$P = 0.1$ atm.

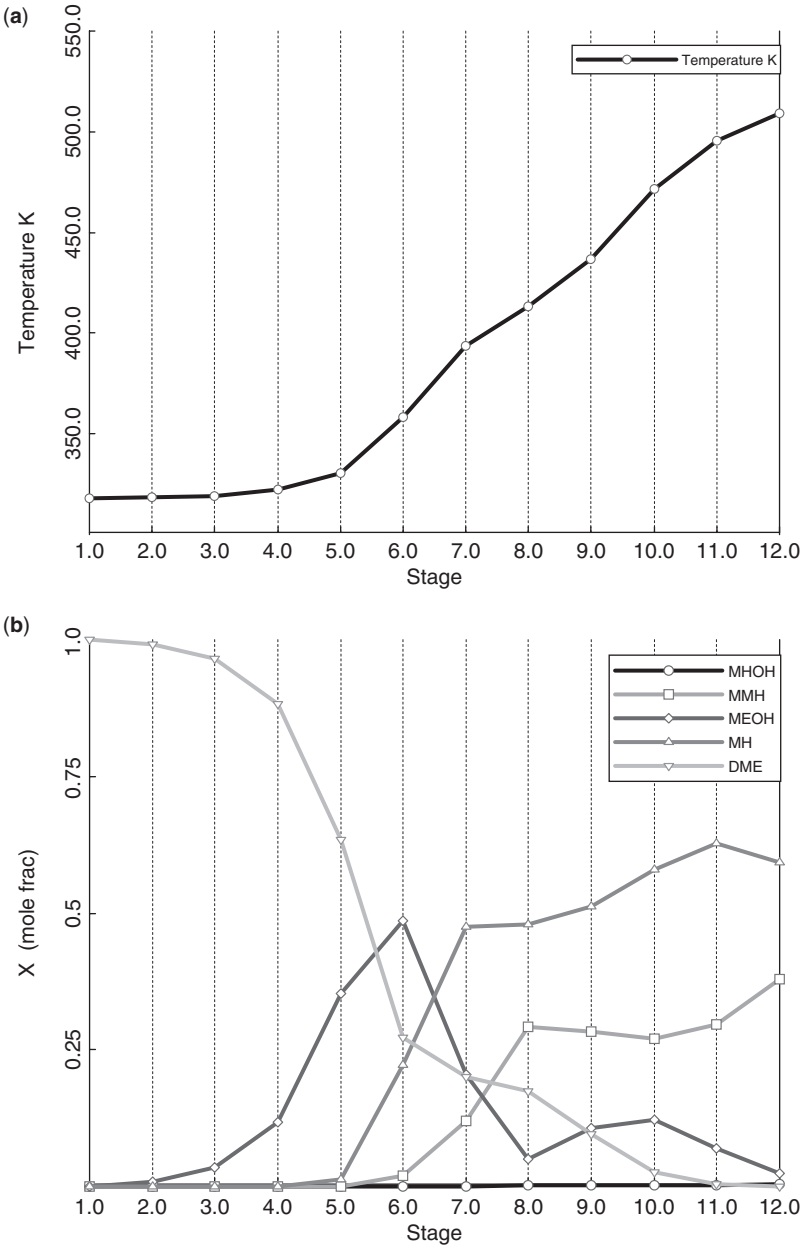


**Figure 12.7.** C1 (a) temperature profile, and (b) composition profiles.

## 12.7 PLANTWIDE CONTROL

In this section, a plantwide control structure is developed for the MMH process. Before the steady-state Aspen Plus simulation can be exported into Aspen Dynamics, the reflux drums and column bases in the three distillation columns are sized to provide 5 min of liquid holdup at 50% level. Pumps and control valves are placed on the flowsheet for achieving a realistic

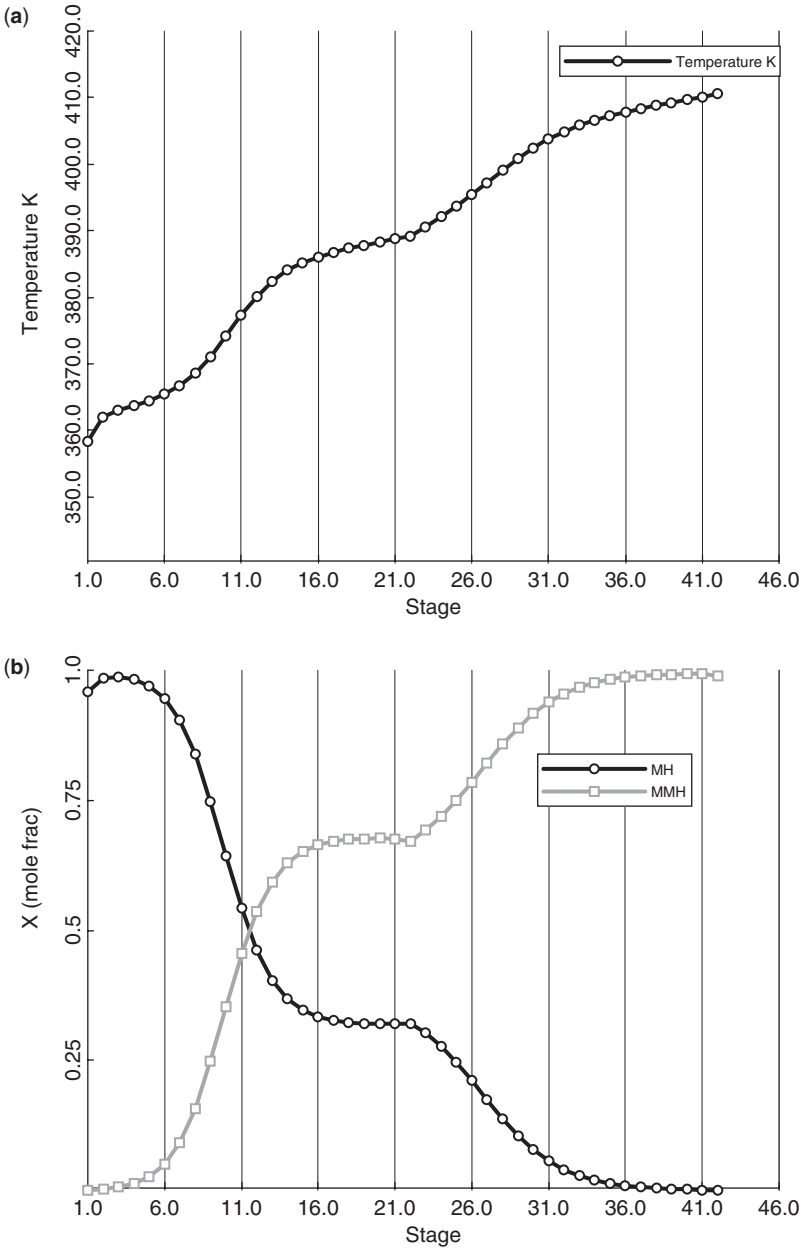


**Figure 12.8.** C2 (a) temperature profile, and (b) composition profiles.

pressure-driven dynamic simulation. Design pressure drops over control valves are set at 2 to 4 atm to provide the necessary rangeability for handling large disturbances without valve saturation.

The dynamic heat-transfer option selected in the reactor is *Dynamic*. This model assumes a perfectly mixed cooling jacket surrounding the reactor. The jacket heat-transfer area is 25.1 $m^2$. With an overall heat-transfer coefficient of 0.57 kW $m^{-2}$ $K^{-1}$ and a heat duty

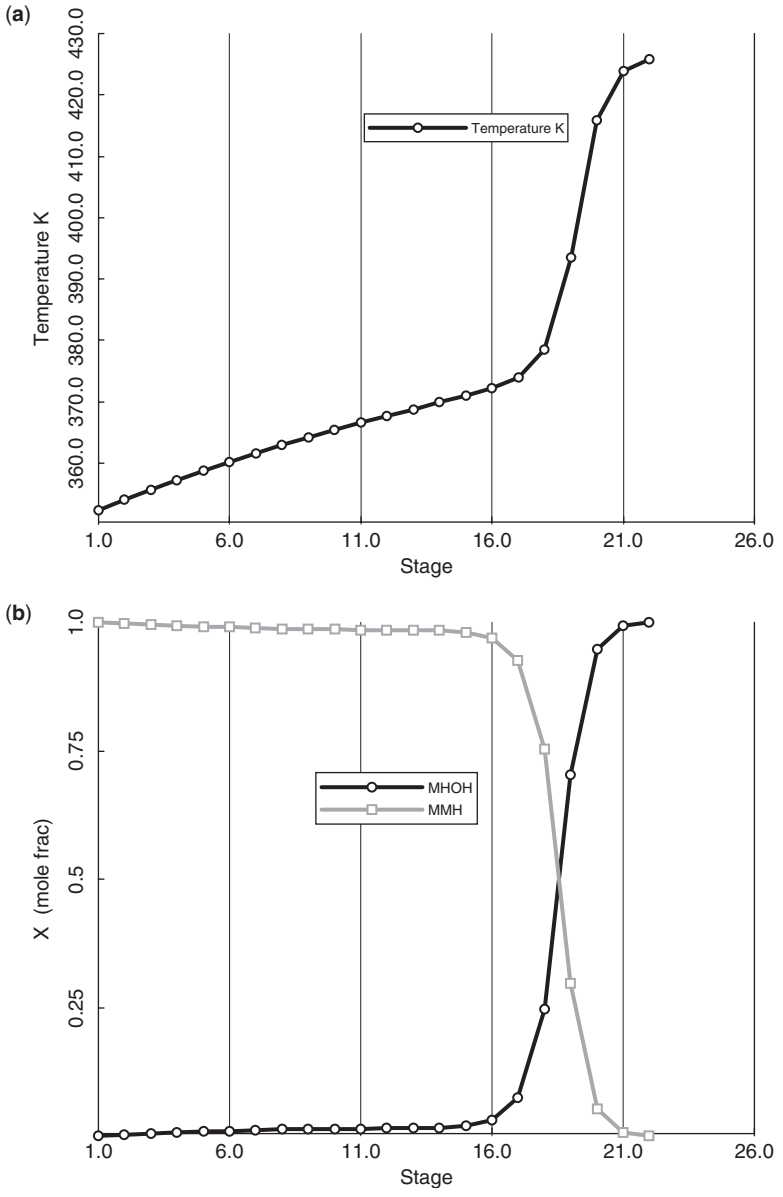


**Figure 12.9.** C3 (a) temperature profile, and (b) composition profiles.

of 0.426 MW, the jacket temperature is 380 K. The flowrate of cooling water is 12,175 kg/h, with an inlet temperature of 350 K.

### 12.7.1 Control Structure

Figure 12.10 shows the plantwide control structure developed for this process. Conventional PI controllers are used in all loops. All level loops are proportional with $K_C = 2$, except for

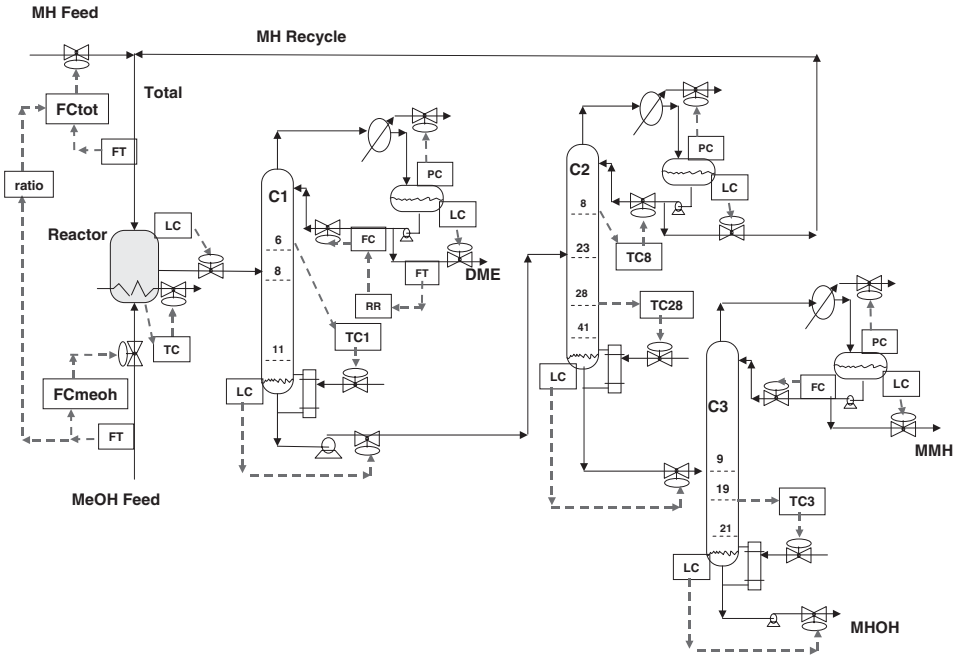


**Figure 12.10.** Plantwide control structure.

the reactor level controller that uses a gain of 5. The column tray temperature controllers and the reactor temperature controller have 1-min deadtimes. These temperature controllers are tuned by using relay-feedback tests to obtain ultimate gains and periods and then applying Tyreus–Luyben tuning rules.

All of the loops are listed below with their controlled and manipulated variables.

1. The fresh feed of methanol is flow-controlled. Since the per-pass conversion of methanol is very high, this fresh feed can be flow-controlled into the process.
2. The fresh feed of MH is manipulated to control the total flow of MH into the reactor. The setpoint of this flow controller is ratioed to the fresh methanol.
3. Reactor liquid level is controlled by manipulating reactor effluent.
4. Reactor temperature is controlled by manipulating the flowrate of the cooling medium to the jacket.
5. Pressures in all three columns are controlled by manipulating condenser heat removal.
6. The base levels in all three columns are controlled by manipulating bottoms flowrates.
7. The reflux-drum levels in all three columns are controlled by manipulating distillate flowrates.
8. In column C1, the RR is maintained by manipulating reflux flowrate based on the distillate flowrate.
9. Stage 6 temperature in column C1 is controlled by manipulating reboiler heat input.

**TABLE 12.8 Controller Parameters**

| | TCR | TC1 | TC8 | TC28 | TC3 |
|---|---|---|---|---|---|
| Controlled variable | Reactor temperature | Stage 6 temperature in column C1 | Stage 8 temperature in column C2 | Stage 28 temperature in column C2 | Stage 19 temperature in column C3 |
| Manipulated variable | Coolant flowrate | Reboiler heat input | Reflux flowrate | Reboiler heat input | Reboiler heat input |
| SP | 400 K | 354.4 K | 368.6 K | 400 K | 397.1 K |
| Transmitter range | 350–450 K | 300–400 K | 300–400 K | 350–450 K | 350–450 K |
| OP | 12,175 kg/h | 357 Kcal/s | 19,34 kg/h | 225.5 Kcal/s | 129.3 Kcal/s |
| OP range | 0–36,525 kg/h | 0–686 kcal/s | 0–50,000 kg/h | 0–437 kcal/s | 0–258.4 kcal/s |
| Deadtime | 1 min | 1 min | 1 min | 1 min | 1 min |
| $K_C$ | 16 | 0.43 | 2.1 | 6.0 | 0.55 |
| $\tau_I$ | 25 min | 30 min | 17 min | 13 min | 24 min |

10. Dual-temperature control is used in column C2. Stage 8 temperature is controlled by manipulating reflux flowrate. Stage 28 temperature is controlled by manipulating reboiler heat input.
11. In column 3, reflux is flow-controlled and the temperature on stage 19 is controlled by manipulating reboiler heat input.

Table 12.8 gives controller parameters for all the temperature controllers.

### 12.7.2 Dynamic Performance Results

Several large disturbances are made to test the ability of the proposed plantwide control structure. Figure 12.11 gives responses of the system to a 20% *increase* in the setpoint of the methanol flow controller at time equal 0.2 h. Stable base-level regulatory control is achieved. The setpoint of the total MH recycle controller is increased by the ratio multiplier. The flowrate of fresh MH undergoes a large transient increase before leveling out at about 60 kmol/h. More MMH product (D3) is produced as well as slightly more DME by-product (D1). MHOH by-product (B3) shows little change. The purity of the MMH product ($x$D3) is maintained quite close to its specification. The purities of the by-product streams ($x$D1 and $x$B3) change very little. All temperatures are well controlled. All reboiler heat duties increase as expected. The flowrate of reflux in column C2 and the flowrate of cooling water to the reactor jacket also increase.

Figure 12.12 gives results for a 20% *decrease* in fresh methanol flowrate. Similar results are obtained for this large disturbance.

Figure 12.13 shows the effect of decreasing reactor temperature. The fresh feed of methanol remains at 50 kmol/h, but the lower reaction rates produce a decrease in the fresh feed of MMH. The production of the undesirable by-products (D1 and B3) increase. There is little change in the production of the desired product (D3). These results illustrate the sensitivity of the yield to reactor temperature.

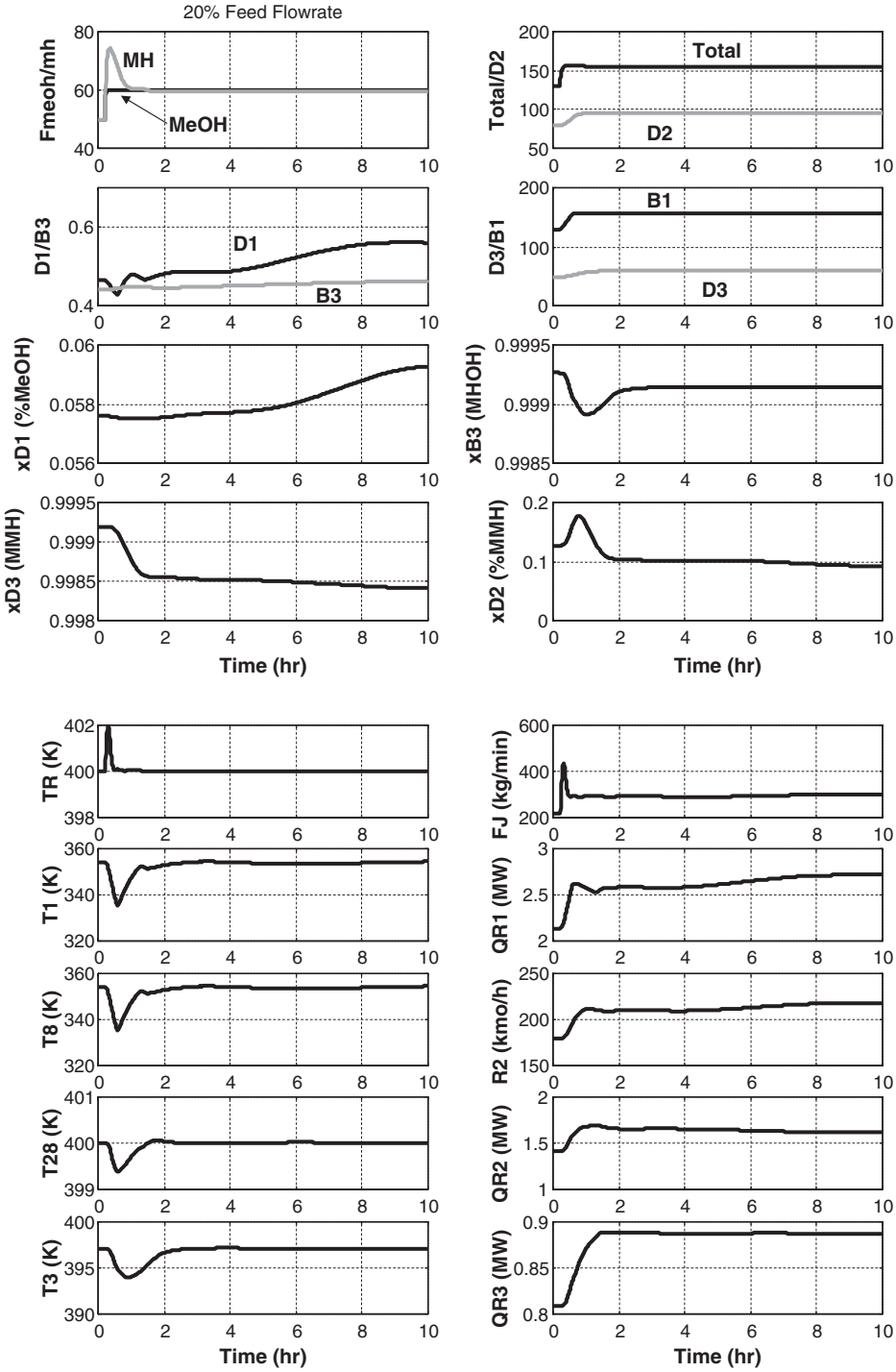


**Figure 12.11.** 20% increase in MeOH flowrate.

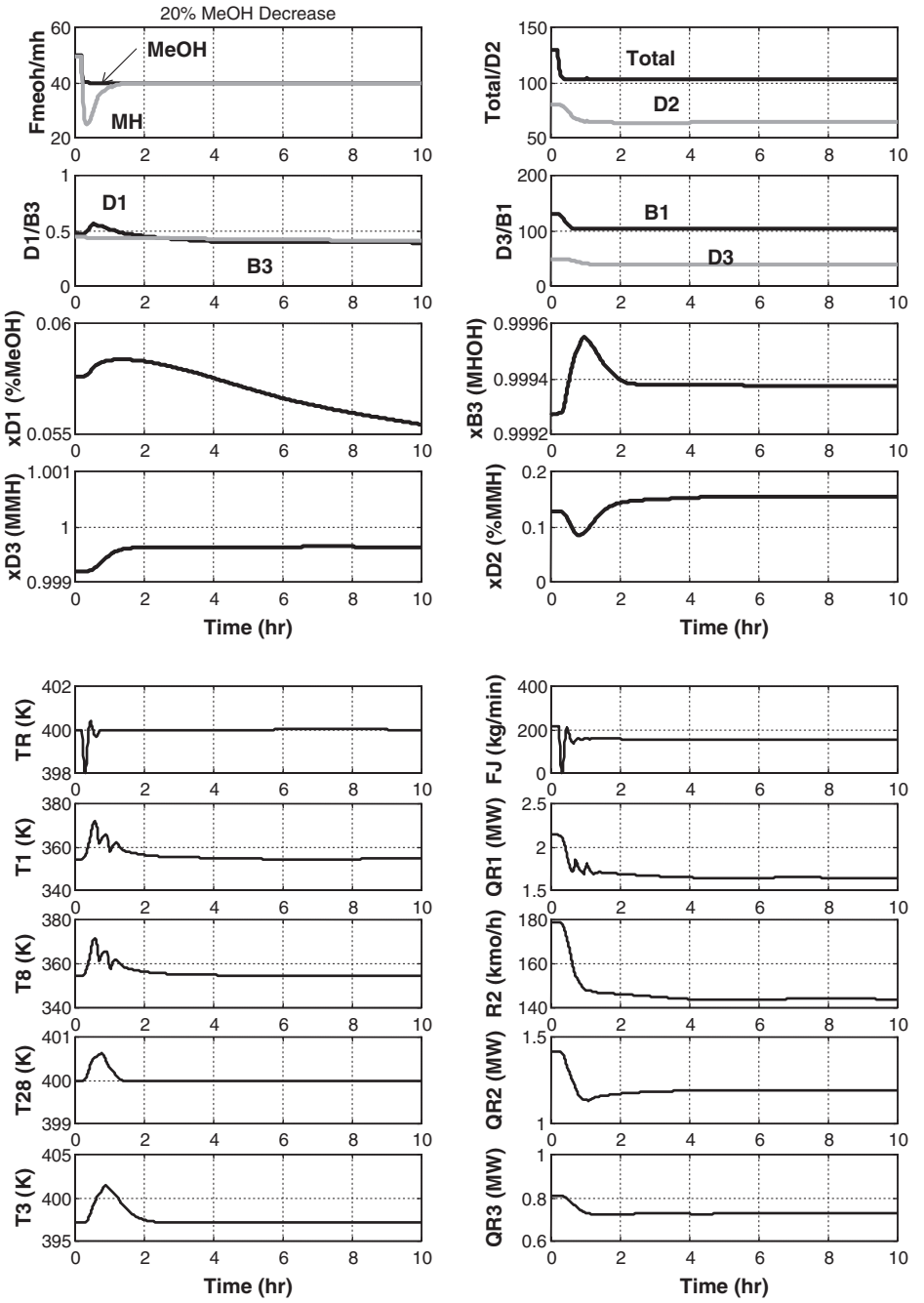


**Figure 12.12.** 20% decrease in MeOH flowrate.

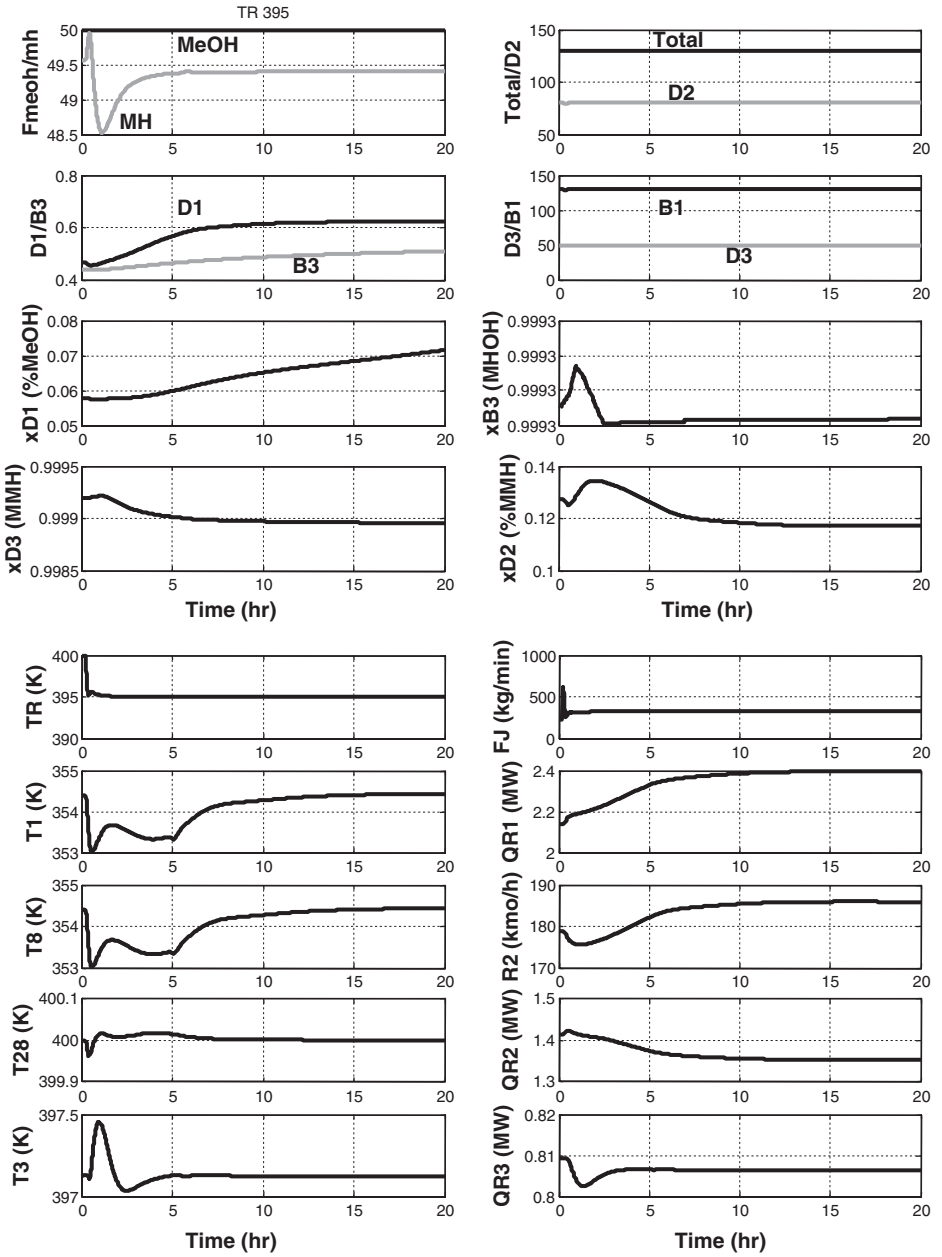


**Figure 12.13.** Reactor temperature 395 K.

## 12.8 CONCLUSION

The MMH process provides an interesting example of the classical trade-off between reactor size and recycle. The balancing of the costs and performance of the reaction section of the process with the costs and performance of the separation section of the process is the key feature in the optimum economic design.

The plantwide control structure provides effective base-level regulatory control of the process using simple PI controllers. Composition controllers are not required in the columns, since temperature controllers provide adequate product-quality control.

## REFERENCES

1. Griffin, D. W., Mellichamp, D. A., Doherty, M. F. Effect of competing reversible reactions on optimal operating policies for plants with recycle, *Ind. Eng. Chem. Res.* 2009, **48**, 8037–8047.
2. Douglas, J. M. *Conceptual Design of Chemical Processes*, McGraw-Hill, New York, 1988.
3. Turton, R., Bailie, R. C., Whiting, W. B., Shaelwitz, J. A. *Analysis, Synthesis and Design of Chemical Processes*, 2nd Edition, Prentice Hall, Englewood Cliffs, NJ, 2003.

# CHAPTER 13

# DESIGN AND CONTROL OF A METHYL ACETATE PROCESS USING CARBONYLATION OF DIMETHYL ETHER

The production of methyl acetate from the raw materials of methanol and carbon monoxide (CO) offers a potentially attractive alternative to other routes. The process has two distinct reaction and separation steps. First, methanol is dehydrated to form dimethyl ether (DME). Then, CO is combined with DME to produce methyl acetate. Each section involves reactors and distillation columns with either liquid or gas recycle.

In this chapter, we develop the economically optimum design of the two-step process and study its dynamic control. The economics consider capital costs (reactors, distillation columns, heat exchangers, and compressors), energy costs (compressor work, reboiler heat input, and condenser refrigeration), the value of steam produced from the exothermic reactions, the cost of the CO, and the heating value of a vent stream that is necessary for purging off the inert hydrogen that enters in the fresh CO feed. The process illustrates a number of important design trade-offs among the many design optimization variables: reactor temperatures, reactor pressures, distillation column pressures, reactor sizes, and purge composition. A plantwide control structure that is capable of effectively handling large disturbances in production rate and fresh feed compositions is developed for the entire two-section process.

## 13.1 INTRODUCTION

Methyl acetate is a commodity chemical with many uses. There are several processes used for its production. Methyl acetate is conventionally made by esterification of acetic acid with methanol over an acid catalyst. However, there is an alternate route in which methanol is first dehydrated to DME and then carbonylated directly to methyl acetate. For a plant with CO available on site, this may be a viable option. Recent advances in carbonylation catalysis promise improved economics for this approach.

*Principles and Case Studies of Simultaneous Design*, First Edition. William L. Luyben

This chapter explores an alternative route that consists of two reaction steps: dehydration of methanol to form DME, followed by carbonylation with CO to form methyl acetate.

In the following sections we develop reasonable conceptual designs of these two sections of the plant. Then plantwide dynamic control of the entire process is considered.

## 13.2 DEHYDRATION SECTION

The dehydration reaction of methanol to form DME and water can be conducted in either the vapor or liquid phases. The kinetics used in this chapter are discussed in detail in Section 13.2.2. A vapor-phase tubular reactor is used. The reaction is exothermic.

There are many alternative reactor configurations. We consider three possible flowsheets:

1. One adiabatic reactor
2. Two adiabatic reactors with intermediate cooling
3. Cooled reactor

The most economically attractive of these three is shown in Section 13.2.4 to be the cooled reactor.

### 13.2.1 Process Description of Dehydration Section

Figure 13.1 shows equipment and stream details of the optimum cooled reactor process. Fresh methanol is fed to a vaporizer at 500 kmol/h. The composition of the fresh feed is

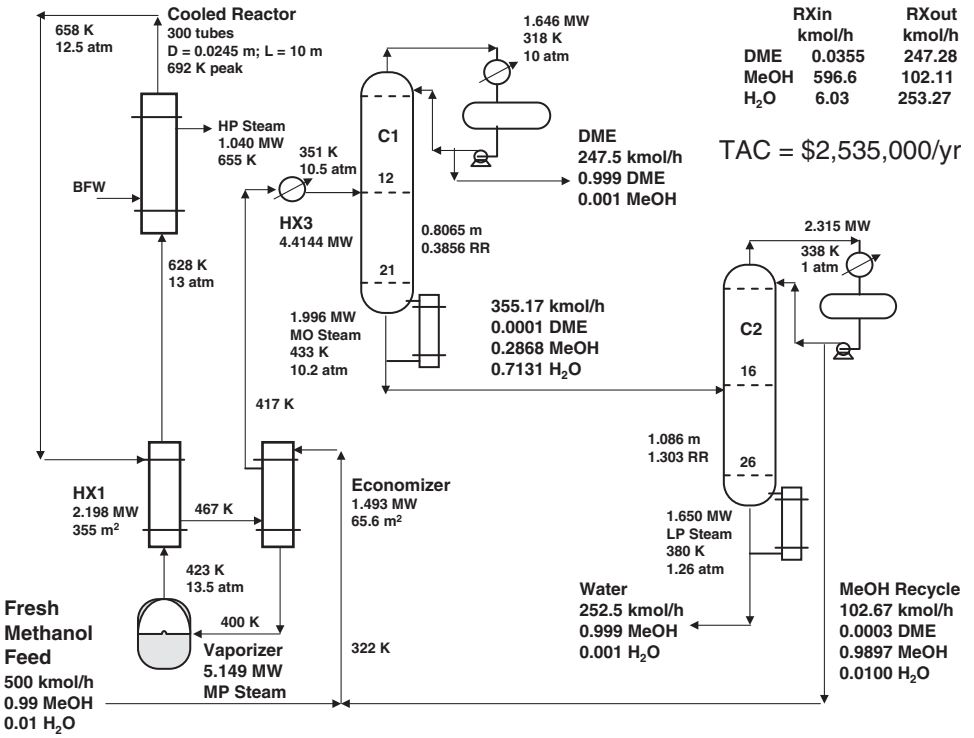


**Figure 13.1.** Dehydration flowsheet for a cooled reactor (300 tubes).

99 mol% methanol and 1 mol% water. A recycle stream of methanol at 102.7 kmol/h is also fed to the vaporizer, which operates at 13.5 atm. This pressure is set by the downstream distillation column pressure of 10 atm, which is determined by the vapor pressure of DME at 318 K so that cooling water can be used in the condenser. The vaporizer temperature is 423 K, which requires medium-pressure steam (11 atm, 457 K). Vaporizer energy consumption is 5.149 MW.

The vapor stream is preheated in a feed-effluent heat exchanger (FEHE) to 628 K before entering the cooled tubular reactor. The reactor has 300 tubes (0.0245 m diameter and 10 m length). The Aspen heat-transfer model with *Constant medium temperature* is used for this cooled tubular reactor. The optimum medium temperature is 665 K, so high-pressure steam is generated (42 atm).

The exothermic heat of reaction is used to generate high-pressure steam on the shell side of the reactor, which provides a credit for the economics of the process at \$9.88/GJ. An overall heat-transfer coefficient of 0.28 kW $K^{-1}$ $m^{-2}$ is used. The per-pass conversion of methanol is 82.9%. The catalyst has a density of 2500 kg/$m^3$, with a void fraction of 0.4. The catalyst price is \$50/kg.

The hot reactor effluent leaves at 658 K and is fed to the FEHE to preheat the reactor feed. The FEHE transfers 2.198 MW and cools the vapor stream to 467 K. An overall heat-transfer coefficient of 0.17 kW $K^{-1}$ $m^{-2}$ is assumed. The stream is cooled further in a heat exchanger (economizer) that preheats the fresh and recycle methanol streams to 400 K (overall heat-transfer coefficient = 0.28 kW $K^{-1}$ $m^{-2}$). The stream then enters a water-cooled heat exchanger that cools it to 351 K before it enters the first distillation column (overall heat-transfer coefficient = 0.85 kW $K^{-1}$ $m^{-2}$).

Column C1 has 22 stages and is fed on stage 12. We use the Aspen terminology in which stage 1 is the condenser. The separation is an easy one, so few trays are required and the reflux ratio (RR) is only 0.38. Reboiler duty is 1.996 MW using medium-pressure steam, since the base temperature is 433 K. The distillate product is 99.9 mol% DME with 0.1 mol% methanol. This liquid distillate stream is pumped up to the pressure required in the carbonylation section of the plant. The bottoms stream is a mixture of methanol and water, which is fed to column C2 for separation.

Column C2 produces a high-purity methanol distillate (98.97 mol% methanol, 0.03 mol% DME and 1 mol% water), which is recycled back to the vaporizer. The bottoms is high-purity water (99.9 mol%). The column operates at 1 atm, using cooling water in the condenser and low-pressure steam in the reboiler (1.65 MW).

### 13.2.2 Dehydration Kinetics

The chemistry of the dehydration of methanol produces DME and water in a vapor-phase reaction.

$$2CH_3OH \Longleftrightarrow CH_3OCH_3 + H_2O \tag{13.1}$$

The reaction is exothermic, so the chemical equilibrium constant decreases with increasing temperature. Low-temperature operation can produce high conversion, but a large reactor will be required because the specific reaction rates are small. Thus, there is a classical trade-off between reactor size and recycle in this kinetic system.

The forward reaction rate was taken from a rate expression found in a design project on the West Virginia University Chemical Engineering Department's website.[1] This project write-up cites Bandiera and Naccache,[2] who measured methanol dehydration rates over

dealuminated H-mordenite catalyst at temperatures ranging from 473 to 573 K. Under these conditions, Bandiera and Naccache found the rate to be first-order in methanol partial pressure. They also found evidence of product inhibition, which they interpreted as DME adsorption, and the rate constant in the WVU write-up corresponds to inhibition at an average DME mole fraction of 0.055 given their reactor pressure of 16.8 atm and an assumed catalyst bulk density of approximately 1000 $kg/m^3$. At our reactor pressures of 10–13 atm, this corresponds to an average DME mole fraction of 0.070–0.095, which is realistic if not exact.

In this work, the WVU rate expression (having units per unit bed volume) was converted back to a per-unit bed mass basis, assuming a bed bulk density of 1000 $kg/m^3$. The equilibrium constant for the reaction was estimated from known thermodynamic properties so that the final rate expression had the following form:

$$\begin{aligned} r_{\text{dehy}} &= k_{\text{dehy}}\left(p_{\text{MeOH}} - \frac{p_{\text{DME}}p_{\text{W}}}{p_{\text{MeOH}}K_{\text{dehy}}}\right) \\ r_{\text{dehy}} &= \text{MeOH dehydration rate, kmol/kg}_{\text{catalyst}}\text{/s} \\ k_{\text{dehy}} &= \text{dehydration rate constant, kmol/kg}_{\text{catalyst}}\text{/s/Pa} \\ K_{\text{dehy}} &= \text{dehydration equilibrium constant} \end{aligned} \tag{13.2}$$

with

$$\begin{aligned} \ln k_{\text{dehy}}(\text{kmol/kg}_{\text{catalyst}}\text{/s/Pa}) &= -8.00 - 9680/T \\ \ln K_{\text{dehy}} &= -2.8086 + 3061/T \end{aligned} \tag{13.3}$$

where $T$ = temperature, K.

Table 13.1 gives the kinetic and adsorption parameters entered into the Aspen LHHW reaction model to implement these kinetics.

### 13.2.3 Alternative Flowsheets

The flowsheet shown in Figure 13.1 is for a cooled reactor. Adiabatic reactors were also studied. The separation section is essentially the same in all flowsheets with small differences in reboiler duties for different methanol recycle flowrates.

***One Adiabatic Reactor.*** Figure 13.2 shows the effects of changing reactor size ($D_{\text{R}}$) and reactor inlet temperature ($T_{\text{in}}$) on the amount of methanol recycle required when one adiabatic reactor is used. A reactor aspect ratio of $L_{\text{R}}/D_{\text{R}} = 10$ is assumed, so a $D_{\text{R}} = 0.5$ corresponds to a reactor with diameter of 0.5 m and length of 5 m. For each reactor size, there is an optimum reactor inlet temperature that minimizes methanol recycle. This is equivalent to maximizing per-pass conversion of methanol. Larger reactors require less recycle because the lower temperatures produce larger chemical equilibrium constants.

Figure 13.3 shows the flowsheet using one adiabatic reactor. The economic optimum size vessel has a diameter of 0.7 m and a length of 7 m. The fresh and recycle methanol are preheated in an economizer and vaporized. The vapor stream is preheated to 570 K in a FEHE, and leaves the adiabatic reactor at 686 K. The per-pass conversion is 81.7%. The flowrate of recycle methanol is 111.4 kmol/h.

**TABLE 13.1 Kinetic LHHW Parameters**

*Dehydration* ($CH_3OH \rightarrow \frac{1}{2}CH3{-}O{-}CH3 + \frac{1}{2}H_2O$)
- Kinetic factor $k = 0.000336$
  $E = 80{,}480$ kJ/kmol
- *Driving-force expressions*
  - Term 1
    - Concentration exponents for reactants: $CH_3OH = 1$
    - Concentration exponents for products: DME = 0; $H_2O = 0$
    - Coefficients: A = 0; B = C = D = 0
  - Term 2
    - Concentration exponents for reactants: $CH_3OH = -1$
    - Concentration exponents for products: DME = 1; $H_2O = 1$
    - Coefficients: A = 2.8086; B = −3061; C = D = 0
- *Adsorption expression*
  - Adsorption term exponent = 1
  - Concentration exponents
    - Term 1: $H_2O = 0$
    - Term 2: $H_2O = 0$
  - Adsorption constants
    - Term 1: A = −0.61395; B = 0; C = 0, D = 0
    - Term 2: A = −0.61395; B = 0; C = 0, D = 0

*Carbonylation* ($CO + CH3{-}O{-}CH3 \rightarrow CH3{-}CO{-}O{-}CH3$)
- Kinetic factor $k = 1.7 \times 10^{-12}$
  $E = 1663$ cal/mol
  $T_o = 473.15$ K
- *Driving-force expressions*
  - Term 1
    - Concentration exponents for reactants: CO = 1; DME = 1
    - Concentration exponents for products: MeOAc = 0
    - Coefficients: A = B = C = D = 0
  - Term 2
    - Concentration exponents for reactants: CO = 0; DME = 0
    - Concentration exponents for products: MeOAc = 0
    - Coefficients: A = −20; B = C = D = 0
- *Adsorption expression*
  - Adsorption term exponent = 1
  - Concentration exponents
    - Term 1: DME = 0
    - Term 2: DME = 1
  - Adsorption constants
    - Term 1: A = B = C = D = 0
    - Term 2: A = B = C = D = 0

The hot reactor effluent goes to a steam generator that produces high-pressure steam (1.194 MW), which is an economic credit. The stream is then cooled in three heat exchangers in series before entering the first distillation column.

***Two Adiabatic Reactors.*** Figure 13.4 shows the flowsheet using two adiabatic reactors in series with intermediate cooling. The advantage of having two reactors with interstage

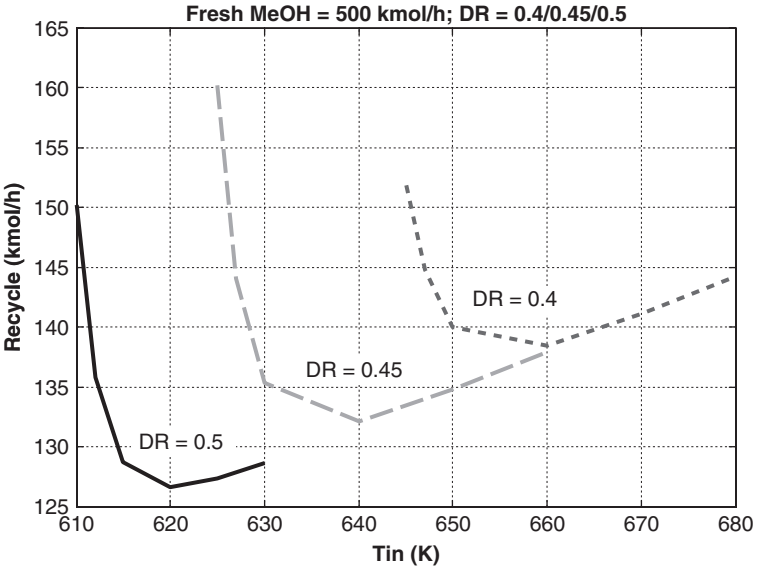


**Figure 13.2.** Effect of inlet temperature and reactor size dehydration: One adiabatic reactor.

cooling is that higher reactor inlet temperatures can be used to obtain faster kinetics, while at the same time having lower reactor exit temperatures, which give a higher chemical equilibrium constant. We assume that each reactor is the same size. The economic optimum size of each vessel is a diameter of 0.5 m and a length of 5 m.

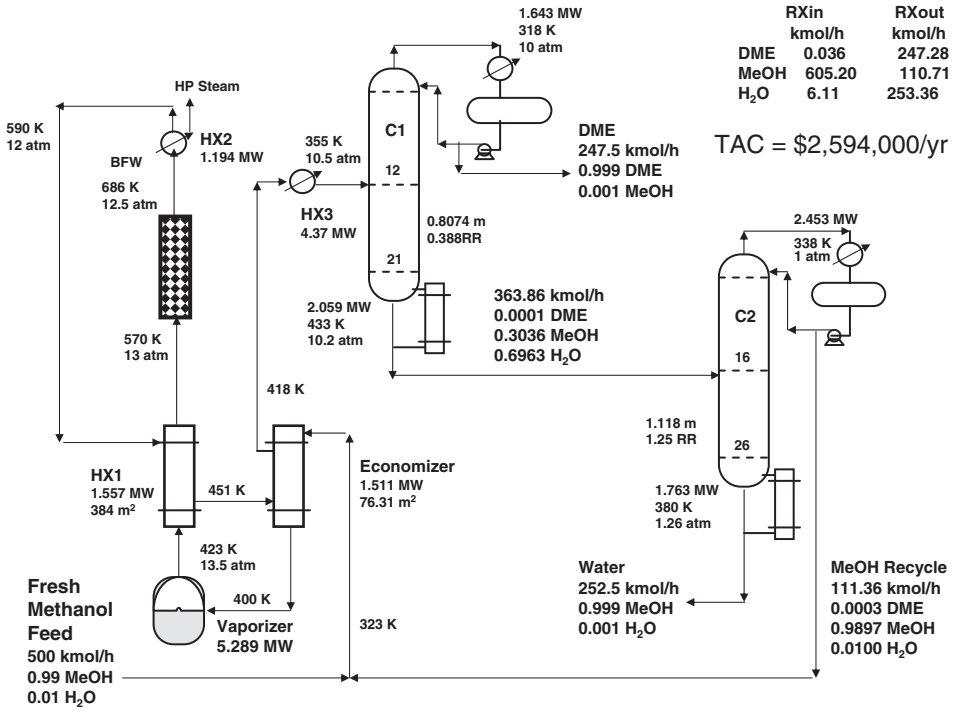


**Figure 13.3.** Dehydration; one adiabatic reactor (0.7 m × 7 m).

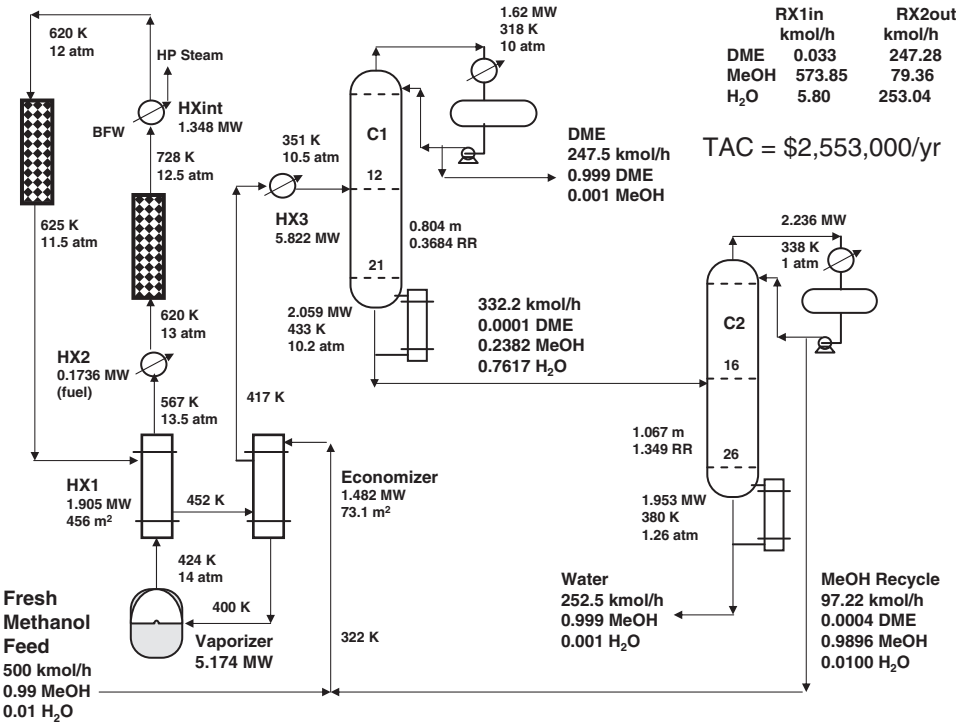


**Figure 13.4.** Dehydration; two adiabatic reactors (0.5 m × 5 m).

After the vaporizer and FEHE, a small fired heater is required to attain the 620 K inlet temperature to the first reactor. Notice that this is higher than the reactor inlet temperature in the one-adiabatic reactor flowsheet (570 K). The effluent from this reactor leaves at 728 K and is cooled to 620 K by generating high-pressure steam in an intermediate heat exchanger. The cooled stream is fed to the second reactor, in which a small additional conversion of methanol occurs, giving an exit temperature of only 625 K. The per-pass conversion through the two reactors is 86.2%. The flowrate of recycle methanol is 97.23 kmol/h, which should be compared to the methanol recycle flowrate of 111.4 kmol/h in the one-adiabatic flowsheet.

***Cooled Reactor.*** This flowsheet has been described in detail in Section 13.2.1 and is shown in Figure 13.1. Note that the reactor cooling medium temperature is 655 K, which gives a reactor exit temperature of 658 K (and a peak temperature of 692 K). This exit temperature is lower than those of the one-adiabatic reactor flowsheet (668 K) and the first reactor in the two-adiabatic reactor flowsheet (728 K), which gives a larger chemical equilibrium constant. The methanol recycle flowrate is 102.7 kmol/h, which is intermediate between the one-adiabatic and two-adiabatic flowsheet recycle flowrates.

Figure 13.5 compares the temperature profiles through the reactors in the three alternative flowsheets. The one-adiabatic reactor must have a low inlet temperature (570 K) and a large methanol recycle flowrate (111.36 kmol/h) in order to keep the reactor exit temperature from going too high (686 K).

In the two-adiabatic flowsheet, the inlet temperatures can be higher (620 K) than in the one-adiabatic flowsheet. The first reactor has a high exit temperature because of the high inlet temperature and because the methanol recycle flowrate is lower (97.23 kmol/h). But

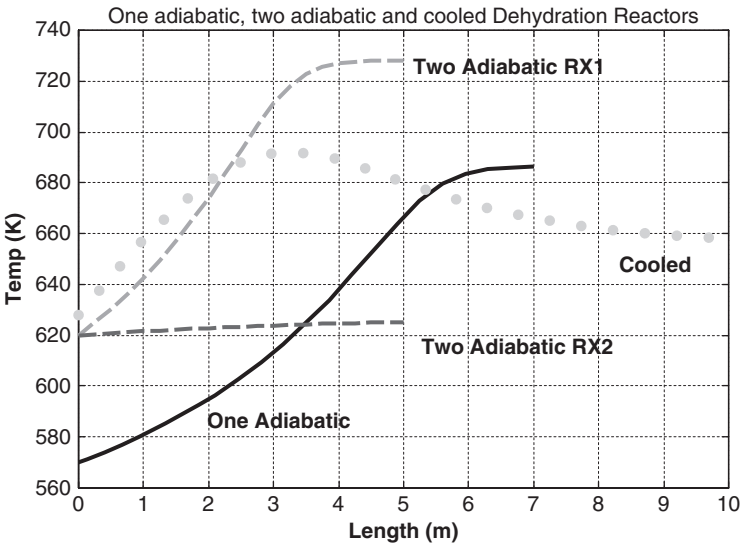


**Figure 13.5.** Dehydration; temperature profiles.

the low temperatures in the second reactor raise the chemical equilibrium constant and permit higher methanol conversion.

The cooled reactor with a 655 K cooling medium temperature has a peak temperature of 692 K at about 3 m down the reactor, as shown in the dotted curve in Figure 13.5. Conversion is not as high in the cooled reactor as in the two-adiabatic flowsheet because of the higher temperatures, so the recycle flowrate is higher (102.7 kmol/h). The economic analysis given in Section 13.2.4 shows that the cooled reactor flowsheet has the minimum total annual cost (TAC), primarily because less catalyst is needed.

### 13.2.4 Optimization of Three Flowsheets

The three flowsheets have similar but slightly different design optimization variables. Reactor size and reactor temperature are the dominant variables. The basis for cost and sizing calculations are given in Table 13.2. These parameters are taken from Douglas[3] and Turton et al.[4]

Total annual cost is the economic criterion used for choosing the optimum design. The cost of energy in the vaporizer and column reboilers is reduced by the credit for steam produced (in the heat exchanger after the reactor in the one-adiabatic flowsheet, in the intermediate heat exchanger in the two-adiabatic flowsheet, or in the reactor in the cooled reactor flowsheet). The annual cost of capital is the total capital investment divided by a 3-yr payback period. Capital investment includes the vaporizer, economizer, FEHE, reactor(s), partial condenser, column vessels, column condensers, and column reboilers.

***Single Adiabatic Reactor.*** For a single adiabatic reactor, the size of the reactor (represented by $D_R$) and the reactor inlet temperature are the dominant variables. The flowsheet is optimized by selecting a reactor size and finding the reactor inlet temperature that gives the minimum required methanol recycle flowrate. This minimizes vaporizer energy and

**TABLE 13.2 Basis of Economics and Equipment Sizing**

Column diameter: Aspen tray sizing
Column length: NT trays with 2 ft spacing plus 20% extra length
Columns, separator, and adiabatic reactor vessels (diameter and length in meters)
  Capital cost = $17{,}640(D)^{1.066}(L)^{0.803}$

*Condensers (area in $m^2$)*
  Heat-transfer coefficient = 0.852 kW/K-$m^2$
  Differential temperature: C1 and C2 = Reflux-drum temperature − 310 K
    C3 = 300 − 253 K
  Capital cost = $7296(A)^{0.65}$

*Reboiler (area in $m^2$)*
  Heat-transfer coefficient = 0.568 kW/K-$m^2$
  Differential temperature: C1 (MP steam) = 457 − base temperature
    C2 (LP steam) = 433 − base temperature
    C3 (LP steam) = 433 − base temperature
  Capital cost = $7296(A)^{0.65}$

*Economizer, feed-effluent, partial condenser, and vaporizer heat exchanger (area in $m^2$)*
  Capital cost = $7296(A)^{0.65}$
  Heat-transfer coefficients: Economizer = 0.28 kW $K^{-1}$ $m^{-2}$
    FEHE = 0.17 kW $K^{-1}$ $m^{-2}$
    Partial condenser = 0.852 kW $K^{-1}$ $m^{-2}$
    Vaporizer = 0.85 kW $K^{-1}$ $m^{-2}$

*Cooled reactor vessel (based on heat-transfer area of tubes)*
  Heat-transfer coefficient = 0.28 kW $K^{-1}$ $m^{-2}$
    Dehydration reactor: Cooling medium temperature = 655 K
    Carbonylation reactor: Cooling medium temperature = 460 K
  Capital cost = $7296(A)^{0.65}$

Catalyst cost = \$50/kg; density = 2500 kg/$m^3$; void fraction = 0.4

*Energy cost*
  LP steam = \$7.78/GJ
  MP steam = \$8.22/GJ
  HP steam = \$9.88/GJ
  Electricity = \$16.6/GJ

$$\text{TAC} = \frac{\text{Capital cost}}{\text{Payback period}} + \text{Energy cost}$$

Payback period = 3 yr

separation cost in column C2, in which the methanol is taken overhead and recycled. The TAC for each reactor size is evaluated and the minimum case is selected.

The TAC considers both energy and capital costs. The annual cost of the energy comes from the duties in the vaporizer and in the two column reboilers. There is an energy credit for the high-pressure steam generated in the heat exchanger after the reactor. Capital costs include the capital cost of the heat exchangers (vaporizer, FEHE, economizer, partial condenser, column condensers, and column reboilers) and distillation column vessels. The TAC is energy costs plus annual capital cost (total capital divided by a 3-yr payback period).

Table 13.3 gives economic results for a single adiabatic flowsheet for three different reactor sizes ($D_R$ = 0.6, 0.7, and 0.8 m). For each case, the reactor inlet temperature ($T_{in}$)

**TABLE 13.3 Optimum One-Adiabatic Reactor Flowsheet**

| | | | |
|---|---|---|---|
| $D_R$ (m) | 0.6 | 0.7 | 0.8 |
| $L_R$ (m) | 6 | 7 | 8 |
| $T_{in}$ (K) | 590 | 570 | 555 |
| Recycle $D_2$ (kmol/h) | 117.9 | 111.4 | 106.2 |
| $Q_{R2}$ (MW) | 1.849 | 1.763 | 1.696 |
| $Q_{vaporizer}$ (MW) | 5.345 | 5.289 | 5.244 |
| Steam value ($10^6$ \$/yr) | 0.3674 | 0.3720 | 0.3755 |
| Reactor vessel ($10^6$ \$) | 0.0659 | 0.0879 | 0.1128 |
| Catalyst ($10^6$ \$) | 0.2121 | 0.3367 | 0.5027 |
| C1 capital ($10^6$ \$) | 0.6172 | 0.6149 | 0.6131 |
| C2 capital ($10^6$ \$) | 0.5218 | 0.5085 | 0.4979 |
| Total capital ($10^6$ \$) | 1.756 | 1.886 | 2.063 |
| Energy cost ($10^6$ \$/yr) | 2.010 | 1.965 | 1.930 |
| TAC ($10^6$ \$/yr) | 2.596 | **2.594** | 2.618 |

that minimizes the flowrate of recycle is found. The optimum inlet temperature decreases as reactor size is increased. Recycle flowrates, vaporizer duty, and C2 reboiler duty decrease as reactor size increases.

Naturally, the capital cost of the reactor vessel and the catalyst increase directly with reactor size. The capital cost of column C1 changes very little, but the capital cost of column C2 decreases slightly with increasing reactor size.

Total capital cost increases, while total energy cost decreases, as the reactor is made larger. The net effect is a minimum TAC of \$2,594,000/yr for the one-adiabatic reactor flowsheet when a 0.7 m by 7 m reactor is used.

***Two Adiabatic Reactors.*** We assume that the reactors are of equal size, but the inlet temperatures can be different. A range of reactor inlet temperatures for the two reactors is explored for a specified reactor size. The values of the two inlet temperatures that minimize recycle flowrate are found. In all the cases considered, it turned out that the inlet temperatures are the same. Then, a different reactor size is specified, and the calculations are repeated. The reactor size and set of reactor inlet temperatures that give the minimum total annual cost is selected.

Table 13.4 gives economic results for the two-adiabatic flowsheet for three different reactor sizes ($D_R = 0.4, 0.5$ and 0.6 m). These are the dimensions of each of the two reactors. The optimum inlet temperatures decrease as reactor size is increased, as do recycle flowrates, vaporizer duty, and C2 reboiler duty. The capital cost of the two reactor vessels is somewhat higher than the capital cost of the larger single reactor in the one-adiabatic flowsheet. However, the cost of the catalyst is smaller, since the total reactor volume is smaller in the two vessels than in the single larger vessel. The capital cost of column C1 is about same in the two flowsheets, but the capital cost of column C2 is somewhat smaller in the two-adiabatic flowsheet because of the smaller recycle flowrate.

Total capital cost increases, while energy cost decreases, as the reactors are made larger. The net effect is a minimum TAC of \$2,553,000/yr for the two-adiabatic reactor flowsheet when two 0.5 m by 5 m reactors are used. Note that this is somewhat smaller than the TAC of the one-adiabatic flowsheet.

***Cooled Reactor.*** The cooled reactor vessel capital cost is based on its heat-transfer area. The optimum design has 300 tubes (diameter = 0.0245 m, length = 10 m). High-pressure

**TABLE 13.4 Optimum Two-Adiabatic Reactor Flowsheet**

| | | | |
|---|---|---|---|
| $D_R$ (m) | 0.4 | 0.5 | 0.6 |
| $L_R$ (m) | 4 | 5 | 6 |
| $T_{in}$ (K) | 650 | 620 | 575 |
| Recycle $D_2$ (kmol/h) | 107.1 | 97.23 | 106.2 |
| $Q_{R2}$ (MW) | 1.724 | 1.593 | 1.696 |
| $Q_{vaporizer}$ (MW) | 5.260 | 5.174 | 5.244 |
| Steam value ($10^6$ \$/yr) | 0.4153 | 0.4191 | 0.4191 |
| Two reactor vessels ($10^6$ \$) | 0.0618 | 0.0937 | 0.1318 |
| Catalyst ($10^6$ \$) | 0.1257 | 0.2454 | 0.4241 |
| C1 capital ($10^6$ \$) | 0.6153 | 0.6117 | 0.6091 |
| C2 capital ($10^6$ \$) | 0.5014 | 0.4803 | 0.4648 |
| Total capital ($10^6$ \$) | 1.709 | 1.842 | 2.044 |
| Energy cost ($10^6$ \$/yr) | 2.009 | 1.939 | 1.888 |
| TAC ($10^6$ \$/yr) | 2.579 | **2.553** | 2.569 |

steam is generated in the reactor and is an energy credit. The number of tubes is specified and the temperature of the cooling medium is varied to find the value that gives the minimum recycle flowrate.

Table 13.5 gives designs with different numbers of tubes. The optimum cooling medium temperature and the methanol recycle flowrate decrease as the number of tubes increases. The cost of the reactor vessel and the catalyst increase as more tubes are used. Notice that the cost of the vessel (\$256,800 for the tube-in-shell reactor) for the cooled reactor with the optimum 300 tubes is much larger than the two simple vessels in the two-adiabatic flowsheet (\$93,700). However, the catalyst cost is lower (\$190,000 vs. \$245,400), since the cooled reactor requires the smallest amount of catalyst.

Total capital cost increases and total energy cost decreases as more reactor tubes are used. The minimum TAC of \$2,535,000 occurs with 300 tubes. The cooled reactor flowsheet has the smallest TAC.

Figure 13.6 give direct comparisons among the three flowsheets, showing how methanol recycle, reactor temperatures, energy costs, and TAC vary with the total catalyst. The cooled

**TABLE 13.5 Optimum Cooled Reactor Flowsheet**

| | | | |
|---|---|---|---|
| Tubes | 200 | 300 | 400 |
| $L_R$ (m) | 10 | 10 | 10 |
| Tube ID (m) | 0.0245 | 0.0245 | 0.0245 |
| $T_{medium}$ (K) | 665 | 655 | 645 |
| Recycle $D_2$ (kmol/h) | 109.9 | 102.7 | 98.14 |
| $Q_{R2}$ (MW) | 1.745 | 1.650 | 1.592 |
| $Q_{vaporizer}$ (MW) | 5.276 | 5.214 | 5.174 |
| Steam value ($10^6$ \$/yr) | 0.3190 | 0.3240 | 0.3276 |
| Reactor vessel ($10^6$ \$) | 0.1973 | 0.2568 | 0.3095 |
| Catalyst ($10^6$ \$) | 0.1267 | 0.1900 | 0.2534 |
| C1 capital ($10^6$ \$) | 0.6137 | 0.6109 | 0.6092 |
| C2 capital ($10^6$ \$) | 0.5056 | 0.4905 | 0.4811 |
| Total capital ($10^6$ \$) | 1.651 | 1.754 | 1.858 |
| Energy cost ($10^6$ \$/yr) | 2.000 | 1.950 | 1.918 |
| TAC ($10^6$ \$/yr) | 2.550 | **2.535** | 2.538 |

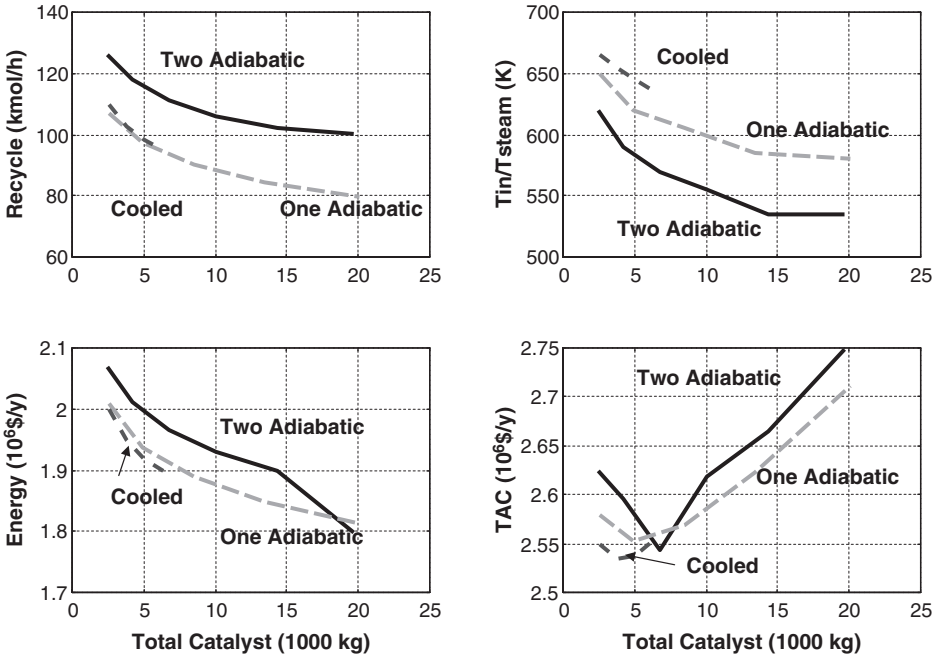


**Figure 13.6.** Alternative reactor designs.

reactor is selected for the dehydration section of the plant. Figure 13.7 shows the composition profiles down the length of the cooled reactor.

***Optimization of Distillation Columns.*** The two distillation columns in the dehydration section are optimized by finding the total number of trays in each column that

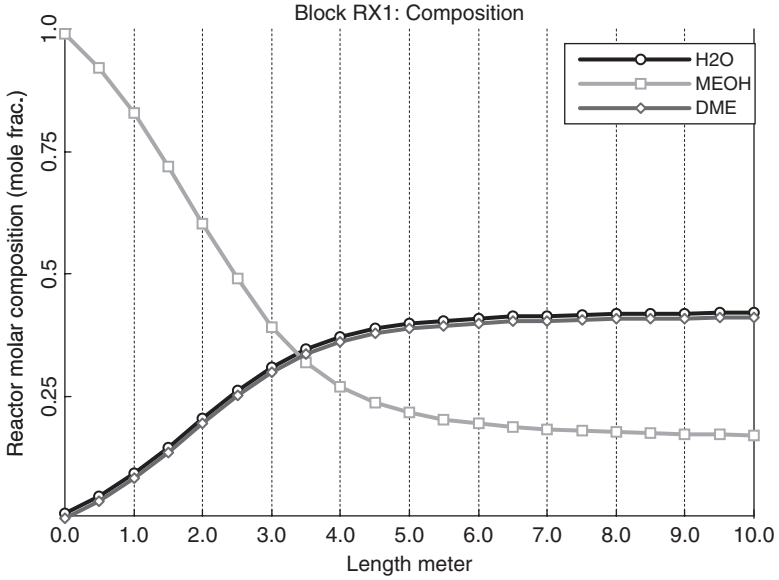


**Figure 13.7.** Cooled reactor (300 tubes): Composition profiles.

**TABLE 13.6 Optimum Column Designs**

| | | | |
|---|---|---|---|
| Column C1 | | | |
| NT | 17 | 22 | 27 |
| NF | 9 | 12 | 14 |
| $Q_R$ (MW) | 2.064 | 2.019 | 2.018 |
| ID (m) | 0.8095 | 0.7978 | 0.7984 |
| Total capital ($10^6$ \$) | 0.5782 | 0.6062 | 0.6418 |
| Total energy ($10^6$ \$/y) | 0.5350 | 0.5233 | 0.5232 |
| TAC ($10^6$ \$/y) | 0.7278 | **0.7254** | 0.7371 |
| Column C2 | | | |
| NT | 22 | 27 | 32 |
| NF | 14 | 16 | 18 |
| $Q_R$ (MW) | 1.695 | 1.650 | 1.649 |
| ID (m) | 1.098 | 1.086 | 1.084 |
| Total capital ($10^6$ \$) | 0.4646 | 0.4905 | 0.5208 |
| Total energy ($10^6$ \$/y) | 0.4159 | 0.4049 | 0.4046 |
| TAC ($10^6$ \$/y) | 0.5707 | **0.5683** | 0.5782 |

minimize TAC. The feed flowrates and compositions found in the optimum cooled reactor design are used in these calculations. The specifications for distillate and bottoms purities are those previously discussed. The feed-tray location is for each case that minimizes reboiler duty.

Table 13.6 gives results of the economic analysis over a range of column sizes. Capital costs increase as more stages are added, while energy costs decrease. The optimum design for column C1 is a 22-stage column, fed on stage 12. The optimum design for column C2 is 27-stage column, fed on stage 16.

In the following section, the steady-state design of the carbonylation section is developed. Section 13.4 of the chapter considers the dynamic control of both sections coupled together.

## 13.3 CARBONYLATION SECTION

The liquid DME produced in the first section of the plant is fed into the carbonylation section. Carbon monoxide is available at 5 atm, so this gaseous fresh feed stream must be compressed to the pressure selected for operation of the carbonylation reactor. This makes system pressure a critically important design optimization variable. As discussed in Section 13.3.2, higher pressures favor reaction kinetics, so reactor size is reduced and less recycle is required to attain high conversion. This saves capital investment in the reactor vessel, the catalyst, and the recycle compressors. However, higher system pressure means higher capital and energy costs for the fresh feed CO compressor that must increase the pressure from the supply pressure of 5 atm.

The fresh CO feed contains an impurity of 2 mol% hydrogen, which is assumed to be inert in the system and must be purged from the process. This makes the concentration of hydrogen in the gas recycle and purge stream another important design optimization variable. The higher the hydrogen concentration in the purge steam, the lower the losses of CO, DME, and methyl acetate in the purge stream. However, higher hydrogen concentrations

require higher gas recycle flowrates and larger reactors to maintain conversion. The purge stream only has heating value.

The economic optimization of the process is discussed in Section 13.3.5. The final design flowsheet features a reactor with 1000 tubes, an operating pressure of 30 atm, and a hydrogen impurity level of 40 mol%.

### 13.3.1 Process Description

Figure 13.8 shows the flowsheet of the carbonylation section of the process. The liquid DME from the first section of the plant is pumped to 32 atm and fed to a vaporizer, which operates at 372 K, so low-pressure steam can be used (6 atm, 433 K). The flowrate of the DME is fixed in the steady-state design of this section at 250 kmol/h and has a composition of 99.9 mol% DME and 0.1 mol% methanol. The vapor stream is combined with three gas streams: the fresh CO feed, a recycle gas stream from a separator tank and a vapor distillate stream from the top of the reflux-drum of a distillation column.

The required flowrate of the fresh CO feed is 262 kmol/h, which is higher than the stoichiometric amount needed to react with the 250 kmol/h of DME because of the loss of CO in the purge stream. The gas is compressed from 5 to 32 atm in compressor $K_{CO}$, which requires 636 kW of compression work. Compressor work is priced at the cost of electricity ($16.8/GJ).

The total vapor stream is fed to a multi-tube tubular reactor that is packed with solid catalyst. The reactor has 1000 tubes, 0.05 m in diameter and 10 m in length. The catalyst has a density of 2500 kg/m$^3$ and a void fraction of 0.4. The total weight of catalyst is 48,800 kg. At a cost of $50/kg, the catalyst cost is $2,440,000. The capital cost of the reactor vessel is estimated from its heat-transfer area (1570 m$^2$) to be $872,000.

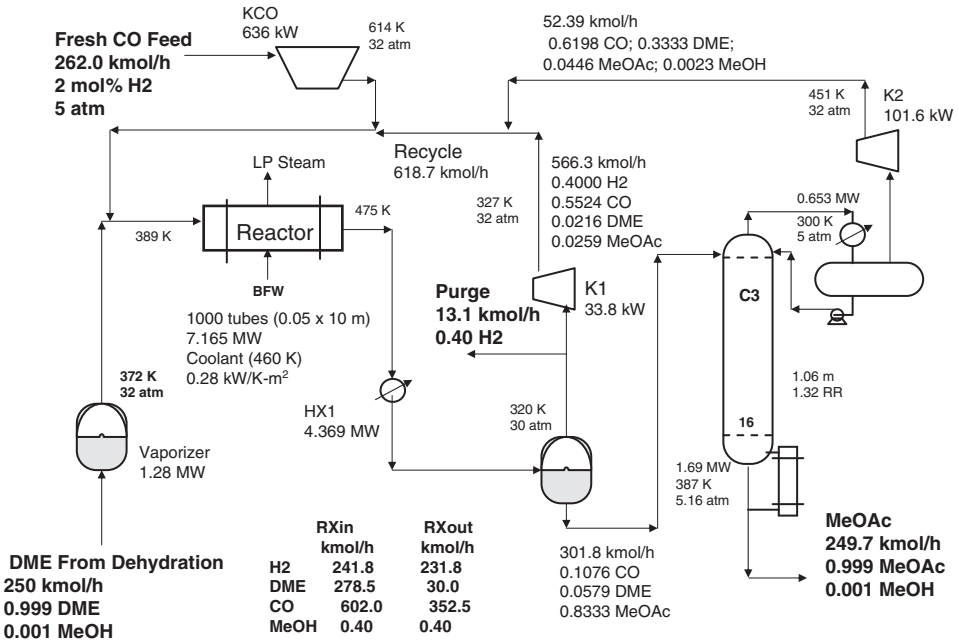


**Figure 13.8.** Carbonylation flowsheet (30 atm, 1000 tubes, purge 40 mol% $H_2$).

The heat from the exothermic reaction is removed by generating low-pressure steam. A plug flow reactor model in Aspen Plus is used with the cooling option of *Constant medium temperature* at 460 K. The heat removal rate is 7.165 MW of energy, using an overall heat-transfer coefficient of $0.28\,\text{kW}\,\text{K}^{-1}\,\text{m}^{-2}$. The low-pressure steam generated in the reactor represents a credit of \$1,760,000/yr. The Ergun equation is used to calculate pressure drop through the reactor tubes. Total pressure drop through the gas loop is 2 atm.

The hot vapor stream from the reactor at 475 K is partially condensed in a water-cooled heat exchanger (4.369 MW) and fed to a separator tank, which operates at 320 K and 30 atm. Most of the gas from the separator is compressed back to 32 atm in compressor K1, which requires 33.8 kW of compression work with a gas flowrate of 566.6 kmol/h.

A small portion of the separator gas is purged from the system in order to remove all the hydrogen entering in the fresh CO feed. The required purge flowrate is 13.1 kmol/h when the hydrogen composition is 40 mol%. The other components lost in the purge stream are CO (55.24 mol%) and small amounts of DME (2.16 mol%) and methyl acetate (2.59 mol%). As discussed in Section 13.3.5, lower hydrogen compositions result in higher losses of CO, which necessitate more fresh feed of CO. The purge stream represents a small credit to the operation, since it has heating value. Using a value of \$6/GJ and estimating the useful energy obtained from burning the gas in 5% excess air, the value of the purge stream is estimated to be \$1.6/kmol, with a purge gas composition of about 50:50 CO and hydrogen.

The liquid from the separator is fed on stage 2 of a 17-stage distillation column operating at 5 atm. Aspen notation is used for tray numbers, with the reflux drum being stage 1. The separator liquid contains small amounts of dissolved light components (essentially no hydrogen but some CO and DME) that go overhead in the column and are recycled.

The column operating pressure of 5 atm is selected so that low-pressure steam can be used in the reboiler. The base temperature is 387 K when the bottoms methyl acetate product is 99.9 mol% methyl acetate and 0.1 mol% methanol. The condenser temperature is set at 300 K by including about 5 mol% methyl acetate in the vapor distillate. This means that refrigeration is required (at 253 K and \$7.89/GJ). However, the condenser duty is fairly small (0.653 MW) since the vapor distillate is relatively small (52.39 kmol/h) and the RR is 1.32. The vapor distillate is compressed in compressor K2 to 32 atm, requiring 101.6 kW of compression work.

The optimization of the column in terms of the number of trays and feed-tray location is discussed in Section 13.3.5. The methyl acetate product is produced at a rate of 249.7 kmol/h and a purity of 99.9 mol%. The impurity is the small amount of methanol that comes in with the DME feed.

### 13.3.2 Carbonylation Kinetics

The chemistry of the carbonylation involves the reaction of CO with DME.

$$CO + CH_3OCH_3 \iff CH_3COOCH_3 \tag{13.4}$$

According to recent research, DME can be carbonylated with high selectivity to form MeOAc (Cheung et al.[5]). The reaction rate data given by Cheung et al. may be reasonably

represented under steady operating conditions by a rate expression in the following form derived from their mechanism:

$$r_{\text{carbonyl}} = k_{\text{carbonyl}}\left(\frac{p_{\text{CO}}}{1 + K_{\text{W}} p_{\text{W}}}\right)$$

$$r_{\text{carbonyl}} = \text{carbonylation, kmol/kg}_{\text{catalyst}}\text{/s} \tag{13.5}$$

$$k_{\text{carbonyl}} = \text{carbonylation rate constant, kmol/kg}_{\text{catalyst}}\text{/s/Pa}$$

$$K_{\text{W}} = \text{H}_2\text{O adsorption equilibrium constant, Pa}$$

Data in Cheung et al. suggest that for DME-pretreated H-mordenite catalysts:

$$k_{\text{carbonyl}} = 8.2 \times 10^{-5} \exp\left(-\frac{8370}{T}\right) \text{kmol/kg}_{\text{catalyst}}\text{/s/Pa} \tag{13.6}$$

where $T$ = temperature, K.

In practice, the inhibiting effect of water is so strong that it must be removed from the DME stream prior to feeding the carbonylation step. In this work, it has been assumed that the DME feed stream is sufficiently dry that the water adsorption term can be neglected. That is reflected in the constants given in Table 13.1 for implementation in Aspen Plus.

An additional issue for simulation arises because this expression is zero-order in one of the reactants, DME. In the event that DME is the limiting reactant, and because the reaction is irreversible, this could result in calculated conversions of DME in excess of 100% (with corresponding negative DME outflows). To avoid this occurrence, the above expression was multiplied by a factor that is equal to unity except at very low DME partial pressures as shown below:

$$r_{\text{carbonyl}} = k_{\text{carbonyl}}\left(\frac{p_{\text{CO}}}{1 + K_{\text{W}} p_{\text{W}}}\right)\left(\frac{K_{\text{DME}}\, p_{\text{DME}}}{1 + K_{\text{DME}}\, p_{\text{DME}}}\right) \tag{13.7}$$

$$K_{\text{DME}} = \text{DME pseudo-adsorption equilibrium constant} = 1\,\text{Pa}^{-1}$$

This overall rate expression remains zero-order in DME up to very high conversions but approaches first-order behavior as 100% DME conversion is approached, so that the rate goes to zero as DME approaches complete disappearance.

### 13.3.3 Effect of Parameters

Preliminary exploration of the effects of temperature and pressure on the carbonylation reaction reveal some important findings. A plug flow reactor is modeled in Aspen Plus with 1500 tubes. The reactor is fed with 250 kmol/h of CO and 250 kmol/h of DME.

In the upper graph in Figure 13.9, the pressure is fixed at 30 atm, and the cooling medium temperature is varied over a wide range. The methyl acetate produced is plotted versus temperature. Remember, this is the temperature of the heat-removal medium low-pressure steam in the shell side of the reactor, not the reactor temperature, which varies down the length of the reactor. It is clear that higher temperatures favor methyl acetate production. The maximum cooling medium temperature for effective operation of the catalyst is assumed to be 460 K. Therefore, the cooling medium temperature is set to this value.

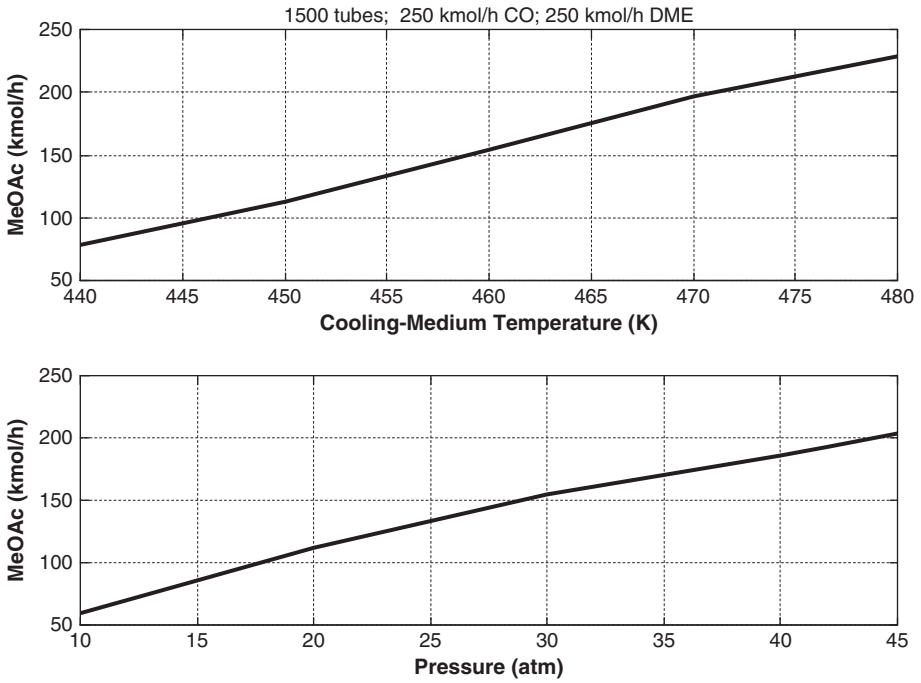


**Figure 13.9.** Carbonylation kinetics: Effect of temperature and pressure.

In the lower graph in Figure 13.9, the cooling medium temperature is fixed at 460 K, and the pressure is varied over a wide range. The methyl acetate produced is plotted versus pressure. It is clear that higher pressures favor methyl acetate production. However, the higher the pressure, the more compression work required in the fresh CO compressor. So the optimum system pressure involves an economic trade-off between compression costs and reactor size.

There is an additional consideration that can limit reactor pressure. The reaction is a gas-phase reaction. Therefore, the pressure in the reactor cannot be so high that liquid is formed in the reactor at the selected cooling medium temperature of 460 K. The vapor fraction of the reactor effluent stays at unity up to a pressure of 40 atm. At 42 atm, the vapor fraction is 0.831. At 45 atm, it is 0.588. Therefore, a conservative maximum pressure of 30 atm is used in the design. In Section 13.3.5, an economic evaluation will demonstrate that this maximum 30-atm operating pressure is the optimum. The cost of additional compression is not as large as the savings in purge losses and lower recycle flowrates.

The second preliminary exploratory study looked at the effects of excess amounts of the two reactants to see if the reactor should operate with excess CO or with excess DME in order to drive the reaction to higher conversion to methyl acetate. Figure 13.10 shows how the production of methyl acetate changes as the flowrate of either CO or DME fed to the reactor is varied with the other reactant feed fixed. A reactor with 1500 tubes, operating at 30 atm with a cooling medium temperature of 460 K, is used in all these cases. The dashed line gives results for the case when the flowrate of DME is fixed at 250 kmol/h, and the flowrate of CO is varied over a wide range. It is clear that increasing CO improves methyl acetate production, even when a large excess of CO used.

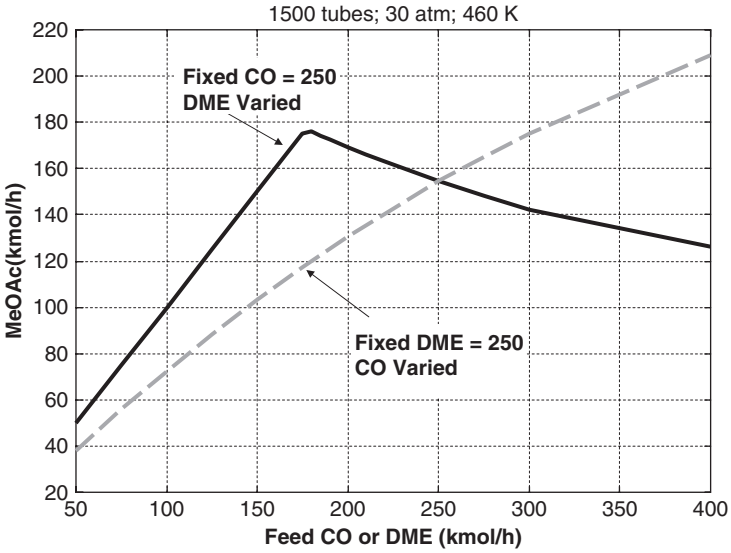


**Figure 13.10.** Carbonylation kinetics: Effect of fresh feeds.

The solid line gives results for the case when the flowrate of CO is fixed at 250 kmol/h, and the flowrate of DME is varied over a wide range. At low DME flowrates, methyl acetate production increases as more DME is fed. The DME is essentially completely consumed in this region. However, above a certain DME feed rate, methyl acetate production starts to decrease. The kinetics become inhibited at high DME concentrations.

These results indicate that the carbonylation reactor must be run with an excess of CO, not DME. This means that the flowsheet will feature a recycle of gaseous CO, which will involve a recycle compressor.

### 13.3.4 Flowsheet Convergence

The carbonylation flowsheet involves two gas recycle streams: vapor from the separator and the vapor distillate from the distillation column. It is also necessary to balance the stoichiometry of the reaction so that the amount of CO fed is exactly equal to the CO consumed in the reaction with the DME feed plus the losses in the purge stream.

Convergence of the recycle loop could not be achieved in Aspen Plus despite numerous approaches to the problem. What did work was a technique suggested many years ago that involves exporting the steady-state Aspen Plus file, without the recycle loop closed, into Aspen Dynamics as a pressure-driven dynamic simulation (see Luyben[6]). The recycle stream is then connected, and a control structure is installed to drive the system to the desired steady-state conditions. This control structure may or may not be the same as that used later in plantwide control studies.

The flowrate of DME is flow-controlled at 250 kmol/h. The fresh feed of CO into the process is manipulated to maintain a high conversion of DME in the reactor. The flow of the fresh CO is flow-controlled by manipulating the work to compressor $K_{CO}$. The flow controller is "on cascade," with its setpoint coming from a "conversion controller" with a process variable of 30 kmol/h of DME leaving the reactor. The DME entering the reactor is 278.5 kmol/h, so the specified conversion is 89%.

Other control loops involve holding liquid level in the vaporizer by manipulating heat input, holding separator pressure at 30 atm by manipulating the work to compressor K1, holding column C3 pressure at 5 atm by manipulating the work to compressor K2, holding separator temperature by manipulating heat removal in partial condenser HX1, fixing reflux flow in column C3 at 70.8 kmol/h, and holding reflux-drum temperature in column C3 at 300 K by manipulating reboiler heat input. The last two loops maintained the high purity (99.9 mol%) of the methyl acetate bottoms product from the distillation column. Liquid levels in the separator and in the column base are held by manipulating the liquid stream leaving the vessel.

### 13.3.5 Optimization

Now that the reactor temperature has been selected from basic kinetic considerations to be at its maximum, the remaining dominant design optimization variables are pressure, reactor size, and purge composition.

***Economic Basis.*** The economics consider both capital investment (compressors, vaporizer, partial condenser, reactor, catalyst, separator tank, distillation column, condenser, and reboiler) and energy costs (compressor work, steam used in the vaporizer, steam used in the column reboiler, and refrigeration used in the column condenser). The two credits are the value of the steam generated in the reactor and the heating value of purge.

Table 13.2 summarizes the sizing and cost basis used in this analysis. These parameters are taken from Douglas[3] and Turton et al.[4] The compressors use electricity at \$16.8/GJ. The partial condenser uses cooling water; this cost is neglected. The vaporizer and reboiler use low-pressure steam at \$7.78/GJ. The condenser uses 253 K refrigerant at \$7.89/GJ.

There are two credits in the economics. One is for the steam generated in the reactor. It is low-pressure saturated steam with a value of \$7.78/GJ. The second is the heating value of the purge stream, which contains mostly hydrogen and CO with small amounts of DME and methyl acetate. The stream can be burned to recover heat. The amount of air to completely combust each component, the component heats of combustion, and the mean heat capacities of the resulting nitrogen, carbon dioxide, and water gas stream are used to find the net heating value of the purge stream (0.259 kJ/kmol). The sensible heat of changing the combustion products from ambient up to a 260 °C stack gas temperature is subtracted from the heat of combustion. A value of \$6/GJ is used for this fuel, which corresponds to \$1.6/kmol.

The assessment of economics assumes the DME feed is fixed at 250 kmol/h. The stoichiometric amount of CO would be 250 kmol/h. The incremental amount of CO that must be fed to satisfy reaction and losses is counted as an operating cost. A price of CO fresh feed is assumed to be \$13.2/kmol (\$370/tonne). The annual capital cost uses a payback period of 3 yr. Total capital investment includes the vaporizer and reactor, with cost based on heat-transfer area. The size of the separator tank is set by have 10 min of liquid holdup. Other capital investments are the three compressors, the partial condenser, and the distillation column with its vessel, reboiler, and condenser.

The TAC is defined as the annual cost of capital plus the cost of energy (reboiler, vaporizer, refrigerant, and compressor work), plus the cost of CO fresh feed above the 250 kmol/h stoichiometric amount, minus the credits for reactor steam and purge heating value. The amount of methyl acetate produced in all cases is essentially constant at 249.7 kmol/h.

This method of economic analysis avoids the necessity of specifying the cost of DME and the value of methyl acetate, which always have quite a bit of uncertainty.

$$\begin{aligned}\text{TAC} = {} & \text{Cost incremental CO} + \text{compressor energy} + \text{reboiler energy} \\ & + \text{vaporizer energy} + \text{condenser refrigerant} + (\text{total capital})/3 \\ & - \text{credit for reactor steam} - \text{credit for purge heating value} \end{aligned} \tag{13.8}$$

The optimum number of stages and the feed-stage location in the distillation column are found by minimizing TAC. The optimum is a 17-stage column fed on the top tray (stage 2). This column has a TAC of \$403,000/yr compared to a TAC of \$690,000/yr for a smaller 12-stage column.

***Effect of Reactor Size and Purge Composition.*** The number of tubes in the reactor and the hydrogen composition of the purge stream are dominant design optimization variables. A big reactor requires smaller recycle flowrates, so compression costs are lower. But the capital cost of the reactor vessel and the expensive catalyst are high. Letting the hydrogen concentration build up reduces purge losses and CO fresh feed requirements. But recycle flowrates increase, so compression costs are large.

Figure 13.11 shows these effects for three different reactor sizes (800, 1000, and 1500 tubes) over a range of purge gas compositions. For all these results, the DME feed flowrate and the methyl acetate product flowrate are essentially fixed. Other fixed variables are separator pressure (30 atm) and temperature (320 K), column pressure (5 atm), reflux-drum temperature (300 K), DME leaving the reactor (30 kmol/h), and column reflux flowrate (70.8 kmol/h).

The top left graph in Figure 13.11a shows how recycle flowrates increase with purge hydrogen composition. This occurs because the hydrogen reduces the concentrations of the reactant, so more recycle is required to maintain the high per-pass conversion of DME. As the number of reactor tubes is increased, the required recycle decreases.

The right three graphs in Figure 13.11a show how the work of each of the three compressors changes with purge concentration and reactor size. The recycle compressor on the separator gas stream (K1) increases rapidly as purge composition increases, but is lowered when a larger reactor is used. The compressor on the vapor distillate (K2) decreases with increasing purge composition because fewer light components are fed to the column from the separator tank at the higher gas flowrates. Reactor size has little effect.

The fresh CO feed compressor is most strongly affected by reactor size. The separator tank pressure is constant at 30 atm for all these cases, but the higher recycle flowrates result in higher pressure drops through the gas loop (reactor and partial condenser) that raise the discharge pressure of the $K_{CO}$ compressor. The large reactor has lower recycle flowrates and lower pressure drops, so the compressor work is lower and less affected by purge composition.

The middle and bottom left graphs in Figure 13.11a show how less purge and less fresh CO feed are required as purge hydrogen composition is increased, with essentially the same effect for any reactor size. The "Delta CO" variable is the flowrate of CO above the 250 kmol/h stoichiometric amount. Thus, increasing purge hydrogen composition lowers CO feed costs.

Figure 13.11b gives economic results. The value of the steam generated in the reactor is shown in the upper left graph. Larger reactors generate more steam because they require lower recycle flowrates. Higher recycle flowrate carries more sensible heat out of the reactor into the partial condenser, the heat duty of which increases as recycle flowrate increases.

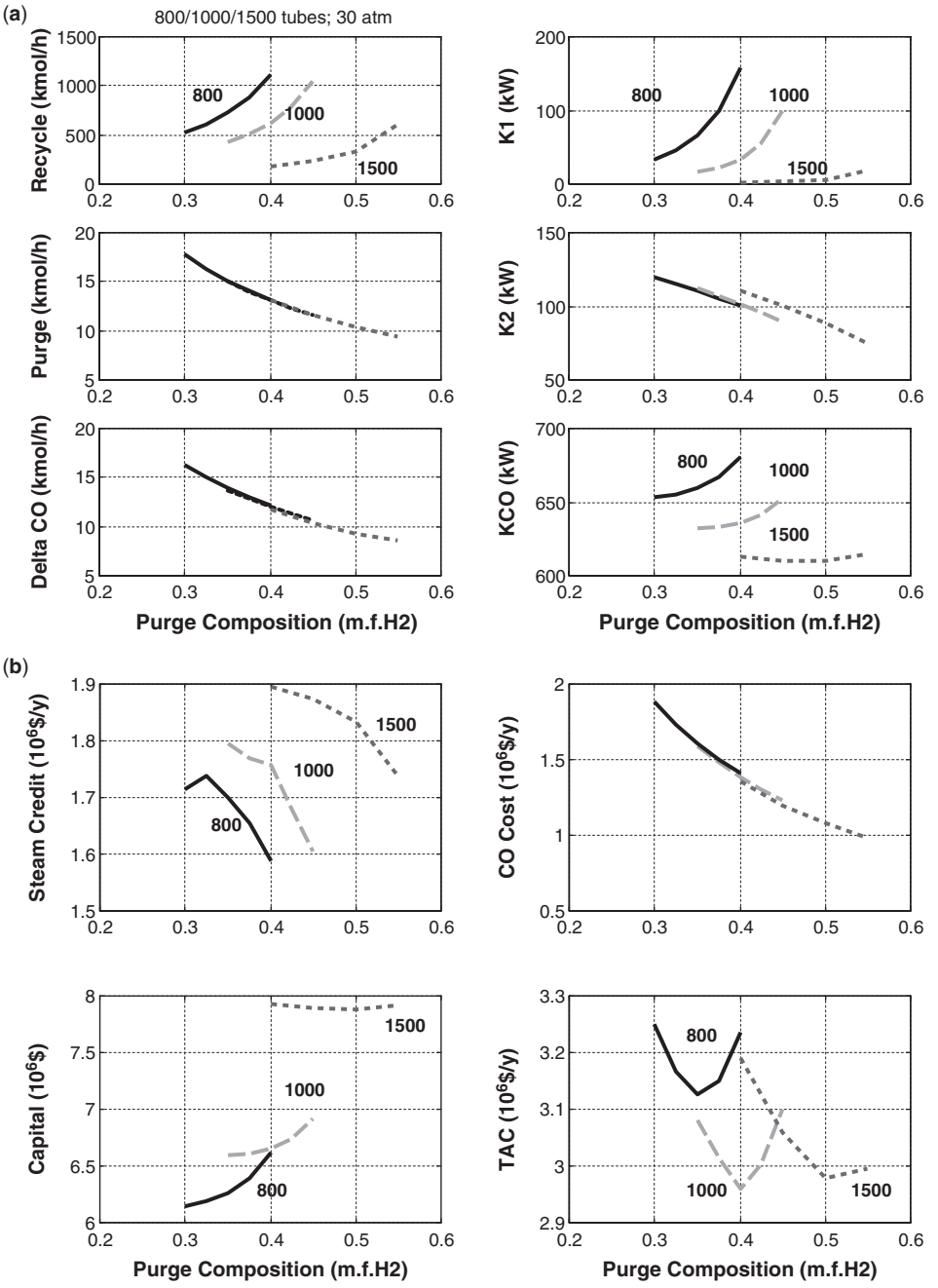


**Figure 13.11.** (a) Effect of purge composition and reactor tubes (30 atm, 460 K). (b) Economics effects of purge composition and reactor tubes.

Since higher purge gas hydrogen composition requires higher recycle flowrates, reactor steam generation decreases as purge composition increases. A comparison of the top left graph in Figure 13.11a (showing recycle) with the top left graph in Figure 13.11b (showing steam) clearly shows this inverse relationship.

The bottom left graph in Figure 13.11b shows the strong effect of reactor size on total capital cost. This is due to the large contribution of the cost of the reactor vessel ($872,000) and the catalyst ($2,420,000), which are significant components of the total capital cost. In the final design, the capital cost of all three compressors is $2,570,000; the capital cost of the distillation column and associated heat exchangers is $282,000; the capital cost of the separator tank is $200,000; the capital cost of the vaporizer is $120,000; and the capital cost of the partial condenser is $300,000. So, the reactor cost and the compressor costs dominate the economics of capital investment.

In contrast, the economics of operating costs are dominated by compression costs ($408,000/yr), the cost of excess fresh CO feed ($1,360,000/yr), and the value of the reactor steam ($1,760,000/yr). The energy cost of the reboiler steam is $414,000/yr, and the cost of condenser refrigeration is $163,000/yr.

The effect of reactor size and purge composition on TAC is shown in the bottom right graph of Figure 13.11b. There is an optimum purge composition for each reactor size that increases as the reactor becomes larger. The minimum TAC design has a reactor with 1000 tubes and a purge composition of 40 mol% hydrogen.

***Effect of Pressure.*** The final important design optimization variable is system pressure. Figure 13.12 shows that higher pressures reduce the required recycle flowrate and the purge flowrate, which reduce recycle compression costs and the cost of fresh CO feed. However, the compression cost of $K_{CO}$ increases. Since reactant cost is an important variable, TAC continues to decrease as pressure increases. The assumed 30-atm pressure limitation then fixes system pressure. The results shown in Figure 13.12 are for a 1500-tube reactor with the optimum purge composition for each pressure (35 mol% at 20 atm, 45 mol% at

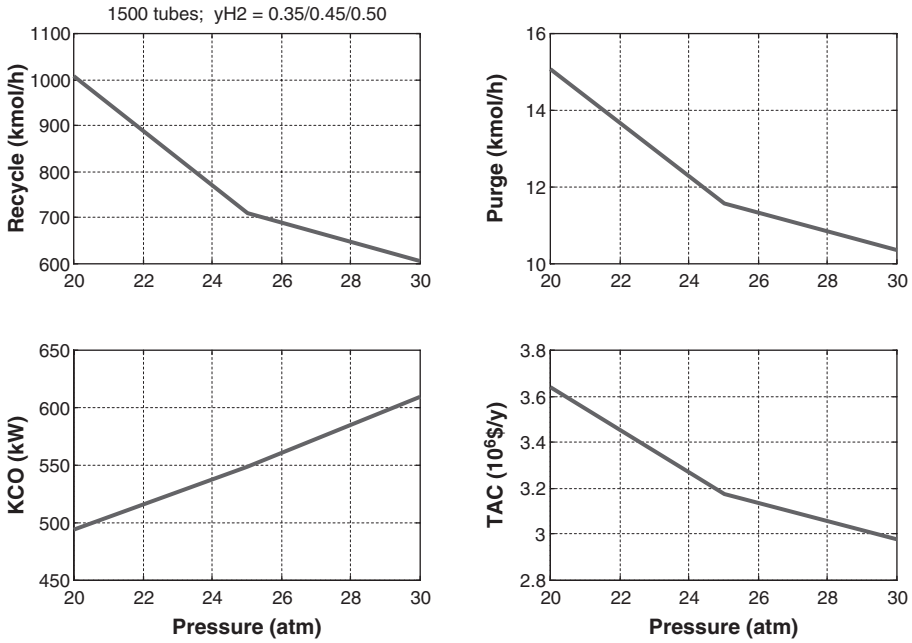


**Figure 13.12.** Effect of pressure (1500 tubes, 460 K).

25 atm, and 50 mol% at 30 atm). A 1500-tube reactor is used because very high recycle flowrates and low purge compositions are needed at the low system pressures.

## 13.4 PLANTWIDE CONTROL

Before exporting the steady-state Aspen Plus simulation into Aspen Dynamics, the size of the reflux drums and column bases in the distillation columns are specified to provide 5 min of liquid holdup at 50% level. The sizes of the reactors and column vessels are known from the steady-state design. The size of the separator is also determined during steady-state design so that its capital investment costs can be calculated. The compressors and heat exchangers are assumed to have negligible dynamic lags. The "Gear" numerical integration algorithm was used because it gave much faster computing speed than the default "Implicit Euler" algorithm.

The development of the plantwide control structure presented in Section 13.4.1 is based on the heuristic procedure proposed a decade ago, which has been successfully applied to many industrial processes (see Luyben et al.[7]).

### 13.4.1 Control Structure

Figures 13.13 and 13.14 show the plantwide control structure for the two sections. Conventional PI controllers are used in all loops. All level loops are proportional with $K_C = 2$. The flow controller that manipulates the CO feed compressor uses a gain of

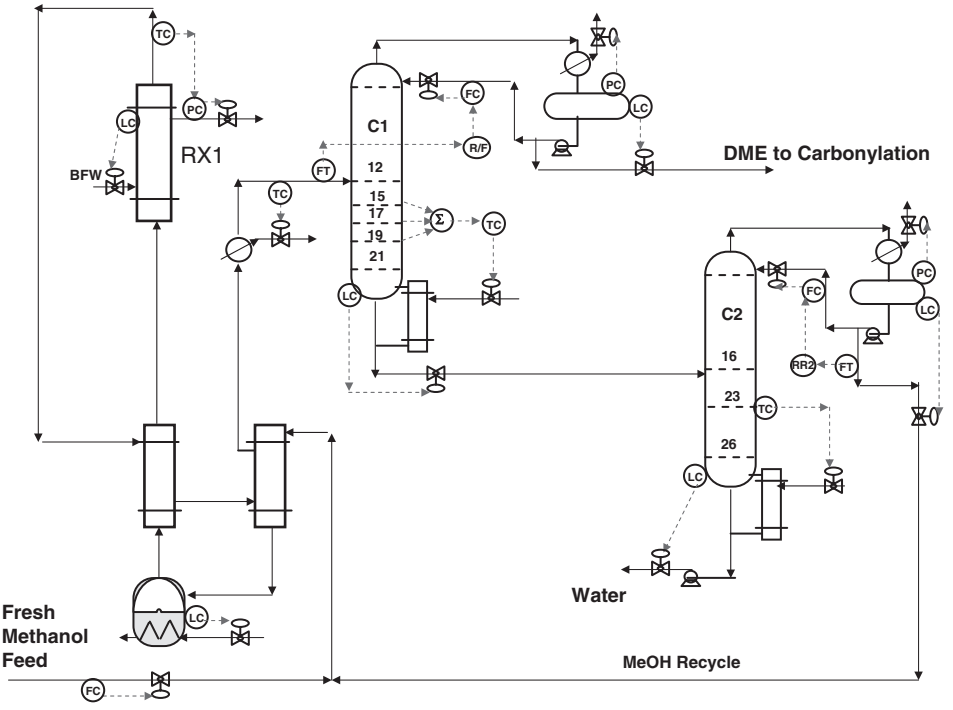


**Figure 13.13.** Dehydration control structure.

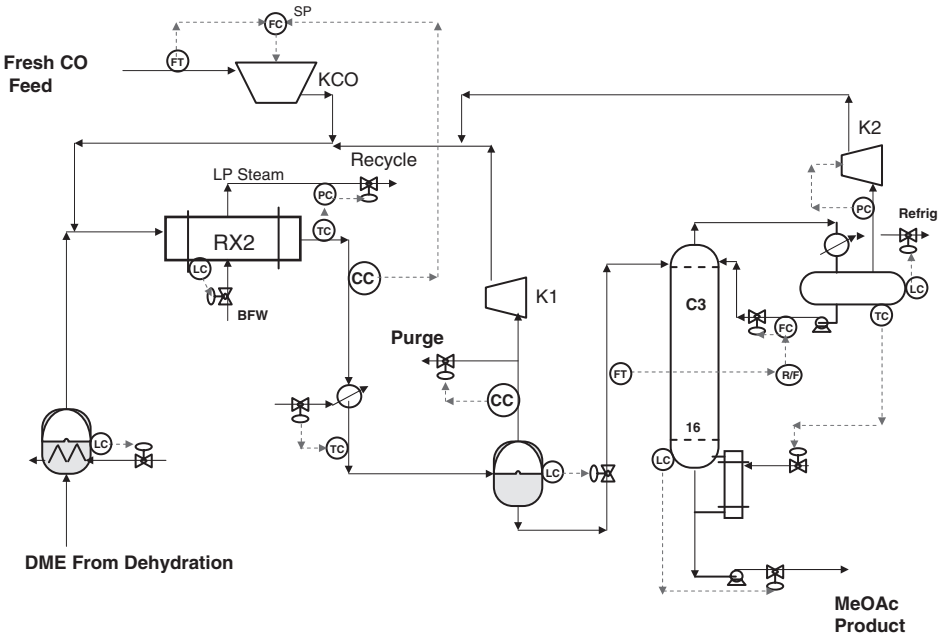


**Figure 13.14.** Carbonylation control structure.

0.5 and an integral time of 0.5 min. The column tray temperature controllers have 1-min deadtimes. The reactor temperature loops have 2-min deadtimes to account for the steam generation dynamics. The composition controllers have 3-min deadtimes. These temperature and composition controllers are tuned by using relay-feedback tests to obtain ultimate gains and periods and then applying Tyreus-Luyben tuning rules.

All of the loops are listed below with their controlled and manipulated variables.

***Dehydration Section.*** Please see Figure 13.13.

1. The fresh feed of liquid methanol is flow-controlled.
2. The liquid level in the methanol vaporizer is controlled by manipulating the heat input.
3. The exit temperature of the dehydration reactor RX1 is controlled by manipulating the cooling medium temperature (pressure of steam).
4. The temperature of the feed to column C1 is controlled by manipulating cooling water to the heat exchanger.
5. Reflux-to-feed (R/F) is controlled in C1 by manipulating reflux flowrate.
6. Pressures in C1 and C2 are controlled by manipulating condenser heat removal
7. Base levels are controlled in C1 and C2 by manipulating bottoms flowrate.
8. Reflux-drum levels in C1 and C2 are controlled by manipulating distillate flowrates.
9. An average temperature in C1 (stages 15, 17, and 19) is controlled by manipulating reboiler heat input.

10. The RR in C2 is controlled by manipulating reflux flowrate.
11. The temperature on stage 23 in C2 is controlled by manipulating reboiler heat input.

***Carbonylation Section.*** Please see Figure 13.14.

1. The liquid level in the DME vaporizer is controlled by manipulating the heat input.
2. The exit temperature of the carbonylation reactor RX2 is controlled by manipulating the cooling medium temperature (pressure of steam).
3. The composition of DME in the effluent of the reactor is controlled by manipulating the fresh feed of CO through a cascade flow-controller with an output signal that manipulates the work to compressor $K_{CO}$.
4. The temperature of the feed to the separator tank is controlled by manipulating cooling water to the heat exchanger.
5. The liquid level in the separator is controlled by manipulating the feed to column C3.
6. The hydrogen composition of the gas from the separator is controlled at 40 mol% hydrogen by manipulating the gas purge.
7. The work to compressor K1 is fixed.
8. The temperature in the reflux drum of column C3 is controlled by manipulating reboiler heat input.
9. The reflux in column C3 is ratioed to the feed.
10. The base level in C3 is controlled by manipulating bottoms flowrate.
11. The pressure in C3 is controlled by manipulating work to compressor K2.
12. The reflux-drum level in C3 is controlled by manipulating condenser heat removal.

There are several key loops in this structure that are discussed in detail below. Notice that there is no control of the pressure in the gas loop in the carbonylation section. Pressure floats up and down with the load on the plant to force the complete consumption of both reactants.

***Average Temperature Control in Column C1.*** As shown in Figure 13.15, the temperature difference between the top and the bottom of column C1 is quite large (320 to 430 K) because the DME distillate is much lighter than the other components. The steep part of the temperature profile is in the stripping section. In this situation, an average temperature control structure instead of a single temperature structure is often used to improve controllability.

Figure 13.16 demonstrates this improvement. The solid lines show when the temperature on stage 17 is controlled. The dashed lines show when the sum of the temperatures on stages 15, 17, and 19 are controlled. The disturbance is a 20% decrease in the fresh feed of methanol to the plant. Note that Aspen Dynamics uses metric units, so the "average" temperature (actually the sum of the three temperatures) is in degrees Celsius. The single stage 17 temperature is in Kelvin.

The big improvement is in the purity of the DME distillate. With single temperature control, a large transient drop in purity (bottom right graph in Figure 13.16) from 99.9 mol% down to 97.5 mol% DME results. With average temperature control, the transient drop in purity is greatly reduced.

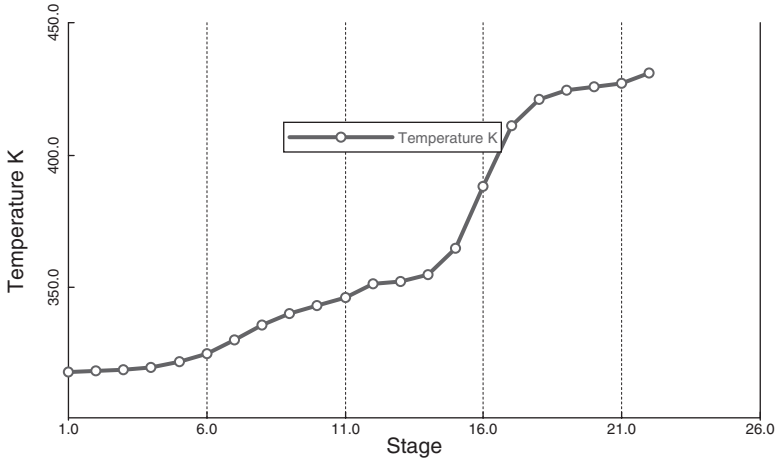


**Figure 13.15.** Temperature profile in column C1.

***R/F Control in Column C1 and RR in Column C2.*** Temperature control is used in both columns. To decide how the other control degree of freedom should be selected, a feed composition sensitivity analysis was performed on both columns. The two design specifications in each column were fixed and feed compositions of the light- and heavy-key components were varied around their design values. The required changes in reflux flowrate and RR were determined.

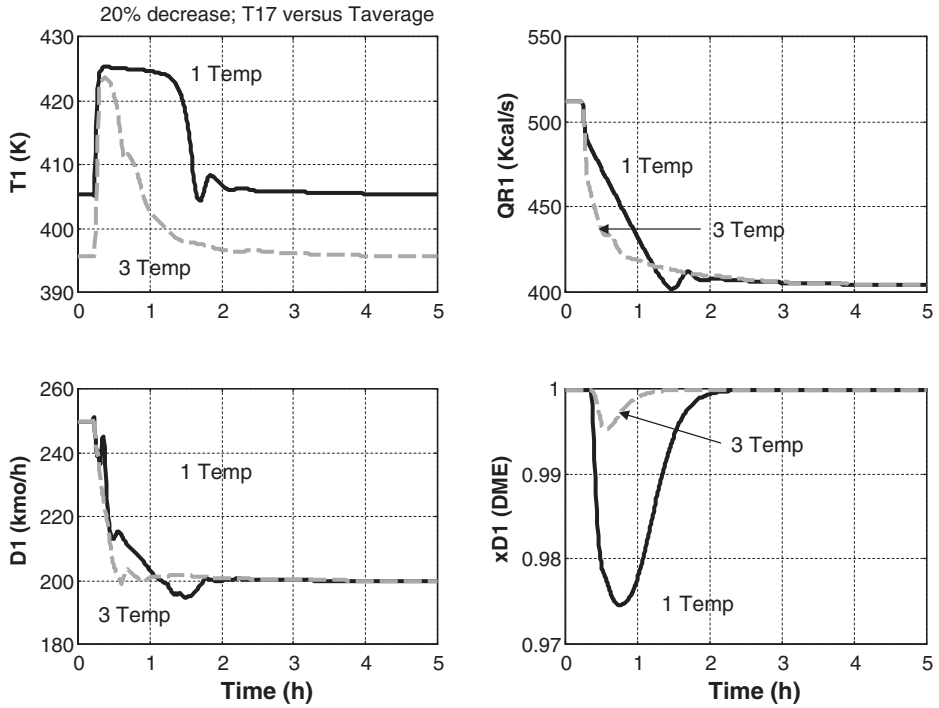


**Figure 13.16.** Average temperature control of column C1.

In column C1, the required changes in the R/F ratio were much smaller than the required changes in RR. Therefore, the R/F structure was selected.

In column C2, the required changes in RR were smaller than required changes in the R/F ratio. Therefore, the RR structure was selected.

***Conversion in Carbonylation Reactor.*** The most important loop in the whole plant is the one that controls the concentration of DME in the reactor effluent leaving the carbonylation reactor. If DME is increasing, more fresh feed of CO is added.

This structure requires an online measurement of composition. Several other alternative structures were explored that avoided composition measurement, but none was found that could handle the difficult problem of precisely balancing the addition rate of CO to satisfy the stoichiometry of the reaction.

Many plants with a gas fresh feed can be successfully controlled by bringing in the gas on pressure control. If more reactant is being fed than consumed, the pressure will rise, and the pressure control cuts back on the fresh gas feed. This technique eliminates a composition measurement.

However, in this process there are two gas streams into the carbonylation reactor. If pressure is increasing, it can be due to too much or too little CO. This pressure control structure did not provide stable regulatory control.

***Control Structure in Column C3.*** Because of the high pressure in the separator, the liquid phase contains quite a bit of lighter components in addition to the product (methyl acetate). The liquid composition is 10.76 mol% CO and 5.79 mol% DME, and these light components must be removed and recycled back to the reactor. The C3 distillation column has this job.

The very light CO and DME would require a very high pressure if cooling water were used in the condenser, so refrigeration is used. To keep the reflux-drum temperature from

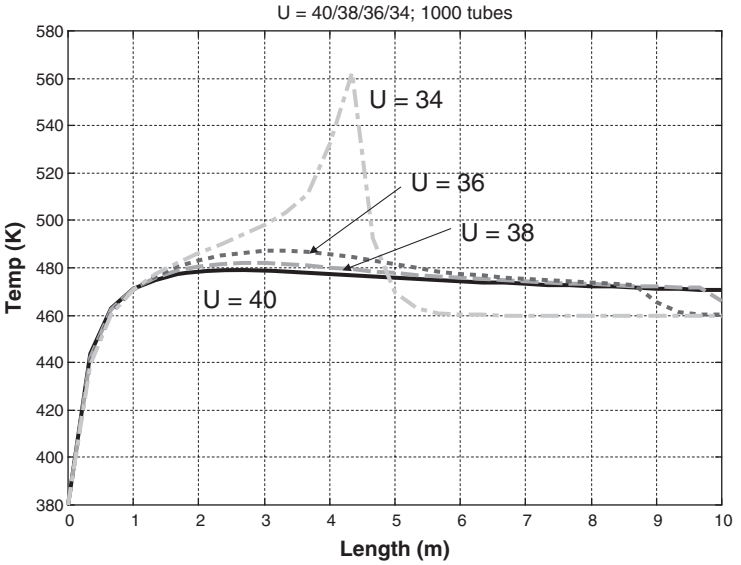


**Figure 13.17.** Carbonylation temperature profiles.

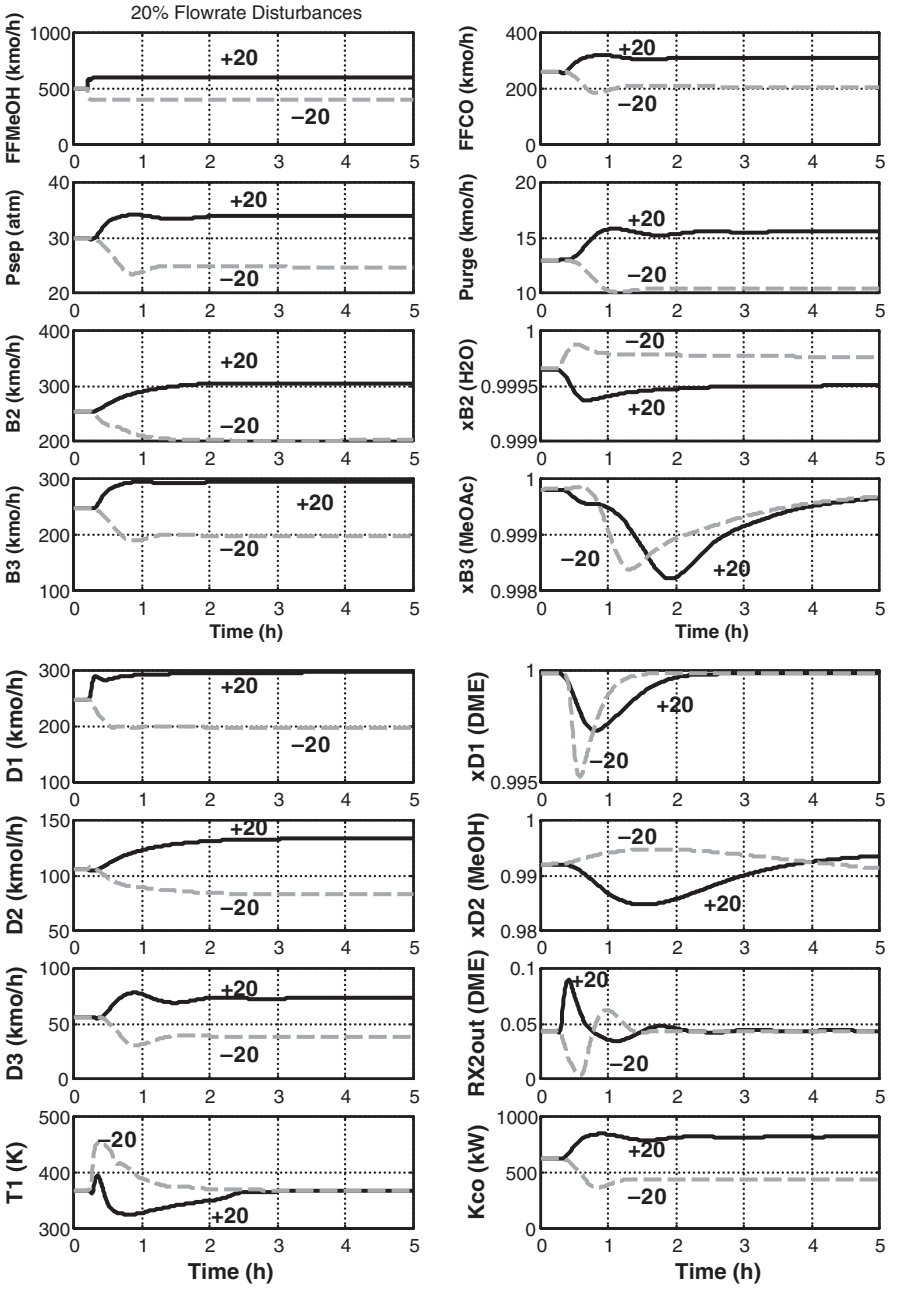


**Figure 13.18.** 20% flowrate disturbances.

being very low, some methyl acetate is taken overhead. The distillate is taken as a vapor from the top of the reflux drum and is compressed and recycled.

A simple control structure was found to be quite effective since the basic separation is an easy one (few trays and modest RR). The reflux flowrate is ratioed to the feed flowrate. Reflux-drum temperature is controlled at 300 K (so medium-cold refrigerant can be used)

by manipulating reboiler duty. Pressure is controlled by manipulating compressor K2 work. Reflux-drum level is controlled by manipulating condenser refrigerant duty.

***Control Structure for Reactors.*** The exit temperatures of the two cooled reactors are controlled by manipulating the cooling medium temperature. Physically, this corresponds to manipulating the pressure of the steam being generated. Temperature control of the dehydration reactor was easy to set up and provided effective control.

Temperature control of the carbonylation reactor was found to be quite difficult. Relay-feedback tests could not be run because of numerical integration errors. To overcome these problems, the value of the overall heat-transfer coefficient was increased from the design value of 0.28 to 0.40 kW $K^{-1}$ $m^{-2}$. Figure 13.17 shows the strong dependence of the temperature profile on the value of the overall heat-transfer coefficient. These numerical problems may indicate real physical problems in this highly exothermic system. This issue is under study.

### 13.4.2 Dynamic Performance

The coupled system was subjected to large disturbances in throughput and feed compositions. Figure 13.18 gives the responses of several important variables to 20% disturbances in the setpoint of the fresh methanol flow controller. The solid lines are 20% increases, and the dashed lines are 20% decreases. Stable regulatory control is achieved for these large disturbances.

Figure 13.18 shows that the pressure in the separator ($P_{sep}$) floats up and down with throughput. Higher feed rates require higher pressures, which result in higher power

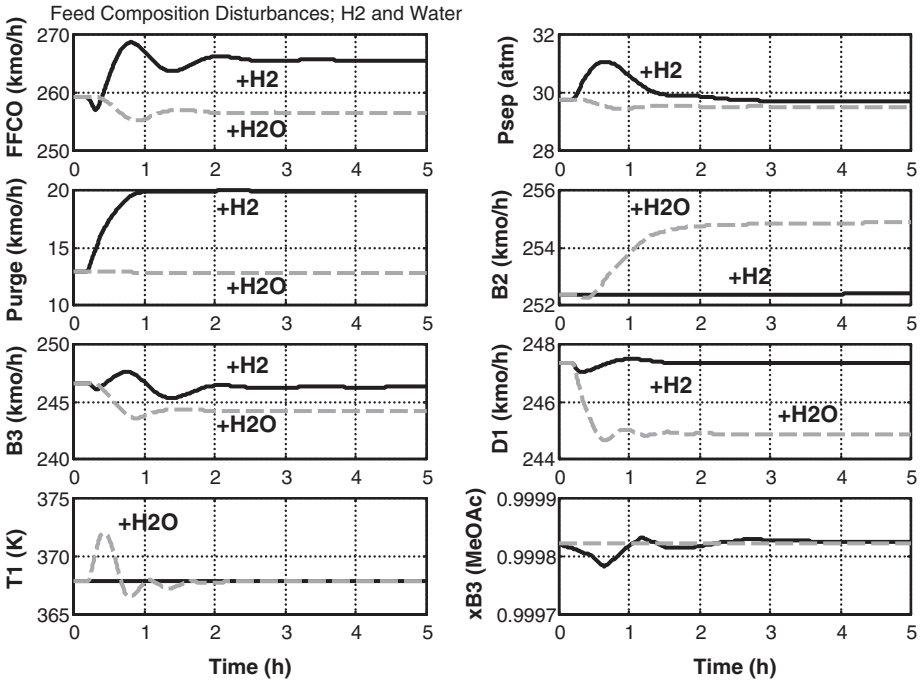


**Figure 13.19.** Feed composition disturbances.

consumption in the fresh CO compressor. The production rates of methyl acetate (B3) and water (B2) change directly with throughput, as does the flowrate of the purge stream.

The purities of these streams [$x_{B3(MeOAc)}$ and $x_{B2(H2O)}$] are held quite close to their specifications. The purity of the DME ($x_{D1(DME)}$) drops slightly for both disturbances, which puts more methanol into the carbonylation section and causes the small transient drop in the methyl acetate purity.

Figure 13.19 shows how disturbances in the compositions of the two fresh feeds affect the system. The solid lines show when the hydrogen impurity in the CO increases from 2 to 3 mol%. The major effect, as expected, is an increase in the purge flowrate. The flowrate of fresh CO also must increase since the amount of fresh methanol fed and the resulting DME produced require the same amount of CO to react and the CO losses are larger.

The dashed lines indicate when the water impurity in the fresh methanol increases from 0.1 to 0.2 mol%. Since slightly less methanol is being fed, there is a small reduction in the DME produced [shown as D1 in Figure 13.19 right graph, third from the top]. Naturally, slightly less methyl acetate is produced (B3) and slightly more water is produced (B2).

## 13.5 CONCLUSION

The design and control of a fairly complex chemical process has been studied. The two sections of the plants have their individual reaction and separations sections with a recycle stream in each. Steady-state design involves a number of economic trade-offs between the many design optimization variables. Reactor size, temperature, and pressure affect separation and compression costs, as well as reactant losses in a purge stream.

A plantwide control structure is developed and demonstrated to provide effective control for large disturbances.

## REFERENCES

1. http://www.che.cemr.wvu.edu/publications/projects/large_proj/dimethyl_ether.PDF.
2. Bandiera, J., Naccache, C. Kinetics of methanol dehydration in dealuminated H-mordenite: Model with acid and base active centers, *Appl. Catal.* 69, 139–149, 1991.
3. Douglas, J. M. *Conceptual Design of Chemical Processes*, McGraw-Hill, New York, 1988.
4. Turton, R., Bailie, R. C., Whiting, W. B., Shaelwitz, J. A. *Analysis, Synthesis and Design of Chemical Processes*, 2nd Edition, Prentice Hall, Englewood Cliffs, NJ, 2003.
5. Cheung, P., Bhan, A., Sunley, G. J., Law, D. J., Iglesia, E. Site requirements and elementary steps in DME carbonylation catalyzed by acidic zeolites, *J. Catal.* 2007, **245**, 110–123.
6. Luyben, W. L. Use of dynamic simulation to converge complex process flowsheets, *Chem. Eng. Educ.* 2004, **38**, 2.
7. Luyben, W. L., Tyreus, B. D., Luyben, M. L. *Plantwide Process Control*, McGraw-Hill, New York, 1999.

# CHAPTER 14

# DESIGN AND CONTROL OF THE MONO-ISOPROPYL AMINE PROCESS

The mono-isopropyl amine (MIPA) process provides an interesting example of plantwide economic design optimization and plantwide control. The process consists of a tubular reactor and three distillation columns. There are both gas and liquid recycles. Fresh feed streams of isopropyl alcohol and ammonia are introduced into the process. The desired products are MIPA and water. An undesirable by-product of di-isopropyl amine (DIPA) is also produced and is recycled to extinction since its formation reaction is reversible. An excess of ammonia in the reactor inhibits the DIPA reaction, so ammonia is also recycled.

The purpose of this chapter is to present the details of the process for use by other workers as a test case for use in plantwide design and control studies. A heuristic economic optimum design and a control structure are developed. The process illustrates the classical design trade-off between reactor costs versus separation costs. In addition, the process has two recycles, which are both distillate products from different distillation columns, and this leads to another trade-off. Using more ammonia recycle produces less DIPA recycle. So the optimum design must balance the separation costs of the two recycles. Two of the distillation columns can be effectively controlled using a single temperature and the reflux-to-feed (R/F) ratio. The third column requires a dual control structure (one temperature and one composition).

## 14.1 INTRODUCTION

A number of typically large processes have been described in the literature over the years and have been the subjects of both steady-state design studies and plantwide control studies. The pioneering work by Douglas[1] presented the first example, the hydro-dealkylation of toluene to form benzene (HDA). This flowsheet has been the subject of many studies. The Tennessee

*Principles and Case Studies of Simultaneous Design*, First Edition. William L. Luyben

Eastman process developed by Downs and Vogel[2] was a favorite process considered in a large number of academic studies because it is relatively simple. A plantwide control book (see Luyben[3]) considered these two processes and two other complex industrial systems (isomerization and alkylation). A dynamic simulation book (see Luyben[4]) provided other examples (ethyl benzene and methyl amine). A recent paper by Vasudevan et al.[5] presents flowsheet information dealing with the styrene process.

All of these processes involve multiple units with reaction sections coupled with separation sections connected by recycle streams. They present challenging design and control problems. Many design trade-offs are illustrated in these examples: reactor size versus recycle flowrate, reactor size versus inlet temperature (for tubular reactors), separation costs versus individual recycle flowrates (for multiple recycles), heat exchanger area (capital cost) versus energy costs, pressure drop through valves and equipment versus pumping and compression costs.

The purpose of this chapter is to present a new example that has some interesting and somewhat unusual features.

## 14.2 PROCESS STUDIED

### 14.2.1 Reaction Kinetics

The production of MIPA involves the reaction of isopropanol (IPA) with ammonia.

$$\mathrm{IPA} + \mathrm{NH_3} \longrightarrow \mathrm{MIPA} + \mathrm{H_2O} \tag{14.1}$$

There is also a sequential reaction of MIPA and IPA to form DIPA.

$$\mathrm{IPA} + \mathrm{MIPA} \longrightarrow \mathrm{DIPA} + \mathrm{H_2O} \tag{14.2}$$

An additional reversible reaction is

$$\mathrm{DIPA} + \mathrm{NH_3} \Longleftrightarrow 2\,\mathrm{MIPA} \tag{14.3}$$

Table 14.1 gives the reaction kinetics assumed to apply in the system. Reaction 3 is modeled as two reactions ($\Re_{3F}$ and $\Re_{3R}$). All reaction rates have units of kmol $\mathrm{sec}^{-1}$ $\mathrm{m}^{-3}$. Concentration units are molarity ($\mathrm{kmol/m^3}$). The reactions occur in the vapor phase in the presence of a solid catalyst (0.5 void fraction, 200 $\mathrm{lb/ft^3}$ solid density).

These kinetic parameters indicated that the concentration of ammonia should be kept large and the concentration of MIPA should be kept small to avoid the production of the undesirable by-product, DIPA. Increasing the concentration of ammonia in the reactor

**TABLE 14.1 Reaction Kinetics**[a]

| | $\Re 1$ | $\Re 2$ | $\Re 3F$ | $\Re 3R$ |
|---|---|---|---|---|
| $K$ | $2.533 \times 10^{13}$ | $1.086 \times 10^{16}$ | $8.53 \times 10^{15}$ | $8.53 \times 10^{15}$ |
| $E$ (Btu/lb-mol) | 54,000 | 67,500 | 67,500 | 67,500 |
| Concentration terms ($\mathrm{kmol/m^3}$) | $C_{\mathrm{IPA}}C_{\mathrm{NH3}}$ | $C_{\mathrm{IPA}}C_{\mathrm{MIPA}}$ | $C_{\mathrm{NH3}}C_{\mathrm{DIPA}}$ | $(C_{\mathrm{MIPA}})^2$ |

[a]Overall reaction rates have units of kmol $\mathrm{sec}^{-1}$ $\mathrm{m}^{-3}$.

results in more ammonia recycle and less DIPA recycle. As discussed in Section 14.2.3, each of these two components is recycled from the top of a distillation column. Increasing the ammonia recycle flowrate means larger energy consumption and larger capital investment in the column shell and heat exchangers (reboiler and condenser) in the ammonia column. However, increasing ammonia recycle flowrate means lower DIPA recycle flowrate, which results in lower energy consumption and lower capital investment in the column shell and heat exchangers in the DIPA column. Thus, there is an optimum design that balances these two effects.

The desired MIPA reaction has a smaller activation energy than the undesirable DIPA reaction. Therefore, low reactor temperatures favor the MIPA reaction. However, low reactor temperatures lower specific reaction rates, resulting in a lower conversion of IPA for a given size reactor or a larger reactor for a given IPA conversion. In this work, the IPA per-pass conversion is set at 99.5% so that very little IPA must be recycled.

Hydrogen improves catalyst life and lowers dew-point temperatures, so hydrogen is circulated around in the reaction separation in two gas recycle streams. Hydrogen is not consumed in the reactions. The inlet stream to the reactor must be vapor, so the inlet temperature must be higher than the dew-point temperature of the reactor feed mixture. The presence of hydrogen permits lower reactor inlet temperatures before a liquid phase begins to appear, so a wider range of inlet temperature can be used if desired. The main hydrogen circulation stream has a composition of about 58 mol% hydrogen and 40 mol% ammonia and a flowrate of 32 lb-mol/h. The smaller hydrogen stream has a composition of about 95 mol% hydrogen and 5 mol% ammonia and a flowrate of 8.3 lb-mol/h.

### 14.2.2 Phase Equilibrium

The components that must be separated in the system are fairly easily separated by distillation. The normal boiling points of ammonia, MIPA, IPA, DIPA, and water are −28.1, 89.2, 180.2, 183.2, and 212 °F, respectively. Notice that the boiling points of IPA and DIPA are very close, so any unreacted IPA is recycled back to the reactor in the DIPA recycle.

The separation of ammonia is easy, but a high-pressure column is required if cooling water is to be used in the condenser. The NRTL physical property package is used in this study. At a pressure of 300 psia, the reflux-drum temperature is 120 °F, which permits cooling water to be used in the condenser. The separation is fairly easy, so the column will not require many trays. A column with 12 stages is used. Aspen simulation is used in this study, so the number of stages is counted from the top with the reflux drum being stage 1 and the reboiler being stage NT. The resulting reflux ratio (RR) required for the separation is only about 0.4. There is a very large temperature change over the column (reflux drum at 120 °F and base at 360 °F because of the very light ammonia in the distillate and all the heavier components in the bottoms). This large temperature difference affects the control structure, as discussed in Section 14.4.

The column for the MIPA/DIPA separation is operated at 30 psia. The reflux-drum temperature at this the pressure is about 120 °F. The separation is not quite as easy as in the ammonia/MIPA system, so a column with 22 stages is used. The resulting RR required for the separation is 1.6.

The column for DIPA/water separation operates at 5 psia. The reflux-drum temperature at this pressure is about 120 °F. This separation is the most difficult of the three, so a column with 52 stages is used. The resulting RR required for the separation is 4.88.

### 14.2.3 Flowsheet

Figure 14.1 shows the flowsheet of the process. The fresh feeds of IPA and ammonia enter the process as liquids. The fresh feed flowrate of IPA is set at 100 lb-mol/h. The fresh feeds are combined with two liquid recycle streams: ammonia recycle D1 (the distillate from the column C1) and DIPA recycle D3 (the distillate from the column C3).

***Reaction Section.*** Two vapor recycle streams are also added. The first comes from a flash tank and the second comes from a vapor vent off the reflux drum in the first column. The first stream contains mostly hydrogen and ammonia, and it is compressed and recycled. The compressor suction and discharge pressures are 335 and 350 psia, respectively, so the compressor work is small.

The purpose of the vent stream from the reflux drum of the first column is to remove the small amount of hydrogen that is in the liquid feed to this column (0.05 mol%) in order to give reasonable temperatures and pressures in the condenser. The vent stream is also compressed (300 to 350 psia) and recycled.

The liquid streams are fed to a feed-effluent heat exchanger (FEHE) that recovers some energy from the hot reactor effluent stream. An overall heat-transfer coefficient of 50 Btu $h^{-1}$ $ft^{-2}$ $F^{-1}$ is assumed, which results in a heat-transfer area of 1375 $ft^2$ to transfer $4.94 \times 10^6$ Btu/h. The preheated stream is fed into a vaporizer along with the two gas recycle streams. The vaporizer operates at 345 psia and produces vapor at its dew point (308 °F), which is fed to another heat exchanger that provides the desired reactor inlet temperature $T_{in}$. As discussed in Section 14.3, the reactor inlet temperature is adjusted to give the

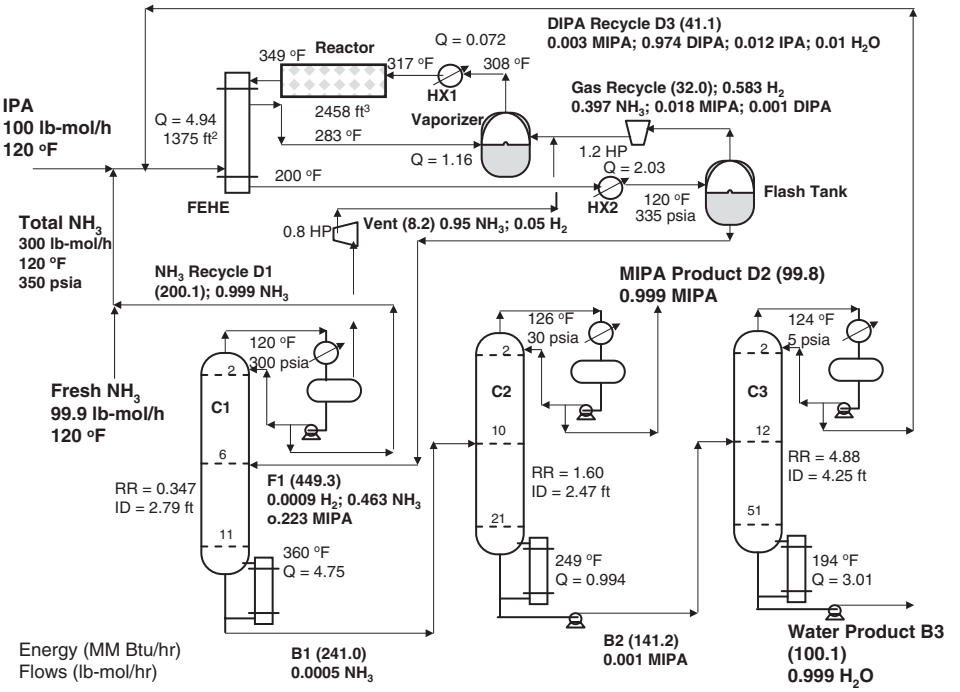


**Figure 14.1.** MIPA flowsheet.

desired conversion of IPA. The higher the inlet temperature, the higher the conversion of IPA. An Aspen *Flowsheet design spec* feature is used to give a reactor outlet component molar flowrate of IPA of 0.5 lb-mol/h (fresh IPA feed flowrate is 100 lb-mol/h). The pressure of the steam used in the vaporizer depends on the composition, and this varies in the designs with the recycle flowrates. With high ammonia recycles, low-pressure steam (100 psia) can be used. With low ammonia recycles, high-pressure steam (600 psia) must be used because the high concentration of DIPA raises the vaporizer temperature.

The reactor is a gas-phase tubular reactor operating adiabatically. Its aspect ratio $L/D$ is 10. A second Aspen *Flowsheet design spec* is used to adjust the size of the reactor to maintain a 6-min residence time. This residence time is somewhat large for a gas-phase reactor, but a high conversion of IPA is desired. The resulting reactor size is not unreasonably large (2458 $ft^3$ with diameter of 6.8 ft). The reactor contains a solid catalyst with a void fraction of 0.5 and a solid density of 200 $lb/ft^3$. The reaction is exothermic. With an inlet temperature of 317 °F, the exit temperature $T_{out}$ is 349 °F.

The reactor effluent is cooled and partially condensed in the FEHE before going to a condenser in which it is cooled to 120 °F using cooling water. The two-phase stream from the heat exchanger is fed to a flash tank. The vapor from the tank is compressed and recycled. The liquid is fed into the first distillation column (C1).

***Ammonia Recycle Column C1.*** This column has 12 stages and is fed on stage 6, which is the optimum feed stage to minimize reboiler heat input. The operating pressure is 300 psia. A partial condenser is used with a small vent stream removed from the reflux drum to keep hydrogen from suppressing the temperature in the condenser. The design specification in the condenser is a temperature of 120 °F, and the vent rate is automatically adjusted in the Aspen Plus Radfrac model to maintain this specified temperature.

There are two design specifications in this column. The first sets the ratio of the ammonia to the sum of the ammonia and the MIPA in the bottoms to 0.001. This limits the ammonia leaving in the bottoms to a small amount so that the MIPA purity in the second column can be achieved. Obtaining this ratio is achieved in the Radfrac simulation by opening the *Components* page tab in the design spec and specifying ammonia as the *Component* and specifying both ammonia and MIPA as the *Basic Components*. The distillate flowrate is the *Vary* variable for this design spec. The second design specification is a distillate impurity of 0.1 mol% MIPA. The *Vary* variable is the RR.

The case shown in Figure 14.1 is the optimum economic design, which corresponds to a total ammonia flowrate (fresh ammonia plus the distillate from C1) of 300 lb-mol/h. Under these conditions the energy consumption in the first column ($Q_{R1}$) is $4.75 \times 10^6$ Btu/h and the RR is 0.347. Column diameter is 2.79 ft. Notice that the base temperature is high (360 °F) because of the high operating pressure of the column. High-pressure steam (600 psia) is required in this reboiler. The base temperatures in the other two columns are low enough to use low-pressure steam (100 psia).

***MIPA Product Column C2.*** This column has 22 stages and is fed on stage 10. The operating pressure is 30 psia, which gives a reflux-drum temperature of 126 °F. The two design specifications are 0.05 mol% DIPA impurity in the distillate (which produces a MIPA product with 99.9 mol% purity) and 0.1 mol% MIPA impurity in the bottoms. Energy consumption ($Q_{R2}$) is $0.994 \times 10^6$ Btu/h, and the RR is 1.6. Column diameter is 2.47 ft.

***DIPA Recycle Column C3.*** This column has 52 stages and is fed on stage 12. The operating pressure is 5 psia, which gives a reflux-drum temperature of 124 °F. The two design specifications are 1 mol% water impurity in the distillate and 0.1 mol% DIPA impurity in the bottoms. Energy consumption ($Q_{R3}$) is $3.01 \times 10^6$ Btu/h, and the RR is 4.88. Column diameter is 4.25 ft. Notice that the column is operating under vacuum to maximize relative volatilities.

Theoretical trays are assumed in all distillation columns, and capital costs are not adjusted for tray efficiencies.

## 14.3 ECONOMIC OPTIMIZATION

### 14.3.1 Design Optimization Variables

This process has a large number of potential design optimization variables. The number has been greatly reduced by using a number of heuristics. The number of stages has been selected to match the degree of difficulty of the separation and balance the number of trays against RR. Column pressures have been minimized and still permit the use of cooling water in condensers. Reactor inlet temperature has been set to give a high conversion of IPA. Reactor size has been set to give a reasonable residence time. Stream compositions have been selected to provide reasonable separations and to achieve high-purity product streams (MIPA in stream D2 and water in stream B3).

The remaining important design optimization variable is the ammonia-to-IPA ratio. This is set by selecting the total ammonia flowrate that minimizes total annual cost (TAC), which is a simple economic objective function that balances capital and energy costs. Table 14.2

**TABLE 14.2 Basis of Economics and Equipment Sizing**[a]

Column diameter: Aspen Tray Sizing
Column length: NT trays with 2-ft spacing plus 20% extra length

*Condensers (area in $m^2$)*
Heat-transfer coefficient = 0.852 kW/K-$m^2$
Differential temperature = 13.9 K
Capital cost = $7296(A)^{0.65}$

*Reboilers, FEHE and preheater (area in $m^2$)*
Heat-transfer coefficient = 0.568 kW/K-$m^2$
Differential temperature = 34.8 K
Capital cost = $7296(A)^{0.65}$

*Column and reactor vessel (diameter and length in meters)*
Capital cost = $17{,}640(D)^{1.066}(L)^{0.802}$

*Energy cost*
LP steam = $\$6.08/10^6$ GJ
LP steam = $\$6.87/10^6$ GJ
LP steam = $\$9.83/10^6$ GJ

$$\text{TAC} = \frac{\text{Capital cost}}{\text{Payback period}} + \text{Energy cost}$$

Payback period = 3 yr

[a]Based on information in Luyben.[6]

gives the economic basis and equipment-sizing relationships used in the economic calculations. Notice that the cost of energy is different for the different units and for different cases. High-pressure steam is used in the reboiler of the ammonia column and in the reactor preheater (HX1) in all cases. Low-pressure steam is used in the other reboilers in all cases. The vaporizer uses high-pressure steam for the low ammonia recycle cases (150 and 200 lb-mol/h total ammonia) because the high concentration of DIPA produces a high vaporizer temperature. For the medium ammonia recycle case (300 lb-mol/h total ammonia), medium-pressure steam can be used. For the high ammonia recycle cases (>400 lb-mol/h total ammonia), low-pressure steam can be used.

### 14.3.2 Optimization Results

Figure 14.2 shows how several important variables change as the ammonia recycle is varied. The top graph on the left shows there is an optimum value for the total ammonia fed to the reactor of 300 lb-mol/h that minimizes TAC. This occurs because of the opposite effects of total ammonia on distillate D1 from the ammonia column and distillate D3 from the DIPA recycle column. Distillate D1 increases directly with total ammonia recycle. Distillate D3 *decreases* as total ammonia recycle increases. Results for the optimum case are shown in Figure 14.1. Details of equipment sizes and parameter values for this case are given in Table 14.3.

Figure 14.3 gives the temperature and composition profiles in the reactor. Figure 14.4 gives the temperature and composition profiles in the ammonia column, C1. Figures 14.5 and 14.6 give the profiles for C2 and C3.

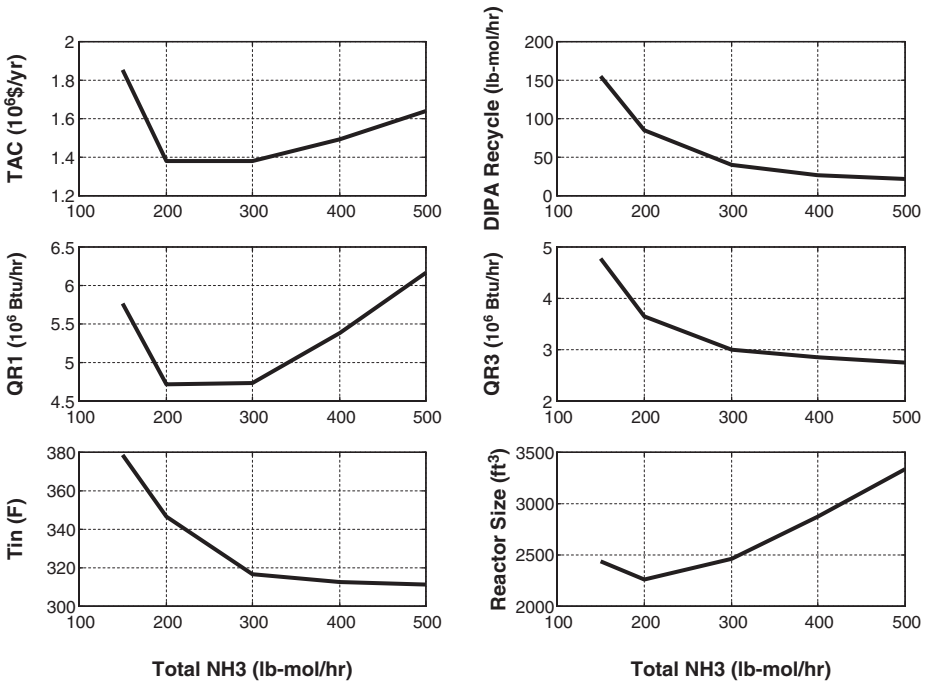


**Figure 14.2.** Effect of ammonia recycle.

**TABLE 14.3 Equipment Sizes and Variables for Optimum Case[a]**

| | | C1 | C2 | C3 | |
|---|---|---|---|---|---|
| NT/NF | | 12/6 | 22/10 | 52/12 | |
| ID | ft | 2.79 | 2.47 | 4.26 | |
| $Q_C$ | $10^6$ Btu/h | 2.12 | 2.95 | 3.46 | |
| $Q_R$ | $10^6$ Btu/h | 4.73 | 0.991 | 4.01 | |
| $A_C$ | $ft^2$ | 578 | 716 | 906 | |
| $A_R$ | $ft^2$ | 753 | 158 | 479 | |
| Vessel cost | $10^6$ $ | 0.0732 | 0.112 | 0.418 | |
| Heat exchangers | $10^6$ $ | 0.213 | 0.154 | 0.216 | |
| Energy | $10^6$ $/yr | 0.430 | 0.0557 | 0.169 | |
| Total capital cost | $10^6$ $ | 0.286 | 0.266 | 0.634 | |
| | | FEHE | Vaporizer | HX1 | HX2 |
| $A$ | $ft^2$ | 1375 | 185 | 11.5 | 532 |
| $Q$ | $10^6$ Btu/h | 4.94 | 1.16 | 0.072 | 2.03 |
| Capital cost | $10^6$ $ | 0.179 | 0.0464 | 0.00768 | 0.0928 |
| Energy | $10^6$ $/yr | 0 | 0.0740 | 0.00654 | 0 |
| | | Reactor | | | |
| Volume | $ft^3$ | 2458 | | | |
| Diameter | ft | 6.80 | | | |
| Capital cost | $10^6$ $ | 0.417 | | | |

Total capital cost = $1.94 \times 10^6$ $.
Total energy = $0.734 \times 10^6$ $/yr.
Total annual cost = $1.38 \times 10^6$ $/yr.
[a]TOTNH3 = 300 lb-mol/h.

The selection of the number of trays in the columns has been made heuristically based on the degree of difficulty of the separation. The largest column in terms of capital investment is the DIPA recycle column (C3) with 52 stages. To justify this selection, a number of cases were run with different numbers of trays. Table 14.4 gives results for columns having from 22 to 52 stages. The feed to the column is the bottoms from C2 for the case with 300 lb-mol/h of total ammonia. The distillate and bottoms streams have exactly the same compositions for all designs, but the equipment sizes and energy consumptions change. As more stages are added, capital cost increases but energy cost decreases. The economic optimum design is a 42-stage column. However, the TAC of the 52-stage column is less than 2% larger than that of the optimum 42-stage column. Distillation wisdom suggests that several additional trays should be added to improve dynamic controllability and the ability to handle changing process conditions. Therefore a 52-stage column is used in this study.

## 14.4 PLANTWIDE CONTROL

The first step in studying dynamics using a pressure-driven dynamic simulation is to add pumps and control valves and to size all column bases and reflux drums.

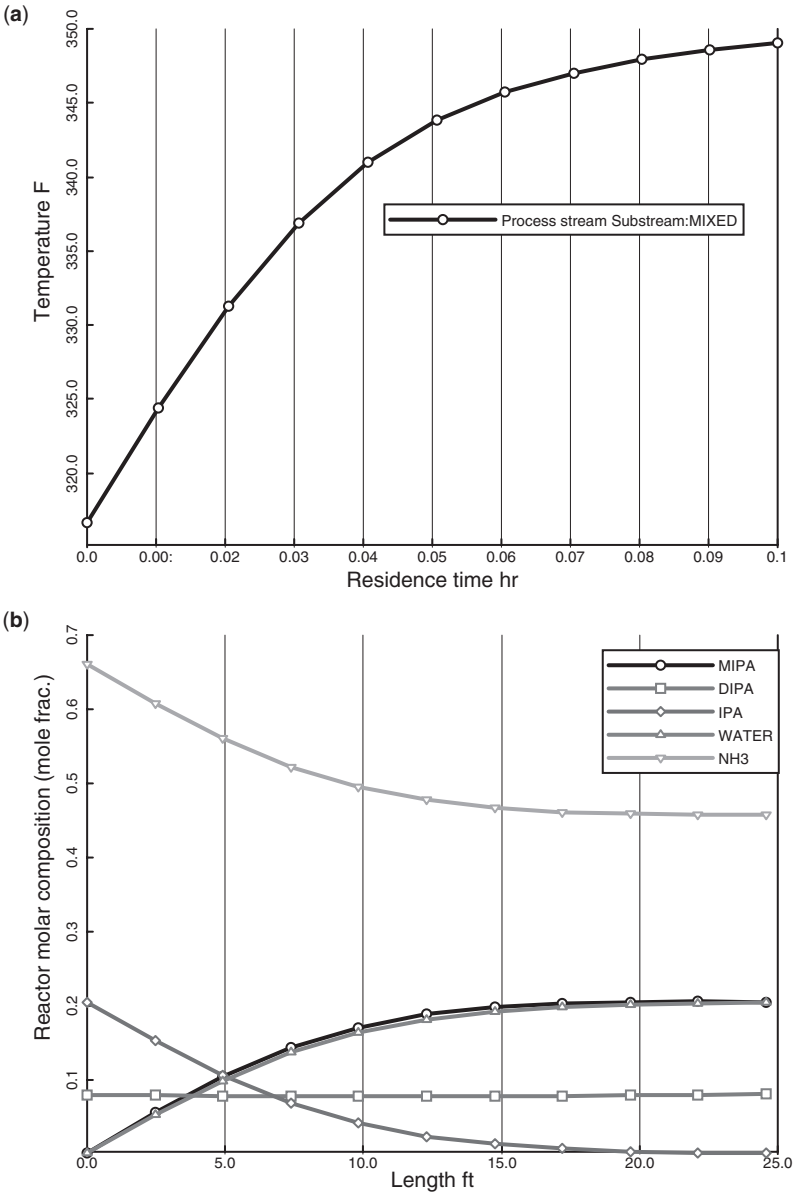


**Figure 14.3.** (a) Reactor temperature profile, (b) reactor composition profiles.

### 14.4.1 Dynamic Model Sizing

Pumps and control valves are inserted into the flowsheet, as shown in Figure 14.7. A pressure-driven simulation is used in order to study realistic control limitations and performance. Control valve pressure drops at design conditions are about 50 psi, and pump heads are selected to provide these pressure drops. Reflux drums, column bases, the vaporizer, and the flash drum are sized to provide 5 min of holdup at 50% level.

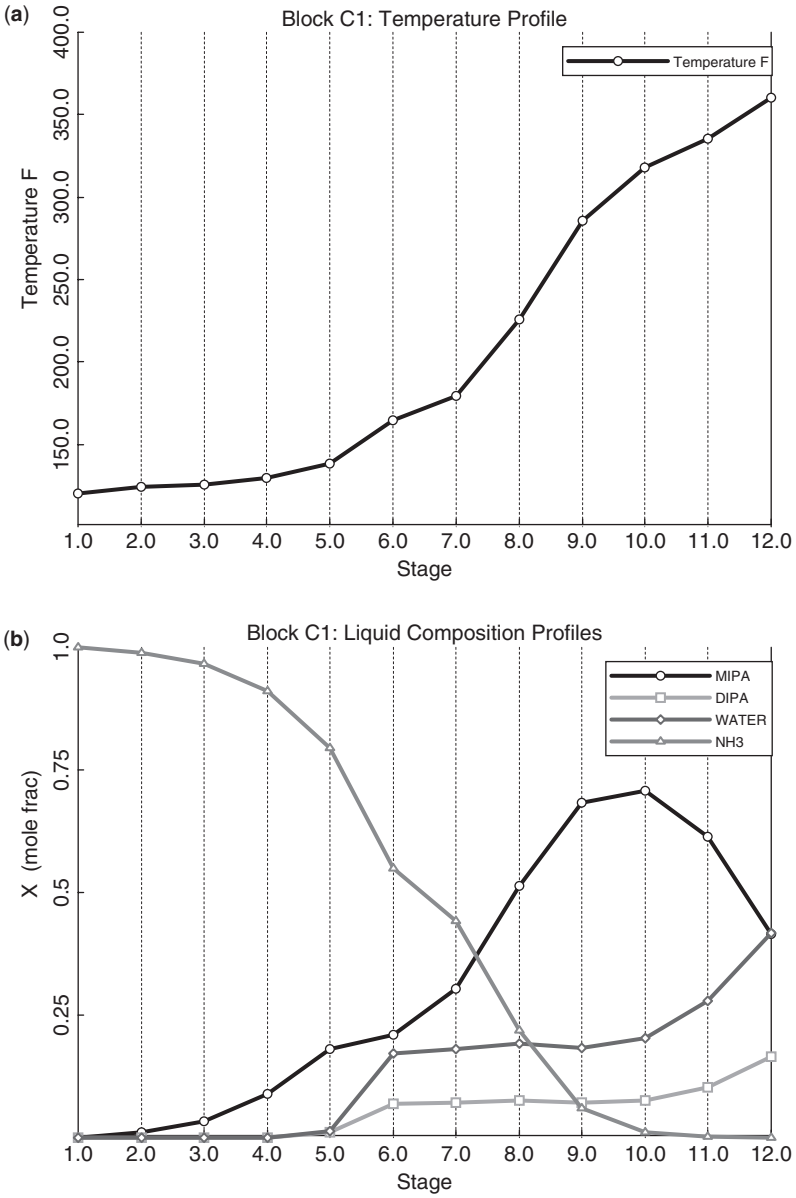


**Figure 14.4.** (a) Column C1 temperature profile, (b) column C1 composition profiles.

The tube side and shell side volumes of the FEHE are calculated using the heat-transfer area of 1375 $ft^2$ and assuming 2-inch tubes that are 10 ft in length. The tube volume is 575 $ft^3$ in 263 tubes. Shell volume is assumed equal to tube volume.

### 14.4.2 Distillation Column Control Structures

Most practical distillation column control structures use some sort of single-end control instead of the theoretically optimum dual-composition control. Typically, an industrial

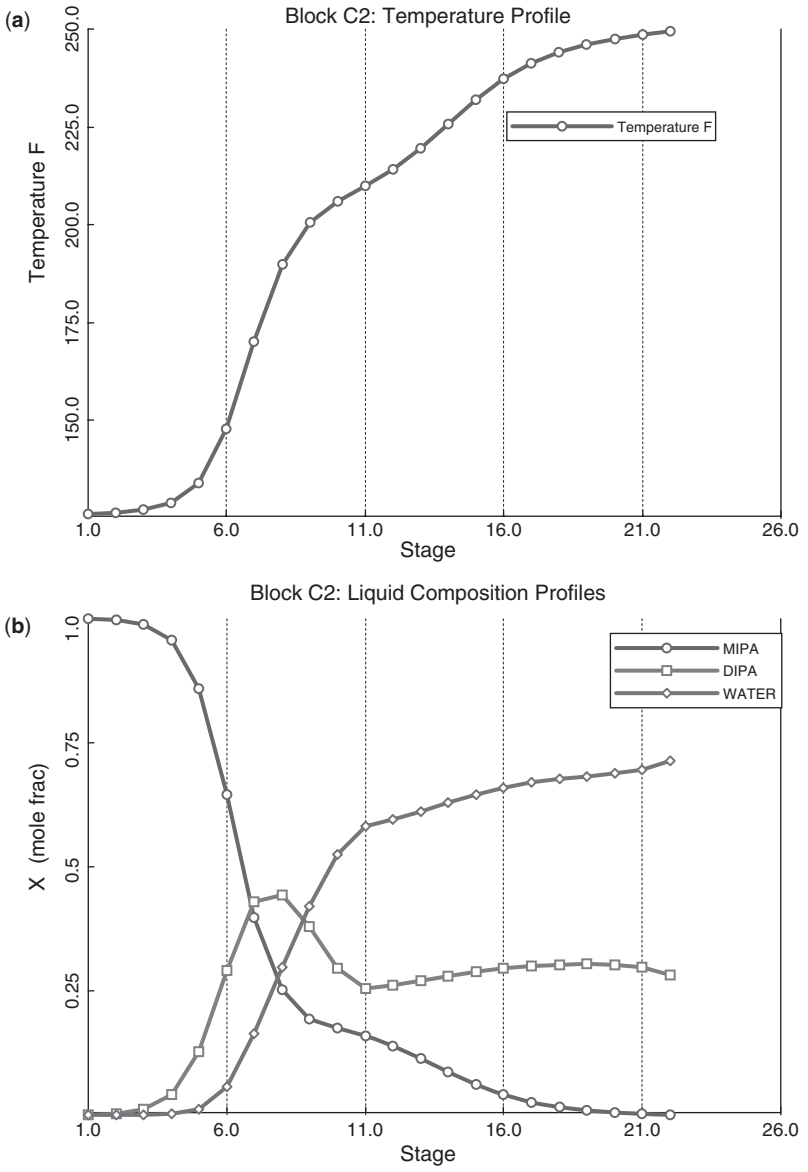


**Figure 14.5.** (a) Column C2 temperature profile, (b) column C2 composition profiles.

column controls a single tray temperature by manipulating reboiler heat input. The remaining control degree of freedom is satisfied by setting either a R/F ratio of a RR. However, there are columns that require dual-end control schemes to handle disturbances. The first thing to do is to explore if single-end control may be effective or not, and if so, which ratio scheme is better.

This can be accomplished by generating some steady-state results in Aspen Plus to see how reflux and RR must change to maintain products purities in the face of feed composition disturbances. The two *design spec/vary* are activated in each column, and the feed composition is varied over a range around the design feed composition. The required changes

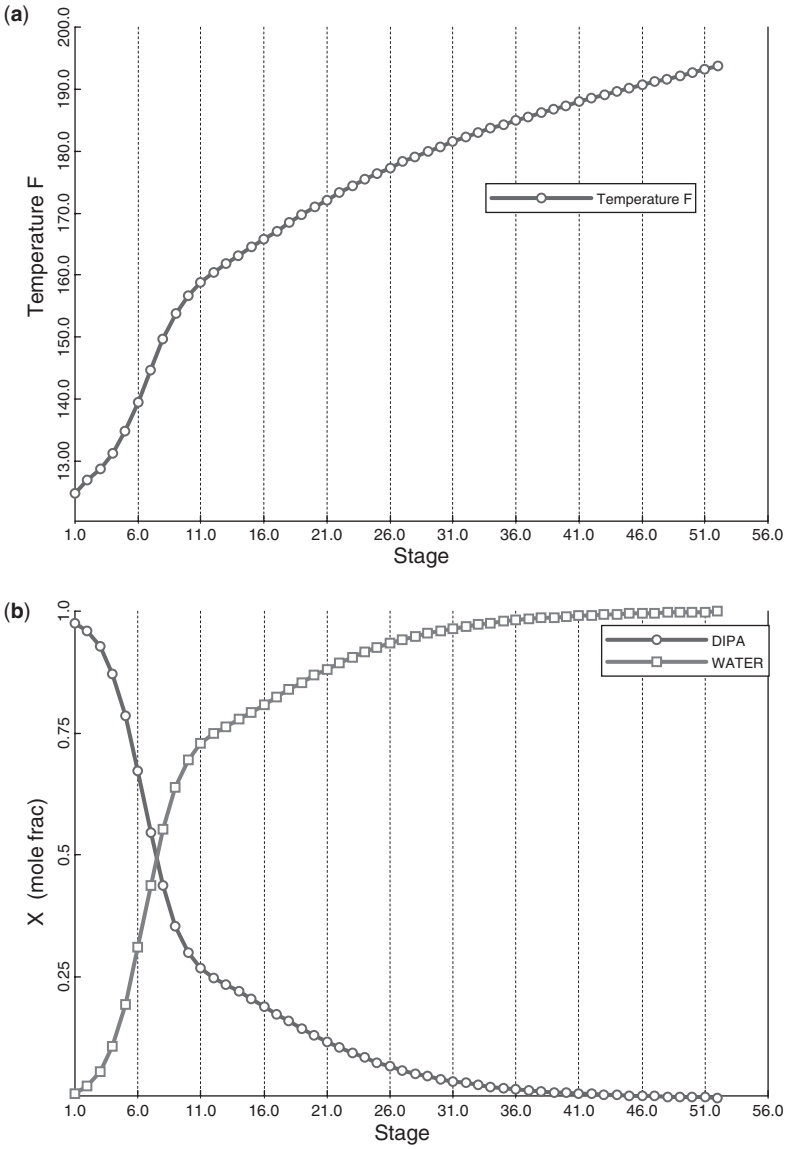


**Figure 14.6.** (a) Column C3 temperature profile, (b) column C3 composition profiles.

in reflux flowrate and RR are recorded. If the changes in one of these is small, single-end control may be effective.

Table 14.5 gives the results of these calculations for the three columns. The required changes in R/F are fairly small for C1 and C2, so a control structure that holds a single tray temperature and maintains a fixed R/F may work well for these columns.

Column C3 is quite different. Here the change in R/F is very large, so the RR structure may be better. However, the changes in RR are also fairly large, so a dual-end control structure may be required in this column. These alternative structures are explored in Section 14.4.3.

**TABLE 14.4 Economics of Column C3**

| | | | | | |
|---|---|---|---|---|---|
| NT3 | | 22 | 32 | 42 | 52 |
| $NF_{opt}$ | | 9 | 11 | 12 | 12 |
| ID | ft | 6.16 | 4.72 | 4.39 | 4.26 |
| $Q_C$ | MM Btu/h | 7.04 | 4.22 | 3.67 | 3.46 |
| $Q_R$ | MM Btu/h | 6.56 | 3.76 | 3.21 | 3.00 |
| $A_C$ | $ft^2$ | 1842 | 1106 | 960 | 906 |
| $A_R$ | $ft^2$ | 1044 | 598 | 511 | 479 |
| Shell | $10^3$ \$ | 297 | 310 | 361 | 418 |
| Heat exchangers | $10^3$ \$ | 349 | 248 | 225 | 216 |
| Total capital | $10^3$ \$ | 646 | 557 | 586 | 634 |
| Energy | $10^3$ \$/yr | 369 | 211 | 280 | 169 |
| **TAC** | $10^3$ \$/yr | 584 | 398 | **375** | 381 |

It is interesting to note that the changes in R and RR are not monotonic with feed composition $z$. Reflux flowrates and RRs are sometimes higher at both ends of the feed composition range than at the design value.

The location of the tray with the temperature that should be controlled can be determined by looking at the column temperature profiles and seeing where a temperature break occurs (large changes in temperature from tray to tray). In Column C1 (Figure 14.4a) there is only one break location, and stage 10 is selected. In Column C2 (Figure 14.5a) the largest break occurs in the rectifying section, which is fortunate because the MIPA product is the distillate stream. Stage 6 is selected.

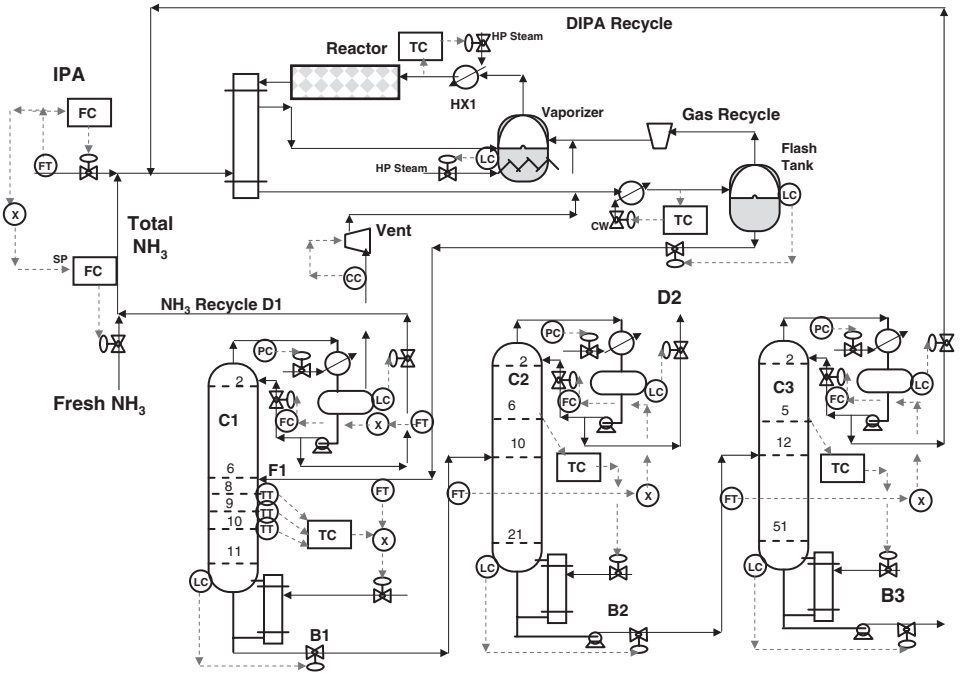


**Figure 14.7.** Plantwide control structure.

**TABLE 14.5 Effect of Feed Composition on R/F and RR**

| | | | R | RR |
|---|---|---|---|---|
| C1 | LK/HK | NH3/MIPA | | |
| | Design $z_{LK/HK}$ | 0.464/0.223 | 71.96 | 0.3449 |
| | Plus LK | 0.414/0.273 | 72.57 | 0.3898 |
| | Minus LK | 0.494/0.193 | 70.71 | 0.3183 |
| | % Change | | **4.3** | 26 |
| C2 | LK/HK | MIPA/DIPA | | |
| | Design $z_{LK/HK}$ | 0.414/0.167 | 159.3 | 1.598 |
| | Plus LK | 0.464/0.117 | 169.2 | 1.515 |
| | Minus LK | 0.364/0.217 | 169.0 | 1.930 |
| | % Change | | **6** | 26 |
| C3 | LK/HK | DIPA/H2O | | |
| | Design $z_{LK/HK}$ | 0.284/0.711 | 201.3 | 4.896 |
| | Plus LK | 0.334/0.661 | 272.1 | 5.640 |
| | Minus LK | 0.234/0.761 | 209.8 | 6.174 |
| | % Change | | 35 | **11** |

Column C3 (Figure 14.6a) has only one temperature break, which is in the rectifying section. However, the water product comes out the bottoms. So, controlling a temperature high in the column may not be effective. Also, remember that this is a vacuum column, so the temperature changes from tray to tray are significantly affected by pressure changes. Notice the almost linear changes in temperature in the stripping section.

In the next section, we will explore several alternative control structures for C3 because its inherent characteristics indicate difficulty in control.

### 14.4.3 Plantwide Control Structure

***Initial Control Structure.*** A plantwide control structure is shown in Figure 14.7. The various loops are listed below with their controlled and manipulated variables.

1. Fresh IPA feed is flow-controlled. This is the throughput handle. This fresh feed can be flow-controlled because the per-pass conversion of this reactant is very high (see Luyben[3]).
2. Total ammonia (fresh feed plus ammonia recycle D1 from column C1) is ratioed to the IPA flowrate. The fresh feed of ammonia is manipulated to hold the total flowrate of ammonia.
3. Vaporizer level is controlled by vaporizer heat input. There is no liquid outlet stream.
4. Reactor inlet temperature is controlled by heat input to HX1.
5. Temperature leaving the condenser, HX2, is controlled by heat removal.
6. Pressures in all columns are controlled by condenser heat removal.
7. Base levels in all columns are controlled by bottoms flowrates.
8. Reflux drum levels in all columns are controlled by distillate flowrates.
9. Reflux flowrates are ratioed to column feed flowrates in all columns. Several alternatives for column C3 will be discussed later.

10. An average temperature is controlled in column C1 by manipulating reboiler heat input. This structure is used because of the large temperature change over the column( see Luyben[6]). Temperatures on stages 8, 9, and 10 are measured and averaged. Notice that this average temperature is displayed in degrees Celsius since Aspen Dynamics uses metric units. The alternative of ratioing the reboiler heat input to the feed flowrate with the ratio reset by the temperature controller will be discussed later.
11. Hydrogen composition in the vent stream is controlled by manipulating compressor power.
12. Single temperatures in C2 (stage 6) and C3 (stage 5) are controlled by manipulating reboiler heat inputs.

All liquid level controllers are proportional-only using $K_c = 2$. There is one exception to this tuning, which is the reflux-drum level in recycle column C3. The tuning of this level controller will be discussed later. Column temperature loops contain 1-min deadtimes and are tuned using relay-feedback tests and Tyreus-Luyben tuning rules. Table 14.6 gives controller tuning parameters for various cases.

The solid lines in Figure 14.8 give results for column C1 with a very small (5%) increase in the setpoint of the IPA flow-controller. Stable regulator control is achieved with the ammonia impurity in the bottoms and the MIPA impurity in the distillate returned close to their desired levels. However, there is a very large transient drop in the average temperature of over 10 °C for about an hour, which causes a large temporary increase in the ammonia impurity in the bottoms (peaks at over twice the desired value) even for this small increase in throughput. Clearly, this initial structure needs modification to improve the effectiveness of control. In the next section, a straightforward change is made to provide better dynamic regulation.

***Modified Control Structure for C1.*** The transient problem can be greatly improved by using a feedforward ratio scheme. The reboiler heat input $Q_{R1}$ is ratioed to the feed to column $F_1$. The average temperature controller changes this ratio. The output signal from the temperature controller is the $Q_{R1}/F_1$ ratio.

Despite the base units of measure used in any simulation, Aspen Dynamics uses metric units in its calculations. Therefore the $Q_{R1}/F_1$ ratio must be in terms of GJ/h for heat input and kmol/h for flowrate. The steady-state value of heat input $Q_{R1}$ is $4.75 \times 10^6$ Btu/h (5.077 GJ/h), and the feed flowrate is 451 lb-mol/h (250.6 kmol/h), giving a ratio of 0.02438. Of course, the tuning constants for the temperature controller change with this new structure (see Table 14.6).

The dashed lines in Figure 14.8 give results for a 5% increase in IPA feed flowrate with the $Q_{R1}/F_1$ ratio. The peaks in the temperature and ammonia impurity deviations are greatly reduced.

The dotted lines in Figure 14.8 give results for a much larger 20% increase in IPA feed flowrate. The transient deviations naturally increase for this big disturbance, but stable regulatory control is attained with column specifications held close to their desired values.

Figure 14.9 shows how variables in all sections of the process respond to a 20% increase in IPA feed flowrate. Figure 14.9a gives results for the reaction section. As IPA increases, the ratio structure increases the flowrate of the total ammonia, which is achieved by manipulating the fresh ammonia feed flowrate. The left middle graph shows that the fresh ammonia peaks

**TABLE 14.6 Controller Parameters**

| | Ammonia Column (C1) | | Product Column (C2) | Recycle Column | | | |
|---|---|---|---|---|---|---|---|
| | | | | C3 (R/F) | C3 (RR) | C3 (dual) | C3 (dual) |
| | TC1 Average | TC1 Average | TC2 | TC3 | TC3 | TC3 | CC3 |
| SP | 135.7 °C | 135.7 °C | 150 °F | 134.8 °F | 134.8 °F | 134.8 °F | 0.0425 DIPA |
| Transmitter range | 100–200 °C | 100–200 °C | 100–200 °F | 100–200 °F | 100–200 °F | 100–200 °F | 0–0.1 DIPA |
| OP | $4.75 \times 10^6$ Btu/h | 0.0248 $Q_{R1}/F_1$ GJ/kmol | $0.994 \times 10^6$ Btu/h | $3.01 \times 10^6$ Btu/h | $3.01 \times 10^6$ Btu/h | 19,600 lb/h reflux | $3.01 \times 10^6$ Btu/h |
| OP range | $0–9.46 \times 10^6$ Btu/h | 0–0.1 | $0–1.99 \times 10^6$ Btu/h | $0–6.03 \times 10^6$ Btu/h | $0–6.03 \times 10^6$ Btu/h | 0–40,000 lb/h | $0–6.03 \times 10^6$ Btu/h |
| Deadtime | 1 min | 1 min | 1 min | 1 min | 1 min | 1 min | 5 min |
| $K_C$ | 0.20 | 0.11 | 0.43 | 3.6 | 3.4 | 2.3 | 0.20 |
| $\tau_I$ (min) | 16 | 16 | 24 | 29 | 26 | 17 | 46 |

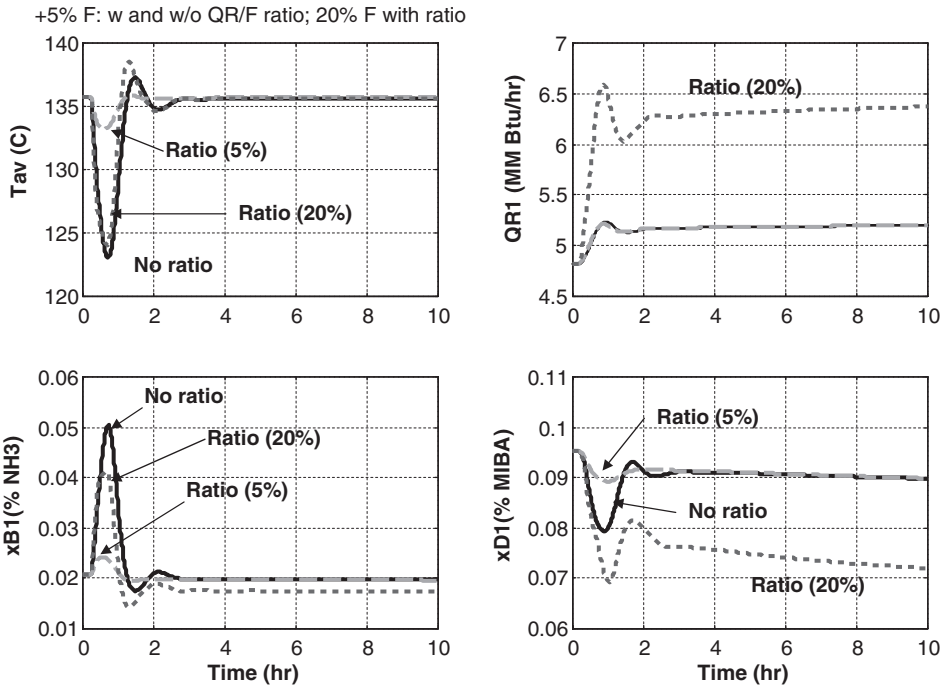


**Figure 14.8.** Effect of steam-to-feed ratio.

up to about 150 lb-mol/h before leveling out at the new steady-state value of 120 lb-mol/h, which is necessary to satisfy the stoichiometry of the reaction (every mole of IPA consumes one mole of ammonia).

Figure 14.9b shows how variables in column C1 change for this disturbance. The feed to column $F_1$ increases about 20%, as does the distillate D1 and bottoms B1 flowrates. The reflux is ratioed to the feed flowrate. The average temperature controller adjusts the $Q_{R1}/F_1$ ratio. The new steady-state reboiler duty is about 35% larger than the initial duty for the 20% increase in throughput. Notice that the vent increases to maintain the hydrogen composition in the vent.

Figure 14.9c shows how variables in column C2 change. The feed to the column $F_2$ increases more slowly than that to C1 because of the upstream proportional level controllers. The reflux is ratioed to the feed flowrate. The temperature controller increases reboiler heat input $Q_{R2}$. The purity of the MIPA distillate product $x_{D2(MIPA)}$ is held very close to the desired specification. There is a temporary increase in the MIPA impurity $x_{B2(MIPA)}$ in bottoms B2. This will go overhead in the next column and appear in the recycle stream D3.

Figure 14.9d gives results for column C3. Remember that an R/F ratio structure has been used, despite the analysis that indicated it would not be too effective. The simulation results confirm this prediction. The second and third graphs on the right show that the bottoms water purity is not maintained. The DIPA impurity in this stream increases from the desired 0.1 mol% to over 0.25 mol%. Clearly, the control structure for column C3 needs to be modified to maintain the purity of the bottoms water product and prevent the loss of DIPA.

***Modified Control Structures for C3.*** Our earlier analysis indicated that holding an RR instead of an R/F ratio would be better for the separation in C3. Figure 14.10 shows this

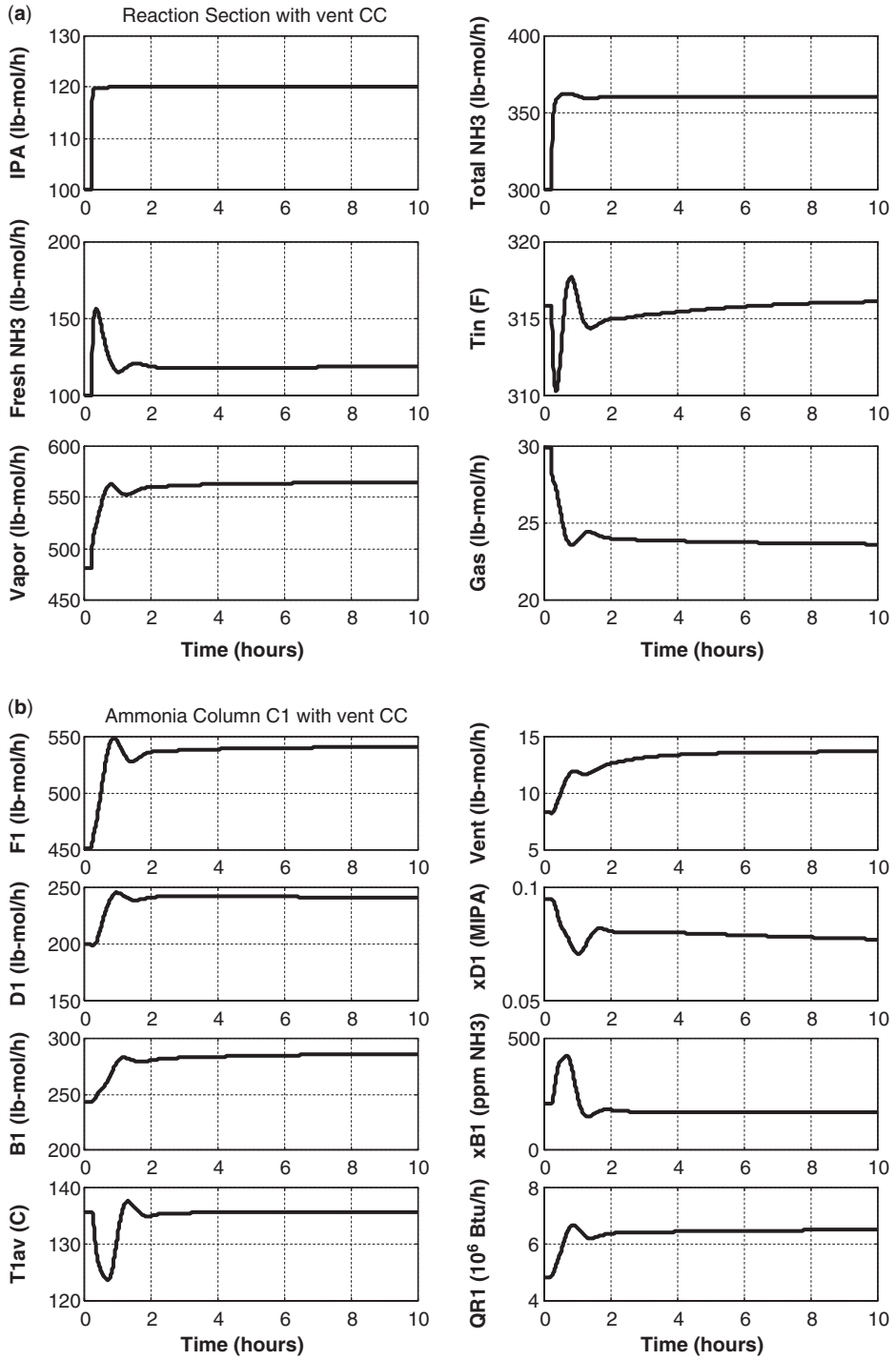


**Figure 14.9.** (a) Reaction section, (b) column C1.

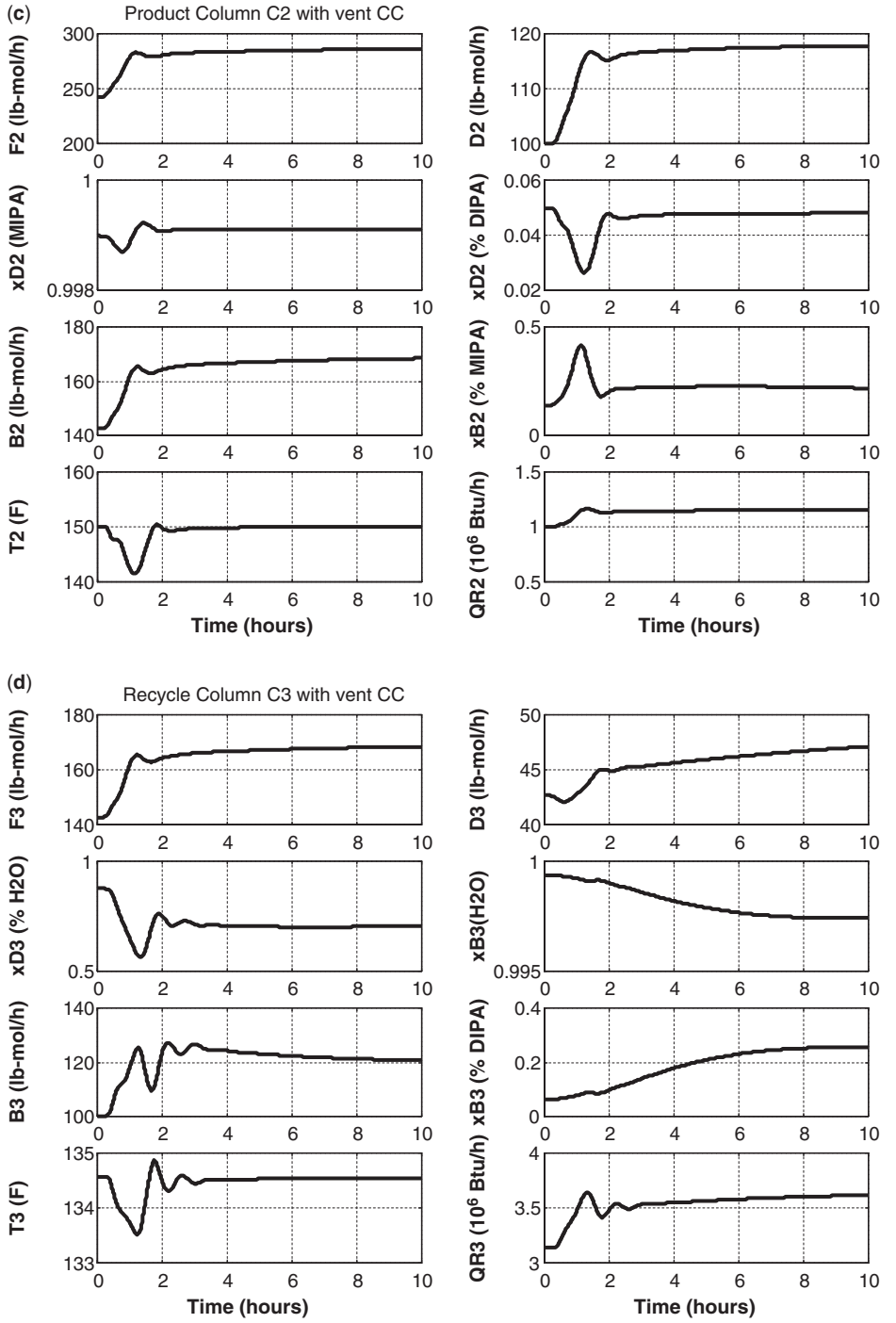


**Figure 14.9.** (*Continued*). (c) Column C2, (d) column C3.

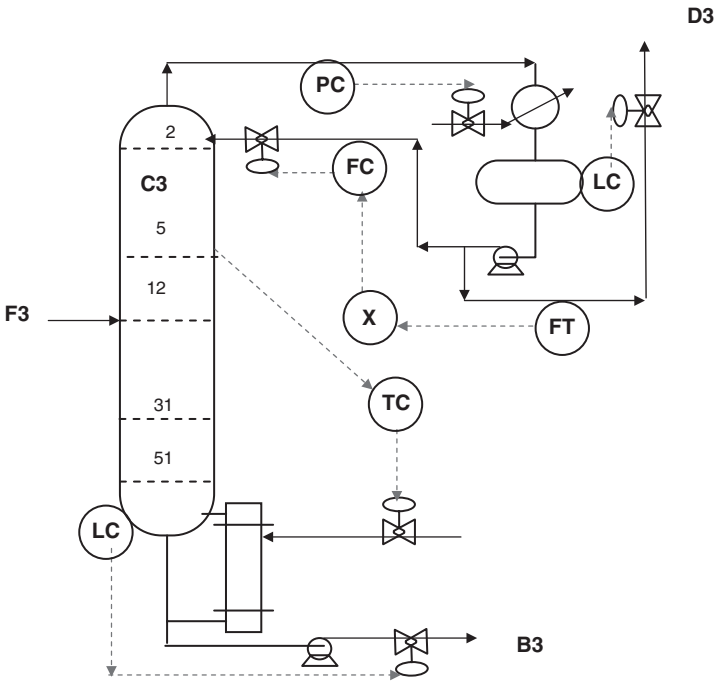


**Figure 14.10.** Reflux ratio control structure.

alternative structure. Results for the R/F and RR structures are compared in Figure 14.11. The solid lines are the R/F results. The dashed lines are the RR results. Somewhat surprisingly, the RR results are much worse than the R/F results. In fact, it appears that this structure leads to an unworkable plantwide system. The DIPA recycle stream D3 keeps slowly decreasing over the 10-h simulation time as more and more DIPA is lost in the water product.

It is clear that neither of these structures provides effective control, so a dual-end control scheme is tested. Figure 14.12 shows a structure in which stage 5 temperature is controlled by reflux flowrate and the composition DIPA on stage 31 is controlled by reboiler duty. We could try to directly control the DIPA concentration in the bottoms, but this is a high-purity separation. The desired bottoms impurity is 0.1 mol% DIPA. The response of the bottoms composition would be very nonlinear and present difficult control problems.

Distillation control wisdom suggests that it is much better to control a composition at an intermediate tray where the composition of DIPA is not so small and the responses are much more linear. Stage 31 where the DIPA composition has built up to 4.25 mol% is selected (see Figure 14.6b).

The two loops interact in this dual-end structure, so loop interaction must be taken into account. A practical way to achieve this is to use a sequential tuning approach. Since a 1-min deadtime is used in the temperature loop and a 5-min deadtime is used in the composition loop, the T5-to-R loop is tuned first with a fixed reboiler heat input. Then the temperature loop is placed on automatic, and the composition loop is tuned. Table 14.6 gives tuning results.

Dynamic responses for column C3 (the dotted lines) using the dual-end structure are compared with other structures in Figure 14.11. Effective control is achieved with both products

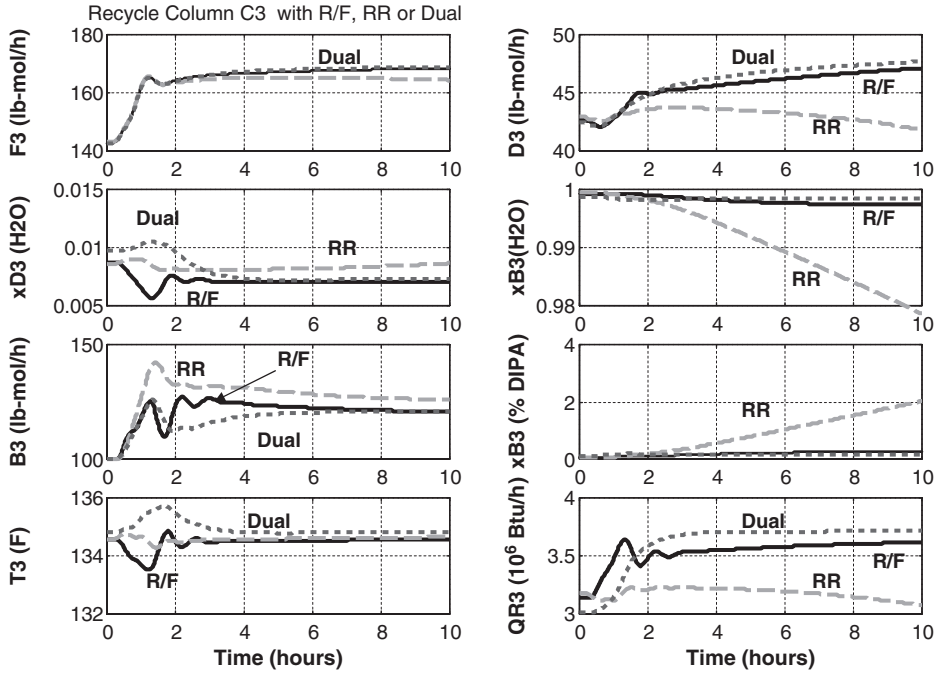


**Figure 14.11.** Comparison of alternative C3 control structures.

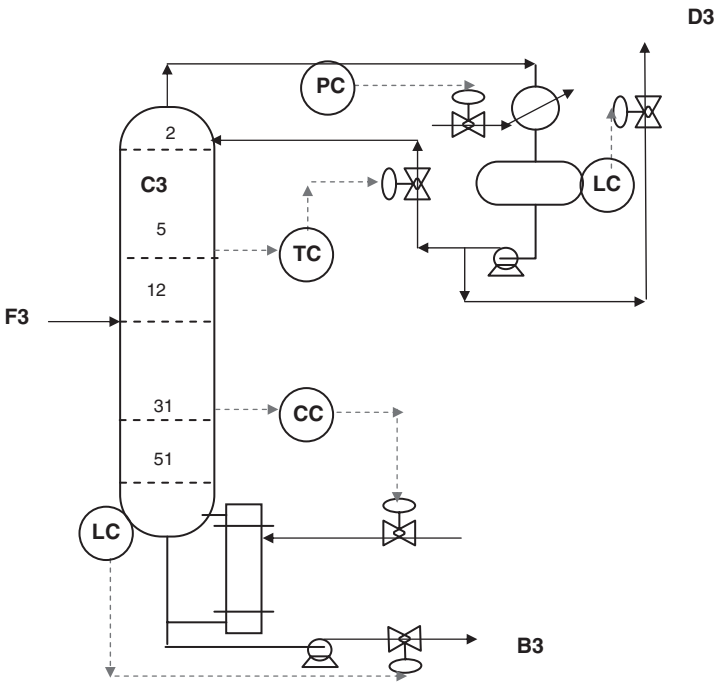


**Figure 14.12.** Dual-end control structure.

held close to their specifications. The Aspen Dynamics implementation of the final plant-wide control structure is given in Figure 14.13a, and controller faceplates are shown in Figure 14.13b. Notice that the total ammonia flow-controller ($FC_{tot}$) is on cascade.

Figure 14.14 gives results for the entire process for positive (solid lines) and negative (dashed lines) disturbances in the IPA flowrate. Figure 14.14a shows variables in the reaction section. The control structure effectively handles these large disturbances. Notice that the

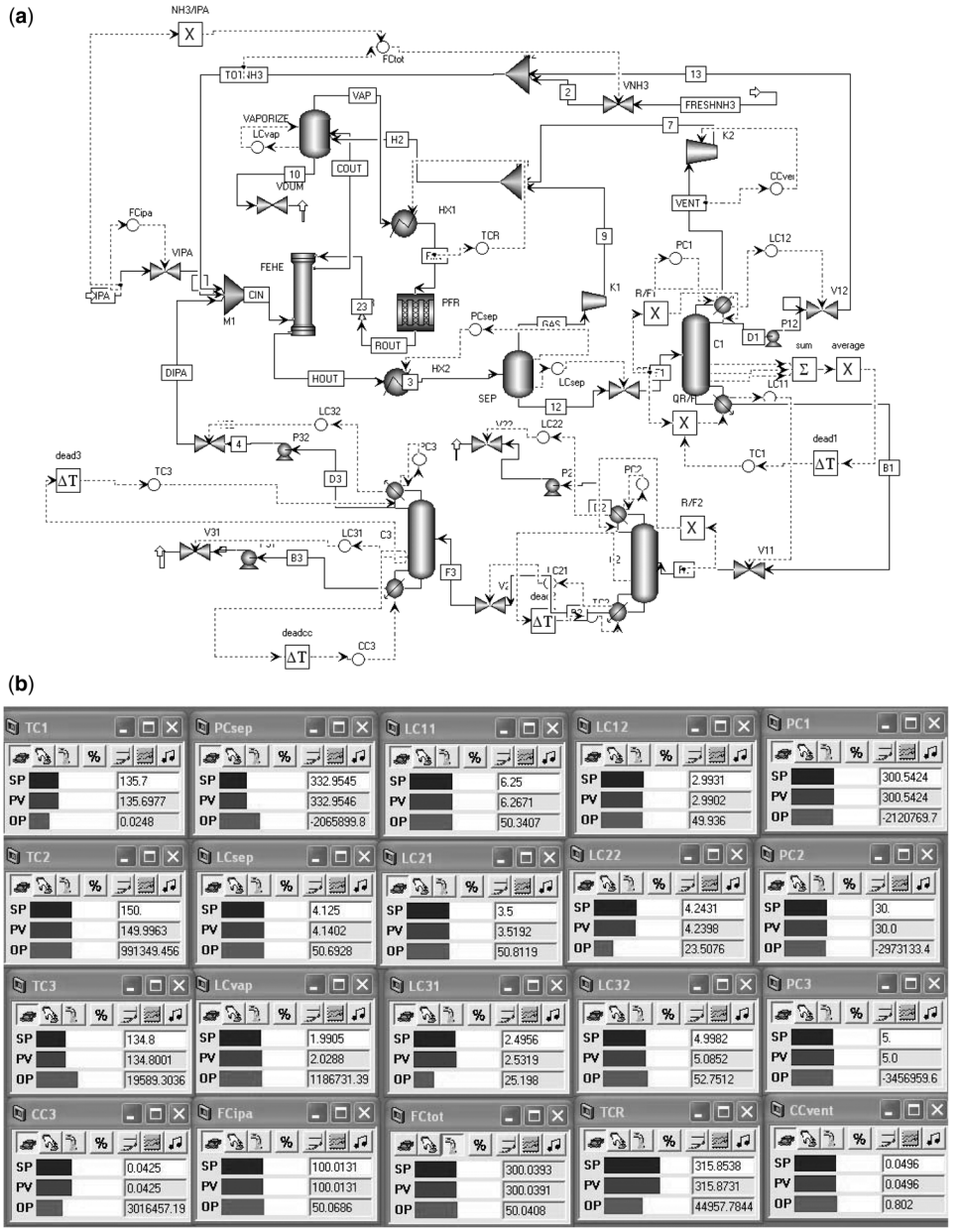


**Figure 14.13.** (a) Aspen Dynamics flowsheet, (b) controller faceplates.

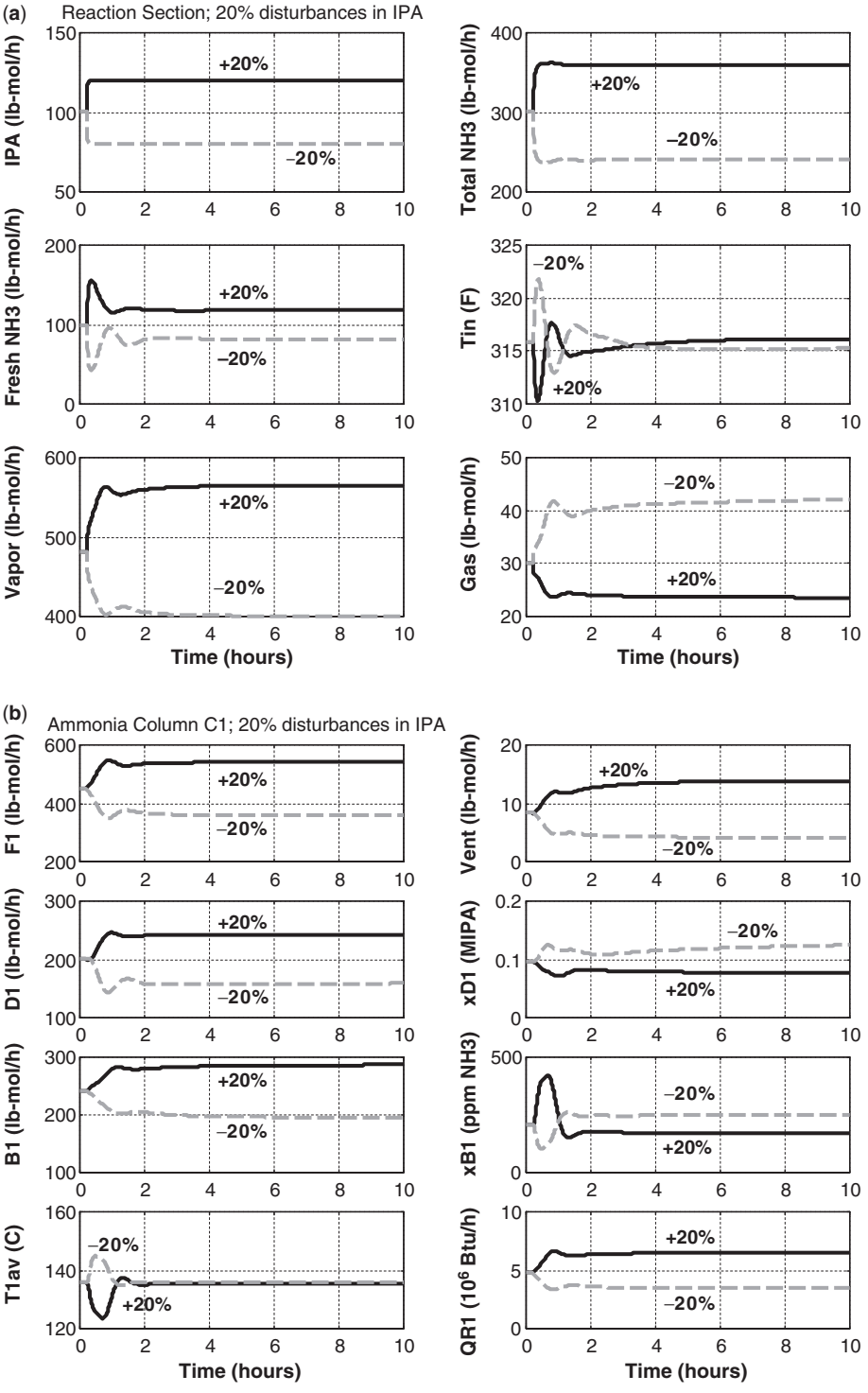


**Figure 14.14.** 20% disturbance in IPA (a) reaction section, (b) column C1.

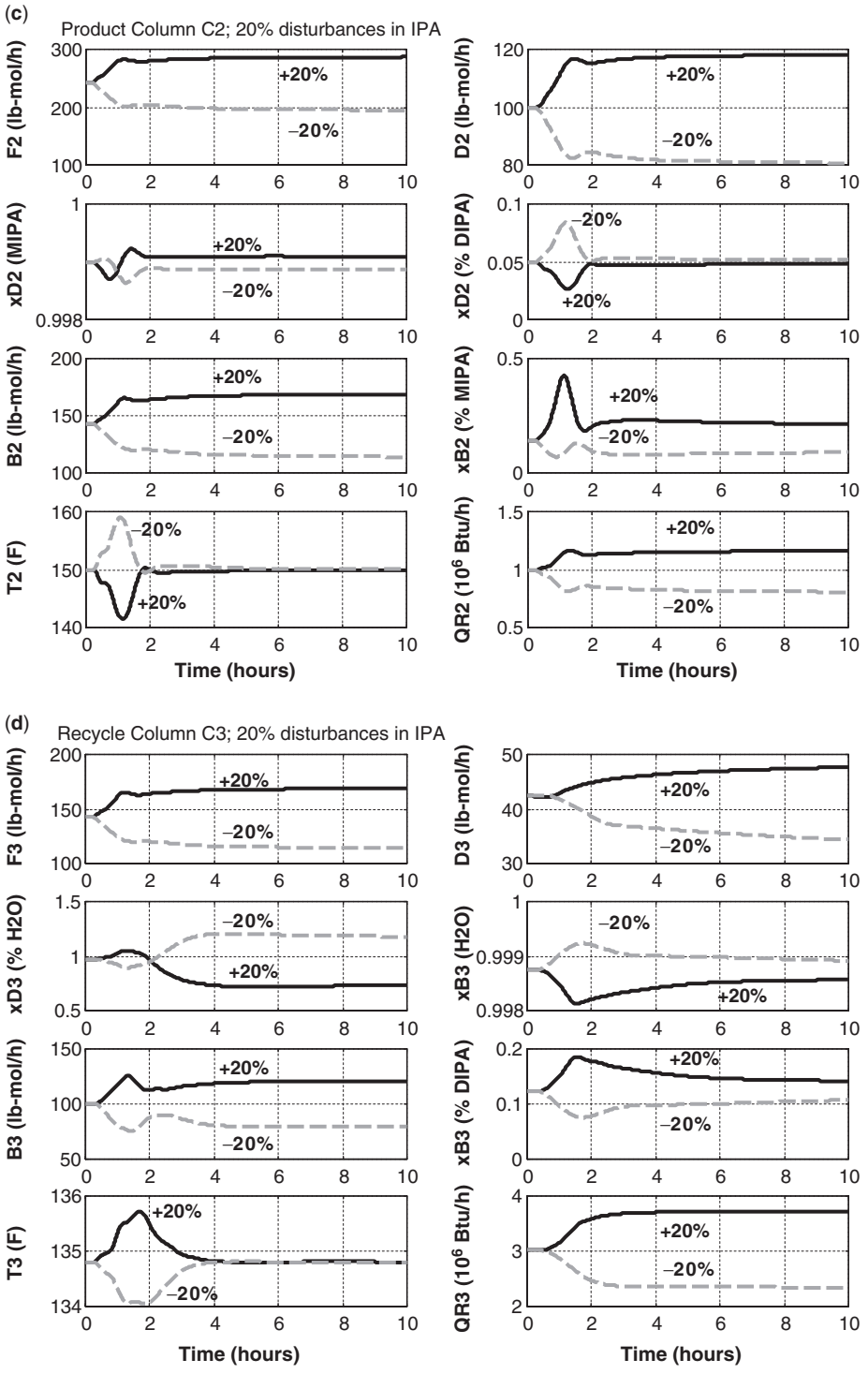


**Figure 14.14.** (*Continued*). (c) Column C2, (d) column C3.

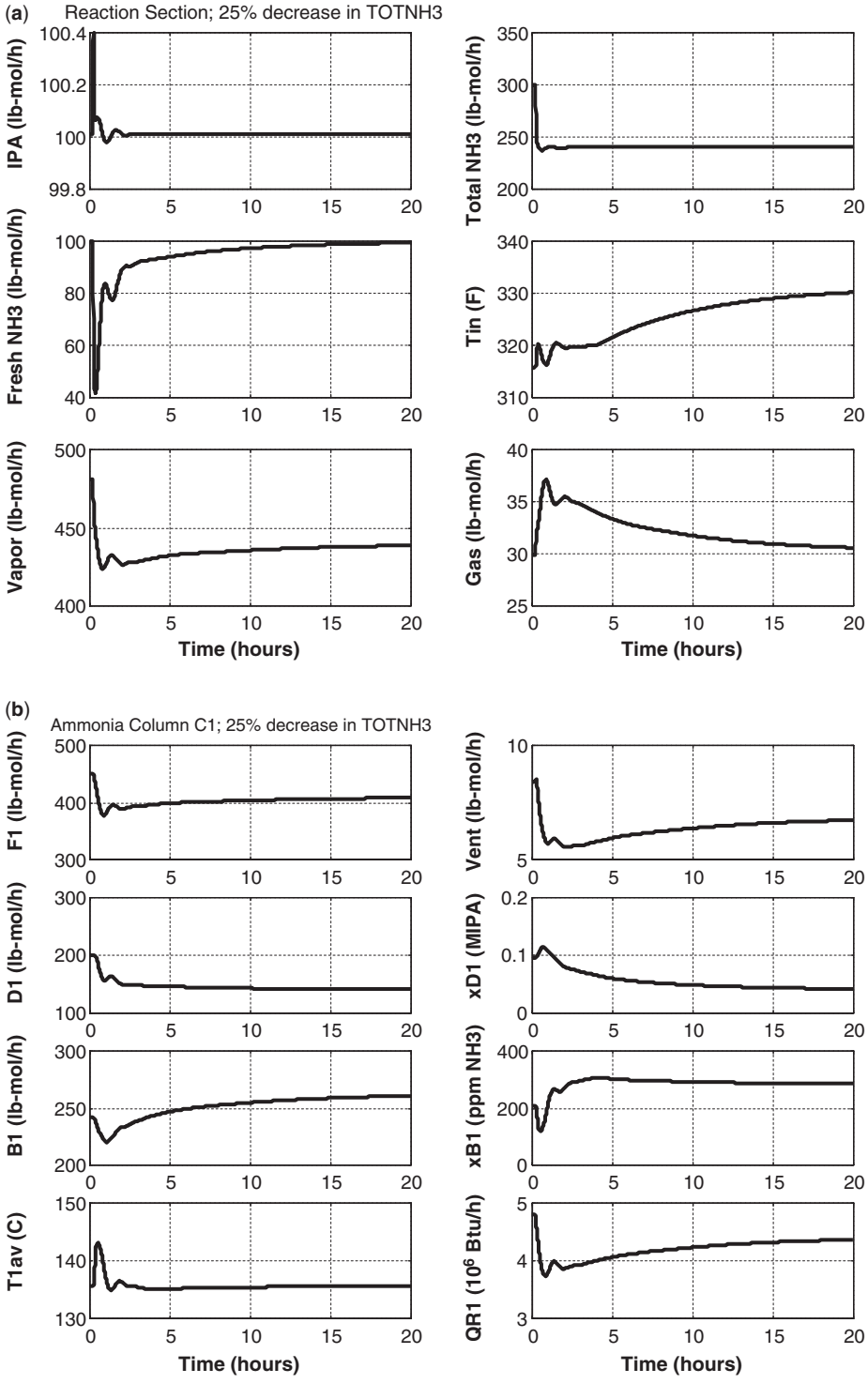


**Figure 14.15.** 25% decrease in total $NH_3$-to-IPA ratio (a) reaction section, (b) column C1.

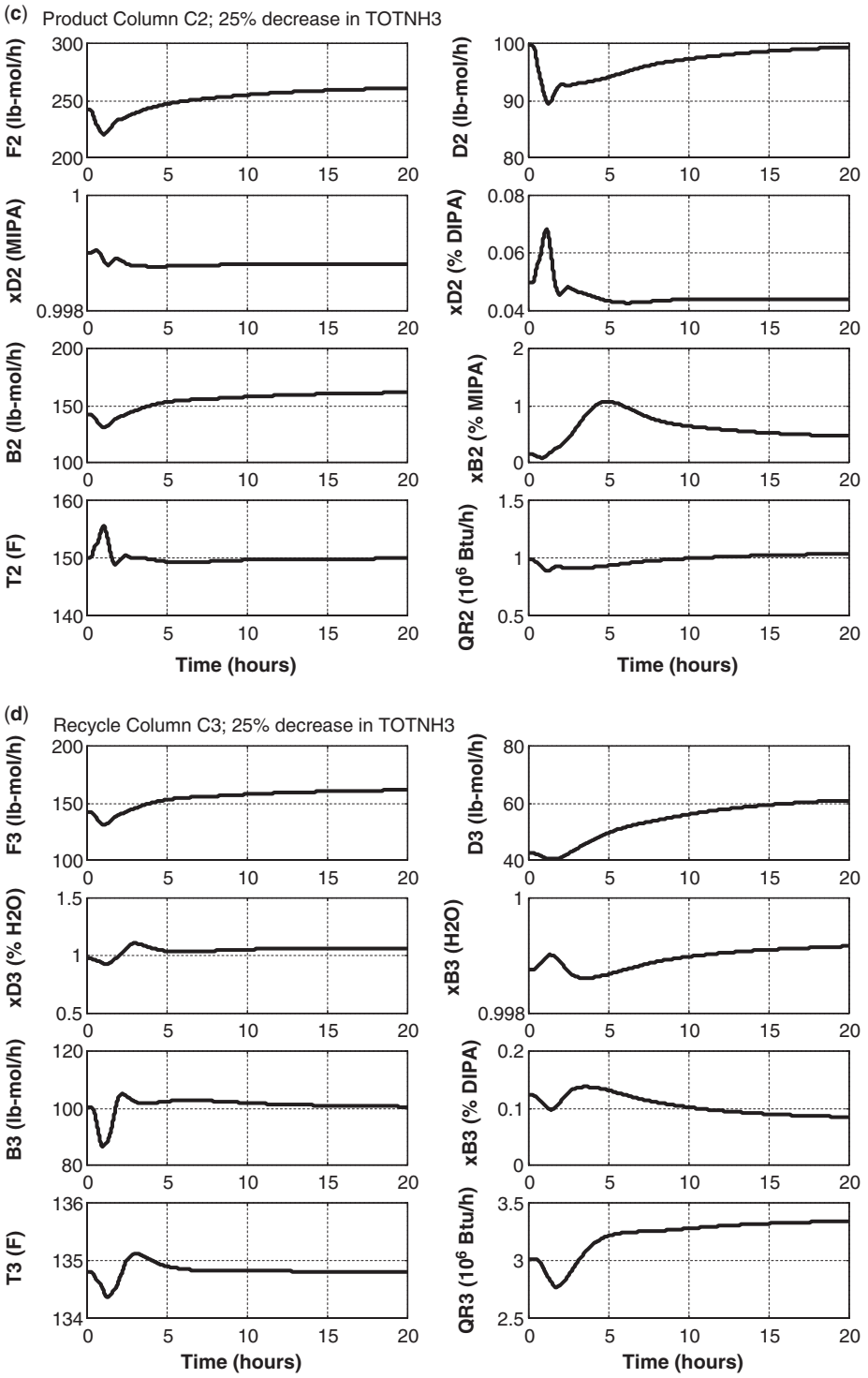


**Figure 14.15.** (*Continued*). (c) Column C2, (d) column C3.

reactor inlet temperature $T_{in}$ is not held at its setpoint for the increase in IPA feed flowrate. The heat input to the heat exchanger goes to zero, but the preheating in the FEHE is so large that the temperature from the heat exchanger is greater than the specified reactor inlet temperature. This causes no problem because the IPA conversion is even higher at the higher inlet temperature.

Figure 14.14b gives results for column C1. The impurities levels in both the distillate and the bottoms are maintained close to the desired levels. Figure 14.14c gives results for column C2. The purity of the MIPA distillate product is held very close to the specified value. The impurity of MIPA in the bottoms increases slightly for the 20% disturbance, which results in a small increase the MIPA in the D3 recycle stream. Figure 14.14d shows the responses of the variable in column C3. The purity of the water bottoms product is held very close to the specified value. Notice that the reactor inlet temperature climbs to 330 °F, which is far above the setpoint value of 317 °F because of the increase in heat transfer in the FEHE.

Other disturbances were made to further test the robustness of the control structure. The system was found to be insensitive to changes in reactor inlet temperature. Disturbances were made in the ratio of ammonia to IPA. This represents a severe disturbance because it has a large effect on the DIPA recycle. Figure 14.15 gives results for a 20% decrease in this ratio ($NH_{3(tot)}$/IPA ratio changed from 3 to 2.4). The control structure successfully handles the large disturbance. Notice that the time scale has been increased to 20 h. It takes a long time for the DIPA recycle (see Figure 14.15d) to increase up to its new level to counteract the effect of the lower reaction selectivity due to the lower ammonia to IPA ratio. The IPA feed flowrate is fixed at 100 lb-mol/h, so eventually the fresh ammonia must also stabilize at 100 lb-mol/h to satisfy the reaction stoichiometry. Figure 14.15a shows that it takes over 15 h for the fresh ammonia to reach this flowrate.

The tuning of the reflux-drum level controller in recycle column C3 affects the time it takes to come to a new steady state. The value of gain used in these simulations is $Kc = 5$. Using the normal $K_c = 2$ results in even longer times. Low gains slow down the flowrate disturbances. Since D3 is a recycle stream, changing it slowly results in longer times for the entire plantwide system to come to a new steady state.

## 14.5 CONCLUSION

A new complex process has been presented in this chapter. It is hoped that this process will be useful to researchers in their plantwide design and control studies. A heuristic economic design has been developed, which balances the effects of the two liquid recycles on capital investment and energy costs. Increasing one recycle decreases the other, so there is an optimum point.

A plantwide control structure has been developed and tested for very large disturbances. Two of the distillation columns can be effectively controlled using a single-end structure with fixed R/F ratios. The third column requires dual-end control using one temperature and one composition. A composition on an intermediate tray is selected to avoid control difficulties due to severe nonlinearity inherent with a high-purity product. An average temperature scheme is used in one of the columns that has a very large temperature change from top to bottom.

## REFERENCES

1. Douglas, J. M. *Conceptual Design of Chemical Processes*, McGraw-Hill, New York, 1988.
2. Downes, J. J., Vogel, E. F. A plantwide industrial process control problem, *Comp. Chem. Eng*. 1992, **17**, 245–255.
3. Luyben, W. L., Tyreus, B. D., Luyben, M. L. *Plantwide Process Control*, McGraw-Hill, New York, 1999.
4. Luyben, W. L. *Plantwide Dynamic Simulators for Chemical Processing and Control*, Marcel Dekker, New York, 2002.
5. Vasudevan, S., Rangalah, G. P., Murthy Konda, N. V. S. N. Application and evaluation of three methodologies for plantwide control of the styrene monomer plant, *Ind. Eng. Chem. Res.* 2009, **48**, 10941–10961.
6. Luyben, W. L. *Disillation Design and Control Using Aspen Simulation*, John Wiley & Sons, Hoboken, NJ, 2006.

# CHAPTER 15

# DESIGN AND CONTROL OF THE STYRENE PROCESS

A recent paper by Vasudevan et al.[1] presented a flowsheet of the styrene process that has several interesting design and control features (see Figure 15.1). Their study concentrated on a comparison of three plantwide control methodologies. The economic optimum design of the process was given, but no quantitative details were given of how the optimum was obtained.

The chemistry of the styrene process involves the dehydrogenation of ethyl benzene (EB). The reaction is endothermic, nonequimolar, and reversible, so high temperatures and low pressures are conducive to high conversion in the adiabatic vapor-phase reactors. Steam is mixed with the EB fed to the reactors to lower the partial pressure of EB and increase conversion. There are also several other side reactions that produce undesirable by-products (benzene, toluene, ethylene, and carbon dioxide) with reaction rates that increase with temperature and partial pressures.

The main design optimization variables in this process are the steam-to-EB ratio, reactor inlet temperature, EB recycle flowrate, and reactor size. Low reactor temperatures suppress side reactions but require higher EB recycle to achieve the same styrene production rate, which increases separation costs. Higher steam-to-EB ratios also suppress side reactions, but increase furnace fuel costs and steam supply costs.

The purpose of this chapter is to develop the economically optimum design considering capital costs, energy costs, and raw material costs, and then to develop a plantwide control structure capable of effectively handling large disturbances in production rate. The proposed design is significantly different than the design of Vasudevan et al. as it features higher steam-to-EB ratios, lower reactor temperatures, larger EB recycle flowrates, and larger reactors.

*Principles and Case Studies of Simultaneous Design*, First Edition. William L. Luyben

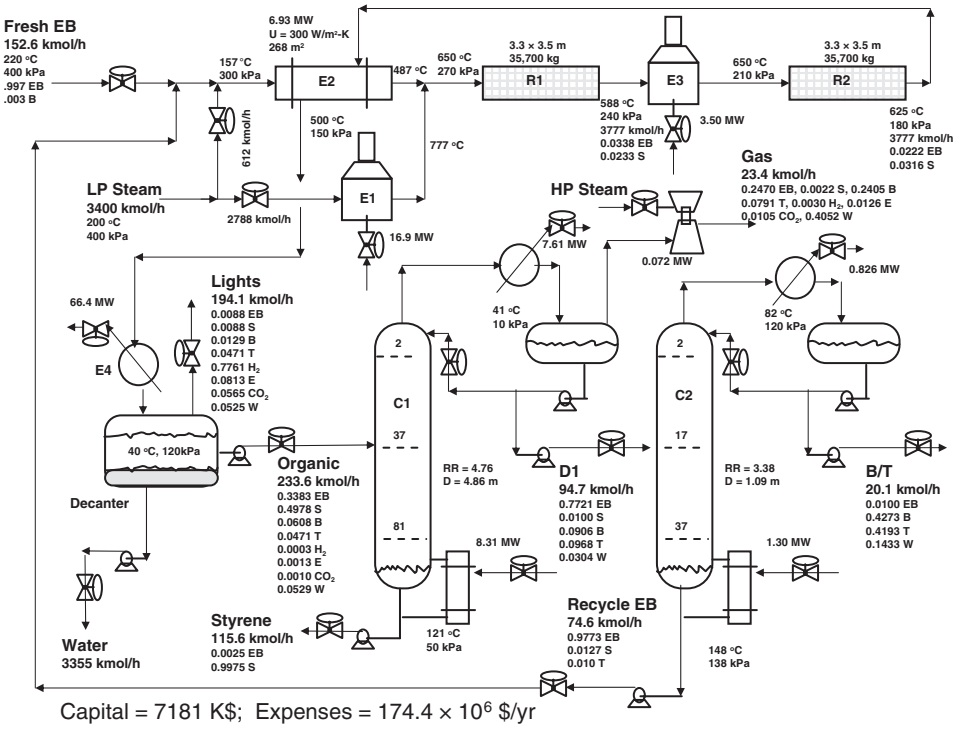


**Figure 15.1.** Vasudevan et al. design.

## 15.1 INTRODUCTION

Jim Douglas was one of the pioneers in conceptual process design. His early book and papers led the way for much of the future practical, nonmathematical design work.[2] One of his contributions was to point out the dominating economic effects of raw material costs in the design of a process. The fresh feed streams are much more costly than the energy used in the process or the cost of the capital invested to build the equipment. Reactant costs are typically an order of magnitude larger than energy or capital costs. This effect is completely generic ("Douglas Doctrine") and is of vital importance in process design.

The styrene process provides an excellent example of the application of the Douglas Doctrine. The consumption of EB fresh feed can be reduced by two methods:

1. Increasing the process steam that is added to the EB feed to the reactor lowers partial pressures and helps to increase conversion of styrene and decrease the production of undesirable by-products. However, it increases the cost of supplying the process steam, and it increases the cost of fuel needed in the furnace to heat the steam and EB to the desired reactor inlet temperature.
2. Lowering reactor temperatures lowers the production of undesirable side products that consume EB without producing styrene. However, lower reactor temperatures require higher EB recycle flowrates to raise EB concentrations so the desired production rate of styrene can be achieved. This increases the capital and energy costs of the separation section of the process.

Thus, there are significant trade-offs that must be made to determine the optimum economic design.

In this chapter, the production rate of styrene is fixed for all cases, and the effects of other design optimization variables are quantitatively explored. The expenses associated with producing this fixed amount of styrene include raw material (EB) cost, process steam cost, furnace fuel cost, column reboiler energy costs, and capital costs (reactors, furnaces, heat exchangers, decanter, and distillation columns). As we will demonstrate, the raw material cost dominates, so investing capital and using energy to reduce the consumption of EB is usually justified, up to the point of diminishing returns. Typically, more capital must be invested to reduce expenses of energy, steam, and raw material. The economic objective is to obtain a reasonable incremental return on incremental investment as changes are made in the design optimization variables.

## 15.2 KINETICS AND PHASE EQUILIBRIUM

### 15.2.1 Reaction Kinetics

The production of styrene involves the dehydrogenation of EB in a high-temperature, low-pressure, gas-phase adiabatic reactor. The reaction is reversible and endothermic.

Styrene reaction:

$$C_6H_5CH_2CH_3 \iff C_6H_5CHCH_2 + H_2 \tag{15.1}$$

There are several other side reactions given by Vasudevan et al.[1] that consume EB and produce undesirable by-products.

Benzene/ethylene reaction

$$C_6H_5CH_2CH_3 \longrightarrow C_6H_6 + C_2H_4 \tag{15.2}$$

Toluene/methane reaction

$$C_6H_5CH_2CH_3 + H_2 \longrightarrow C_6H_5CH_3 + CH_4 \tag{15.3}$$

Carbon monoxide reactions

$$2H_2O + C_2H_4 \longrightarrow 2CO + 4H_2 \tag{15.4a}$$

$$H_2O + CH_4 \longrightarrow CO + 3H_2 \tag{15.4b}$$

**TABLE 15.1 Reaction Kinetics**[a]

| | $k$ | $E$ (kJ/kmol) | Concentrations (Pascals) |
|---|---|---|---|
| Reaction 1 forward | 0.044 | 90,981 | $p_{EB}$ |
| Reaction 1 reverse | $6 \times 10^{-8}$ | 61,127 | $p_S p_H$ |
| Reaction 2 | 27,100 | 207,989 | $p_{EB}$ |
| Reaction 3 | $6.484 \times 10^{-7}$ | 91,515 | $p_{EB} p_H$ |
| Reaction 4 | $4.487 \times 10^{-7}$ | 103,997 | $(p_W)^2 p_E$ |
| Reaction 5 | $2.564 \times 10^{-6}$ | 6723 | $p_W p_M$ |
| Reaction 6 | 1779 | 73,638 | $p_W p_{CO}$ |

[a]Overall reaction rates have units of kmol $s^{-1}$ $m^{-3}$.

Carbon dioxide reaction

$$H_2O + CO \longrightarrow CO_2 + H_2 \tag{15.5}$$

Table 15.1 gives the kinetic parameters used in this study, which are somewhat modified from those of Vasudevan et al.[1] in order to match the reactor exit stream leaving the second reactor. Simple power-law kinetics are used for all reactions. All overall reaction rates have units of kmol $s^{-1}$ $m^{-3}$. Concentration units are partial pressures in Pascals.

$$\Re_{1F} = p_{EB} k_{1F} e^{-E_{1F}/RT} \tag{15.6}$$

$$\Re_{1R} = p_S p_W k_{1R} e^{-E_{1R}/RT} \tag{15.7}$$

$$\Re_2 = p_{EB} k_2 e^{-E_2/RT} \tag{15.8}$$

$$\Re_3 = p_{EB} p_H k_3 e^{-E_3/RT} \tag{15.9}$$

$$\Re_4 = p_W (p_E)^{0.5} k_4 e^{-E_4/RT} \tag{15.10}$$

$$\Re_5 = p_W p_M k_5 e^{-E_5/RT} \tag{15.11}$$

$$\Re_6 = p_W p_{CO} k_6 e^{-E_6/RT} \tag{15.12}$$

The chemistry immediately tells us that high temperatures will favor the first reaction because the activation energy of the forward reaction is greater than the activation energy of the reverse reaction since the reaction is endothermic. The kinetics also tell us low pressure and high EB concentrations will favor the production of styrene.

However, the other reactions have specific reaction rates that increase with temperature. So the production of undesirable by-products that waste the reactant EB can be reduced by keeping temperature low. Thus, there is a fundamental conflict between conversion (favored by high temperatures) and selectivity (favored by low temperatures). Low pressure also slows these undesirable reactions.

### 15.2.2 Phase Equilibrium

The styrene process has a decanter, which involves liquid-liquid-vapor phase equilibrium, and two distillation columns, which involve vapor-liquid equilibrium. Figures 15.2a and 15.2b give the *Txy* diagrams for the EB/styrene system at 10 and 50 kPa, which are the pressures at the top and bottom of the product column C1. The separation is run under vacuum to suppress styrene polymerization. It is a difficult separation, so the column has many trays and a fairly high reflux ratio (RR). Figure 15.3 gives the *Txy* diagram for the toluene/EB separation at 120 kPa. This separation is only modestly difficult, so fewer trays and a lower RR are required.

In the decanter, a multicomponent mixture is separated into two liquid phases (aqueous and organic) and a vapor phase. The major components are water, EB, styrene, and hydrogen, with small amounts of benzene and toluene. Figure 15.4 gives a ternary diagram for the EB/styrene/water system at 10 kPa. The total pressure in the decanter is 120 kPa, but the presence of hydrogen and other light components lowers the effective pressure of the

other heavier components. A pressure of 10 kPa gives a temperature close to the 40 °C temperature in the decanter and illustrates the LLE properties. The aqueous phase is essentially pure water. The organic phase contains a small amount of water.

## 15.3 VASUDEVAN ET AL. FLOWSHEET

Figure 15.1 shows the flowsheet of the process with the equipment sizes and conditions derived from the paper by Vasudevan et al.[1] Flowrates and compositions are similar to those given in their paper, but there are some small differences.

The fresh feed is 152.6 kmol/h of EB. It is combined with 74.6 kmol/h of a recycle stream of mostly EB and 612 kmol/h of low-pressure process steam. The stream is heated in a feed-effluent heat exchanger (E2), which uses the hot reactor effluent to heat the feed stream to 487 °C. Additional low-pressure process steam (2788 kmol/h) is heated in a furnace (E1) to 777 °C and mixed with the stream from E2 to achieve a reactor inlet temperature of 650 °C. The heat duty in the furnace is 16.9 MW. The total process steam is 3400 kmol/h.

### 15.3.1 Reactors

There are two gas-phase adiabatic reactors in series. Each has a diameter of 3.3 m, a length of 3.5 m, and a catalyst loading of 35,700 kg. The exit temperature of the first reactor is 588 °C because of the endothermic reaction. A furnace (E3) heats this stream back up to 650 °C before it enters the second reactor. The furnace heat duty is 3.5 MW.

The total EB entering the first reactor R1 is 225.1 kmol/h. The EB leaving the second reactor has a molar flowrate of 80.9 kmol/h, so the per-pass conversion of EB in the two reactors is 64%. The molar flowrate of styrene leaving the second reactor is 119 kmol/h.

If all of the EB in the fresh feed were converted into styrene, there would be 152.6 kmol/h of styrene produced. Therefore, a significant amount of EB is wasted in producing by-products. In addition, there are significant losses of EB and styrene in the two gas streams leaving the process (to be discussed in Section 15.4). The production rate of stryrene leaving the process from the bottom of the first distillation column is only115.6 kmol/h, giving a styrene yield of only 76%. It is obvious that a lot of EB is not ending up in the styrene product stream. This means that raw material cost is higher than it would be if smaller amounts of by-products were produced and losses of EB and styrene were lower. There appears to be plenty of opportunity for process improvement.

### 15.3.2 Condenser and Decanter

After being cooled in E2 and partially condensed in heat exchanger E4 using cooling water, the process stream enters a decanter operating at 40 °C and 120 kPa. The dimensions to give 20 min of liquid holdup when half full are a diameter of 2.8 m and a length of 5.6 m. Water is withdrawn from the bottom of the vessel at a rate of 3355 kmol/h. The gas phase (“Lights”) leaving the top of the decanter at a flowrate of 194.1 kmol/h contains most of the hydrogen formed in the basic reaction, but it also contains significant amounts of other components. The styrene lost in this stream is 1.71 kmol/h, and the EB loss is also 1.71 kmol/h.

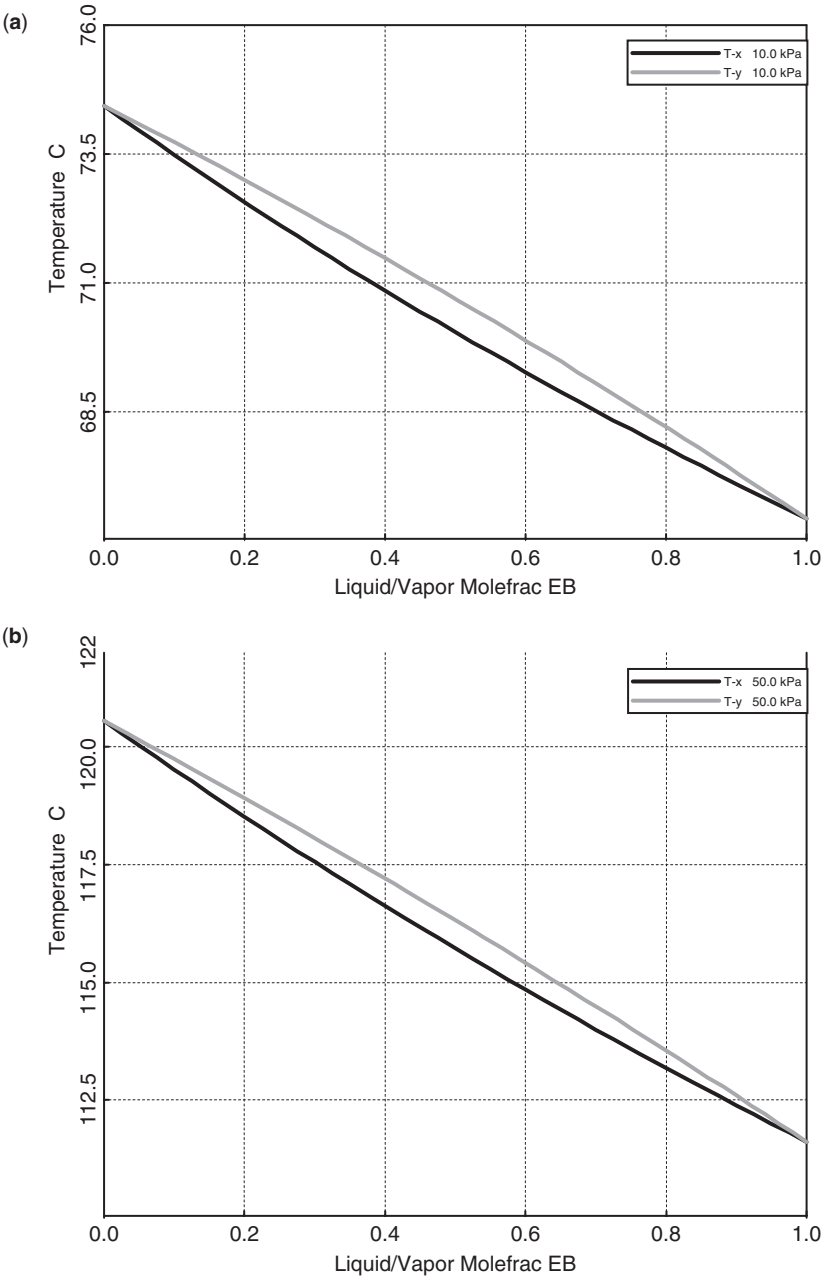


**Figure 15.2.** *Txy* diagram for EB/styrene at (a) 10 kPa, and (b) 50 kPa.

### 15.3.3 Product Column C1

The organic phase is fed to the distillation column C1 at a flowrate of 233.6 kmol/h and a composition of 33.83 mol% EB, 49.78 mol% styrene, 6.08 mol% benzene, 4.71 mol% toluene, 5.29 mol% water, and a small amount of some of the light components.

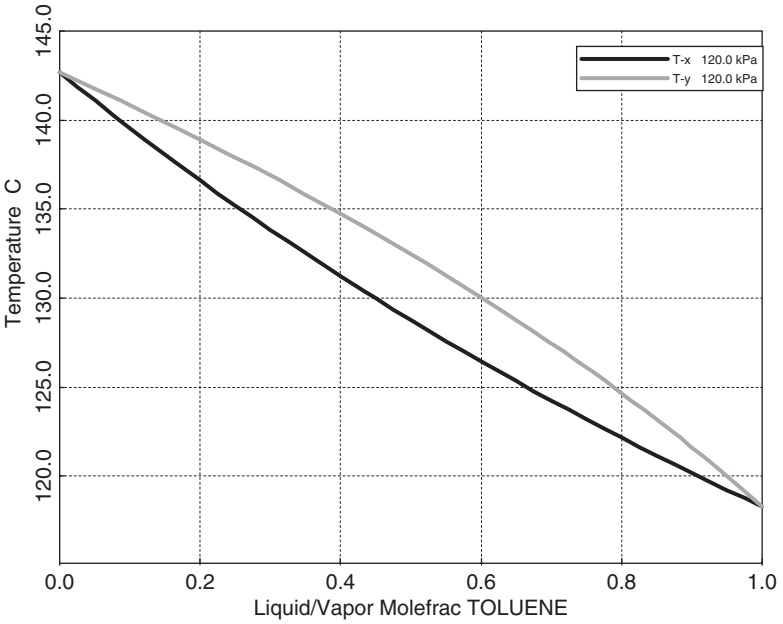


**Figure 15.3.** *Txy* diagram for toluene/EB at 120 kPa.

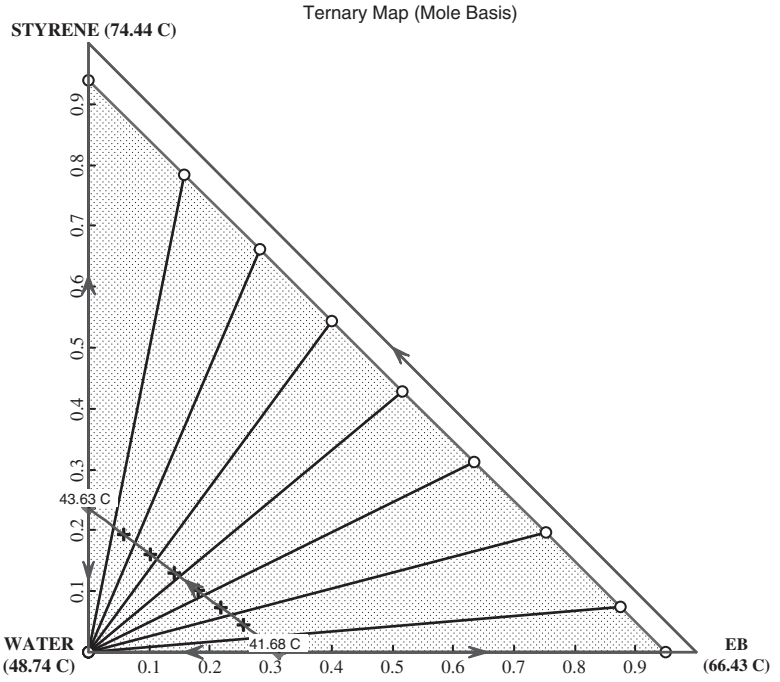


**Figure 15.4.** Ternary diagram for EB/styrene/water at 10 kPa.

The 82-stage column operates under vacuum with a reflux-drum pressure of 10 kPa. The pressure drop per tray is assumed to be 0.5 kPa. A theoretical tray model is used in the Aspen *RadFrac* simulation, but in determining the capital cost of the column, structured packing at a cost of $\$1000/m^3$ is assumed to fill the vessel.

The diameter of the column is 4.86 m, and the reboiler duty (supplied by low-pressure steam) is 8.31 MW. The RR is 4.76. The feed is fed on stage 37, which minimizes reboiler duty.

The two design specifications for the column are a bottoms purity of 99.75 mol% styrene and a distillate impurity of 1 mol% styrene.

### 15.3.4 Recycle Column C2

The bottoms stream from column C1 is fed to stage 17 of a 38-stage distillation column, which recovers EB for recycle. The two design specifications are a bottoms impurity of 1 mol% toluene and a distillate impurity of 1 mol% EB. The distillate is mostly benzene and toluene with some water. The bottoms is recycled back to the reaction section.

The column operates at 120 kPa, has a diameter of 1.09 m, and requires an RR of 3.38. The reboiler duty is 1.3 MW.

As we will show in Section 15.5, the total capital investment of the Vasudevan et al. plant is \$7,181,000. The total expenses for purchasing the fresh EB feed, the process steam, and the energy required in the furnaces and distillation columns is \$174,400,000/yr. A large percentage of this expense is in raw materials cost. To produce 115.6 kmol/h of styrene, the fresh feed of EB is 152.6 kmol/h.

In the proposed design discussed in Section 15.5, the same amount of styrene is produced from less EB fresh feed (132.8 kmol/h). This results in a much lower expense of \$155,800,000/yr. The capital investment is only slightly higher (\$8,764,000).

## 15.4 EFFECTS OF DESIGN OPTIMIZATION VARIABLES

The design discussed in the previous section appears to offer bountiful opportunities for cost reduction, primarily in terms of improving the yield of styrene by reducing the production of unwanted by-products and reducing losses of raw material and product. In this section we explore the effects of the major design optimization variables on the economics of the process.

The major design optimization variables are the process steam, the reactor inlet temperature, the EB recycle flowrate, and the size of the reactors. These will each be explored separately.

### 15.4.1 Effect of Process Steam

Using more process steam lowers partial pressures of the reactant and products in the styrene reversible reaction and helps to drive the reaction to the right. However, steam costs increase, and furnace duties increase. A process steam cost of \$16.27/1000 kg is assumed based on information from Turton et al.[3] Remember that boiler feed water must be generated and converted into steam before it is injected as live steam into the process. The water from the decanter cannot be used as boiler feed water. The cost of the fuel used in the two furnaces is assumed to be \$9.83/GJ based on energy cost data from Turton et al.[3]

The flowrate of process steam was varied to see its effect on process conditions and economic results. In all the results shown below, the production of styrene is kept constant at 115.6 kmol/h. This is achieved by varying the EB recycle flowrate in each case. Reactor inlet temperatures are kept at 650 °C. As we will see, the fresh feed of EB required to produce the 115.6 kmol/h of styrene changes as the process steam flowrate is changed. The cost of EB is assumed to be \$0.50/lb.

The installed costs of the furnaces are calculated from the correlation given in Turton et al.[3] (p. 915).

$$\log_{10} C_n = 7.3488 - 1.168 \log_{10} Q_{En} + 0.2028(\log_{10} Q_{En})^2 \tag{15.13}$$

where $C_n$ is the installed cost of furnace $n$ with an energy requirement of $Q_{En}$ in kW.

Figure 15.5 shows the results of changing process steam from the original 3400 kmol/h up to 4500 kmol/h. As process steam flowrate increases, less EB fresh feed is needed, which translates into significant reductions in raw material cost. This occurs because there is less production of undesirable by-products, as demonstrated by the reduction in "Lights" from the decanter and "Gas" from the reflux drum of C1.

However, the energy consumption in the furnace E1 increases, which raises energy cost and furnace capital cost. There is little change in the EB recycle needed to keep the styrene production constant at 115.6 kmol/h.

Table 15.2 gives details of the costs for each case. We use the incremental savings and the incremental capital investment in going from one case to another to select the optimum process steam flowrate. The savings are the differences between the expenses (EB fresh feed, fuel, and process steam) in moving from one case to the next. Expenses are reduced as

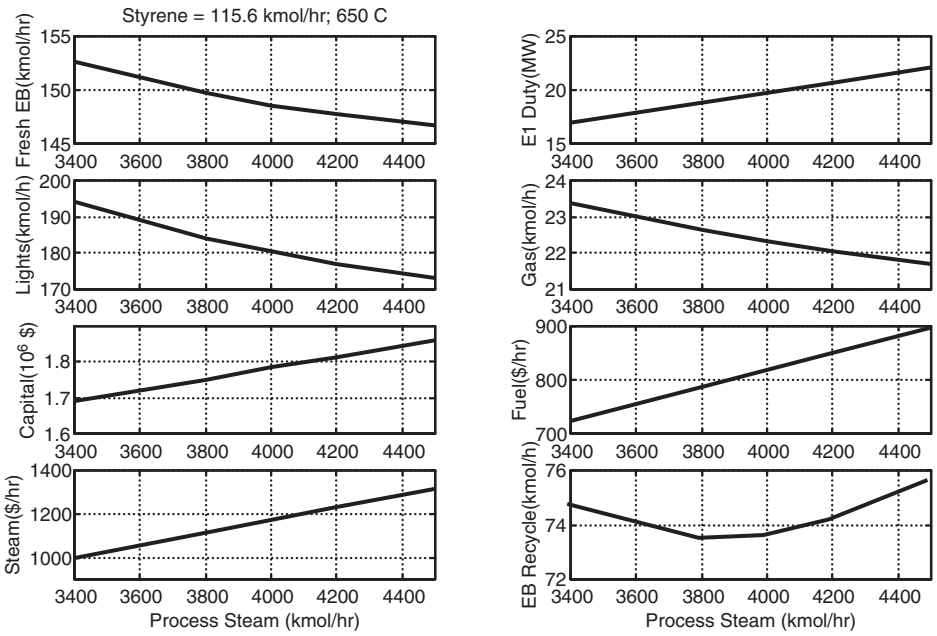


**Figure 15.5.** Effect of process steam.

**TABLE 15.2 Effect of Process Steam Flowrate**[a]

| Process steam flowrate (kmol/h) | 3400 | 3800 | 4000 | 4200 | 4500 |
|---|---|---|---|---|---|
| $Q_{E1}$ (MW) | 16.95 | 18.80 | 19.79 | 20.67 | 22.10 |
| $Q_{E3}$ (MW) | 3.50 | 3.40 | 3.36 | 3.32 | 3.28 |
| Fresh EB (kmol/h) | 152.64 | 149.70 | 148.6 | 147.77 | 146.72 |
| Lights (kmol/h) | 194.1 | 183.9 | 180.4 | 177.0 | 173.3 |
| Gas (kmol/h) | 23.38 | 22.63 | 22.34 | 22.07 | 21.72 |
| EB recycle (kmol/h) | 74.61 | 73.35 | 73.46 | 74.05 | 75.47 |
| Furnace energy cost ($/h) | 724.0 | 785.6136 | 819.2322 | 848.9581 | 898.0006 |
| Process steam cost ($/h) | 995.7 | 1112.9 | 1171.4 | 1230.0 | 13179 |
| Capital investment furnace ($ $10^6$) | 1.690 | 1.7506 | 1.7838 | 1.8130 | 1.861 |
| Incremental furnace capital ($) | – | 61.171 | 33.200 | 29.135 | 47.977 |
| Fresh EB savings ($/h) | – | 343.8634 | 128.6564 | 97.0771 | 122.8084 |
| Energy and process steam cost increase ($/h) | – | 178.7191 | 92.1906 | 88.2979 | 136.9058 |
| Net savings ($ $10^6$/y) | – | 1.4467 | 0.31944 | 0.076906 | −0.12349 |
| Incremental ROI | – | 23.64 | 9.6217 | 2.6396 | −2.574 |

[a]Styrene production = 115.6 kmol/h; 650 °C reactor inlet temperatures.

process steam flowrate is increased because the reduction in EB fresh feed is much larger than the increase in the cost of process steam and furnace energy, up to some point of diminishing returns. However, capital investment increases.

For example, with a process steam flowrate of 3800 kmol/h (second column in Table 15.2), the capital investment in the furnaces is $1,750,600. With a process steam flowrate of 4000 kmol/h, the capital investment is $1,783,800. The incremental capital investment is $33,200. At 3800 kmol/h, the cost of steam is $1112.9/h and the cost of furnace fuel is $785.61/h. At 4000 kmol/h, these increase to $1171.4 and $819.23/h, respectively. This is an increase in total cost of $92.19/h.

However, the reduction in EB fresh feed (149.7 – 148.6 = 1.1 kmol/h) represents a raw material savings of $128.65/h. So the net savings is $128.65/h minus $92.19/h, which amounts to $319,440/yr.

The increase in furnace capital investment in designing for 4000 kmol/h of process steam instead of 3800 kmol/h is $33,200. Investing this amount to save almost ten times this amount is an attractive investment.

Going from 4000 kmol/h up to 4200 kmol/h of process steam requires an incremental investment of $29,135 and yields a net savings of $76,906/yr, which is still attractive. However, in going up to 4500 kmol/h, steam and fuel costs increase by $136.90/h while EB fresh feed savings only increase by $122.81/h and capital investment increases by $47,977.

In order to remain on the conservative side, a process steam flowrate of 4000 kmol/h is selected as the design point.

### 15.4.2 Effect of Reactor Inlet Temperature

With process steam fixed at 4000 kmol/h, the effect of reactor inlet temperature is explored. Styrene production is held at 115.6 kmol/h for all cases. The inlet temperatures of both reactors are assumed to be the same.

Figure 15.6 shows how several important variables change as reactor inlet temperature is changed from the original 650 °C down to 550 °C. As the top graph on the left shows, the consumption of raw material EB decreases as reactor inlet temperatures are decreased. This is reflected in the decreases in the flowrates of vapor from the decanter shown in Figure 15.6 ("Lights" shown in the second graph from the top on the left) and gas from the reflux drum of the first distillation column ("Gas," shown in the second graph from the top on the right). However, the rate of reduction of the required EB fresh feed slows up as temperatures are reduced, so there is a point of diminishing returns. The third graph from the top on the right shows that net expenses (raw material savings minus the costs of process steam, furnace energy, and reboiler energy) reach a minimum at about 560 °C.

Figure 15.6 also shows (top graph on the right) that the required recycle of EB increases as reactor inlet temperatures are decreased. Higher EB concentrations are required in the reactors to achieve the desired styrene production rate. The higher recycle raises separation costs in the distillation columns. Energy costs in the large E1 furnace and in the reboiler of the first column increase. Capital investments in the furnace and in the first distillation column increase as reactor inlet temperatures are reduced.

Table 15.3 gives details of the economics for each case. The incremental savings in going from 580 °C to 560 °C is the difference between the total expenses: \$158,050,000/yr − \$157,520,000/yr = \$530,000/yr. The incremental increase in capital investment is \$11,485,000 − \$9,965,900 = \$1,519,000, giving a return on investment of 35%.

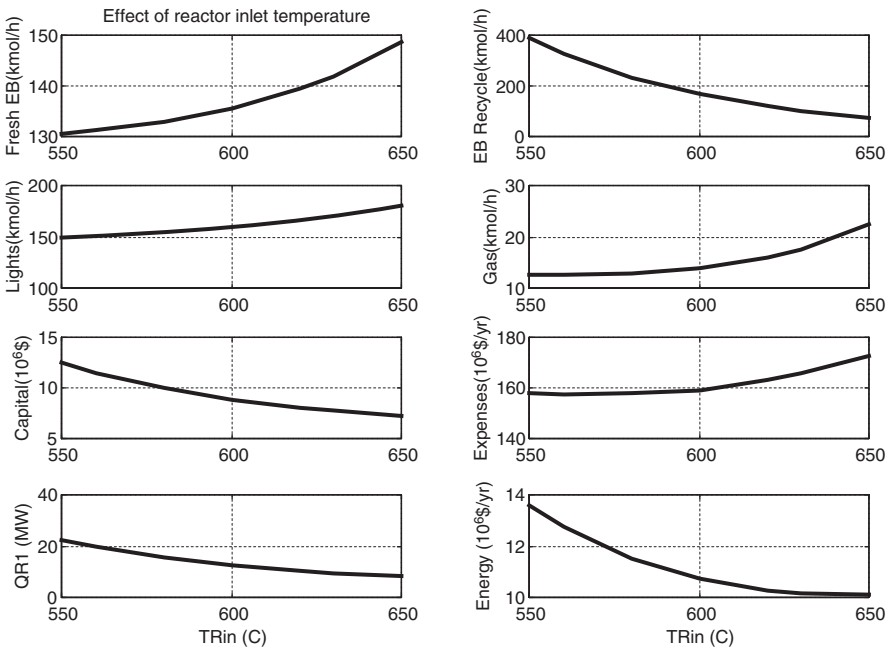


**Figure 15.6.** Effect of reactor inlet temperature.

**TABLE 15.3 Effect of Reactor Inlet Temperature**[a]

| | | | | | | |
|---|---|---|---|---|---|---|
| Reactor inlet temperature (°C) | 550 | 560 | 580 | 600 | 650 | 650 |
| Process steam (kmol/h) | 4000 | 4000 | 4000 | 4000 | 4000 | 3400 |
| Fresh EB (kmol/h) | 130.6469 | 131.268 | 132.996 | 135.618 | 148.63 | 152.6426 |
| EB recycle (kmol/h) | 391.7 | 327.8 | 232.2 | 165.9 | 73.46 | 74.61 |
| Lights (kmol/h) | 149.7 | 151.1 | 154.8 | 159.5 | 180.4 | 194.1 |
| Gas (kmol/h) | 12.67 | 12.55 | 12.96 | 14.01 | 22.34 | 23.38 |
| $Q_{E1}$ (MW) | 14.68 | 15.23 | 16.25 | 17.22 | 19.73 | 16.95 |
| $Q_{R1}$ (MW) | 22.53 | 19.75 | 15.47 | 12.42 | 8.236 | 8.313 |
| ID1 (m) | 8.355 | 7.783 | 6.823 | 6.06 | 4.839 | 4.86 |
| Total capital ($10^6$ $) | 12.458 | 11.485 | 9.9659 | 8.8467 | 7.2156 | 7.1808 |
| Total expenses ($10^6$ $/yr) | 157.72 | 157.52 | 158.05 | 159.95 | 172.63 | 174.44 |
| Total energy ($10^6$ $/yr) | 13.603 | 12.764 | 11.529 | 10.733 | 10.08 | 9.321 |

[a]Styrene production = 115.6 kmol/h.

Going from 560 °C to 550 °C increases total expenses instead of decreasing them, and requires an increase in capital investment. Therefore, a reactor inlet temperature of 560 °C is selected for the design.

### 15.4.3 Effect of Reactor Size

The next design optimization variable considered is reactor size. The diameters of the two reactors are held constant at 3.3 m, and their lengths are varied from the base-case 3.5 m up to 10 m. Process steam is 4000 kmol/h and reactor inlet temperature is 560 °C in all these cases.

Figure 15.7 shows that the consumption of fresh EB increases slowly as the reactor length is increased. This occurs because less EB recycle is required to maintain styrene production, which increases the production of undesirable by-products. The vapor from the decanter increases as reactor length increases.

However, the very significant reduction in EB recycle reduces energy and capital costs in the separation section, so total capital investment decreases despite the increase in reactor capital investment. The net result in the balance between raw material cost and energy cost is a reduction in total expenses as we move up from 3.5 m to 7 m in reactor length, where a minimum is encountered.

As shown in Table 15.4, going from 10 m to 8 m in reactor length increases expenses slightly (raw material cost increases while energy consumption in the separation section decreases) by $580,000/yr. The required increase in capital investment in going from 10 m to 8 m is $225,000, which is a 250% return on incremental investment. So the 8 m reactor is better than the 10 m reactor.

Going from 8 m to 7 m in reactor length again results in a slight increase in expenses, but reduces capital investment still further. The savings in expenses in going from 8 m down to 7 m is $70,000/yr. The required increase in capital investment is $279,400, which is only a 35% return on incremental investment.

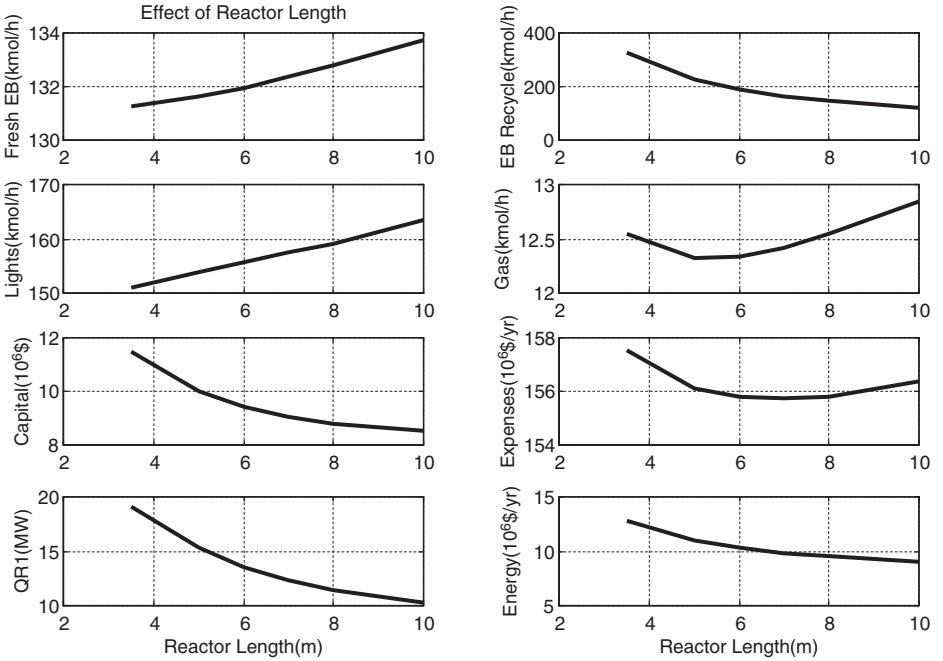


**Figure 15.7.** Effect of reactor length.

Going from 7 m down to 6 m results in increases in both expenses and capital investment, which obviously is unattractive. The 8-m reactor is selected for the proposed design.

### 15.4.4 Optimum Distillation Column Design

The number of stages in each of the distillation columns was optimized by finding the number that minimized total annual cost (TAC). The results are shown in Table 15.5. The optimum values are the same as those given in the Vasudevan et al. design.

**TABLE 15.4 Effect of Reactor Size**[a]

| Reactor length (m) | 3.5 | 5 | 6 | 7 | 8 | 10 |
|---|---|---|---|---|---|---|
| Fresh EB (kmol/h) | 131.268 | 131.6287 | 131.9723 | 132.356 | 132.7634 | 133.7437 |
| EB recycle (kmol/h) | 327.8 | 328.3 | 191.0 | 165.0 | 146.0 | 121.2 |
| Lights (kmol/h) | 151.1 | 153.9 | 155.7 | 157.5 | 159.2 | 163.6 |
| Gas (kmol/h) | 12.55 | 12.31 | 12.34 | 12.42 | 12.54 | 12.85 |
| $Q_{E1}$ (MW) | 15.23 | 14.76 | 14.59 | 14.47 | 14.38 | 14.27 |
| $Q_{R1}$ (MW) | 19.75 | 15.28 | 13.56 | 12.35 | 11.46 | 10.31 |
| ID1 (m) | 7.783 | 6.778 | 6.356 | 6.043 | 5.804 | 5.479 |
| Total capital ($10^6$ $) | 11.485 | 9.9912 | 9.4365 | 9.0432 | 8.7638 | 8.5388 |
| Total expenses ($10^6$ $/yr) | 157.52 | 156.12 | 155.80 | **155.73** | 155.80 | 156.38 |
| Total energy ($10^6$ $/yr) | 12.764 | 10.764 | 10.326 | 9.858 | 9.517 | 9.090 |

[a]Styrene production = 115.6 kmol/h; process steam flowrate = 4000 kmol/h; reactor inlet temperatures = 560 °C.

**TABLE 15.5 Optimum Distillation Column Design**

| | | | |
|---|---|---|---|
| Column C1 | | | |
| NT | 72 | 82 | 102 |
| $NF_{opt}$ | 32 | 37 | 45 |
| ID1 (m) | 5.979 | 5.806 | 5.674 |
| $Q_{R1}$ (MW) | 12.05 | 11.45 | 11.056 |
| $Q_{C1}$ (MW) | 11.47 | 10.87 | 10.41 |
| TAC ($10^6$ \$/yr) | 5.468 | **5.372** | 5.491 |
| Column C2 | | | |
| NT | 32 | 38 | 42 |
| $NF_{opt}$ | 16 | 17 | 18 |
| ID2 (m) | 1.408 | 1.381 | 1.371 |
| $Q_{R2}$ (MW) | 2.077 | 1.987 | 1.965 |
| $Q_{C2}$ (MW) | 1.174 | 1.099 | 1.072 |
| TAC ($10^6$ \$/yr) | 0.8206 | **0.8127** | 0.8153 |

### 15.4.5 Number of Reactors

The flowsheets considered above used two reactors in series with two furnaces for preheating. A flowsheet with three reactors and three furnaces was studied to see if there was any economic incentive to add an additional reaction stage. Process steam flowrate was kept at 4000 kmol/h, and reactor inlet temperature was kept at 560 °C.

A third reactor and a third furnace were added. Capital investment increased because of this change and its effect on other parameters.

With three 8-m reactors, the consumption of fresh EB jumped from 132.76 to 136.28 kmol/h, indicating poor economics. With three 3.5-m reactors, the consumption of fresh EB was reduced from the base-case of 132.76 to 132.19 kmol/h. However, the required EB recycle climbed from the base-case of 146.0 to 194.8 kmol/h. The resulting increase in column energy and capital made capital investment climb from \$8,763,800 to \$9,921,000, and expenses increased from \$155,800,000/yr to \$156,820,000/yr. Therefore, a two-stage reaction section is better than three-stage.

### 15.4.6 Reoptimization

In the previous sections, the design optimization variables have been changed one at a time to find the best values. Several additional cases were examined in which parameters were changed from the optimum values to see if there were better conditions. The independent variation of parameters appears to have resulted in the optimum economic design.

For example, with a 8-m reactor and 560 °C reactor inlet temperatures, the process steam flowrate was varied from its optimum value of 4000 kmol/h. Results showed that 4000 kmol/h is still the optimum.

Increasing steam flowrate to 4200 kmol/h reduced fresh EB feed from 132.7634 to 132.1605 kmol/h. But total energy increased from \$9,517,000/yr to \$9,765,000/yr, and capital investment increased from \$8,763,800 to \$8,817,300. The net effect on expenses was an increase from \$155,800,000/yr to \$155,950,000/yr. So, increasing process steam flowrate from the proposed value is unattractive.

Decreasing steam flowrate to 3800 kmol/h increased fresh EB feed from 132.7634 to 133.4902 kmol/h. Total energy decreased from \$9,517,000/yr to \$9,277,600/yr and capital

investment also decreased from $8,763,800 to $8,719,800. But the increase in raw material cost produced a net increase in expenses from $155,800,000/yr to $156,820,000/yr. So, decreasing process steam flowrate from the proposed value is also unattractive. The "sweet spot" appears to be 4000 kmol/h.

### 15.4.7 Other Improvements

There are several other features that could be explored to improve the flowsheet. First, the feed to C1 could be preheated by the bottoms from the column to reduce reboiler energy consumption.

Second, the hot stream from the feed-effluent heat exchanger (FEHE) E2 is at a high enough temperature (392 °C) that it could be used to generate steam or be heat-integrated with the reboilers in the distillation columns instead of throwing the energy away to cooling water. After generating steam, a water-cooled condenser would be required to get the stream down to 40 °C.

Neither of these features is included in the proposed flowsheet because they could also be applied in the Vasudevan et al. flowsheet and would not affect the comparison.

## 15.5 PROPOSED DESIGN

Figure 15.8 shows the flowsheet with the revised parameters. Process steam flowrate is 4000 kmol/h. Reactor inlet temperature is 560 °C. Reactors are 8 m in length.

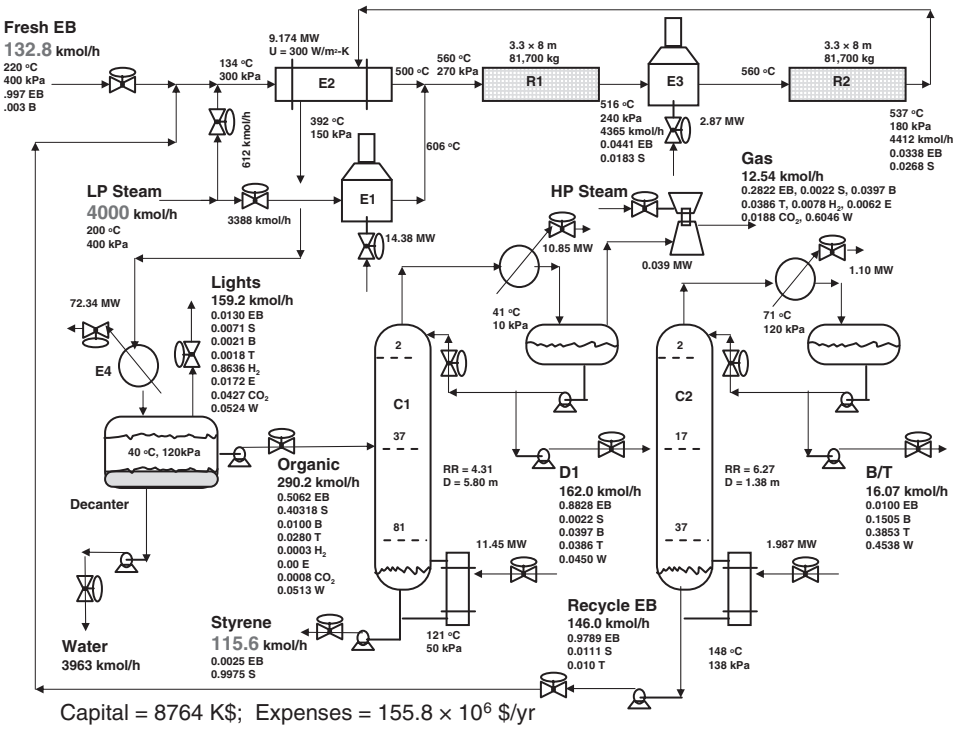


**Figure 15.8.** Proposed design.

Notice that the styrene production rate from the bottom of the product column C1 is exactly the same as that in the Vasudevan et al. design. However, the fresh EB feed has been reduced from 152.6 to 132.8 kmol/h.

Recycle EB has almost doubled (74.6 to 146 kmol/h). Decanter vapor has dropped from 194.1 to 159.2 kmol/h. Gas from the reflux drum of C1 has dropped from 23.4 to 12.54 kmol/h. Styrene yield has increased from 76% to 87%.

The economic result of these changes in equipment and operating conditions is a reduction in total expenses from \$174,400,000/yr to \$155,800,000/yr, which is a very significant savings in operating costs. This improvement requires an increase in capital investment from \$7,181,000 to \$8,764,000, which is well justified to attain the cost reduction.

Figure 15.9 gives the composition profiles in the two reactors. Figure 15.10 gives the temperature and composition profiles in the product column. Figure 15.11 gives these profiles in the recycle column.

## 15.6 PLANTWIDE CONTROL

Before the steady-state Aspen Plus simulation is exported into Aspen Dynamics, column reflux drums and bases are sized to provide 5 min of liquid holdup at 50% level. The decanter is sized to provide 20-min holdup. Deadtimes of 5 min are inserted in the two furnace temperature control loops to account for the dynamic lags in furnace firing.

It is interesting to note that the steady state predicted by the dynamic model in Aspen Dynamics is slightly different than that predicted by the steady-state model in Aspen Plus. Running the Aspen Dynamics simulation out in time until all variables stopped changing gave somewhat different conditions. The total EB was fixed at 278.6 kmol/h. The resulting fresh feed of EB was 129.53 kmol/h instead of 132.8 kmol/h found in Aspen Plus. The styrene product changed from 115.6 to 112.5 kmol/h. The production of "Lights" changed from 159.2 to 155.9 kmol/h. The production of "Gas" changed from 12.54 to 12.39 kmol/h. The explanation for this small difference in the two steady states probably lies in the difference in the plug flow reactor models. In Aspen Plus, a distributed ordinary differential equation model is used. In Aspen Dynamics, a multicell "lumped" model is used.

### 15.6.1 Control Structure

Figure 15.12 shows the plantwide control structure developed for this process. Conventional PI controllers are used in all loops. All level loops are proportional with $K_C = 2$. The C2 column temperature loop has a 1-min deadtime. The composition loops have 3-min deadtimes. All are tuned by using relay-feedback tests (see Yu[4]) to obtain ultimate gains and periods, and then applying Tyreus–Luyben tuning rules. The various loops are listed below with their controlled and manipulated variables.

1. The total EB flowrate (fresh plus recycle from the recycle column) is controlled by manipulating the fresh feed of EB.
2. The flowrate of the steam that is mixed with the total EB stream before feeding into FEHE E1 is ratioed to the flowrate of the total EB.
3. The flowrate of the steam that is heated in furnace E2 is ratioed to the flowrate of the total EB, with the ratio adjusted by the output signal from a temperature controller holding the inlet temperature to the first reactor (TCR1).

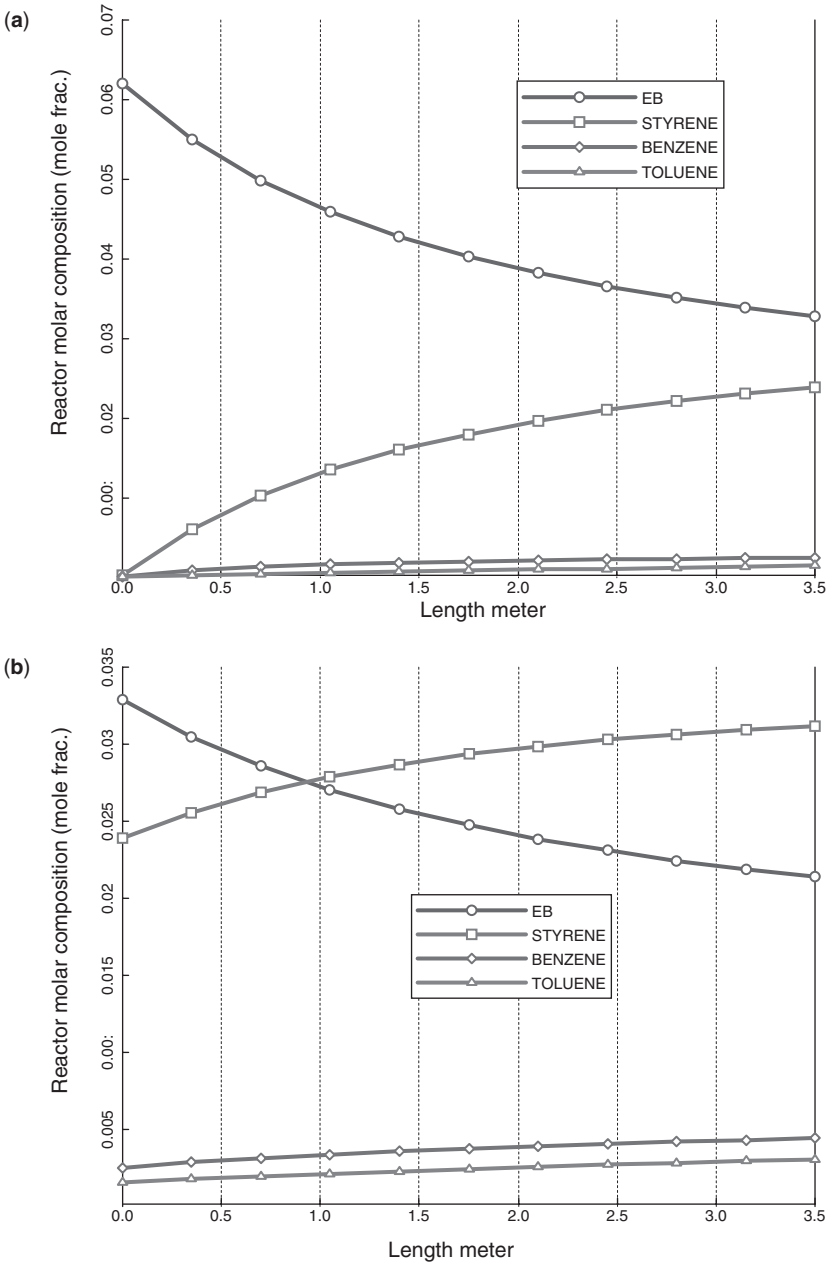


**Figure 15.9.** Composition profiles in (a) Reactor R1, and (b) Reactor R2.

4. The inlet temperature to the second reactor is controlled by manipulating the fuel to furnace E3 (TCR2).
5. Decanter temperature is controlled by manipulating the heat removal in condenser E4.
6. Decanter pressure is controlled by manipulating the vapor stream ("Lights").

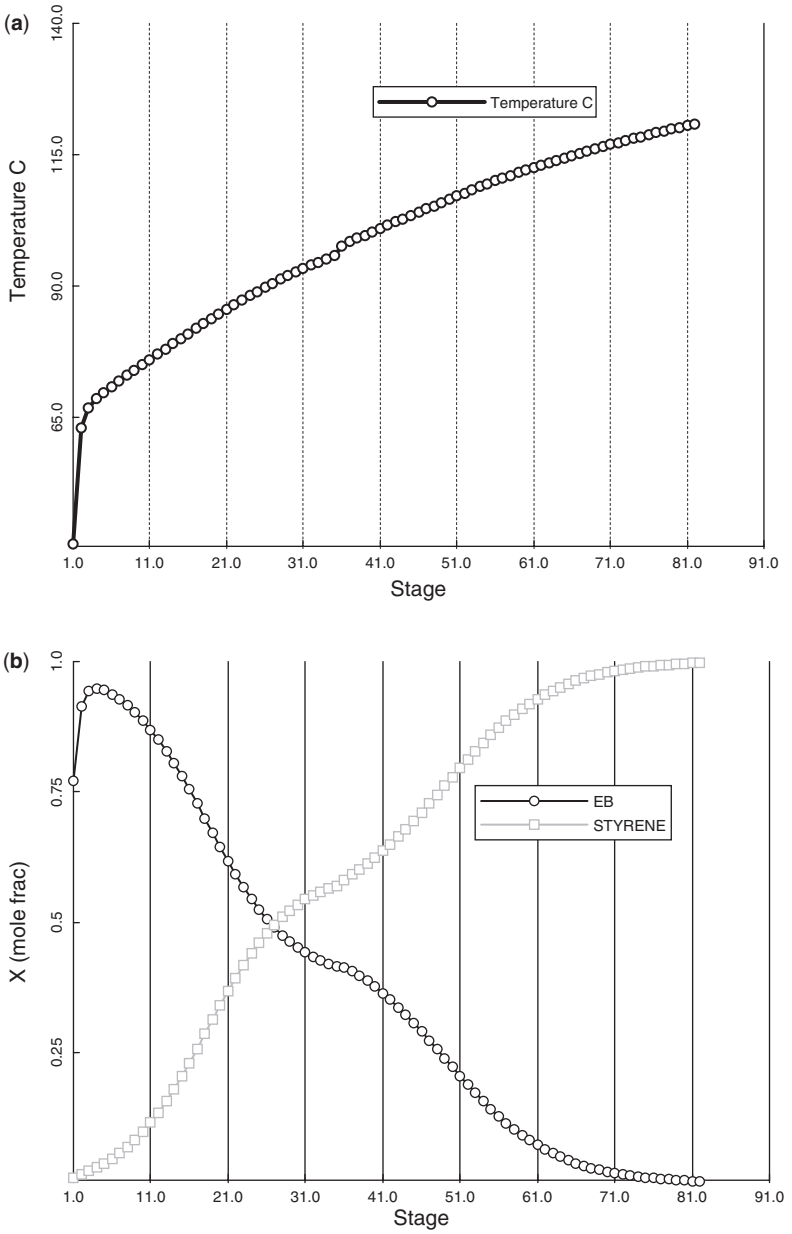


**Figure 15.10.** Column C1: (a) temperature profile, and (b) composition profiles.

7. The water/organic level in the decanter is controlled by the aqueous phase drawoff rate.
8. The organic level is controlled by the organic drawoff rate, which is the feed to the product column.
9. Reflux in the product column is ratioed to the feed to the column, but a 5-min lag is inserted between the feed flow signal and the reflux flow to account for the dynamic difference between the effect of feed flowrate and reflux flowrate.

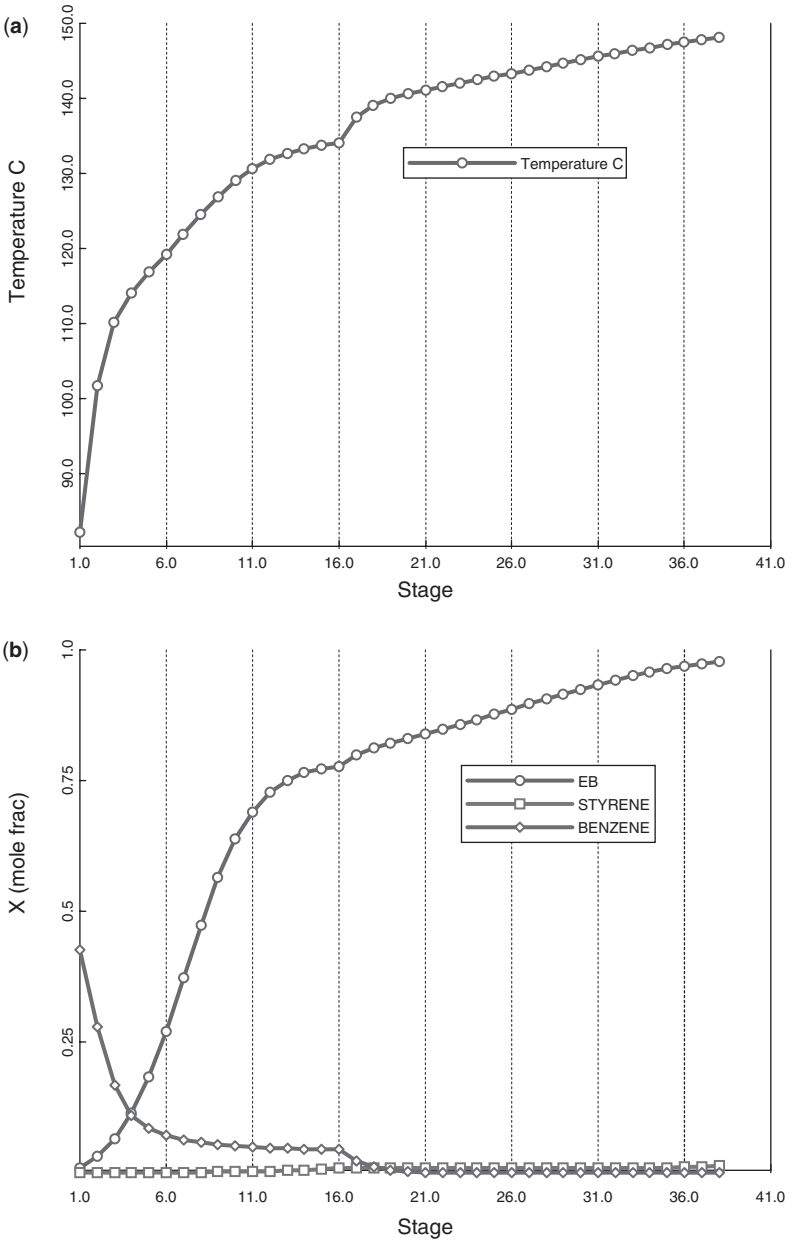


**Figure 15.11.** Column C2: (a) temperature profile, and (b) composition profiles.

10. Gas from the reflux drum of the product column is removed by changing compressor speed to control reflux-drum temperature.
11. The EB impurity on stage 65 is controlled by manipulating reboiler heat input (CC1).
12. Base level is controlled by manipulating bottoms flowrate, which is the styrene product from the process.
13. Distillate controls reflux-drum level and is the feed to the recycle column.

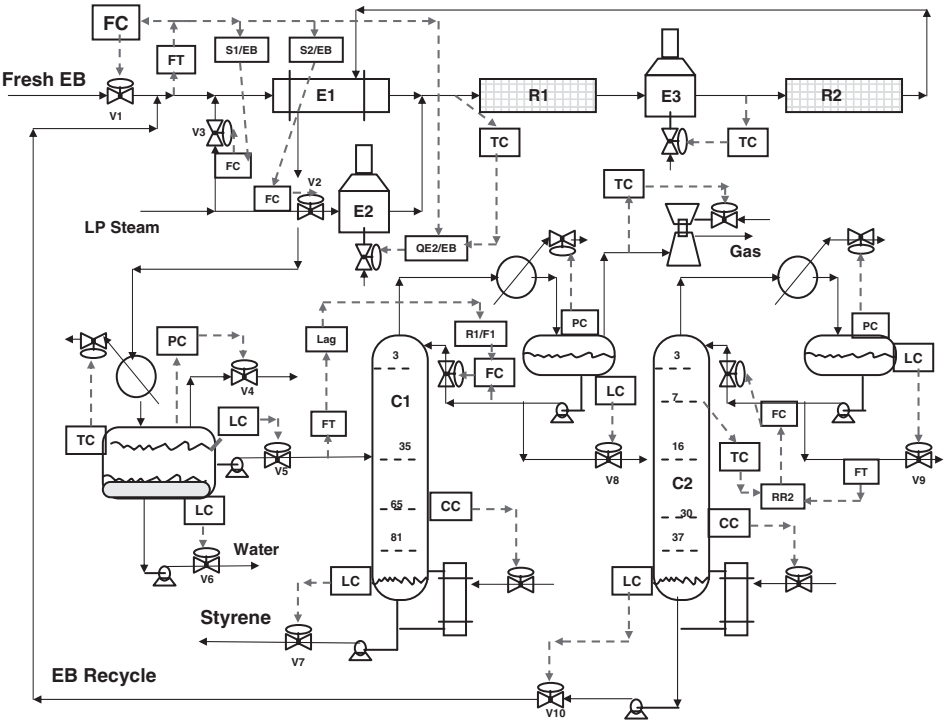


**Figure 15.12.** Control structure.

14. Distillate in the recycle column controls reflux-drum level.
15. Reflux in the recycle column is manipulated to keep a specified RR, with the RR being adjusted by a stage 7 temperature controller (TC2).
16. Base level is controlled by manipulating bottoms flowrate; this is the EB recycle stream back to the reaction section.
17. Toluene impurity on stage 30 in the recycle column is controlled by manipulating reboiler heat input (CC2).
18. Pressures in both columns are controlled by manipulating condenser heat removal rates.

The rationale for the selection of the distillation control structures outlined above is discussed in the next section. Since the product styrene leaves from the bottom of the first column, an effective column control structure for this column is vital in terms of product-quality control.

### 15.6.2 Column Control Structure Selection

For reasons of simplicity and low maintenance cost, many industrial distillation columns use some type of single-end temperature control. However, this simple structure may not provide effective control for some columns. Even if a single-end control structure is possible, we have to decide how to select the other control degree of freedom. The most common choices are holding a constant reflux-to-feed (R/F) ratio or holding a constant RR.

***Selecting Reflux Ratio or Reflux-to-Feed Ratio.*** To explore this question, a series of steady-state runs were made in which the effects of changes in feed composition on the required changes in R/F ratio and RR were determined while holding both products at their specified composition. Table 15.6 gives results of these calculations for the two distillation columns.

*Product Column C1.* In the first distillation column, the feed compositions of the light-key component EB and the heavy-key component styrene are varied around the design point (50.61 mol% EB and 40.31 mol% styrene). As more EB and less styrene are fed to the column, there is very little change in the R/F ratio (see Table 15.6). On the other hand, the RR changes about 17% over the range. Therefore, an R/F ratio should work well.

There may be some difficulties with this structure because of the high RR in this column. Conventional distillation wisdom suggests that reflux-drum level should be controlled using reflux when RRs are high. A recent paper (see Luyben[5]) suggests a method for handling the situation in which an R/F ratio structure can be used even in a high RR column by using reboiler heat input to control reflux-drum level. Since the product column operates under vacuum conditions, rapid manipulation of reboiler heat input is undesirable. Therefore the R/F structure is selected. Dynamic performance results presented in Section 15.6.3 show that effective control is achieved.

*Recycle Column.* In the second distillation column, the feed compositions of the light-key component toluene and the heavy-key component EB are varied around the design point (4.722 mol% toluene and 88.28 mol% EB). The changes in the R/F ratio over the range of feed compositions are about 34% (see Table 15.6), and the changes in the RR are about 8%. These results suggest that a single-end structure may not provide effective control for feed composition disturbances. Therefore a dual-end structure is selected for this column. A composition controller and a temperature controller are used, as discussed below.

**TABLE 15.6 Column Control Structure Selection**

| | Feed Composition | Reflux-to-Feed Ratio | Reflux Ratio |
|---|---|---|---|
| C1 | 0.55615 EB<br>0.35307 Styrene | 2.587 | 3.966 |
| Design | 0.50615 EB<br>0.40307 Styrene | 2.590 | 4.305 |
| | 0.45615 EB<br>0.45307 Styrene | 2.595 | 4.711 |
| C2 | 0.02722 Toluene<br>0.9028 EB | 0.4787 | 6.078 |
| Design | 0.04722 Toluene<br>0.8828 EB | 0.6202 | 6.254 |
| | 0.06722 Toluene<br>0.8628 EB | 0.6913 | 5.782 |

***Selecting Temperature/Composition Control Tray Location.*** Another important issue in distillation control structure selection is the location of the tray used for temperature or composition control. A simple approach for temperature control that usually works quite well is to select a location where the temperatures are changing significantly from tray to tray.

*Product Column.* The EB/styrene separation is a difficult one (low relative volatility), which requires many trays and gives a flat temperature profile. The vacuum operation results in significant pressure changes through the column, and the resulting temperature profile is more affected by pressure than composition (see Figure 15.10a). Therefore, temperature cannot be used in this column. A direct composition measurement and composition control are required.

The natural choice of what composition to control would be the EB impurity in the bottoms. However, trying to control bottoms composition in this high-purity column (99.75 mol% styrene) would result in slow closed-loop dynamic response and a high degree of nonlinearity.

Distillation control wisdom suggests that it is better to move away from the high-purity end of the column to a tray having larger compositions. Process gains are larger, and there is less nonlinearity to complicate closed-loop performance. Figure 15.10b shows that the EB impurity on stage 65 is 6.38 mol% EB. We select this stage to control.

*Recycle Column.* Figure 15.11a shows that there are significant changes in temperature from tray to tray in the rectifying section of the column. So we should be able to control one temperature. Since this temperature is near the top of the column, it should do an effective job of maintaining the EB impurity in the distillate. Stage 7 is selected. The temperature controller adjusts the RR.

The second loop in the recycle column must be a composition loop since there is only one temperature break in the column. The bottoms recycle stream is fairly pure EB with only 1 mol% toluene. We might consider controlling it directly. Control might be better if we control a composition higher up in the column.

Both of these alternatives were tested. Controller tuning with a 3-min deadtime produced an integral time of 65 min for control of bottoms composition. Controller tuning with the same 3-min deadtime for controlling the toluene impurity on stage 30 produced a 33-min integral time. These results demonstrate that much tighter control can be achieved by using a composition away from the high-purity base of the column.

### 15.6.3 Dynamic Performance Results

Several large disturbances were made to test the ability of the proposed plantwide control structure to provide stable regulatory control and hold product streams near their desired specifications. Table 15.7 gives controller parameters for the major loops.

***Throughput Disturbances.*** Figure 15.13 gives the responses of a number of important variables when 20% changes in the setpoint of the flow controller on the total EB fed to the reactors are made at time equal 0.2 h. The solid lines are for 20% increases, and the dashed lines are for 20% decreases. Stable regulatory control is achieved for these large disturbances.

The change in the total EB immediately changes the two steam addition rate through the action of the ratio elements. Notice that there are large transient changes in the flow of the

**TABLE 15.7 Controller Parameters**

| | TCR1 | TCR2 | CC1 | CC2 | TC2 |
|---|---|---|---|---|---|
| Controlled variable | $R_1$ inlet temperature | $R_2$ inlet temperature | Stage 65 liquid composition | Stage 30 liquid composition | Stage 7 liquid composition |
| Manipulated variable | Furnace E2 heat duty | Furnace E3 heat duty | Reboiler heat input | Reboiler heat input | RR |
| SP | 560 °C | 560 °C | 0.0665 mole fraction EB | 0.0463 mole fraction toluene | 125.9 °C |
| Transmitter range | 500–700 °C | 500–700 °C | 0–0.133 mole fraction EB | 0–0.10 mole fraction toluene | 100–200 °C |
| OP | 0.1859 $Q_{E2}/EB_{tot}$ | 9.958 GJ/h | 41.33 GJ/h | 7.254 GJ/h | 7.254 RR2 |
| OP range | 0–0.3 $Q_{E2}/EB_{tot}$ | 0–20.67 GJ/h | 0–100 GJ/h | 0–14.31 GJ/h | 0–10 RR2 |
| Deadtime | 3 min | 3 min | 3 min | 3 min | 1 min |
| $K_C$ | 0.225 | 0.915 | 0.271 | 0.193 | 1.60 |
| $\tau_I$ | 14.5 min | 13.2 min | 37 min | 33 min | 15.8 min |

fresh EB feed. The fresh EB feed climbs to almost 300 kmol/h for an increase in total EB flow, and drops to zero for a while for a decrease in total EB flow. The result of the 20% changes in total EB are 16% changes in the fresh feed of EB and 16% changes in the styrene product (from 112.5 up to 129.3 kmol/h or down to 94.7 kmol/h). The change in EB recycle is about 23%, and the change in "Lights" is about 18%.

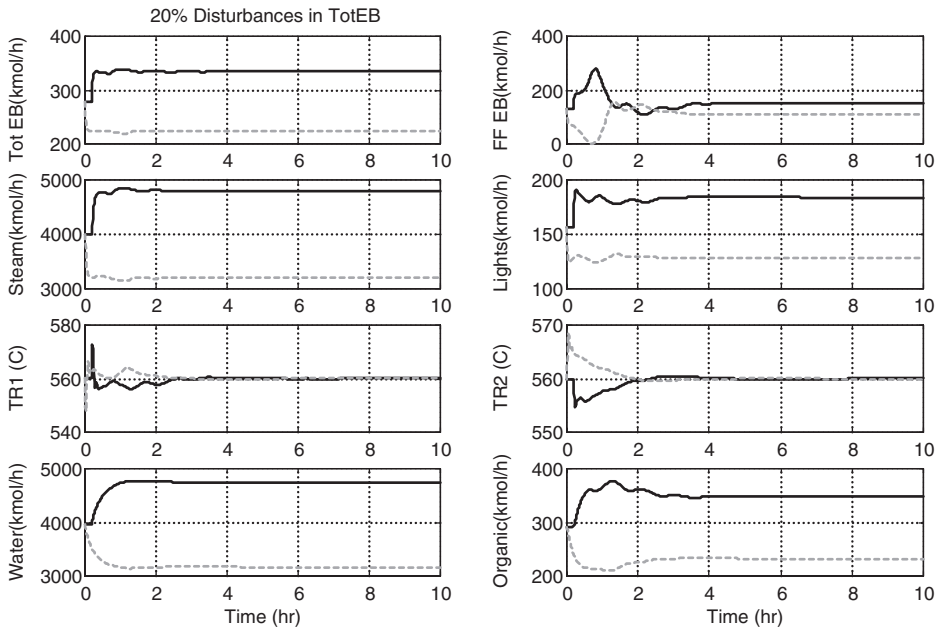


**Figure 15.13.** 20% disturbances in $EB_{tot}$.

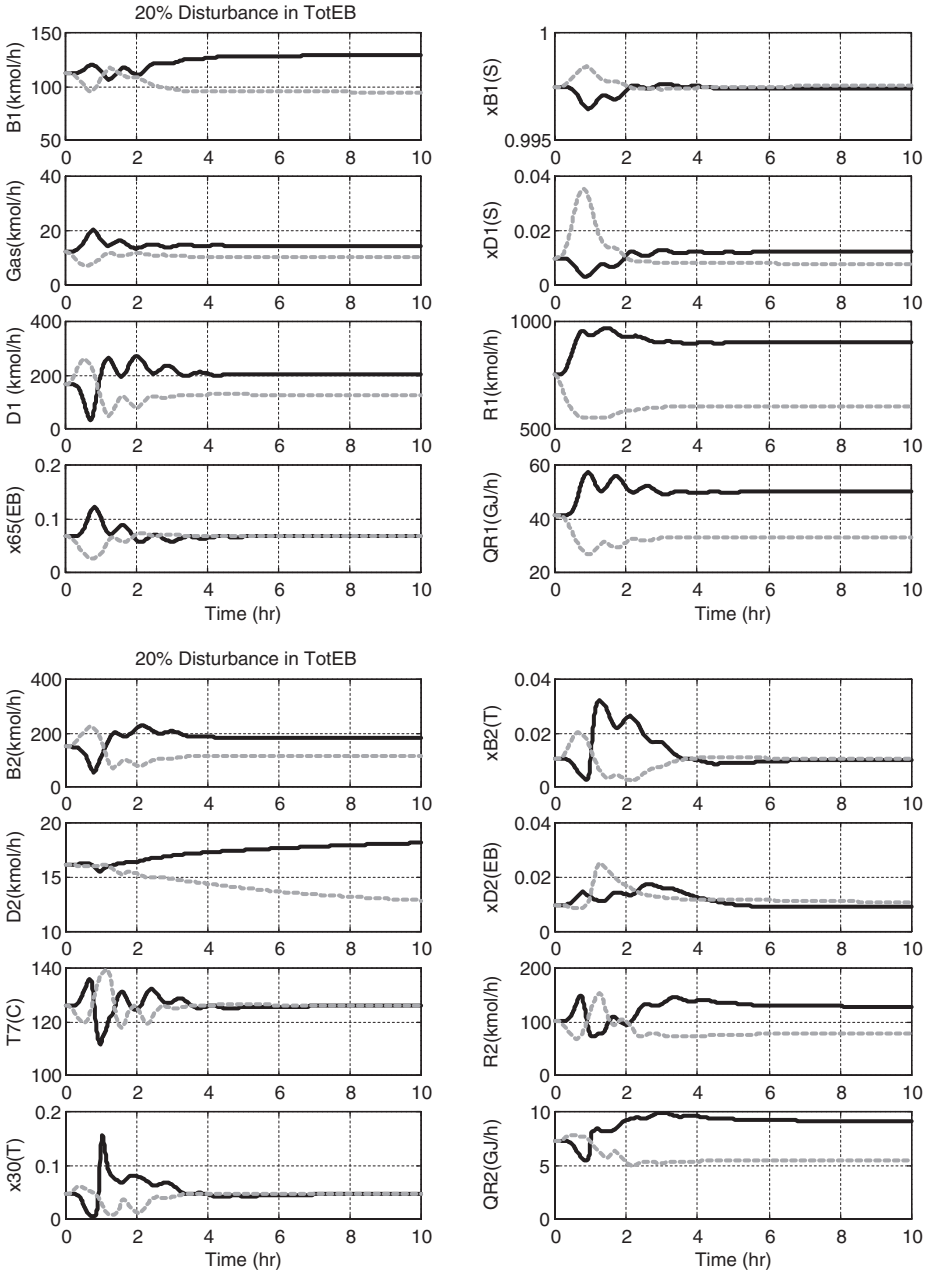


**Figure 15.13.** *Continued*.

The control of reactor R1 inlet temperature ($T_{R1}$) is quite good, with a deviation of only 10 °C. This is due to the $Q_{E2}$-to-$EB_{tot}$ ratio that makes immediate changes in the furnace fuel as inlet flows change. The reflux changes (through the lag) as the feed to the column ("Organic") changes.

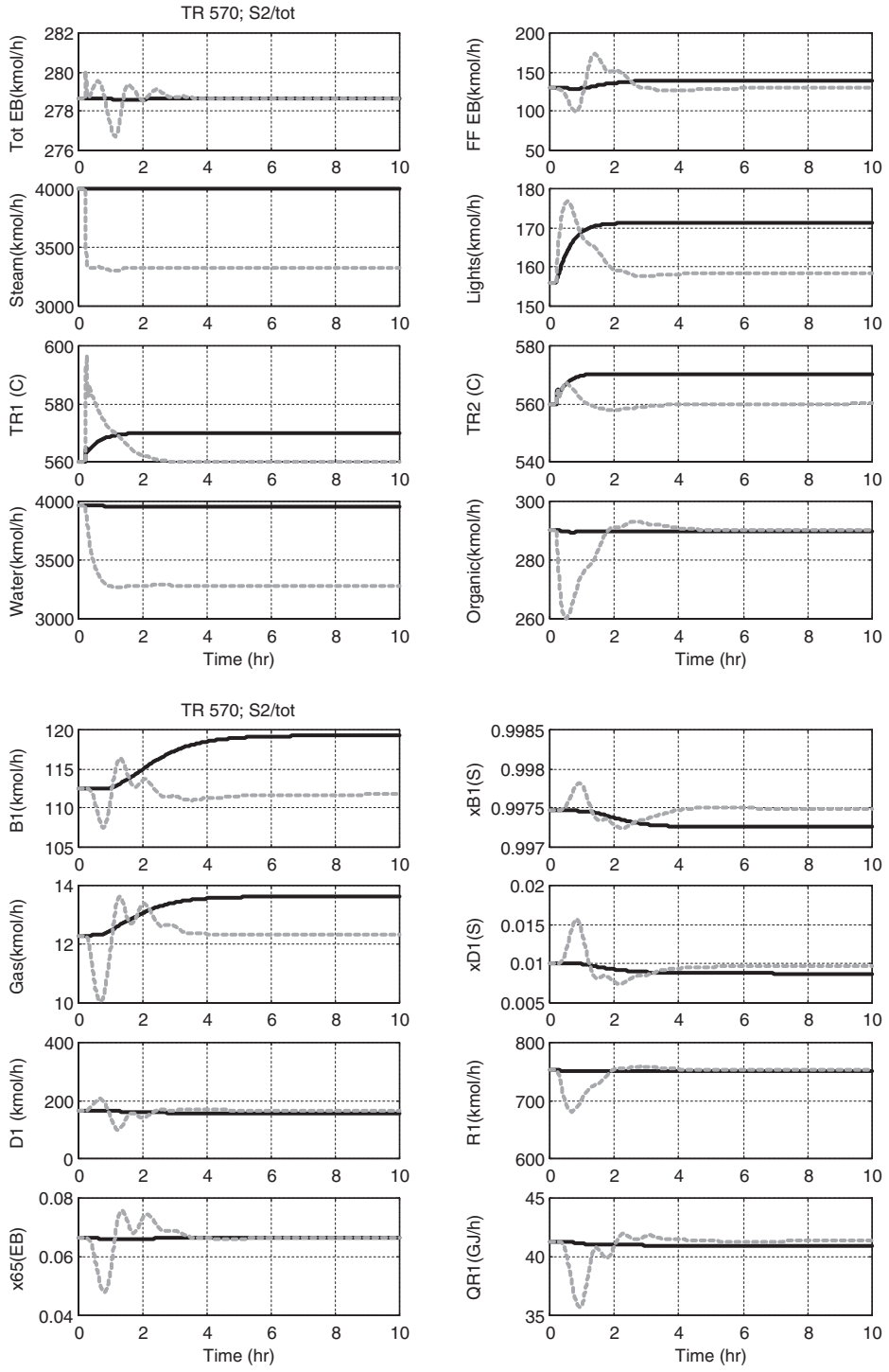


**Figure 15.14.** Disturbances in inlet reactor temperature and steam/EB ratio.

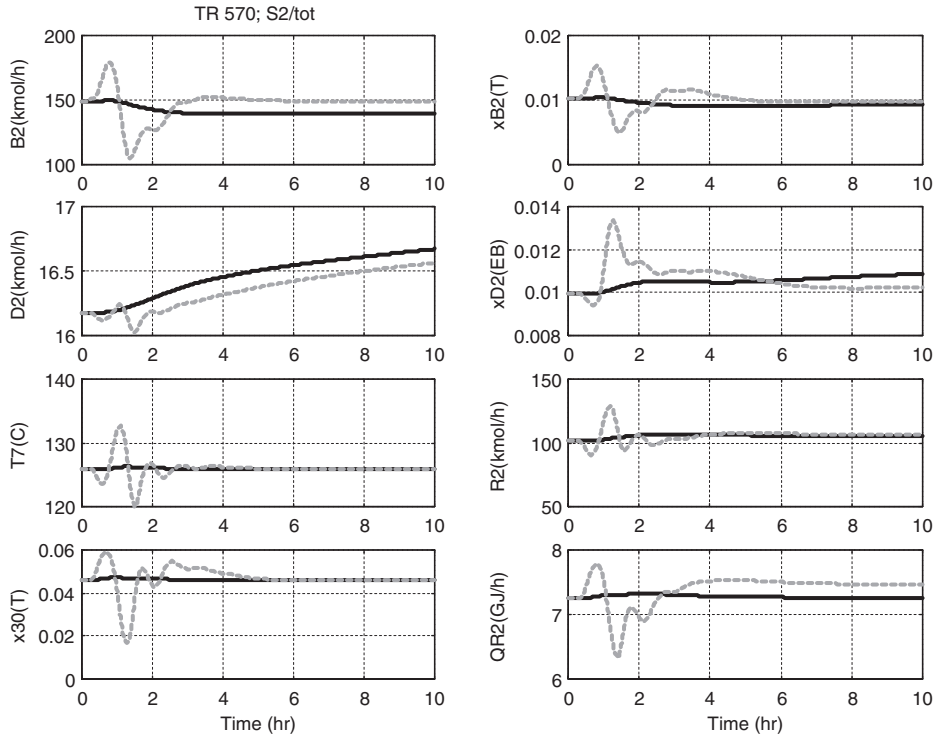


**Figure 15.14.** *Continued*.

The purity of the styrene product $x_{B1(S)}$ is maintained very close to its specification. Remember that this composition is not directly controlled. The composition of stage 65 is controlled by manipulating reboiler heat input.

The impurity of EB in the distillate of the recycle column undergoes some transient disturbances but is brought back to very close to its specified value in about 3 h. The changes in the flowrate of the distillate D2 from the recycle column are very slow, taking almost 10 h to come to a new steady state. The changes in the flowrate of the EB recycle (B2) occur fairly quickly, taking only about 2 h to come to steady state.

***Reactor Inlet Temperature Disturbances.*** The solid lines in Figure 15.14 give the responses of the system when the setpoints of the two reactor inlet temperature controllers are increased from 560 to 570 °C at time equal 0.2 hours. Total EB is held constant.

The higher reactor temperatures lead to increases in "Lights" (155.9 to 171.1 kmol/h), "Gas" (12.29 to 13.62 kmol/h), and fresh EB (129.5 to 139.4 kmol/h). There is only a small increase in styrene product (112.5 to118.3 kmol/h), so the styrene yield drops from 86.8 to 85.6% as a result of the higher temperature.

***Steam-to-EB Ratio Disturbances.*** The dashed lines in Figure 15.14 give the responses when the ratio between the steam fed to furnace E2 and the total EB is reduced from 12.155 to 9.724. There are some small transients, but the long-term effect on the process is small. There are small increases in the reflux and reboiler heat input in the recycle column.

## 15.7 CONCLUSION

The styrene process illustrates a number of interesting design trade-offs. Low reactor temperatures improve styrene yield, but require more EB recycle to maintain conversion, which increases energy and capital costs in the separation section of the process. Higher process steam flows improve yield and selectivity but increase furnace capital and fuel costs and increase the cost of providing the process steam. Economics are dominated by improving yield to reduce raw material costs.

The control of the process requires effective control structures for the distillation columns from which the styrene product and the recycle EB come. The product column uses an R/F single-end control structure, but temperature control cannot be used because of the flat temperature profile. Composition control on an intermediate tray avoids slow dynamics and nonlinearity. A dual-end control structure is required in the recycle column (one temperature controller and one composition controller).

## REFERENCES

1. Vasudevan, S., Rangaiah, G. P., Murthy Konda, N. V. S. N., Tay, W. H. Application and evaluation of three methodologies for plantwide control of the styrene monomer plant, *Ind. Eng. Chem. Res.* 2009, **48**, 10,941–10,961.
2. Douglas, J. M. *Conceptual Design of Chemical Processes*, McGraw-Hill, New York, 1988.
3. Turton, R., Bailie, R. C., Whiting, W. B., Shaelwitz, J. A. *Analysis, Synthesis and Design of Chemical Processes*, 2nd Edition, Prentice Hall, Englewood Cliffs, NJ, 2003.
4. Yu, C. C. *Autotuning of PID Controllers*, 2nd Edition, Springer-Verlag, London, 2006.
5. Luyben, W. L. Unusual control structure for high reflux ratio distillation columns, *Ind. Eng. Chem. Res.* 2009, **48**, 11,048–11,059.